

Supplementary information

Discovery and molecular basis of subtype-selective cyclophilin inhibitors

In the format provided by the authors and unedited

Supplementary Information

Discovery and molecular basis of subtype-selective cyclophilin inhibitors

Alexander A. Peterson, Aziz M. Rangwala, Manish K. Thakur, Patrick S. Ward, Christie Hung, Ian R. Outhwaite, Alix I. Chan, Dmitry L. Usanov, Vamsi K. Mootha, Markus A. Seeliger*, David R. Liu*

* Correspondence: drliu@fas.harvard.edu, markus.seeliger@stonybrook.edu

Supplementary Table 1 | Calculated abundance of each human cyclophilin family member from paxdb^{4,1}

Supplementary Table 2 | Overview of all cyclophilin-selective inhibitors reported in this work

Supplementary Table 3 | Plasmids and primers used for USER cloning of CypD mutant expression constructs

Supplementary Table 4 | Plasmids and primers used for cloning of CypA, CypB, and CypE mutant expression constructs

Supplementary Table 5 | Plasmids used for recombinant expression of cyclophilin proteins

Supplementary Table 6 | Concentrations of cyclophilins used in competition anisotropy binding assay with A26-FI

Supplementary Table 7 | High-resolution mass spectroscopy results for intermediates reported in this work

Supplementary Table 8 | High-resolution mass spectroscopy results for macrocycles reported in this work

Supplementary Table 9 | Crystal diffraction statistics for all CypD-inhibitor co-crystal structures reported in this work

Supplementary Figure 1 | Cyclosporine A interactions with active site residues of CypD

Supplementary Figure 2 | Surface plasmon resonance measurement of JOMBt and JOBBt binding to immobilized CypD

Supplementary Figure 3 | Prolyl isomerase activity of cyclophilins on Suc-AAPF-AMC

Supplementary Figure 4 | Functionalization of piperidine α -carbon improves CypD potency, while replacing the second building block improves CypD selectivity

Supplementary Figure 5 | Large S2 binding groups improve selectivity for CypD

Supplementary Figure 6 | Large hydrophobic S2 binding groups impart selectivity for CypD over CypG, CypH, NKTR, and PPWD1

Supplementary Figure 7 | Biphenyl and bi-aromatic derivatives of B2 showing no improvement in selectivity for CypD

Supplementary Figure 8 | Para-carbonyl-containing biphenyl moieties show partial selectivity over CypC

Supplementary Figure 9 | Para-carboxy-containing biphenyl groups provide enhanced selectivity and potency for CypD

Supplementary Figure 10 | Masking or moving the carboxylate of B23 results in loss in potency and selectivity for CypD

Supplementary Figure 11 | Inverting ligand charge abrogates CypD potency and shifts the cyclophilin selectivity profile

Supplementary Figure 12 | Nitrile-containing biphenyl groups show similar CypD inhibition potencies and linker dependencies as carboxylates

Supplementary Figure 13 | Residue K118 is necessary for potent CypD inhibition with carboxylate-containing inhibitors

Supplementary Figure 14 | S123 gatekeeper position dictates inhibitor potency

Supplementary Figure 15 | Prolyl isomerase inhibition activity on CypD gatekeeper mutants

Supplementary Figure 16 | Derivatives of B23 that show similar selectivity and potency profiles for CypD

Supplementary Figure 17 | Derivatives of B23 that show reduced potency and selectivity for CypD

Supplementary Figure 18 | B23 derivatives that can simultaneously interact with CypD residues K118 and S119 and present a carboxylate near gatekeeper residues

Supplementary Figure 19 | The CypB E121S gatekeeper mutant is inhibited more potently compared to wild-type CypB by carboxylate-containing inhibitors

Supplementary Figure 20 | The CypA E81S/K82R gatekeeper mutant is inhibited more potently compared to wild-type CypA with carboxylate-containing inhibitors

Supplementary Figure 22 | Prolyl isomerase inhibition by CypD-selective inhibitors used in mitochondrial models of mPTP

Supplementary Figure 23 | Additional independent replicates of calcium retention assays in mitochondria

Supplementary Figure 24 | Representative images of Cy5-conjugated CypD inhibitor localization in HeLa cells

Supplementary Figure 25 | CypD inhibition of Cy5-conjugated CypD inhibitors

Supplementary Figure 26 | Fluorescence polarization competition with A26-FI against lysine-containing cyclophilins

Supplementary Figure 27 | Fluorescence polarization competition with A26-FI against CypE with control compounds C5A and C6A

Supplementary Figure 28 | Prolyl isomerase inhibition by C1A, C3A, C5A, and C6A

Supplementary Figure 29 | Mass spectroscopy analysis of C3A covalent modification on 13 cyclophilins

Supplementary Figure 30 | CypE mutant FP analysis

Supplementary Figure 31 | Prolyl isomerase inhibition screening of CypE lysine mutants reveals K217 residue as site of C3A covalent modification

Supplementary Figure 32 | Ligand-dependent conformation of primary gatekeeper residues S123 and R124 in the S2 pocket

Supplementary Figure 33 | Molecular footprinting analysis demonstrates that key binding interactions of B52 are unique to CypD

Supplementary Figure 34 | Electron densities of ligands from CypD-inhibitor co-crystal structures

Supplementary Figure 35 | SDS-PAGE of recombinantly expressed cyclophilin proteins

Supplementary Note 1:

Python Scripts

Analysis of CypD selection high-throughput sequencing data

Calculating enrichment values of library members

Supplementary Note 2:

Synthetic Methods

Generalized procedures

Synthesis of intermediates

Synthesis of final macrocycles

¹H-NMR Spectra

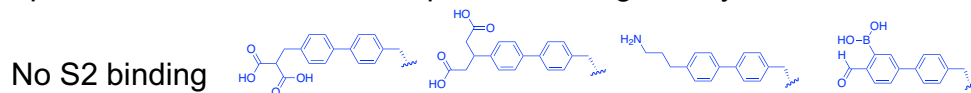
HPLC Chromatograms

Supplementary References

Supplementary Table 1 | Calculated abundance of each human cyclophilin family member from paxdb^{4.1}. CypD is the third most abundant cyclophilin, while CypB and CypA are the second and first, respectively (see Wang, M., Herrmann, C. J., Simonovic, M., Szklarczyk, D. & von Mering, C. Version 4.0 of PaxDb: Protein abundance data, integrated across model organisms, tissues, and cell-lines. *Proteomics* **15**, 3163–3168 (2015)). CypA is one of the most abundantly expressed proteins in human cells. Therefore, selectivity over CypA is the most important for CypD selective inhibition in biological models. Compounds **B52/B53**, **B32**, and **C3A** *in vitro* show >100-fold selectivity for CypD, CypD K118E/R124A, and CypE, respectively, over CypA.

Cyclophilin	Gene	Protein abundance: H.Sapiens whole integrated (ppm)	Normalized CypD abundance
CypD	PPIF	187	1
CypA	PPIA	4317	23.1
CypB	PPIB	248	1.33
CypC	PPIC	0.226	0.00121
Cyp40	PPID	13.5	0.0722
CypE	PPIE	61.7	0.330
CypG	PPIG	24.2	0.129
CypH	PPIH	11.9	0.0636
PPIL1	PPIL1	17.8	0.0952
PPIL2	PPIL2	3.14	0.0168
CypJ/PPIL3	PPIL3	4.62	0.0247
PPIL4	PPIL4	2.14	0.0114
PPIL6	PPIL6	0.167	0.000893
PPWD1	PPWD1	29.2	0.156
RanBP2	RanBP2	35.5	0.190
SDCCAG	CWC27	1.82	0.00973
NKTR	NKTR	0.108	0.000577

Supplementary Table 2 | Overview of all cyclophilin-selective inhibitors reported in this work. Inhibitor IC₅₀ values from prolyl-isomerase inhibition on the targeted cyclophilin are highlighted in dashed boxes. The inhibition potencies against all other cyclophilins are normalized to this IC₅₀ value and are shown as a fold-difference. Boxes are shaded according to the fold-difference value. Each cyclophilin is inhibited selectively due to the identity of its unique S2 pocket residues and the S2 pocket binding moiety of the inhibitor.



Non-selective	CypD selective		CypD K118E/R124A selective	CypE selective	
CsA	B52	B53	B32	C3A	Residues proximal to biphenyl
13 nM (1x)	10 nM (1x)	57 nM (1x)	100x	46x	CypD (Lys, Ser, Arg)
2x	31x	14x	120x	13 nM (1x)	CypE (Lys, Lys, Lys)
1x	21x	19x	50x	310x	CypB (Lys, Glu, Arg)
1x	110x	60x	130x	230x	CypA (Lys, Glu, Lys)
2x	600x	750x	33x	31x	PPIL1 (Ala, Lys, Gln)
11x	2200x	>900x	67x	140x	Cyp40 (Glu, Glu, Lys)
1x	>10000x	>900x	20x	1300x	CypC (Val, Glu, Thr)
2x	>10000x	>900x	180x	3100x	CypG (Glu, Gly, Phe)
15x	>10000x	>900x	13x	620x	PPWD1 (Glu, Gly, Glu)
6x	>10000x	>900x	>830x	>3800x	CypH (Ala, Gly, Pro)
38x	>10000x	>900x	>830x	2500x	NKTR (Glu, Gly, Tyr)
			60 nM (1x)		CypD K118E/R124A (Glu, Ser, Ala)
Reported non-binder for PPIL2, PPIL6, SDCCAG-10. Unknown for PPIL3, PPIL4.	No active site binding by fluorescence polarization B52-FI .	No active site binding by fluorescence polarization B53-FI .	Predicted weak binding due to weak potency of A26-FI by fluorescence polarization, which has poor S2-pocket occupancy		PPIL2, PPIL3, PPIL4, PPIL6, SDCCAG-10

Color Gradient: 100.00 90.00 80.00 70.00 60.00 50.00 40.00 30.00 20.00 10.00 9.00 8.00 7.00 6.00 5.00 4.00 3.00 2.00 1.00
 Formatting Rules: Red ≥100x Gray=10x Green ≤1x

Supplementary Table 3 | Plasmids and primers used for USER cloning of CypD mutant expression constructs.

Mutation (plasmid name)	Starting plasmid	Primer (forward, reverse)
CypD K118A (2BT-CypD (45-207) K118A)	2BT-CypD (45-207)	AGGCGGGGCG/ideoxyU/CCATCTACGGAAGCCGCTTTC ACGCCCGCC/ideoxyU/GTGCCATTGTGGTTGGTG
CypD K118E (2BT-CypD (45-207) K118E)	2BT-CypD (45-207)	AGGCGGGGAA/ideoxyU/CCATCTACGGAAGCCGCTTTC ATTCCCGCC/ideoxyU/GTGCCATTGTGGTTGGTG
CypD S123E (2BT-CypD (45-207) S123E)	2BT-CypD (45-207)	ACGGAGAACGC/ideoxyU/TTCCTGACGAGAACTTAC AGCGTTCTCCG/ideoxyU/AGATGGACTTCCCG
CypD R124A (2BT-CypD (45-207) R124A)	2BT-CypD (45-207)	AGCGCGTTTCC/ideoxyU/GACGAGAACTTTACTGAAG AGGAAACGCGC/ideoxyU/TCCGTAGATGGACTTCC
CypD R124K (2BT-CypD (45-207) R124K)	2BT-CypD (45-207)	AGCAAATTTCC/ideoxyU/GACGAGAACTTTACTGAAG AGGAAATTTGC/ideoxyU/TCCGTAGATGGACTTCC
CypD K118E/R124A (2BT-CypD (45-207) K118E/R124A)	2BT-CypD-R124A (45-207)	AGCGCGTTTCC/ideoxyU/GACGAGAACTTTACTGAAG AGGAAACGCGC/ideoxyU/TCCGTAGATGGATTCCC

Supplementary Table 4 | Plasmids and primers used for cloning of CypA, CypB, and CypE mutant expression constructs.

Mutation (plasmid name)	Starting plasmid	Primer (forward, reverse)
CypD K175I (2BT-CypD (45-207) K175I)	2BT-CypD (45-207)	5'-GTTCCGGTCACGTCATAGAGGGCATGGAC-3' 5'-GTCCATGCCCTCTATGACGTGACCGAAC-3'
CypB E121S (2BT-CypB (34-216) E121S)	2BT-CypB (34-216)	5'-GGAAAGAGCATCTACGGTAGCCGCTTCCCCGATGAG-3' 5'-CTCATCGGGGAAGCGGCTACCGTAGATGCTCTTTCC-3'
CypA K82R (2BT-CypA (1-165) K82R)	2BT-CypA (1-165)	5'-GCAAGTCCATCTATGGGGAGCGCTTTGAAGATGAGAACTTCATCC-3' 5'-GGATGAAGTTCTCATCTTCAAAGCGCTCCCATAGATGGACTTGC-3'
CypA E81S/K82R (2BT-CypA (1-165) E81S/K82R)	2BT-CypA K82R (1-165)	5'-GCAAGTCCATCTATGGGGAGCGCTTTGAAGATGAGAACTTCATCC-3' 5'-GGATGAAGTTCTCATCTTCAAAGCGCTCCCATAGATGGACTTGC-3'
CypE K212A (pET28α LIC-CypE (131-301) K212A)	pET28α LIC-CypE (131-301)	5'-CCACAATGGCACTGGGGGCGCGTCCATCTATGGGAAG-3' 5'-CGAACTTCTCCCATAGATGGACGCGCCCCAGTGCCATTG-3'
CypE K217A (pET28α LIC-CypE (131-301) K217A)	pET28α LIC-CypE (131-301)	5'-GGGCAAGTCCATCTATGGGGCGAAGTTTCGATGATG-3' 5'-GTTTTTCATCATCGAACTTCGCCCCATAGATGGAC-3'
CypE K218A (pET28α LIC-CypE (131-301) K218A)	pET28α LIC-CypE (131-301)	5'-GCAAGTCCATCTATGGGAAGCGTTTCGATGATGAAAAC-3' 5'-GGATAAAGTTTTTCATCATCGAACGCTTCCCATAGATGG-3'

Supplementary Table 5 | Plasmids used for recombinant expression of cyclophilin proteins.

Expression plasmid	Cyclophilin protein
2BT-CypD (45-207)	CypD
2BT-CypD (45-207) K118A	CypD K118A
2BT-CypD (45-207) K118E	CypD K118E
2BT-CypD (45-207) S123E	CypD S123E
2BT-CypD (45-207) R124A	CypD R124A
2BT-CypD (45-207) R124K	CypD R124K
2BT-CypD (45-207) K118E/R124A	CypD K118E/R124A
2BT-CypD (45-207) K175I	CypD K175I
2BT-CypA (1-165)	CypA
2BT-CypA (1-165) K82R	CypA K82R
2BT-CypA (1-165) E81S/K82R	CypA E81S/K82R
2BT-CypB (34-216)	CypB
2BT-CypB (34-216) E121S	CypB E121S
pET28 α LIC-CypC (24-212)	CypC
pET28 α LIC-CypE (131-301)	CypE
pET28 α LIC-CypE (131-301) K212A	CypE K212A
pET28 α LIC-CypE (131-301) K217A	CypE K217A
pET28 α LIC-CypE (131-301) K218A	CypE K218A
pET28 α LIC-CypG (1-179)	CypG
2BT-CypH (1-177)	CypH
2BT-Cyp40 (1-183)	Cyp40
pET28 α LIC-NKTR (7-179)	NKTR
2BT-PPIL1 (1-166)	PPIL1
pET28 α LIC-PPIL2 (280-457)	PPIL2
2BT-PPIL3 (1-161)	PPIL3
pET28 α LIC-PPWD1 (473-646)	PPWD1

Supplementary Table 6 | Concentrations of cyclophilins used in competition anisotropy binding assay with A26-FI.

Cyclophilin	Concentration (nM)
CypD	40
CypA	80
CypB	100
CypE	150
CypE K212A	150
CypE K217A	150
CypE K218A	150
Cyp40	300
PPIL1	600
PPIL3	2000

Supplementary Table 7 | High-resolution mass spectroscopy results for intermediates reported in this work. Experiments and formula confirmation were performed by Harvard University's Center for Mass Spectroscopy.

Compound ID	Molecular Formula	Calculated [M+H] ⁺	Found [M+H] ⁺	Calculated Δ ppm					
4F	C ₂₃ H ₂₄ N ₂ O ₆	425.171	425.1707	-0.7	I19d	C ₁₂ H ₁₃ BO ₅	247.0783	247.0782	-0.4
I1	C ₂₁ H ₁₉ NO ₄	348.1241	348.1245	1.1	I19e	C ₁₀ H ₉ BO ₅	219.047	219.0469	-0.5
I2	C ₂₁ H ₁₉ NO ₄	348.1241	348.1245	1.1	I20a	C ₁₂ H ₁₁ F ₃ O ₆ S	341.0301	341.0309	2.3
I3	C ₂₀ H ₁₉ NO ₄	336.1241	336.1246	1.5	I20b	C ₁₇ H ₂₃ BO ₅	341.1531	341.1526	-1.5
I4	C ₂₂ H ₂₃ NO ₄	366.17	366.1701	0.3	I20c	C ₁₁ H ₁₃ BO ₅	235.0783	235.0783	0
I5	C ₂₉ H ₂₄ N ₂ O ₄	465.1809	465.1811	0.4	I20d	C ₁₀ H ₁₁ BO ₅	221.0627	221.0626	-0.5
I6a	C ₁₉ H ₂₅ BO ₄	329.1919	329.1921	0.6	I21a	C ₁₆ H ₂₁ BO ₄	287.146	287.1463	1
I6b	C ₁₃ H ₁₅ BO ₄	245.0991	245.099	-0.4	I21b	C ₁₀ H ₁₁ BO ₄	205.0678	205.0676	-1
I7a	C ₁₆ H ₂₁ BO ₅	303.1409	303.1411	0.7	I22a	C ₁₆ H ₂₀ NO ₄	324.1378	324.138	0.6
I7b	C ₁₀ H ₁₁ BO ₅	221.0627	221.0625	-0.9	I22b	C ₁₀ H ₁₀ NO ₄	218.063	218.0628	-0.9
I8a	C ₁₀ H ₉ BO ₅	219.047	219.0469	-0.5	I22c	C ₉ H ₈ NO ₄	204.0474	204.047	-2
I8b	C ₉ H ₇ BO ₅	205.0314	205.031	-2	I23	C ₁₈ H ₂₇ BO ₆	373.1793	373.1792	-0.3
I9a	C ₁₂ H ₁₁ F ₃ O ₆ S	341.0301	341.0304	0.9	I24a	C ₁₉ H ₂₇ BrO ₄	421.0985	421.0986	0.2
I9b	C ₁₇ H ₂₃ BO ₅	341.1531	341.1526	-1.5	I24b	C ₂₅ H ₃₉ BO ₆	469.2732	469.2732	0
I9c	C ₁₁ H ₁₃ BO ₅	235.0783	235.0783	0	I24c	C ₁₉ H ₂₉ BO ₆	387.1949	387.1949	0
I9d	C ₁₀ H ₁₁ BO ₅	221.0627	221.0626	-0.5	I25a	C ₂₃ H ₂₆ BrNO ₅	476.1067	476.1067	0
I10	C ₉ H ₈ NO ₄	204.0474	204.047	-2	I25b	C ₃₂ H ₂₆ BrNO ₅	606.0887	606.088	-1.2
I11	C ₁₄ H ₁₇ BO ₅	275.1096	275.1098	0.7	I25c	C ₄₇ H ₄₉ BrNeO ₇	911.2738 (Na ⁺ adduct)	911.2718	-2.2
I12a	C ₁₆ H ₂₃ BO ₄	289.1617	289.1619	0.7	I26a	C ₂₃ H ₂₆ BrNO ₅	476.1067	476.1061	-1.3
I12b	C ₁₀ H ₁₃ BO ₄	207.0834	207.0832	-1	I26b	C ₃₂ H ₂₆ BrNO ₅	606.0887	606.0877	-1.6
I13a	C ₁₆ H ₂₁ BO ₄	287.146	287.1461	0.3	I26c	C ₄₇ H ₄₉ BrNeO ₇	911.2738 (Na ⁺ adduct)	911.2715	-2.5
I13b	C ₁₆ H ₂₁ BO ₄	205.0678	205.0675	-1.5	I27a	C ₂₂ H ₂₄ BrNO ₅	484.073	484.0728	-0.4
I14a	C ₁₂ H ₁₅ BrO ₄ S	356.9767	356.9769	0.6	I27b	C ₃₁ H ₂₄ BrNO ₅	592.073	592.0724	-1
I14b	C ₁₈ H ₂₇ BO ₆ S	405.1514	405.1512	-0.5	I27c	C ₄₆ H ₄₇ BrNeO ₇	875.2762	875.2757	-0.6
I14c	C ₁₂ H ₁₇ BO ₆ S	323.0731	323.0734	0.9	I28a	C ₂₂ H ₂₄ BrNO ₅	484.073	484.0725	-1
I15a	C ₁₁ H ₁₁ F ₃ O ₆ S	351.0121	351.0124	0.9	I28b	C ₃₁ H ₂₄ BrNO ₅	592.073	592.0727	-0.5
I15b	C ₁₆ H ₂₃ BO ₅	329.1531	329.1531	0	I28c	C ₄₆ H ₄₇ BrNeO ₇	875.2762	875.2753	-1
I15c	C ₁₀ H ₁₃ BO ₅	223.0783	223.0782	-0.4	I29a	C ₂₀ H ₂₉ BO ₆	399.1949	399.1951	0.5
I15d	C ₉ H ₁₁ BO ₅	209.0627	209.0624	-1.4	I29b	C ₁₄ H ₁₉ BO ₆	317.1167	317.117	0.9
I16a	C ₁₅ H ₂₁ BO ₅	291.1409	291.1413	1.4	I30a	C ₁₅ H ₁₉ BrO ₄	365.0359	365.0359	0.0
I16b	C ₉ H ₁₁ BO ₅	209.0627	209.0624	-1.4	I30b	C ₂₁ H ₃₁ BO ₆	413.2106	413.2106	0.0
I17a	C ₁₁ H ₉ BrO ₃	268.9808	268.9809	0.4	I30c	C ₁₆ H ₂₁ BO ₆	331.1323	331.1327	1.2
I17b	C ₁₇ H ₂₁ BO ₅	317.1555	317.1558	0.9	(4Br)B6	C ₄₃ H ₅₂ BrN ₇ O ₇	858.3184	858.3193	1
I17c	C ₁₁ H ₁₁ BO ₅	235.0772	235.0768	-1.7	(4Br)B6-A	C ₃₉ H ₄₃ BrNeO ₆	771.25	771.25	0
I17d	C ₉ H ₇ BO ₅	205.0314	205.0311	-1.5	(4Br)B6-B	C ₄₁ H ₄₈ BrN ₇ O ₆	814.2922	814.2908	-1.7
I18a	C ₁₇ H ₂₁ BO ₅	317.1555	317.1557	0.6	(4Br)B6-FI	C ₃₉ H ₄₃ BrNeO ₆	1332.4499	1332.4489	-0.8
I18b	C ₁₁ H ₁₁ BO ₅	235.0772	235.0766	-2.6	*(4Br)B6-A	C ₃₉ H ₄₃ BrNeO ₆	771.25	771.25	0
I18c	C ₉ H ₇ BO ₅	205.0314	205.0311	-1.5	*(4Br)B6-B	C ₄₁ H ₄₈ BrN ₇ O ₆	814.2922	814.291	-1.5
I19a	C ₁₂ H ₁₂ O ₄	221.0808	221.081	0.9					
I19b	C ₁₃ H ₁₁ F ₃ O ₆ S	375.0121	375.0123	0.5					
I19c	C ₁₈ H ₂₃ BO ₅	353.1531	353.1532	0.3					

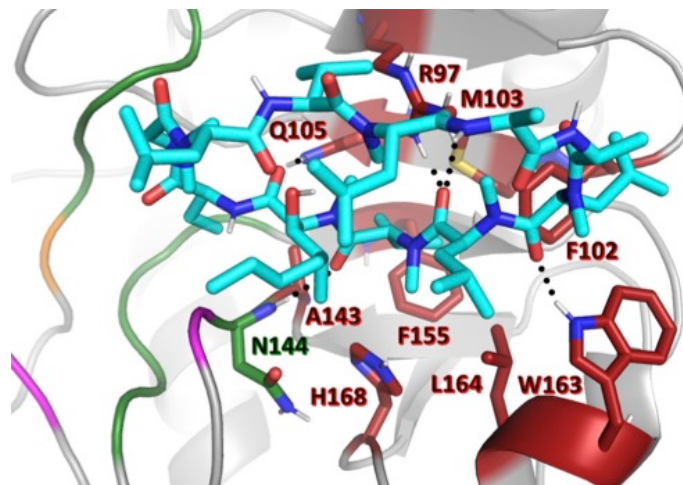
Supplementary Table 8 | High-resolution mass spectroscopy results for macrocycles reported in this work. Experiments and formula confirmation were performed by Harvard University's Center for Mass Spectroscopy.

Compound ID	Molecular Formula	Calculated [M+H] ⁺	Found [M+H] ⁺	Calculated Δ ppm					
JOMbT	C34H45N7O8	680.3402	680.3398	-0.6	B14	C51H57N7O8	896.4341	896.4343	0.2
JOMbC	C34H45N7O8	680.3402	680.3404	0.3	B15	C51H59N7O8	898.4498	898.4497	-0.1
JOMbT-A	C30H36N6O7	593.2718	593.2721	0.5	B16	C49H56N8O9	901.4243	901.4237	-0.7
JOMbT-D	C40H57N7O10	796.424	796.4238	-0.3	B17	C51H59N7O9	914.4447	914.4448	0.1
JOBBt	C35H47N7O8	694.3559	694.3556	-0.4	B18	C50H58N8O8	899.445	899.4453	0.3
JOBBc-A	C31H38N6O7	607.2875	607.2874	-0.2	B19	C50H59N7O9S	934.4168	934.4166	-0.2
JOGAt	C34H45N7O8	680.3402	680.3403	0.1	B20	C50H57N7O9	900.4291	900.4289	-0.2
JOGAc	C34H45N7O8	680.3402	680.3405	0.4	B21	C51H59N7O9	914.4447	914.4443	-0.4
JOGbT-A	C31H38N6O7	607.2875	607.2875	0	B22	C51H59N7O9	914.4447	914.4448	0.1
JOGbC-A	C31H38N6O7	607.2875	607.2876	0.2	B23	C52H61N7O9	928.4604	928.4604	0
JOCbT	C34H45N7O8	680.3402	680.3402	0	B24	C52H59N7O9	926.4447	926.445	0.3
JOCbC	C34H45N7O8	680.3402	680.3403	0.1	B25	C52H57N7O9	924.4291	924.4295	0.4
JOMAt	C33H43N7O8	666.3246	666.324	-0.9	B26	C52H61N7O9	928.4604	928.4607	0.3
JOMAc	C33H43N7O8	666.3246	666.3246	0	B27	C53H63N7O9	942.476	942.4762	0.2
JOMCt	C35H47N7O	694.3559	694.3559	0	B28	C53H63N7O9	942.476	942.4754	-0.6
JOMCc	C35H47N7O	694.3559	694.356	0.1	B29	C54H65N7O9	956.4917	956.4918	0.1
JOMFt	C34H45N7O8	680.3402	680.3403	0.1	B30	C51H60N8O9	929.4556	929.4558	0.2
JOMFc	C34H45N7O8	680.3402	680.3399	-0.4	B31	C51H62N8O7	899.4814	899.4813	-0.1
HOJjT	C37H51N7O8	722.3872	722.387	-0.3	B32	C52H64N8O7	913.4971	913.4974	0.3
HOJjC	C37H51N7O8	722.3872	722.3867	-0.7	B33	C50H56N8O7	881.4345	881.4344	-0.1
HJJjT	C39H59N7O7	738.4549	738.4544	-0.7	B34	C51H58N8O7	895.4501	895.4499	-0.2
HJJjC	C39H59N7O7	738.4549	738.4543	-0.8	B35	C53H61N7O10	956.4553	956.4552	-0.1
A1	C33H43N7O8	666.3246	666.3246	0.0	B36	C52H57N7O10	940.424	940.4244	0.4
A2	C33H43N7O8	666.3246	666.3244	-0.3	B37	C53H61N7O10	956.4553	956.4553	0
A3	C30H45N7O8	632.3402	632.3404	0.3	B38	C51H59N7O10	930.4396	930.4401	0.5
A4	C31H43N7O8	642.3246	642.3245	-0.2	B39	C52H58N8O9	939.44	939.4404	0.4
A5	C31H43N7O8	642.3246	642.3245	-0.2	B40	C51H57N7O10	928.424	928.4243	0.3
A6	C32H41N7O8	652.3089	652.3088	-0.2	B41	C53H63N7O9	942.476	942.476	0
A7	C34H45N7O8	680.3402	680.3401	-0.1	B42	C53H61N7O9	940.4604	940.4605	0.1
A8	C30H43N7O7	614.3297	614.3295	-0.3	B43	C51H59N7O11S	978.4066	978.4062	-0.4
A9	C36H47N7O7	690.361	690.3608	-0.3	B44	C52H61N7O10	944.4553	944.4553	0
A10	C33H49N7O7	656.3766	656.3765	-0.2	B45	C52H61N7O10	944.4553	944.456	0.7
A11	C38H49N7O7	716.3766	716.3763	-0.4	B46	C52H57N7O10	940.424	940.424	0
A12	C36H53N7O7	696.4079	696.4075	-0.6	B47	C52H57N7O10	940.424	940.4243	0.3
A13	C40H49N7O7	740.3766	740.3767	0.1	B48	C53H59N7O10	954.4396	954.4397	0.1
A14	C43H51N7O8	794.3872	794.3872	0.0	B49	C53H61N7O10	956.4553	956.455	-0.3
A15	C42H51N7O7	766.3923	766.3921	-0.3	B50	C53H61N7O9	940.4604	940.4606	0.2
A16	C37H49N7O7	704.3766	704.3762	-0.6	B51	C52H58N8O9	939.44	939.4401	0.1
A17	C34H45N7O7S	696.3174	696.3174	0.0	B52	C53H61N7O11	972.4502	972.4488	-1.4
A18	C37H49N7O7	704.3766	704.3764	-0.3	B53	C54H63N7O11	986.4658	986.4653	-0.5
A19	C37H49N7O7	704.3766	704.3763	-0.4	A26-FI	C68H73N7O16	1244.5187	1244.5199	1
A20	C40H55N7O7	746.4236	746.4234	-0.3	B52-FI	C80H83N7O19	1446.5816	1446.5822	0.4
A21	C34H45N7O8	680.3402	680.3402	0.0	B53-FI	C81H85N7O19	1460.5973	1460.5986	0.9
A22	C35H47N7O8	694.3559	694.3556	-0.4	B52-A	C49H52N6O10	885.3818	885.3819	0.1
A23	C34H45N7O8	680.3402	680.3404	0.3	B53-A	C50H54N6O10	899.3974	899.3976	0.2
A24	C33H43N7O8	666.3246	666.3244	-0.3	*B52-A	C49H52N6O10	885.3818	885.3822	0.5
A25	C35H47N7O8	694.3559	694.3557	-0.3	*B53-A	C50H54N6O10	899.3974	899.3978	0.4
A26	C41H51N7O8	770.3872	770.3866	-0.8	C1A	C47H51BN6O9	855.3883	855.3872	-1.7
A27	C35H47N7O8	694.3559	694.3554	-0.7	C2A	C47H51BN6O9	855.3883	855.3878	-1.5
A28	C35H47N7O8	694.3559	694.3557	-0.3	C3A	C46H49BN6O9	841.3727	841.3725	-0.2
A29	C35H47N7O8	694.3559	694.3551	-1.2	C4A	C46H49BN6O9	841.3727	841.3726	-0.1
A30	C34H47N7O8	682.3559	682.3559	0.0	C5A	C46H48N6O7	797.3657	797.3643	-1.8
B1	C50H57N7O8	884.4341	884.4338	-0.3	C6A	C45H49BN6O8	813.37789	813.3779	0
B2	C49H57N7O7	856.4392	856.4383	-1.1	B52-Cy5	C83H94N9O11+	1392.7067	1392.7074	0.5
B3	C44H55N7O	794.4236	794.423	-0.8	B53-Cy5	C84H96N9O11+	1406.7224	1406.72	-1.7
B4	C45H55N7O7	806.4236	806.4234	-0.2	*B52-Cy5	C83H94N9O11+	1392.7067	1392.7048	-1.4
B5	C47H61N7O7	836.4705	836.4704	-0.1	*B53-Cy5	C84H96N9O11+	1406.7224	1406.72	-1.7
B6	C43H53N7O7	780.4079	780.4075	-0.5	B52-Et-Cy5	C87H102N9O11+	1448.7693	1448.7652	-2.8
B7	C43H53N7O8	796.4028	796.4021	-0.9	B53-Et-Cy5	C88H104N9O11+	1462.785	1462.7824	-1.8
B8	C50H59N7O7	870.4549	870.4546	-0.3	*B52-Et-Cy5	C87H102N9O11+	1448.7693	1448.7672	-1.4
B9	C50H59N7O7	870.4549	870.4546	-0.3	*B53-Et-Cy5	C88H104N9O11+	1462.785	1462.7844	-0.4
B10	C50H59N7O8	886.4498	886.45	0.2	Cy5-enAc	C36H47N4O2+	567.3694	567.3687	-1.2
B11	C51H59N7O8	898.4498	898.4495	-0.3					
B12	C49H57N7O8	872.4341	872.4341	0					
B13	C48H56N6O7	857.4345	857.4343	-0.2					

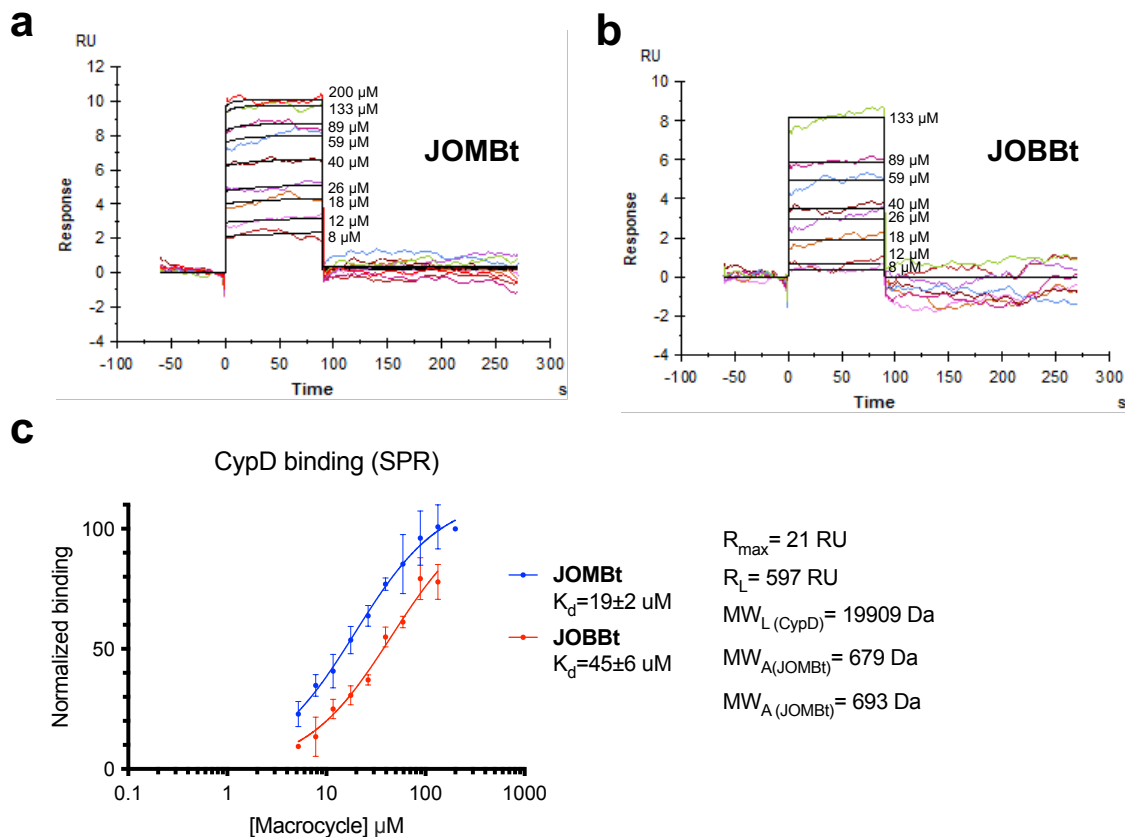
Supplementary Table 9 | Crystal diffraction statistics for all CypD-inhibitor co-crystal structures reported in this work. Statistics for the highest-resolution shell are shown in parentheses.

	CypD + JOMBt	CypD + A26	CypD + B1	CypD + B2	CypD + B3	CypD + B21	CypD + B23	CypD + B25	CypD + B52	CypD + B53
Wavelength	0.97933 Å	0.97933 Å	0.97933 Å	0.97933 Å	0.97933 Å	0.92016 Å	0.97931 Å	0.92011 Å	0.92011 Å	0.92011 Å
Resolution range	46.482 - 1.746 (1.776 - 1.746)	37.923 - 1.055 (1.073 - 1.055)	44.534 - 1.211 (1.232 - 1.211)	37.700 - 1.461 (1.486 - 1.461)	44.684 - 1.522 (1.549 - 1.522)	30.96 - 0.97 (1.000 - 0.97)	25.72 - 1.18 (1.21 - 1.18)*	25.83 - 1.572 (1.61 - 1.572)	25.73 - 1.16 (1.19 - 1.16)	25.68 - 1.104 (1.143 - 1.104)
Space group	P 2 ₁ 2 ₁ 2 ₁	P 1 2 ₁ 1	P 2 ₁ 2 ₁ 2 ₁	P 1 2 ₁ 1	P 2 ₁ 2 ₁ 2 ₁	P 4 ₃	P 2 ₁ 2 ₁ 2 ₁	P 2 ₁ 2 ₁ 2 ₁	P 2 ₁ 2 ₁ 2 ₁	P 2 ₁ 2 ₁ 2 ₁
Unit cell	38.505 57.879 78.01 90.90 90	36.061 67.087 38.662 90 101.218 90	40.195 60.141 66.264 90 90 90	35.838 67.41 38.455 90 101.371 90	40.279 60.265 66.592 90 90 90	38.632 38.632 103.509 90 90 90	38.542 67.177 69.071 90 90 90	38.564 67.19 69.58 90 90 90	38.408 67.032 69.324 90 90 90	38.492 66.885 68.968 90 90 90
Total reflections	219423 (11765)	495647 (7380)	470396 (2064)	138577 (7413)	302677 (16985)	1028544 (9410)	528630 (783)	196553 (168)	804168 (37928)	934857 (53061)
Unique reflections	17266 (869)	78970 (2430)	43493 (799)	31004 (1557)	25507 (1301)	82203 (2612)	46222 (393)	18407 (161)	62319 (4063)	71217 (4690)
Multiplicity	12.7 (13.5)	6.3 (3.0)	10.8 (2.6)	4.5 (4.8)	11.9 (13.1)	12.5 (3.6)	11.4 (2.0)	10.7 (1.0)	12.9 (9.3)	13.1 (11.3)
Completeness (%)	94.2 (99.9)	95.5 (59.6)	87.8 (33.4)	99.70 (99.8)	99.9 (100.0)	92.15 (61.6)	76.6 (9.1)	71.1 (8.7)	99.0 (88.5)	98.6 (89.1)
Mean I/sigma(I)	12.5 (2.3)	15.03 (2.3)	23.0 (2.1)	9.9 (3.8)	9.1 (3.2)	13.1 (0.9)	19.00 (1.80)	33.70 (5.30)	13.50 (2.90)	9.60 (3.00)
Wilson B-factor		19.17	9.05	11.42	9.55	13.97	7.71	9.38	9.58	9.65
R-merge	0.136 (1.195)	0.057 (0.461)	0.051 (0.428)	0.116 (1.046)	0.165 (1.607)	0.107 (1.364)	0.078 (0.508)	0.056 (0.035)	0.112 (0.595)	0.180 (0.596)
R-meas	0.142 (1.241)	0.062 (0.558)	0.053 (0.538)	0.131 (1.167)	0.173 (1.671)	0.112 (1.615)	0.02682 (0.1685)	0.01992 (0.06542)	0.03362 (0.2297)	0.0529 (0.2299)
R-pim	0.040 (0.333)	0.024 (0.307)	0.015 (0.317)	0.060 (0.507)	0.050 (0.456)	0.029 (0.828)	0.01896 (0.1192)	0.01409 (0.04626)	0.02377 (0.1625)	0.0374 (0.1625)
CC1/2	0.996 (0.772)	0.999 (0.798)	1 (0.766)	0.994 (0.574)	0.996 (0.911)	0.997 (0.241)	0.998 (0.803)	0.998 (0.963)	0.995 (0.921)	0.994 (0.888)
CC*	0.999 (0.954)	1 (0.961)	1 (0.951)	0.998 (0.91)	0.999 (0.98)	0.999 (0.635)	1 (0.987)	1 (0.997)	1 (0.987)	0.999 (0.98)
Reflections used in refinement	17146 (1755)	78345 (5507)	43488 (1922)	30862 (3055)	25407 (2507)	82203 (4868)	42114 (2767)	18375 (288)	62243 (5800)	71160 (6445)
Reflections used for R-free	848 (80)	3807 (270)	2108 (103)	1531 (157) 0.1654	1275 (117)	1997 (108)	1831 (120)	1826 (27) 0.1339	2011 (188) 0.1357	1998 (186) 0.1369
R-work	0.1702 (0.1894)	0.1364 (0.2102)	0.1513 (0.2112)	0.1734 (0.1734)	0.1690 (0.2280)	0.1365 (0.3333)	0.1350 (0.1812)	0.1678 (0.1678)	0.1795 (0.1795)	0.1698 (0.1698)
R-free	0.1842 (0.2096)	0.1447 (0.2210)	0.1604 (0.2189)	0.1786 (0.1975)	0.1886 (0.2689)	0.1519 (0.3275)	0.1473 (0.1933)	0.1635 (0.2256)	0.1516 (0.1875)	0.1477 (0.1917)
CC(work)	0.946 (0.932)	0.974 (0.915)	0.969 (0.896)	0.962 (0.935)	0.962 (0.923)	0.978 (0.650)	0.972 (0.927)	0.966 (0.946)	0.969 (0.955)	0.970 (0.940)
CC(free)	0.946 (0.892)	0.977 (0.931)	0.956 (0.909)	0.952 (0.922)	0.952 (0.929)	0.983 (0.689)	0.967 (0.915)	0.949 (0.821)	0.952 (0.960)	0.955 (0.940)
Number of non-hydrogen atoms		1387	1570	1462	1454	1524	1539	1557	1555	1479
macromolecules		1248	1258	1270	1279	1275	1277	1269	1244	1244
ligands		49	56	65	63	58	67	68	68	71
solvent		90	256	127	112	191	195	220	243	164
Protein residues		163	163	163	163	163	163	163	163	163
RMS(bonds)		0.007	0.007	0.008	0.012	0.008	0.012	0.009	0.007	0.011
RMS(angles)		0.99	1.04	1.08	1.51	1.299	1.28	1.2	1.062	1.327
Ramachandran favored (%)		96.3	95.68	95.65	95.68	96.32	96.89	95.65	95.65	95.03
Ramachandran allowed (%)		3.7	4.32	4.35	4.32	3.68	3.11	4.35	4.35	4.97
Ramachandran outliers (%)		0	0	0	0	0	0	0	0	0
Rotamer outliers (%)		0	0	0	0.72	1.44	0.71	0	0	0
Clashscore		1.18	0	0.77	0	2.31	2.68	1.14	1.57	2.35
Average B-factor		22.3	12.17	15.3	12.06	18.44	10.72	12.77	13.25	12.43
macromolecules		21.31	9.54	14.69	11.39	16.8	9.09	10.43	10.64	10.56
ligands		25.97	12.59	14.13	12.8	19.38	9.61	11.32	12.01	11.04
solvent		33.89	24.99	21.98	19.23	29.13	21.78	26.7	26.97	27.18
Number of TLS groups		8	10	7	8	9	9	9	7	9

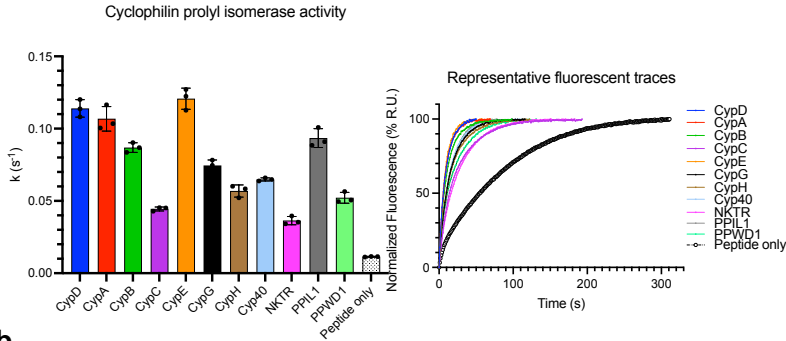
*Data was collected to 1.18 Å resolution but cut off for refinement to 1.3 Å resolution to improve completeness.



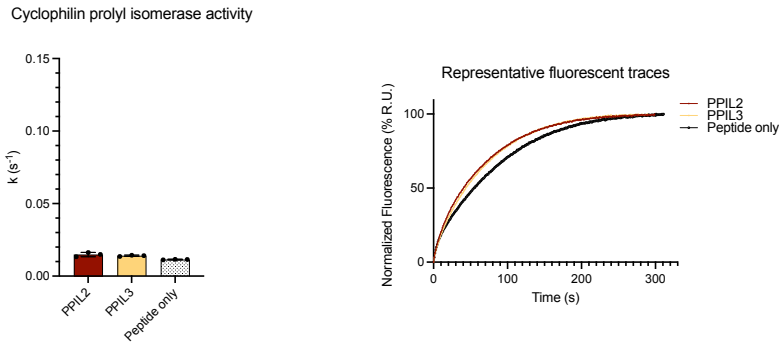
Supplementary Figure 1 | Cyclosporine A interactions with active site residues of CypD (PDB ID 2Z6W). CsA makes primary contacts with active site residues (red) and minimally interacts with S2 pocket residues (green, magenta, orange), with the exception of N144 which lies at the interface between the two pockets. Primary hydrophobic interactions are between Val on CsA and F155 at the base of the active site pocket, surrounded by M103, L164 and H168. Predicted hydrogen bond contacts with CypD residues (black dashes) are shown with R97, Q105, N144, and W163. These residues are highly conserved between isoforms, contributing to the promiscuous cyclophilin inhibition by CsA (Extended Data 1c).



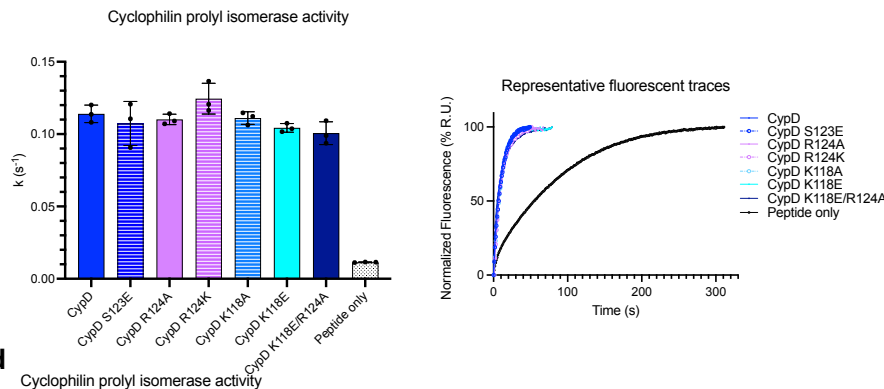
Supplementary Figure 2 | Surface plasmon resonance measurement of JOMBt and JOBBt binding to immobilized CypD. Representative sensorgram of **a**, JOMBt and **b**, JOBBt, flowed over amine immobilized CypD. Black lines are calculated kinetic fits for each dose. **c**, Binding dose response of JOMBt and JOBBt, where sensorgram RU values were normalized to DMSO treated baseline and 200 μ M JOMBt. Individual replicates represent fitted kinetic RU value during compound administration at each dose. Shown are SPR parameters including theoretical R_{max} , based off amount of immobilized CypD (R_L) and molecular weights of assayed material ($MW_{L(CypD)}$, $MW_{A(JOMBt)}$, $MW_{A(JOMBt)}$). K_d values reflect mean \pm SEM of three technical replicates. Data points and error bars reflect mean \pm SD of individual assays at one dose.

a

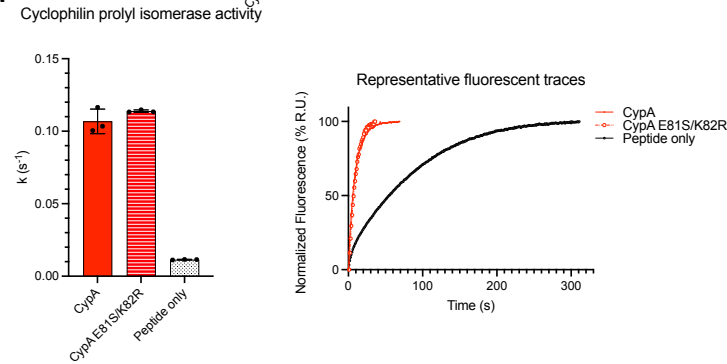
Cyclophilin	Prolyl-isomerization rate constant (k , s^{-1})	Signal/Background	Z' Factor
CypD	0.114±0.006	10.4	0.82
CypA	0.107±0.009	9.7	0.71
CypB	0.087±0.003	7.9	0.87
CypC	0.044±0.001	4	0.89
CypE	0.121±0.007	11	0.80
CypG	0.074±0.004	6.7	0.80
CypH	0.057±0.004	5.2	0.73
CypM0	0.065±0.001	5.9	0.93
NKTR	0.036±0.003	3.3	0.62
PPIL1	0.093±0.007	8.5	0.74
PPWD1	0.052±0.004	4.7	0.69
Peptide only	0.0110±0.0002	-	-

b

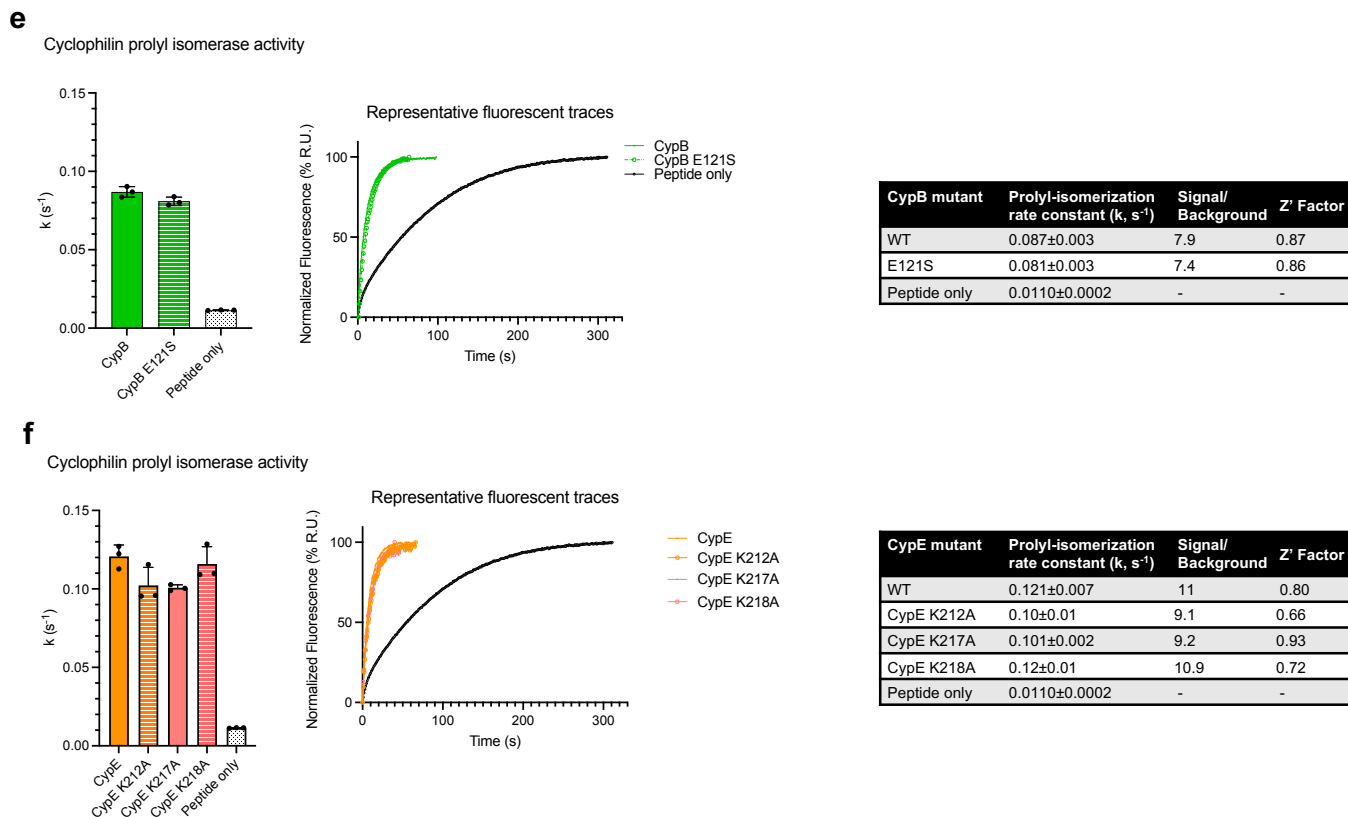
Cyclophilin	Prolyl-isomerization rate constant (k , s^{-1})	Signal/Background	Z' Factor
PPIL2	0.015±0.002	1.4	-0.65
PPIL3	0.0140±0.0005	1.3	0.30
Peptide only	0.0110±0.0002	-	-

c

CypD mutant	Prolyl-isomerization rate constant (k , s^{-1})	Signal/Background	Z' Factor
WT	0.114±0.006	10.4	0.82
K118A	0.111±0.004	10.1	0.87
K118E	0.104±0.003	9.5	0.90
S123E	0.11±0.01	10	0.69
R124A	0.110±0.004	10	0.87
R124K	0.12±0.01	10.9	0.72
K118E/R124K	0.101±0.008	9.2	0.73
Peptide only	0.0110±0.0002	-	-

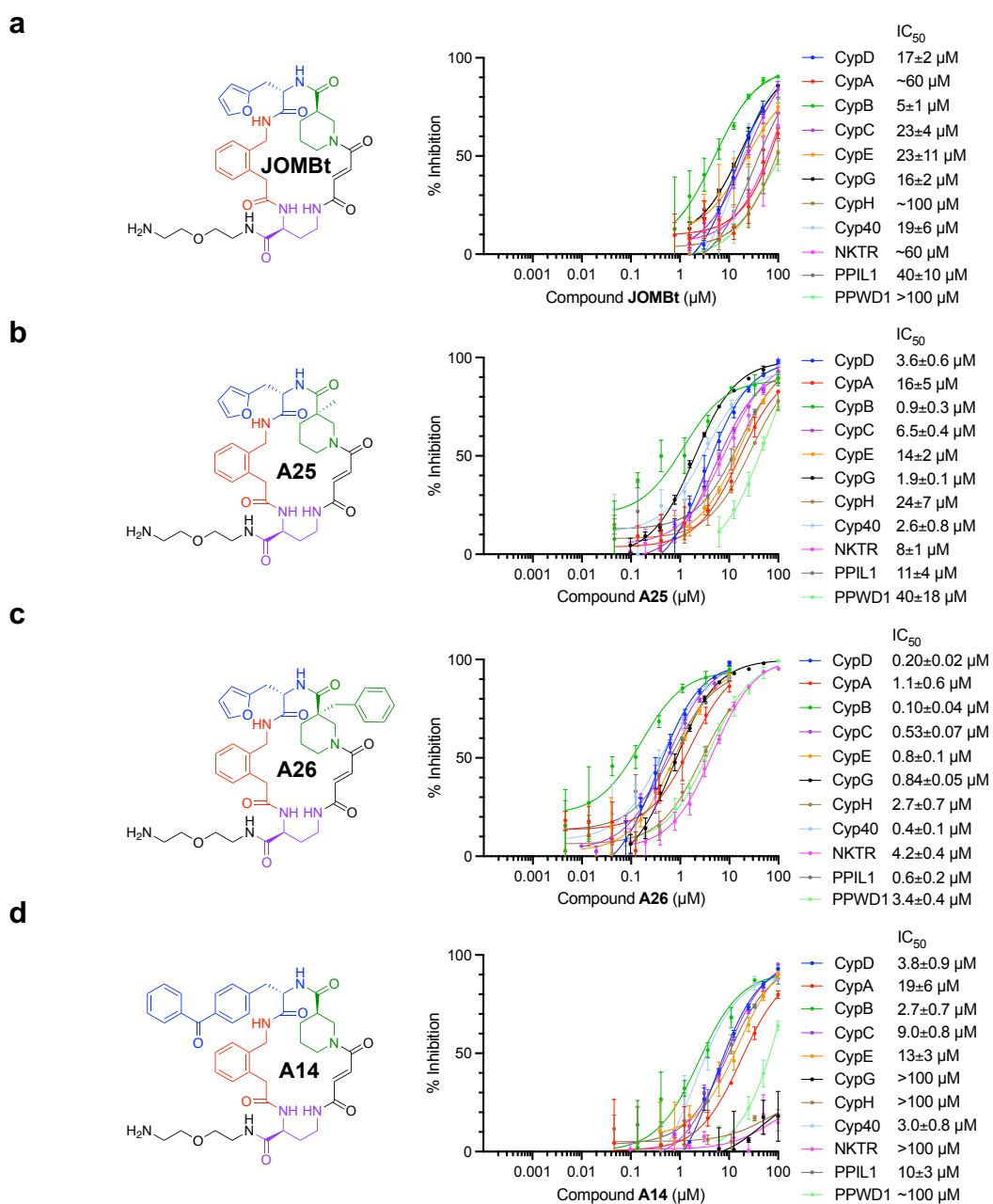
d

CypA mutant	Prolyl-isomerization rate constant (k , s^{-1})	Signal/Background	Z' Factor
WT	0.107±0.009	9.7	0.71
E81S/K82R	0.114±0.008	10.4	0.76
Peptide only	0.0110±0.0002	-	-

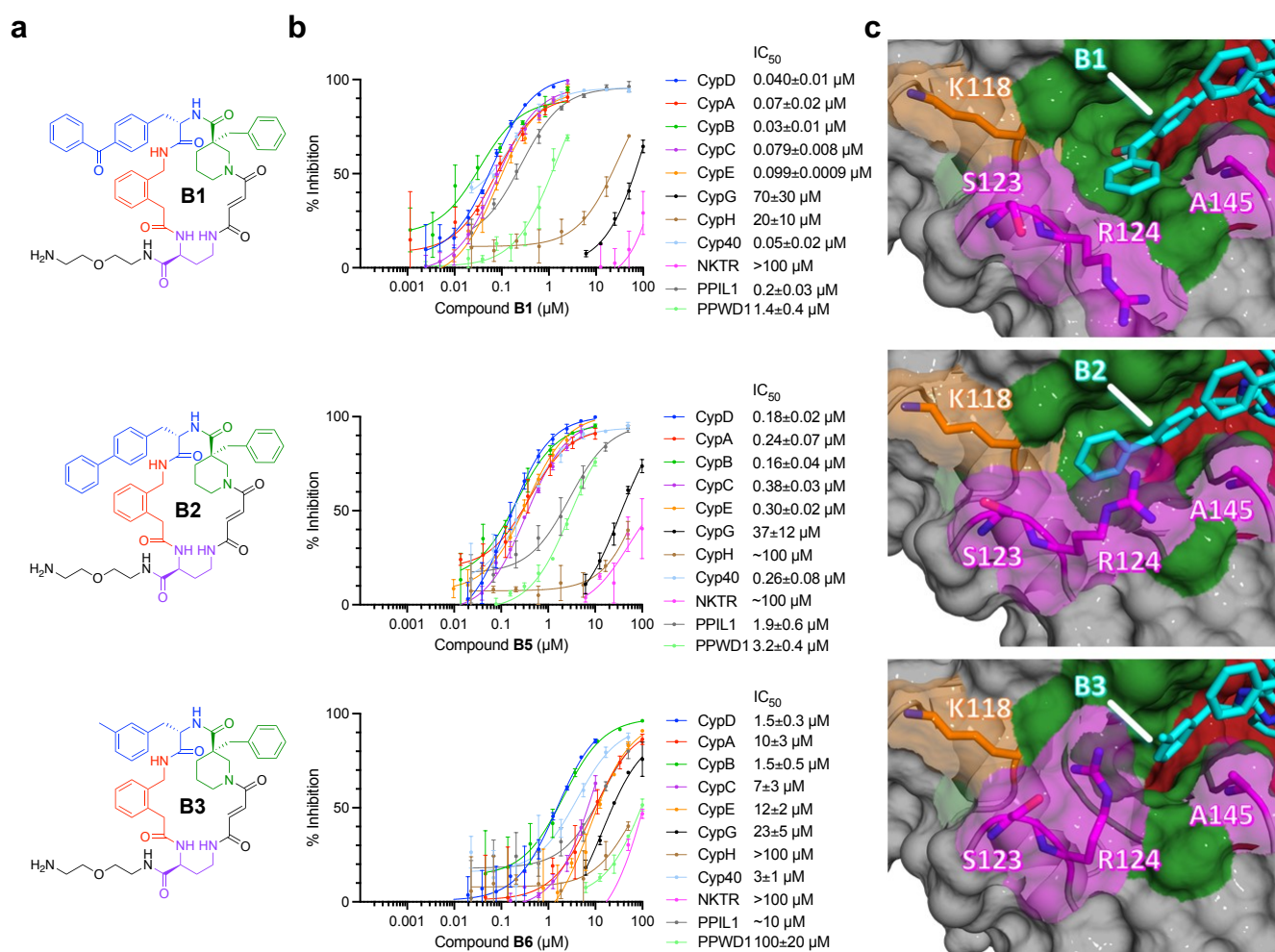


Supplementary Figure 3 | Prolyl isomerase activity of cyclophilins on Suc-AAPF-AMC.

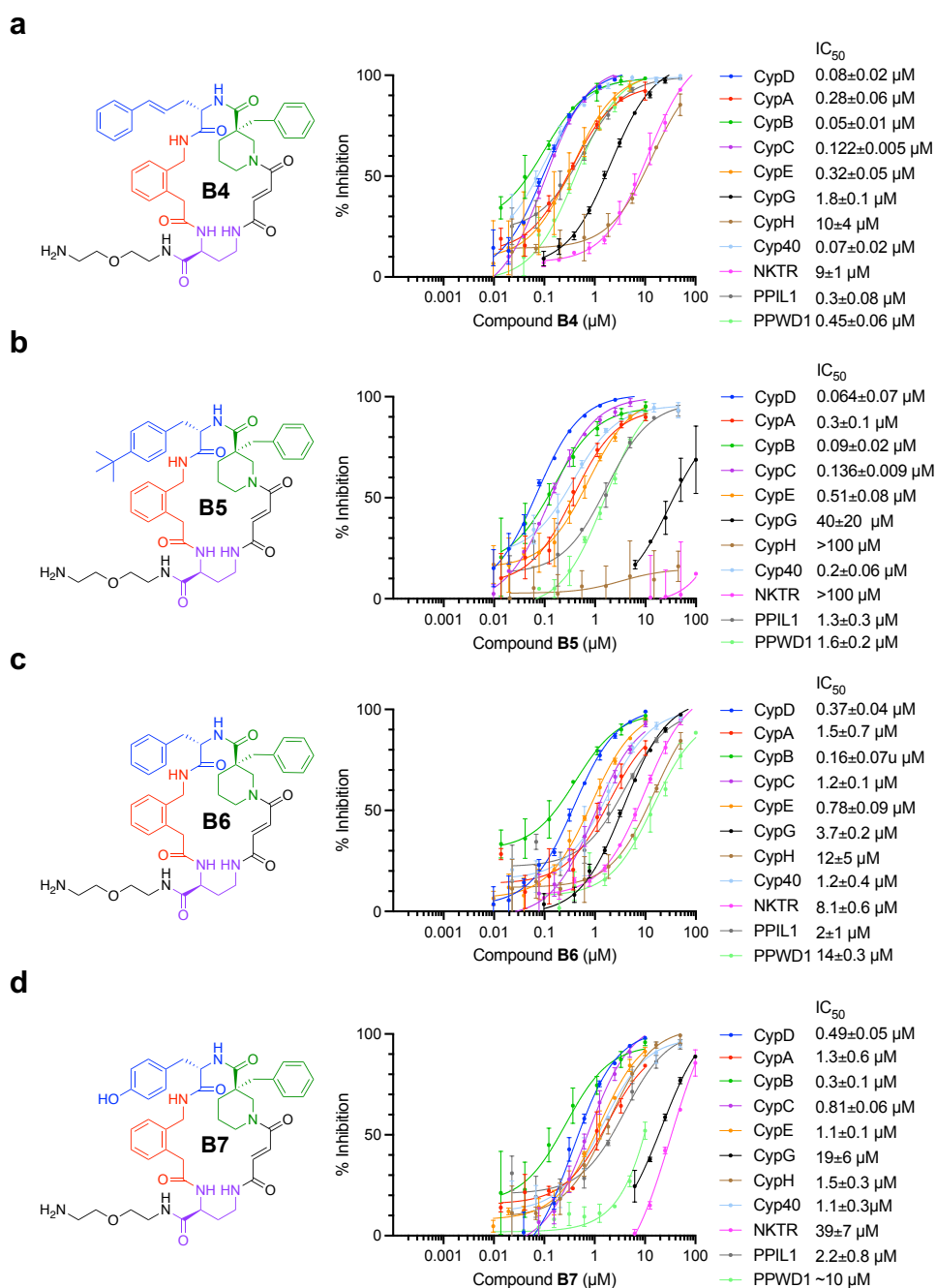
Rate constant, signal to background ratio (rate constant of cyclophilin divided by rate constant of peptide), and Z' values for: **a**, all wild-type cyclophilins screened; **b**, prolyl isomerase-inactive cyclophilins; **c**, CypD mutants; **d**, CypA E81S/K82R double mutant; **e**, CypB E121S mutant; **f**, CypE mutants. Also included are one representative kinetic trace of each cyclophilin during the assay timescale, normalized to fluorescence at $t=0$ and maximum fluorescent value. Analyses were halted after calculated maximum fluorescent value due to observed fluorescent bleaching during the sustained fluorescent plateau. Values and error bars reflect mean±SD of three technical replicates.



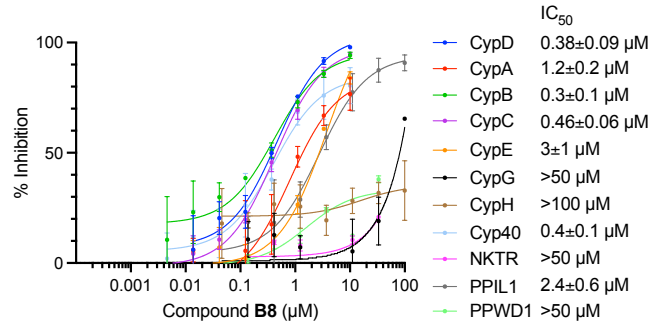
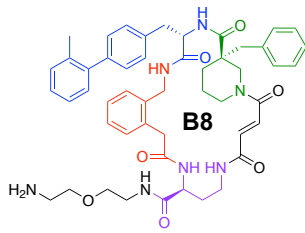
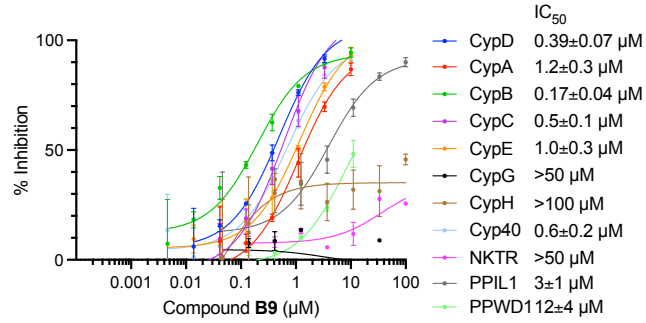
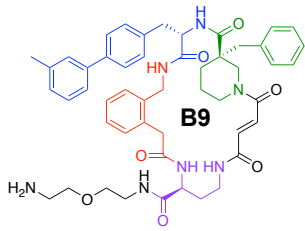
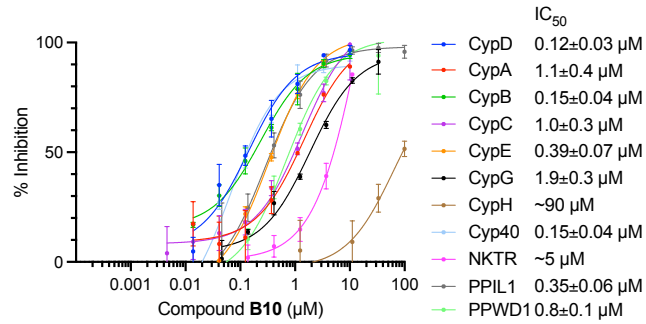
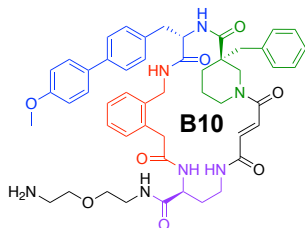
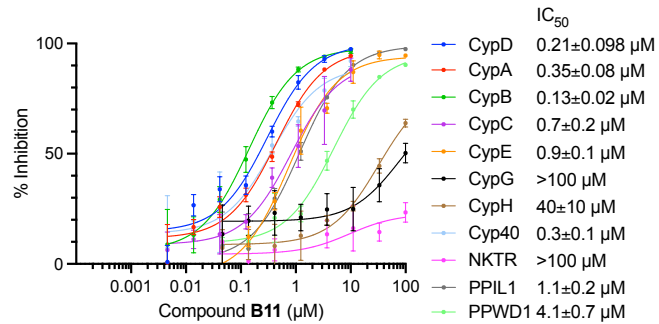
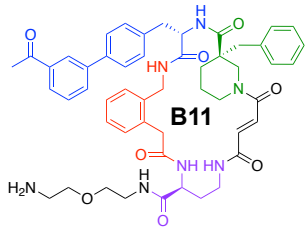
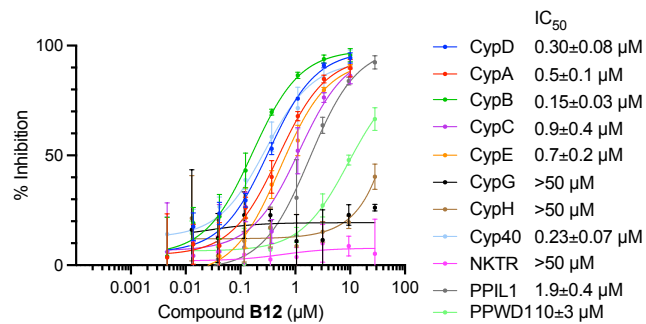
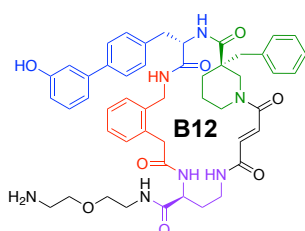
Supplementary Figure 4 | Functionalization of piperidine α -carbon improves CypD potency, while replacing the second building block improves CypD selectivity. a, Structure and cyclophilin inhibition dose response profile shown for a, JOMBt; b, A25; c, A26; and d, A14. While iterative functionalization of the α -carbon with a methyl or benzyl group improves potency for CypD, these compounds are still promiscuous cyclophilin inhibitors, with no gain in selectivity compared to JOMBt. In contrast, diversifying the second building block with larger moieties such as a benzophenone only marginally improve potency, but greatly increase selectivity over CypG, CypH, NKTR, and PPWD1. Crystal structures of JOMBt and A26 corroborate these observations, as the second building block is positioned within the S2 pocket, while the α -carbon on the piperidine is near a conserved Thr residue (Fig. 1f, Extended Data 3b). IC_{50} values reflect mean \pm SEM of three technical replicates. Data points and error bars reflect mean \pm SD of individual assays at one dose.

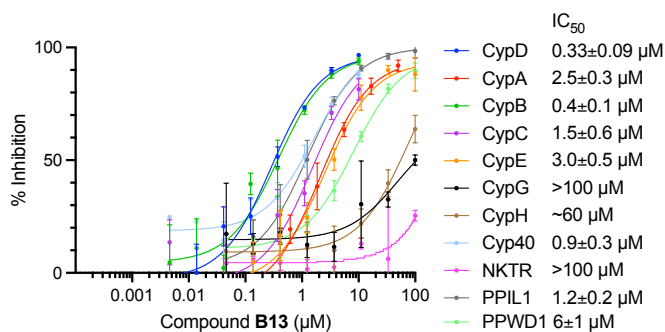
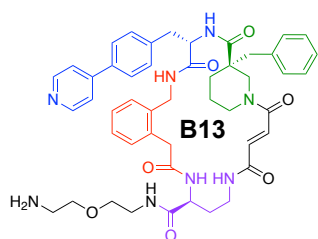
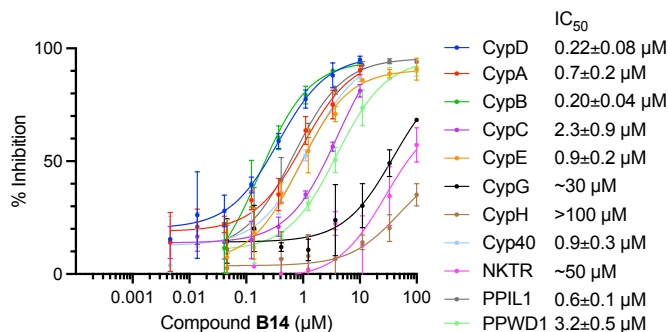
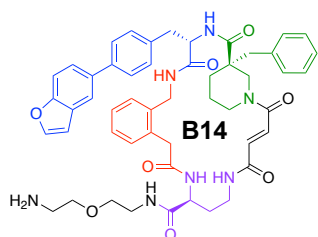


Supplementary Figure 5 | Large S2 binding groups improve selectivity for CypD. **a**, Structure of **B1**, **B2**, and **B3**. **b**, Prolyl-isomerase cyclophilin inhibition profile for **B1**, **B2**, and **B3**. **c**, Co-crystal structures of **B1** (PDB ID 7TGU, 1.21 Å resolution), **B2** (PDB ID 7TGV, 1.46 Å resolution), and **B3** (PDB ID 7TH1 1.52 Å resolution) bound to CypD, viewing the S2 pocket. Active site binding is identical to that of **A26** (Fig. 1e). The large benzophenone and biphenyl of **B1** and **B2**, respectively, fill the S2 pocket more completely than **B3**, which contains a *m*-methylphenyl group. This interaction imparts selectivity over CypG, CypH, NKTR, and PPWD1, which have sterically occluded or more structurally rigid S2 pocket residues. Macrocycles with larger S2-binding groups cause R124 to flip out of the S2 pocket in CypD (see Supplementary Fig. 32, Supplementary Video 1). IC₅₀ values reflect mean±SEM of three technical replicates. Data points and error bars reflect mean±SD of individual assays at one dose.

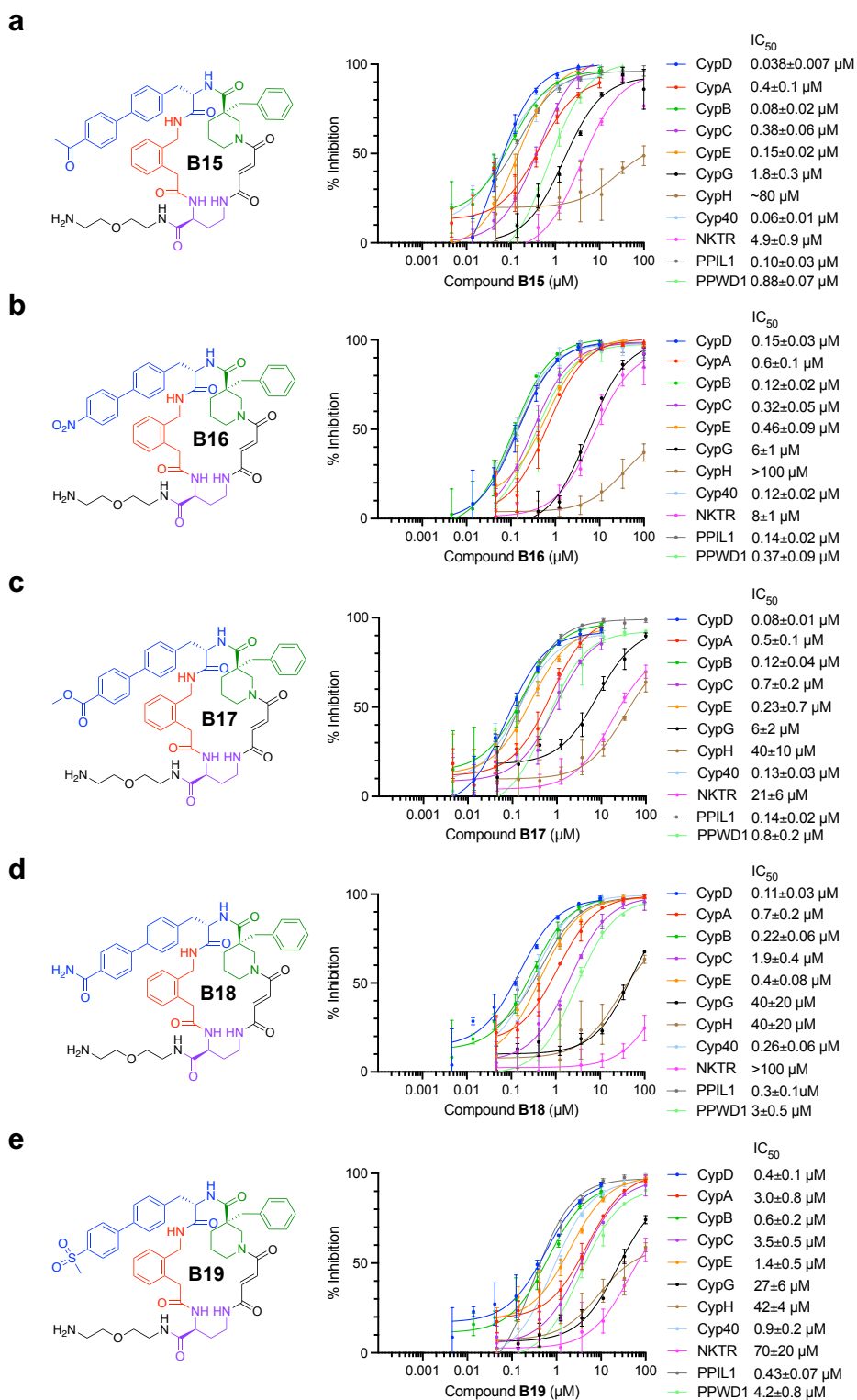


Supplementary Figure 6 | Large hydrophobic S2 binding groups impart selectivity for CypD over CypG, CypH, NKTR, and PPWD1. Structure and cyclophilin inhibition dose response data for **a**, **B4**; **b**, **B5**; **c**, **B6**; and **d**, **B7**. Small S2 binding moieties such as the phenylalanine in **B6** do not provide sufficient steric clash with S2 residues, even for cyclophilins with sterically occluded S2 pockets. Binding deeper into S2 pocket with *tert*-butyl phenylalanine in **B5** results in selectivity over CypG, CypH, and NKTR. An intermediate size styryl-alanine in **B4** offers moderate selectivity. **B4** and **B5** also exhibit slightly improved potency for CypD compared to **B6**. Using a tyrosine in **B7** offers little selectivity for CypH, and selectivity over NKTR and CypG, but a decrease in potency compared to **B4** and **B5**. IC₅₀ values reflect mean±SEM of three technical replicates. Data points and error bars reflect mean±SD of individual assays at one dose.

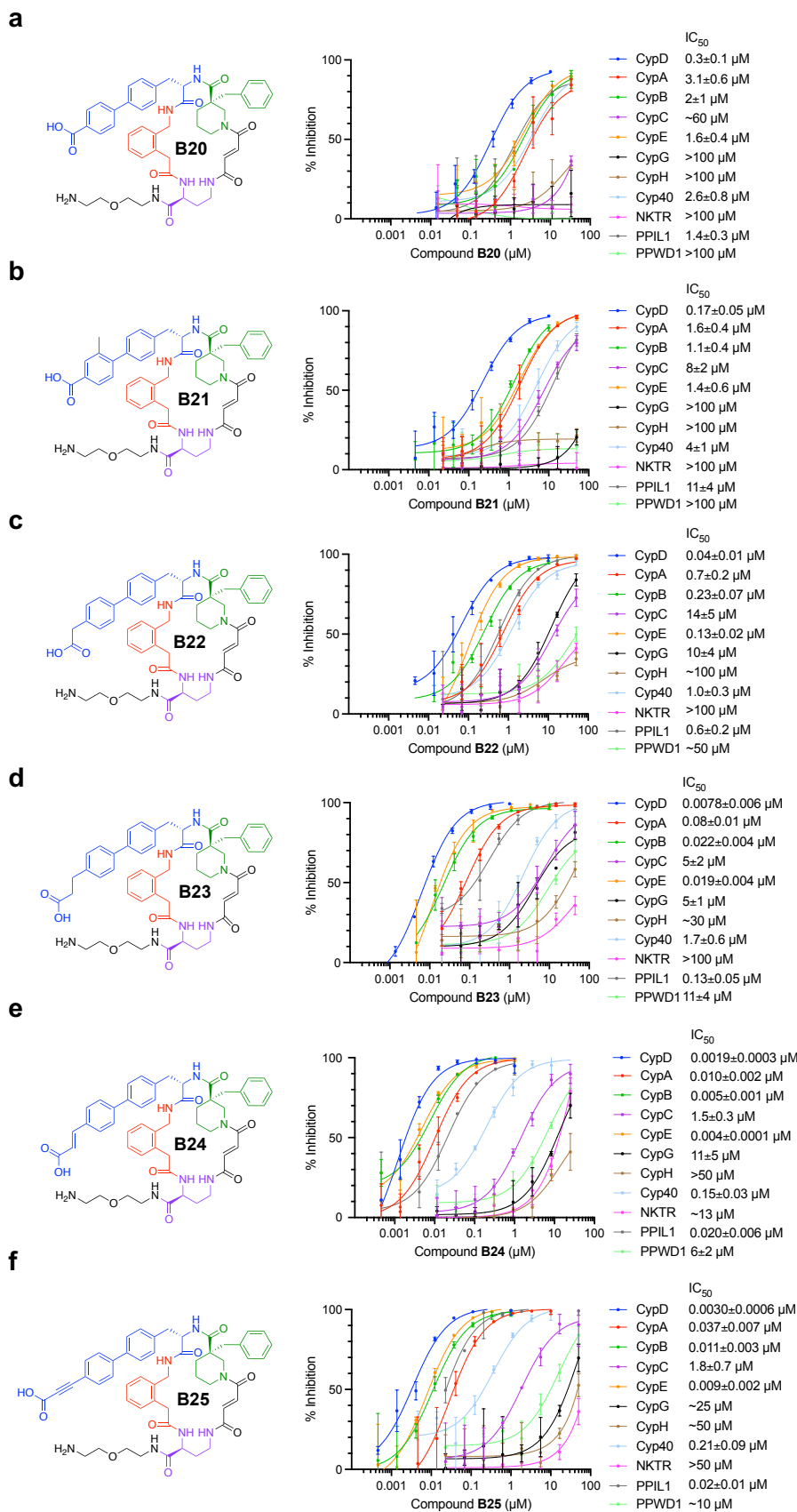
a**b****c****d****e**

f**g**

Supplementary Figure 7 | Biphenyl and bi-aromatic derivatives of B2 showing no improvement in selectivity for CypD. Structure and cyclophilin inhibition dose response data for **a**, B8; **b**, B9; **c**, B10; **d**, B11; **e**, B12; **f**, B13; and **g**, B14. These compounds exhibit similar gain in selectivity over CypG, CypH, NKTR, and PPWD1 as in B2, but no further selectivity for CypD. IC₅₀ values reflect mean±SEM of three technical replicates. Data points and error bars reflect mean±SD of individual assays at one dose.

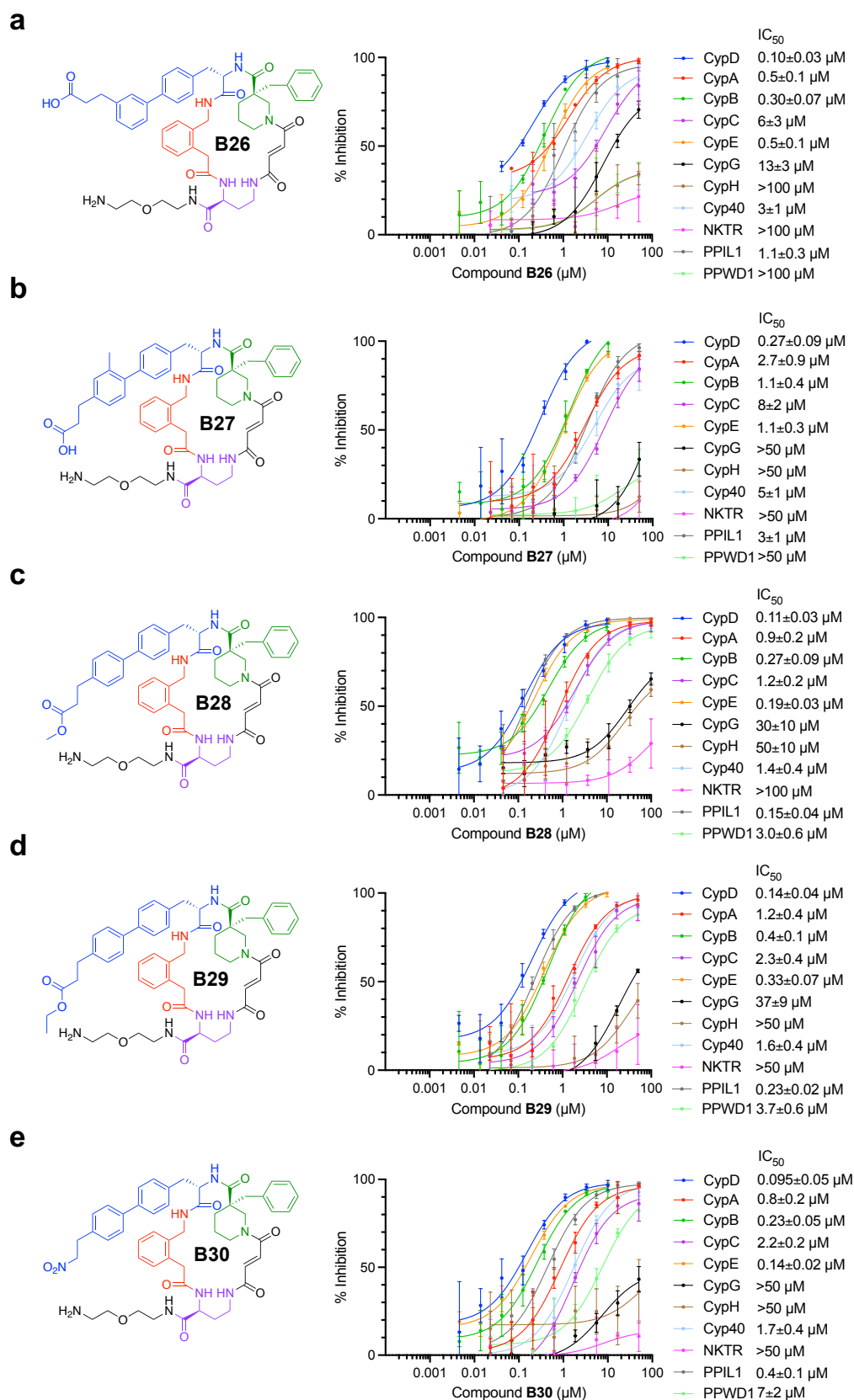


Supplementary Figure 8 | Para-carbonyl-containing biphenyl moieties show partial selectivity over CypC. Structure and cyclophilin inhibition dose response data for **a**, **B15**; **b**, **B16**; **c**, **B17**; **d**, **B18**; and **e**, **B19**. **B15**, **B17**, **B18**, and **B19** show reduced potency for CypC compared to CypD. These para-carbonyl biphenyl groups maintain a similar selectivity profile over CypG, CypH, and NKTR as **B2**. IC₅₀ values reflect mean±SEM of three technical replicates. Data points and error bars reflect mean±SD of individual assays at one dose.



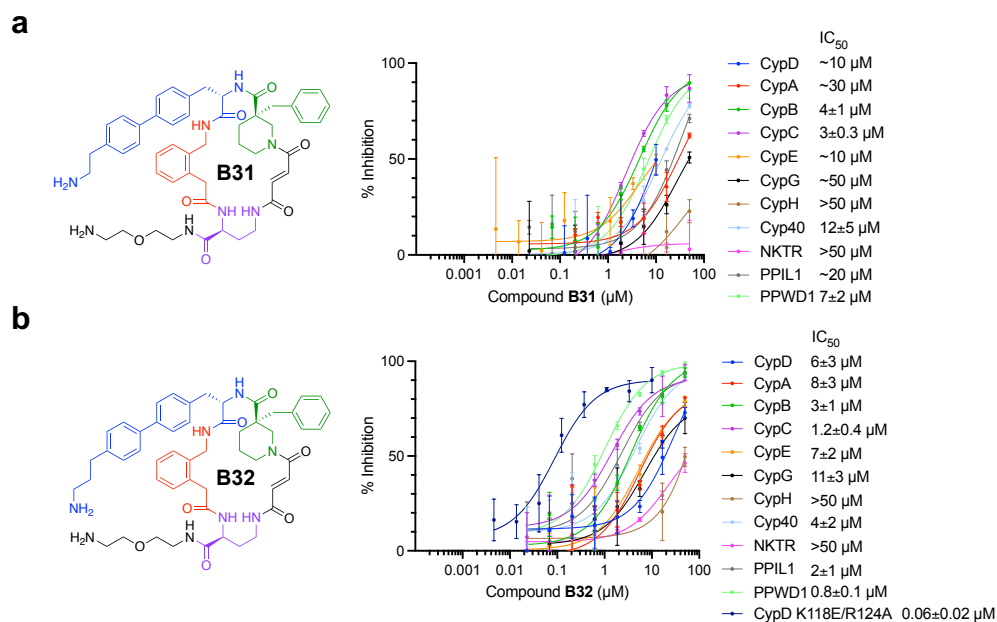
Supplementary Figure 9 | Para-carboxy-containing biphenyl groups provide enhanced selectivity and potency for CypD. Structure and cyclophilin inhibition dose response data for

a, B20; b, B21; c, B22; d, B23; e, B24; and f, B25. The carboxylate in **B20** and **B21** provides a high degree selectivity over CypC and Cyp40. Extension of the carboxylate from the biphenyl with a methylene in **B22** further improves potency for CypD and selectivity over CypC, Cyp40, PPIL1 and CypA. Extension with an ethylene in **B23** gives high potency for CypD, strong selectivity over CypC and Cyp40, and appreciable selectivity over CypA and PPIL1. Replacement of **B23**'s ethylene linker between the biphenyl and carboxylate with a vinyl or ethynyl linker in **B24** and **B25**, respectively, mimics **B23** potency and selectivity profile, but with slightly lower selectivity over PPIL1. IC₅₀ values reflect mean±SEM of three technical replicates. Data points and error bars reflect mean±SD of individual assays at one dose.

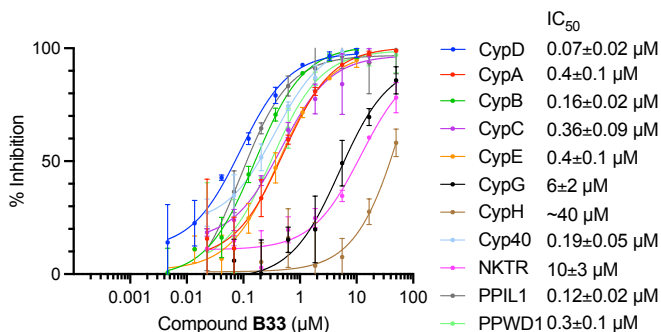
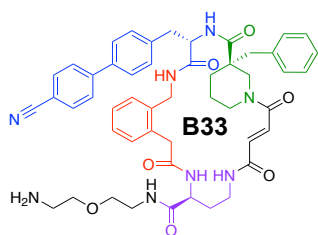
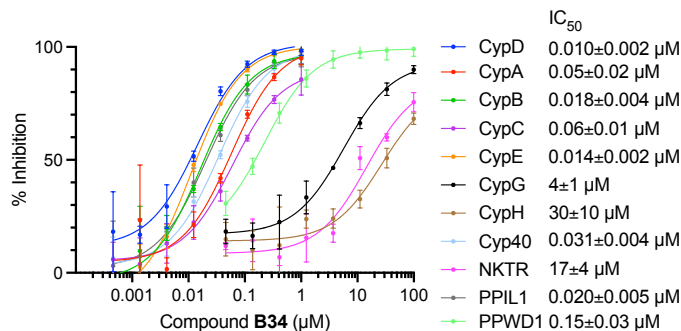
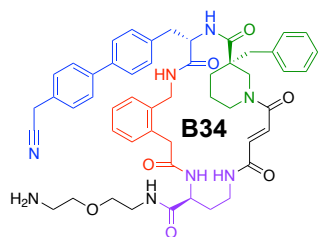


Supplementary Figure 10 | Masking or moving the carboxylate of B23 results in loss in potency and selectivity for CypD. Structure and cyclophilin inhibition dose response data for

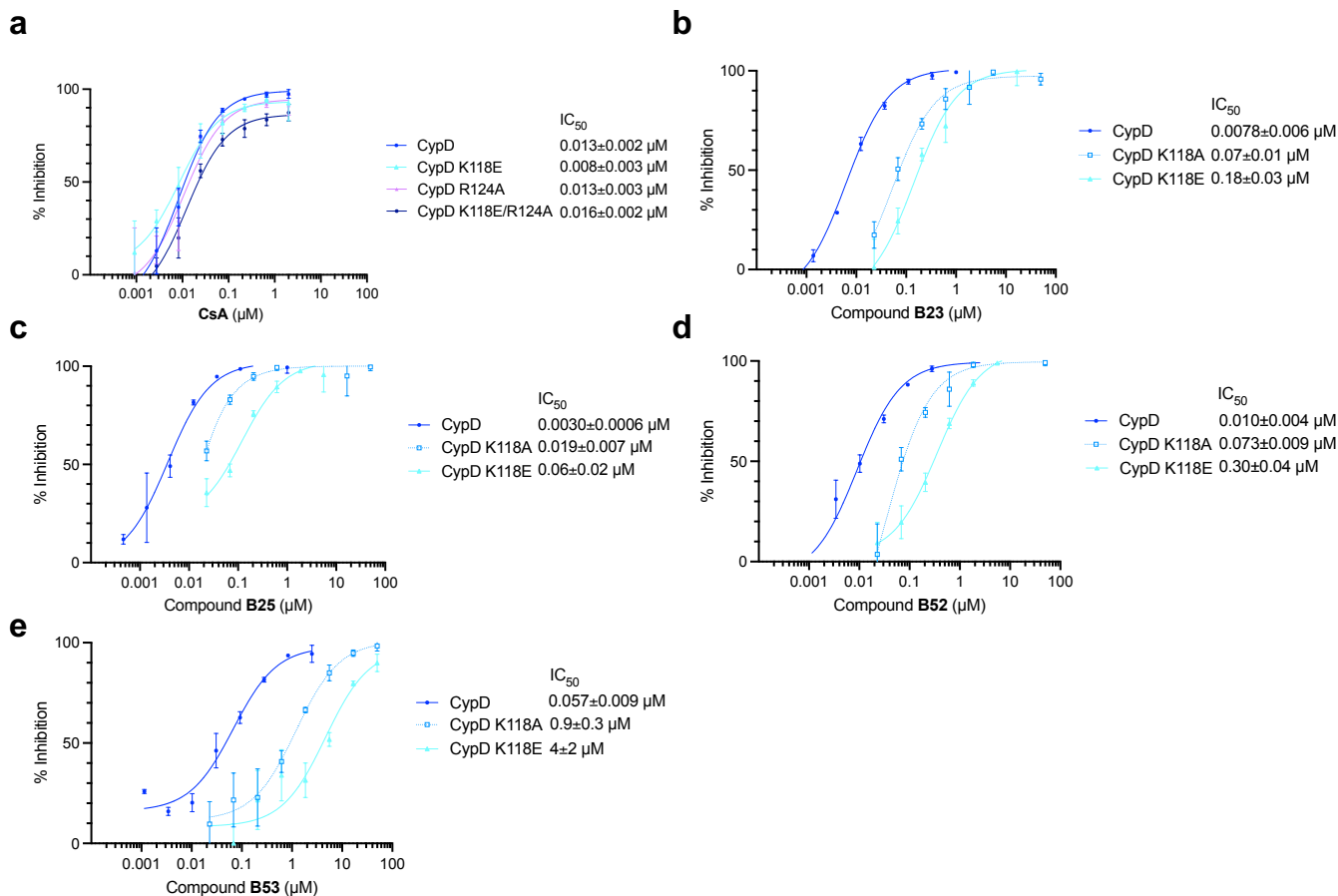
a, B26; b, B27; c, B28; d, B29; and e, B30. Compared to **B23**, alternate placement of the carboxylate on the biphenyl results in decreased potency and selectivity, shown with *meta* placement of the carboxylate in **B26** or adjusting biphenyl substitution in **B27**. Presumably, **B27** exhibits a binding mode similar to that shown in the **B21** co-crystal structure (PDB ID 7TH6, 0.97 Å resolution), where the *ortho*-methyl migrates the biphenyl out of the S2 pocket. Masking the negative charge of the carboxylate with a methyl ester, ethyl ester, or a net-neutral nitro group in **B28**, **B29**, and **B30** respectively, results in the same loss in potency and selectivity. IC₅₀ values reflect mean±SEM of three technical replicates. Data points and error bars reflect mean±SD of individual assays at one dose.



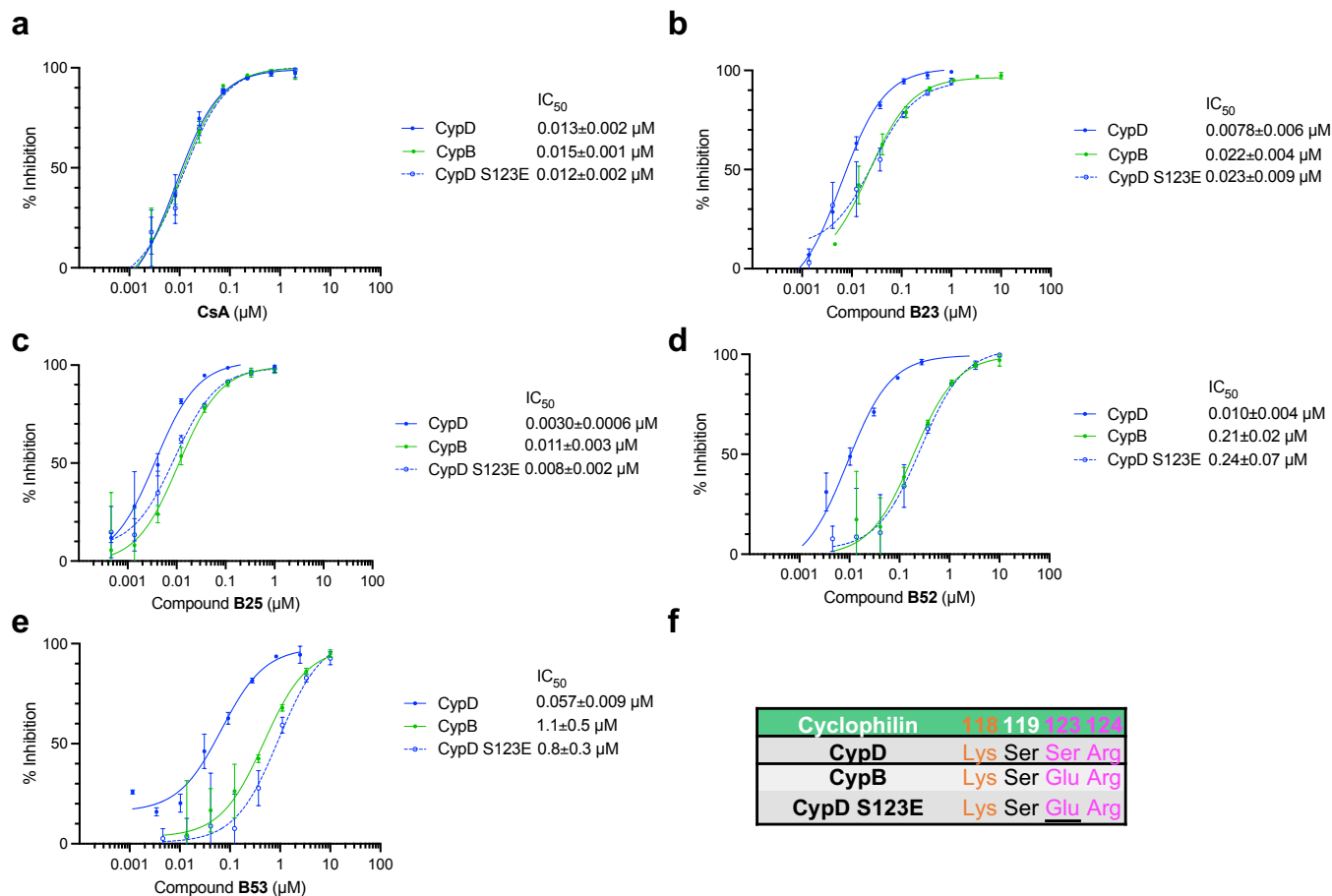
Supplementary Figure 11 | Inverting ligand charge abrogates CypD potency and shifts the cyclophilin selectivity profile. Structure and cyclophilin inhibition dose response data for **a**, **B31**; and **b**, **B32**. Inserting an amine with a net positive charge results in >1,000-fold reduction in CypD potency, presumably due to charge-charge repulsion at the K118 residue. **B31** and **B32** also show some selectivity preference for CypC and PPWD1, respectively. Both of these cyclophilins have a negatively charged glutamate residue replacing CypD's K118 residue. The inhibition potency of **B32** is restored against the charge-inverted mutant CypD K118E/R124A, preferentially inhibiting this mutant over any wild-type cyclophilin. IC₅₀ values reflect mean±SEM of three technical replicates. Data points and error bars reflect mean±SD of individual assays at one dose.

a**b**

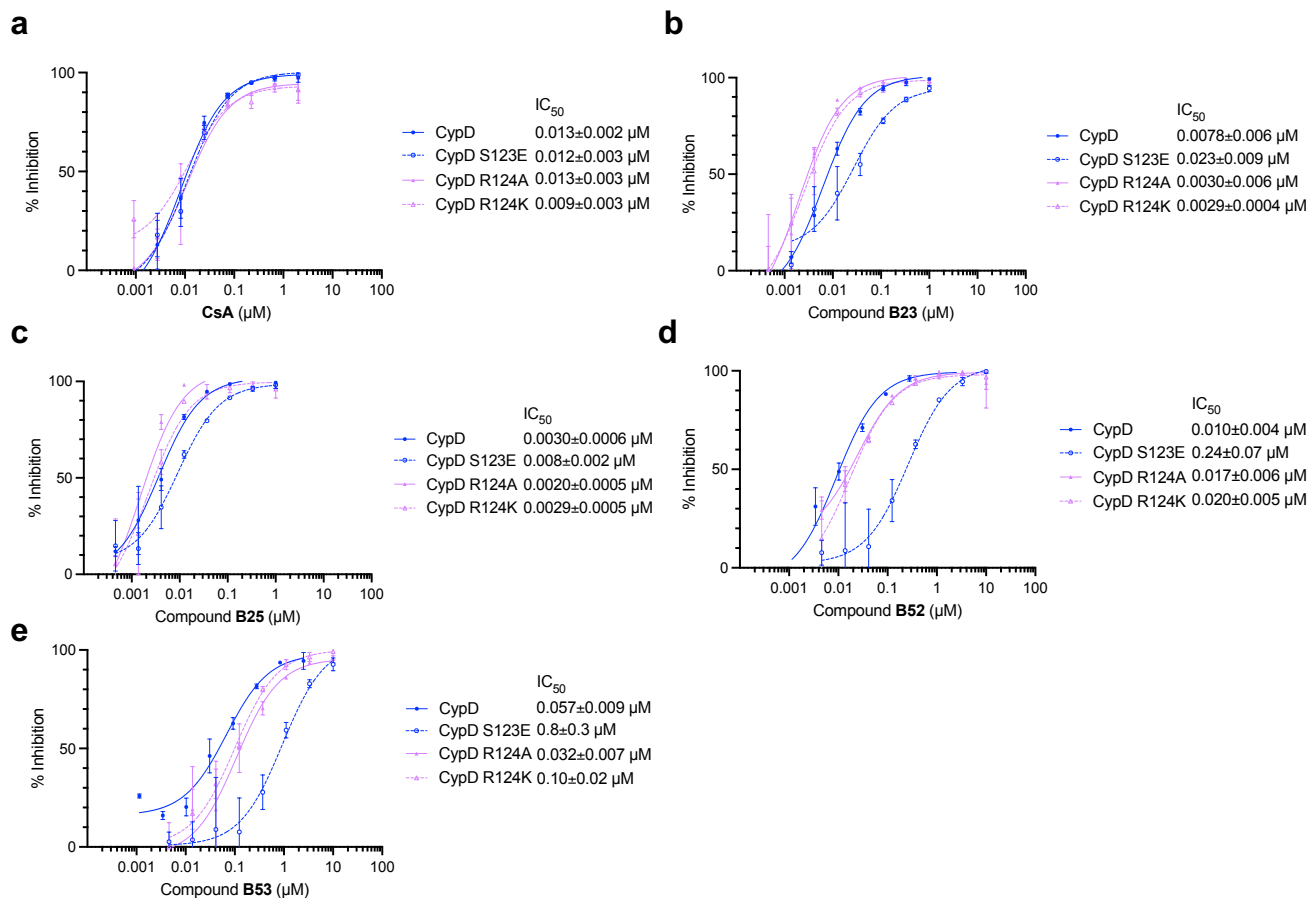
Supplementary Figure 12 | Nitrile-containing biphenyl groups show similar CypD inhibition potencies and linker dependencies as carboxylates. Structure and cyclophilin inhibition dose response data for **a**, **B33**; and **b**, **B34**. The increased potency of **B34** compared to **B33** is consistent with the same trend we observed for **B22** and **B23**. IC₅₀ values reflect mean±SEM of three technical replicates. Data points and error bars reflect mean±SD of individual assays at one dose.



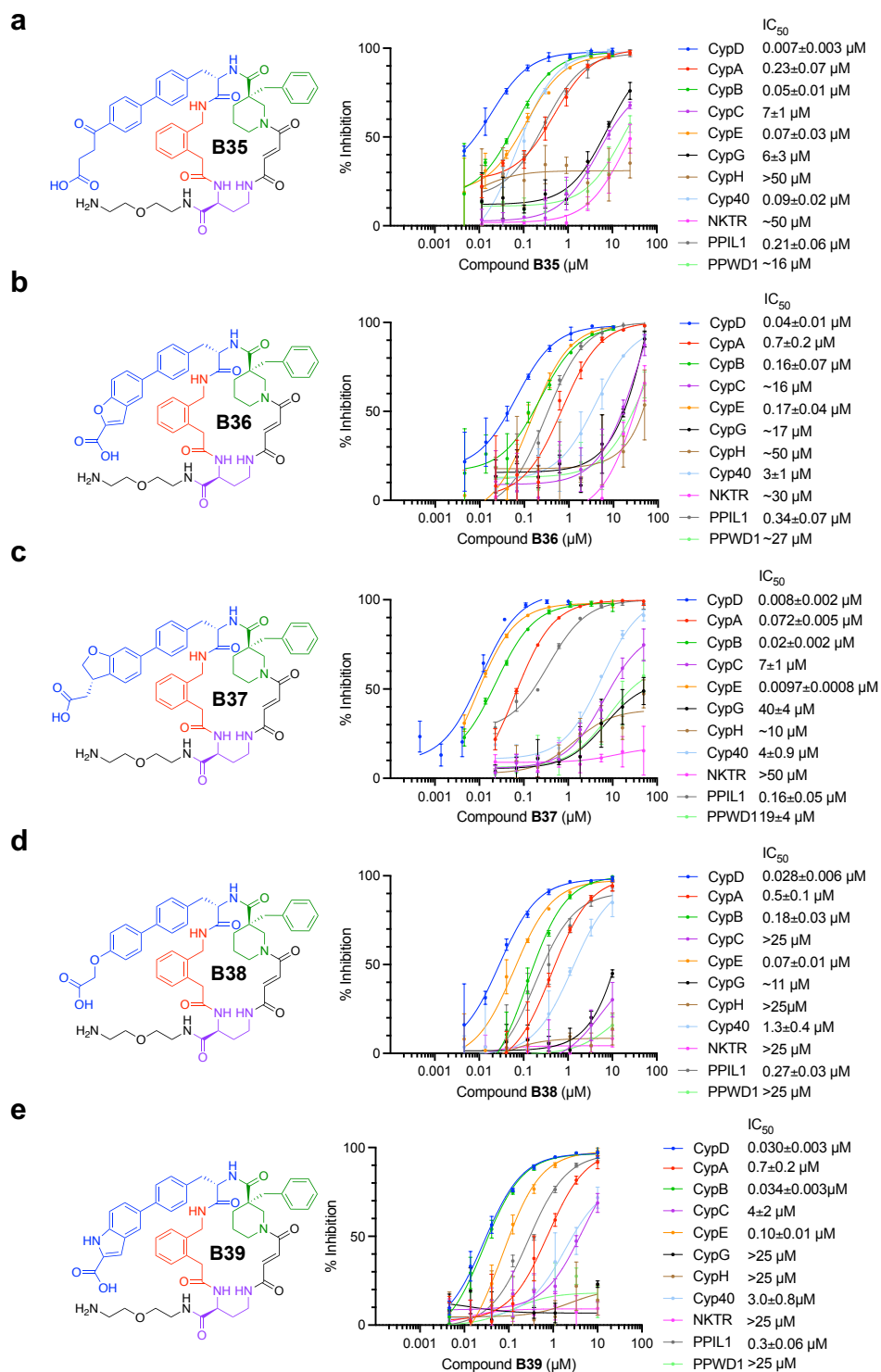
Supplementary Figure 13 | Residue K118 is necessary for potent CypD inhibition with carboxylate-containing inhibitors. Dose response curves of CypD, CypD K118A, and CypD K118E with **a**, CsA; **b**, B23; **c**, B25; **d**, B52; and **e**, B53. CsA as an active site ligand does not show appreciable changes in potency for CypD mutants compared to wild-type CypD. A salt bridge was observed in each crystal structure between a carboxylate on B23, B25, B52, and B53, and residue K118 (Fig. 3c, Fig. 4c). Mutation to a neutral alanine results in a 6- to 20-fold decrease in potency compared to wild-type CypD. Mutation to a negatively charged glutamate results in a 20- to 100-fold decrease in potency compared to wild-type CypD. For CypD wild-type IC₅₀ data with B52 and B53, values reflect mean±SD of four independent replicates (each comprising three technical replicates). Graphs show a representative single independent replicate (Independent replicate 1 is shown, containing three technical replicates) with data points and error bars reflecting mean±SD of individual assays at one dose. Further independent replicates are shown in Supplementary Fig. 18b-c. All other IC₅₀ values reflect mean±SEM of three technical replicates, with data points and error bars reflecting mean±SD of individual assays at one dose.



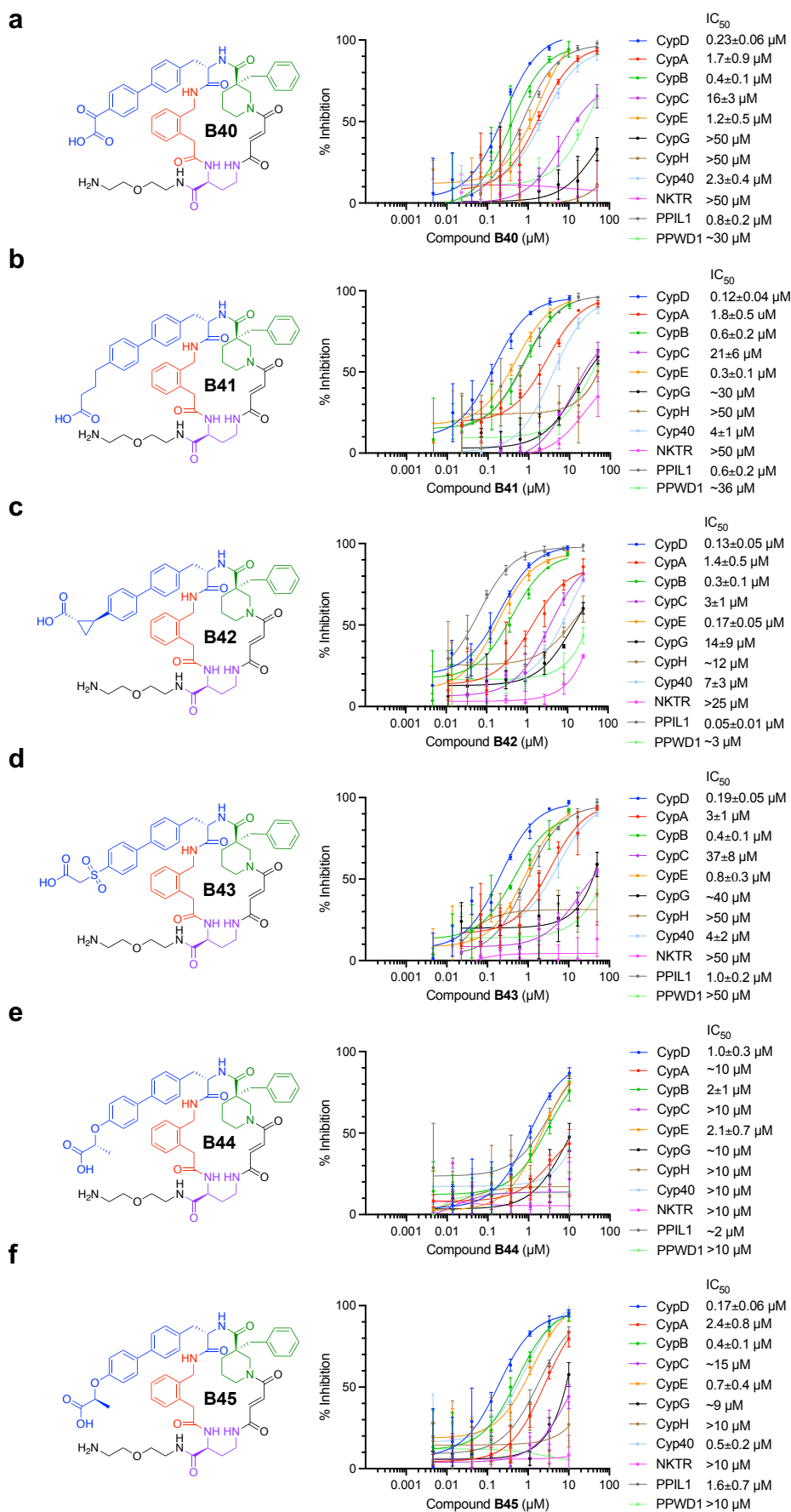
Supplementary Figure 14 | S123 gatekeeper position dictates inhibitor potency. Dose response curves of CypD, CypB, and CypD S123E, shown for **a**, CsA; **b**, B23; **c**, B25. **d**, B52; and **e**, B53. **f**, List of residues on the far side of the S2 pocket of cyclophilins that are proximal to the ligand carboxylates, with the CypD mutation underlined. CsA as an active site ligand does not show appreciable differences in potency between wild-type CypD, wild-type CypB, and CypD S123E. Wild-type CypB and wild-type CypD share identical S2 pockets with the exception of the analogous CypD S123 residue, which is a glutamate in CypB. CypD S123E thus provides the same S2 pocket as CypB WT, resulting in almost identical potencies for these two proteins for all inhibitors shown. For CypD and CypB wild-type IC₅₀ data with B52 and B53, values reflect mean±SD of four independent replicates (each comprising three technical replicates). Graphs show a representative single independent replicate (Independent replicate 1 is shown, containing three technical replicates) with data points and error bars reflecting mean±SD of individual assays at one dose. Further independent replicates are shown in Supplementary Fig. 18b-c. All other IC₅₀ values reflect mean±SEM of three technical replicates, with data points and error bars reflecting mean±SD of individual assays at one dose.

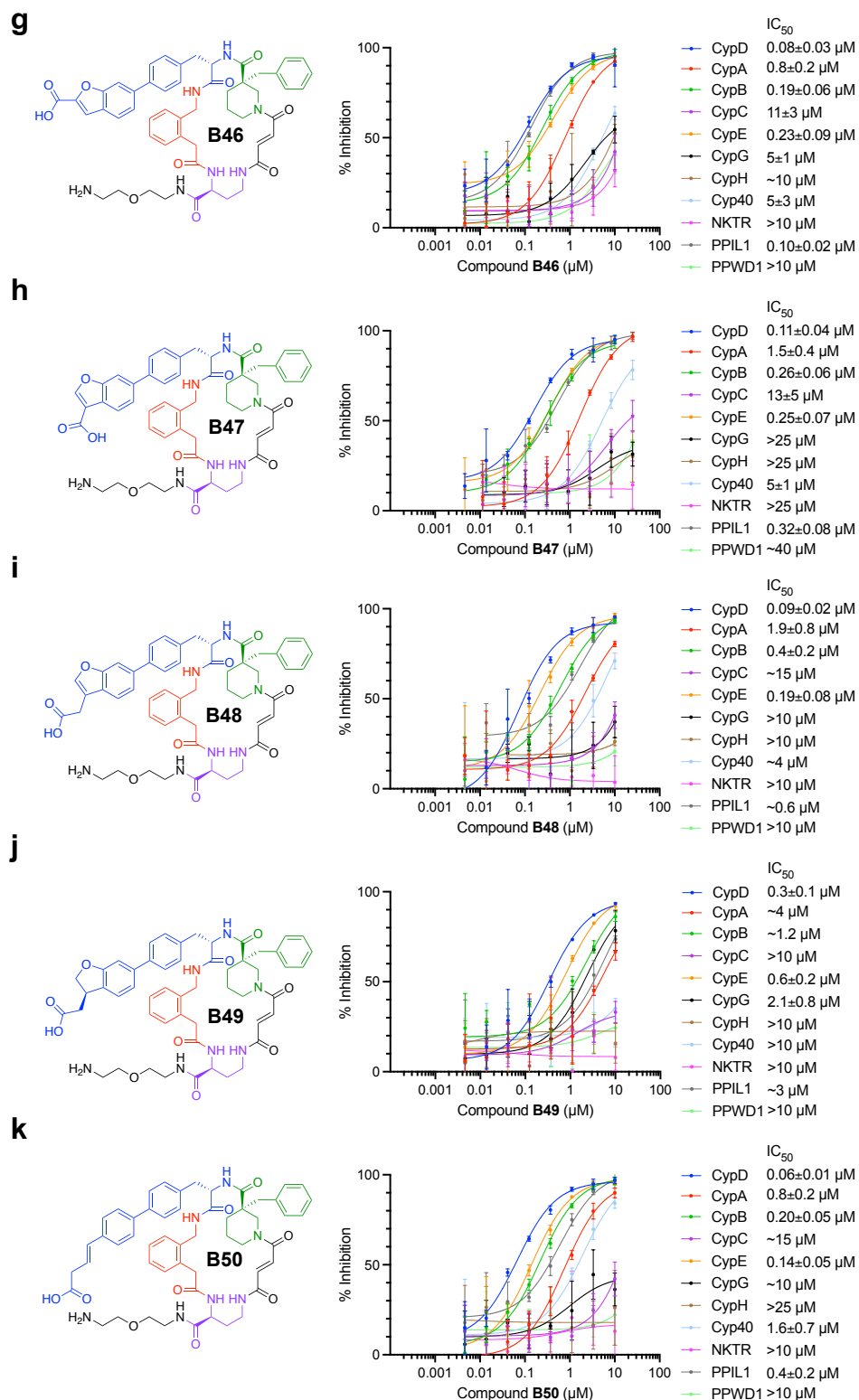


Supplementary Figure 15 | Prolyl isomerase inhibition activity on CypD gatekeeper mutants. Dose response curves of CypD and CypD S123E, CypD R124A, and CypD R124K mutants, shown for **a**, CsA; **b**, B23; **c**, B25; **d**, B52; and **e**, B53. CsA as an active site ligand does not show appreciable differences in potency between wild-type CypD and CypD mutants. Each carboxylate-containing ligand shows a modest drop in potency for CypD S123E compared to wild-type CypD, indicating a transient interaction with this residue. Little to no drop-in potency for R124A or R124K mutants suggest that the carboxylates for each compound do not interact with this residue directly. For CypD wild-type IC₅₀ data with B52 and B53, values reflect mean±SD of four independent replicates (each comprising three technical replicates). Graphs show a representative single independent replicate (Independent replicate 1 is shown, containing three technical replicates) with data points and error bars reflecting mean±SD of individual assays at one dose. Further independent replicates are shown in Supplementary Fig. 18b-c. All other IC₅₀ values reflect mean±SEM of three technical replicates, with data points and error bars reflecting mean±SD of individual assays at one dose.



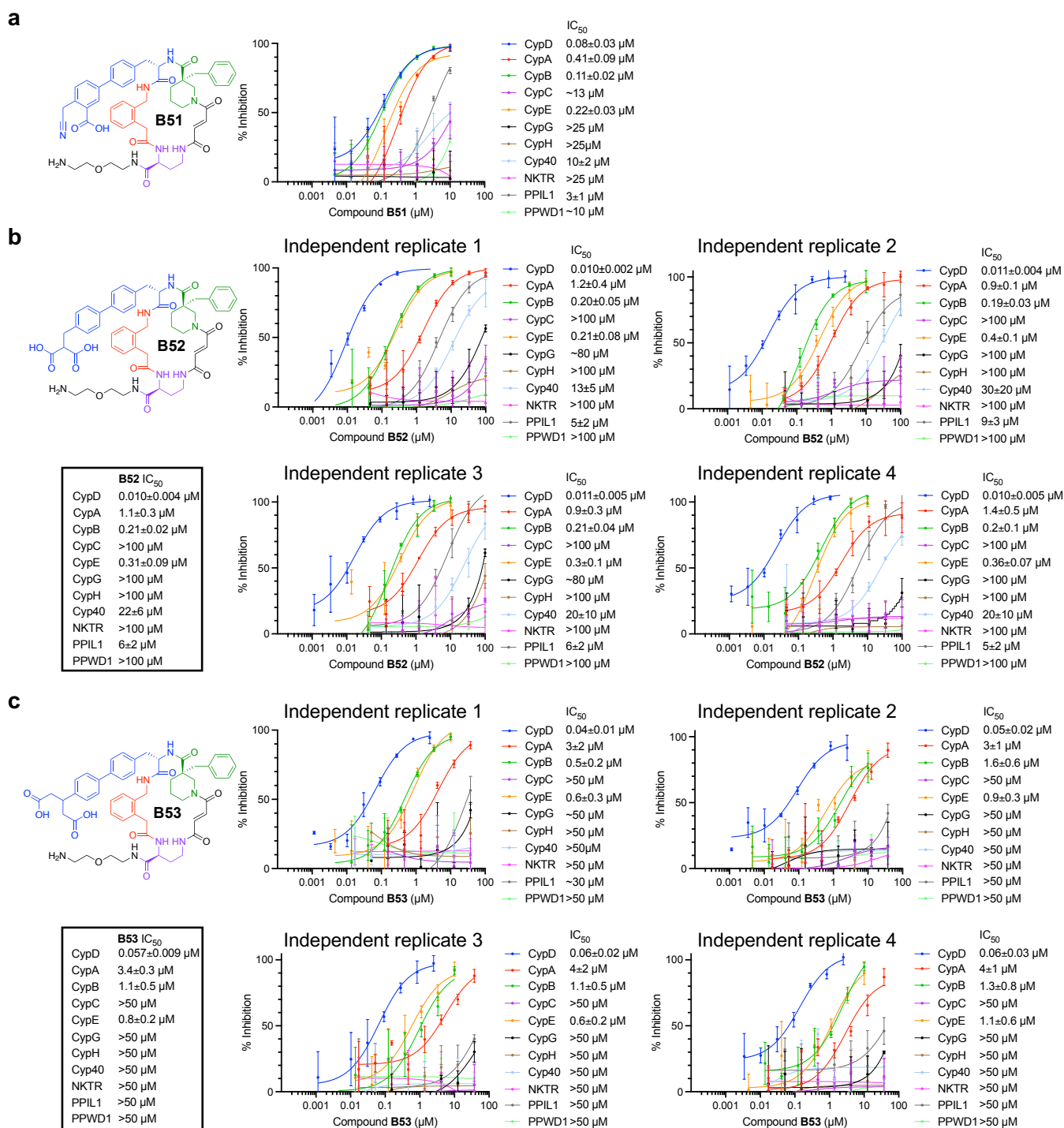
Supplementary Figure 16 | Derivatives of B23 that show similar selectivity and potency profiles for CypD. Structure and cyclophilin inhibition dose response data for **a**, B35; **b**, B36; **c**, B37; **d**, B38; and **e**, B39. Compared to B23, all compounds maintain the same CypD potency and selectivity profile. Presumably, these compounds retain the interactions with K118 and S119 shown in the B23 co-crystal structure (Fig. 3c). IC_{50} values reflect mean \pm SEM of three technical replicates. Data points and error bars reflect mean \pm SD of individual assays at one dose.





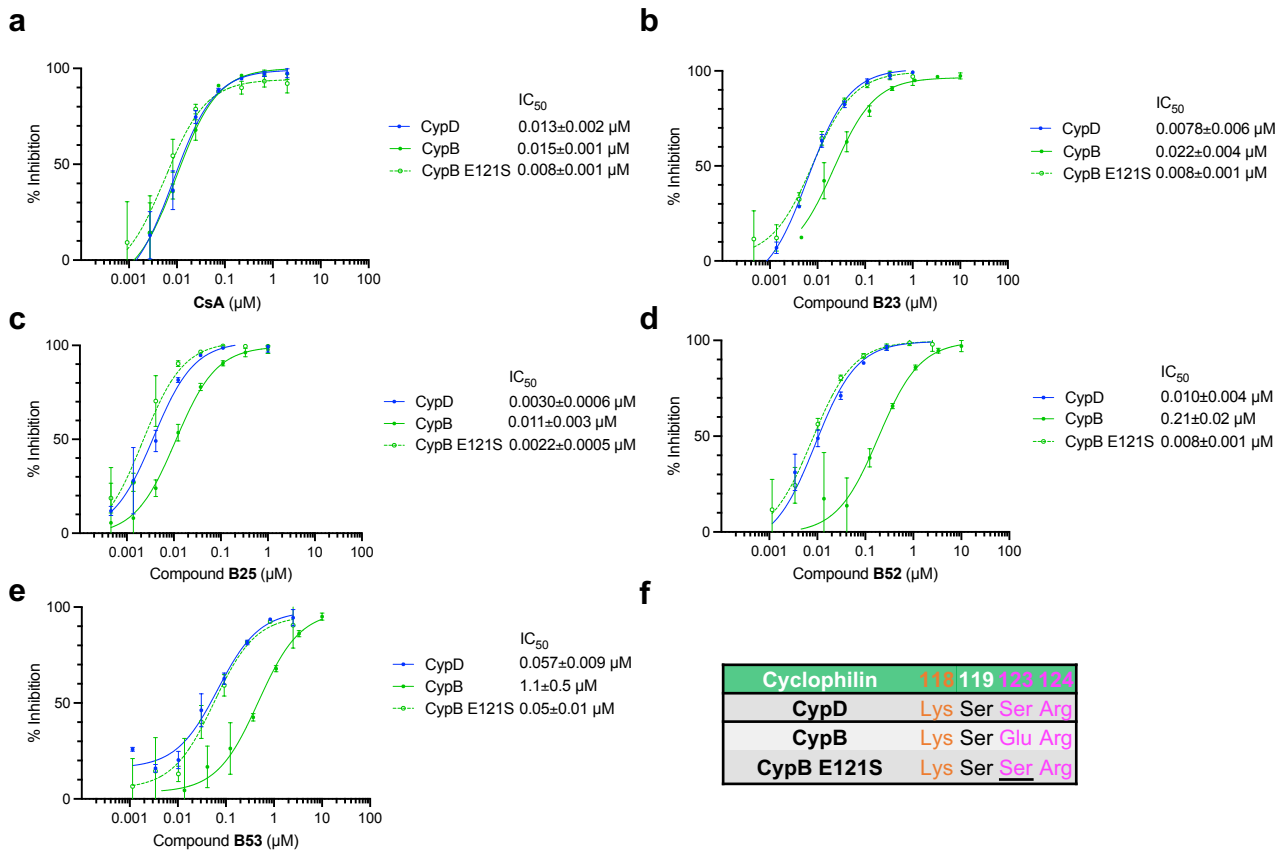
Supplementary Figure 17 | Derivatives of B23 that show reduced potency and selectivity for CypD. Structure and cyclophilin inhibition dose response data for **a, B40; b, B41; c, B42; d, B43; e, B44; f, B45; g, B46; h, B47; i, B48; j, B49; and k, B50**. Functionalization of the ethylene linker for **B23** commonly results in loss of potency and selectivity, shown in **B40, B42, B43, B44, and B45**, suggesting these extra functional groups interfere with the carboxylate's binding with

K118 and S119 residues. Extension of the linker further than **B23**'s ethylene (**B41** and **B50**) also reduces CypD potency. Other versions of structural rigidity introduced to the carboxylate, such as heterocycles, must be precisely placed, as **B42**, **B46**, **B47**, **B48**, and **B49** all show reduced potency compared to other heterocycle-carboxylates, such as **B37** and **B39** (Supplemental Fig. 16). IC₅₀ values reflect mean±SEM of three technical replicates. Data points and error bars reflect mean±SD of individual assays at one dose.

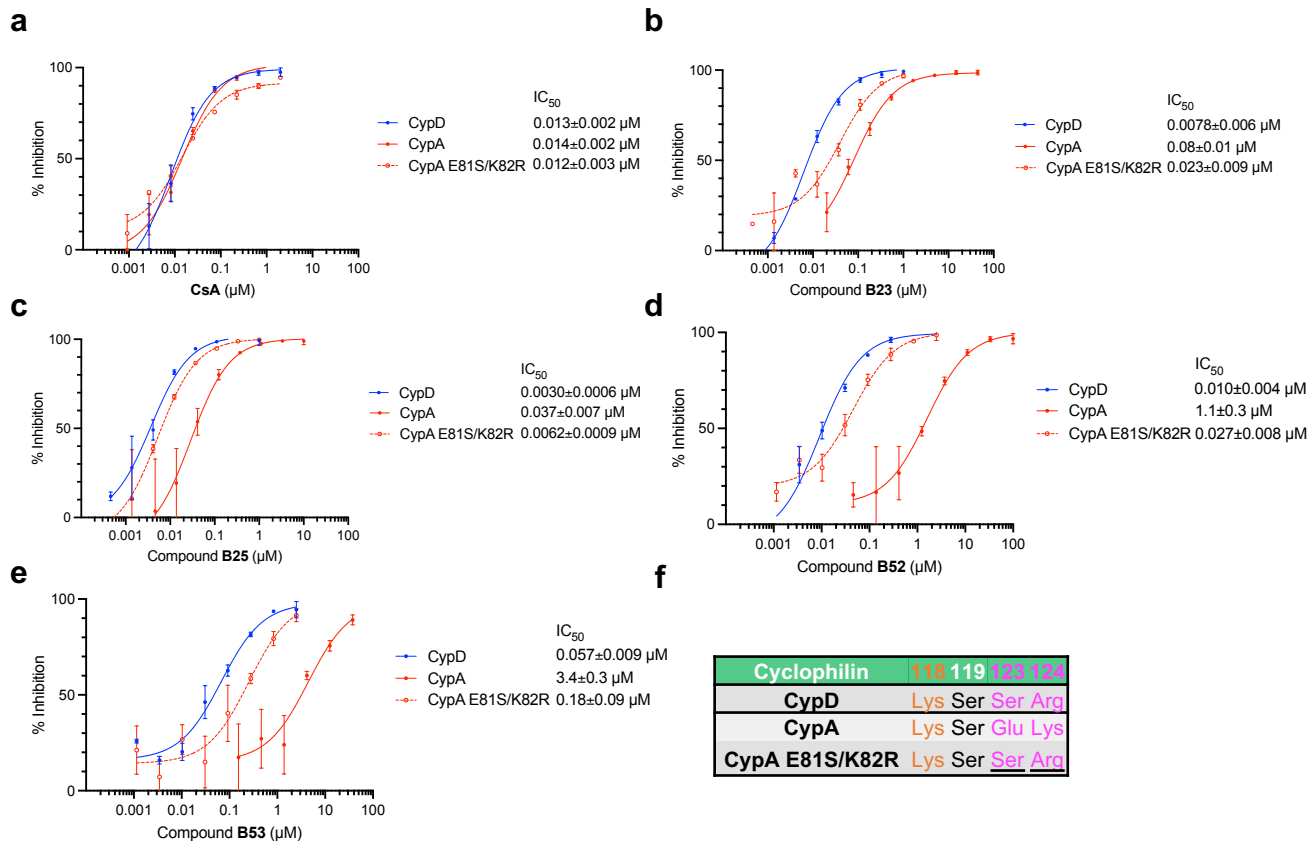


Supplementary Figure 18 | B23 derivatives that can simultaneously interact with CypD residues K118 and S119 and present a carboxylate near gatekeeper residues. Structure and cyclophilin inhibition dose response data for a, B51; b, B52; and c, B53. Nitrile derivatives that previously showed high potency but poor selectivity for CypD (Supplemental Fig. 12) were functionalized with a carboxylate, shown in B51. This change resulted in loss of potency, but similar selectivity profiles as B23. A large improvement in selectivity was observed when dicarboxylate groups were used. For both B52 and B53, one carboxylate is oriented to interact with K118 and S119, while the second carboxylate is directed towards the gatekeeper residue

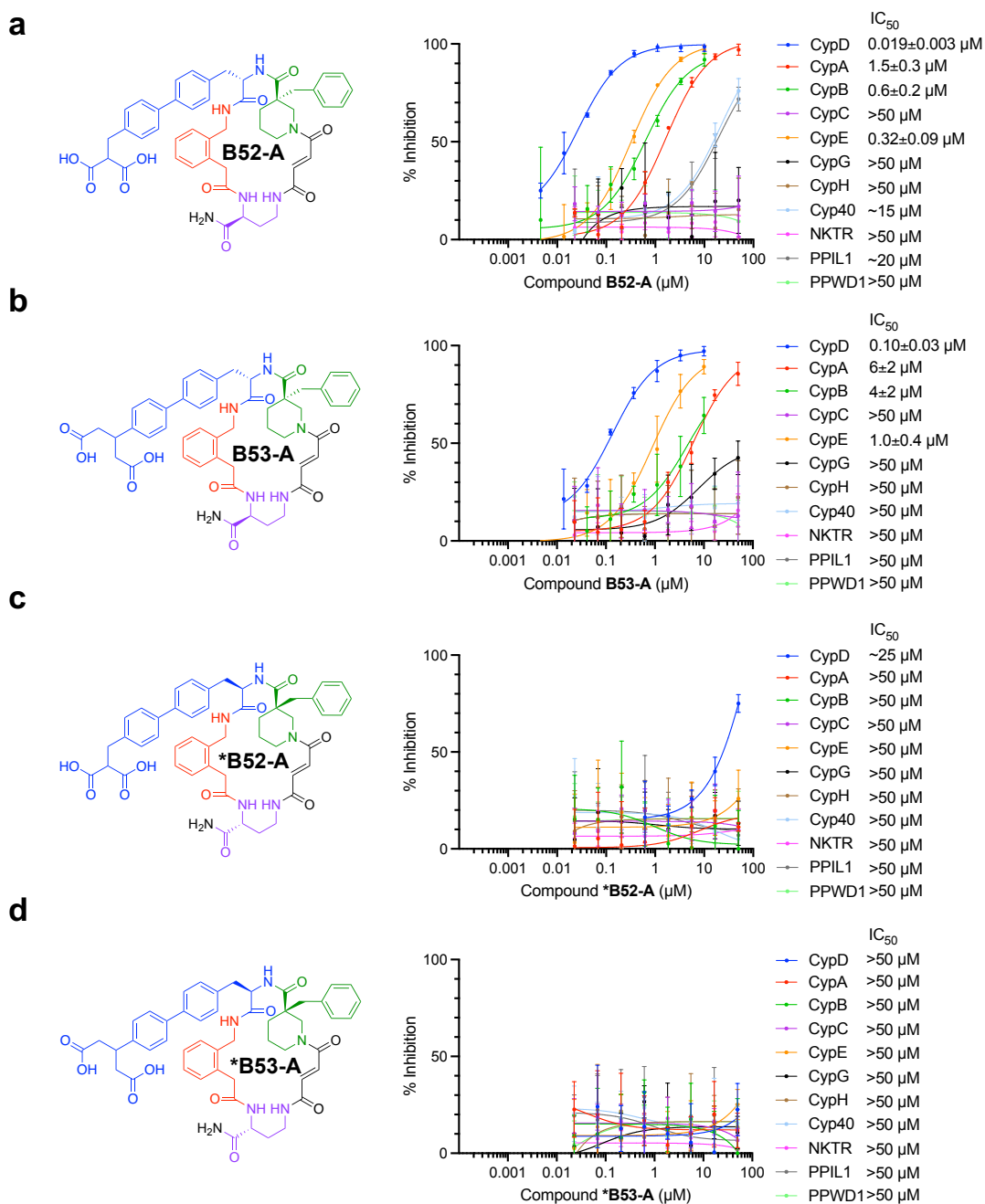
S123 of CypD (Fig. 4c). For **B52** and **B53**, four independent replicates (each comprising three technical replicates) are shown, with their respective fitted values that reflect mean \pm SEM of three technical replicates. Data points and error bars reflect mean \pm SD of individual assays at one dose. Tables show final reported IC₅₀ values that reflect mean \pm SD of four independent replicates, whose values are used for the entirety of this work. Independent replicate 1 was collected with a separately synthesized compound batch than independent replicates 2, 3, and 4. For **B51**, IC₅₀ values reflect mean \pm SEM of three technical replicates, with data points and error bars reflecting mean \pm SD of individual assays at one dose.



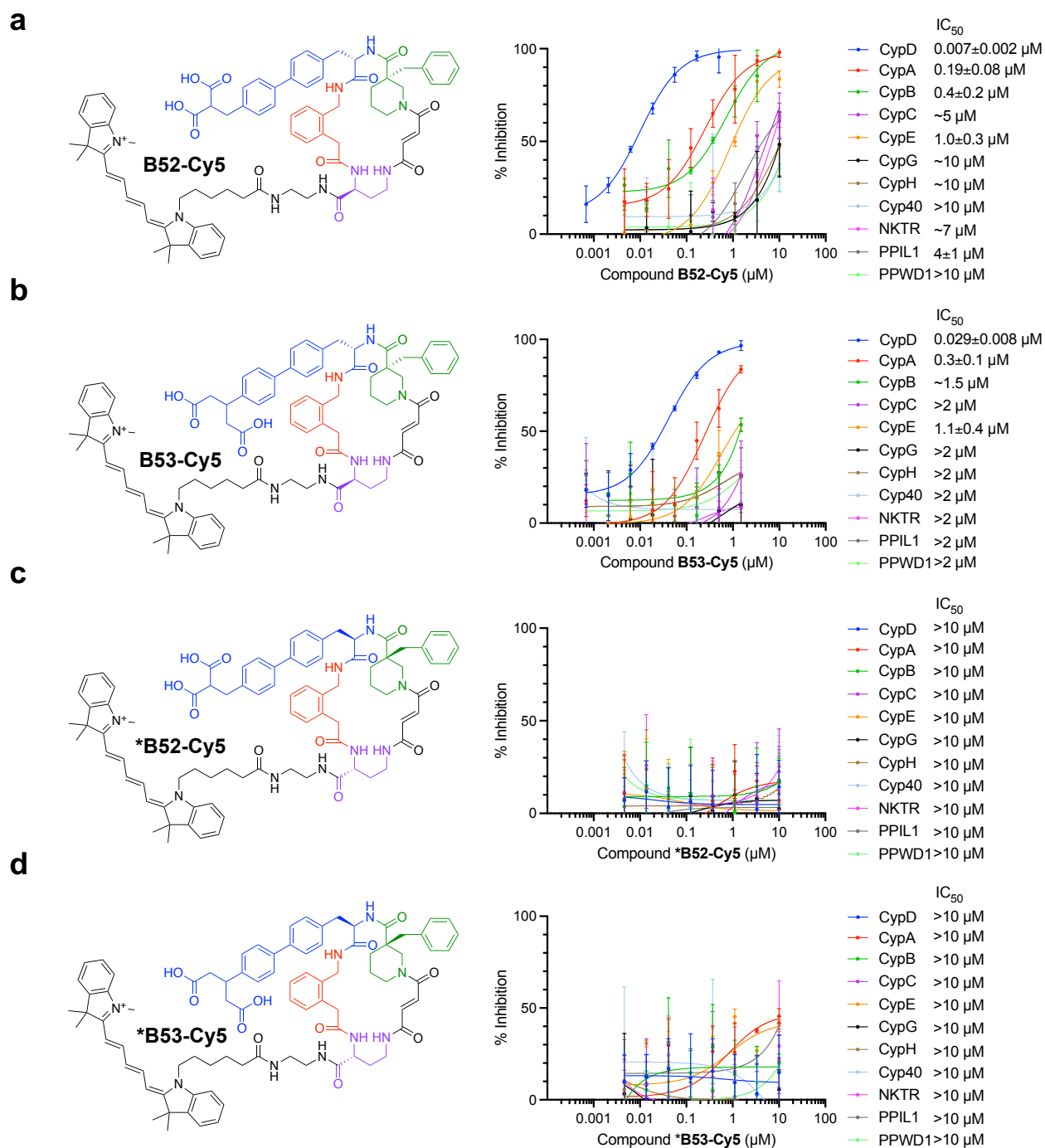
Supplementary Figure 19 | The CypB E121S gatekeeper mutant is inhibited more potently compared to wild-type CypB by carboxylate-containing inhibitors. Dose response curves of CypD, CypB, and CypB E121S, shown for **a**, **CsA**; **b**, **B23**; **c**, **B25**; **d**, **B52**; and **e**, **B53**. **f**, List of residues on the far side of the S2 pocket of cyclophilins that are proximal to ligand carboxylates, with the CypB mutation underlined. **CsA** as an active site ligand does not show appreciable differences in potency between wild-type cyclophilins and the tested cyclophilin mutants. For carboxylate-containing inhibitors, wild-type CypB shows attenuated potency compared to wild-type CypD. Carboxylate-containing compounds inhibit wild-type CypD and CypB E121S equipotently, as this CypB mutant contains S2 pocket residues that mimic those in CypD's S2 pocket. For wild-type CypD and CypB IC₅₀ data with **B52** and **B53**, values reflect mean±SD of four independent replicates (each comprising three technical replicates). Graphs show a representative single independent replicate (Independent replicate 1 is shown, containing three technical replicates) with data points and error bars reflecting mean±SD of individual assays at one dose. Further independent replicates are shown in Supplementary Fig. 18b-c. All other IC₅₀ values reflect mean±SEM of three technical replicates, with data points and error bars reflecting mean±SD of individual assays at one dose.



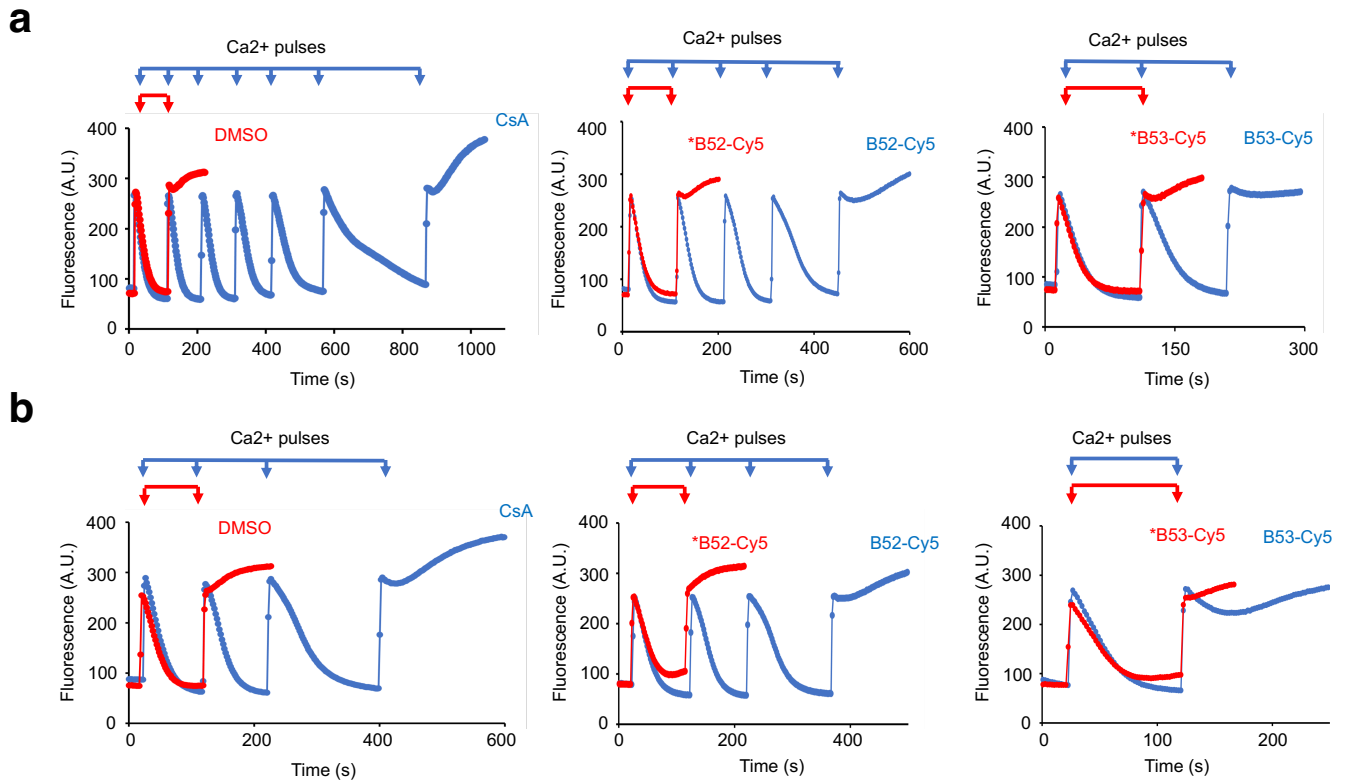
Supplementary Figure 20 | The CypA E81S/K82R gatekeeper mutant is inhibited more potently compared to wild-type CypA with carboxylate-containing inhibitors. Dose response curves of CypD, CypA, and CypA E81S/K82R, shown for a, CsA; b, B23; c, B25; d, B52; e, B53. f, List of residues on the far side of the S2 pocket of cyclophilins that are proximal to the ligand carboxylates, with CypA mutations underlined. CsA as an active site ligand does not show appreciable changes in potency between the wild-type cyclophilins and mutants. For carboxylate-containing inhibitors, wild-type CypA shows attenuated potency compared to wild-type CypD. Carboxylate-containing compounds inhibit wild-type CypD and CypA E81S/K82R equipotently, as this CypA mutant contains S2 pocket residues that mimic those in CypD's S2 pocket. For CypD and CypA wild-type IC₅₀ data with B52 and B53, values reflect mean±SD of four independent replicates (each comprising three technical replicates). Graphs show a representative single independent replicate (Independent replicate 1 shown, containing three technical replicates) with data points and error bars reflecting mean±SD of individual assays at one dose. Further independent replicates are shown in Supplementary Fig. 18b-c. All other IC₅₀ values reflect mean±SEM of three technical replicates, with data points and error bars reflecting mean±SD of individual assays at one dose.



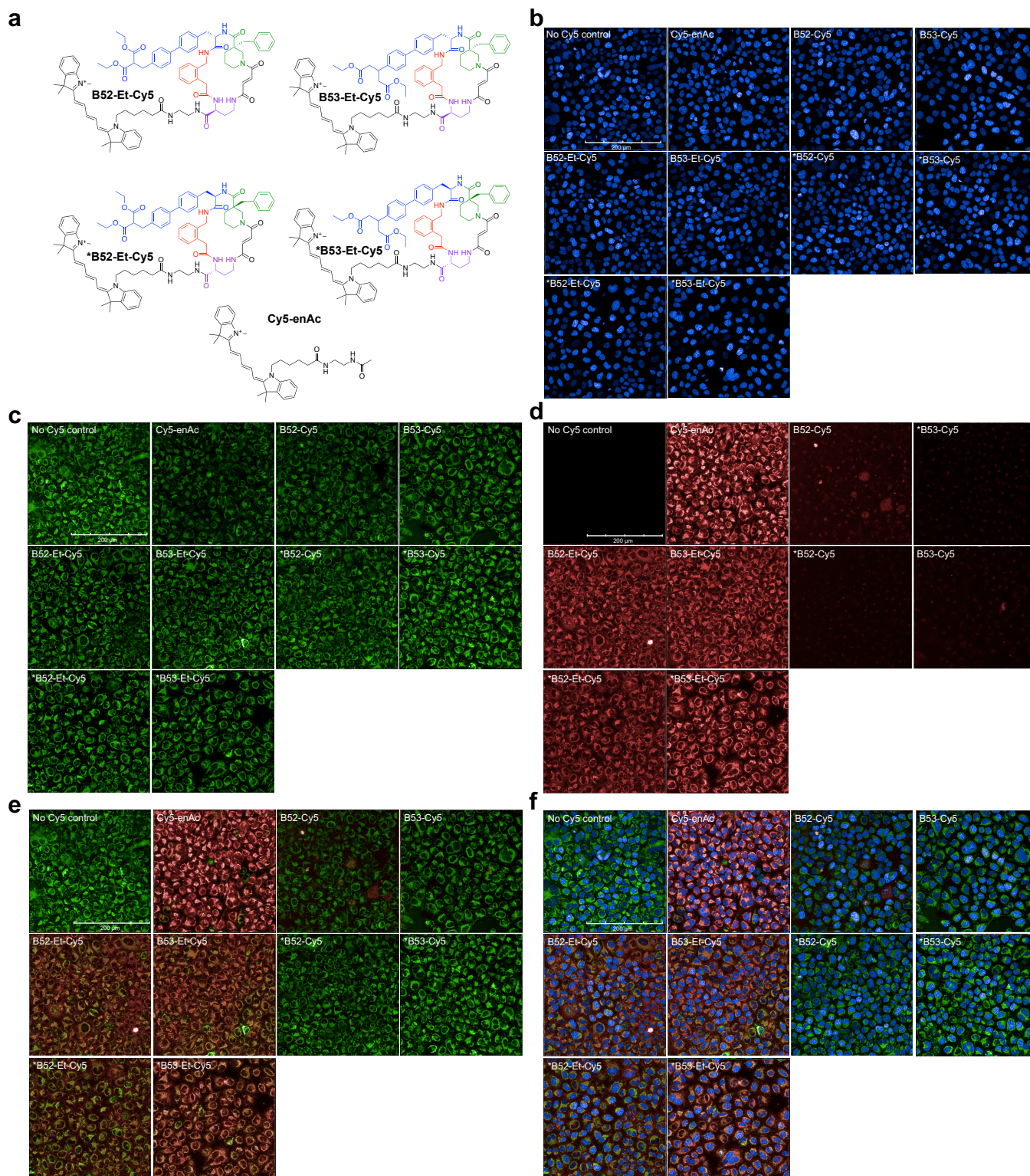
Supplementary Figure 21 | Prolyl isomerase inhibition of additional CypD-selective inhibitors. Structure and cyclophilin inhibition dose response data for **a**, **B52-A**; **b**, **B53-A**; **c**, ***B52-A**; and **d**, ***B53-A**. **B52-A** and **B53-A** retain the same selectivity profile as their associated analogs **B52** and **B53**, respectively, with a 2- to 3-fold decrease in potency. Enantiomers ***B52-A** and ***B53-A** show no substantial inhibition activity on any cyclophilins tested. IC₅₀ values reflect mean±SEM of three technical replicates. Data points and error bars reflect mean±SD of individual assays at one dose.



Supplementary Figure 22 | Prolyl isomerase inhibition by CypD-selective inhibitors used in mitochondrial models of mPTP. Structure and cyclophilin inhibition dose response data for **a**, B52-Cy5; **b**, B53-Cy5; **c**, *B52-Cy5; and **d**, *B53-Cy5. B52-Cy5 and B53-Cy5 retain the same selectivity profile as their associated analogs, B52 and B53, respectively. Enantiomers *B52-Cy5 and *B53-Cy5 show no substantial inhibition profile on any cyclophilins tested. IC₅₀ values reflect mean±SEM of three technical replicates. Data points and error bars reflect mean±SD of individual assays at one dose.

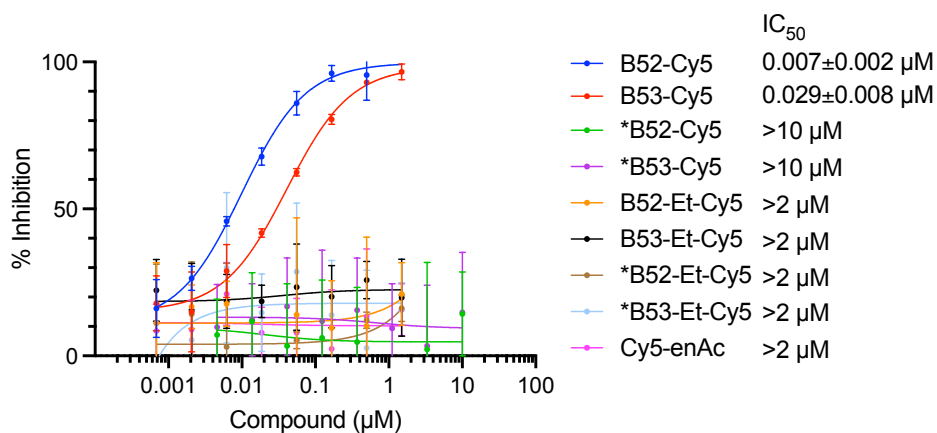


Supplementary Figure 23 | Additional independent replicates of calcium retention assays in mitochondria. The calcium retention capacity was determined in additional preparations of isolated mouse liver mitochondria (0.5 $\mu\text{g}/\text{mL}$) in response to pulses of 60 μM CaCl_2 in the presence of the indicated CypD inhibitors (or inactive enantiomers). Concentrations used were 2 μM **CsA**, 10 μM **B52-Cy5**, 10 μM ***B52-Cy5**, 20 μM **B53-Cy5**, and 20 μM ***B53-Cy5**. Mitochondrial uptake of extra-mitochondrial Ca^{2+} was assessed by monitoring the fluorescence of Calcium-green 5n, depicted in arbitrary units (A.U.). The rapid increase in fluorescence after several pulses of Ca^{2+} are taken up corresponds to mitochondrial Ca^{2+} release via mPTP. **a** All assays performed on the same mitochondrial preparation and day. **b**, All assays performed on a different mitochondrial preparation and day.

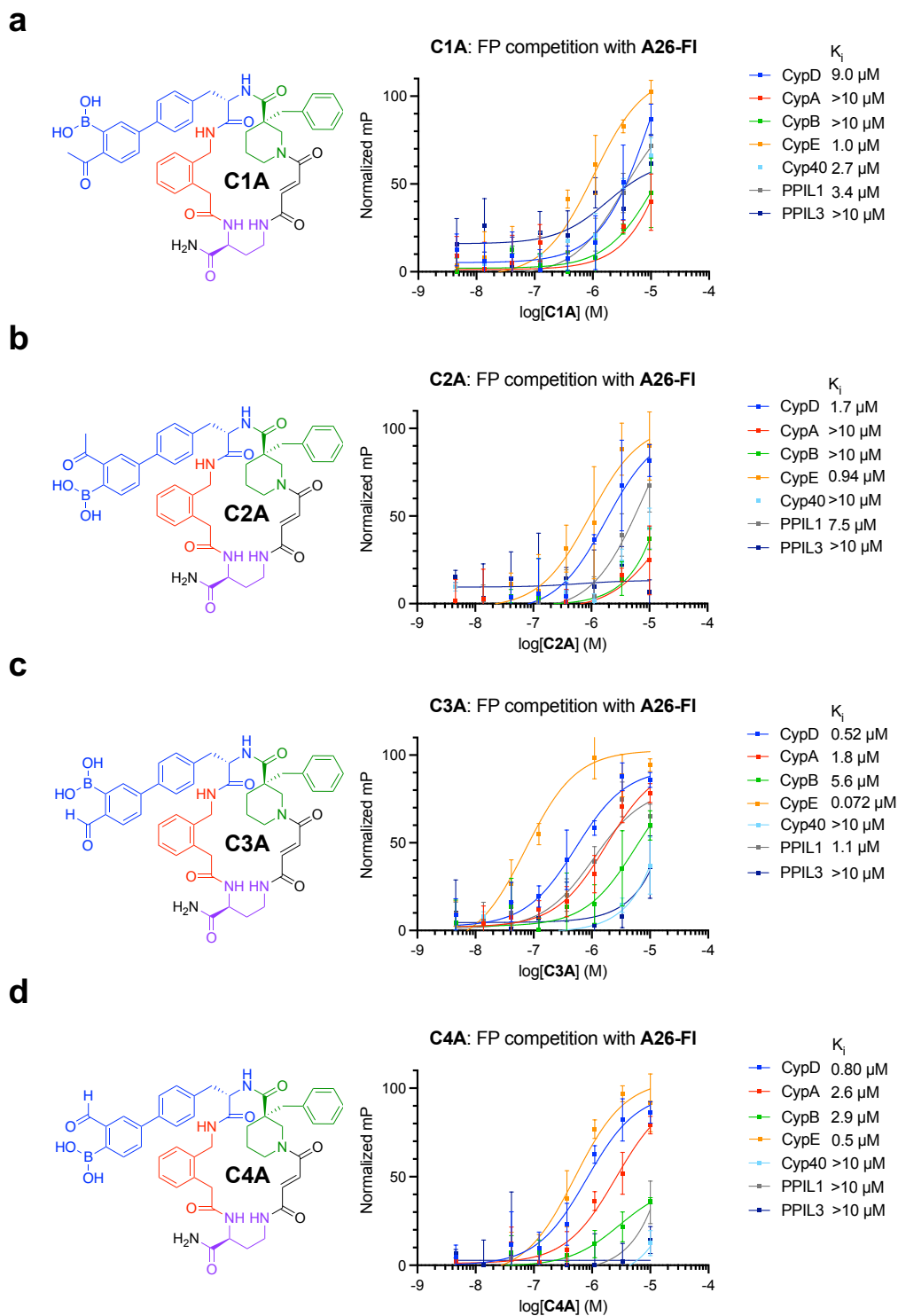


Supplementary Figure 24 | Representative images of Cy5-conjugated CypD inhibitor localization in HeLa cells. HeLa cells were co-treated with Cy5 conjugated compounds shown in (a) and Supplemental Fig. 22, and co-stained with Mitotracker Green, Hoechst 33342 and imaged by fluorescence microscopy. Images include the following channels; **b**, Hoechst 33342 nuclear stain; **c**, Mitotracker Green mitochondrial stain; **d**, Deep red channel showing Cy5-

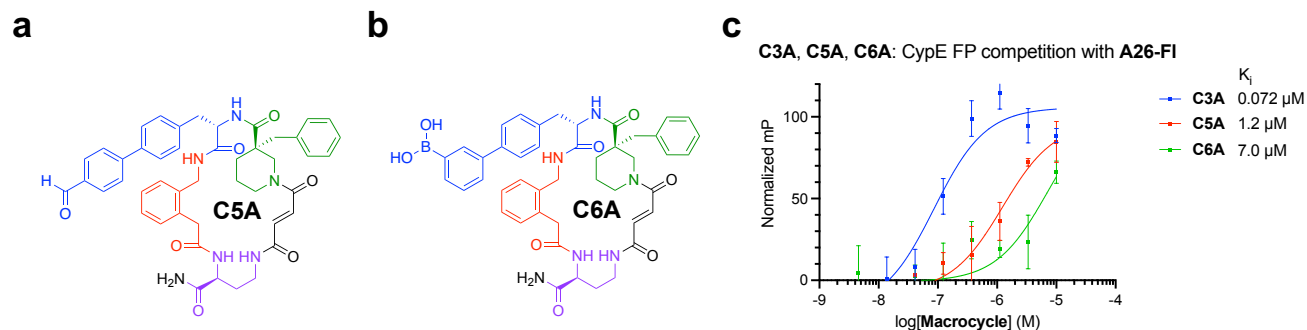
conjugated compound; **e**, overlay of Mitotracker Green and Cy5 channels; **f**, overlay of Hoechst 33342, Mitotracker Green, and Cy5 channels. **Cy5-enAc** (and ester derivatives **B52-Et-Cy5**, **B53-Et-Cy5**, ***B52-Et-Cy5**, and ***B53-Et-Cy5** show both good mitochondrial localization via overlap with Mitotracker Green and sufficient mitochondrial fluorescence. In contrast, dicarboxylate derivatives **B52-Cy5**, **B53-Cy5**, ***B52-Cy5**, and ***B53-Cy5** show poor mitochondrial localization and fluorescence. Microscopy images shown are a representative image of three technical replicates. Scale bars, 200 μm .



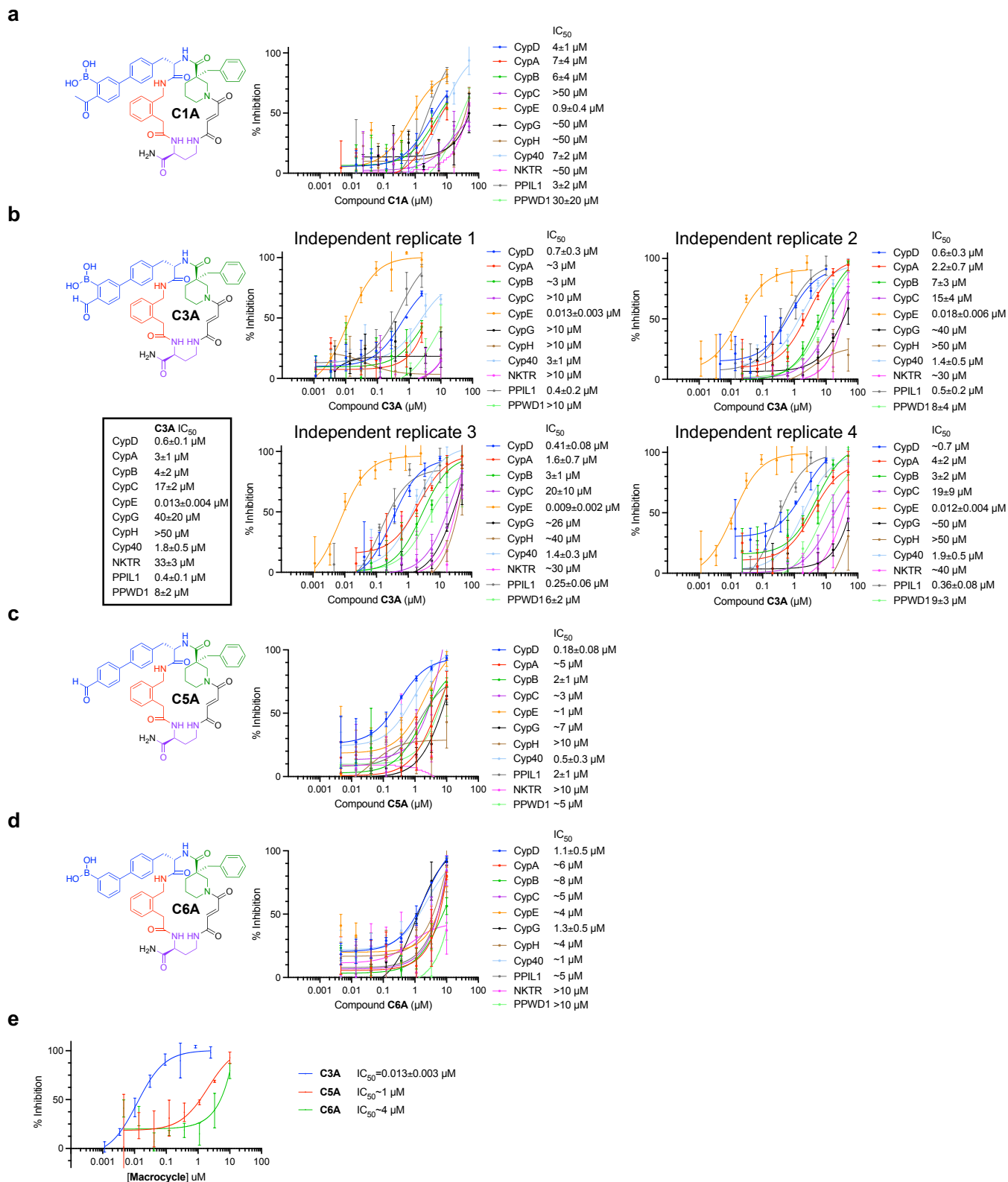
Supplementary Figure 25 | CypD inhibition of Cy5-conjugated CypD inhibitors. CypD prolyl-isomerase inhibition of Cy5-conjugated compounds is shown. Only compounds with correct stereochemistry and exposed dicarboxylate moieties are potent CypD inhibitors. **Cy5-enAc** alone does not inhibit CypD. IC₅₀ values reflect mean ± SEM of three technical replicates. Data points and error bars reflect mean ± SD of individual assays at one dose.



Supplementary Figure 26 | Fluorescence polarization competition with A26-FI against lysine-containing cyclophilins. Structure and FP competition with 0.5 nM A26-FI dose response data for **a**, C1A; **b**, C2A; **c**, C3A; and **d**, C4A. C3A shows selectivity for CypE, while regioisomer C4A and acetyl derivatives C1A and C2A show attenuated binding to CypE. Y-axes are normalized to internal control wells containing A26-FI only (100%) and A26-FI with cyclophilin (0%). Data points and error bars reflect mean \pm SD of three technical replicates. K_i values reflect the mean of three technical replicates.



Supplementary Figure 27 | Fluorescence polarization competition with A26-FI against CypE with control compounds C5A and C6A. Structures of compounds **a**, **C5A**; and **b**, **C6A**. **c**, Dose response of **C3A**, **C5A**, and **C6A** against CypE. Removal of either the aldehyde or boronic acid from **C3A** results in attenuated inhibition of CypE. Y-axes are normalized to internal control wells containing **A26-FI** only (100%) and **A26-FI** with cyclophilin (0%). Data points and error bars reflect mean \pm SD of three technical replicates. K_i values reflect mean of three technical replicates.

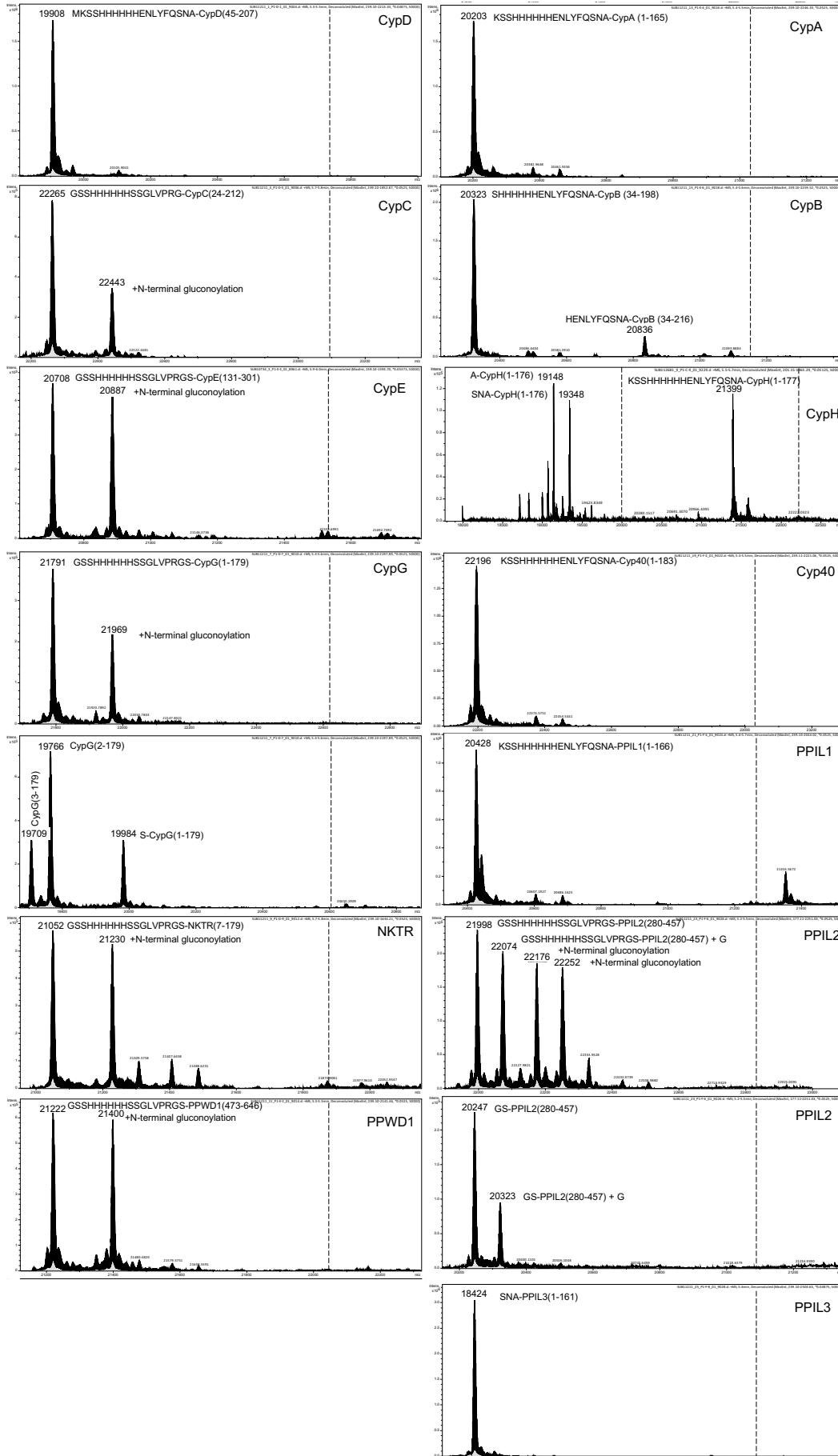


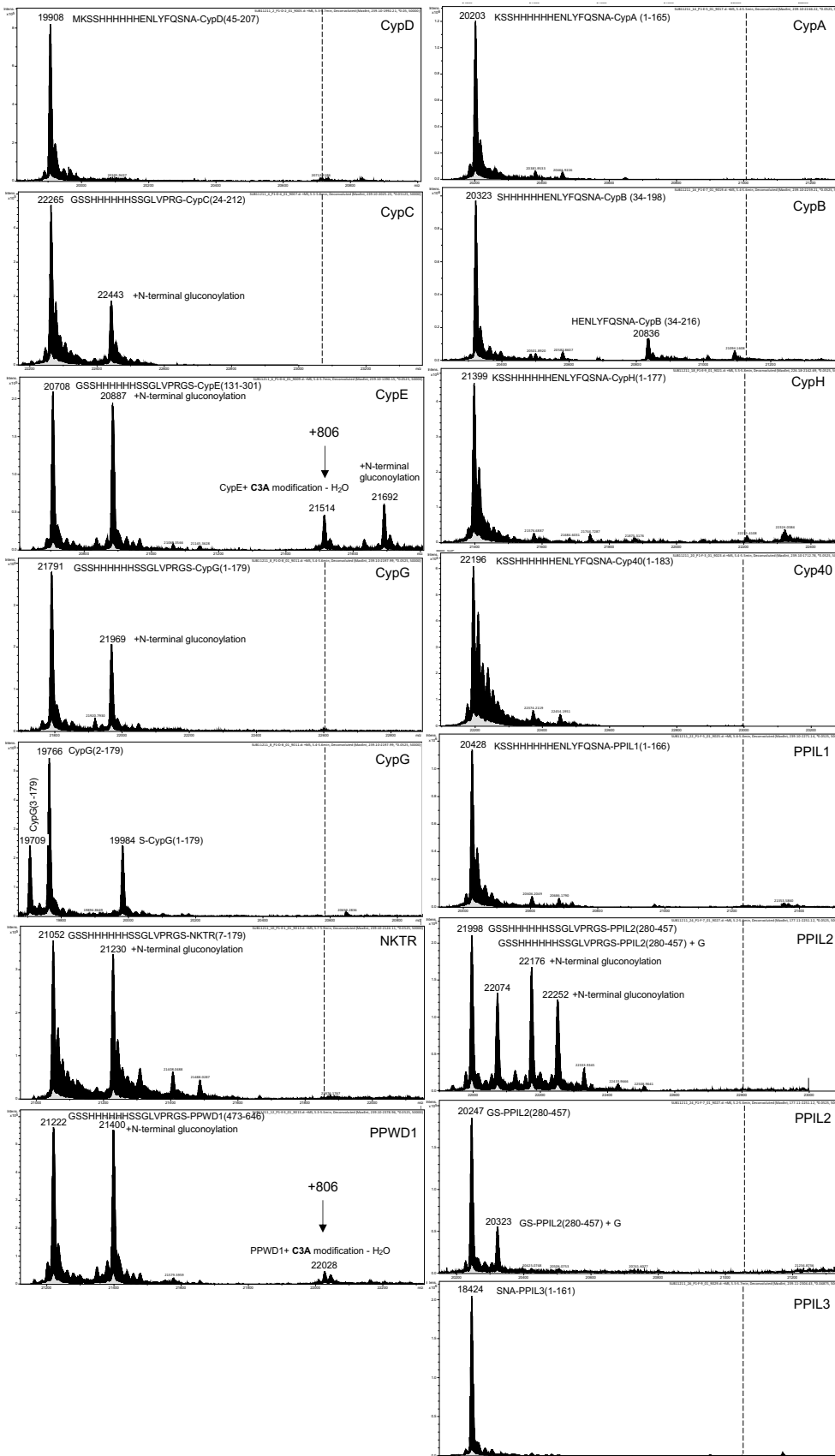
Supplementary Figure 28 | Prolyl isomerase inhibition by C1A, C3A, C5A, and C6A.

Structure and cyclophilin inhibition dose response data for **a**, C1A; **b**, C3A; **c**, C5A; and **d**, C6A.

C3A shows good selectivity and potency for CypE, while retaining only the aldehyde in C4A or the boronic acid in C5A results in loss in CypE potency and promiscuous cyclophilin inhibition.

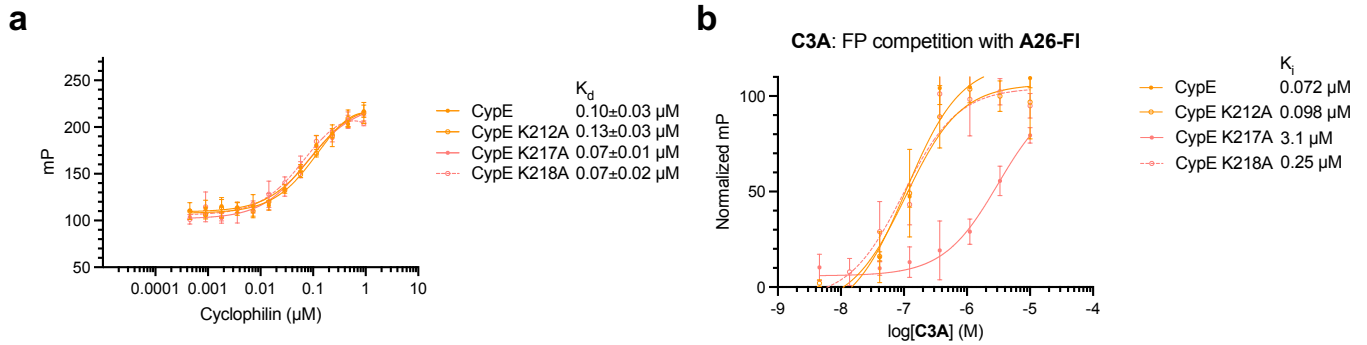
Replacing the aldehyde with an acetyl group in **C1A** also results in loss of potency and selectivity for CypE. **e**, Dose response curves of **C3A**, **C4A**, and **C5A** against CypE, showing the necessity of both parts of the covalent warhead for CypE potency. For **C3A**, four independent replicates (each comprising three technical replicates) are shown, with their respective fitted values that reflect mean \pm SEM of three technical replicates. Data points and error bars reflect mean \pm SD of individual assays at one dose. Table shows final reported IC₅₀ values that reflect mean \pm SD of four independent replicates for CypD, CypA, CypB, CypE, Cyp40 and PPIL1, and mean \pm SD of three independent replicates (Independent replicates 2-4) for CypC, CypG, CypH, NKTR, and PPWD1. Table IC₅₀ values are used for the entirety of this work. Independent replicate 1 was collected with a separately synthesized compound batch than was used in independent replicates 2, 3, and 4.

a

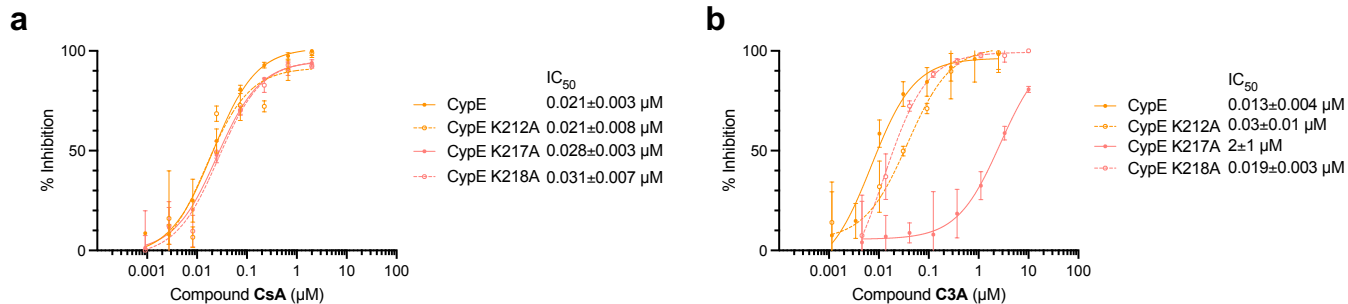
b

Supplementary Figure 29 | Mass spectroscopy analysis of C3A covalent modification on 13 cyclophilins. a, Mass spectroscopy analysis of lysine covalent modification and b, after

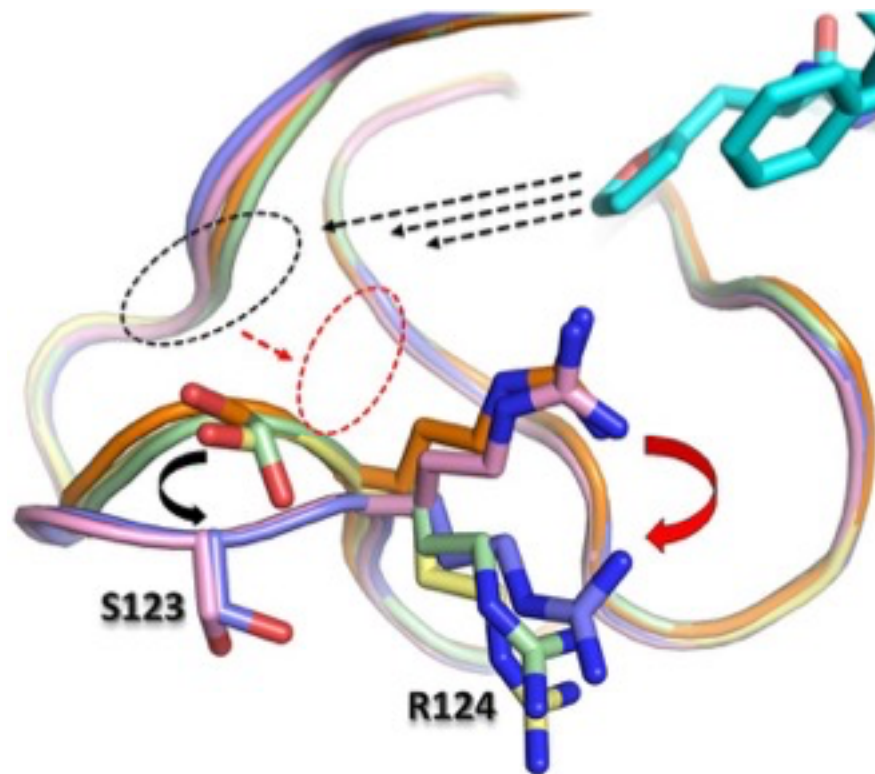
treatment with NaCNBH₃ to trap iminoboronate as lysine-modified secondary amine, highlighting relevant m/z regions. Primary protein peaks are shown along with expected region of **C3A** modification (+824: **C3A** modification non-reductive, represented as a dashed line for the most abundant ion peak(s) in panel **a**, +806: **C3A** –H₂O reductive amination covalent adduct, represented as a dashed line on cyclophilins with no observed covalent modification for the most abundant ion peak in panel **b**). We observed small amounts of covalent modification for PPWD1, however with a diminished peak intensity compared to CypE's +806 covalent adduct, suggesting minimal adduct formation in solution. We observed some C-terminal truncation for CypB of residues that are not anticipated to affect active site or S2 pocket integrity, prolyl-isomerase catalytic activity, or inhibitor binding. We also observed a mixture of CypH, CypG and PPIL2 constructs that include various cleaved and non-cleaved His-tag forms, with representative mass spectra shown for each primary peak. N-terminal His-tag or cleaved cyclophilin constructs are not anticipated to affect active site or S2 pocket integrity, prolyl-isomerase catalytic activity, or inhibitor binding. Various recombinantly expressed constructs show N-terminal gluconoylation. Some proteins when co-treated with NaCNBH₃ showed +14 mass off the primary peak not present in non-reductive conditions (see CypC, CypH, NKTR, Cyp40, and PPIL1) suggesting various methylation events via reductive amination.



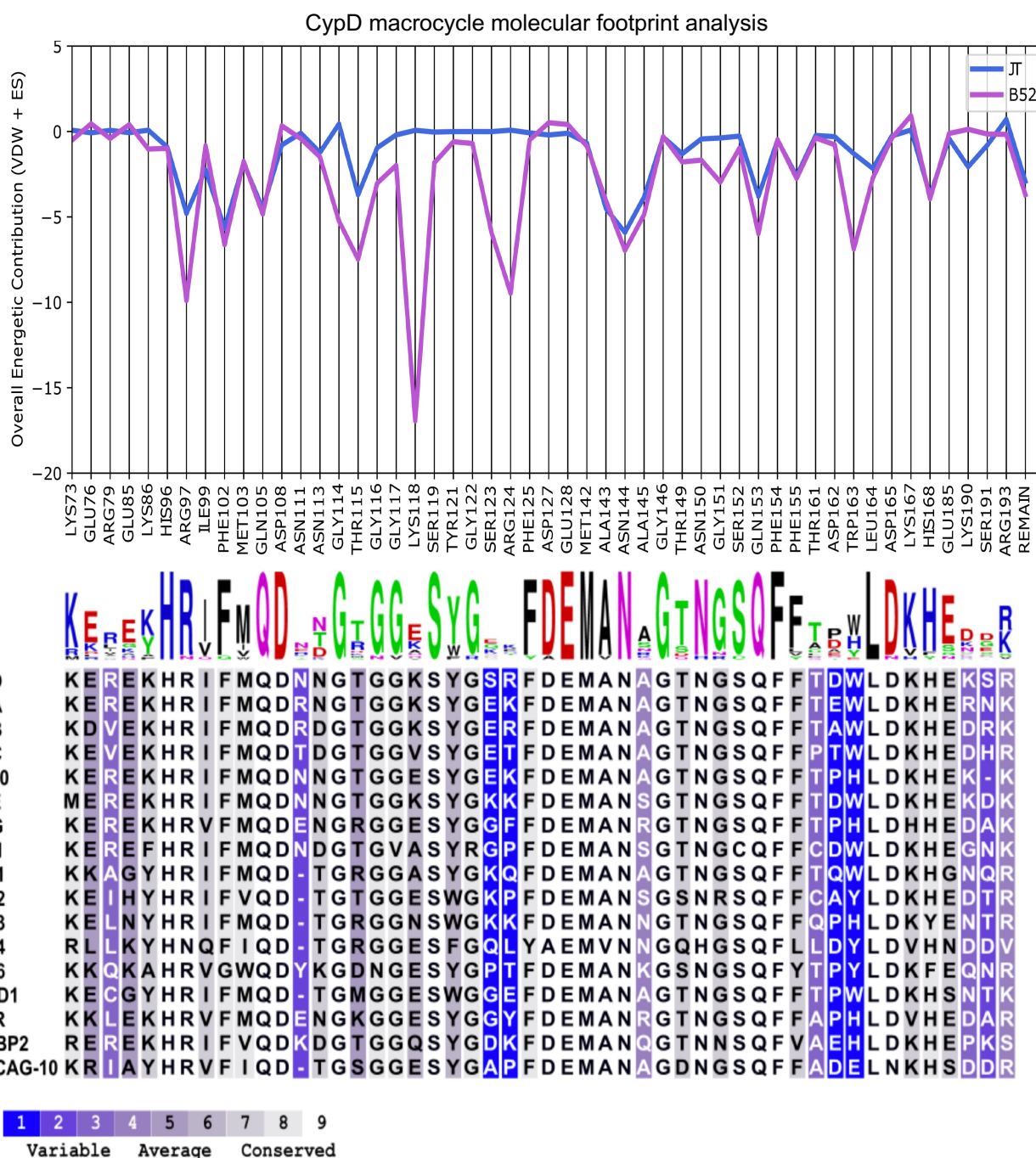
Supplementary Figure 30 | CypE mutant FP analysis. a, Protein titration against 0.5 nM **A26-FI**. K_d values and error bars reflect mean \pm SEM of three technical replicates. Data points and error bars reflect SD of individual assays at one dose. **b**, FP competition with 0.5 nM **A26-FI** dose response data **C3A** CypE proteins. **C3A** has significantly attenuated binding for only the K217A mutant compared to wild-type. Y-axes are normalized to internal control wells containing **A26-FI** only (100%) and **A26-FI** with cyclophilin (0%). Data points and error bars reflect mean \pm SD of three technical replicates. K_i values reflect the mean of three technical replicates.



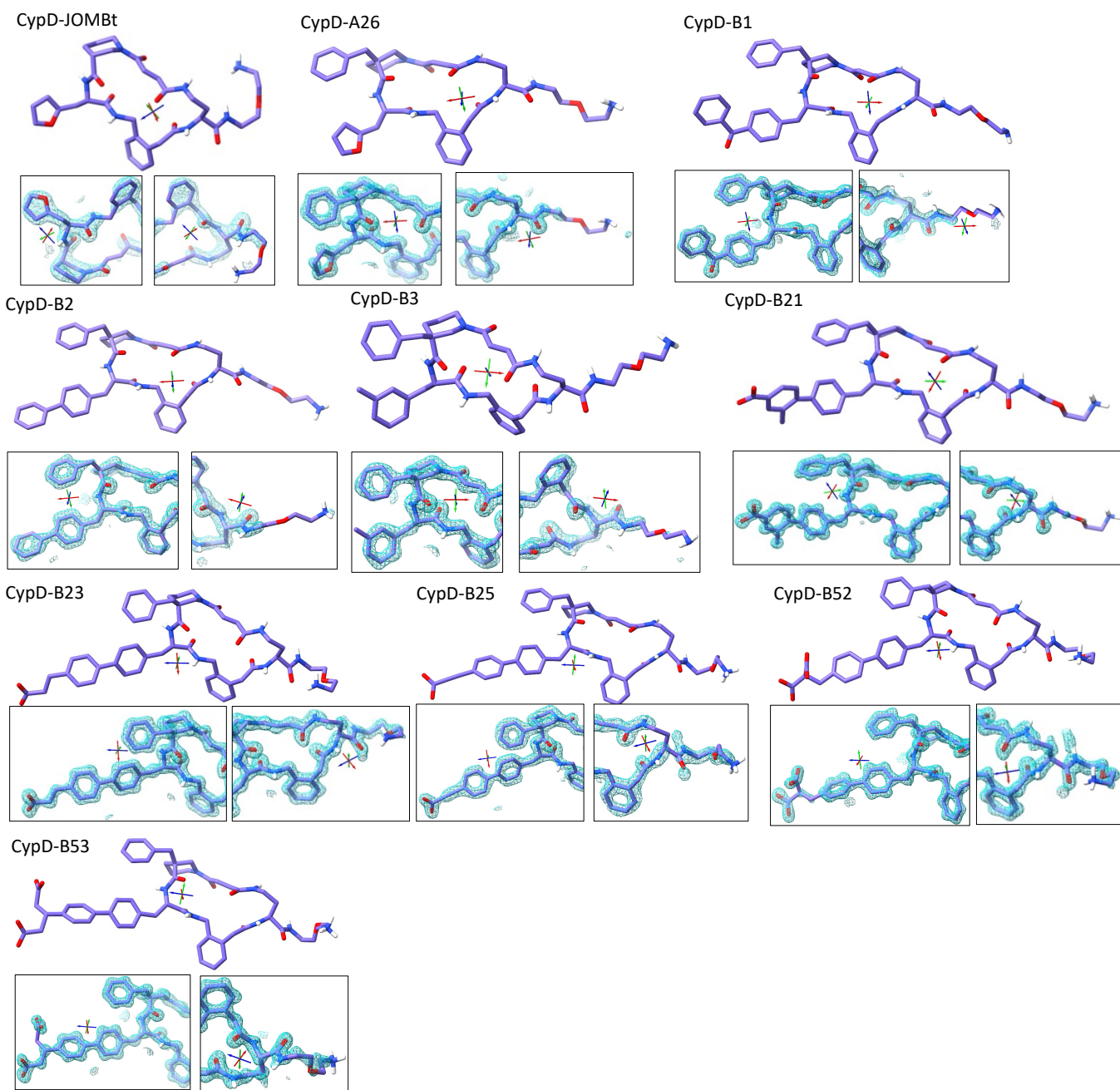
Supplementary Figure 31 | Prolyl isomerase inhibition screening of CypE lysine mutants reveals K217 residue as site of C3A covalent modification. Dose response curves of CypD, CypE K212A, CypE K217A, and CypE K218A shown for **a**, **CsA** and **b**, **C3A**. **CsA** as an active site ligand does not show appreciable differences in potency between wild-type CypE and the tested CypE mutants. Loss of **C3A** inhibition potency for only the K217A mutant compared to wild-type or K212A and K218A mutants verifies that K217 is the being covalently modified by **C3A**. For wild-type CypE IC₅₀ data with **C3A**, values reflect mean±SD of four independent replicates (each comprising three technical replicates). Graphs show a representative single independent replicate (Independent replicate 3 is shown, containing three technical replicates) with data points and error bars reflecting mean±SD of individual assays at one dose. Further independent replicates are shown in Supplementary Fig. 28b. All other IC₅₀ values reflect mean±SEM of three technical replicates, with data points and error bars reflecting mean±SD of individual assays at one dose.



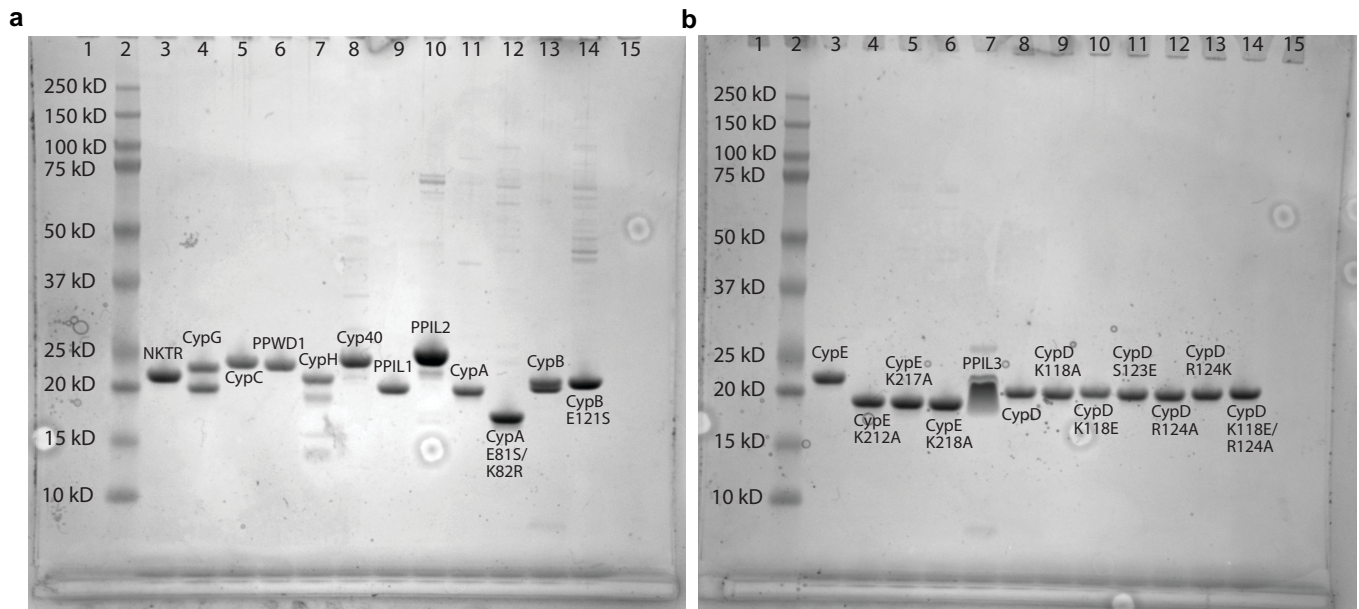
Supplementary Figure 32 | Ligand-dependent conformation of primary gatekeeper residues S123 and R124 in the S2 pocket. Superposition of co-crystal structures containing various inhibitors bound to CypD. **A26** co-crystal structure (orange) shown along with **A26** (cyan) as a reference for gatekeeper positions, shows little influence of ligand on residue conformation. Binding deeper into the S2 pocket (black arrows and circle) with larger carboxylate-containing ligands such as **B25** (pink) causes the S123 containing loop region to flip outwards of the pocket. Binding deeper and out of the pocket (red circles and arrows) causes the R124 residue to flip out of the pocket, shown by **B1** (green) and **B21** (yellow). Dicarboxylate-containing ligands such as **B53** (purple) exhibit conformational change of both the S123 loop as well as the side-chain of R124.



Supplementary Figure 33 | Molecular footprinting analysis demonstrates that key binding interactions of B52 are unique to CypD. Graph of the predicted overall energetic contribution (sum of Van der Waals and electrostatic energy) of the top fifty contributing residues in CypD to compounds **JOMBt** and **B52** aligned with a sequence alignment and web logo of all 17 human cyclophilins. Energetic contributions calculated using footprinting function in DOCK6.9. Coloring scheme of sequence alignment corresponds to sequence conservation score as calculated by the ConSurf webserver (<https://consurf.tau.ac.il/>). Note, this analysis shows R124 as a contributing residue for **B52** binding, in contrast to CypD mutant data, which suggested that this residue does not interact with **B52**. But we attribute this discrepancy to **B52**'s observed hydrogen bond with backbone atoms between S123 and R124, instead of side-chain moieties.



Supplementary Figure 34 | Electron densities of ligands from CypD-inhibitor co-crystal structures



Supplementary Figure 35 | SDS-PAGE of recombinantly expressed cyclophilin proteins.

a, The gel shows representative samples of the following:

Lane 1-Blank;

Lane-2: Protein Ladder;

Lane 3- GSSHHHHHHSSGLVPRGS-NKTR(7-179);

Lane 4-Mixture of GSSHHHHHHSSGLVPRGS-CypG(1-179), S-CypG(1-179), CypG(2-179), CypG(3-179), see Supplementary Figure 29 for confirmation of mixture;

Lane 5- GSSHHHHHHSSGLVPRG-CypC(24-212);

Lane 6- GSSHHHHHHSSGLVPRGS-PPWD1(473-646);

Lane 7- Mixture of KSSHHHHHHENLYFQSNA-CypH(1-177), A-CypH(1-176), and SNA-CypH(1-176), Supplementary Figure 29 for confirmation of mixture;

Lane 8-KSSHHHHHHENLYFQSNA-Cyp40(1-183);

Lane 9- KSSHHHHHHENLYFQSNA-PPIL1(1-166);

Lane 10- Mixture of GS-PPIL2(280-457), GSSHHHHHHSSGLVPRGS-PPIL2(280-457), GS-PPIL2(280-457) + G, and GSSHHHHHHSSGLVPRGS-PPIL2(280-457) + G, see Supplementary Figure 29 for confirmation of mixture

Lane 11- KSSHHHHHHENLYFQSNA-CypA (1-165);

Lane 12- SNA-CypA E81S/K82R (1-165);

Lane 13- Mixture of SHHHHHHHENLYFQSNA-CypB (34-198) and HENLYFQSNA-CypB (34-216); see Supplementary Figure 29 for confirmation of mixture

Lane 14- SNA-CypB E121S (34-216);

Lane 15-blank

b, The gel shows representative samples of the following:

Lane 1-Blank;

Lane-2: Protein Ladder;

Lane 3- GSSHHHHHHSSGLVPRGS-CypE(131-301);

Lane 4- GS-CypE K212A (131-301);

Lane 5- GS-CypE K217A (131-301);

Lane 6- GS-CypE K218A (131-301);

Lane 7- SNA-PPIL3(1-161);

Lane 8- MKSSHHHHHHENLYFQSNA-CypD(45-207);

Lane 9- MKSSHHHHHHENLYFQSNA-CypD K118A (45-207);
Lane 10- MKSSHHHHHHENLYFQSNA-CypD K118E (45-207);
Lane 11- MKSSHHHHHHENLYFQSNA-CypD S123E (45-207);
Lane 12- MKSSHHHHHHENLYFQSNA-CypD R124A (45-207);
Lane 13- MKSSHHHHHHENLYFQSNA-CypD R124K (45-207);
Lane 14- MKSSHHHHHHENLYFQSNA-CypD K118E/R124A (45-207);
Lane 15-blank.

All wild-type recombinant proteins were also verified by LC-MS through experiments conducted in Supplemental Figure 29.

Supplementary Note 1

Python Scripts

Analysis of CypD selection high-throughput sequencing data

a few notes about this code:

- * assumes your files fastq files are all unzipped (not fastq.gz's) and in the same folder
- * set your filepath and directory of this folder below
- * assumes filenames follow the form 'proteinName_L001_R1_001.fastq' (MiSeq output format).
- * the 'S#' indices (e.g. S1) should be mapped to whatever variable bases are in the primer in a separate .csv (barcode keys.csv), saved in the same file as your fastq data (in the form ['S1' , 'TCACT']). these should be the first bases in each line of the sequence.
- * don't put underscores in the sample filename, it messes up the regex to do the offset mapping (e.g. use input-library instead of input_library)

```
""

import collections #for Counter
#import itertools
import glob #useful for getting all files in a directory
import os # for filepaths http://stackoverflow.com/questions/3964681/find-all-files-in-directory-with-extension-
txt-with-python
import re # for regex
import csv # for converting to/from csv
#import pandas # for dealing with arrays (calculating enrichments)

""

****CHANGE THE FILEPATH****

#first, find the sequence files, place filepath below
filepath = '---'
os.chdir(filepath) # sets the directory to look in

#dictionaries of anticodons
scaffolds={"TGGA": "A", "CAAC": "B", "TTAA": "C", "ACAA": "D",
"TGAG": "E", "TTCC": "F", "TATA": "G", "AAAT": "H",
"CTAC": "I", "TCTA": "J", "AAAC": "K", "AAAA": "L",
"CAAA": "M", "ACCT": "N", "TCCT": "O", "TTAC": "P",
"TAAT": "Q", "TAAC": "R", "AATC": "S", "CTAT": "T",
"TGAT": "U", "TTTT": "V", "CTTT": "W", "AATT": "X",
"TATC": "Y", "AACC": "Z", "TCAC": "UU", "CACA": "VV",
"CATT": "WW", "ACTT": "XX", "TATT": "YY", "TCTT": "ZZ"}

codons_1 = {"AAAGCC": "A", "AAGCCT": "B", "TTTGCC": "C", "GTTTCCT": "D",
"CATACG": "E", "CTCATG": "F", "TGTCTC": "G", "CTACAG": "H",
"CAGCTA": "I", "CTGAGA": "J", "AGCTCT": "K", "TGTTCCG": "L",
"AAGAGC": "M", "AGCAGA": "N", "GATCGA": "O", "TCAGTC": "P",
"TACTGC": "Q", "ATACGC": "R", "GATTCC": "S", "TGAAGC": "T"}
codons_2 = {"TTCAGC": "A", "ATCGAC": "B", "GCAATC": "C", "AAGTCC": "D",
"ATCCGT": "E", "ACTCGA": "F", "TCTTGC": "G", "CACAAG": "H",
"TTAGCC": "I", "AGTCCT": "J", "GCATGA": "K", "CAGACT": "L",
"TTCCAG": "M", "GGCAAT": "N", "TCGAGA": "O", "CTAAGG": "P",
"AGGCTA": "Q", "TCACTG": "R", "TTGCTC": "S", "AGCTTC": "T"}
codons_3 = {"TCCGAT": "A", "TGCACA": "B", "GAGTCT": "C", "CTGAAG": "D",
"TCGACT": "E", "CGTCAT": "F", "AGGTTG": "G", "TACGGA": "H",
"GTAAGC": "I", "CGTAGA": "J", "TGACAC": "K", "GTAGTG": "L",
"GTTTCAG": "M", "GACTAG": "N", "AAACCG": "O", "AATGGG": "P",
"AGAGAG": "Q", "CGGTAA": "R", "ACAGCA": "S", "ACAAGG": "T"}
```

```

# list of all codons, making a Counter object with all codons value 1 to compare enrichments
allcodons = []
for SKey in scaffolds.iterkeys():
    for key1 in codons_1.iterkeys():
        for key2 in codons_2.iterkeys():
            for key3 in codons_3.iterkeys():
                allcodons.append(codons_1[key1] + codons_2[key2] + codons_3[key3] + scaffolds[SKey])
allCodonCount = collections.Counter()
for codon in allcodons:
    allCodonCount[codon]+=1
writer = csv.writer(open('allcodons.csv', 'wb')) # adapted from
http://stackoverflow.com/questions/8685809/python-writing-a-dictionary-to-a-csv-file-with-one-line-for-every-key-
value
for barcode, count in allCodonCount.iteritems():
    writer.writerow([barcode, count])

#open the file of the selection to be analyzed. extract out the sequences.
allFiles = glob.glob('*.*fastq') # makes a list of all the fastq files in that directory
#print allFiles
# https://docs.python.org/2/library/csv.html#module-csv
#with open(filepath + 'barcode keys.csv', 'rU') as csvfile: # rU prevents the universal newline error
http://stackoverflow.com/questions/6726953/open-the-file-in-universal-newline-mode-using-csv-module-django
# keyDict = {}
# keys = csv.reader(csvfile, delimiter = ',')
# for row in keys:
# keyDict[row[0]] = row[1] # makes a dictionary for the offsets

summarycsv = csv.writer(open('sequencing summary.csv', 'wb')) # adapted from
http://stackoverflow.com/questions/8685809/python-writing-a-dictionary-to-a-csv-file-with-one-line-for-every-key-
value
summarycsv.writerow(['Selection', 'Total Reads', 'Valid Reads'])

for filename in allFiles:
    file = filepath + filename
    fasta = open(file) # opens the fasta file
    fastaList = fasta.readlines() # converts the file to a list http://stackoverflow.com/questions/328059/create-
a-list-that-contain-each-line-of-a-file
    seqList = fastaList[1::4] # gets every 4th line, the sequences

    """CHANGE THIS IF FILENAME FORMAT HAS CHANGED"""
    findIndices = re.search('(?!<=_.)*(?!=_L)', filename) # for MiSeq: get the selection indices, which are the first
strings between the underscores. adapted from http://stackoverflow.com/questions/15033905/regex-that-extracts-
text-between-tags-but-not-the-tags
    # findIndices = re.search('(?!<=_.)*(?!=_R1.fastq)', filename) # for NextSeq: get the selection indices, which are the
first strings between the underscores. adapted from http://stackoverflow.com/questions/15033905/regex-that-
extracts-text-between-tags-but-not-the-tags
    indices = findIndices.group(0) # yields S# (whatever the sequencing index is) from the filename

    validseqs = [] # list of valid sequences
    offset = ""
    # offset = keyDict[indices] # is there an offset in the first 0-5 bases?
    for seq in seqList:
        if offset == seq[0:len(offset)]: # if the first bases match the offset
            matchedSeq = re.search('GAGTGGGATG....TAG.....ATCAT.....AACTT.....GTGTACAGGG', seq) #changed to
be 4Ns for scaffold
            # regex that finds the library sequence within the sequences nucleotides
            if matchedSeq is not None: # if a matching sequence is found, add it
                template = matchedSeq.group(0) # this should only find one result in matchedSeq.group, hence the 0
index

```

```

#match sequences to codons
if template[10:14] in scaffolds.keys():    #check if all 4 codons are valid
    if template[17:23] in codons_1.keys():
        if template[28:34] in codons_2.keys():
            if template[39:45] in codons_3.keys():
                scaff = scaffolds[template[10:14]] #all 4 are valid, so start mapping
                A = codons_1[template[17:23]]
                B = codons_2[template[28:34]]
                C = codons_3[template[39:45]]
                decoded = A + B + C + scaff
                validseqs.append(decoded + '\n') #add this sequence to the list

"""**CHANGE THIS IF FILENAME FORMAT HAS CHANGED**"""
findProtein = re.search('.*(?!=_S)', filename) #find the protein name, similar logic as for the indices. same for
MiSeq and NextSeq
protein = findProtein.group(0)

#extractedFileName = indices + '_' + protein + '_decoded.txt'
#testSeqsExtracted = open(extractedFileName, 'w') #make a new file to write extracted sequences to
(https://docs.python.org/2/tutorial/inputoutput.html)
#testSeqsExtracted.writelines(validseqs)
print 'Selection ' + indices + ' (' + protein + ') has ' + str(len(validseqs)) + ' valid sequences out of ' +
str(len(seqList)) + ' reads.'
summarycsv.writerow([protein, str(len(seqList)), str(len(validseqs))])

#now looking through these decoded sequence files and counting them
seqCounts = collections.Counter()
for seq in validseqs:
    seqCounts[seq.rstrip()] +=1 #rstrip() to get rid of the newline \n to make keys match
#print 'done with counter'
totCount = seqCounts + allCodonCount #add one to each so that we have all codons represented, and don't
divide by 0.
for count in totCount.iteritems():
    #print type(count[1])
    #print len(validseqs)
    totCount[count[0]] = float(count[1])/float(len(validseqs)) #normalize to that selection

#print len(seqCounts.keys())
#print len(allCodonCount.keys())
#print len(totCount.keys())
counterFileName = indices + '_' + protein + '_seqCounts.csv'
#export to csv
writer = csv.writer(open(counterFileName, 'wb')) # adapted from
http://stackoverflow.com/questions/8685809/python-writing-a-dictionary-to-a-csv-file-with-one-line-for-every-key-value
# writer.writerow(['Sequence', 'Scaffold', 'A Codon', 'B Codon', 'C Codon', 'Raw Count']) #header row
for barcode, count in totCount.iteritems():
# writer.writerow([barcode, barcode[0:2], barcode[2:5], barcode[5:8], barcode[8:11], count]) #barcodes, split by
individual codon, and total count
    writer.writerow([barcode, count, seqCounts[barcode]])
#print 'done writing lines'

#dictionaries of REV codons
# scaffolds = {"4A":'TCCA', "4B":'GTTG', "4C":'TTAA', "4D":'TTGT', "4E":'CTCA',
# "4F":'GGAA', "4G":'TATA', "4H":'ATTT', "4I":'GTAG', "4J":'TAGA',
# "4K":'GTTT', "4L":'TTTT', "4M":'TTTG', "4N":'AGGT', "4O":'AGGA',
# "4P":'GTAA', "4Q":'ATTA', "4R":'GTTA', "4S":'GATT', "4T":'ATAG',

```

```

# "4U":'ATCA', "4V":'AAAA', "4W":'AAAG', "4X":'AATT', "4Y":'GATA',
# "4Z":'GGTT',"4UU":'GTGA',"4VV":'TGTG',"4WW":'AATG',"4XX":'AAGT',
# "4YY":'AATA',"4ZZ":'AAGA'}
# codons_1 = {"1A":'GGCTTT', "1B":'AGGCTT', "1C":'GCCAAA', "1D":'AGGAAC',
# "1E":'CGTATG', "1F":'CATGAG', "1G":'GAGACA', "1H":'CTGTAG',
# "1I":'TAGCTG', "1J":'TCTCAG', "1K":'AGAGCT', "1L":'CGAACA',
# "1M":'GCTCTT', "1N":'TCTGCT', "1O":'TCGATC', "1P":'GACTGA',
# "1Q":'GCAGTA', "1R":'GCGTAT', "1S":'GGAATC', "1T":'GCTTCA'}
# codons_2 = {"2A": 'GCTGAA', "2B": 'GTCGAT', "2C": 'GATTGC', "2D": 'GGACTT',
# "2E": 'ACGGAT', "2F": 'TCGAGT', "2G": 'GCAAGA', "2H": 'CTTGTG',
# "2I": 'GGCTAA', "2J": 'AGGACT', "2K": 'TCATGC', "2L": 'AGTCTG',
# "2M": 'CTGGAA', "2N": 'ATTGCC', "2O": 'TCTCGA', "2P": 'CCTTAG',
# "2Q": 'TAGCCT', "2R": 'CAGTGA', "2S": 'GAGCAA', "2T": 'GAAGCT'}
# codons_3 = {"3A": 'ATCGGA', "3B": 'TGTGCA', "3C": 'AGACTC', "3D": 'CTTCAG',
# "3E": 'AGTCGA', "3F": 'ATGACG', "3G": 'CAACCT', "3H": 'TCCGTA',
# "3I": 'GCTTAC', "3J": 'TCTACG', "3K": 'GTGTCA', "3L": 'CACTAC',
# "3M": 'CTGAAC', "3N": 'CTAGTC', "3O": 'CGGTTT', "3P": 'CCCATT',
# "3Q": 'CTCTCT', "3R": 'TTACCG', "3S": 'TGCTGT', "3T": 'CCTTGT'}

```

Calculating enrichment values of library members

this code will calculate enrichments. Put all of the *seqCounts.csv files from the other code into a new folder.

Set the input lib and file path

updated 10/24/2016 for ULib notation (ABCXX)

updated regenerated library input 11/8/2017

"""

```

import glob
import csv
import os
import re

```

#first, find the sequence files

filepath = '----' #insert filepath for selection sequencing reads (from sequencing script)

os.chdir(filepath) # sets the directory to look in

inputLibFile = '---' #set the filepath for the input library

with open(filepath + inputLibFile,'rU') as csvfile:

```
inputDict = {}
```

```
keys = csv.reader(csvfile, delimiter = ',')
```

```
for row in keys:
```

```
inputDict[row[0]] = [row[1],row[2]] # makes a dictionary for the input enrichments
```

"""change input text string if not input"""

```
allFiles = [i for i in glob.glob("*.csv") if 'seqCounts' in i and 'reg_lib' not in i]
```

makes a list of all the seq Counts files in that directory except for the input lib

#print allFiles

for file in allFiles:

```
with open(filepath + file,'rU') as csvfile:
```

```
selectDict = {}
```

```
keys = csv.reader(csvfile, delimiter = ',')
```

```
for row in keys:
```

```
selectDict[row[0]] = [row[1],row[2]] # makes a dictionary for the {barcode: selection enrichments, seq counts}
```

```
enrichCalc = {}
```

```
for key in selectDict.keys():
```



```

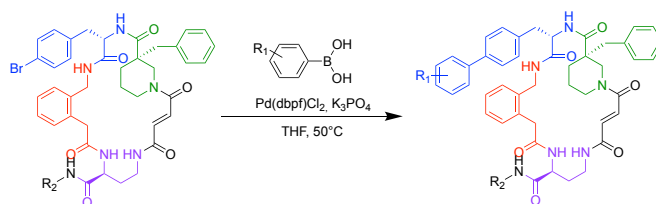
    enrichCalc[key] = float(selectDict[key][0])/float(inputDict[key][0])
# print file
# findIndices = re.search('.*?(?=_)',file) # get the selection indices. .*? is non-greedy
# indices = findIndices.group(0) # yields A-1, or whatever the sequencing index is, from the filename

findProtein = re.search('(?!<=[0-9]_).*?(?=_seqCounts)', file) #find the protein name, similar logic as for the indices
protein = findProtein.group(0)

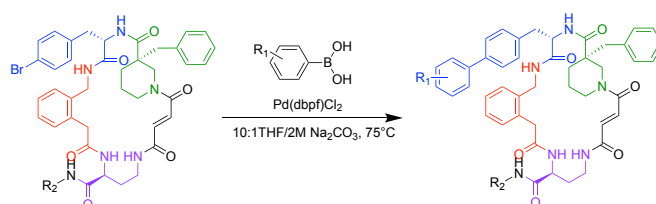
counterFileName = protein + '_enrichment_vs_input.csv'
writer = csv.writer(open(counterFileName, 'wb')) # adapted from
http://stackoverflow.com/questions/8685809/python-writing-a-dictionary-to-a-csv-file-with-one-line-for-every-key-value
writer.writerow(['Sequence', 'A Codon', 'B Codon', 'C Codon', 'Scaffold', 'Raw Selection Freq', 'Raw Selection
Count', 'Pre-enrich Freq', 'Pre-enrich Count', 'Enrichment']) #header row
for barcode, enrich in enrichCalc.iteritems():
    writer.writerow([barcode, barcode[0], barcode[1], barcode[2], barcode[3:],
        selectDict[barcode][0], selectDict[barcode][1], inputDict[barcode][0], inputDict[barcode][1], enrich]) #barcodes,
split by individual codon, and total count

```

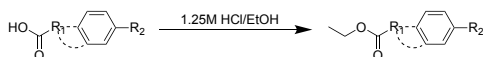

For both *cis* and *trans* isomer, final macrocyclization was afforded by treating resin with pentafluorophenyl diphenylphosphinate (5 eq), anhydrous DIPEA (10 eq) dissolved in ~10 mL anhydrous DMF for 3-16 hours. Resin was then washed three times with DMF, three times with CH₂Cl₂ and allowed to dry in the fume hood. Macrocycle product was then cleaved off resin with two treatments of ~15 mL solution containing 95% trifluoroacetic acid (TFA), 2.5% triisopropylsilane (TIPS) and 2.5% water. Macrocycles sensitive to hydrosilane reduction were cleaved without TIPS. Resin was then washed two times with TFA. Combined supernatants were then dried to an oily residue through rotary evaporation. The peptide was precipitated out of solution with Et₂O cooled to -78°C. Ether was then decanted and isolated precipitate was dissolved in a minimal amount of 3:1 DMF/water, and filtered through 0.22 μL Ultrafree-MC Centrifugal Filters (Millipore Sigma). For hydrophobic macrocycles, no ether precipitation was conducted and sample was directly dissolved in 3:1 DMF/water. Sample was then purified by reverse phase HPLC, with a gradient of 10-60% acetonitrile/water containing 0.1% TFA over 40 minutes. Fractions that contained product was then freeze dried to produce a white powder. Yields for reported macrocycles varied from 1-10% of the initial resin loading.



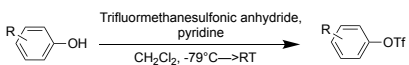
Generalized procedure A for Suzuki-Miyaura cross-coupling of macrocycles: Adapting conditions described previously², into a 10 mL screw-top vial, bromo-macrocycle (0.011 mmol, 1.0 eq), boronic acid (0.11 mmol, 10 eq), [1,1'-Bis(di-*tert*-butylphosphino)ferrocene]dichloropalladium (II) (0.0002 mmol, 0.2 eq), and potassium phosphate tribasic (0.23 mmol, 20 eq) was combined and sealed with a septum. Flask was evacuated and refilled with N₂ three times and left under N₂. Degassed THF (0.05 M), by cycling between vacuum and N₂ with concurrent sonication, was then added to the sealed flask and allowed to stir at 50° C for 16 hours. After cooling, the reaction was cooled and solvent was removed under high-vac. Solid residue was dissolved in a minimal amount of 3:1 DMF/water with 5% TFA and filtered through 0.22 μL Ultrafree®-MC Centrifugal Filters (Millipore-Sigma). Sample was then purified by reverse HPLC, with a 10-60% or 10-100% gradient of acetonitrile/water containing 0.1%TFA depending on hydrophobicity of compound. Fractions that contained product was then freeze dried to produce a white powder.



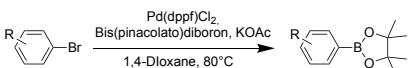
Generalized procedure B for Suzuki-Miyaura cross-coupling of macrocycles: Into a 10 mL screw-top vial, bromo-macrocycle (0.011 mmol, 1.0 eq), boronic acid (0.11 mmol, 10 eq), [1,1'-Bis(di-*tert*-butylphosphino)ferrocene]dichloropalladium (II) (0.0002 mmol, 0.2 eq), were combined and sealed with a septum. Flask was evacuated and refilled with N₂ three times and left under N₂. Degassed 10:1 THF/2M Na₂CO₃ (0.05 M) was added and reaction as heated to at 75° C for 16 hours. After cooling, the reaction was cooled and solvent was removed under high-vac. Solid residue was dissolved in a minimal amount of 3:1 DMF/water with 5% TFA and filtered through 0.22 μL Ultrafree®-MC Centrifugal Filters (Millipore-Sigma). Sample was then purified by reverse HPLC, with a 10-60% or 10-100% gradient of acetonitrile/water containing 0.1%TFA depending on hydrophobicity of compound. Fractions that contained product was then freeze dried to produce a white powder.



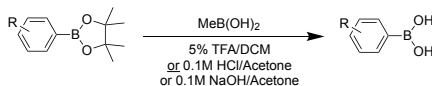
General conditions for ethyl ester protection of carboxylic acids: In a 50 mL roundbottom flask, ester (1 mmol, 1 eq) was suspended in 1.25M HCl/EtOH at RT for 16 hours. Reaction was then diluted slowly with 100 mL saturated NaHCO₃, and aqueous layer was extracted three times with EtOAc. Combined organic layers were washed with saturated NaCl, dried over Na₂SO₄, and concentrated by rotary evaporation to afford ester product.



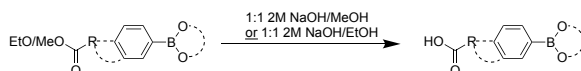
Generalized conditions for triflation of phenols: Into a N₂ flushed 100 mL roundbottom flask, phenol derivative (1.0 mmol, 1.0 eq), was dissolved in CH₂Cl₂ and cooled to -78°C in a dry ice/acetone bath. After sequential dropwise addition of pyridine (3.0 mmol, 3.0 eq) and trifluoromethanesulfonic anhydride (1.1 mmol, 1.1 eq), reaction was allowed to stir for 16 hours, warming up to RT. Reaction was then diluted with 100 mL saturated NaHCO₃, and aqueous layer was extracted three times with EtOAc. Combined organic layers were washed with saturated NaCl, dried over Na₂SO₄, and concentrated by rotary evaporation to afford triflate product.



Generalized Miyaura borylation conditions: Into a 100 mL roundbottom flask, aryl bromide (1.0 mmol, 1.0 eq), bis(pinacolato)diboron (2.0 mmol, 2. eq), [1,1'-bis(diphenylphosphino)ferrocene]dichloropalladium (II) (0.1 mmol, 0.1 eq), and potassium acetate (3.0 mmol, 3 eq) was combined and sealed with a septum. Flask was evacuated and refilled with N₂ three times and left under N₂. Degassed 1,4-Dioxane (0.1 M), by cycling between vacuum and N₂ with concurrent sonication, was then added to the sealed flask and allowed to stir at 80° C for 16 hours. After cooling, the reaction was cooled and diluted with 1M HCl and transferred to a separatory funnel. Aqueous layer was extracted three times with EtOAc and combined organic layers were washed with saturated NaCl, dried over Na₂SO₄, and concentrated by rotary evaporation. Residue was purified by column chromatography to afford product.



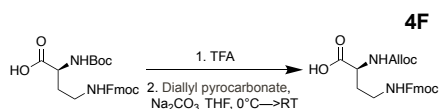
General pinacol deprotection conditions: Adapting conditions described previously³, In a 50 mL roundbottom flask, pinacol boronic ester (1 mmol, 1 eq) and methylboronic acid (10 mmol, 10 eq) were suspended in 5% TFA/CH₂Cl₂, 0.1M HCl/Acetone, or 0.1M NaOH/Acetone depending on acid sensitivity of substrate and allowed to stir at RT for 16 hours. Solvent was removed by rotary evaporation and the residue was resuspended in 0.1M HCl. HCl was removed by rotary evaporation, removing excess methylboronic acid and methylboronic acid pinacol ester. This cycle was repeated three times until no methylboronic acid was present by NMR analysis. For acid sensitive substrates, residue was resuspended in water during rotary evaporation steps. For substrates dissolved in 0.1M NaOH/Acetone, solution was neutralized to ~pH 3, filtered, and concentrated by rotary evaporation. Excess MeB(OH)₂ was removed as described above using water.



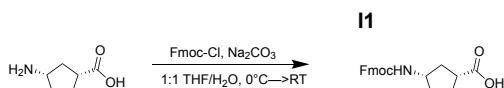
General conditions for saponification of methyl/ethyl esters: In a 50 mL roundbottom flask, ester (1 mmol, 1 eq) was suspended in 1:1 2M NaOH/MeOH (0.1M) for methyl esters or 1:1 2M NaOH/EtOH (0.1M) for ethyl esters and stirred at RT for 15 hours. Reaction was neutralized by diluting reaction with 50 mL 1M HCl, and aqueous layer was extracted three times with EtOAc. Combined organic layers were washed with saturated NaCl, dried over Na₂SO₄, and concentrated by rotary evaporation to isolated carboxylic acid.

Synthesis of intermediates

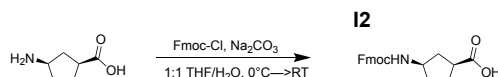
¹H-NMR spectra are provided in a separate part of the Supplementary Information. HRMS characterization for intermediates are shown in Supplementary Table 7.



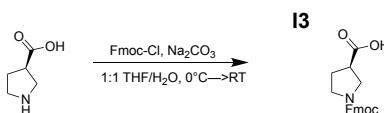
4F (128): In a 500 mL roundbottom flask, *N*^t-Boc-*N'*-Fmoc-L-2,4-diaminobutyric acid (10 mmol) was dissolved in 20 mL TFA and stirred at RT for 1 hour. TFA was then removed by rotary evaporation, leaving an oily solution. Oil was dissolved in 1:1 tetrahydrofuran (THF)/water (0.05 M), sodium carbonate (30 mmol, 3 eq) was added to the flask, and cooled to 0°C. Diallyl pyrocarbonate (15 mmol, 1.5 eq) was then added dropwise to the flask and the reaction was capped and allowed to stir for 5 hours, warming up to RT. THF was removed by rotary evaporation and the aqueous layer was transferred to a separatory funnel and washed two times with 100 mL Et₂O. Aqueous layer was then acidified to pH 1 with 12N HCl, resulting in white precipitate. Aqueous layer was then extracted three times with 100 mL of ethyl acetate (EtOAc). Combined organic layers were washed with saturated NaCl, dried over Na₂SO₄, and concentrated by rotary evaporation to afford **4F** a yellow foam. Yield: 82%



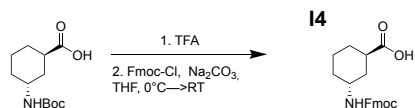
I1 (129): In a 250 mL roundbottom flask, (-)-(1*S*,4*R*)-4-Aminocyclopent-2-enecarboxylic acid (8 mmol), 9-Fluorenylmethoxycarbonyl chloride (8.8 mmol, 1.1 eq), and sodium carbonate (40 mmol, 6 eq) were dissolved in 1:1 THF/water (0.1 M) and stirred at RT for 16 hour. THF was removed by rotary evaporation and ether was added to the aqueous suspension. Aqueous layer was washed two times with ether, then acidified to pH2 with 12N HCl. Aqueous layer was then extracted three times with 100 mL of ethyl acetate (EtOAc). Combined organic layers were washed with saturated NaCl, dried over Na₂SO₄, and concentrated by rotary evaporation to afford **I1** as a white solid. Yield: 96%



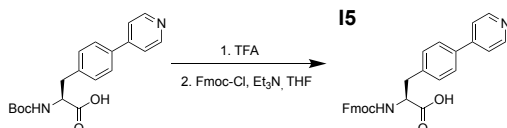
I2 (130): Compound was synthesized as described for compound **I1**. Synthesis afforded **I2** as a white solid. Yield: 89%



I3 (131): In a 250 mL roundbottom flask, (R)-(-)-Pyrrolidine-3-carboxylic acid (2 mmol), 9-Fluorenylmethoxycarbonyl chloride (2.2 mmol, 1.1 eq), and sodium carbonate (12 mmol, 6 eq) were dissolved in 1:1 THF/water (0.1 M) and stirred at RT for 16 hour. THF was removed by rotary evaporation and ether was added to the aqueous suspension. Aqueous layer was washed two times with ether, then acidified to pH2 with 12N HCl. Aqueous layer was then extracted three times with 100 mL of ethyl acetate (EtOAc). Combined organic layers were washed with saturated NaCl, dried over Na₂SO₄, and concentrated by rotary evaporation to afford **I3** as a white solid. Yield: 78%

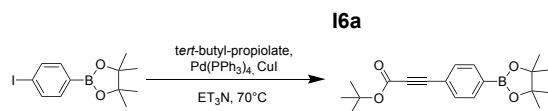


I4 (132): In a 250 mL roundbottom flask, (1*R*,3*R*)-3-[[*tert*-Butoxy]carbonyl]amino)cyclohexane-1-carboxylic acid (1 mmol) was dissolved in 20 mL TFA and stirred at RT for 1 hour. TFA was then removed by rotary evaporation, leaving an oily solution. Residue was dissolved in 1:1 THF/water (0.1M) at 0°C, followed by addition of 9-Fluorenylmethoxycarbonyl chloride (1.1 mmol, 1.1 eq), and sodium carbonate (6 mmol, 6 eq). The reaction was stirred 16 hours, warming to RT. THF was removed by rotary evaporation and ether was added to the aqueous suspension. Aqueous layer was washed two times with ether, then acidified to pH2 with 12N HCl. Aqueous layer was then extracted three times with 100 mL of ethyl acetate (EtOAc). Combined organic layers were washed with saturated NaCl, dried over Na₂SO₄, and concentrated by rotary evaporation to afford **I4** as a yellow solid with some impurities. Compound was carried onto next step without further purification. Yield: 45%



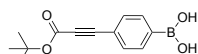
I5 (133): In a 250 mL roundbottom flask, *N*-Boc-4-(4-pyridinyl)-*L*-phenylalanine (0.4 mmol) was dissolved in 20 mL TFA and stirred at RT for 1 hour. TFA was then removed by rotary evaporation, leaving an oily solution. Residue was suspended in THF (0.1M), and water was added until all material dissolved. 9-Fluorenylmethoxycarbonyl chloride (0.44 mmol, 1.1 eq) dissolved in THF was then added, followed by triethylamine (2.0 mmol, 5 eq) and the reaction was stirred 16 hour at RT. THF was removed by rotary evaporation and reaction as partitioned between

EtOAc and 1M HCl. Aqueous layer was then extracted three times with 100 mL of ethyl acetate (EtOAc). Combined organic layers were washed with saturated NaCl, dried over Na₂SO₄, and concentrated by rotary evaporation. Crude product was purified by column chromatography (0-20% MeOH/CH₂Cl₂) to afford **I5** as a white solid. Yield: 88%



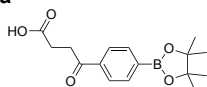
I6a (134): Adapting a previously reported protocol⁴, in a N₂ flushed 100mL roundbottom flask, a solution of 4-iodophenylboronic acid pinacol ester, was dissolved in degassed triethylamine. Then, Tetrakis(triphenylphosphine)-palladium(0), Copper(I) iodide and *tert*-butyl propiolate were added successively and the reaction was heated at 70°C overnight. Reaction was then concentrated by rotary evaporation and crude material was directly purified by column chromatography (0-50% EtOAc/Hex). Product **I6a** was isolated as a yellow solid. Yield: 28%

I6b



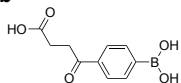
I6b (135): Compound was synthesized using **general pinacol deprotection conditions** with **I6a** as starting material, substituting 0.1N HCl/Acetone as solvent. Solvent was removed by rotary evaporation and the residue was resuspended in H₂O and once again removed by rotary evaporation to remove excess MeB(OH)₂. This step was repeated until all MeB(OH)₂ was removed as seen on ¹H NMR. Product **I6b** was isolated as a white solid with some minor impurities. Product was carried onto next step without further purification. Yield: quantitative

I7a



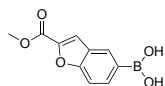
I7a (136): Compound was synthesized using **generalized Miyaura borylation conditions** with 3-(4-Bromobenzoyl)propionic acid. Column chromatography conditions: 0-20% MeOH/CH₂Cl₂. Product **I7a** was isolated as a yellow solid with some excess bis(pinacolato)diboron and extra impurities. Product was carried onto next step without further purification. Yield: approx. quantitative.

I7b



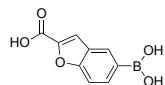
I7b (137): Compound was synthesized using **general pinacol deprotection conditions** with **I7a** and 5% TFA/CH₂Cl₂ as solvent. Product **I7b** was isolated as a yellow solid with some minor impurities. Product was carried onto next step without further purification. Yield: 88%

I8a



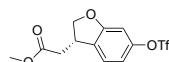
I8a (138): Compound was synthesized using **general pinacol deprotection conditions** with Methyl 5-(tetramethyl-1,3,2-dioxaborolan-2-yl)-1-benzofuran-2-carboxylate and 5% TFA/CH₂Cl₂ as solvent. Product **I8a** was isolated as a white solid. Yield: 98%

I8b



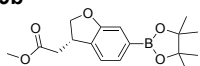
I8b (139): Compound was synthesized using **general conditions for saponification of methyl/ethyl esters** with **I8a**, using 1:1 2M NaOH/MeOH as solvent. Product **I8b** was isolated as white solid with some small impurities. Product was carried onto next step without further purification. Yield: quantitative

I9a



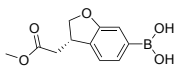
I9a (140): Compound was synthesized using **generalized conditions for triflation of phenols** with (S)-Methyl 2-(6-hydroxy-2,3-dihydrobenzofuran-3-yl)acetate. Product **I9a** was isolated as a brown oil. Yield: 78%

I9b



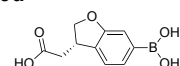
I9b (141): Compound was synthesized using **generalized Miyaura borylation conditions** with **I9a** and no acidic workup. Crude reaction was directly purified by column chromatography (0-50%EtOAc/Hex) to afford product **I9b** as white powder with small amounts of bis(pinacolato)diboron. Product was carried onto next step without further purification. Yield: 67%

I9c



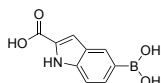
I9c (142): Compound was synthesized using **general pinacol deprotection conditions** with **I9b** and 5% TFA/CH₂Cl₂ as solvent. Product **I9c** was isolated as a white solid. Yield: 90%

I9d



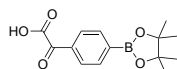
I9d (143): Compound was synthesized using **general conditions for saponification of methyl/ethyl esters** with **I9c**, using 1:1 2M NaOH/MeOH as solvent. Product **I9d** was isolated as white solid with small impurities. Product was carried onto next step without further purification. Yield: 90%

I10



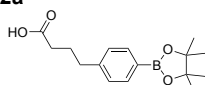
I10 (144): Compound was synthesized using **general pinacol deprotection conditions** with 5-(Tetramethyl-1,3,2-dioxaborolan-2-yl)-1H-indole-2-carboxylic acid and 5% TFA/CH₂Cl₂ as solvent. Product **I10** was isolated as a white solid. Yield: quantitative

I11



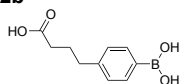
I11 (145): Compound was synthesized using **general conditions for saponification of methyl/ethyl esters** with methyl 2-oxo-2-[4-(tetramethyl-1,3,2-dioxaborolan-2-yl)phenyl]acetate, using 1:1 2M NaOH/MeOH as solvent. Product **I11** was isolated as white solid with small impurities. Product was carried onto next step without further purification. Yield: quantitative

I12a



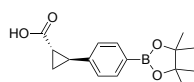
I12a (146): Compound was synthesized using **generalized Miyaura borylation conditions** with 4-(4-Bromophenyl)butanoic acid. Column chromatography conditions: 0-20% MeOH/CH₂Cl₂. Product **I12a** was isolated as a yellow solid with some excess bis(pinacolato)diboron and extra impurities. Product was carried onto next step without further purification Yield: approx. 37%

I12b

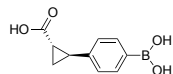


I12b (147): Compound was synthesized using **general pinacol deprotection conditions** with **I12a** and 5% TFA/CH₂Cl₂ as solvent. Product **I12b** was isolated as a yellow solid. Yield: quantitative

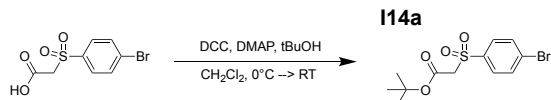
I13a



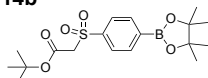
I13a (148): Compound was synthesized using **generalized Miyaura borylation conditions** with (1S,2S)-2-(4-Bromophenyl)cyclopropanecarboxylic acid. Column chromatography conditions: 0-20% MeOH/CH₂Cl₂. Product **I13a** was isolated as a yellow solid with some excess bis(pinacolato)diboron and small impurities. Product was carried onto next step without further purification Yield: approx. quantitative

I13b

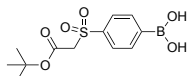
I13b (149): Compound was synthesized using **general pinacol deprotection conditions** with **I13a** and 5% TFA/CH₂Cl₂ as solvent. Product **I13b** was isolated as a yellow solid with minor impurities and trace amounts of **I13a**. Product was carried on without further purification. Yield: 86%



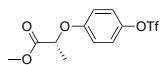
I14a (150): Adapting from a previously reported protocol⁵, into a 50mL roundbottom flask, 2-(4-bromophenyl)acetic acid (0.7 mmol, 1 eq), 4-Dimethylaminopyridine (0.11 mmol, 0.16eq), and *tert*-butanol (2.8 mmol, 4 eq) were dissolved in CH₂Cl₂ (0.1 M) and cooled in an ice bath. N, N'-Dicyclohexylcarbodiimide dissolved in 2 mL CH₂Cl₂ was then added and stirred for 15 minutes, observing a white precipitate. Reaction was then warmed to RT and allowed to stir for 16 hours. Precipitate was filtered through celite and reaction concentrated by rotary evaporation. Residue was dissolved in 100mL EtOAc and 100 mL saturated NaHCO₃. Organic layer was isolated and aqueous layer was extracted two more times with 100 mL EtOAc. Combined organic layers were washed with saturated NaCl, dried over Na₂SO₄, and concentrated by rotary evaporation. Product **I14a** was isolated as a white solid. Yield: 85%

I14b

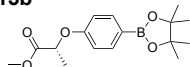
I14b (151): Compound was synthesized using **generalized Miyaura borylation conditions** with **I14a** and no acidic workup. Crude reaction was directly purified by column chromatography (0-50%EtOAc/Hex) to afford product **I14b** as white powder with trace amounts of bis(pinacolato)diboron. Product was carried onto next step without further purification. Yield: 88%.

I14c

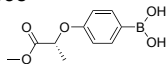
I14c (152): Compound was synthesized using **general pinacol deprotection conditions** with **I14b** and 0.1M NaOH/Acetone as solvent. Product **I14c** was isolated as a white solid with methylboronic acid and other impurities identified on H-NMR. Purification by column chromatography was attempted on crude **I14c** product, but full oxidation of the boronic acid to a phenol was observed. Therefore, crude **I14c** product was carried onto further reactions without further purification. Yield: approx. quantitative

I15a

I15a (153): Compound was synthesized using **generalized conditions for triflation of phenols** with Methyl (r)-(+)-2-(4-hydroxyphenoxy)propanoate. Product **I15a** was isolated as a yellow oil. Yield: quantitative

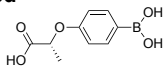
I15b

I15b (154): Compound was synthesized using **generalized Miyaura borylation conditions** with **I15a** and no acidic workup. Crude reaction was directly purified by column chromatography (0-50%EtOAc/Hex) to afford product **I15b** as white powder with trace amounts of bis(pinacolato)diboron. Product was carried onto next step without further purification. Yield: 67%

I15c

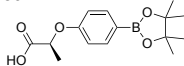
I15c (155): Compound was synthesized using **general pinacol deprotection conditions** with **I15b** and 5% TFA/CH₂Cl₂ as solvent. Product **I15c** was isolated as a white solid with trace amounts of **I15b** excess MeB(OH)₂. Product was carried onto next step without further purification. Yield: quantitative

I15d



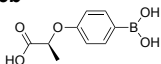
I15d (156): Compound was synthesized using **general conditions for saponification of methyl/ethyl esters** with **I15c**, using 1:1 2M NaOH/MeOH as solvent. Product **I15d** was isolated as brown solid with trace amounts of saponified **I15b**. Product was carried on without further purification. Yield: 61%

I16a



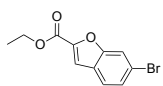
I16a (157): Compound was synthesized using **generalized Miyaura borylation conditions** with (2S)-2-(4-bromophenoxy)propanoic acid. Column chromatography conditions: 0-20% MeOH/CH₂Cl₂. Product **I16a** was isolated as a yellow solid with some excess bis(pinacolato)diboron and extra impurities. Product was carried onto next step without further purification Yield: approx. 89%

I16b



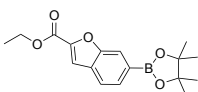
I16b (158): Compound was synthesized using **general pinacol deprotection conditions** with **I16a** and 5% TFA/CH₂Cl₂ as solvent. Product **I16b** was isolated as a white solid with some impurities and excess MeB(OH)₂. Product was carried on without further purification. Yield: quantitative

I17a



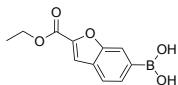
I17a (159): Compound was synthesized using **general conditions for ethyl ester protection of carboxylic acids** using 6-Bromobenzofuran-2-carboxylic acid. Product **I17a** was isolated as a white solid with a small amount of starting material impurities. Product was carried onto next step without further purification. Yield: quantitative

I17b



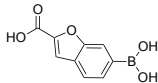
I17b (160): Compound was synthesized using **generalized Miyaura borylation conditions** with **I17a** and no acidic workup. Crude reaction was directly purified by column chromatography (0-50%EtOAc/Hex) to afford product **I17b** as clear solid with small amounts of bis(pinacolato)diboron. Product was carried onto next step without further purification Yield: 88%

I17c



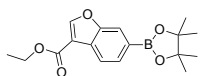
I17c (161): Compound was synthesized using **general pinacol deprotection conditions** with **I17b** and 5% TFA/CH₂Cl₂ as solvent. Product **I17c** was isolated as a white solid. Yield: 83%

I17d



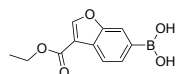
I17d (162): Compound was synthesized using **general conditions for saponification of methyl/ethyl esters** with **I17c**, using 1:1 2M NaOH/EtOH as solvent. Product **I17d** was isolated as brown solid. Yield: quantitative

I18a



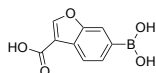
I18a (163): Compound was synthesized using **generalized Miyaura borylation conditions** with Ethyl 6-bromobenzofuran-3-carboxylate and no acidic workup. Crude reaction was directly purified by column chromatography (0-50%EtOAc/Hex) to afford product **I18a** as white solid with trace amounts of bis(pinacolato)diboron. Product was carried onto next step without further purification Yield: 94%

I18b



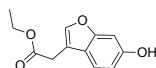
I18b (164): Compound was synthesized using **general pinacol deprotection conditions** with **I18a** and 5% TFA/CH₂Cl₂ as solvent. Product **I18b** was isolated as a white solid. Yield: quantitative

I18c



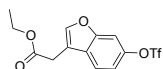
I18c (165): Compound was synthesized using **general conditions for saponification of methyl/ethyl esters** with **I18b**, using 1:1 2M NaOH/EtOH as solvent. Product **I18c** was isolated as white solid. Yield: 98%

I19a



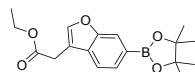
I19a (166): Compound was synthesized using **general conditions for ethyl ester protection of carboxylic acids** using 2-(6-Hydroxybenzofuran-3-yl)acetic acid. Product **I19a** was isolated as a brown oil. Yield: 86%

I19b



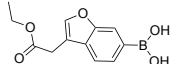
I19b (167): Compound was synthesized using **generalized conditions for triflation of phenols** with **I19a**. Product **I19b** was isolated as a brown oil. Yield: quantitative

I19c



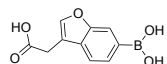
I19c (168): Compound was synthesized using **generalized Miyaura borylation conditions** with **I19b** and no acidic workup. Crude reaction was directly purified by column chromatography (0-50%EtOAc/Hex) to afford product **I19c** as white solid with trace amounts of bis(pinacolato)diboron. Product was carried onto next step without further purification Yield: 76%

I19d



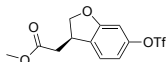
I19d (169): Compound was synthesized using **general pinacol deprotection conditions** with **I19c** and 5% TFA/CH₂Cl₂ as solvent. Product **I19d** was isolated as a white solid. Yield: 82%

I19e



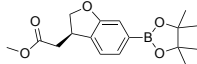
I19e (170): Compound was synthesized using **general conditions for saponification of methyl/ethyl esters** with **I19d**, using 1:1 2M NaOH/EtOH as solvent. Product **I19e** was isolated as white solid. Yield: 96%

I20a



I20a (171): Compound was synthesized using **generalized conditions for triflation of phenols** with (R)-Methyl 2-(6-hydroxy-2,3-dihydrobenzofuran-3-yl)acetate. Product **I20a** was isolated as a clear oil. Yield: quantitative

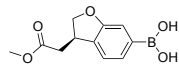
I20b



I20b (172): Compound was synthesized using **generalized Miyaura borylation conditions** with **I20a** and no acidic workup. Crude reaction was directly purified by column chromatography (0-50%EtOAc/Hex) to afford product **I20b**

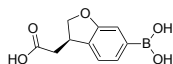
as white powder with small amounts of bis(pinacolato)diboron. Product was carried onto next step without further purification Yield: 81%

I20c



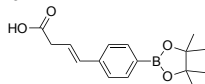
I20c (173): Compound was synthesized using **general pinacol deprotection conditions** with **I20b** and 5% TFA/CH₂Cl₂ as solvent. Product **I20c** was isolated as a white solid. Yield: quantitative

I20d



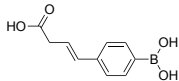
I20d (174): Compound was synthesized using **general conditions for saponification of methyl/ethyl esters** with **I20c**, using 1:1 2M NaOH/MeOH as solvent. Product **I20d** was isolated as white solid with minor impurities. Product was carried on without further purification. Yield: 42%

I21a



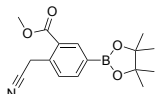
I21a (175): Compound was synthesized using **generalized Miyaura borylation conditions** with (3E)-4-(4-bromophenyl)but-3-enoic acid. Column chromatography conditions: 0-20% MeOH/CH₂Cl₂. Product **I21a** was isolated as a yellow solid with some excess bis(pinacolato)diboron and extra impurities. Product was carried onto next step without further purification Yield: approx. 93%

I21b



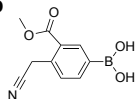
I21b (176): Compound was synthesized using **general pinacol deprotection conditions** with **I21a** and 5% TFA/CH₂Cl₂ as solvent. Product **I21b** was isolated as a yellow solid. Yield: 86%

I22a



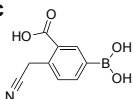
I22a (177): Compound was synthesized using **generalized Miyaura borylation conditions** with Methyl 5-bromo-2-(cyanomethyl)benzoate and no acidic workup. Crude reaction was directly purified by column chromatography (0-50% EtOAc/Hex) to afford product **I22a** as white powder with trace amounts of bis(pinacolato)diboron. Product was carried onto next step without further purification Yield: 97%

I22b

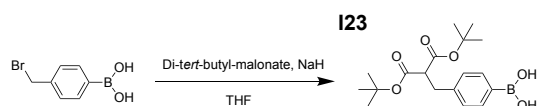


I22b (178): Compound was synthesized using **general pinacol deprotection conditions** with **I22a** and 5% TFA/CH₂Cl₂ as solvent. Product **I22b** was isolated as a white solid. Yield: quantitative 80%

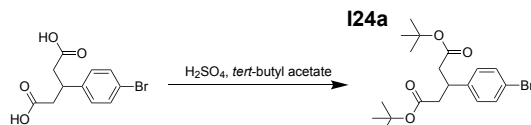
I22c



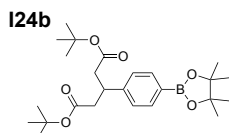
I22c (179): Compound was synthesized using **general conditions for saponification of methyl/ethyl esters** with **I22b**, using 1:1 2M NaOH/MeOH as solvent. Product **I20d** was isolated as white solid with some minor impurities. Product was carried on without further purification. Yield: quantitative



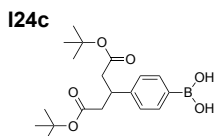
I23 (180): Adapting a previously reported protocol⁶, Into a N₂ flushed 50 mL roundbottom flask, sodium hydride (60% dispersion in mineral oil) (1.47 mmol, 1.05 eq) was dissolved in anhydrous THF (0.1 M) followed by dropwise addition of di-*tert*-butyl-malonate. Once gas finished forming from the solution, 4-(Bromomethyl)phenylboronic acid dissolved in 1mL THF was added to the flask, which was allowed to stir at room temperature for 16 hours. The reaction was then diluted with saturated NH₄Cl and extracted three times with EtOAc. Combined organic layers were washed with saturated NaCl, dried over Na₂SO₄, and concentrated by rotary evaporation. Residue was purified by silica gel chromatography (0-10% MeOH/CH₂Cl₂) to afford product as white solid. Yield: 84%



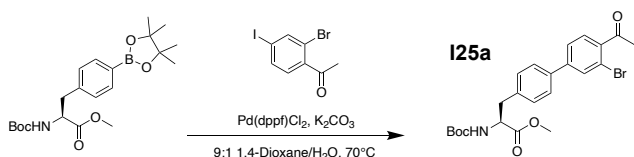
I24a (181): Adopting a previously reported protocol⁷, into a N₂ flushed 50 mL roundbottom flask, B-(4-Bromophenyl)glutaric acid (0.7 mmol, 1.0 eq) was suspended in *tert*-butyl-acetate (0.2M), followed by addition of concentrated H₂SO₄ (0.7 mmol, 1 eq). Reaction was allowed to stir at room temperature for 16 hours. Reaction was diluted with sat. bicarbonate and extracted three times with EtOAc. Combined organic layers were washed with saturated NaCl, dried over Na₂SO₄, and concentrated by rotary evaporation. Residue was purified by column chromatography (0-50% EtOAc/Hex) to afford product as white solid. Yield: 47%



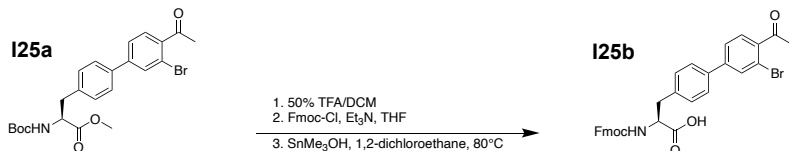
I24b (182): Compound was synthesized using **generalized Miyaura borylation conditions procedure** with **I24a** and no acidic workup. Crude reaction was directly purified by column chromatography (0-50%EtOAc/Hex) to afford product as white powder with trace amounts of bis(pinacolato)diboron. Yield: 97%



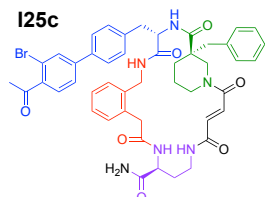
I24c (183): Compound was synthesized **using general pinacol deprotection conditions** with **I24b** and substituting 0.1N NaOH/Acetone as solvent. After 16 hours, reaction was neutralized to ~pH 2-3 with 1N HCl and filtered to remove salts. Solvent was removed by rotary evaporation and the residue was resuspended in H₂O and once again removed by rotary evaporation to remove excess MeB(OH)₂. This step was repeated until all MeB(OH)₂ was removed as seen on ¹H NMR. Product was isolated as a white solid with small impurities. Product was carried on to next step without further purification Yield: quantitative



I25a (184): Adapting a previously reported protocol⁸, a mixture of Boc-4-borono pinacol ester-L phenylalanine methyl ester (1.98 mmol, 1 eq.), 1-(2-Bromo-4-iodophenyl)ethanone (2.56 mmol, 1.3 eq.), [1,1-Bis(diphenylphosphino)ferrocene]dichloropalladium(II) (0.19 mmol, 0.1 eq.), and potassium carbonate (7.90 mmol, 4 eq.) was dissolved in 18 mL of degassed 1,4-dioxane and 2 mL of degassed water (0.1 M) and stirred at 70°C in a sealed round bottom flask overnight. The reaction was then cooled down to room temperature, diluted with water, extracted three times with ethyl acetate (EtOAc), washed with brine, dried over sodium sulfate (Na₂SO₄), and evaporated under reduced pressure. The crude product was then dry loaded onto a 25G SNAP column, purified by flash column chromatography using 0-50% EtOAc/Hexanes, and yielded **I25a** as a yellow foam. Yield: 42% yield



I25b (185): Compound **I25a** (0.84 mmol, 1 eq.) was dissolved in 4.5 mL trifluoroacetic acid and 4.5 mL dichloromethane (0.1 M solution) to remove the Boc protecting group. The reaction was stirred for one hour at room temperature and the solvent was evaporated under reduced pressure and dried on high vacuum overnight. Then, a mixture of the crude Boc deprotected product and sodium bicarbonate (4.21 mmol, 5 eq.) was dissolved in 2 mL of 1,4-dioxane and 4 mL of water and stirred. 9-Fluorenylmethoxycarbonyl chloride (1.05 mmol, 1.25 eq.) was separately dissolved in 2 mL of 1,4-dioxane and added to the reaction. The reaction was stirred overnight at room temperature, then suspended in water, extracted three times with EtOAc, dried over Na₂SO₄, and evaporated under reduced pressure. To deprotect the methyl ester, a mixture of the crude Fmoc protected product and trimethyltin hydroxide (1.26 mmol, 1.5 eq.) was dissolved in 8 mL of 1,2-dichloroethane (0.1 M) and stirred at 80°C under reflux for three hours. The reaction was then cooled down to room temperature, suspended in ethyl acetate, washed two times with 1 M hydrochloric acid, and dried over Na₂SO₄. The crude product was then dry loaded onto a 10G SNAP column, purified by flash column chromatography using 0-100% EtOAc/Hexanes, and yielded **I25b** as a yellow solid. Yield: 76%



I25c (186): Macrocyclic peptide was synthesized using **general procedure for solid-phase peptide synthesis of macrocyclic inhibitors**. **I25c** was obtained as a white powder. Yield: 7%

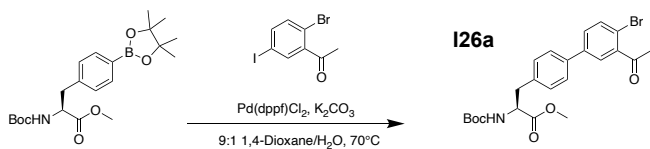
Resin: Rink Amide

4th Building Block: N^α-Fmoc-N^γ-allyloxycarbonyl-L-2,4-diaminobutyric acid

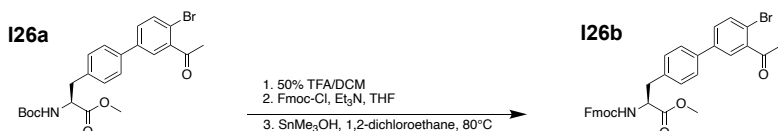
1st Building Block: Fmoc-2-aminomethyl-phenylacetic acid

2nd Building Block: **I25b**

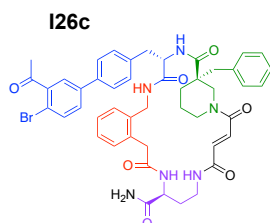
3rd Building Block: (S)-Fmoc-3-benzyl-piperidine-3-carboxylic acid



I26a (187): Compound was synthesized and purified as described in **I25a** with 1-(2-Bromo-5-iodophenyl)ethanone, affording **I26a** as a yellow foam. Yield: 37% yield



I26b (188): Compound was synthesized and purified as described in **I25b**, with **I26a** (0.73 mmol, 1 eq.), affording **I26b** as a yellow solid. Yield: 55%



I26c (189): Macrocyclic peptide was assembled using **general procedure for solid-phase peptide synthesis of macrocyclic inhibitors** and was obtained as a white powder. Yield: 7%

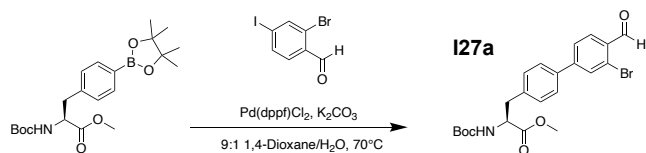
Resin: Rink Amide

4th Building Block: N^α-Fmoc-N^γ-allyloxycarbonyl-L-2,4-diaminobutyric acid

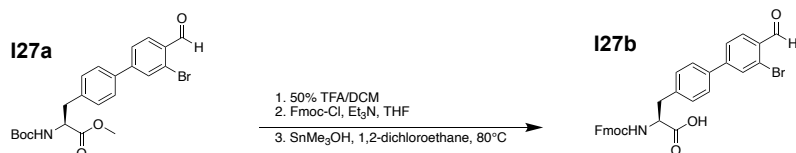
1st Building Block: Fmoc-2-aminomethyl-phenylacetic acid

2nd Building Block: **I26b**

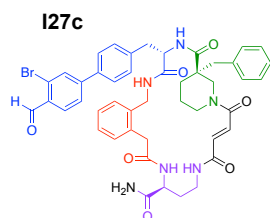
3rd Building Block: (S)-Fmoc-3-benzyl-piperidine-3-carboxylic acid



I27a (190): Compound was synthesized and purified as described in **I25a** with 2-Bromo-4-iodobenzaldehyde, affording **I27a** as a yellow foam. Yield: 46%



I27b (191): Compound was synthesized and purified as described in **I25b**, with **I27a** (0.91 mmol, 1 eq.), affording **I27b** as a yellow solid. Yield: 63%



I27c (192): Macrocycle was assembled using **general procedure for solid-phase peptide synthesis of macrocycle inhibitors** and was obtained as a white powder. Yield: 1%

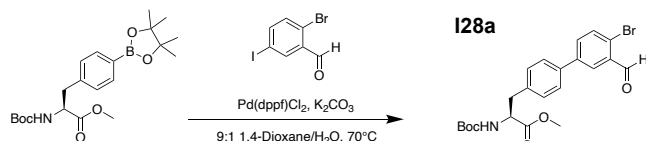
Resin: Rink Amide

4th Building Block: N^α-Fmoc-N^γ-allyloxycarbonyl-L-2,4-diaminobutyric acid

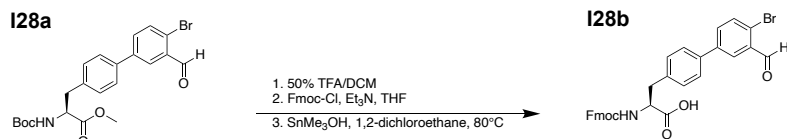
1st Building Block: Fmoc-2-aminomethyl-phenylacetic acid

2nd Building Block: **I27b**

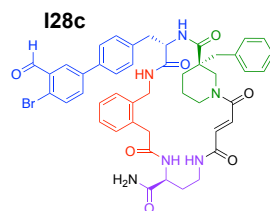
3rd Building Block: (S)-Fmoc-3-benzyl-piperidine-3-carboxylic acid



I28a (193): Compound was synthesized and purified as described in **I25a** with 2-Bromo-5-iodobenzaldehyde, affording **I28a** as a yellow foam. Yield: 42%



I28b (194): Compound was synthesized and purified as described in **I25b**, with **I28a** (0.87 mmol, 1eq.), affording **I28b** as a yellow solid. Yield: 36%



I28c (195): Macrocycle was assembled using **general procedure for solid-phase peptide synthesis of macrocycles inhibitors** and was obtained as a white powder. Yield: 1%

Resin: Rink Amide

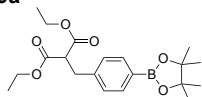
4th Building Block: N^α-Fmoc-N^γ-allyloxycarbonyl-L-2,4-diaminobutyric acid

1st Building Block: Fmoc-2-aminomethyl-phenylacetic acid

2nd Building Block: **I28b**

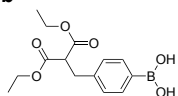
3rd Building Block: (S)-Fmoc-3-benzyl-piperidine-3-carboxylic acid

I29a



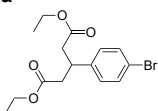
I29a (196): Compound was synthesized using **generalized Miyaura borylation conditions** with Diethyl 2-(4-bromobenzyl)malonate and no acidic workup. Crude reaction was directly purified by column chromatography (0-50%EtOAc/Hex) to afford product as white powder with small amounts of bis(pinacolato)diboron. Yield: approx quantitative

I29b



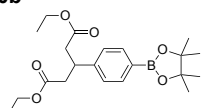
I29b (197): Compound was synthesized using **general pinacol deprotection conditions** with **I29a** and 5% TFA/CH₂Cl₂ as solvent. Product **I29b** was isolated as a white solid. Yield: quantitative

I30a



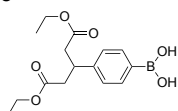
I30a (198): Compound was synthesized using **general conditions for ethyl ester protection of carboxylic acids** using B-(4-bromophenyl)glutaric acid. Product **I30a** was isolated as a brown oil. Yield: 86%

I30b



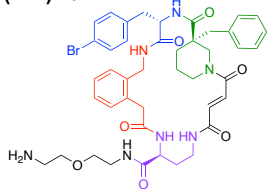
I30b (199): Compound was synthesized using **generalized Miyaura borylation conditions** with **I30a** and no acidic workup. Crude reaction was directly purified by column chromatography (0-50%EtOAc/Hex) to afford product as white powder with trace amounts of bis(pinacolato)diboron. Yield: 88%

I30c



I30c (200): Compound was synthesized using **general pinacol deprotection conditions** with **I30b** and 5% TFA/CH₂Cl₂ as solvent. Product **I30c** was isolated as a white solid. Yield: quantitative

(4Br)B6



(4Br)B6 (201): Macrocycle was assembled using **general procedure for solid-phase peptide synthesis of macrocycle inhibitors**.

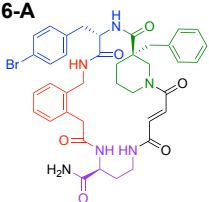
Resin: Bis-(2-aminoethyl)-ether trityl

4th Building Block: N^α-Fmoc-N^γ-allyloxycarbonyl-L-2,4-diaminobutyric acid

1st Building Block: Fmoc-2-aminomethyl-phenylacetic acid

2nd Building Block: Fmoc-4-bromo-L-phenylalanine

3rd Building Block: (S)-Fmoc-3-benzyl-piperidine-3-carboxylic acid

(4Br)B6-A

(4Br)B6-A (202): Macrocyclic was assembled using **general procedure for solid-phase peptide synthesis of macrocyclic inhibitors.**

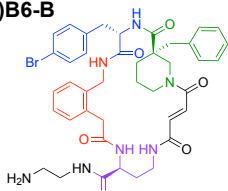
Resin: NovaPEG Rink Amide

4th Building Block: N^α-Fmoc-N^γ-allyloxycarbonyl-L-2,4-diaminobutyric acid

1st Building Block: Fmoc-2-aminomethyl-phenylacetic acid

2nd Building Block: Fmoc-4-bromo-L-phenylalanine

3rd Building Block: (S)-Fmoc-3-benzyl-piperidine-3-carboxylic acid

(4Br)B6-B

(4Br)B6-B (203): Macrocyclic was assembled using **general procedure for solid-phase peptide synthesis of macrocyclic inhibitors.**

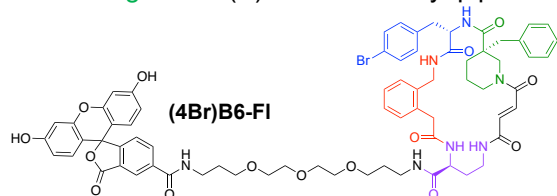
Resin: Universal NovaTag

4th Building Block: N^α-Fmoc-N^γ-allyloxycarbonyl-L-2,4-diaminobutyric acid

1st Building Block: Fmoc-2-aminomethyl-phenylacetic acid

2nd Building Block: Fmoc-4-bromo-L-phenylalanine

3rd Building Block: (S)-Fmoc-3-benzyl-piperidine-3-carboxylic acid

(4Br)B6-FI

(4Br)B6-FI (204): Macrocyclic was assembled using **general procedure for solid-phase peptide synthesis of macrocyclic inhibitors.** Prior to acidic cleavage, resin was suspended with three 1-hour treatments of 1M

hydroxybenzotriazole monohydrate dissolved in 1:1 CH₂Cl₂/trifluoroethanol to remove Mmt group. 5-carboxyfluorescein (5 eq) and (HATU, 4.75 equiv.) were dissolved in a separate flask in ~10-15 mL DMF then treated with *N,N*'-diisopropylethylamine (DIPEA, 10 eq) for 5 minutes, observing a color change. This flask was then transferred to resin swollen in ~10 mL DMF and allowed to mix for 24 hours. Fluorescein labeled peptide were then cleaved from resin and purified as described in general procedure.

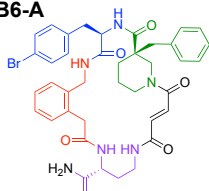
Resin: Universal PEG NovaTag™_Resin

4th Building Block: N^α-Fmoc-N^γ-allyloxycarbonyl-L-2,4-diaminobutyric acid

1st Building Block: Fmoc-2-aminomethyl-phenylacetic acid

2nd Building Block: Fmoc-4-bromo-L-phenylalanine

3rd Building Block: (S)-Fmoc-3-benzyl-piperidine-3-carboxylic acid

*** (4Br)B6-A**

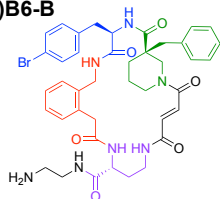
*** (4Br)B6-A (205):** Macrocyclic was assembled using **general procedure for solid-phase peptide synthesis of macrocyclic inhibitors.**

Resin: NovaPEG Rink Amide

4th Building Block: N^α-Fmoc-N^γ-allyloxycarbonyl-D-2,4-diaminobutyric acid

- 1st Building Block: Fmoc-2-aminomethyl-phenylacetic acid
 2nd Building Block: Fmoc-4-bromo-L-phenylalanine
 3rd Building Block: (R)-Fmoc-3-benzyl-piperidine-3-carboxylic acid

***(4Br)B6-B**



***(4Br)B6-B (206):** Macrocyclic was assembled using **general procedure for solid-phase peptide synthesis of macrocycle inhibitors.**

Resin: Universal NovaTag

4th Building Block: N^α-Fmoc-N^γ-allyloxycarbonyl-D-2,4-diaminobutyric acid

1st Building Block: Fmoc-2-aminomethyl-phenylacetic acid

2nd Building Block: Fmoc-4-bromo-L-phenylalanine

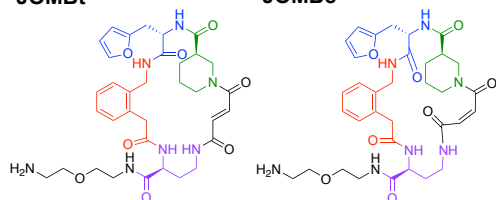
3rd Building Block: (R)-Fmoc-3-benzyl-piperidine-3-carboxylic acid

Synthesis of final macrocycles

¹H-NMR spectra are provided in a separate part of the Supplementary Information. HRMS characterization for intermediates are shown in Supplementary Table 8.

JOMBt

JOMBc



JOMBt/c: Macrocyclic was assembled using **general procedure for solid-phase peptide synthesis of macrocycle inhibitors.**

Resin: Bis-(2-aminoethyl)-ether trityl

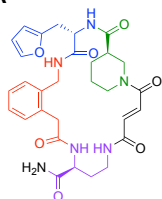
4th Building Block: N^α-Fmoc-N^γ-allyloxycarbonyl-L-2,4-diaminobutyric acid

1st Building Block: Fmoc-2-aminomethyl-phenylacetic acid

2nd Building Block: Fmoc-β-(2-furyl)-Ala-OH

3rd Building Block: Fmoc-D-nipecotic acid

JOMBt-A



JOMBt-A: Macrocyclic was assembled using **general procedure for solid-phase peptide synthesis of macrocycle inhibitors.**

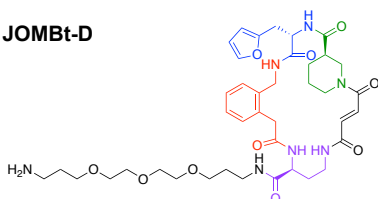
Resin: NovaPEG Rink Amide

4th Building Block: N^α-Fmoc-N^γ-allyloxycarbonyl-L-2,4-diaminobutyric acid

1st Building Block: Fmoc-2-aminomethyl-phenylacetic acid

2nd Building Block: Fmoc-β-(2-furyl)-Ala-OH

3rd Building Block: Fmoc-D-nipecotic acid

JOMBt-D

JOMBt-D: Macrocycle was assembled using **general procedure for solid-phase peptide synthesis of macrocycle inhibitors**.

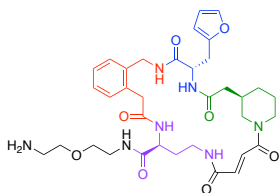
Resin: Universal PEG NovaTag™_Resin

4th Building Block: N^α-Fmoc-N^γ-allyloxycarbonyl-L-2,4-diaminobutyric acid

1st Building Block: Fmoc-2-aminomethyl-phenylacetic acid

2nd Building Block: Fmoc-β-(2-furyl)-Ala-OH

3rd Building Block: Fmoc-D-nipecotic acid

JOBBt

JOBBt: Macrocycle was assembled using **general procedure for solid-phase peptide synthesis of macrocycle inhibitors**.

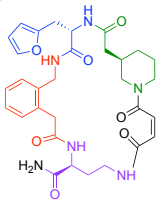
Resin: Bis-(2-aminoethyl)-ether trityl

4th Building Block: N^α-Fmoc-N^γ-allyloxycarbonyl-L-2,4-diaminobutyric acid

1st Building Block: Fmoc-2-aminomethyl-phenylacetic acid

2nd Building Block: Fmoc-β-(2-furyl)-Ala-OH

3rd Building Block: (R)-(1-Fmoc-piperidin-3-yl)acetic acid

JOBBc-A

JOBBc-A: Macrocycle was assembled using **general procedure for solid-phase peptide synthesis of macrocycle inhibitors**.

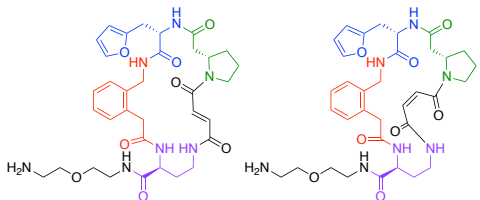
Resin: NovaPEG Rink Amide

4th Building Block: N^α-Fmoc-N^γ-allyloxycarbonyl-L-2,4-diaminobutyric acid

1st Building Block: Fmoc-2-aminomethyl-phenylacetic acid

2nd Building Block: Fmoc-β-(2-furyl)-Ala-OH

3rd Building Block: (R)-(1-Fmoc-piperidin-3-yl)acetic acid

JOCBt**JOCBc**

JOCBt/c: Macrocycle was assembled using **general procedure for solid-phase peptide synthesis of macrocycle inhibitors**.

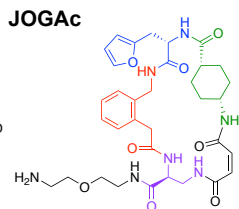
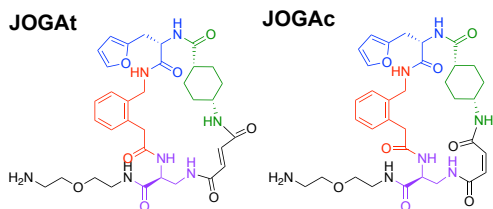
Resin: Bis-(2-aminoethyl)-ether trityl

4th Building Block: N^α-Fmoc-N^γ-allyloxycarbonyl-L-2,4-diaminobutyric acid

1st Building Block: Fmoc-2-aminomethyl-phenylacetic acid

2nd Building Block: Fmoc-β-(2-furyl)-Ala-OH

3rd Building Block: Fmoc-L-β-HomoPro-OH



JOGAt/c: Macrocycle was assembled using **general procedure for solid-phase peptide synthesis of macrocycle inhibitors.**

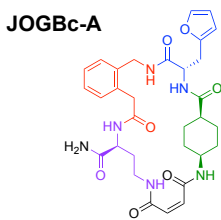
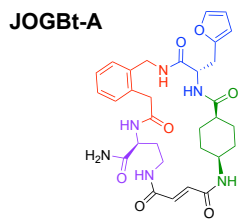
Resin: Bis-(2-aminoethyl)-ether trityl

4th Building Block: N^α-Fmoc-N^β-allyloxycarbonyl-L-2,3-diamino-propionic acid

1st Building Block: Fmoc-2-aminomethyl-phenylacetic acid

2nd Building Block: Fmoc-β-(2-furyl)-Ala-OH

3rd Building Block: Fmoc-cis-4-aminocyclohexane carboxylic acid



JOGBt/c-A: Macrocycle was assembled using **general procedure for solid-phase peptide synthesis of macrocycle inhibitors.**

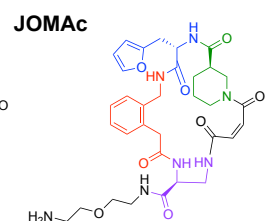
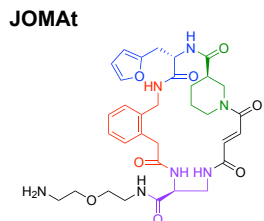
Resin: NovaPEG Rink Amide

4th Building Block: N^α-Fmoc-N^γ-allyloxycarbonyl-L-2,4-diaminobutyric acid

1st Building Block: Fmoc-2-aminomethyl-phenylacetic acid

2nd Building Block: Fmoc-β-(2-furyl)-Ala-OH

3rd Building Block: Fmoc-cis-4-aminocyclohexane carboxylic acid



JOMAt/c: Macrocycle was assembled using **general procedure for solid-phase peptide synthesis of macrocycle inhibitors.**

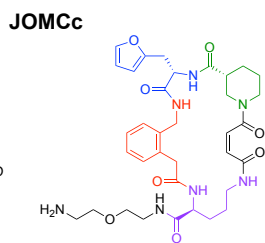
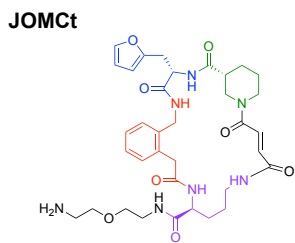
Resin: Bis-(2-aminoethyl)-ether trityl

4th Building Block: N^α-Fmoc-N^β-allyloxycarbonyl-L-2,3-diamino-propionic acid

1st Building Block: Fmoc-2-aminomethyl-phenylacetic acid

2nd Building Block: Fmoc-β-(2-furyl)-Ala-OH

3rd Building Block: Fmoc-D-nipecotic acid



JOMCt/c: Macrocycle was assembled using **general procedure for solid-phase peptide synthesis of macrocycle inhibitors.**

Resin: Bis-(2-aminoethyl)-ether trityl

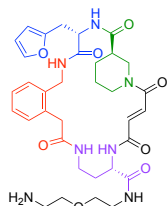
4th Building Block: N^α-Fmoc-N^δ-allyloxycarbonyl-L-ornithine

1st Building Block: Fmoc-2-aminomethyl-phenylacetic acid

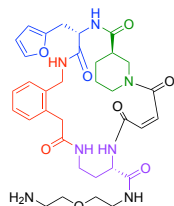
2nd Building Block: Fmoc- β -(2-furyl)-Ala-OH

3rd Building Block: Fmoc-D-nipecotic acid

JOMFt



JOMFc



JOMFt/c: Macrocycle was assembled using **general procedure for solid-phase peptide synthesis of macrocycle inhibitors.**

Resin: Bis-(2-aminoethyl)-ether trityl

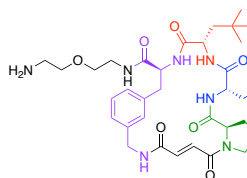
4th Building Block: 4F (N $^{\alpha}$ -allyloxycarbonyl-N $^{\beta}$ -Fmoc-L-2,4-diamino-butyric acid)

1st Building Block: Fmoc-2-aminomethyl-phenylacetic acid

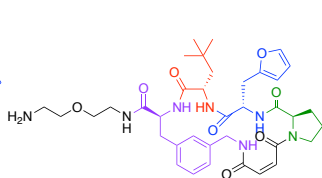
2nd Building Block: Fmoc- β -(2-furyl)-Ala-OH

3rd Building Block: Fmoc-D-nipecotic acid

HOJt



HOJc



HOJt/c: Macrocycle was assembled using **general procedure for solid-phase peptide synthesis of macrocycle inhibitors.**

Resin: Bis-(2-aminoethyl)-ether trityl

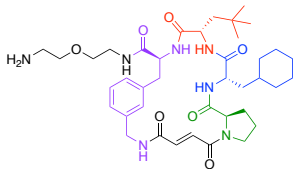
4th Building Block: 4J (Fmoc-3-(allyloxycarbonyl-aminomethyl)-L-phenylalanine)

1st Building Block: Fmoc-neopentylglycine

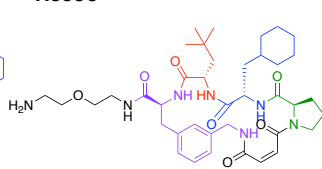
2nd Building Block: Fmoc- β -(2-furyl)-Ala-OH

3rd Building Block: Fmoc-D-Proline

HJt



HJc



HJt/c: Macrocycle was assembled using **general procedure for solid-phase peptide synthesis of macrocycle inhibitors.**

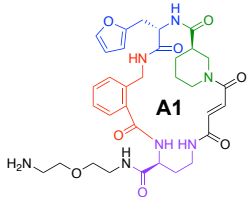
Resin: Bis-(2-aminoethyl)-ether trityl

4th Building Block: 4J (Fmoc-3-(allyloxycarbonyl-aminomethyl)-L-phenylalanine)

1st Building Block: Fmoc-neopentylglycine

2nd Building Block: Fmoc- β -cyclohexyl-L-alanine

3rd Building Block: Fmoc-D-Proline



A1: Macrocycle was assembled using **general procedure for solid-phase peptide synthesis of macrocycle inhibitors.**

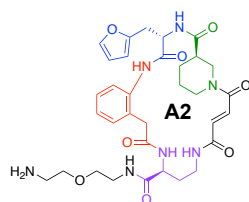
Resin: Bis-(2-aminoethyl)-ether trityl

4th Building Block: N $^{\alpha}$ -Fmoc-N $^{\gamma}$ -allyloxycarbonyl-L-2,4-diaminobutyric acid

1st Building Block: 2-(Fmoc-aminomethyl)benzoic acid

2nd Building Block: Fmoc- β -(2-furyl)-Ala-OH

3rd Building Block: Fmoc-D-nipecotic acid



A2: Macrocycle was assembled using **general procedure for solid-phase peptide synthesis of macrocycle inhibitors**.

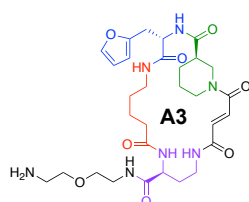
Resin: Bis-(2-aminoethyl)-ether trityl

4th Building Block: N ^{α} -Fmoc-N ^{γ} -allyloxycarbonyl-L-2,4-diaminobutyric acid

1st Building Block: Fmoc-(2-aminophenyl)acetic acid

2nd Building Block: Fmoc- β -(2-furyl)-Ala-OH

3rd Building Block: Fmoc-D-nipecotic acid



A3: Macrocycle was assembled using **general procedure for solid-phase peptide synthesis of macrocycle inhibitors**.

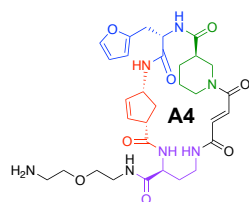
Resin: Bis-(2-aminoethyl)-ether trityl

4th Building Block: N ^{α} -Fmoc-N ^{γ} -allyloxycarbonyl-L-2,4-diaminobutyric acid

1st Building Block: Fmoc-5-aminovaleric acid

2nd Building Block: Fmoc- β -(2-furyl)-Ala-OH

3rd Building Block: Fmoc-D-nipecotic acid



A4: Macrocycle was assembled using **general procedure for solid-phase peptide synthesis of macrocycle inhibitors**.

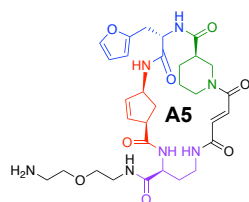
Resin: Bis-(2-aminoethyl)-ether trityl

4th Building Block: N ^{α} -Fmoc-N ^{γ} -allyloxycarbonyl-L-2,4-diaminobutyric acid

1st Building Block: (Fmoc-(-)-(1*S*,4*R*)-4-Aminocyclopent-2-enecarboxylic acid) (AAP_02_046) I1

2nd Building Block: Fmoc- β -(2-furyl)-Ala-OH

3rd Building Block: Fmoc-D-nipecotic acid



A5: Macrocycle was assembled using **general procedure for solid-phase peptide synthesis of macrocycle inhibitors**.

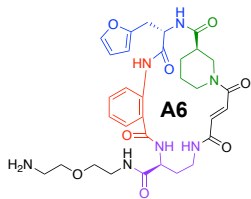
Resin: Bis-(2-aminoethyl)-ether trityl

4th Building Block: N ^{α} -Fmoc-N ^{γ} -allyloxycarbonyl-L-2,4-diaminobutyric acid

1st Building Block: Fmoc-(+)-(1*R*,4*S*)-4-Aminocyclopent-2-enecarboxylic acid (AAP_02_047) I2

2nd Building Block: Fmoc- β -(2-furyl)-Ala-OH

3rd Building Block: Fmoc-D-nipecotic acid



A6: Macrocycle was assembled using **general procedure for solid-phase peptide synthesis of macrocycle inhibitors**.

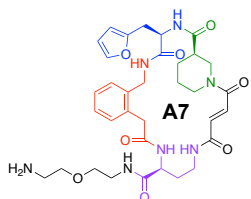
Resin: Bis-(2-aminoethyl)-ether trityl

4th Building Block: N^α-Fmoc-N^γ-allyloxycarbonyl-L-2,4-diaminobutyric acid

1st Building Block: N-Fmoc-anthranilic acid

2nd Building Block: Fmoc-β-(2-furyl)-Ala-OH

3rd Building Block: Fmoc-D-nipecotic acid



A7: Macrocycle was assembled using **general procedure for solid-phase peptide synthesis of macrocycle inhibitors**.

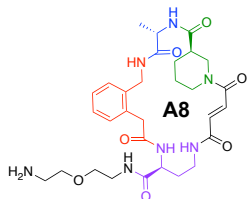
Resin: Bis-(2-aminoethyl)-ether trityl

4th Building Block: N^α-Fmoc-N^γ-allyloxycarbonyl-L-2,4-diaminobutyric acid

1st Building Block: Fmoc-2-aminomethyl-phenylacetic acid

2nd Building Block: Fmoc-β-(2-furyl)-D-Ala-OH

3rd Building Block: Fmoc-D-nipecotic acid



A8: Macrocycle was assembled using **general procedure for solid-phase peptide synthesis of macrocycle inhibitors**.

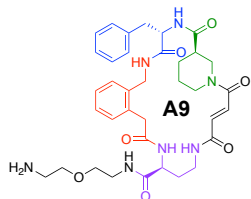
Resin: Bis-(2-aminoethyl)-ether trityl

4th Building Block: N^α-Fmoc-N^γ-allyloxycarbonyl-L-2,4-diaminobutyric acid

1st Building Block: Fmoc-2-aminomethyl-phenylacetic acid

2nd Building Block: Fmoc-L-alanine

3rd Building Block: Fmoc-D-nipecotic acid



A9: Macrocycle was assembled using **general procedure for solid-phase peptide synthesis of macrocycle inhibitors**.

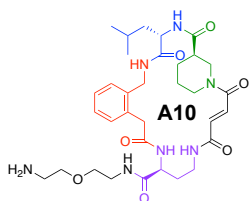
Resin: Bis-(2-aminoethyl)-ether trityl

4th Building Block: N^α-Fmoc-N^γ-allyloxycarbonyl-L-2,4-diaminobutyric acid

1st Building Block: Fmoc-2-aminomethyl-phenylacetic acid

2nd Building Block: Fmoc-L-phenylalanine

3rd Building Block: Fmoc-D-nipecotic acid



A10: Macrocycle was assembled using **general procedure for solid-phase peptide synthesis of macrocycle inhibitors**.

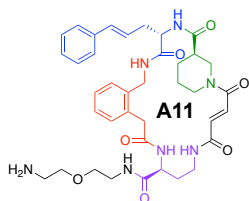
Resin: Bis-(2-aminoethyl)-ether trityl

4th Building Block: N^α-Fmoc-N^γ-allyloxycarbonyl-L-2,4-diaminobutyric acid

1st Building Block: Fmoc-2-aminomethyl-phenylacetic acid

2nd Building Block: Fmoc-L-Leucine

3rd Building Block: Fmoc-D-nipecotic acid



A11: Macrocycle was assembled using **general procedure for solid-phase peptide synthesis of macrocycle inhibitors**.

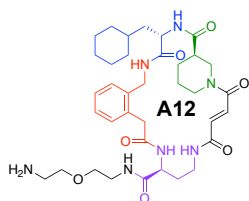
Resin: Bis-(2-aminoethyl)-ether trityl

4th Building Block: N^α-Fmoc-N^γ-allyloxycarbonyl-L-2,4-diaminobutyric acid

1st Building Block: Fmoc-2-aminomethyl-phenylacetic acid

2nd Building Block: Fmoc-3-styryl-L-alanine

3rd Building Block: Fmoc-D-nipecotic acid



A12: Macrocycle was assembled using **general procedure for solid-phase peptide synthesis of macrocycle inhibitors**.

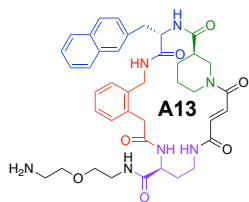
Resin: Bis-(2-aminoethyl)-ether trityl

4th Building Block: N^α-Fmoc-N^γ-allyloxycarbonyl-L-2,4-diaminobutyric acid

1st Building Block: Fmoc-2-aminomethyl-phenylacetic acid

2nd Building Block: Fmoc-β-cyclohexyl-L-alanine

3rd Building Block: Fmoc-D-nipecotic acid



A13: Macrocycle was assembled using **general procedure for solid-phase peptide synthesis of macrocycle inhibitors**.

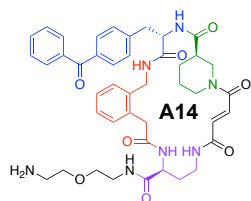
Resin: Bis-(2-aminoethyl)-ether trityl

4th Building Block: N^α-Fmoc-N^γ-allyloxycarbonyl-L-2,4-diaminobutyric acid

1st Building Block: Fmoc-2-aminomethyl-phenylacetic acid

2nd Building Block: Fmoc-3-(2-naphthyl)-L-alanine

3rd Building Block: Fmoc-D-nipecotic acid



A14: Macrocycle was assembled using **general procedure for solid-phase peptide synthesis of macrocycle inhibitors**.

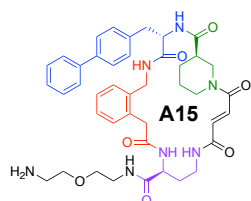
Resin: Bis-(2-aminoethyl)-ether trityl

4th Building Block: N^α-Fmoc-N^γ-allyloxycarbonyl-L-2,4-diaminobutyric acid

1st Building Block: Fmoc-2-aminomethyl-phenylacetic acid

2nd Building Block: Fmoc-4-benzoyl-L-phenylalanine

3rd Building Block: Fmoc-D-nipecotic acid



A15: Macrocycle was assembled using **general procedure for solid-phase peptide synthesis of macrocycle inhibitors**.

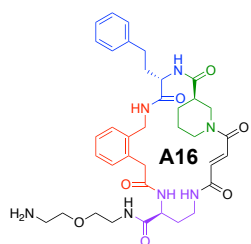
Resin: Bis-(2-aminoethyl)-ether trityl

4th Building Block: N^α-Fmoc-N^γ-allyloxycarbonyl-L-2,4-diaminobutyric acid

1st Building Block: Fmoc-2-aminomethyl-phenylacetic acid

2nd Building Block: Fmoc-*p*-phenyl-L-phenylalanine

3rd Building Block: Fmoc-D-nipecotic acid



A16: Macrocycle was assembled using **general procedure for solid-phase peptide synthesis of macrocycle inhibitors**.

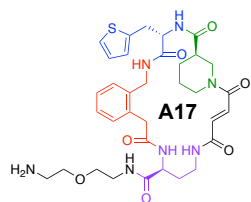
Resin: Bis-(2-aminoethyl)-ether trityl

4th Building Block: N^α-Fmoc-N^γ-allyloxycarbonyl-L-2,4-diaminobutyric acid

1st Building Block: Fmoc-2-aminomethyl-phenylacetic acid

2nd Building Block: Fmoc-L-Homophenylalanine

3rd Building Block: Fmoc-D-nipecotic acid



A17: Macrocycle was assembled using **general procedure for solid-phase peptide synthesis of macrocycle inhibitors**.

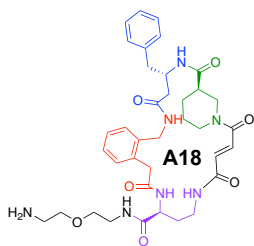
Resin: Bis-(2-aminoethyl)-ether trityl

4th Building Block: N^α-Fmoc-N^γ-allyloxycarbonyl-L-2,4-diaminobutyric acid

1st Building Block: Fmoc-2-aminomethyl-phenylacetic acid

2nd Building Block: Fmoc-β-(2-thienyl)-L-alanine

3rd Building Block: Fmoc-D-nipecotic acid



A18: Macrocycle was assembled using **general procedure for solid-phase peptide synthesis of macrocycle inhibitors**.

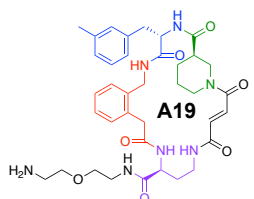
Resin: Bis-(2-aminoethyl)-ether trityl

4th Building Block: N^α-Fmoc-N^γ-allyloxycarbonyl-L-2,4-diaminobutyric acid

1st Building Block: Fmoc-2-aminomethyl-phenylacetic acid

2nd Building Block: Fmoc-L-β-homophenylalanine

3rd Building Block: Fmoc-D-nipecotic acid



A19: Macrocycle was assembled using **general procedure for solid-phase peptide synthesis of macrocycle inhibitors**.

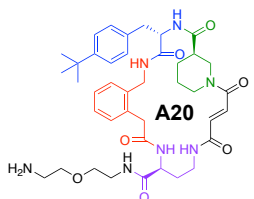
Resin: Bis-(2-aminoethyl)-ether trityl

4th Building Block: N^α-Fmoc-N^γ-allyloxycarbonyl-L-2,4-diaminobutyric acid

1st Building Block: Fmoc-2-aminomethyl-phenylacetic acid

2nd Building Block: Fmoc-3-methyl-L-phenylalanine

3rd Building Block: Fmoc-D-nipecotic acid



A20: Macrocycle was assembled using **general procedure for solid-phase peptide synthesis of macrocycle inhibitors**.

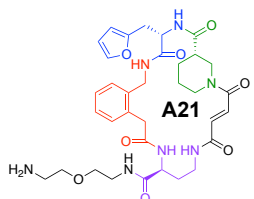
Resin: Bis-(2-aminoethyl)-ether trityl

4th Building Block: N^α-Fmoc-N^γ-allyloxycarbonyl-L-2,4-diaminobutyric acid

1st Building Block: Fmoc-2-aminomethyl-phenylacetic acid

2nd Building Block: Fmoc-4-*tert*-butyl-L-phenylalanine

3rd Building Block: Fmoc-D-nipecotic acid



A21: Macrocycle was assembled using **general procedure for solid-phase peptide synthesis of macrocycle inhibitors**.

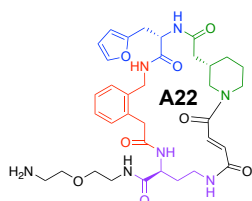
Resin: Bis-(2-aminoethyl)-ether trityl

4th Building Block: N^α-Fmoc-N^γ-allyloxycarbonyl-L-2,4-diaminobutyric acid

1st Building Block: Fmoc-2-aminomethyl-phenylacetic acid

2nd Building Block: Fmoc-β-(2-furyl)-Ala-OH

3rd Building Block: Fmoc-L-nipecotic acid



A22: Macrocycle was assembled using **general procedure for solid-phase peptide synthesis of macrocycle inhibitors**.

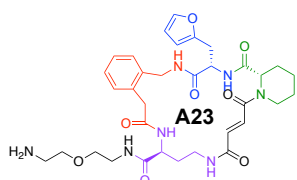
Resin: Bis-(2-aminoethyl)-ether trityl

4th Building Block: N^α-Fmoc-N^γ-allyloxycarbonyl-L-2,4-diaminobutyric acid

1st Building Block: Fmoc-2-aminomethyl-phenylacetic acid

2nd Building Block: Fmoc-β-(2-furyl)-Ala-OH

3rd Building Block: (S)-(1-Fmoc-piperidin-3-yl)acetic acid



A23: Macrocycle was assembled using **general procedure for solid-phase peptide synthesis of macrocycle inhibitors**.

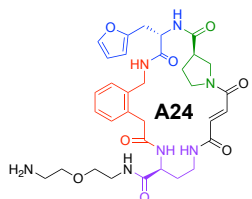
Resin: Bis-(2-aminoethyl)-ether trityl

4th Building Block: N^α-Fmoc-N^γ-allyloxycarbonyl-L-2,4-diaminobutyric acid

1st Building Block: Fmoc-2-aminomethyl-phenylacetic acid

2nd Building Block: Fmoc-β-(2-furyl)-Ala-OH

3rd Building Block: Fmoc-L-homoproline



A24: Macrocycle was assembled using **general procedure for solid-phase peptide synthesis of macrocycle inhibitors**.

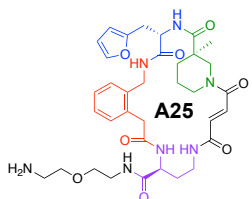
Resin: Bis-(2-aminoethyl)-ether trityl

4th Building Block: N^α-Fmoc-N^γ-allyloxycarbonyl-L-2,4-diaminobutyric acid

1st Building Block: Fmoc-2-aminomethyl-phenylacetic acid

2nd Building Block: Fmoc-β-(2-furyl)-Ala-OH

3rd Building Block: I3



A25: Macrocycle was assembled using **general procedure for solid-phase peptide synthesis of macrocycle inhibitors**.

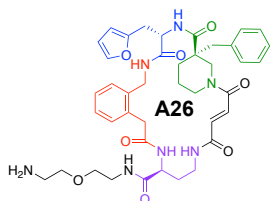
Resin: Bis-(2-aminoethyl)-ether trityl

4th Building Block: N^α-Fmoc-N^γ-allyloxycarbonyl-L-2,4-diaminobutyric acid

1st Building Block: Fmoc-2-aminomethyl-phenylacetic acid

2nd Building Block: Fmoc-β-(2-furyl)-Ala-OH

3rd Building Block: (R)-Fmoc-3-methyl-piperidine-3-carboxylic acid



A26: Macrocycle was assembled using **general procedure for solid-phase peptide synthesis of macrocycle inhibitors**.

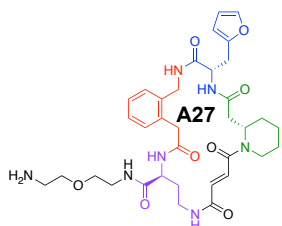
Resin: Bis-(2-aminoethyl)-ether trityl

4th Building Block: N^α-Fmoc-N^γ-allyloxycarbonyl-L-2,4-diaminobutyric acid

1st Building Block: Fmoc-2-aminomethyl-phenylacetic acid

2nd Building Block: Fmoc-β-(2-furyl)-Ala-OH

3rd Building Block: (S)-Fmoc-3-benzyl-piperidine-3-carboxylic acid



A27: Macrocycle was assembled using **general procedure for solid-phase peptide synthesis of macrocycle inhibitors**.

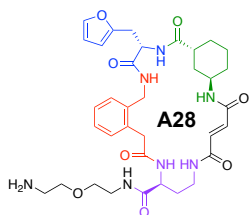
Resin: Bis-(2-aminoethyl)-ether trityl

4th Building Block: N^α-Fmoc-N^γ-allyloxycarbonyl-L-2,4-diaminobutyric acid

1st Building Block: Fmoc-2-aminomethyl-phenylacetic acid

2nd Building Block: Fmoc-β-(2-furyl)-Ala-OH

3rd Building Block: (S)-(1-Fmoc-piperidin-2-yl)acetic acid



A28: Macrocycle was assembled using **general procedure for solid-phase peptide synthesis of macrocycle inhibitors**.

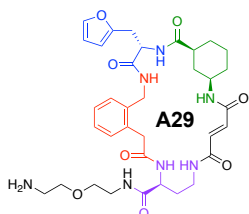
Resin: Bis-(2-aminoethyl)-ether trityl

4th Building Block: N^α-Fmoc-N^γ-allyloxycarbonyl-L-2,4-diaminobutyric acid

1st Building Block: Fmoc-2-aminomethyl-phenylacetic acid

2nd Building Block: Fmoc-β-(2-furyl)-Ala-OH

3rd Building Block: **I4**



A29: Macrocycle was assembled using **general procedure for solid-phase peptide synthesis of macrocycle inhibitors**.

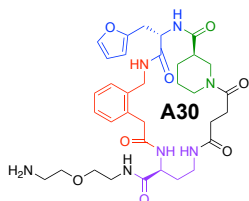
Resin: Bis-(2-aminoethyl)-ether trityl

4th Building Block: N^α-Fmoc-N^γ-allyloxycarbonyl-L-2,4-diaminobutyric acid

1st Building Block: Fmoc-2-aminomethyl-phenylacetic acid

2nd Building Block: Fmoc-β-(2-furyl)-Ala-OH

3rd Building Block: ((1S,3R)-3-(Fmoc-amino)cyclohexane-1-carboxylic acid)



A30: Macrocycle was assembled using **general procedure for solid-phase peptide synthesis of macrocycle inhibitors**, using conditions stipulated in 'trans' isomer procedure, but replacing allyl-fumarate-monoester+HATU with succinic anhydride.

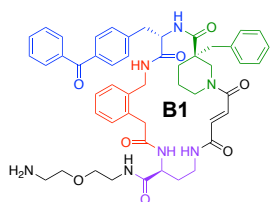
Resin: Bis-(2-aminoethyl)-ether trityl

4th Building Block: N^α-Fmoc-N^γ-allyloxycarbonyl-L-2,4-diaminobutyric acid

1st Building Block: Fmoc-2-aminomethyl-phenylacetic acid

2nd Building Block: Fmoc-β-(2-furyl)-Ala-OH

3rd Building Block: Fmoc-D-nipecotic acid



B1: Macrocycle was assembled using **general procedure for solid-phase peptide synthesis of macrocycle inhibitors**.

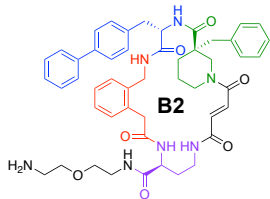
Resin: Bis-(2-aminoethyl)-ether trityl

4th Building Block: N^α-Fmoc-N^γ-allyloxycarbonyl-L-2,4-diaminobutyric acid

1st Building Block: Fmoc-2-aminomethyl-phenylacetic acid

2nd Building Block: Fmoc-4-benzoyl-L-phenylalanine

3rd Building Block: (S)-Fmoc-3-benzyl-piperidine-3-carboxylic acid



B2: Macrocycle was assembled using **general procedure for solid-phase peptide synthesis of macrocycle inhibitors**.

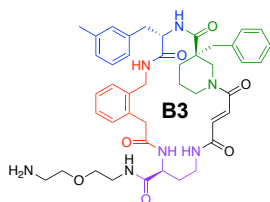
Resin: Bis-(2-aminoethyl)-ether trityl

4th Building Block: N^α-Fmoc-N^γ-allyloxycarbonyl-L-2,4-diaminobutyric acid

1st Building Block: Fmoc-2-aminomethyl-phenylacetic acid

2nd Building Block: Fmoc-*p*-phenyl-L-phenylalanine

3rd Building Block: (S)-Fmoc-3-benzyl-piperidine-3-carboxylic acid



B3: Macrocycle was assembled using **general procedure for solid-phase peptide synthesis of macrocycle inhibitors**.

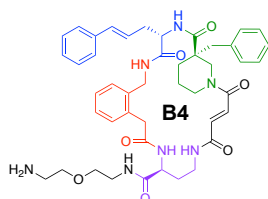
Resin: Bis-(2-aminoethyl)-ether trityl

4th Building Block: N^α-Fmoc-N^γ-allyloxycarbonyl-L-2,4-diaminobutyric acid

1st Building Block: Fmoc-2-aminomethyl-phenylacetic acid

2nd Building Block: Fmoc-3-methyl-L-phenylalanine

3rd Building Block: (S)-Fmoc-3-benzyl-piperidine-3-carboxylic acid



B4: Macrocycle was assembled using **general procedure for solid-phase peptide synthesis of macrocycle inhibitors**.

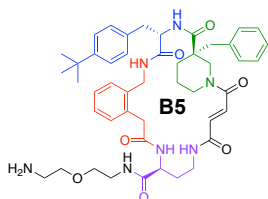
Resin: Bis-(2-aminoethyl)-ether trityl

4th Building Block: N^α-Fmoc-N^γ-allyloxycarbonyl-L-2,4-diaminobutyric acid

1st Building Block: Fmoc-2-aminomethyl-phenylacetic acid

2nd Building Block: Fmoc-3-styryl-L-alanine

3rd Building Block: (S)-Fmoc-3-benzyl-piperidine-3-carboxylic acid



B5: Macrocycle was assembled using **general procedure for solid-phase peptide synthesis of macrocycle inhibitors**.

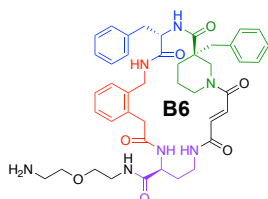
Resin: Bis-(2-aminoethyl)-ether trityl

4th Building Block: N^α-Fmoc-N^γ-allyloxycarbonyl-L-2,4-diaminobutyric acid

1st Building Block: Fmoc-2-aminomethyl-phenylacetic acid

2nd Building Block: Fmoc-4-*tert*-butyl-L-phenylalanine

3rd Building Block: (S)-Fmoc-3-benzyl-piperidine-3-carboxylic acid



B6: Macrocycle was assembled using **general procedure for solid-phase peptide synthesis of macrocycle inhibitors**.

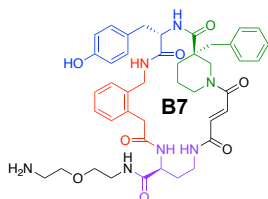
Resin: Bis-(2-aminoethyl)-ether trityl

4th Building Block: N^α-Fmoc-N^γ-allyloxycarbonyl-L-2,4-diaminobutyric acid

1st Building Block: Fmoc-2-aminomethyl-phenylacetic acid

2nd Building Block: Fmoc-L-phenylalanine

3rd Building Block: (S)-Fmoc-3-benzyl-piperidine-3-carboxylic acid



B7: Macrocycle was assembled using **general procedure for solid-phase peptide synthesis of macrocycle inhibitors**.

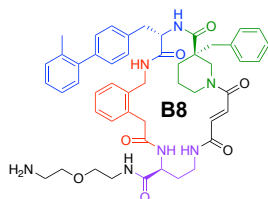
Resin: Bis-(2-aminoethyl)-ether trityl

4th Building Block: N^α-Fmoc-N^γ-allyloxycarbonyl-L-2,4-diaminobutyric acid

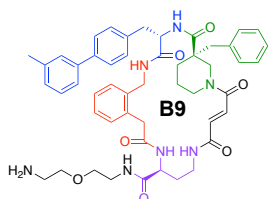
1st Building Block: Fmoc-2-aminomethyl-phenylacetic acid

2nd Building Block: **Fmoc-O-*tert*-butyl-L-tyrosine**

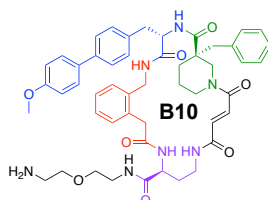
3rd Building Block: (S)-Fmoc-3-benzyl-piperidine-3-carboxylic acid



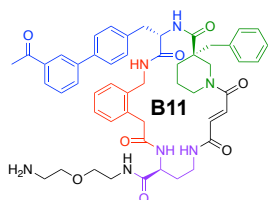
B8: Compound was synthesized using **Generalized procedure A for Suzuki-Miyaura cross-coupling of macrocycles** using **(4Br)B6** and 2-methylphenylboronic acid. Yield: 78%



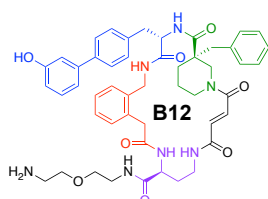
B9: Compound was synthesized using **Generalized procedure A for Suzuki-Miyaura cross-coupling of macrocycles** using **(4Br)B6** and 3-methylphenylboronic acid. Yield: 64%



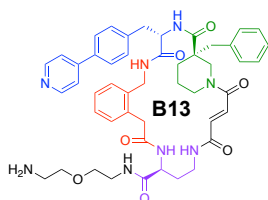
B10: Compound was synthesized using **Generalized procedure A for Suzuki-Miyaura cross-coupling of macrocycles** using **(4Br)B6** and 4-methoxyphenylboronic acid. Yield: 21%



B11: Compound was synthesized using **Generalized procedure A for Suzuki-Miyaura cross-coupling of macrocycles** using **(4Br)B6** and 3-acetylphenylboronic acid. Yield: 37%



B12: Compound was synthesized using **Generalized procedure A for Suzuki-Miyaura cross-coupling of macrocycles** using **(4Br)B6** and 3-hydroxyphenylboronic acid. Yield: 87%



B13: Macrocycle was assembled using **general procedure for solid-phase peptide synthesis of macrocycle inhibitors**.

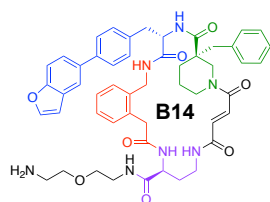
Resin: Bis-(2-aminoethyl)-ether trityl

4th Building Block: N^α-Fmoc-N^γ-allyloxycarbonyl-L-2,4-diaminobutyric acid

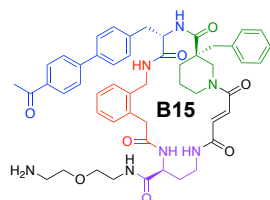
1st Building Block: Fmoc-2-aminomethyl-phenylacetic acid

2nd Building Block: I5

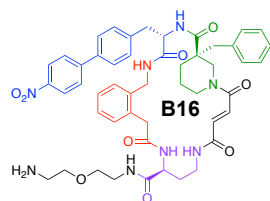
3rd Building Block: (S)-Fmoc-3-benzyl-piperidine-3-carboxylic acid



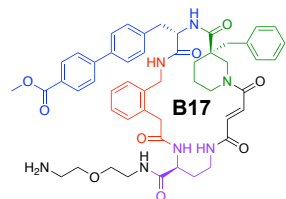
B14: Compound was synthesized using **Generalized procedure A for Suzuki-Miyaura cross-coupling of macrocycles** using **(4Br)B6** and benzofuran-5-yl-5-boronic acid. Yield: quantitative



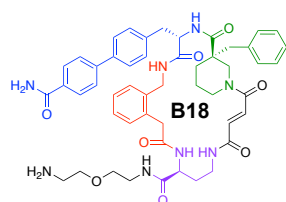
B15 Compound: Compound was synthesized using **Generalized procedure A for Suzuki-Miyaura cross-coupling of macrocycles** using **(4Br)B6** and 4-acetylphenylboronic acid. Yield: 39%



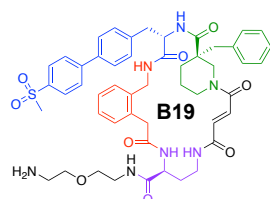
B16: Compound was synthesized using **Generalized procedure A for Suzuki-Miyaura cross-coupling of macrocycles** using **(4Br)B6** and 4-nitrophenylboronic acid. Yield: 60%



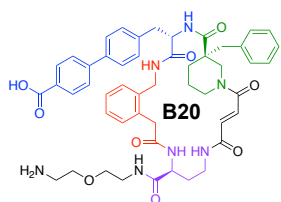
B17: Compound was synthesized using **Generalized procedure A for Suzuki-Miyaura cross-coupling of macrocycles** using **(4Br)B6** and 4-Methoxycarbonylphenylboronic. Yield: 37%



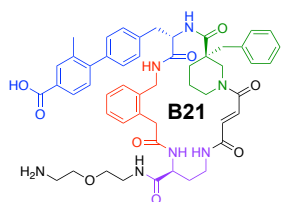
B18: Compound was synthesized using **Generalized procedure A for Suzuki-Miyaura cross-coupling of macrocycles** using **(4Br)B6** and 4-aminocarbonylphenylboronic acid. Yield: 49%



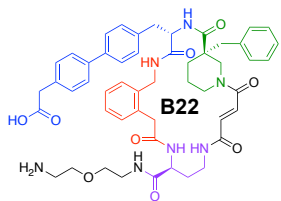
B19: Compound was synthesized using **Generalized procedure A** for **Suzuki-Miyaura cross-coupling of macrocycles** using **(4Br)B6** and 4-(methanesulfonyl)phenylboronic acid. Yield: 86%



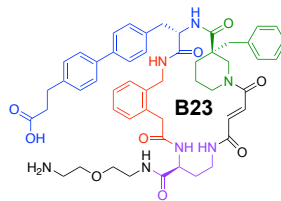
B20: Compound was synthesized using **Generalized procedure A** for **Suzuki-Miyaura cross-coupling of macrocycles** using **(4Br)B6** and 4-(*tert*-Butoxycarbonyl)phenylboronic acid. *Tert*-butyl protected product was treated with 1 mL TFA for 1 hour, and re-purified under same HPLC conditions to yield carboxylic acid product. Yield: 95%



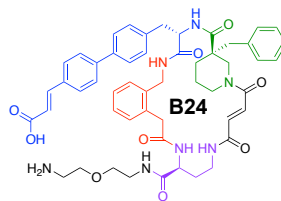
B21: Compound was synthesized using **Generalized procedure A** for **Suzuki-Miyaura cross-coupling of macrocycles** using **(4Br)B6** and 4-carboxy-2-methylphenylboronic acid. Yield: 35%



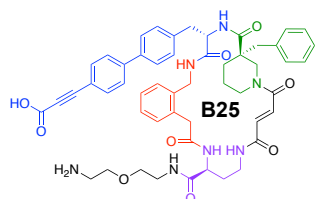
B22: Compound was synthesized using **Generalized procedure A** for **Suzuki-Miyaura cross-coupling of macrocycles** using **(4Br)B6** and 4-carboxymethylphenylboronic acid. Yield: 19%



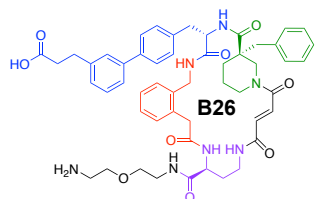
B23: Compound was synthesized using **Generalized procedure A** for **Suzuki-Miyaura cross-coupling of macrocycles** using **(4Br)B6** and 4-cyanomethylphenylboronic acid. Yield: 21%



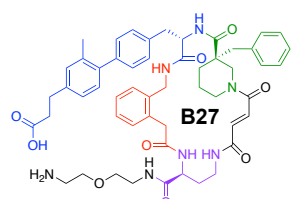
B24: Compound was synthesized using **Generalized procedure B** for **Suzuki-Miyaura cross-coupling of macrocycles** using **(4Br)B6** and 4-(*E*-2-carboxyvinyl)phenylboronic acid. Yield: 20%



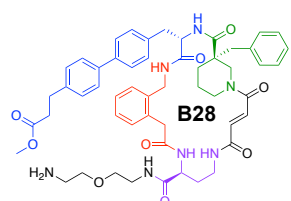
B25: Compound was synthesized using **Generalized procedure A for Suzuki-Miyaura cross-coupling of macrocycles** using **(4Br)B6** and **I6b**. *Tert*-butyl protected product was treated with 1 mL TFA for 1 hour, and re-purified under same HPLC conditions to yield carboxylic acid product. Yield: 15%



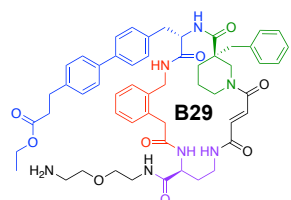
B26: Compound was synthesized using **Generalized procedure A for Suzuki-Miyaura cross-coupling of macrocycles** using **(4Br)B6** and 3-(carboxyethyl)phenylboronic acid. Yield: 9%



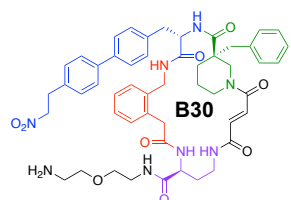
B27: Compound was synthesized using **Generalized procedure A for Suzuki-Miyaura cross-coupling of macrocycles** using **(4Br)B6** and 4-(2-carboxyethyl)-2-methylphenylboronic acid. Yield: 16%



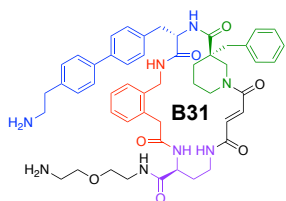
B28: Compound was synthesized using **Generalized procedure A for Suzuki-Miyaura cross-coupling of macrocycles** using **(4Br)B6** and 4-(methoxycarbonyl)ethylphenylboronic acid. Yield: 72%



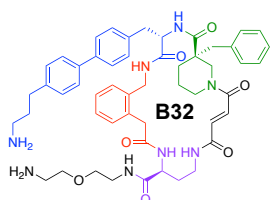
B29: Compound was synthesized using **Generalized procedure A for Suzuki-Miyaura cross-coupling of macrocycles** using **(4Br)B6** and 4-(2-ethoxycarbonyl)ethylphenylboronic acid. Yield: 29%



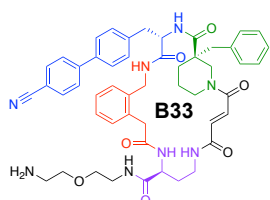
B30: Compound was synthesized using **Generalized procedure A for Suzuki-Miyaura cross-coupling of macrocycles** using **(4Br)B6** and 4-(2-nitroethyl)phenylboronic acid. Yield: 18%



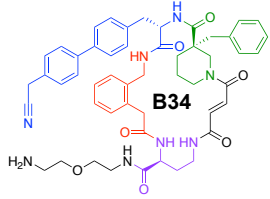
B31: Compound was synthesized using **Generalized procedure A for Suzuki-Miyaura cross-coupling of macrocycles** using **(4Br)B6** and 4-(2-[(tert-Butoxycarbonyl)amino]ethyl)phenyl)boronic acid. Prior to HPLC purification, crude reaction was concentrated under vacuum and treated with 0.3 mL TFA for 1 hour for boc-deprotection. Reaction was concentrated and purified as stipulated in generalized procedure. Yield: 48%



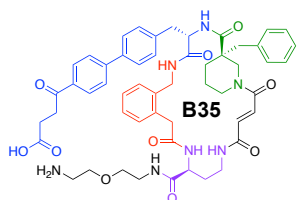
B32: Compound was synthesized using **Generalized procedure A for Suzuki-Miyaura cross-coupling of macrocycles** using **(4Br)B6** and [4-(3-[[[(tert-Butoxy)carbonyl]amino]propyl]phenyl)]boronic acid. Prior to HPLC purification, crude reaction was concentrated under vacuum and treated with 0.3 mL TFA for 1 hour for boc-deprotection. Reaction was concentrated and purified as stipulated in generalized procedure. Yield: 20%



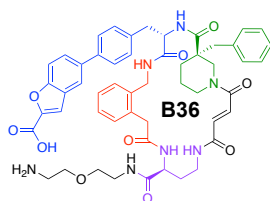
B33: Compound was synthesized using **Generalized procedure A for Suzuki-Miyaura cross-coupling of macrocycles** using **(4Br)B6** and 4-cyanophenylboronic acid. Yield: 30%



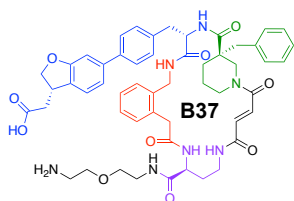
B34: Compound was synthesized using **Generalized procedure A for Suzuki-Miyaura cross-coupling of macrocycles** using **(4Br)B6** and 4-cyanomethylphenylboronic acid. Yield: 46%



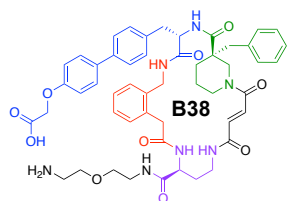
B35: Compound was synthesized using **Generalized procedure A for Suzuki-Miyaura cross-coupling of macrocycles** using **(4Br)B6** and **I7b**. Yield: 6%



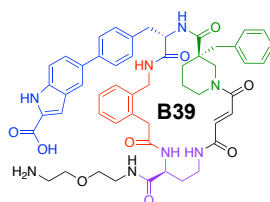
B36: Compound was synthesized using **Generalized procedure A** for Suzuki-Miyaura cross-coupling of macrocycles using **(4Br)B6** and **I8b**. Yield: 12%



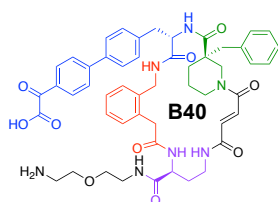
B37: Compound was synthesized using **Generalized procedure A** for Suzuki-Miyaura cross-coupling of macrocycles using **(4Br)B6** and **I9d**. Yield: 25%



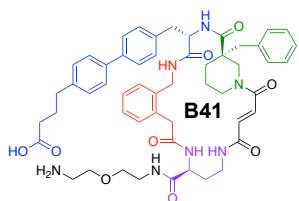
B38: Compound was synthesized using **Generalized procedure A** for Suzuki-Miyaura cross-coupling of macrocycles using **(4Br)B6** and 4-(carboxymethoxy)phenylboronic acid. Yield: 9%



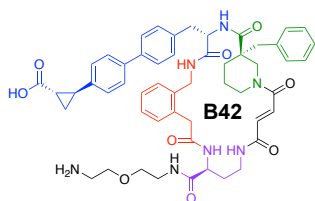
B39: Compound was synthesized using **Generalized procedure B** for Suzuki-Miyaura cross-coupling of macrocycles using **(4Br)B6** and **I10**. Yield: 5%



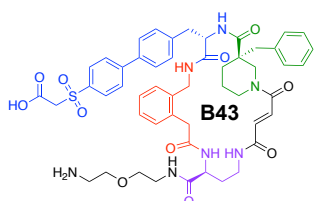
B40: Adopting a previously reported protocol⁹, into a 10 mL screw-top vial, **(4Br)B6** (0.011 mmol, 1.0 eq), **I11** (03_263) (0.11 mmol, 10 eq), Bis(dibenzylideneacetone)palladium(0) (0.0011 mmol, 0.1 eq), Tri-*tert*-butylphosphonium tetrafluoroborate (0.0046 mmol, 0.4 eq), and potassium carbonate (0.11 mmol, 10 eq) were combined and sealed with a septum. Flask was evacuated and refilled with N₂ three times and left under N₂. Degassed 10:1 Toluene/H₂O (0.05 M), was then added to the sealed flask and allowed to stir at 60° C for 16 hours. After cooling, the reaction was cooled and solvent was removed under high-vac. Solid residue was dissolved in a minimal amount of 3:1 DMF/water with 5% TFA and filtered through 0.22 μL Ultrafree®-MC Centrifugal Filters (Milipore-Sigma). Sample was then purified by reverse HPLC, with a 10-60% Fractions that contained product was then freeze dried to produce a white powder. Yield: 10% (03_265)



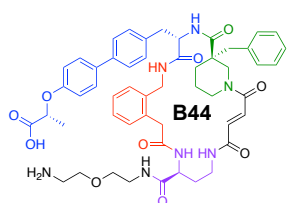
B41: Compound was synthesized using **Generalized procedure A** for Suzuki-Miyaura cross-coupling of macrocycles using **(4Br)B6** and **I12b**. Yield: 14%



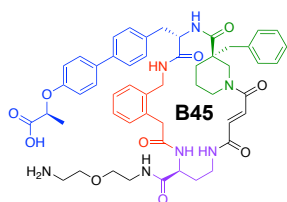
B42: Compound was synthesized using **Generalized procedure B** for Suzuki-Miyaura cross-coupling of macrocycles using **(4Br)B6** and **I13b**. Yield: 31%



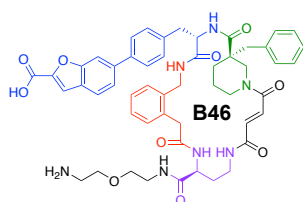
B43: Compound was synthesized using **Generalized procedure A** for Suzuki-Miyaura cross-coupling of macrocycles using **(4Br)B6** and **I14c**. *Tert*-butyl protected product was treated with 1 mL TFA for 1 hour, and re-purified under same HPLC conditions to yield carboxylic acid product. Yield: 11%



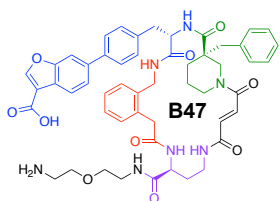
B44: Compound was synthesized using **Generalized procedure A** for Suzuki-Miyaura cross-coupling of macrocycles using **(4Br)B6** and **I15d**. Yield: 8%



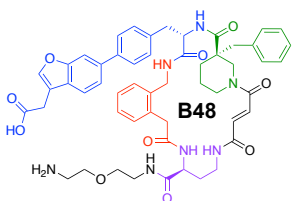
B45: Compound was synthesized using **Generalized procedure A** for Suzuki-Miyaura cross-coupling of macrocycles using **(4Br)B6** and **I16b**. Yield: 16%



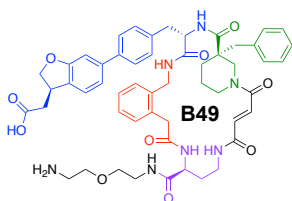
B46: Compound was synthesized using **Generalized procedure B** for Suzuki-Miyaura cross-coupling of macrocycles using **(4Br)B6** and **I17d**. Yield: 4%



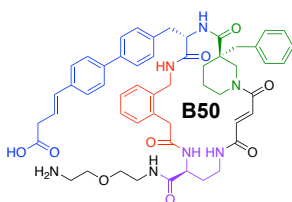
B47: Compound was synthesized using **Generalized procedure B** for Suzuki-Miyaura cross-coupling of macrocycles using **(4Br)B6** and **I18c**. Yield: 8%



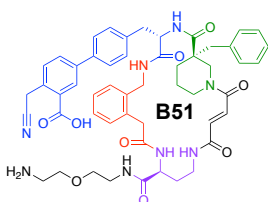
B48: Compound was synthesized using **Generalized procedure A** for Suzuki-Miyaura cross-coupling of macrocycles using **(4Br)B6** and **I19e**. Yield: 5%



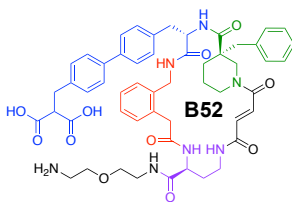
B49: Compound was synthesized using **Generalized procedure A** for Suzuki-Miyaura cross-coupling of macrocycles using **(4Br)B6** and **I20d**. Yield: 5%



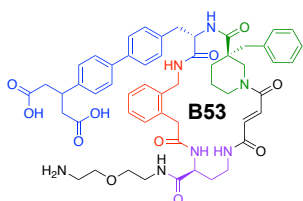
B50: Compound was synthesized using **Generalized procedure B** for Suzuki-Miyaura cross-coupling of macrocycles using **(4Br)B6** and **I21b**. Yield: 8%



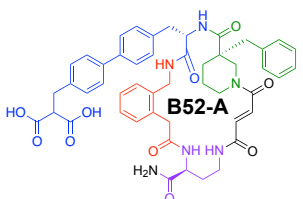
B51: Compound was synthesized using **Generalized procedure B** for Suzuki-Miyaura cross-coupling of macrocycles using **(4Br)B6** and **I22c**. Yield: 18%



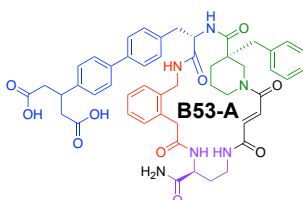
B52: Compound was synthesized using **Generalized procedure A** for Suzuki-Miyaura cross-coupling of macrocycles using **(4Br)B6** and **I23**. *Tert*-butyl protected product was treated with 1 mL TFA for 1 hour, and re-purified under same HPLC conditions to yield carboxylic acid product. Yield: 10%



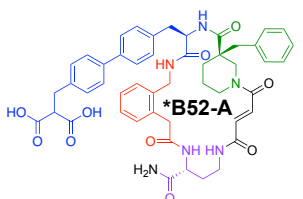
B53: Compound was synthesized using **Generalized procedure A for Suzuki-Miyaura cross-coupling of macrocycles** using **(4Br)B6** and **I24c**. *Tert*-butyl protected product was treated with 1 mL TFA for 1 hour, and re-purified under same HPLC conditions to yield carboxylic acid product. Yield: 21%



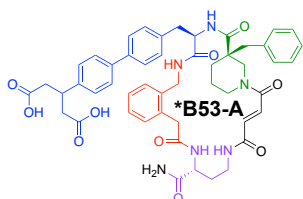
B52-A: Compound was synthesized using **Generalized procedure A for Suzuki-Miyaura cross-coupling of macrocycles** using **(4Br)B6-A** and **I23**. *Tert*-butyl protected product was treated with 1 mL TFA for 1 hour, and re-purified under same HPLC conditions to yield carboxylic acid product. Yield: 40%



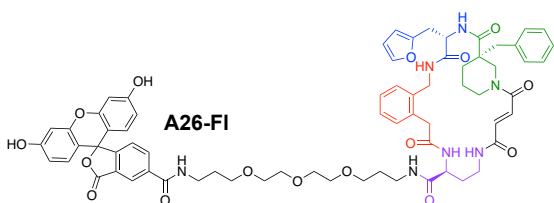
B53-A: Compound was synthesized using **Generalized procedure A for Suzuki-Miyaura cross-coupling of macrocycles** using **(4Br)B6-A** and **I24c**. *Tert*-butyl protected product was treated with 1 mL TFA for 1 hour, and re-purified under same HPLC conditions to yield carboxylic acid product. Yield: 86%



***B52-A:** Compound was synthesized using **Generalized procedure A for Suzuki-Miyaura cross-coupling of macrocycles** using ***(4Br)B6-A** and **I23**. *Tert*-butyl protected product was treated with 1 mL TFA for 1 hour, and re-purified under same HPLC conditions to yield carboxylic acid product. Yield: 21%.



***B53-A:** Compound was synthesized using **Generalized procedure A for Suzuki-Miyaura cross-coupling of macrocycles** using ***(4Br)B6-A** and **I24c**. *Tert*-butyl protected product was treated with 1 mL TFA for 1 hour, and re-purified under same HPLC conditions to yield carboxylic acid product. Yield: 85%.



A26-FI: Macrocycle was assembled using **general procedure for solid-phase peptide synthesis of macrocycle inhibitors**. Prior to acidic cleavage, resin was suspended with three 1-hour treatments of 1M hydroxybenzotriazole monohydrate dissolved in 1:1 CH₂Cl₂/Trifluoroethanol to remove Mmt group. 5-carboxyfluorescein (5 eq) and (HATU, 4.75 equiv.) were dissolved in a separate flask in ~10-15 mL DMF then treated with *N,N'*-diisopropylethylamine (DIPEA, 10 eq) for 5 minutes, observing a color change. This flask was then transferred to resin swollen in ~10 mL DMF and allowed to mix for 24 hours. Fluorescein labeled peptide were then cleaved from resin and purified as described in general procedure.

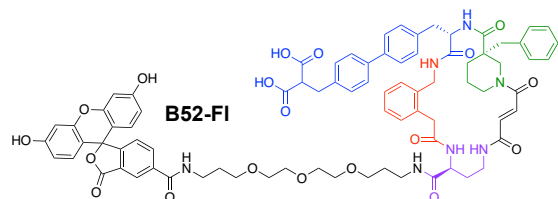
Resin: Universal PEG NovaTag™_Resin

4th Building Block: N^α-Fmoc-N^γ-allyloxycarbonyl-L-2,4-diaminobutyric acid

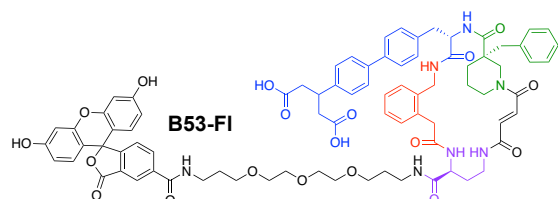
1st Building Block: Fmoc-2-aminomethyl-phenylacetic acid

2nd Building Block: Fmoc-β-(2-furyl)-Ala-OH

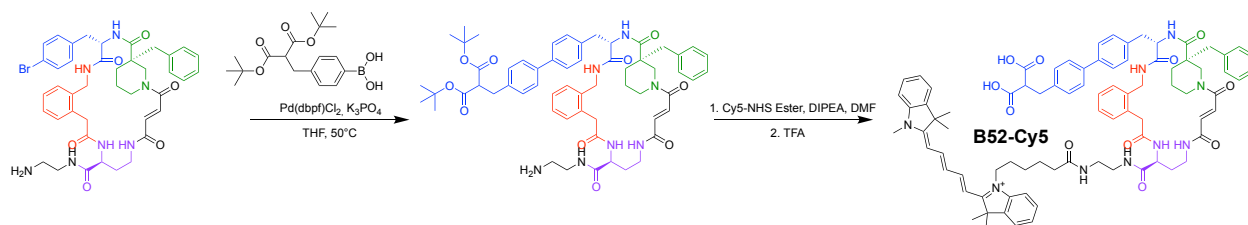
3rd Building Block: (S)-Fmoc-3-benzyl-piperidine-3-carboxylic acid



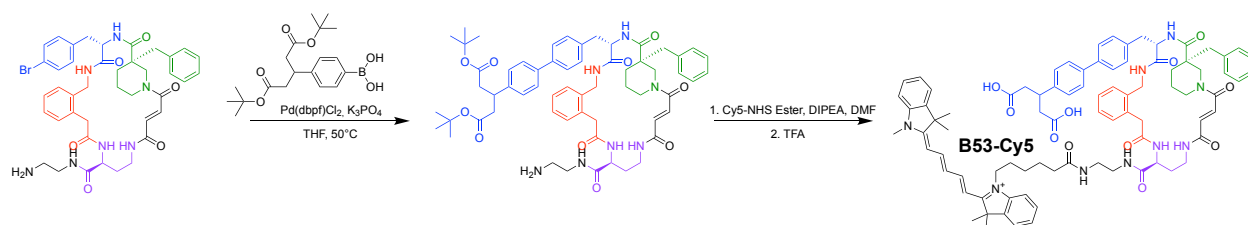
B52-FI: Compound was synthesized using **Generalized procedure A for Suzuki-Miyaura cross-coupling of macrocycles** using **(4Br)B6-FI** and **I23**. *Tert*-butyl protected product was treated with 1 mL TFA for 1 hour, and re-purified under same HPLC conditions to yield carboxylic acid product. Yield: 32%.



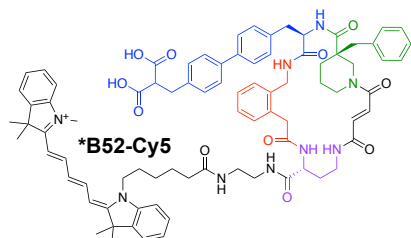
B53-FI: Compound was synthesized using **Generalized procedure A for Suzuki-Miyaura cross-coupling of macrocycles** using **(4Br)B6-FI** and **I24c**. *Tert*-butyl protected product was treated with 1 mL TFA for 1 hour, and re-purified under same HPLC conditions to yield carboxylic acid product. Yield: 33%



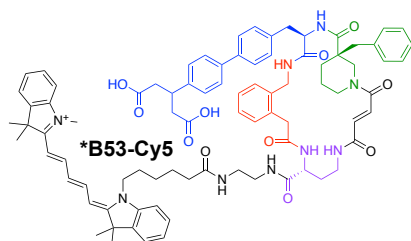
B52-Cy5: Compound was synthesized using **Generalized procedure A for Suzuki-Miyaura cross-coupling of macrocycles** using **(4Br)B6-B** and **I23**. *Tert*-butyl protected product was dissolved in a 1.5 mL Eppendorf tube with 100 μ L DMF and mixed with DIPEA (5 eq.). Cy5-NHS ester (Lumiprobe) (2 eq.) dissolved in 50 μ L DMF was then added to the flask allowed to stir for 1 hour. Resulting crude mixture was purified under same HPLC conditions to yield Cy5 coupled product. This product was then treated with 1 mL TFA for 1 hour, and re-purified under same HPLC conditions to yield carboxylic acid product. Yield: 25%.



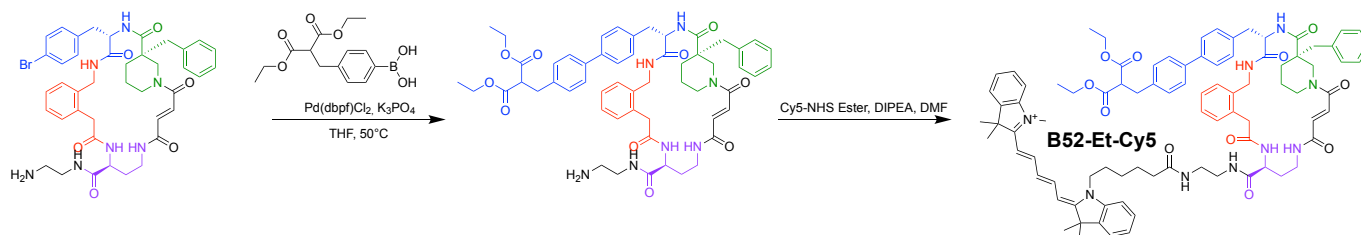
B53-Cy5: Compound was synthesized using **Generalized procedure A for Suzuki-Miyaura cross-coupling of macrocycles** using **(4Br)B6-B** and **I24c**. *Tert*-butyl protected product was dissolved in a 1.5 mL Eppendorf tube with 100 μ L DMF and mixed with DIPEA (5 eq.). Cy5-NHS ester (Lumiprobe) (2 eq.) dissolved in 50 μ L DMF was then added to the flask allowed to stir for 1 hour. Resulting crude mixture was purified under same HPLC conditions to yield Cy5 coupled product. This product was then treated with 1 mL TFA for 1 hour, and re-purified under same HPLC conditions to yield carboxylic acid product. Yield: 6%.



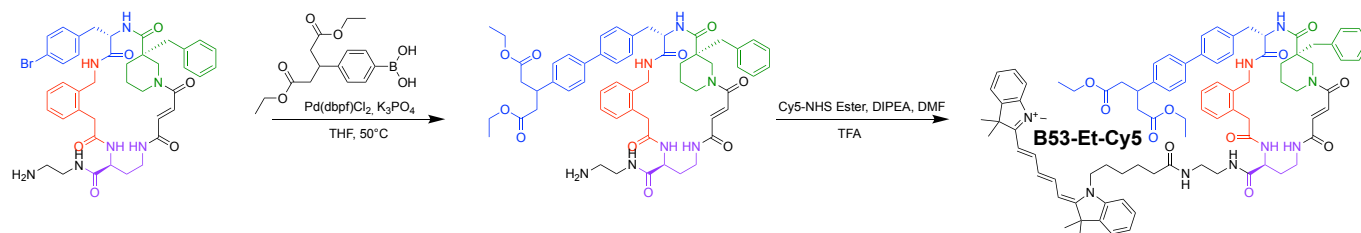
***B52-Cy5:** Compound was synthesized as described in **B52-Cy5** using ***(4Br)B6-B** as starting material. Yield: 6%



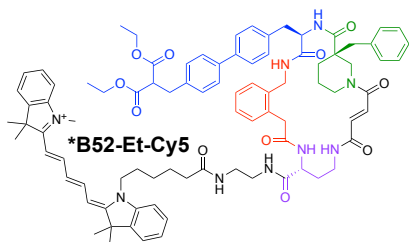
***B53-Cy5:** Compound was synthesized as described in **B53-Cy5** using ***(4Br)B6-B** as starting material. Yield: 8%.



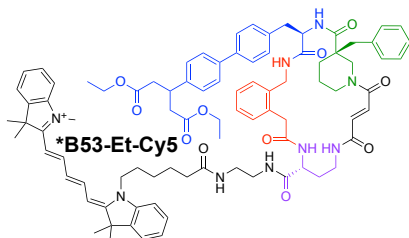
B52-Et-Cy5: Compound was synthesized using **Generalized procedure A for Suzuki-Miyaura cross-coupling of macrocycles** using **(4Br)B6-B** and **I29b**. Suzuki product was dissolved in a 1.5 mL Eppendorf tube with 100 μ L DMF and mixed with DIPEA (5 eq.). Cy5-NHS ester (Lumiprobe) (2 eq.) dissolved in 50 μ L DMF was then added to the flask allowed to stir for 1 hour. Excess Cy5-NHS ester was quenched with N-Acetyethylenediamine (10 eq.), to make **Cy5-enAc**. Resulting crude mixture was purified under same HPLC conditions to yield the two Cy5 coupled products. Yield: 20%



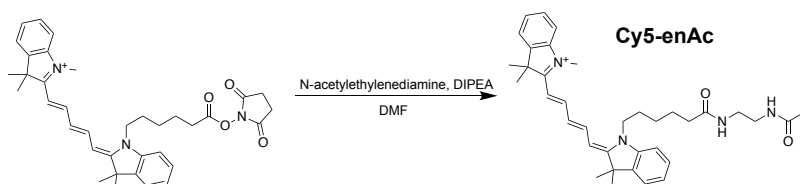
B53-Et-Cy5: Compound was synthesized using **Generalized procedure A for Suzuki-Miyaura cross-coupling of macrocycles** using **(4Br)B6-B** and **I30c**. Suzuki product was dissolved in a 1.5 mL Eppendorf tube with 100 μ L DMF and mixed with DIPEA (5 eq.). Cy5-NHS ester (Lumiprobe) (2 eq.) dissolved in 50 μ L DMF was then added to the flask allowed to stir for 1 hour. Excess Cy5-NHS ester was quenched with N-Acetyethylenediamine (10 eq.), to make **Cy5-enAc**. Resulting crude mixture was purified under same HPLC conditions to yield the two Cy5 coupled products. Yield: 21%



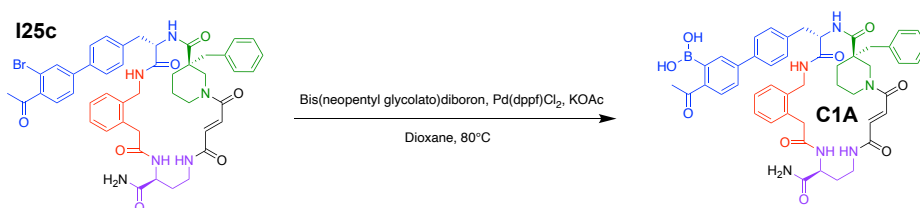
***B52-Et-Cy5:** Compound was synthesized as described in **B52-Et-Cy5** using ***(4Br)B6-B** as starting material. Yield: 18%



***B53-Et-Cy5:** Compound was synthesized as described in **B53-Et-Cy5** using ***(4Br)B6-B** as starting material. Yield: 17%.

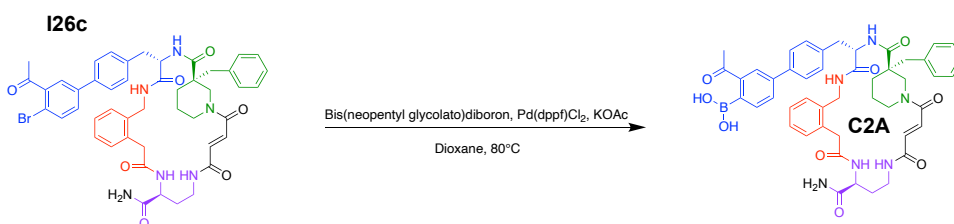


Cy5-enAc: Compound was isolated from excess Cy5-NHS ester that was quenched with N-Acetyllethylenediamine (10 eq.) during syntheses of **B52-Et-Cy5** and **B53-Et-Cy5**. HPLC purification was able to separate **Cy5-enAc** successfully from **B52-Et-Cy5** and **B53-Et-Cy5**.

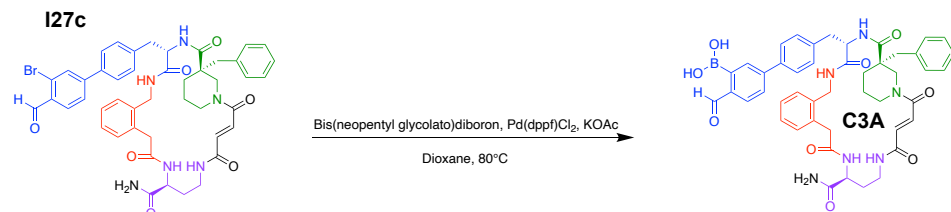


C1A: A mixture of **I25c** (0.008 mmol, 1 eq.), bis (neopentyl glycolato) diboron (0.08 mmol, 10 eq.), [1,1-Bis(diphenylphosphino)ferrocene]dichloropalladium(II) (0.001 mmol, 0.2 eq.), and KOAc (0.08 mmol, 10 eq.) was dissolved in 1 mL 1,4-dioxane (0.008 M). The reaction was stirred for thirty minutes at 80°C. The reaction was then cooled down to room temperature, solvent removed under vacuum, dissolved in DMF, and filtered. The crude product was purified by reverse-phase HPLC using 10-80% acetonitrile in water in 0.1% trifluoroacetic acid and lyophilized to afford **C1A**. Yield: 20% yield

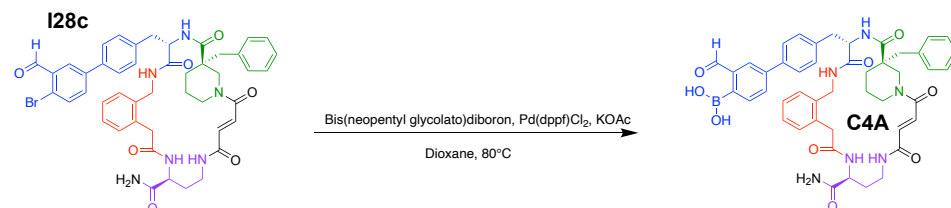
Authors Note: Bis(neopentyl glycolato) and the shorter 30-minute reaction time was due to significant protodeborylation observed with bis(pinacolato)diboron and longer reaction times.



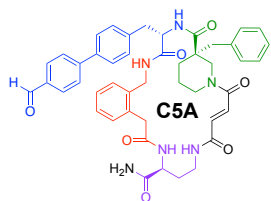
C2A: Compound was synthesized and purified as described in **C1A** with **I26c**, affording **C2A**. Yield: 29%



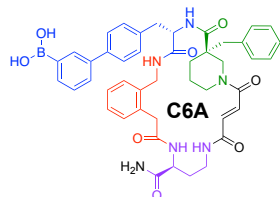
C3A: Compound was synthesized and purified as described in **C1A** with **I27c**, affording **C3A**. Yield: 14%



C4A: Compound was synthesized and purified as described in **C1A** with **I28c**, affording **C4A**. Some impurities were observed by $^1\text{H-NMR}$ that were unable to be removed by HPLC, compound was tested without further purification. Yield: 4%

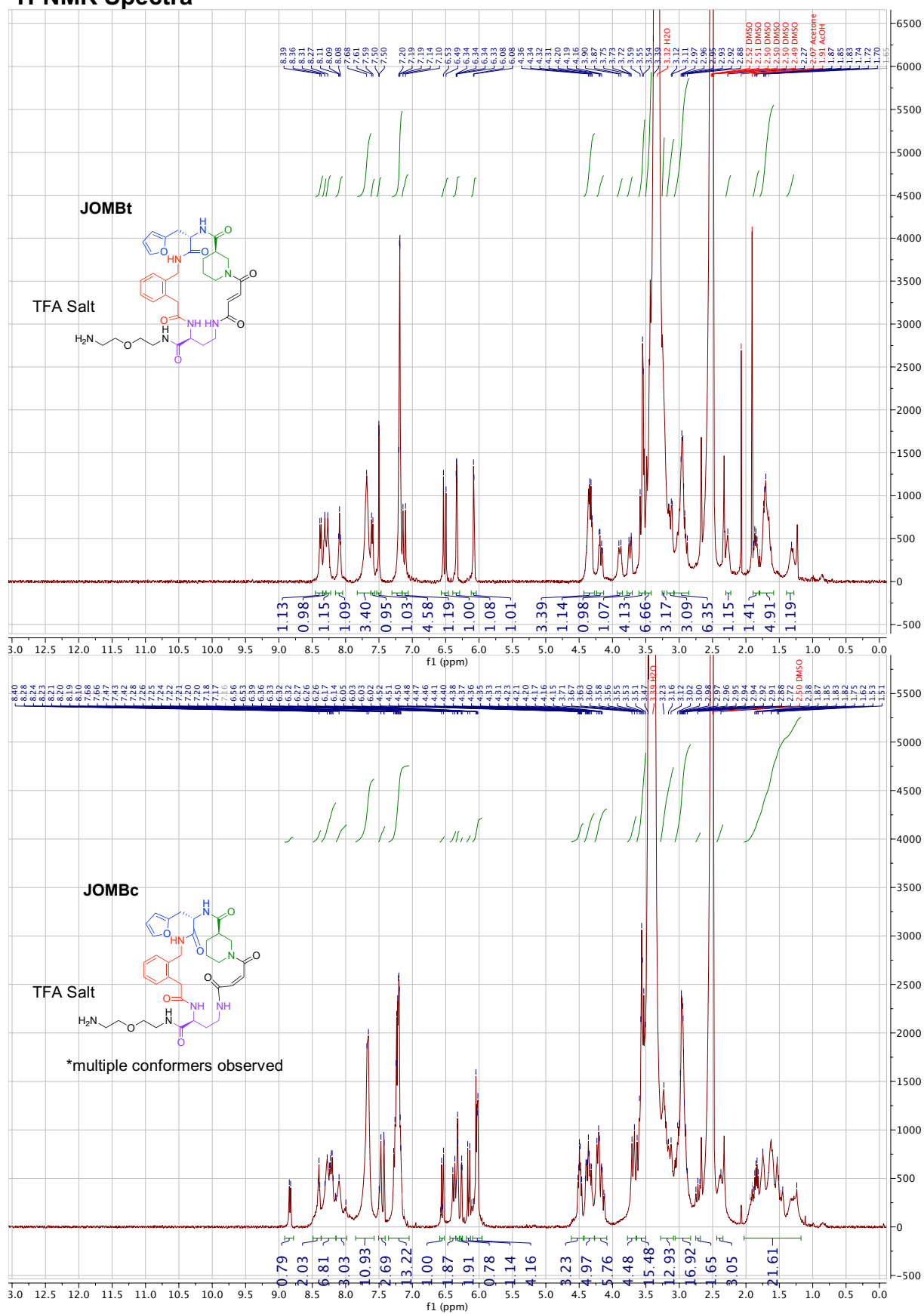


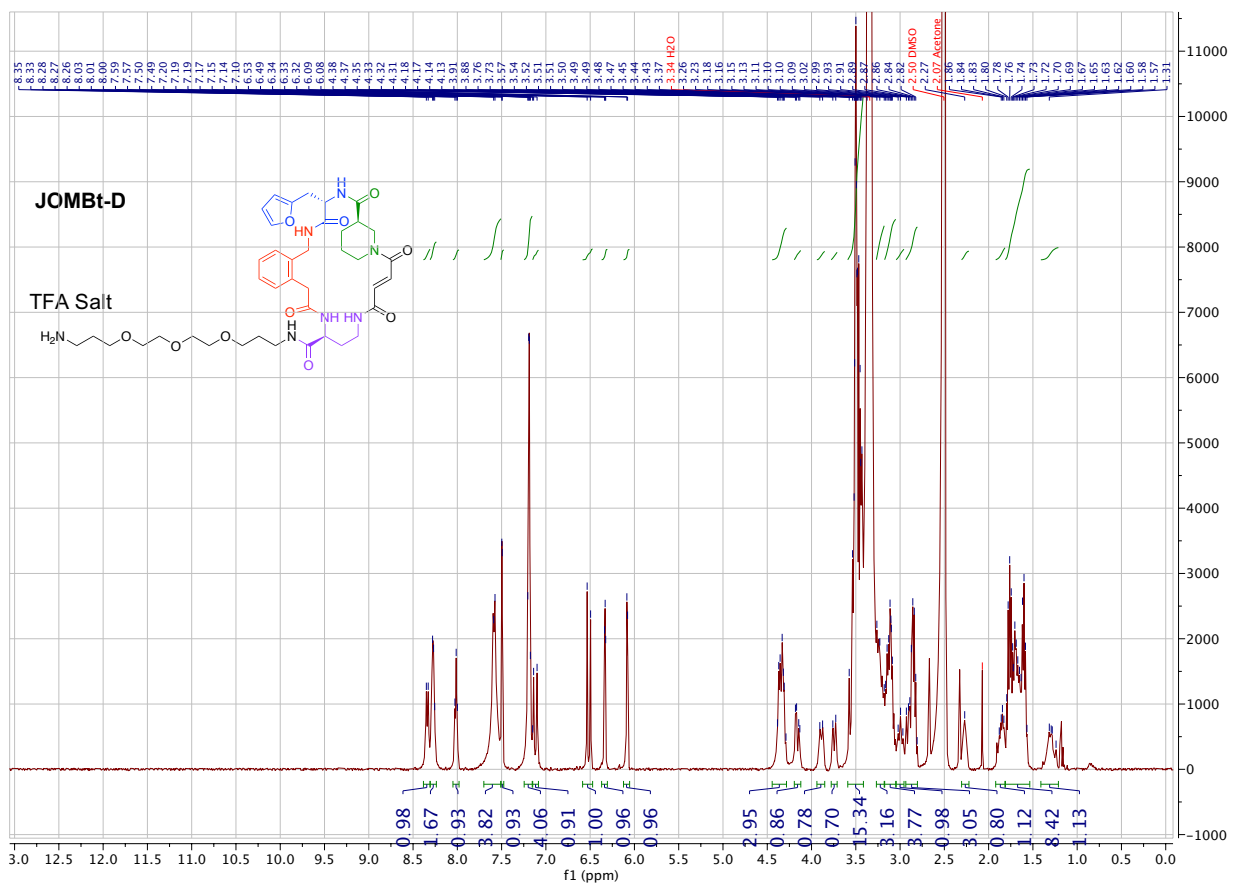
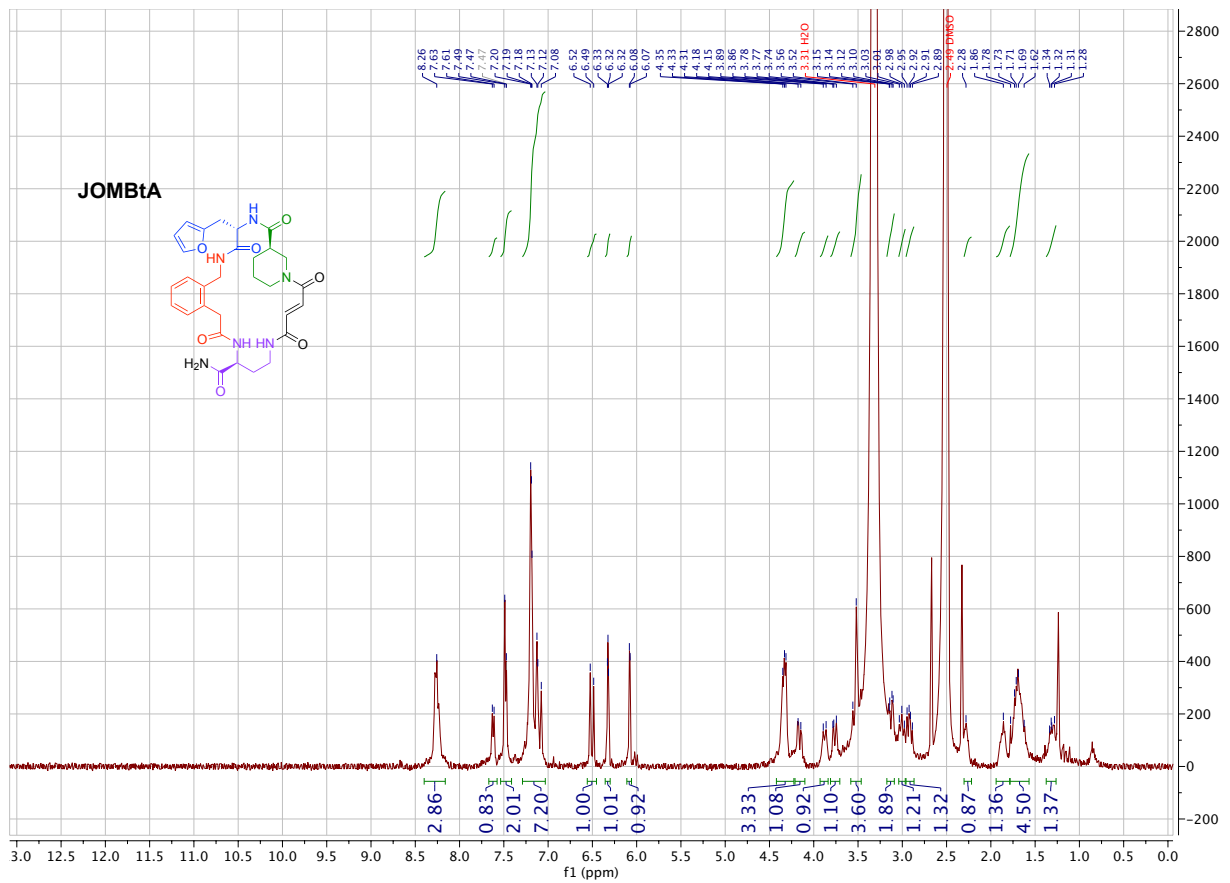
C5A: Compound was synthesized according to **Generalized procedure A for Suzuki-Miyaura cross-coupling of macrocycles** with **(4Br)B6-A** and 4-formylphenylboronic acid, affording **C5A**. Yield: 16%

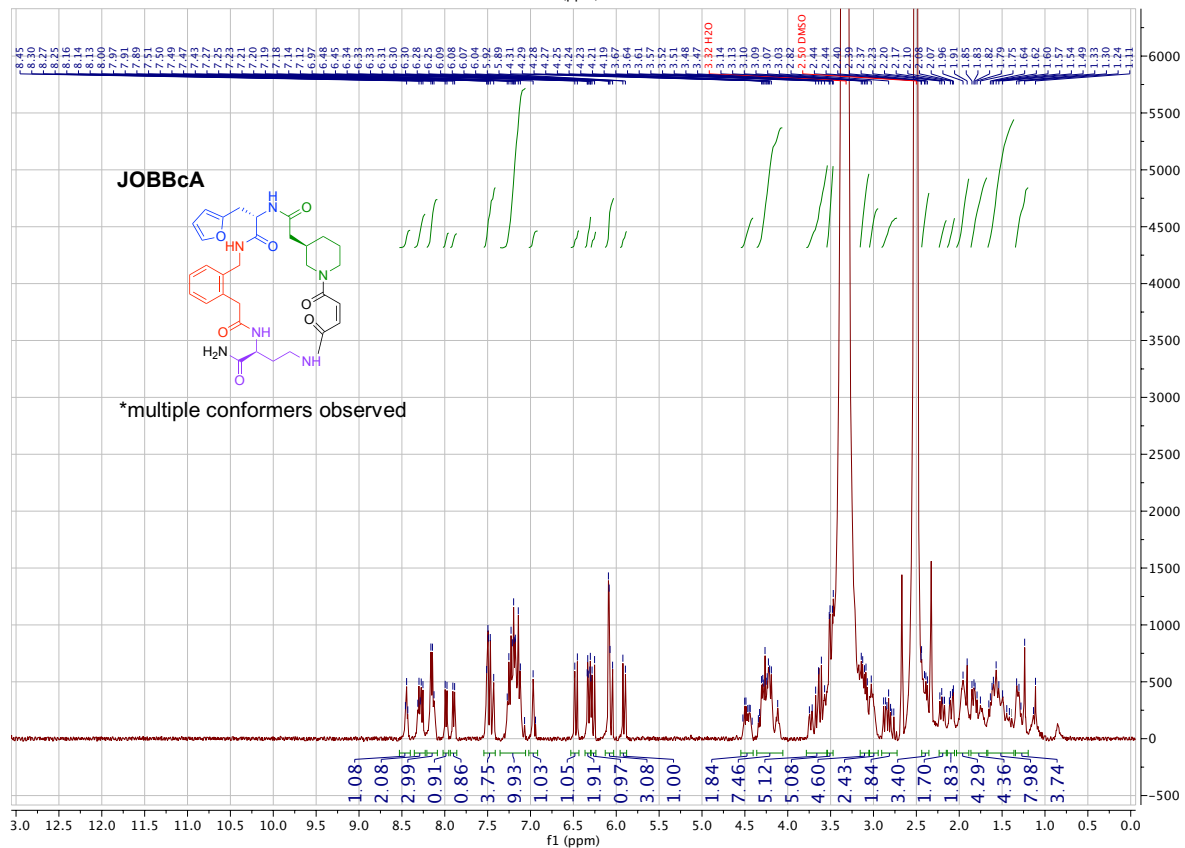
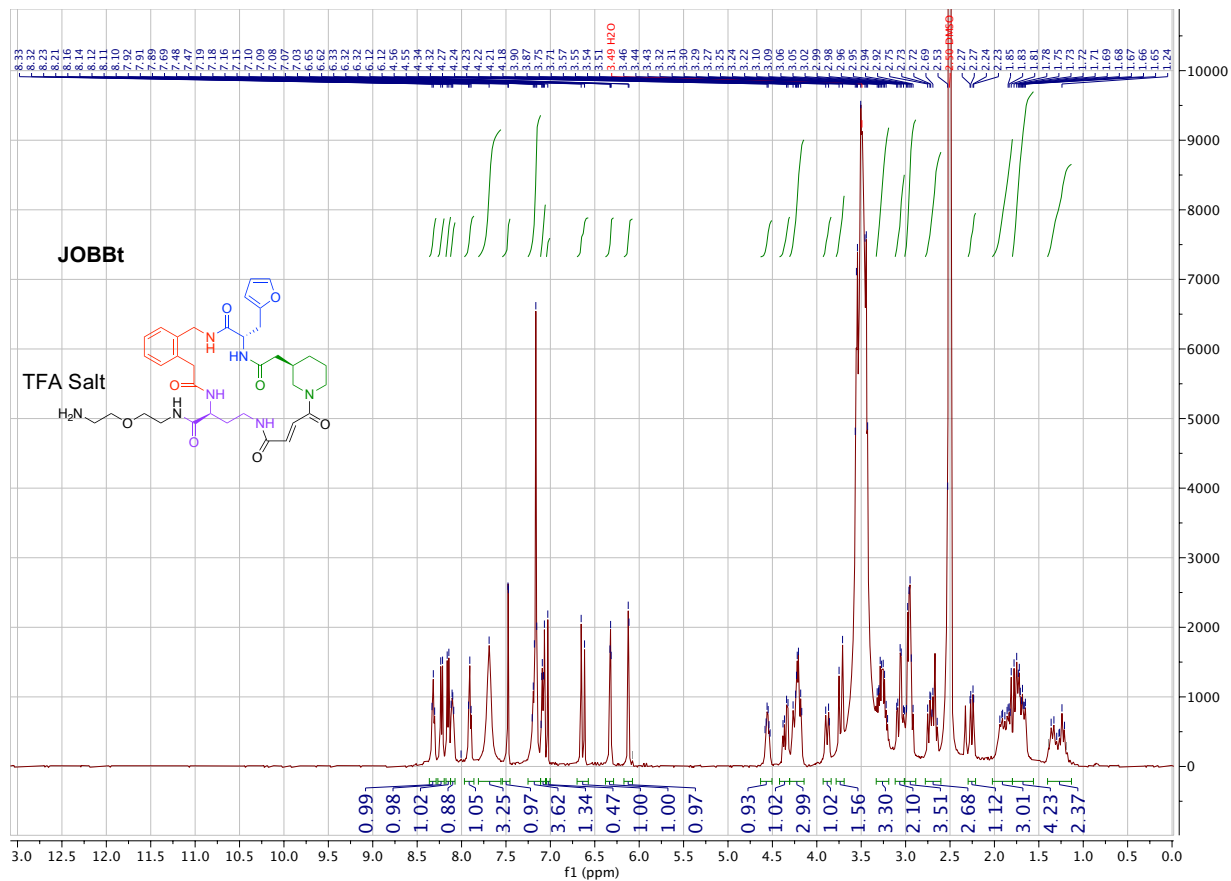


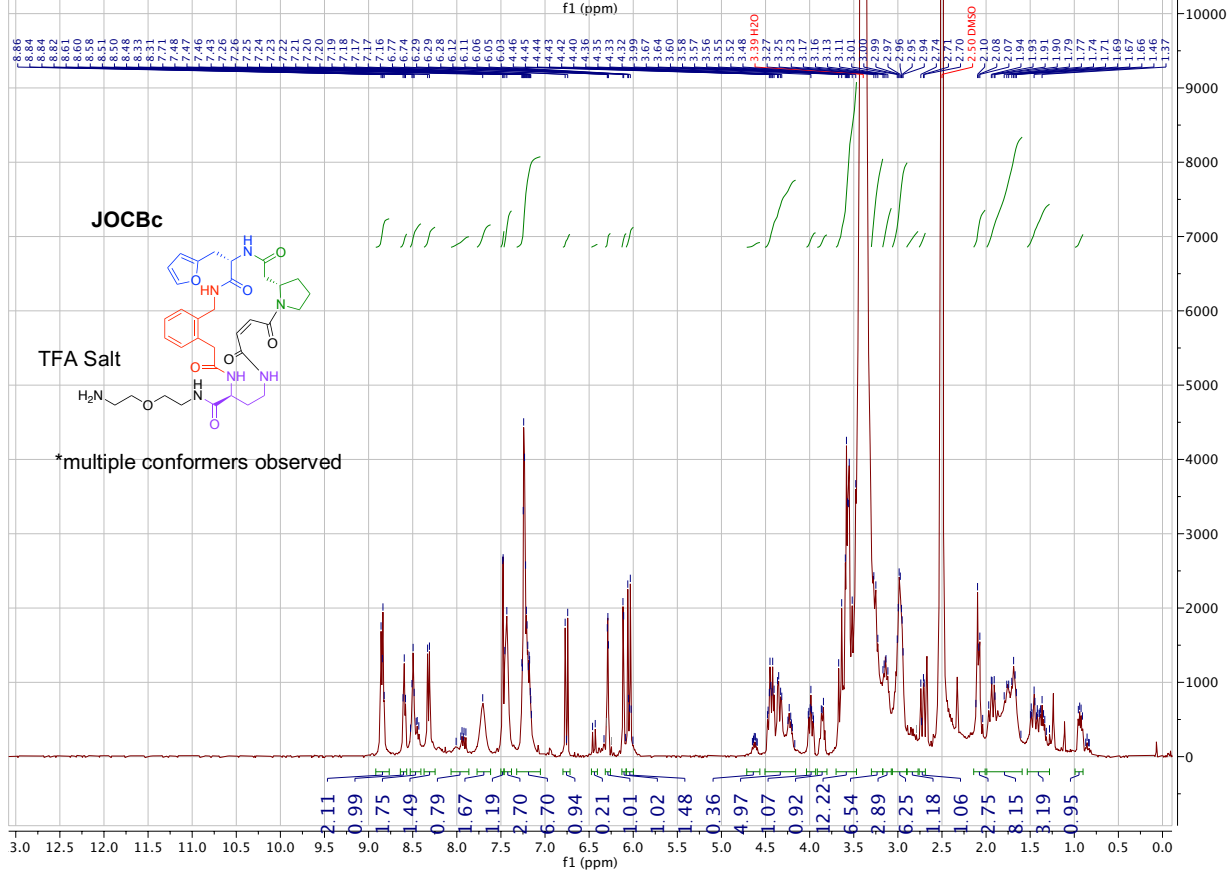
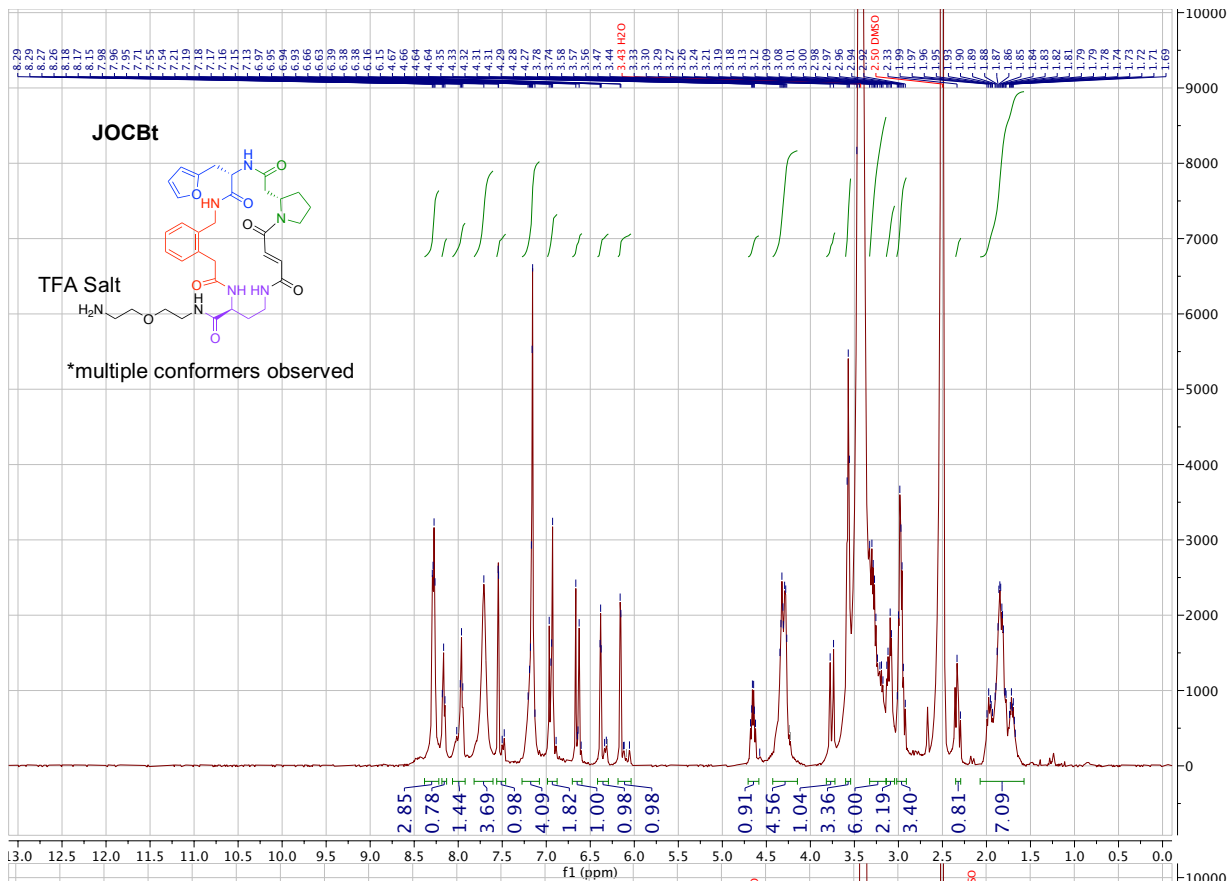
C6A: Compound was synthesized according to **Generalized procedure A for Suzuki-Miyaura cross-coupling of macrocycles** with **(4Br)B6-A** and benzene 1,3-diboronic acid, affording **C6A**. Yield: 13%

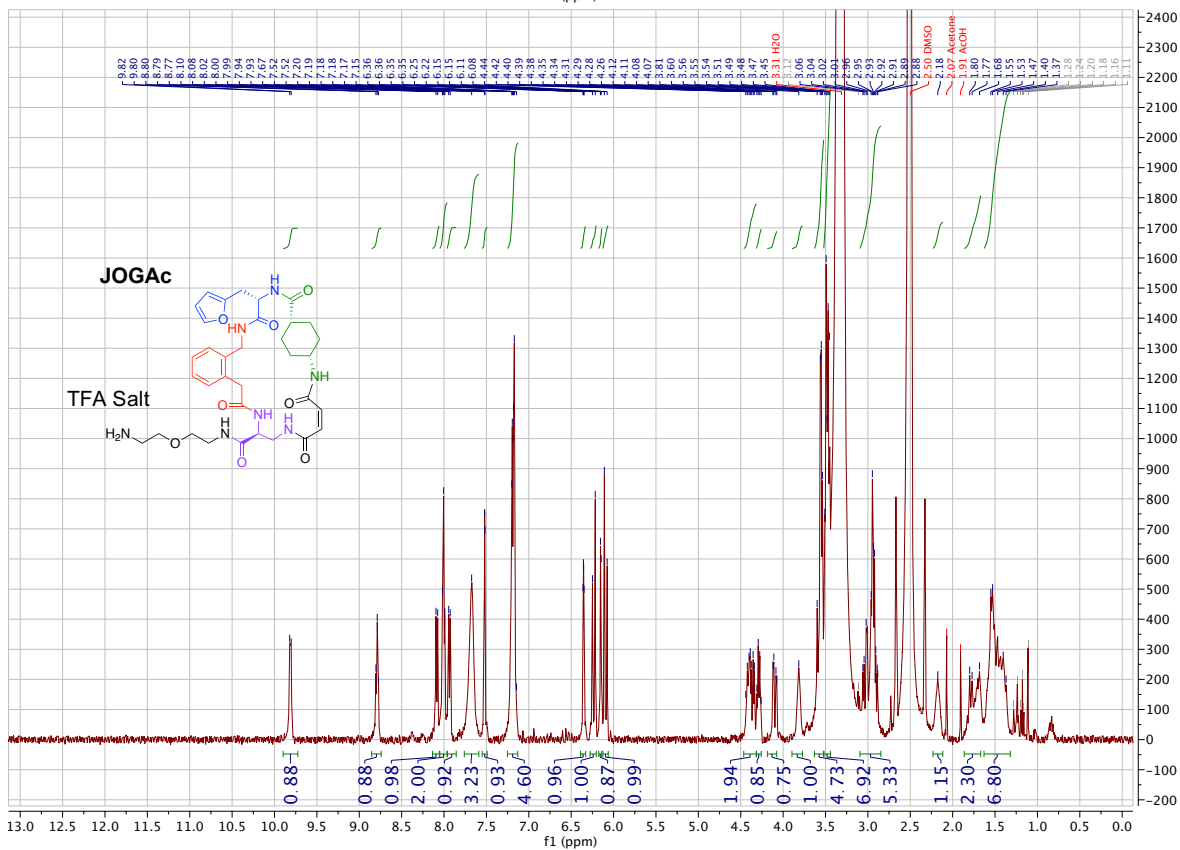
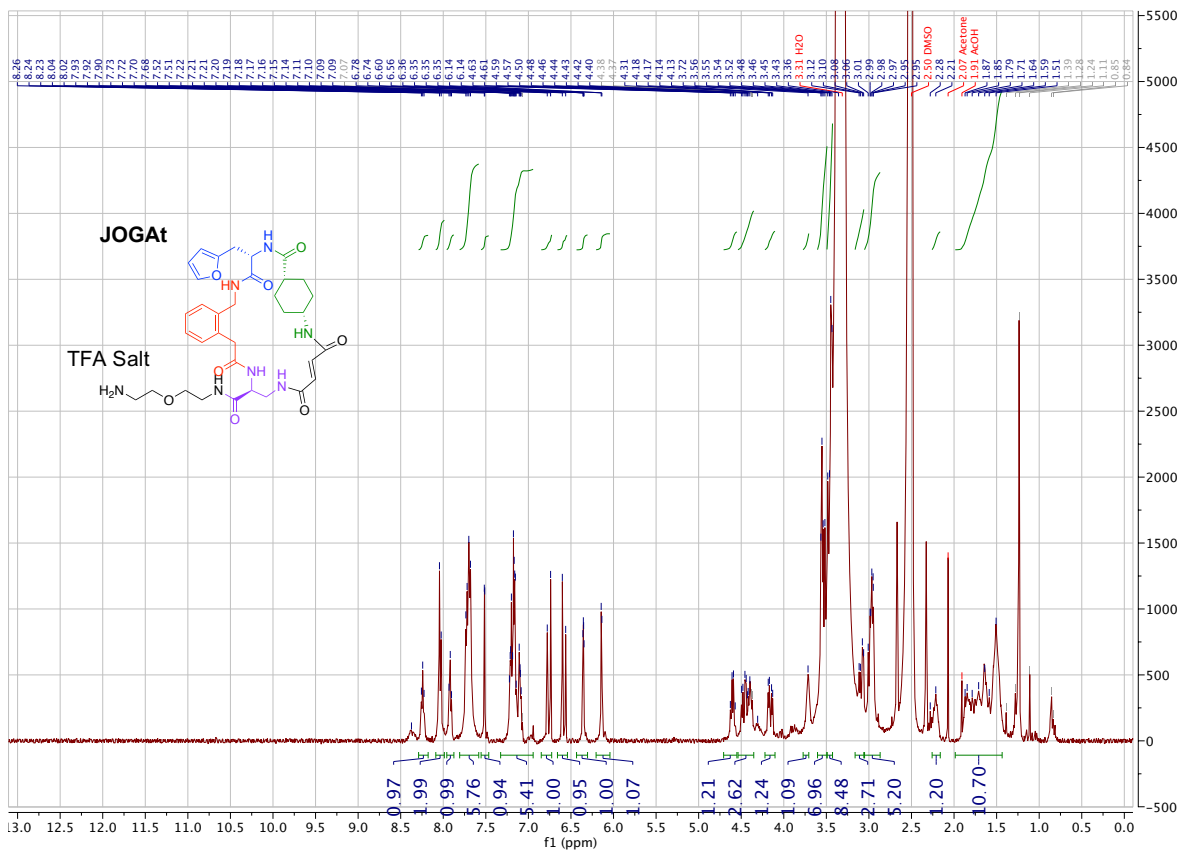
¹H-NMR Spectra

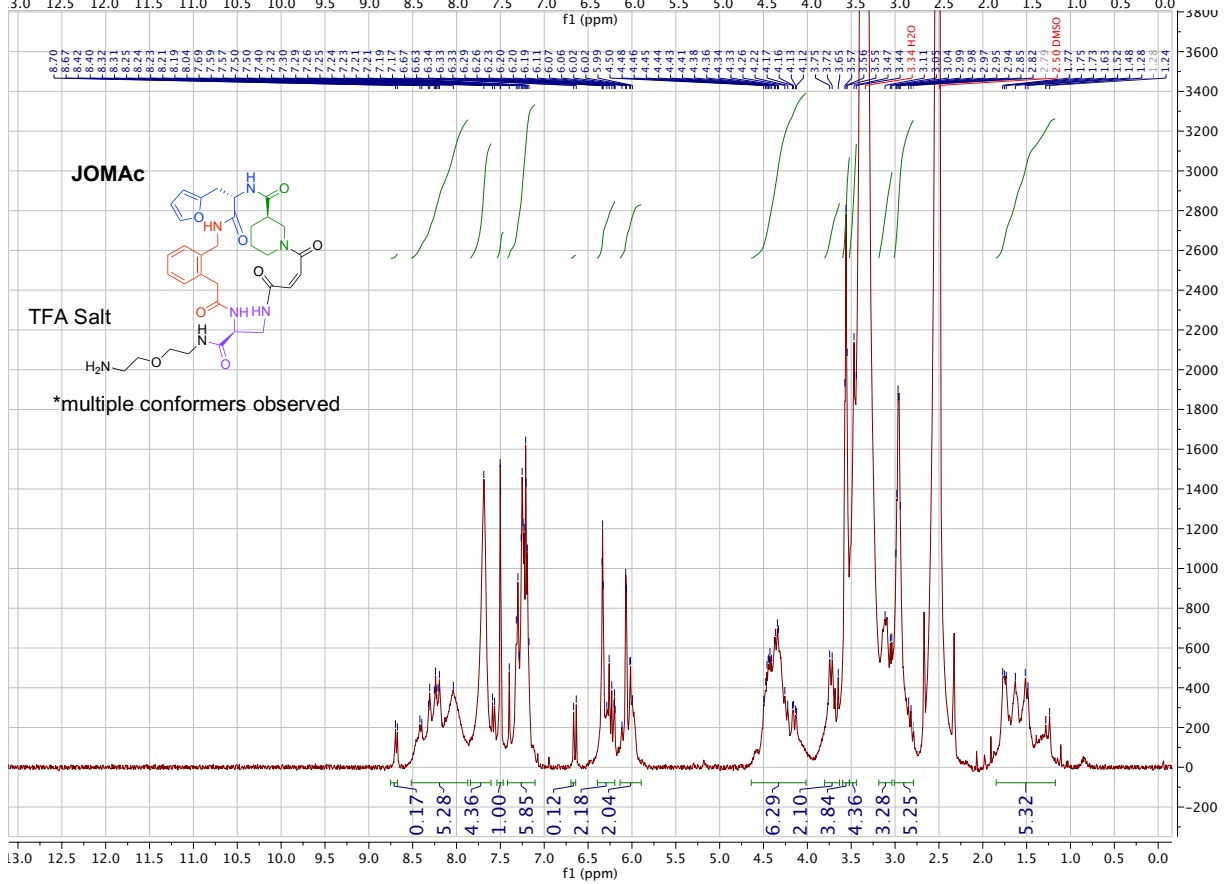
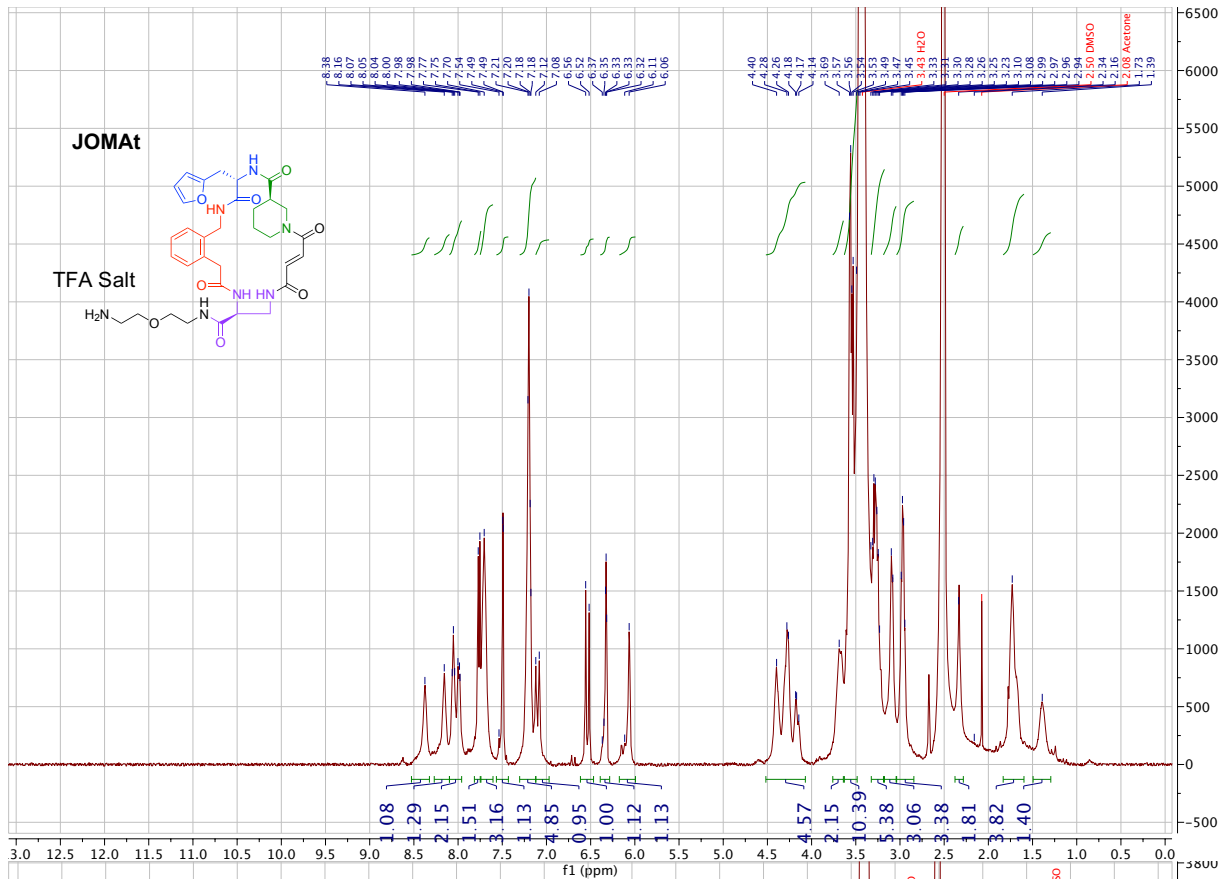


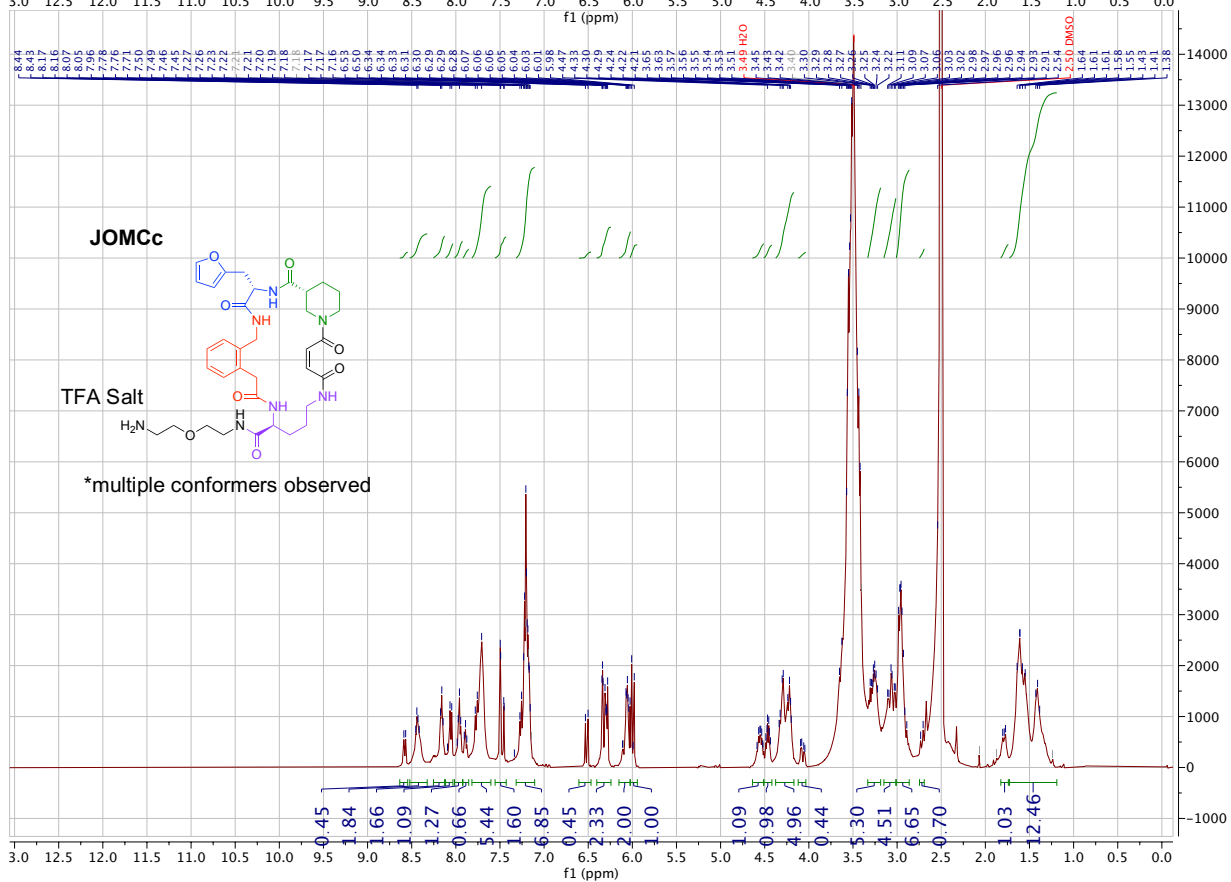
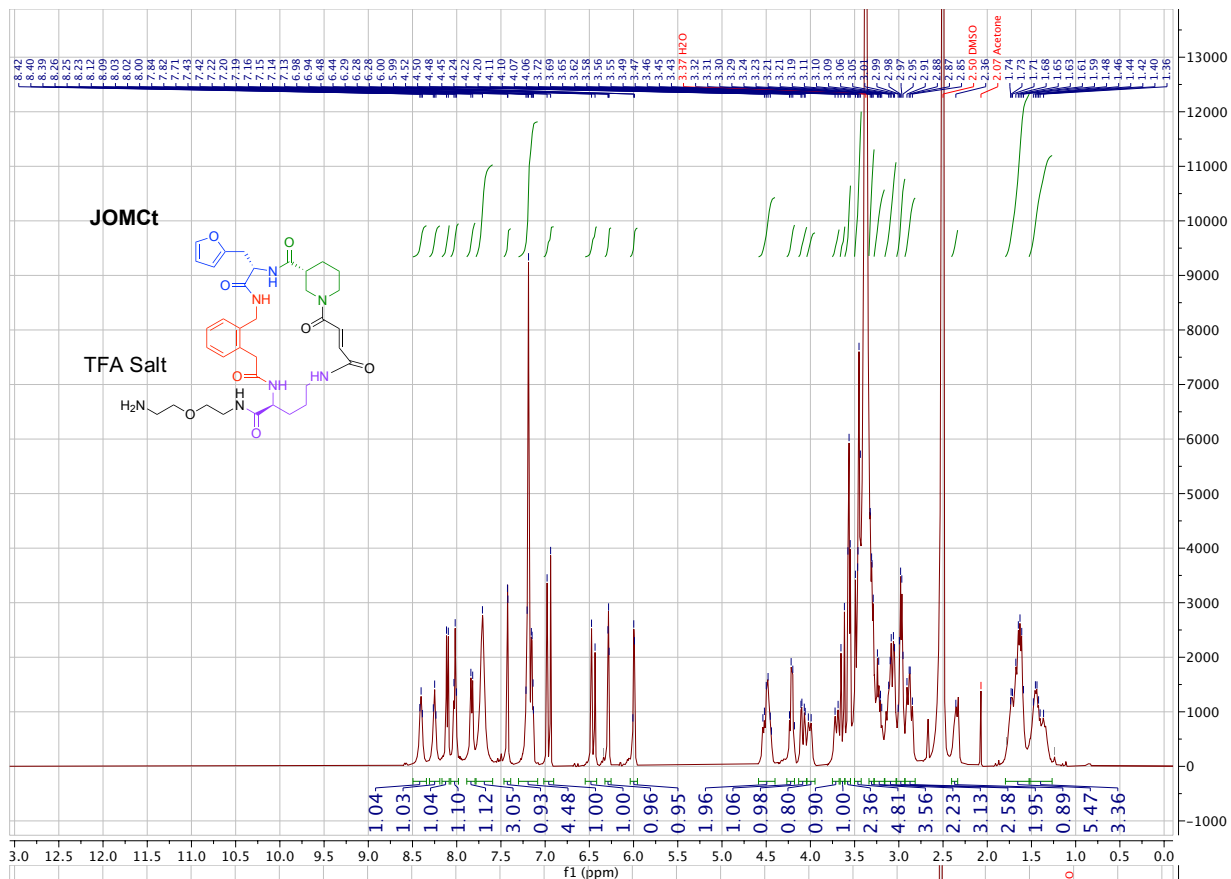


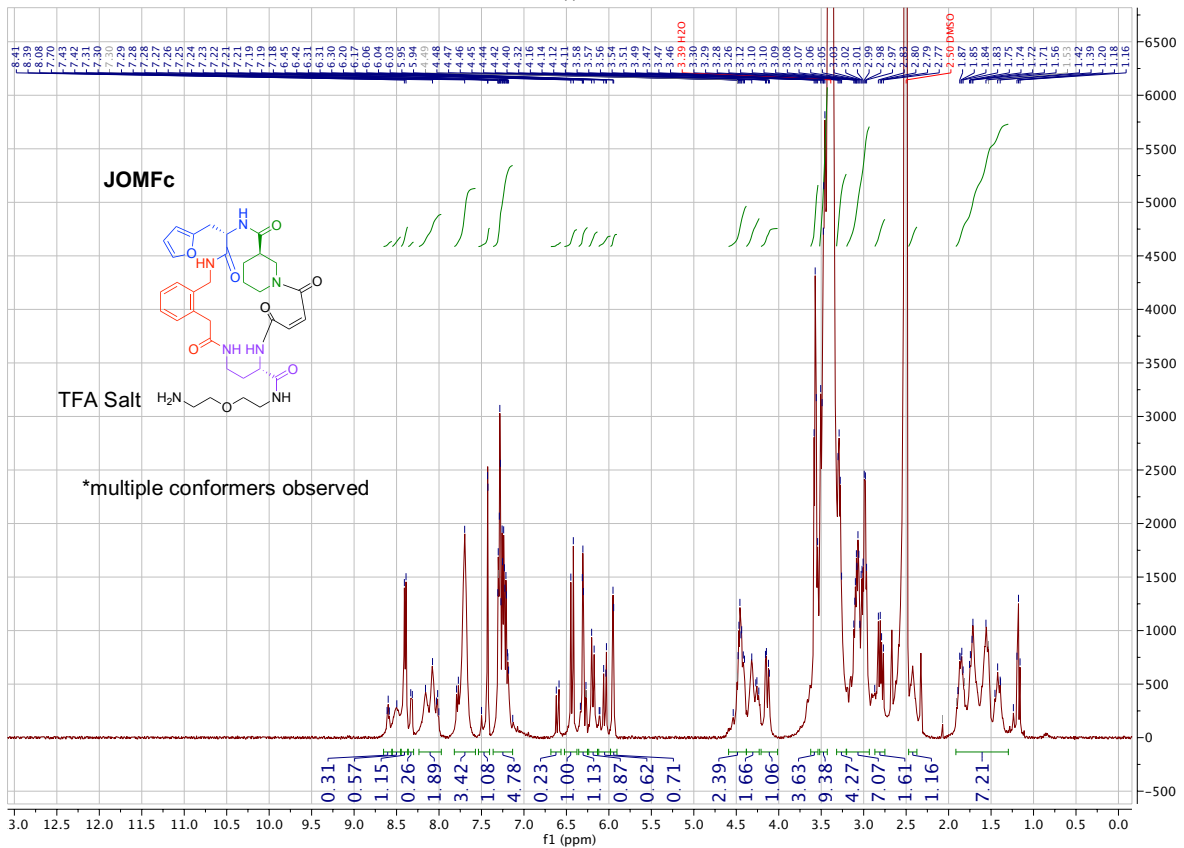
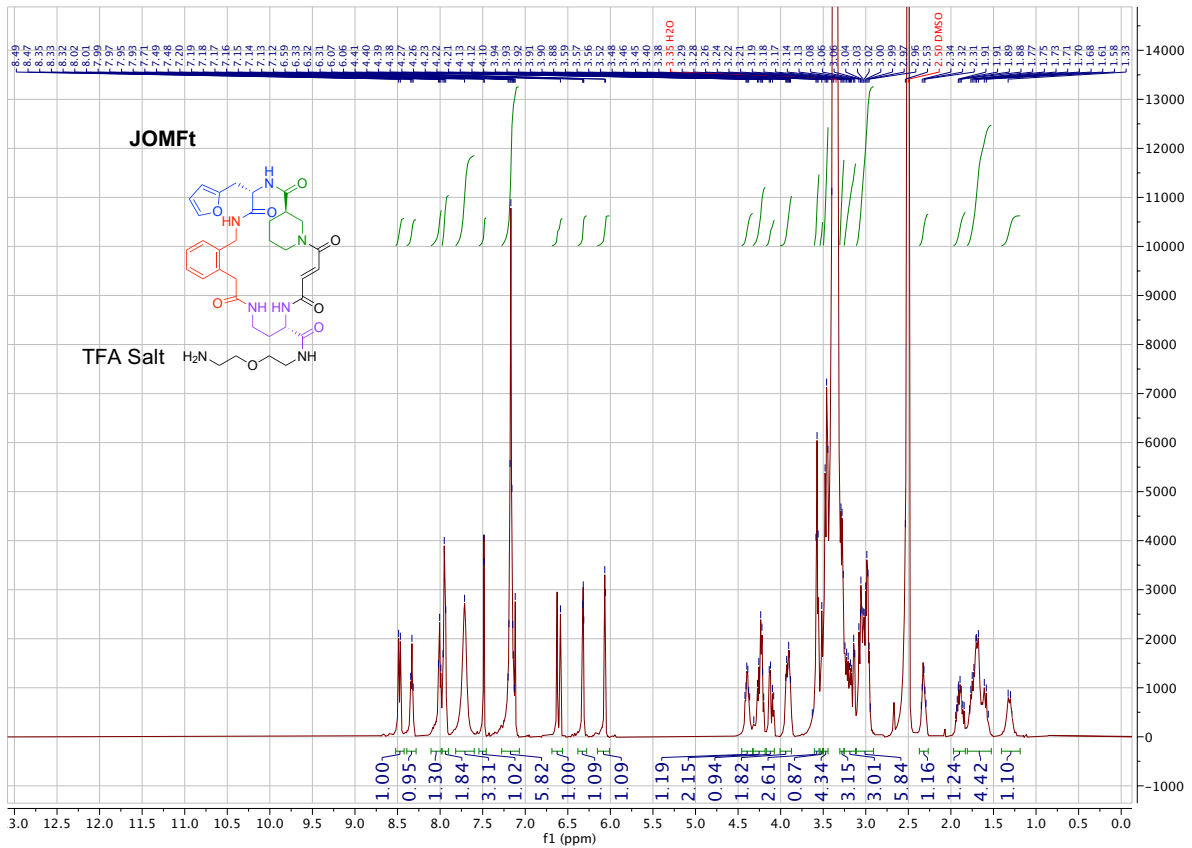


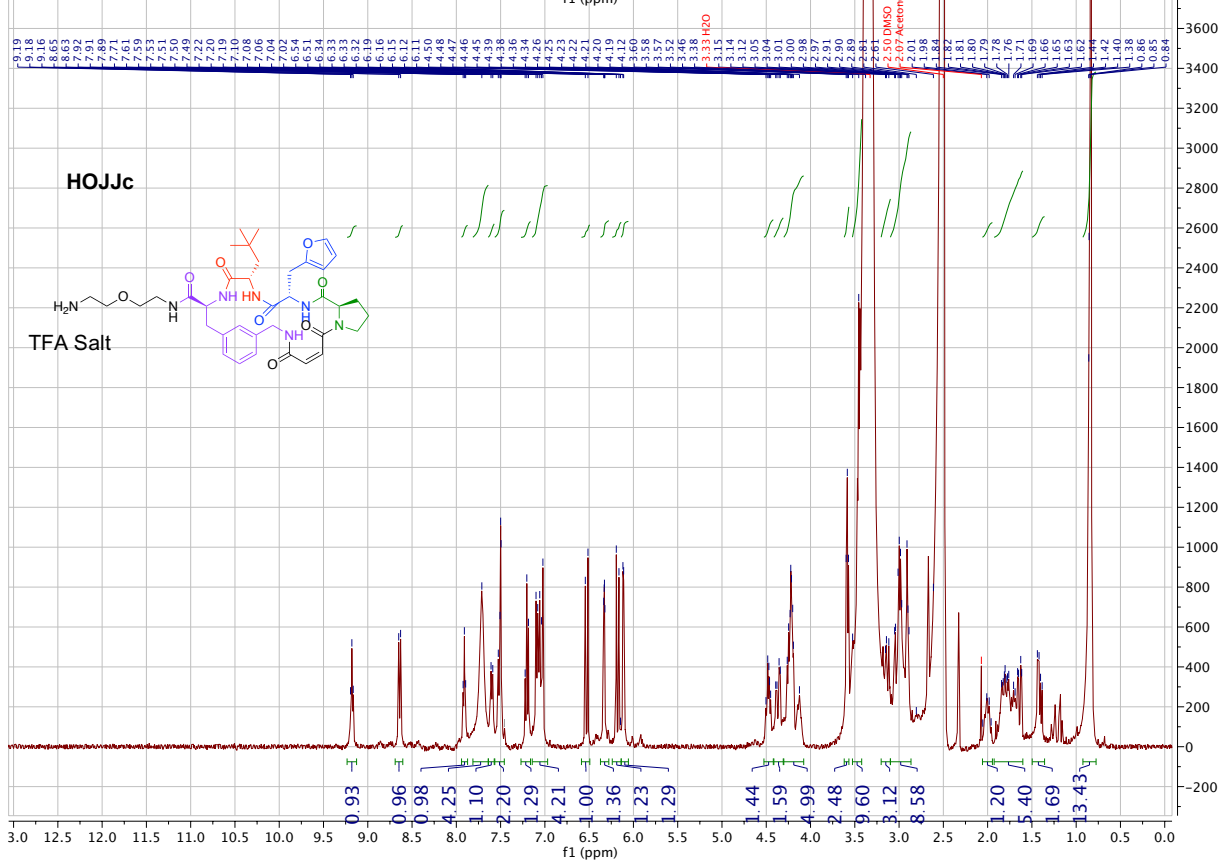
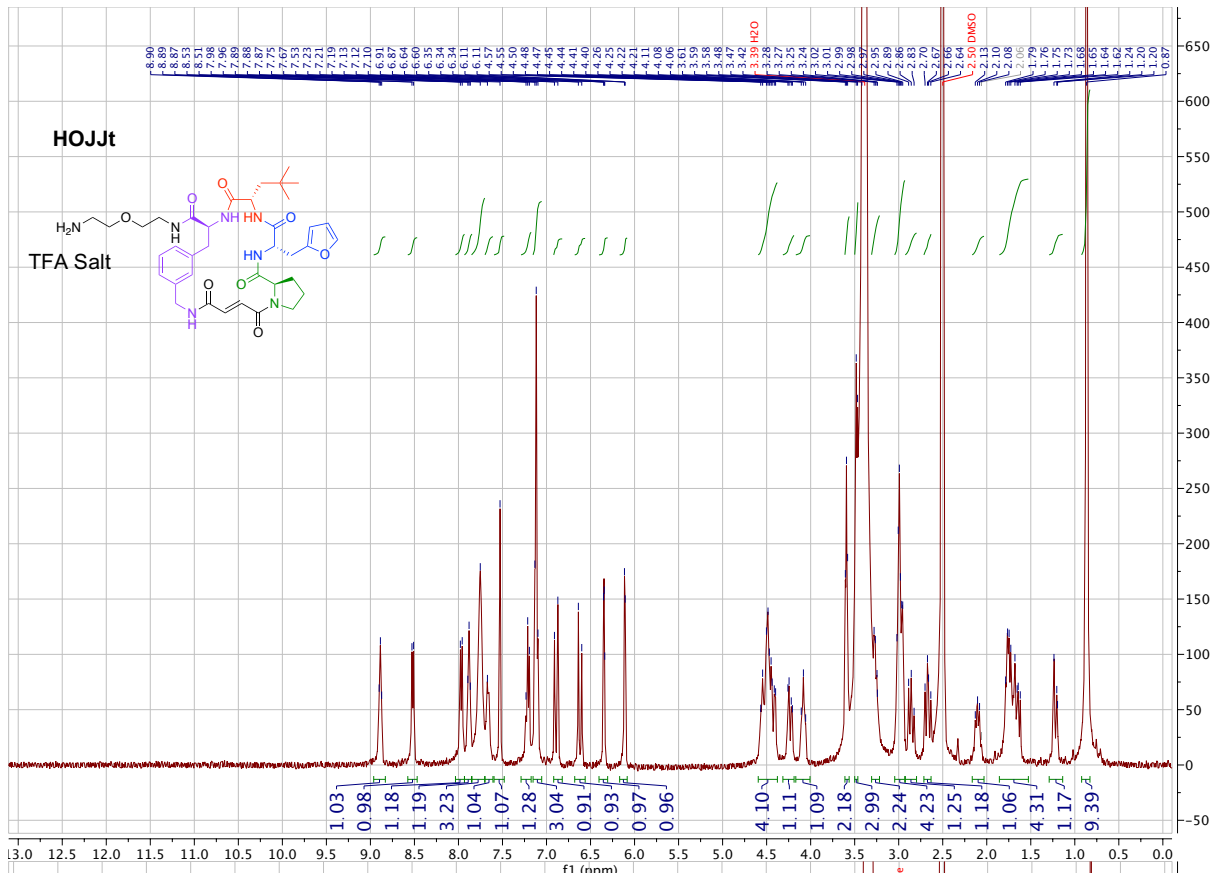


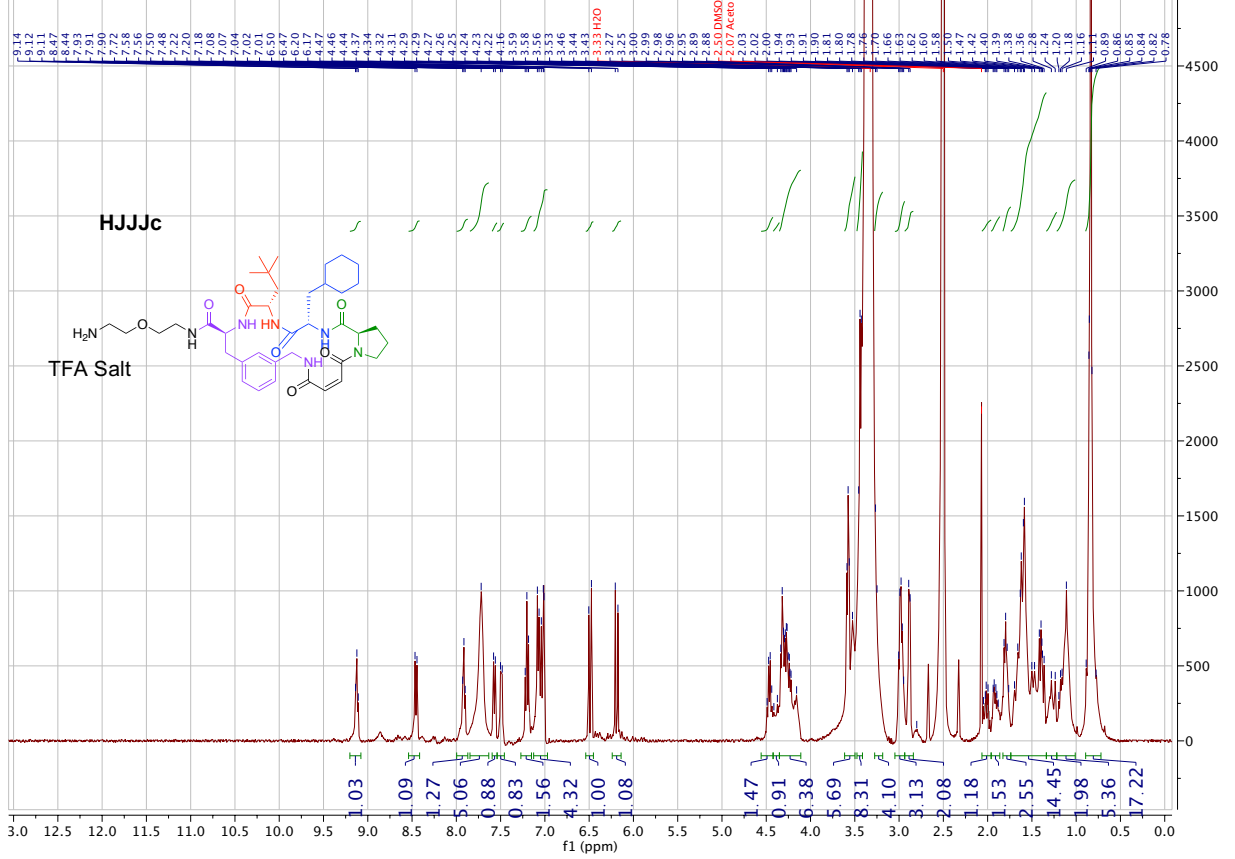
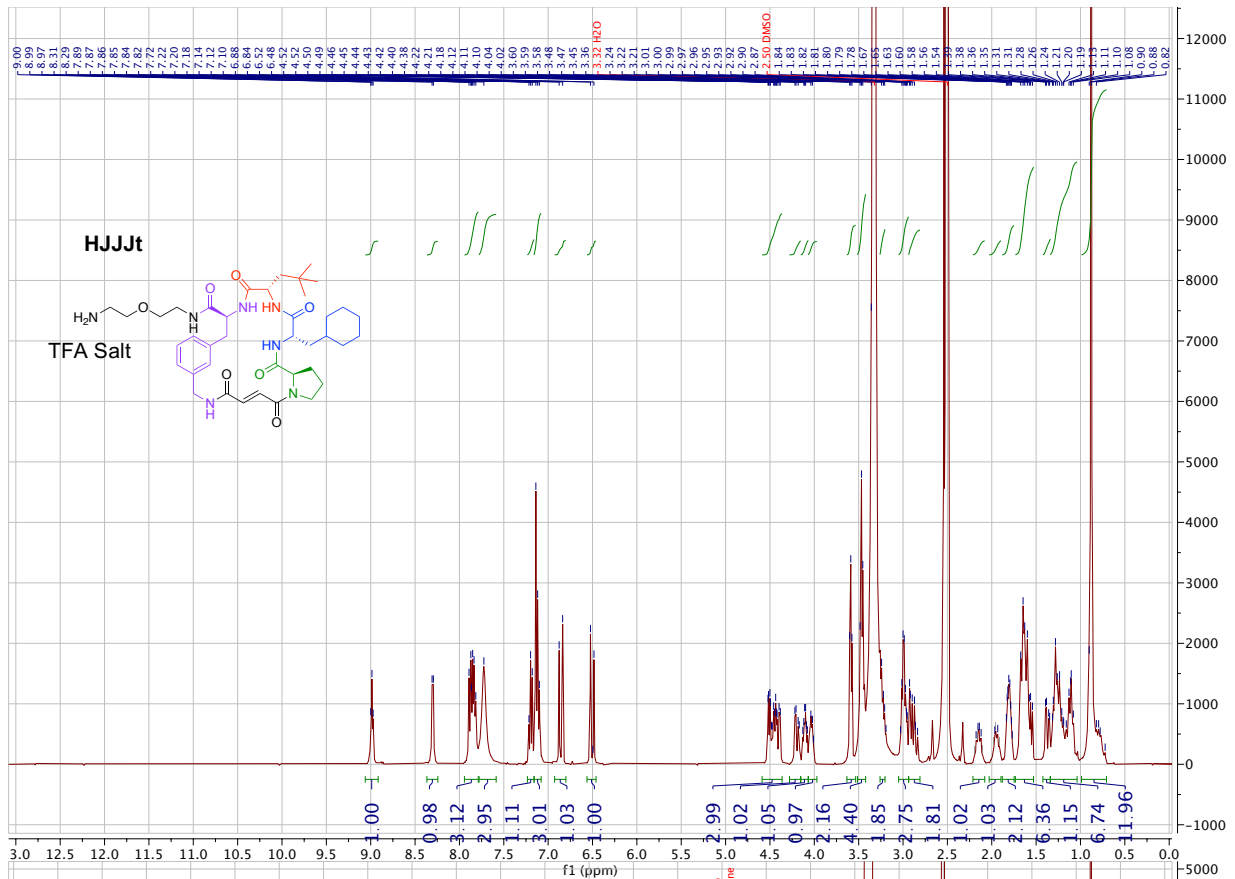


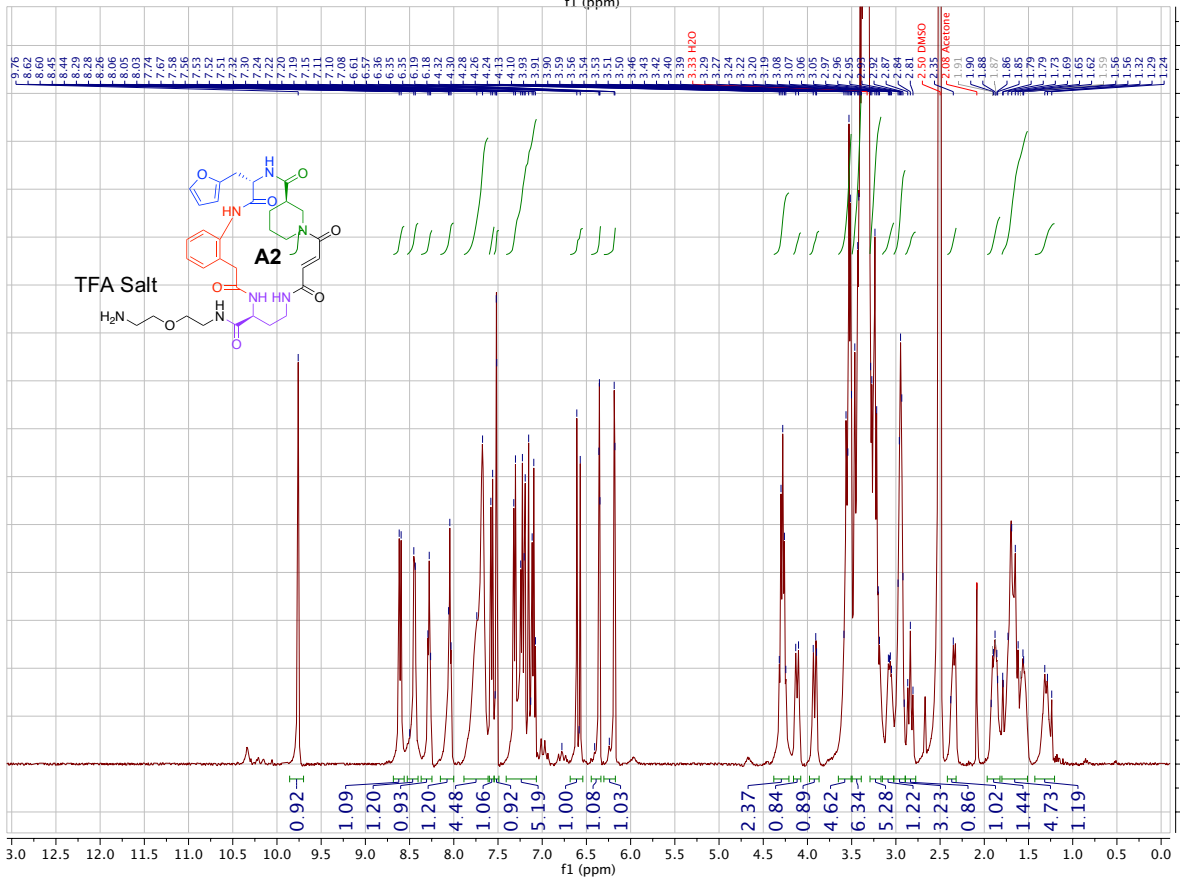
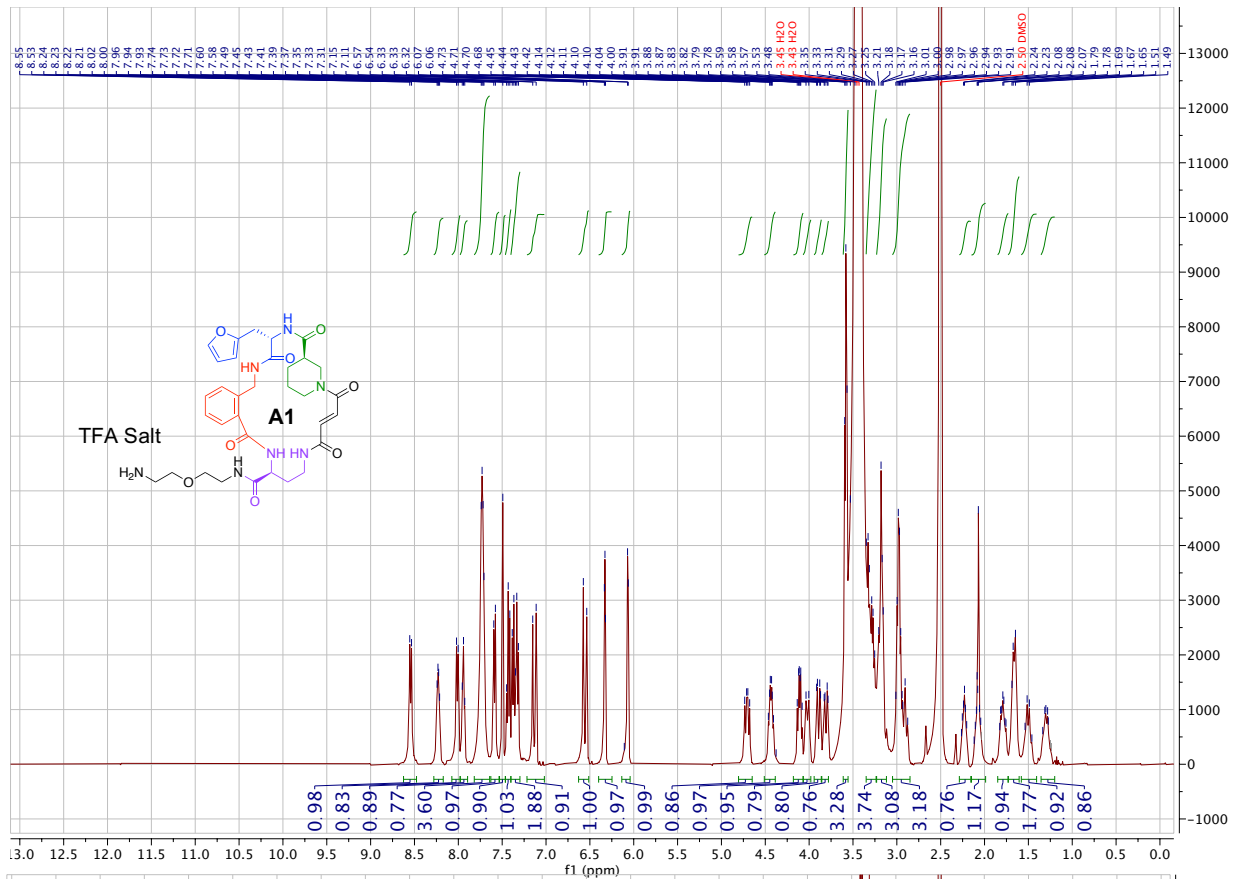


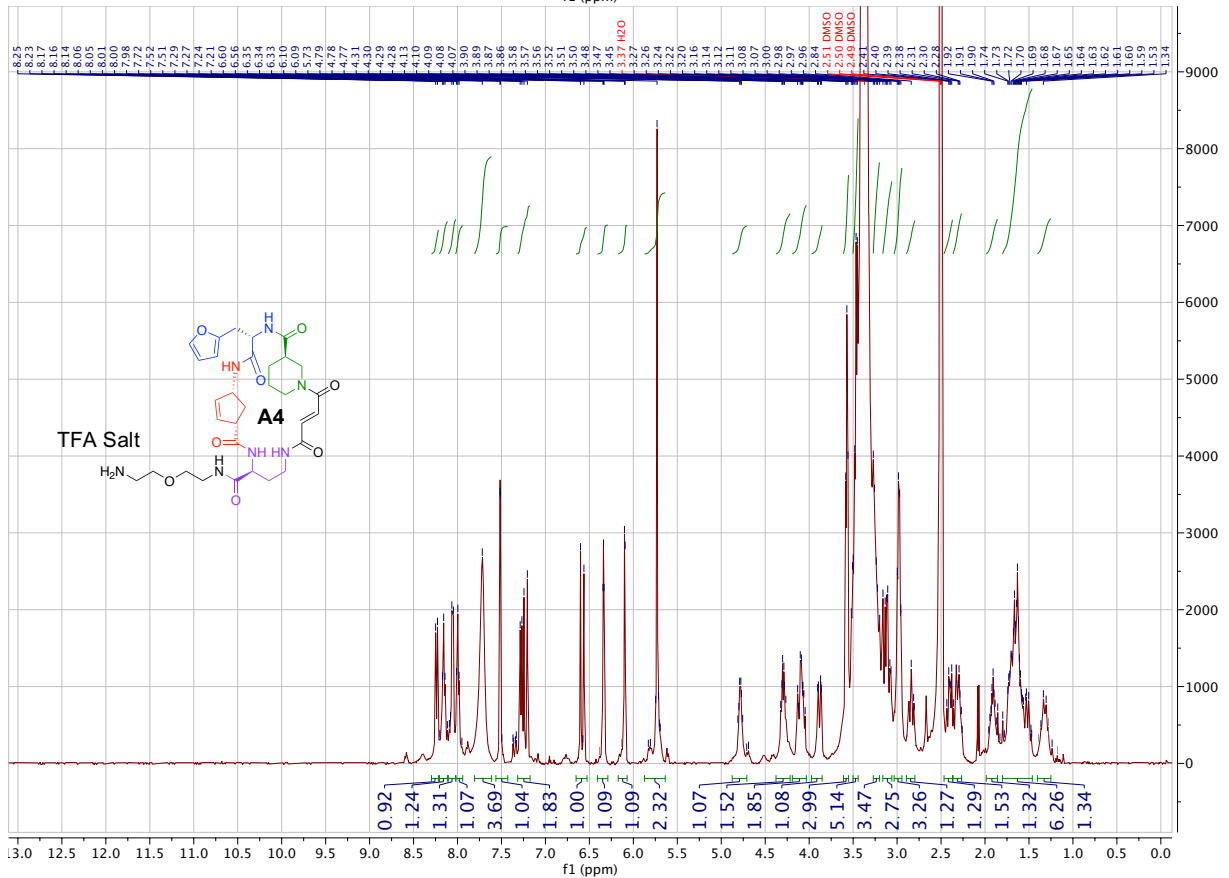
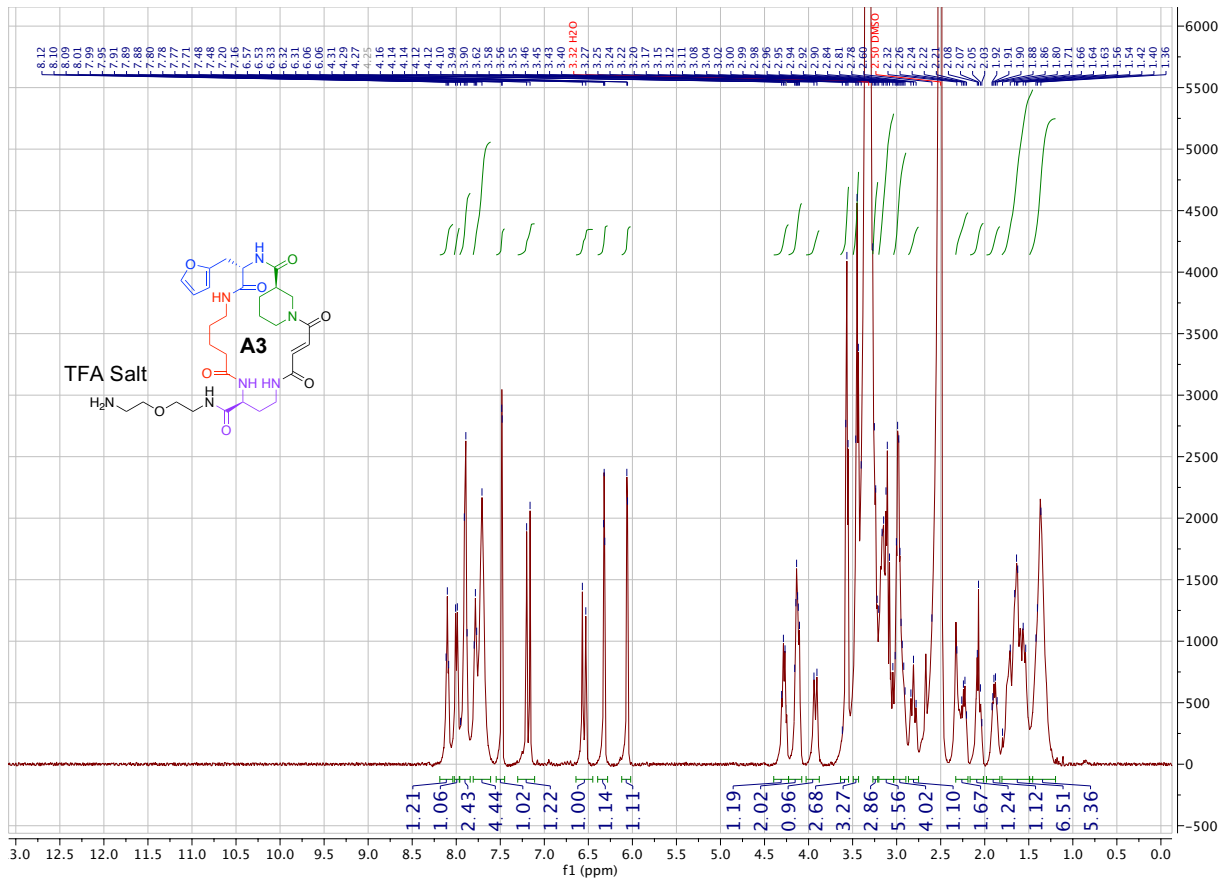


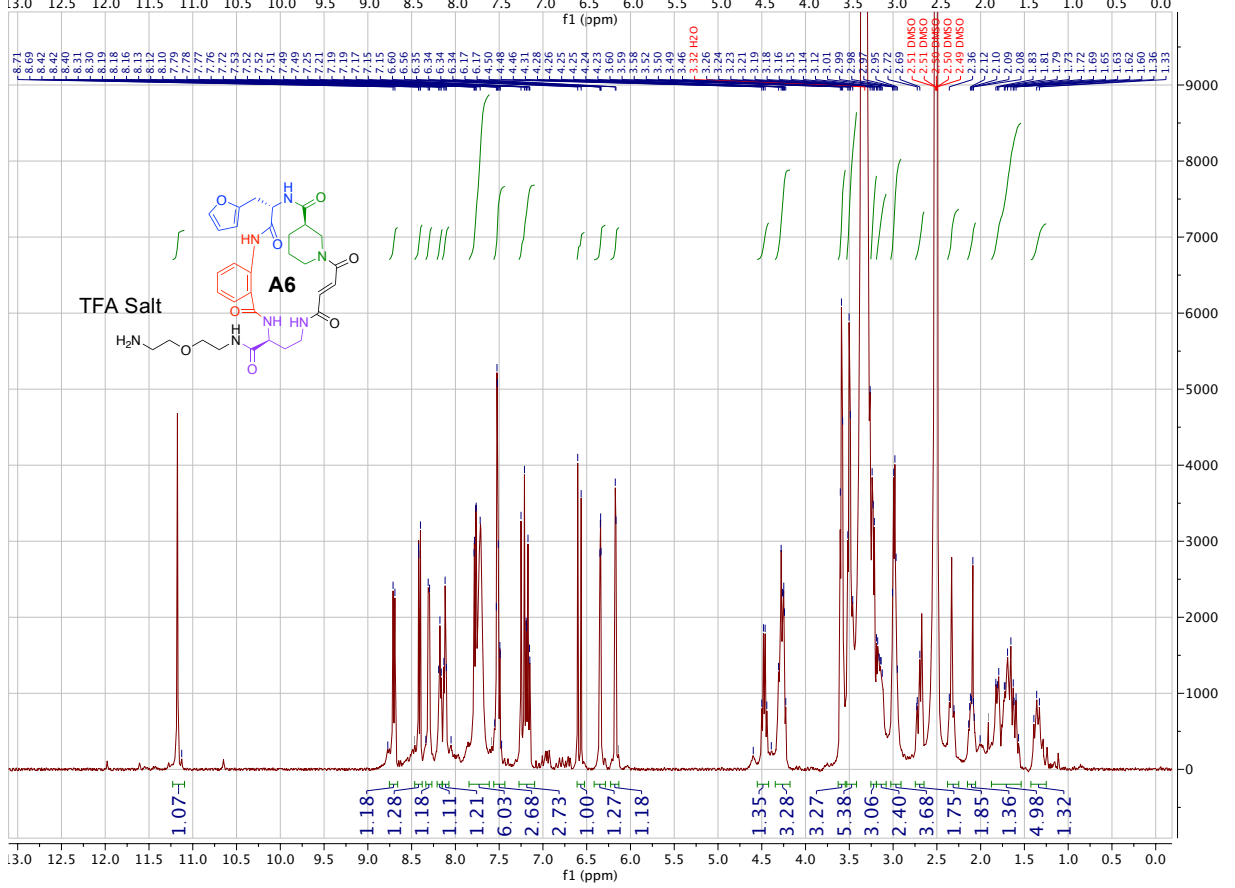
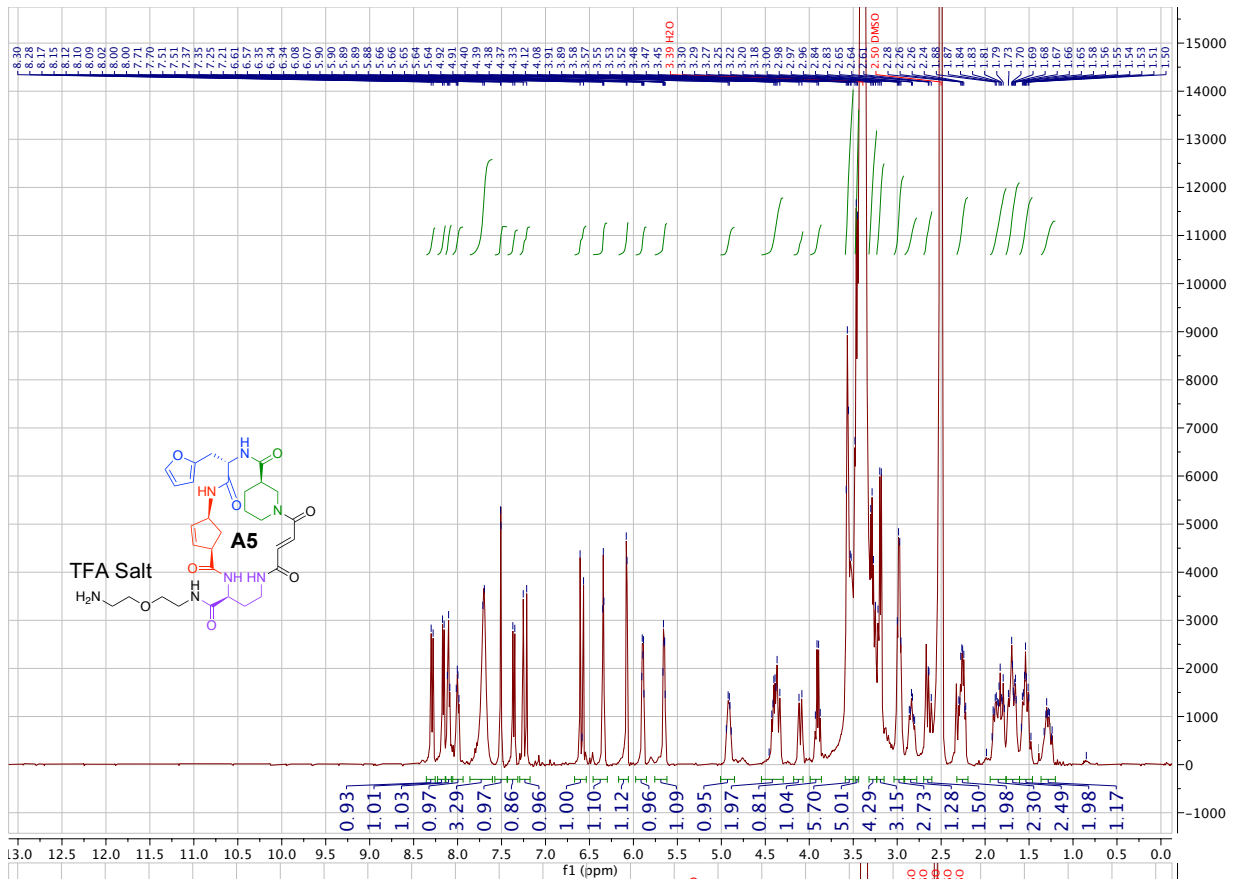


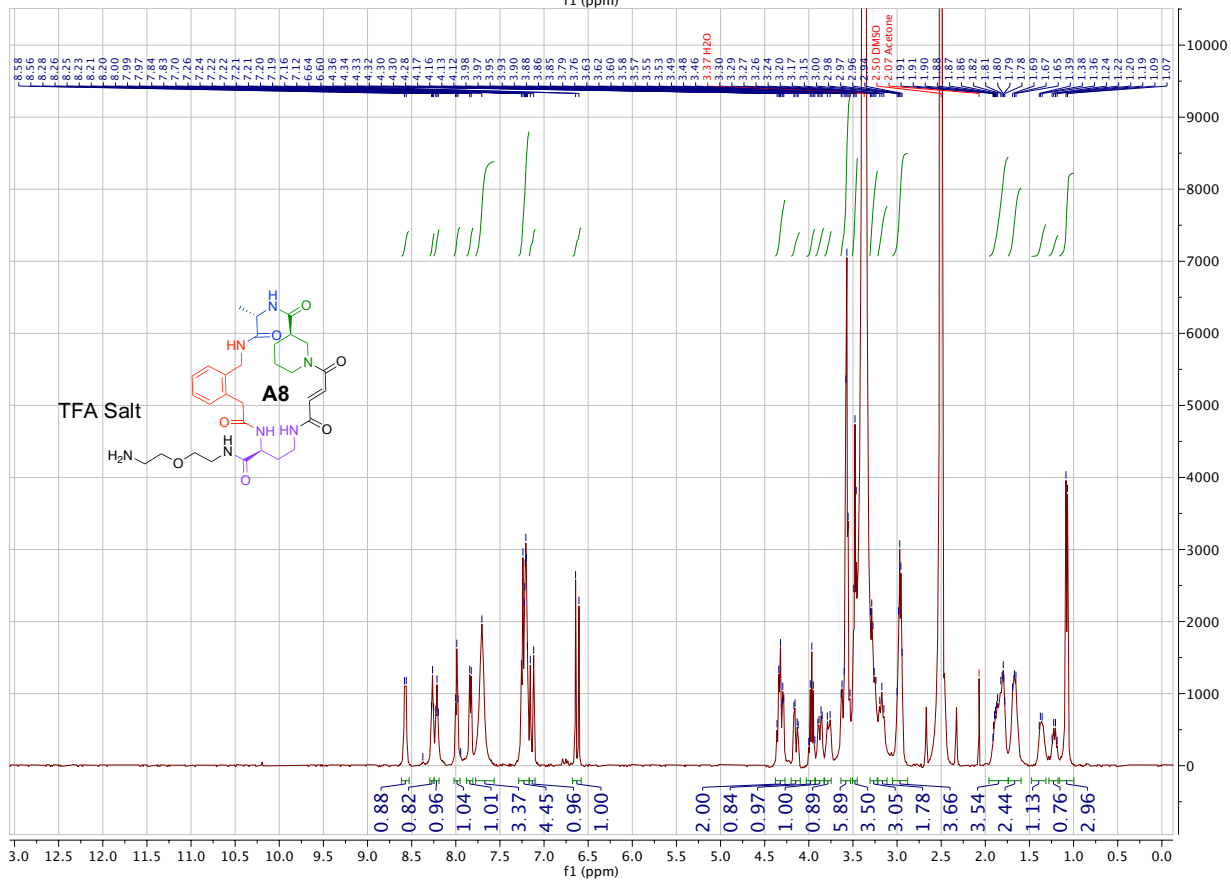
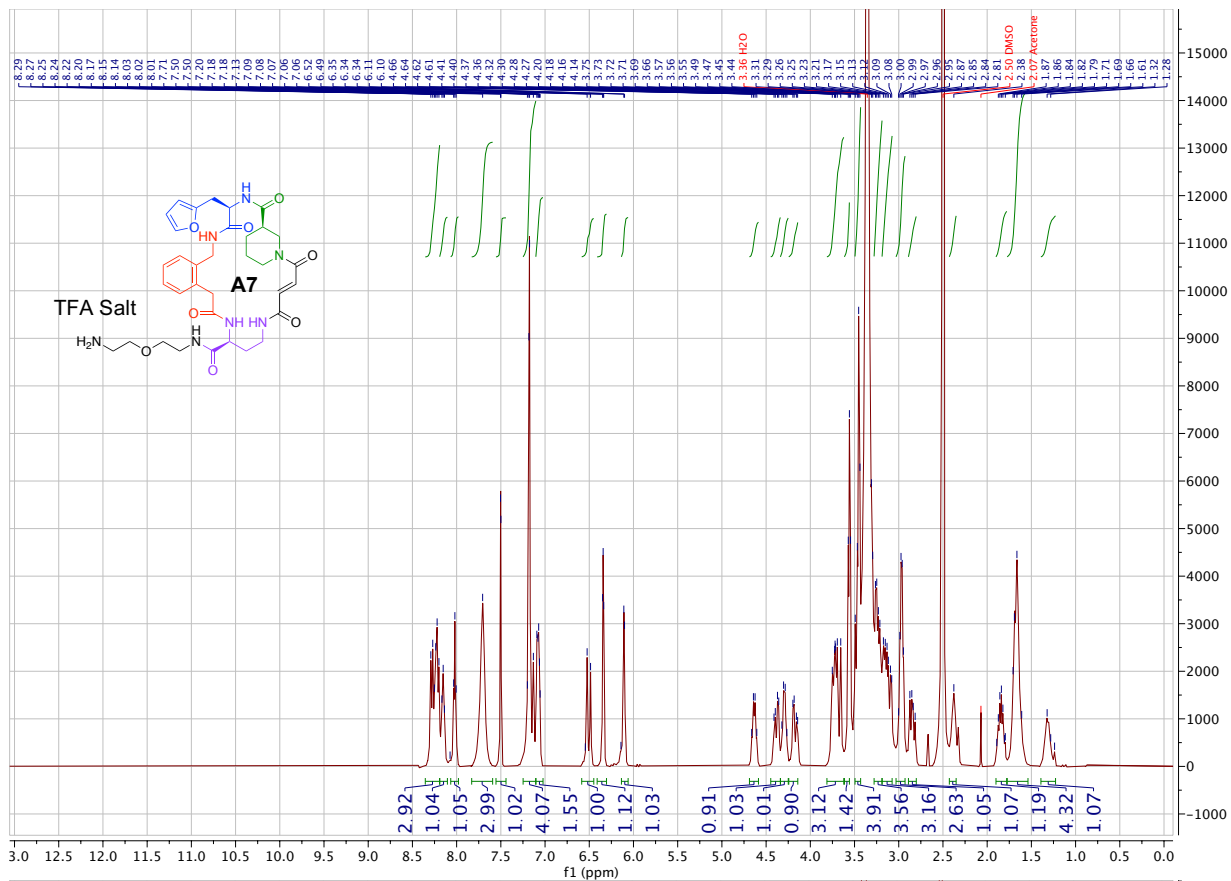


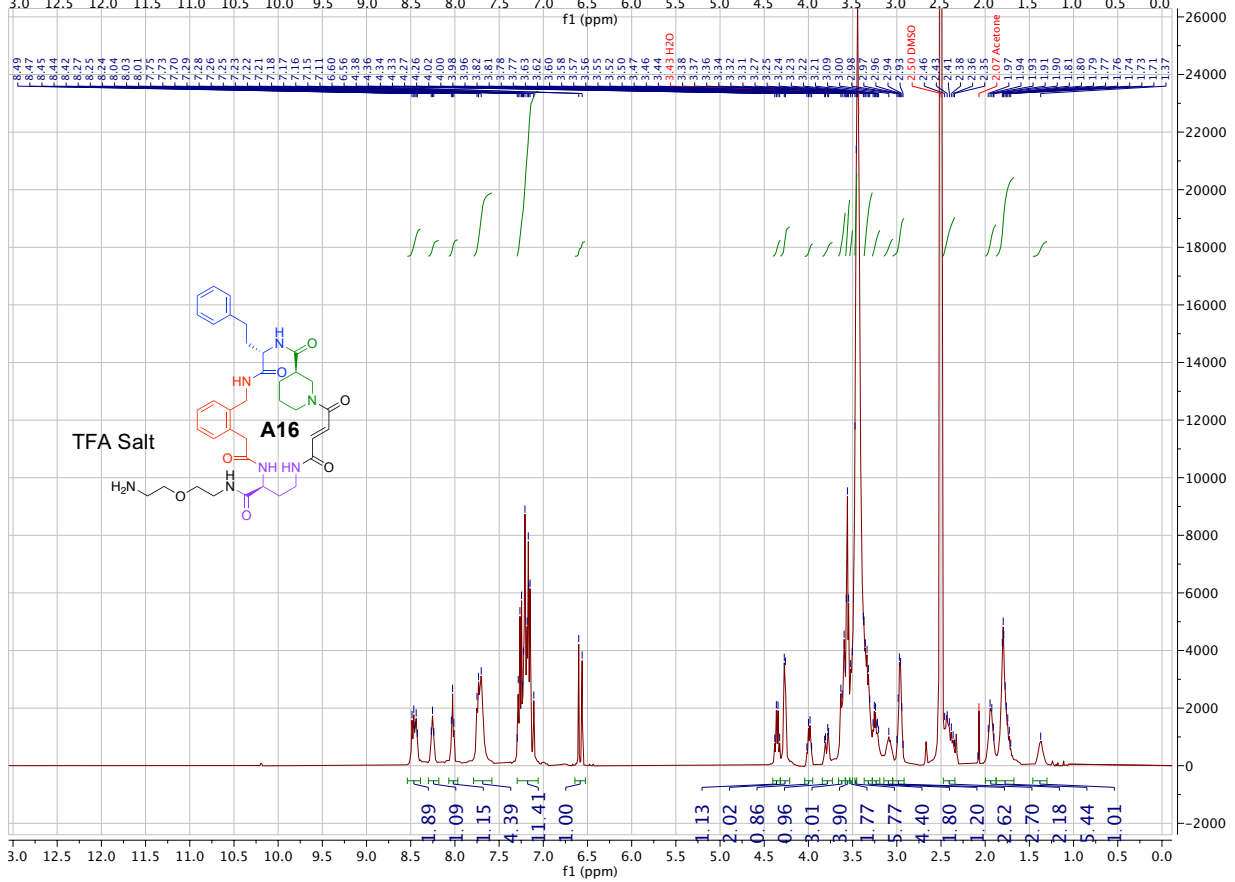
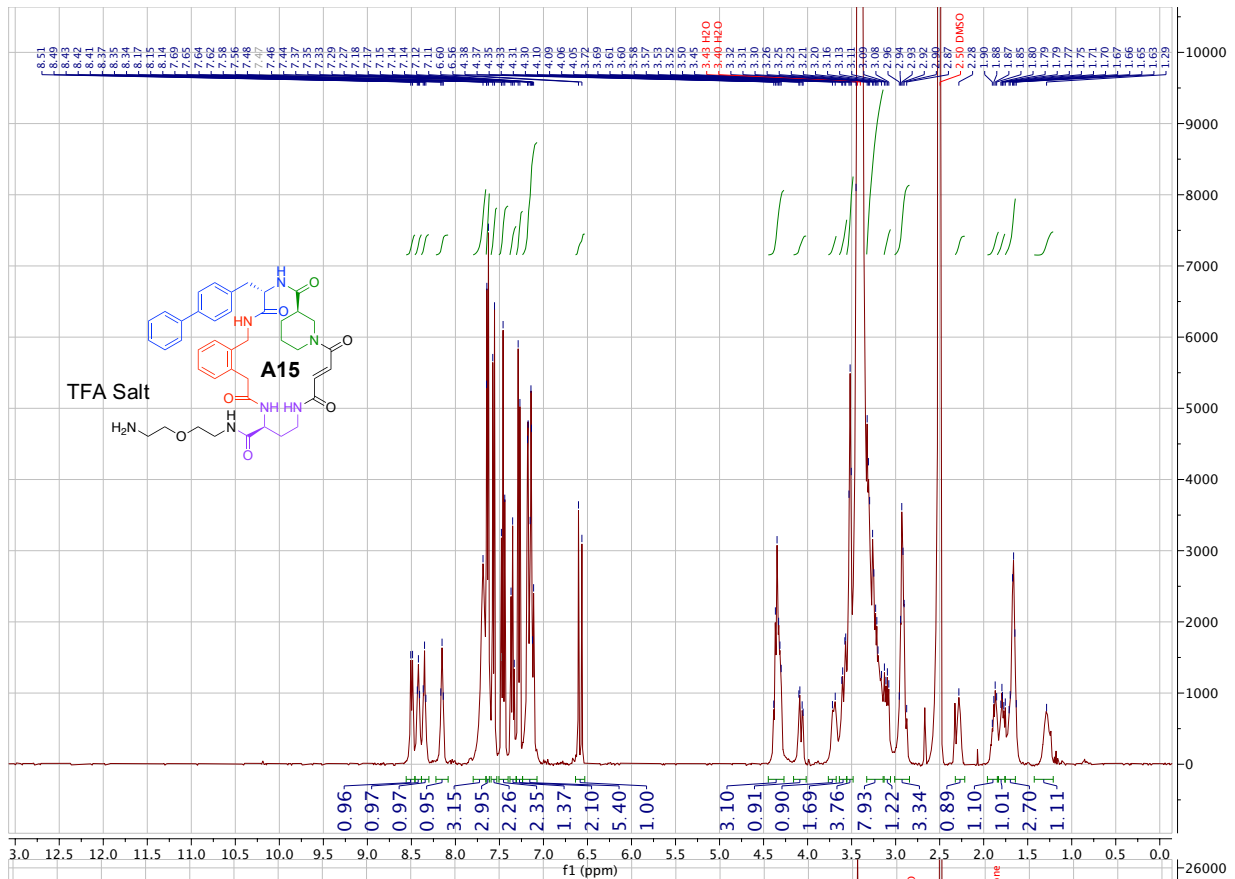


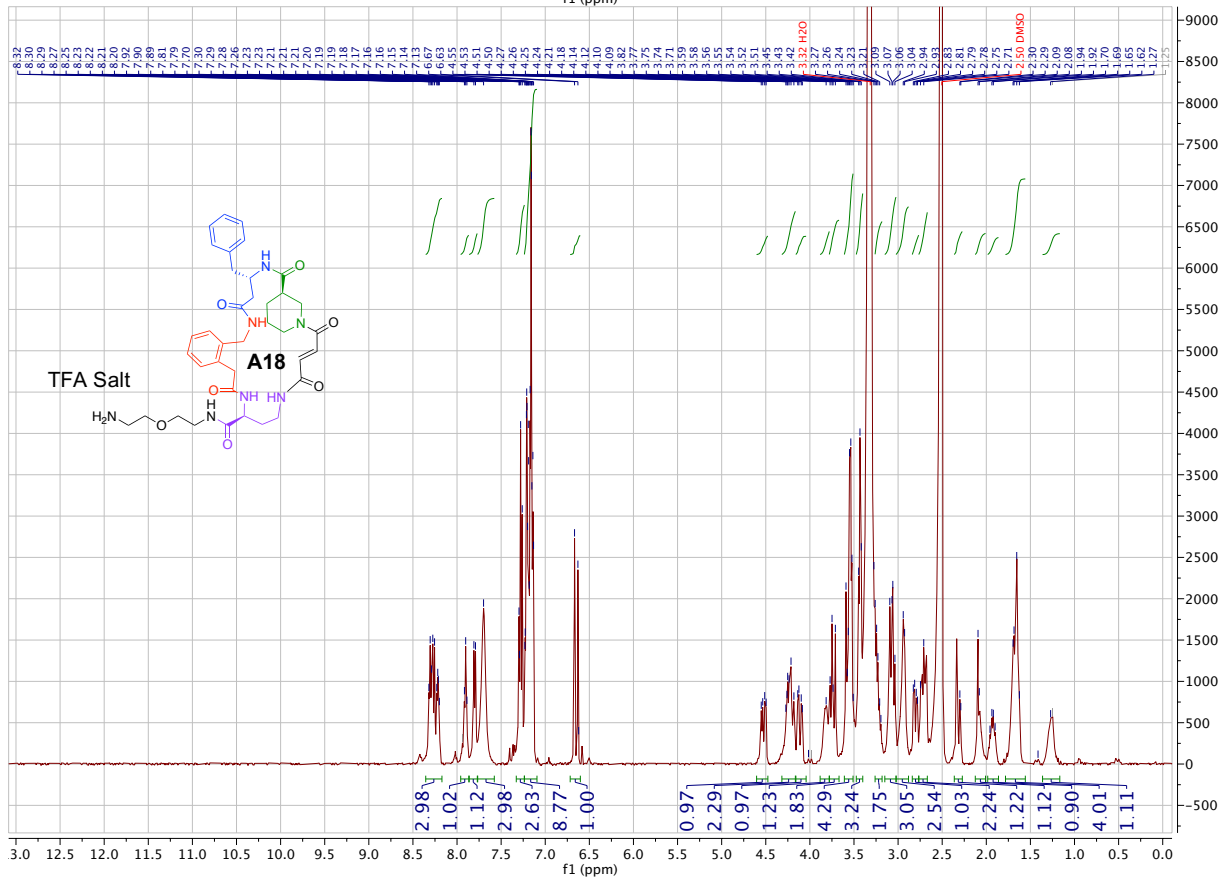
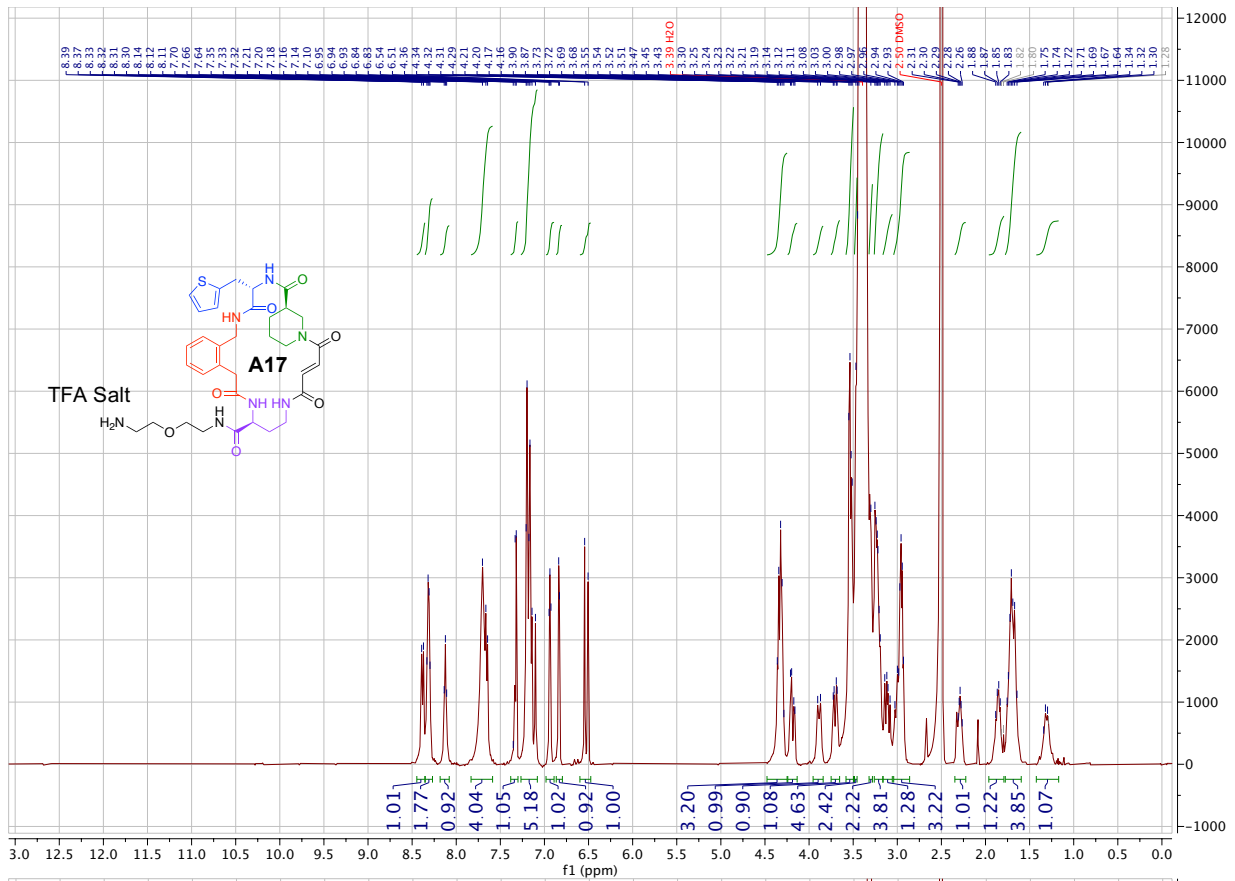


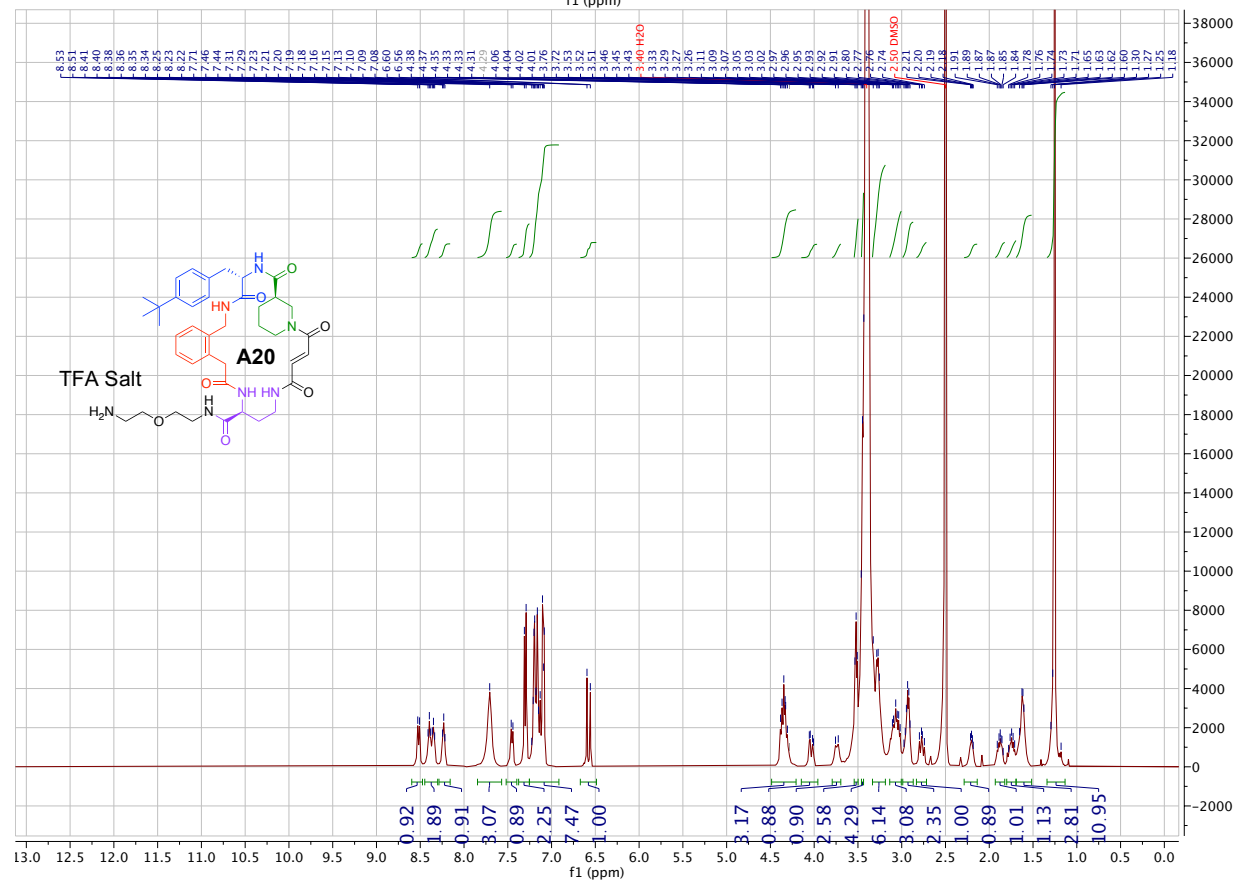
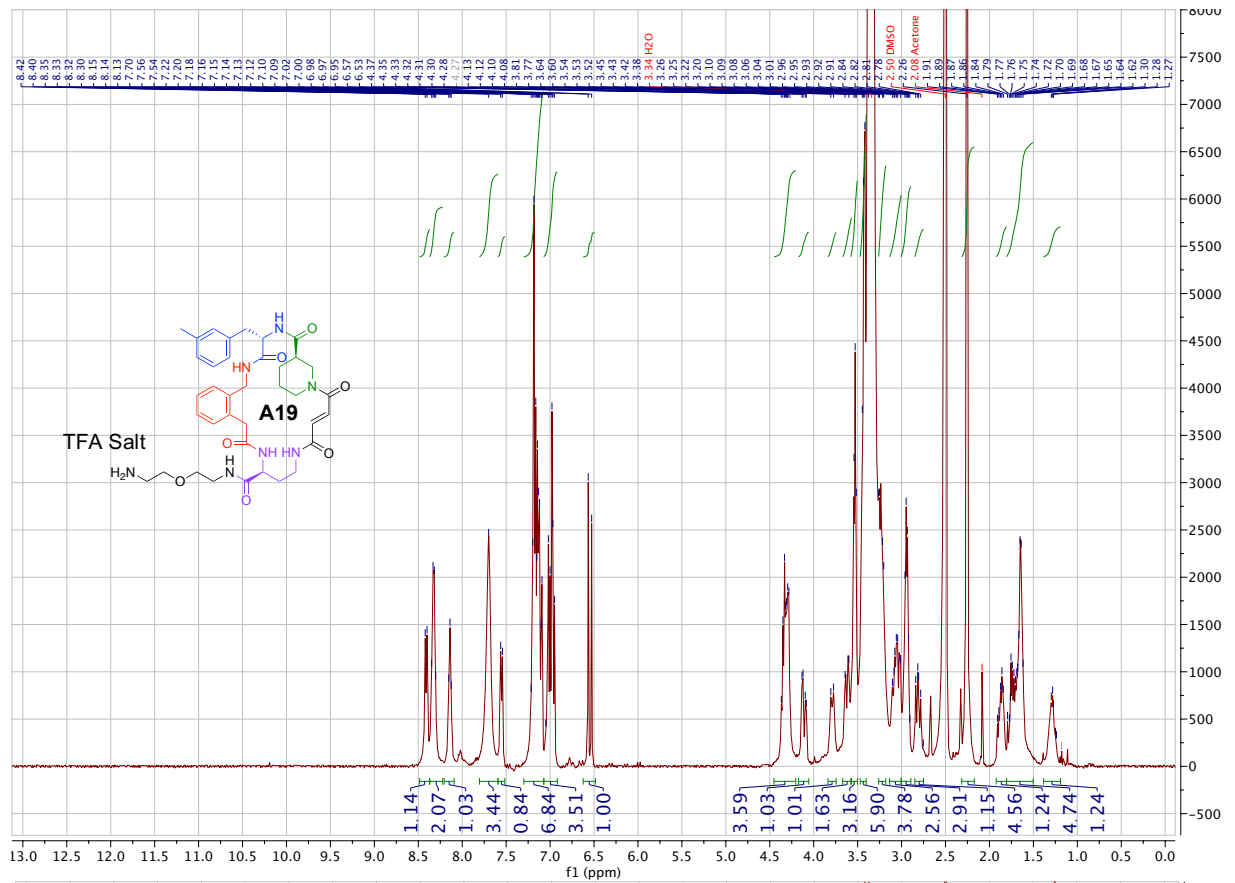


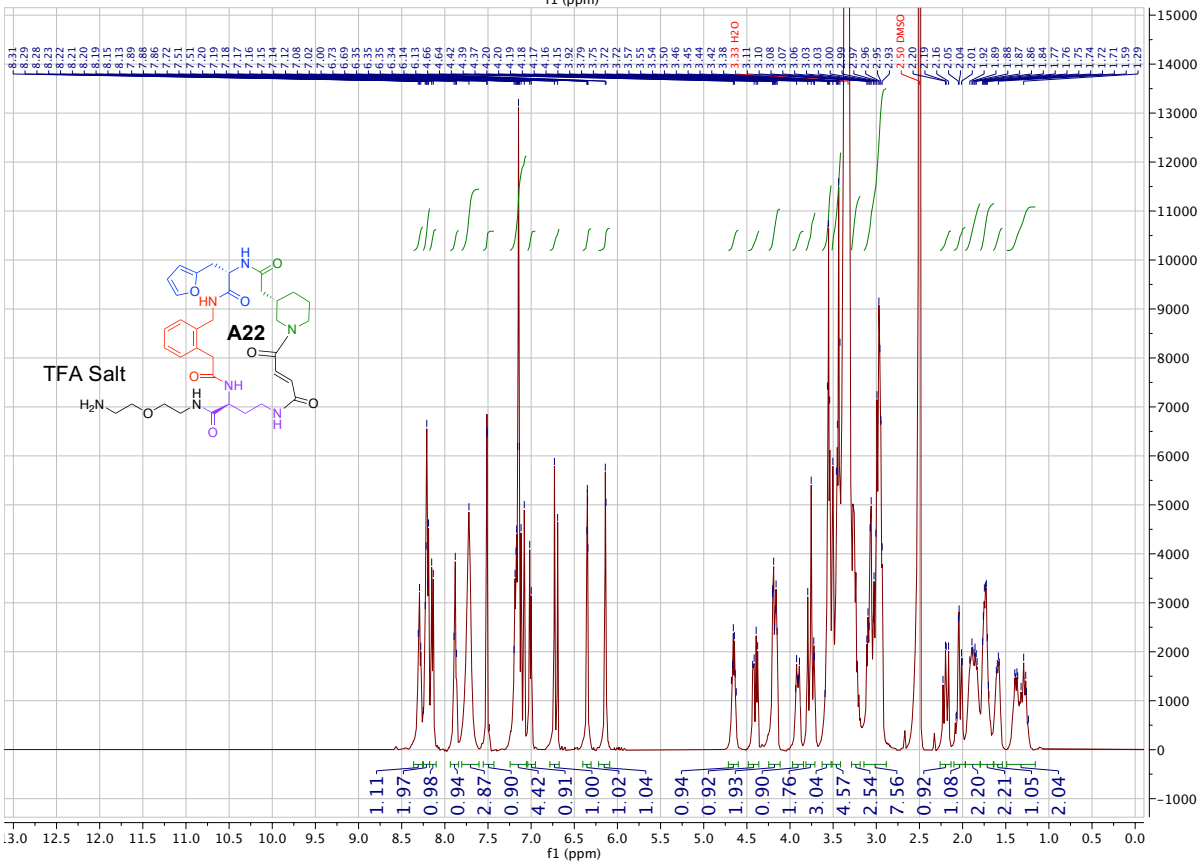
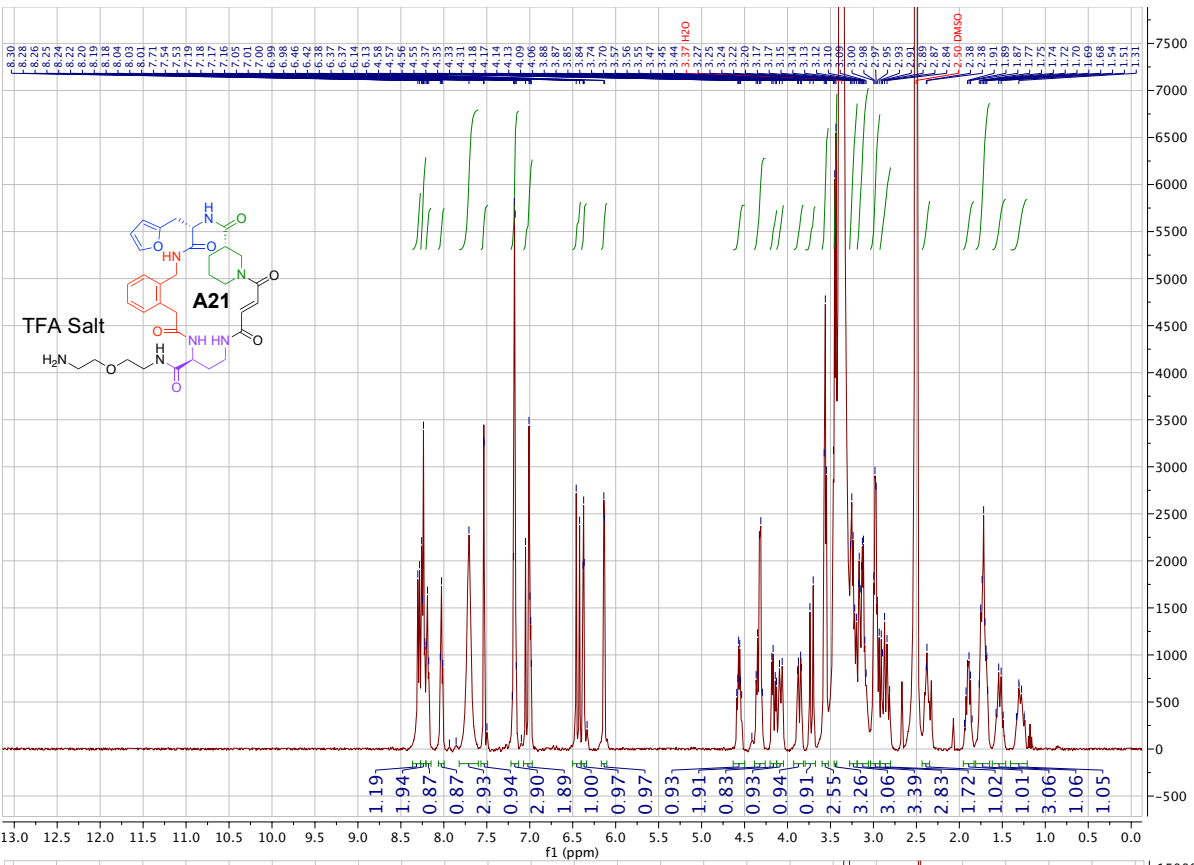


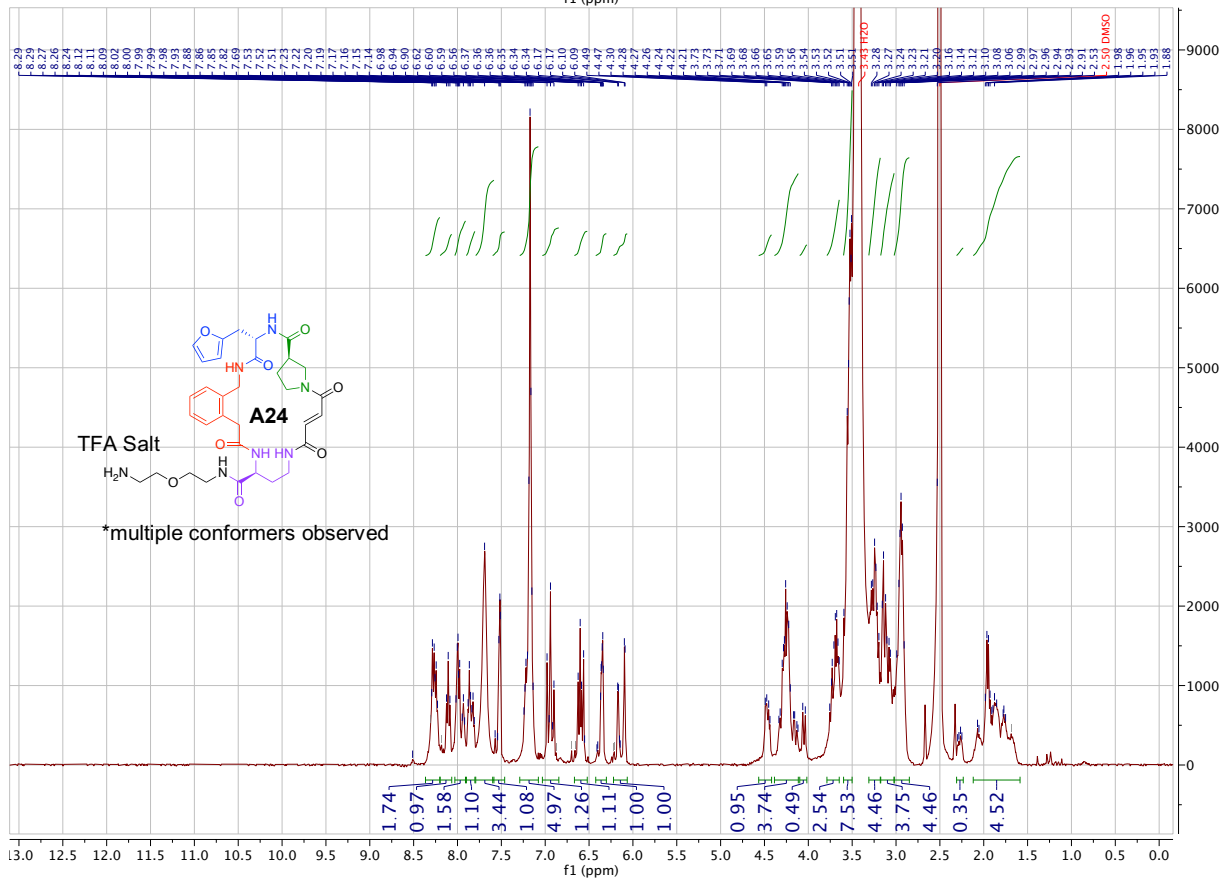
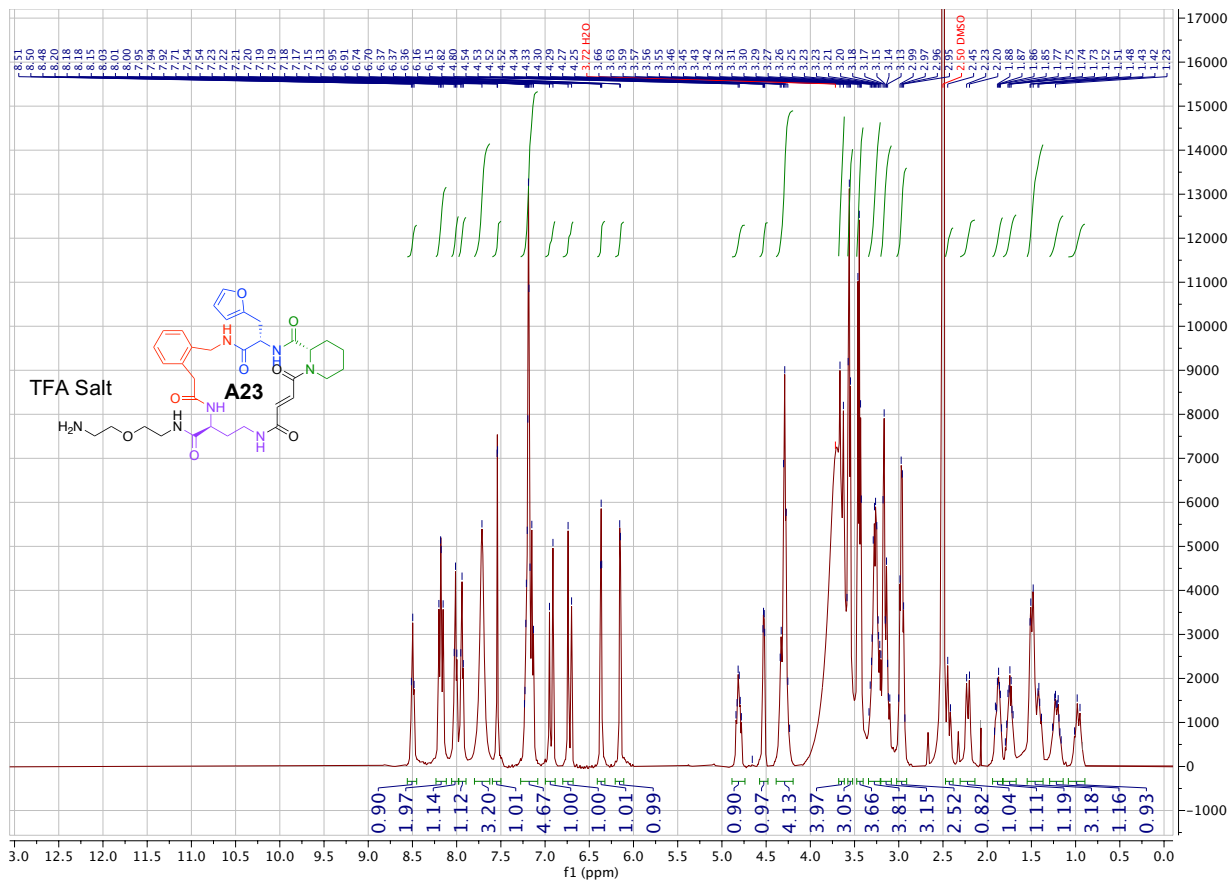


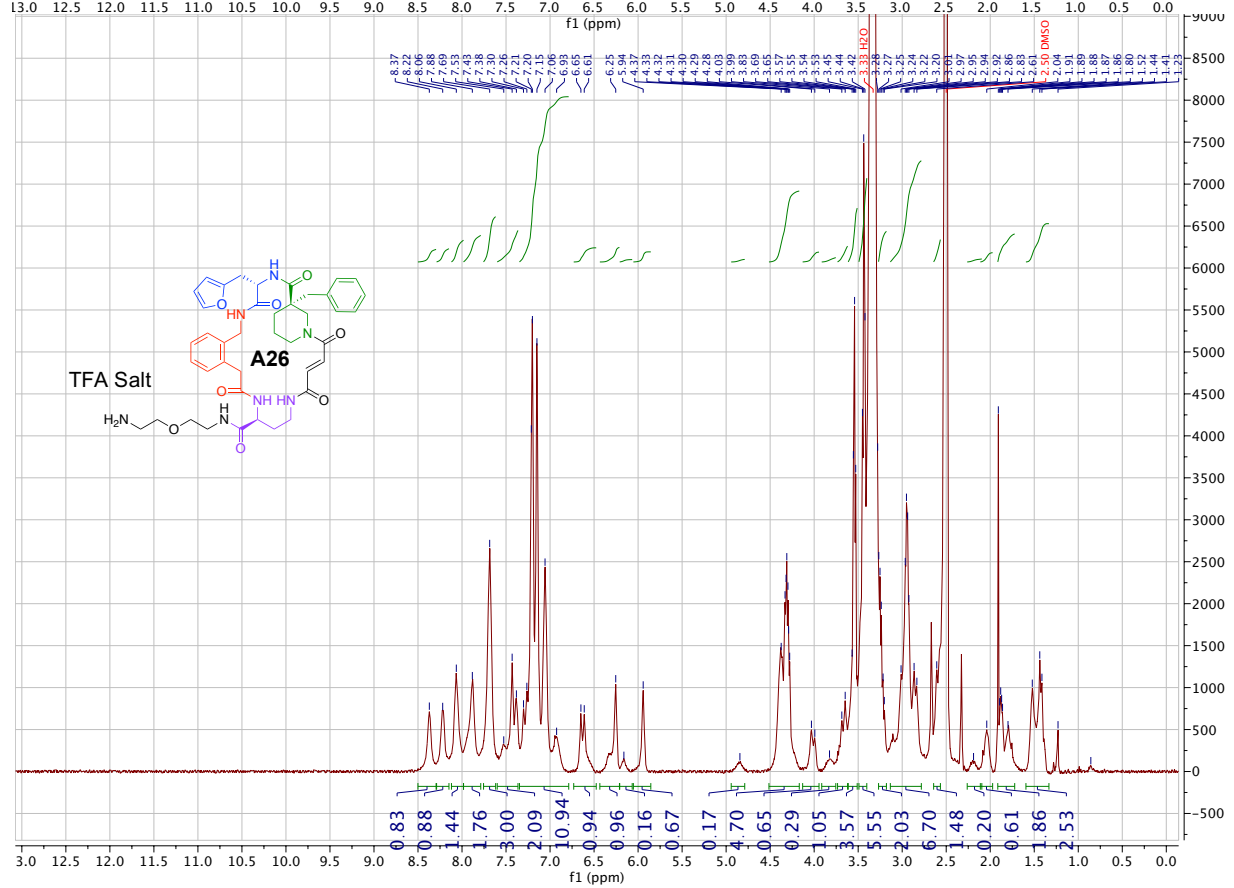
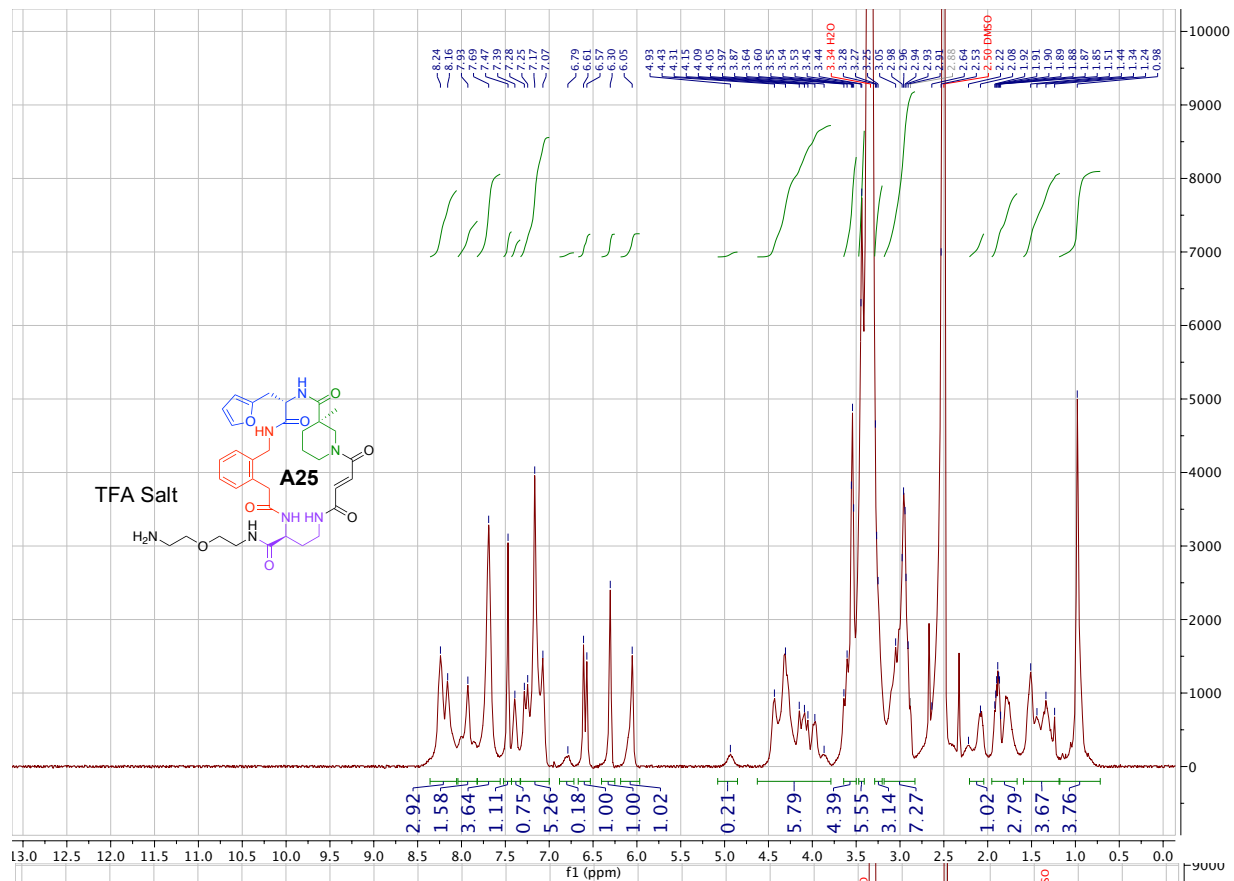


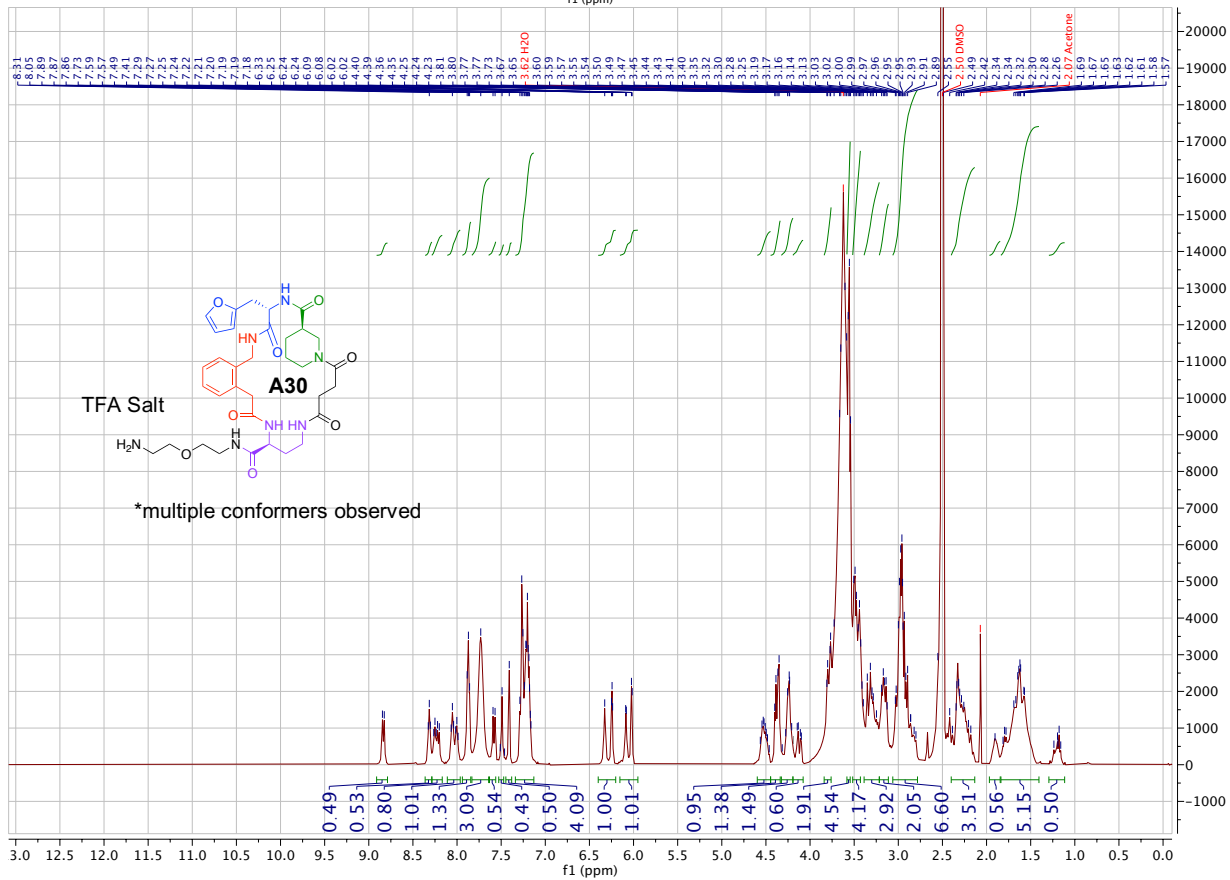
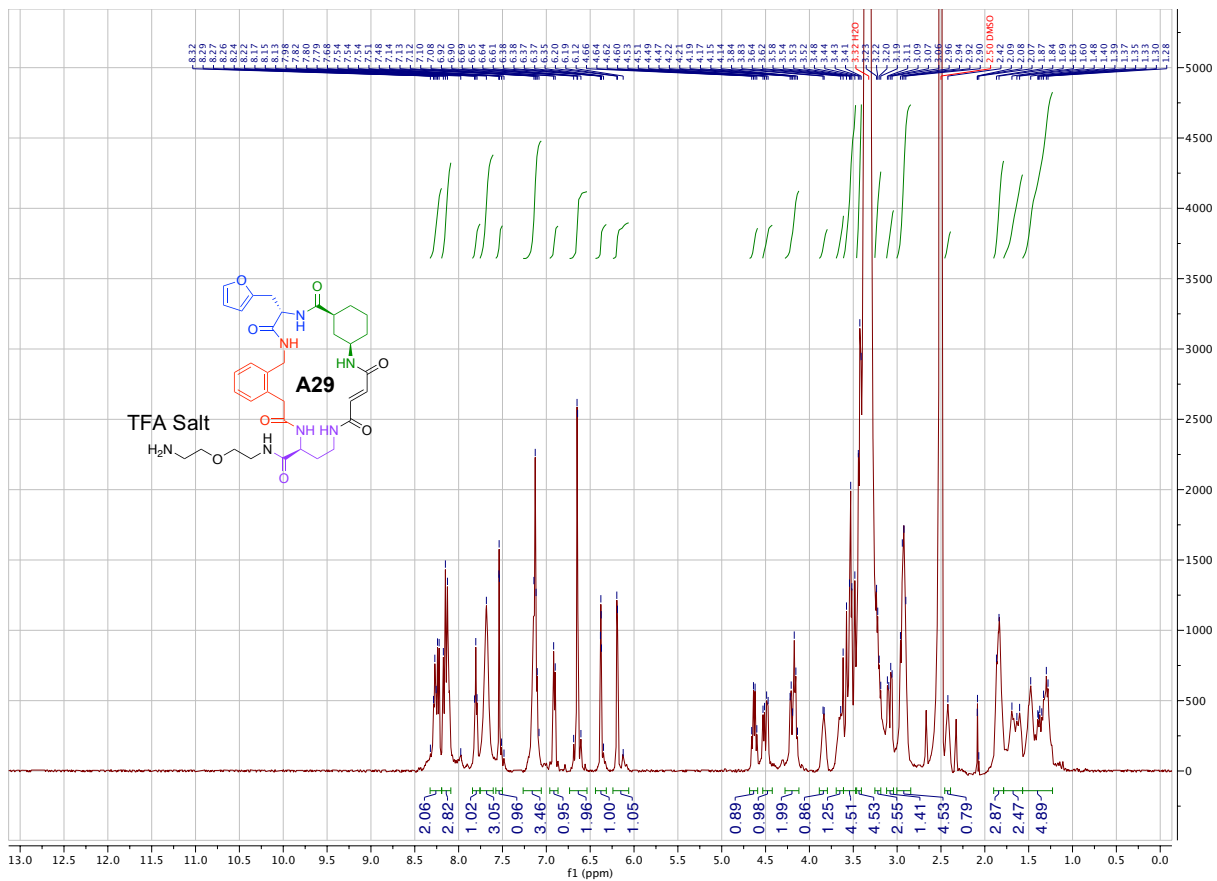


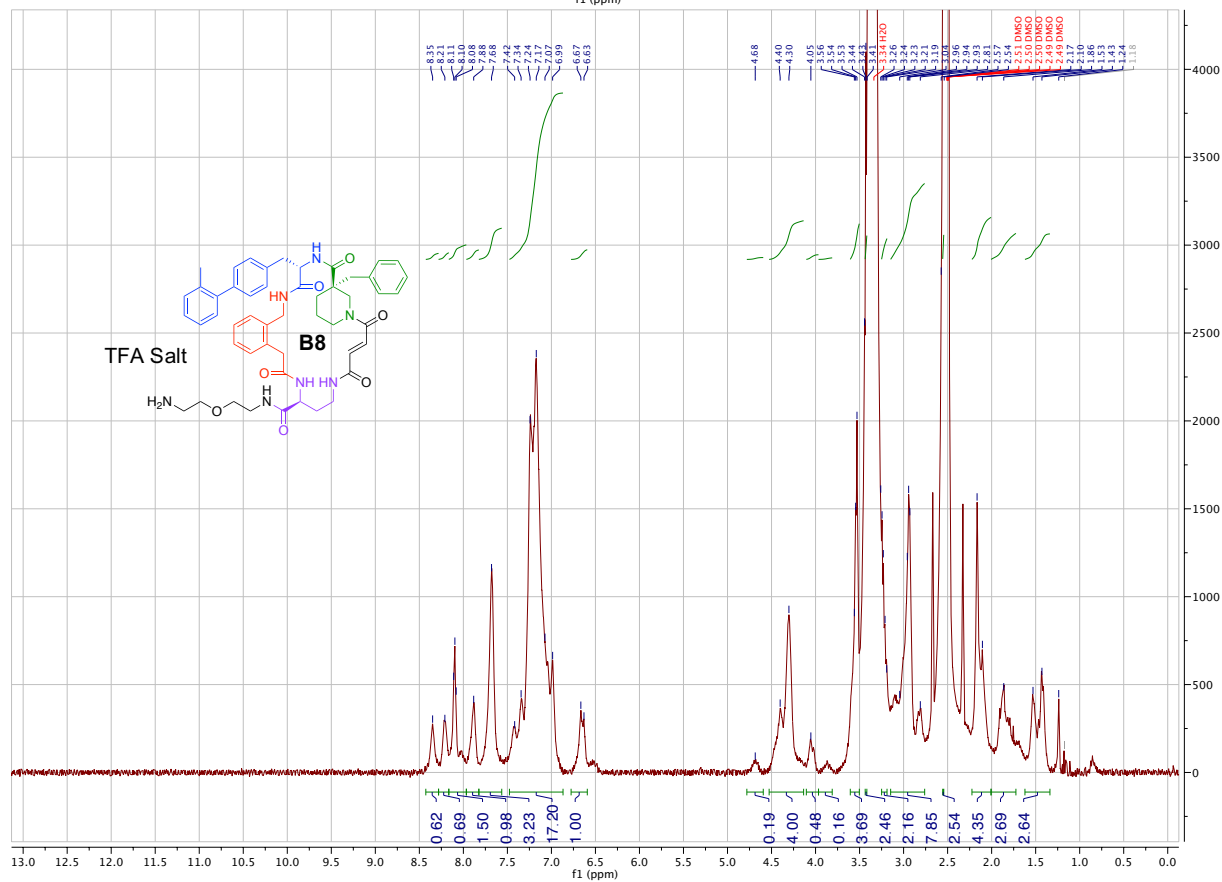
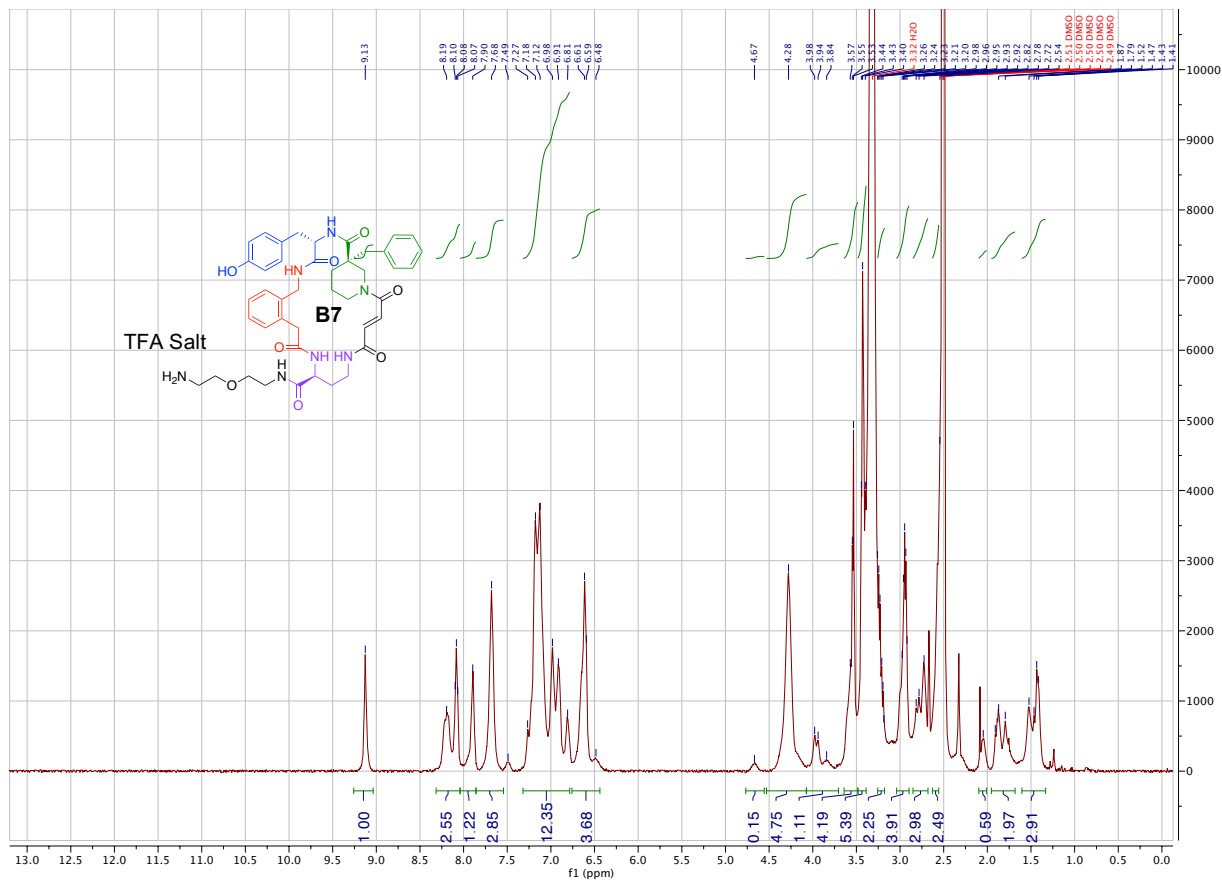


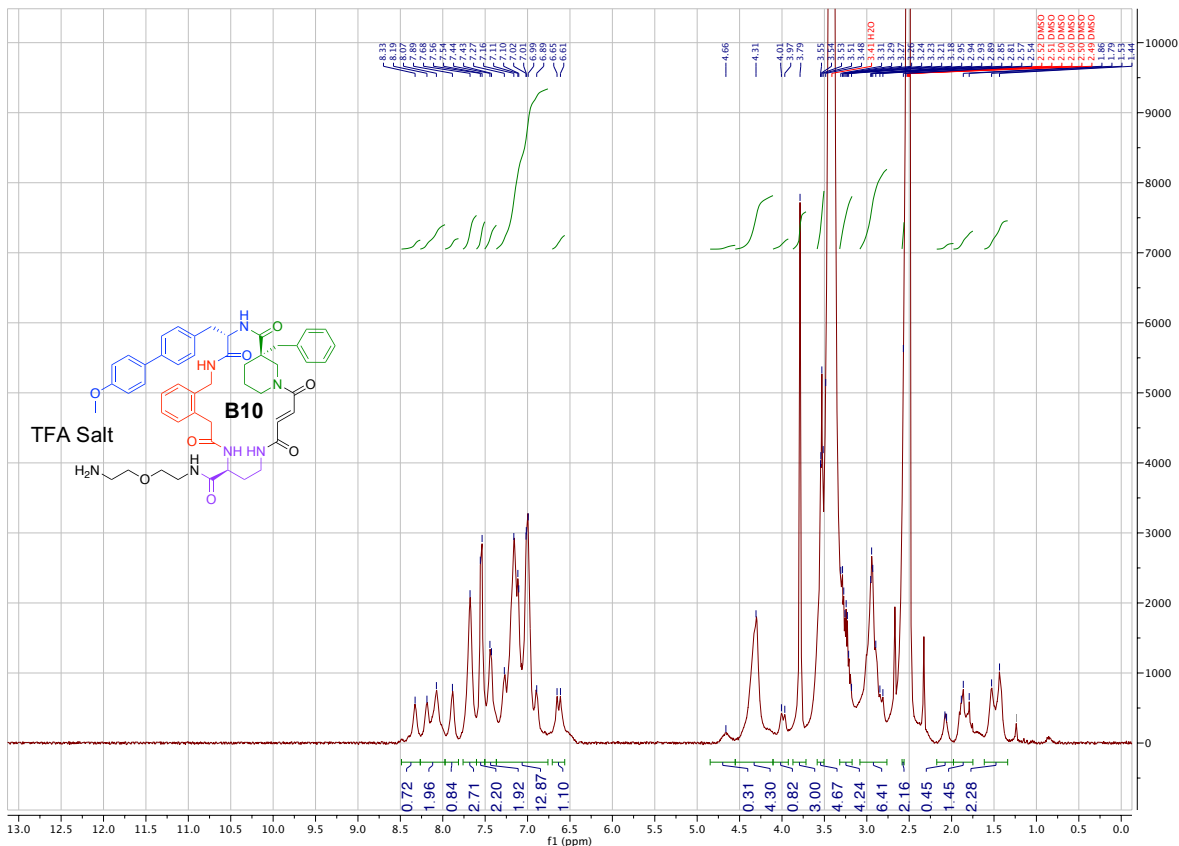
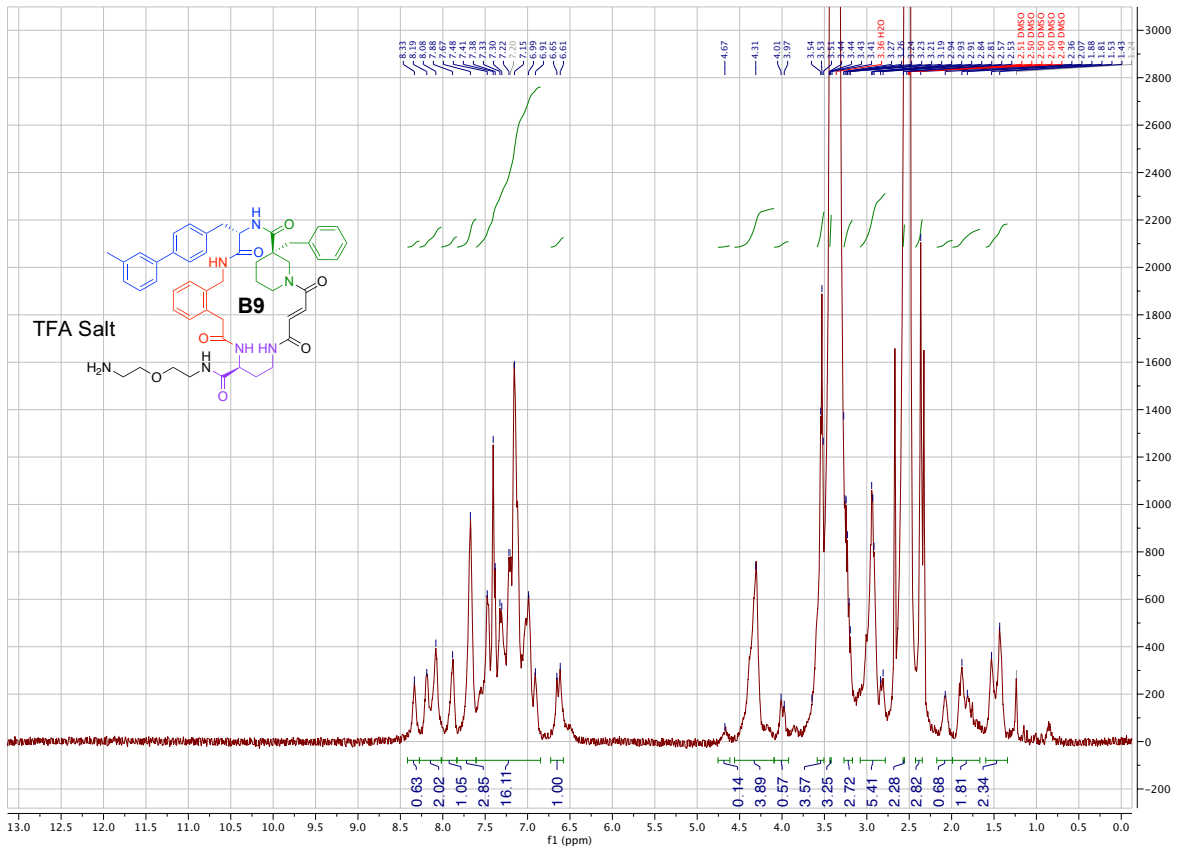


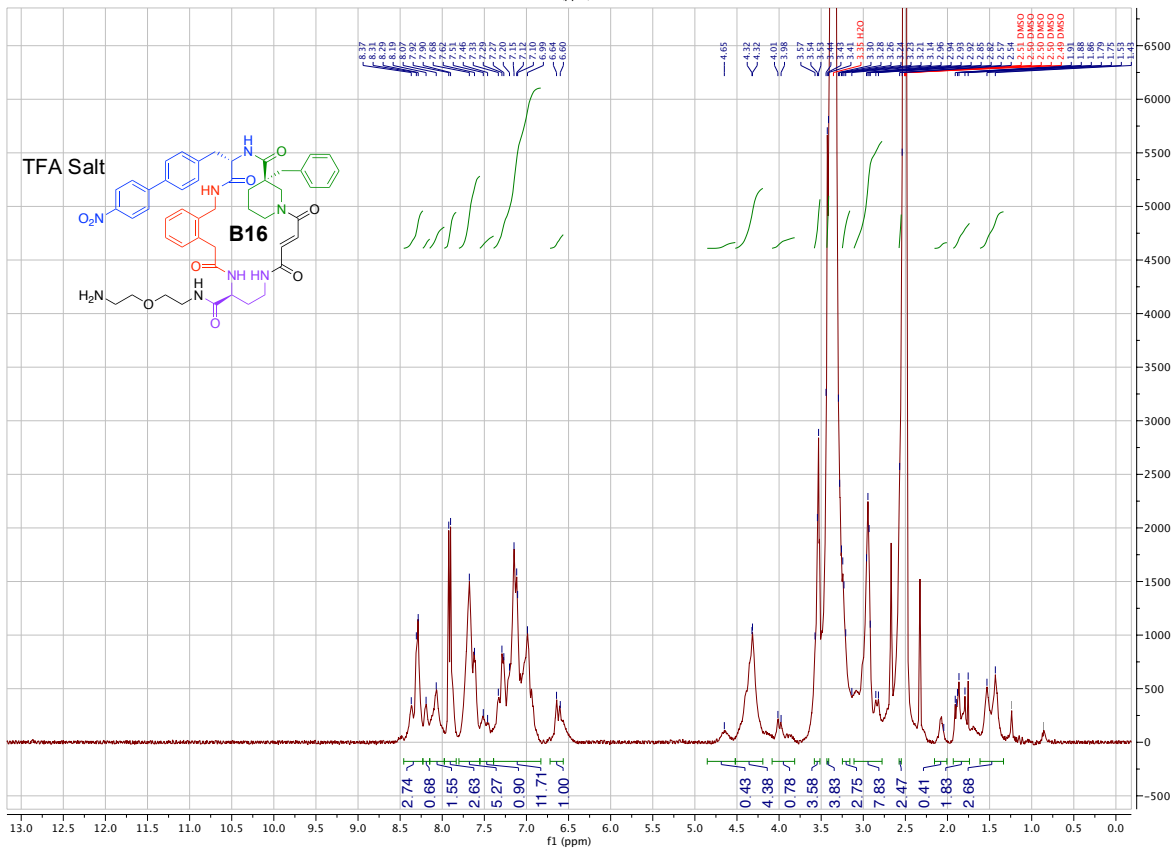
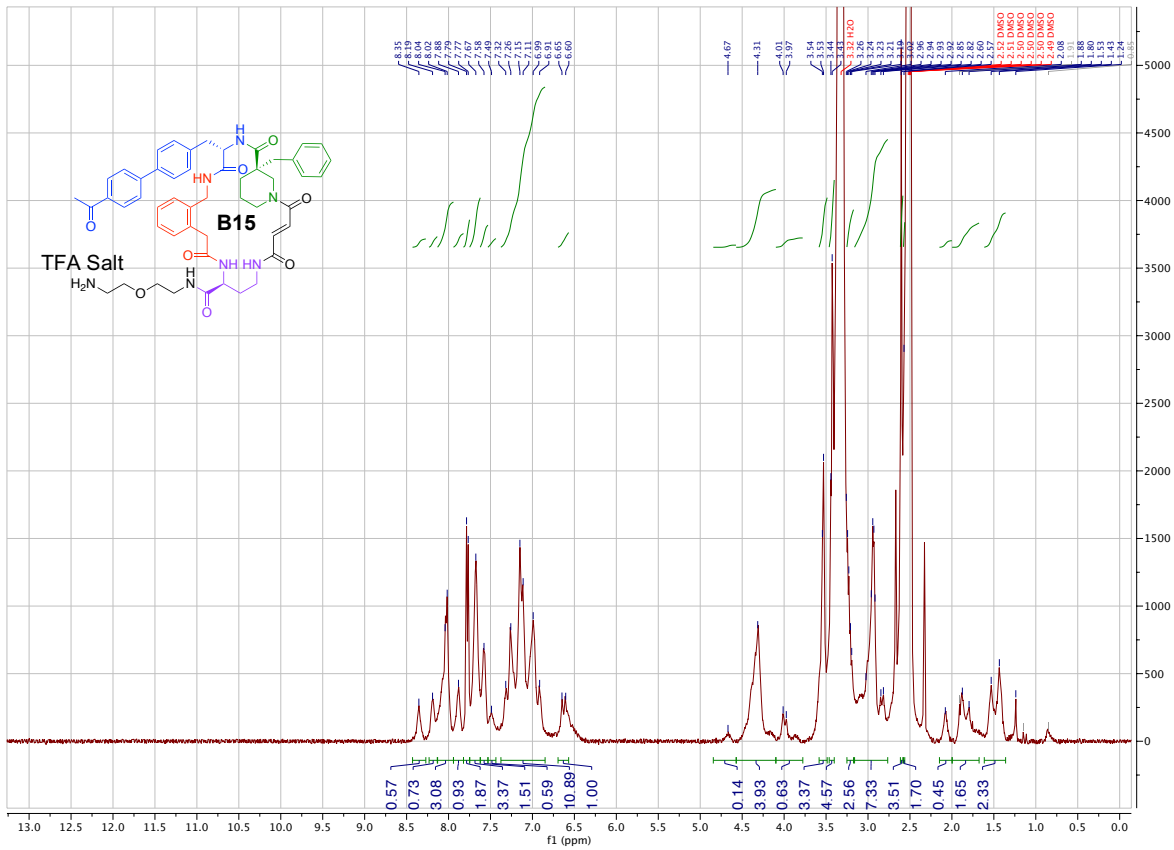


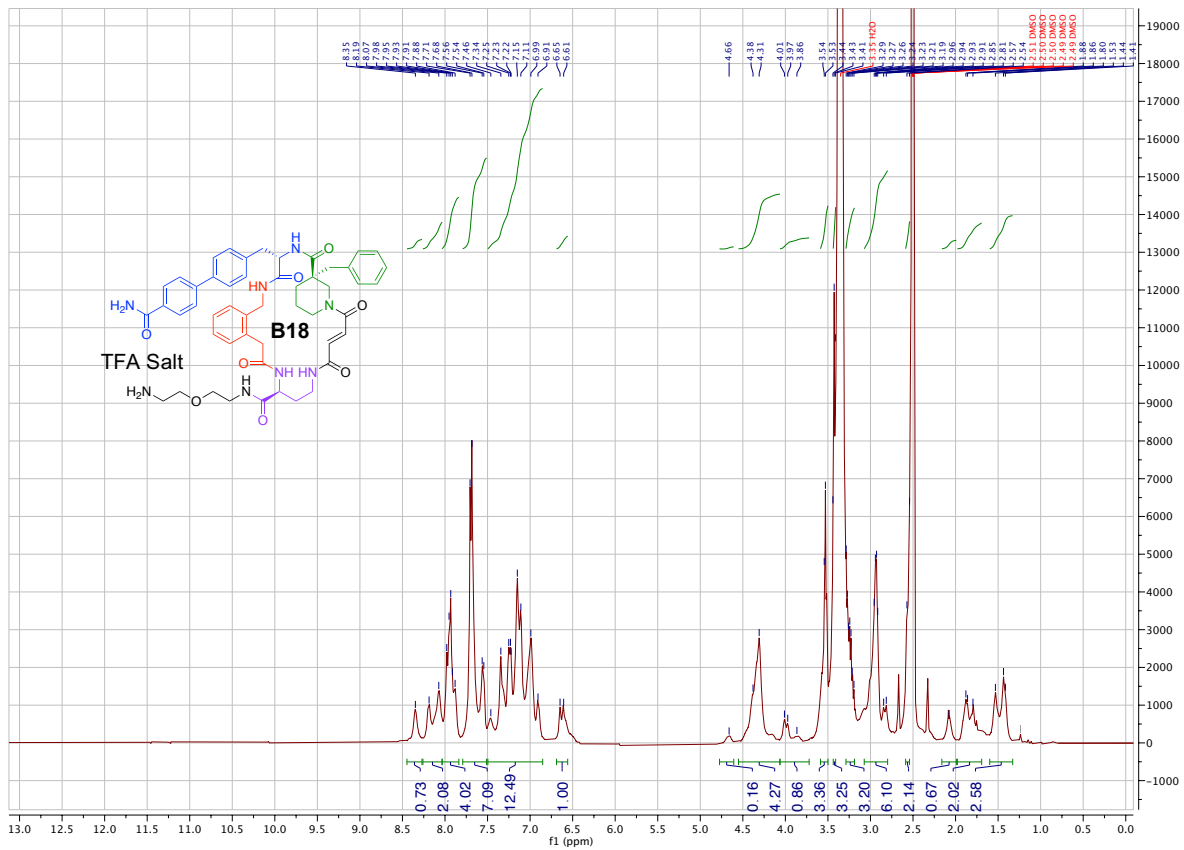
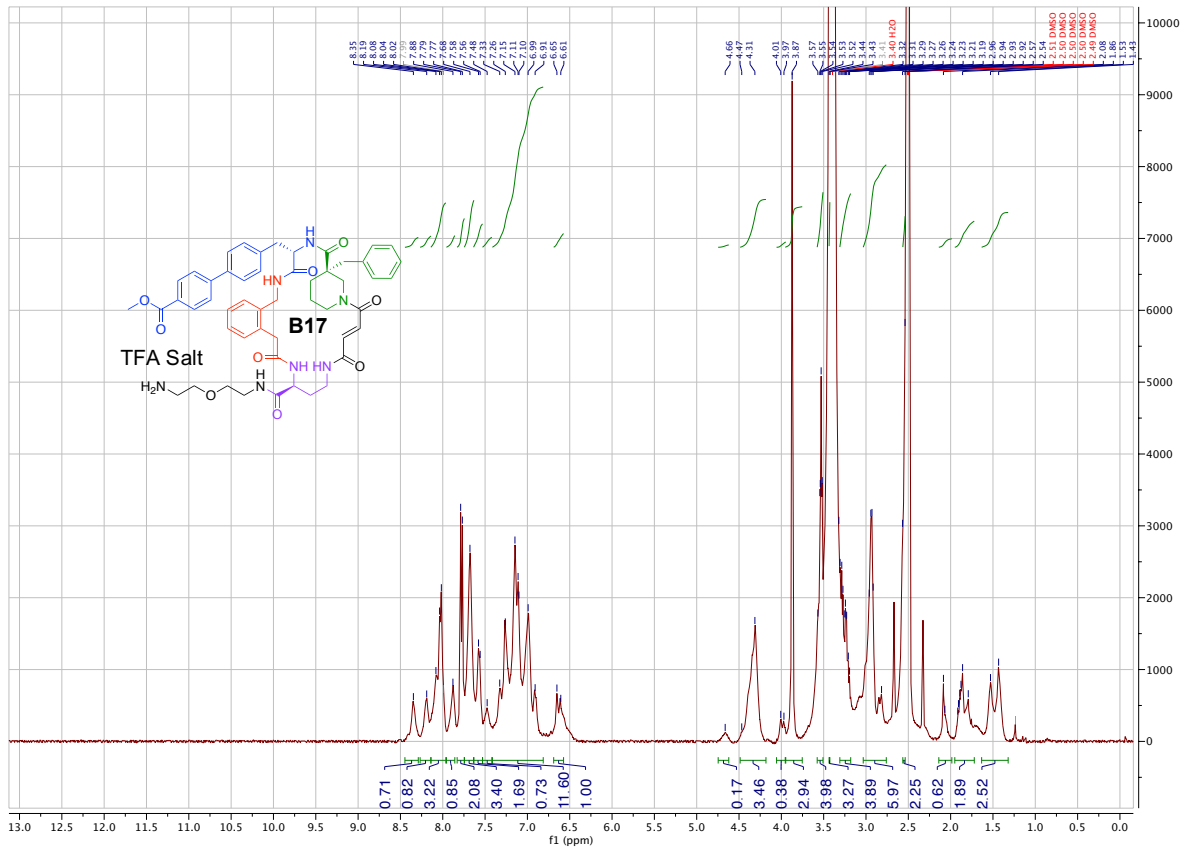


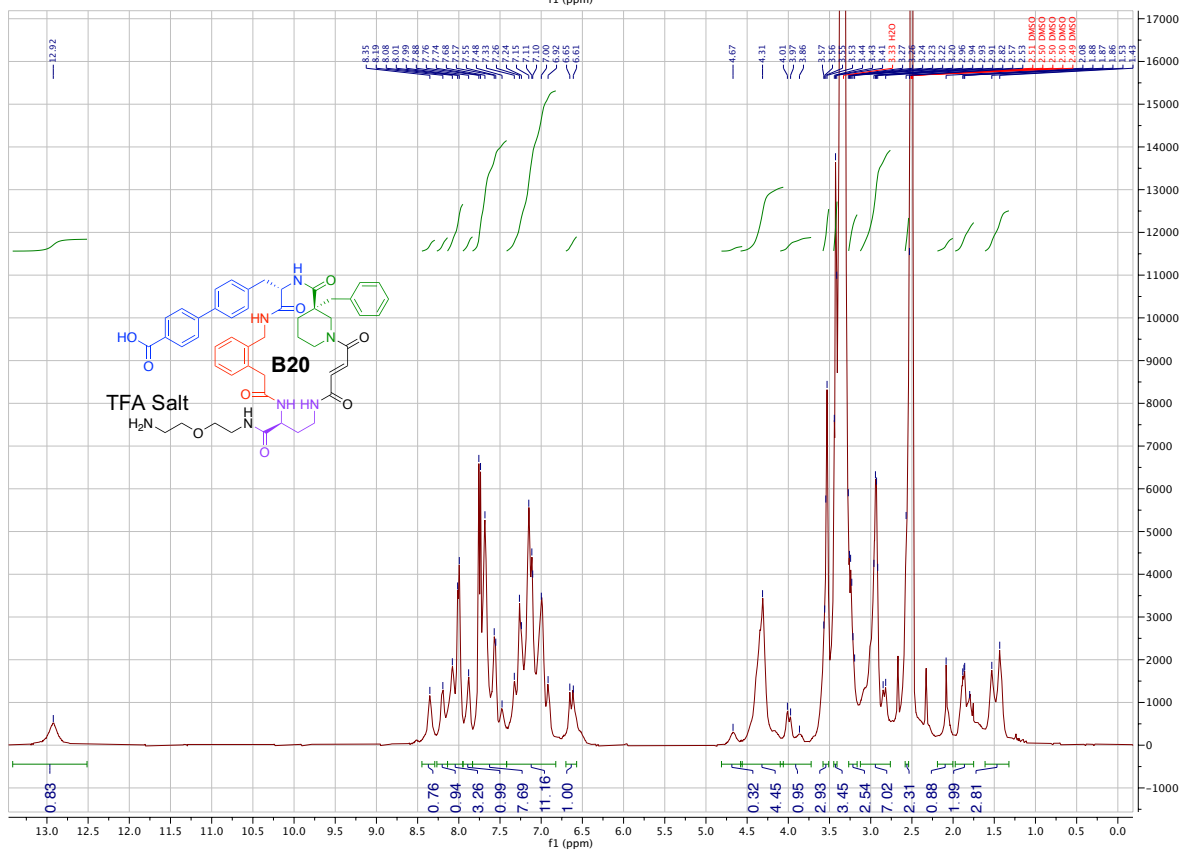
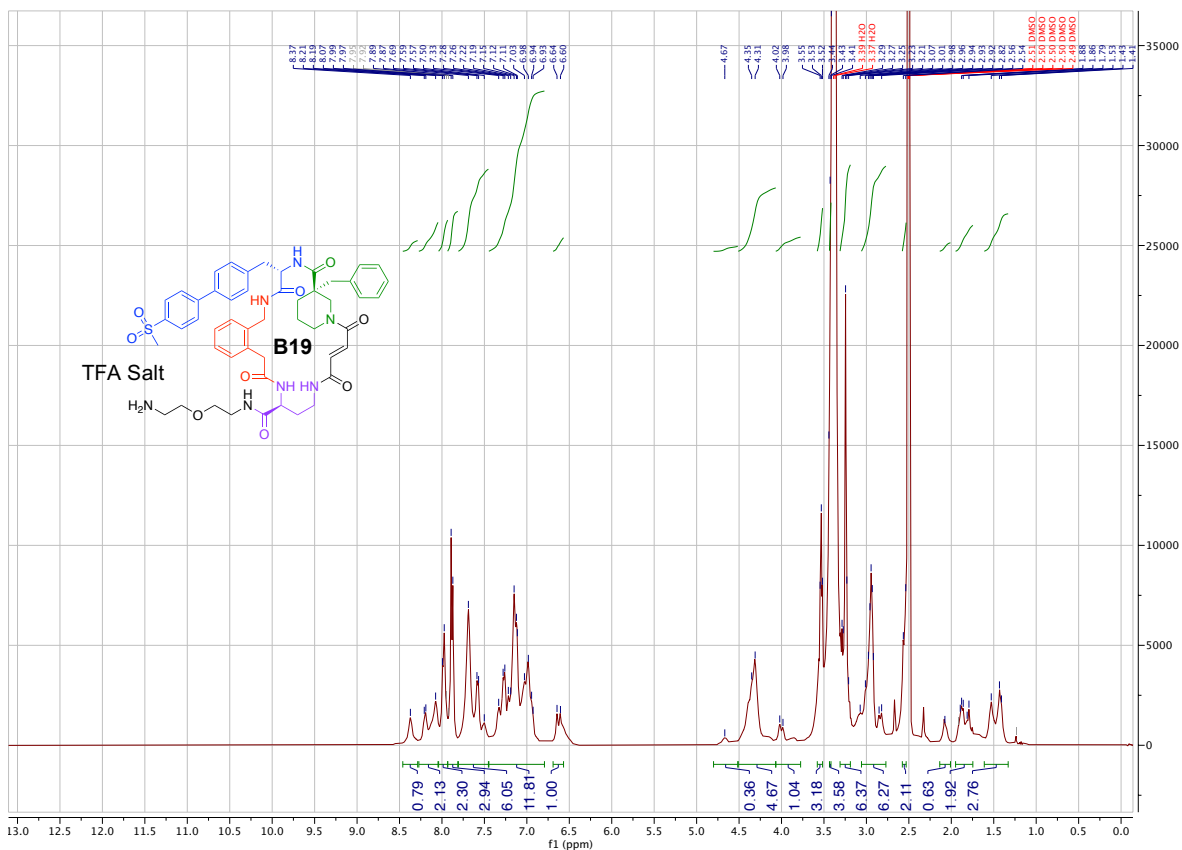


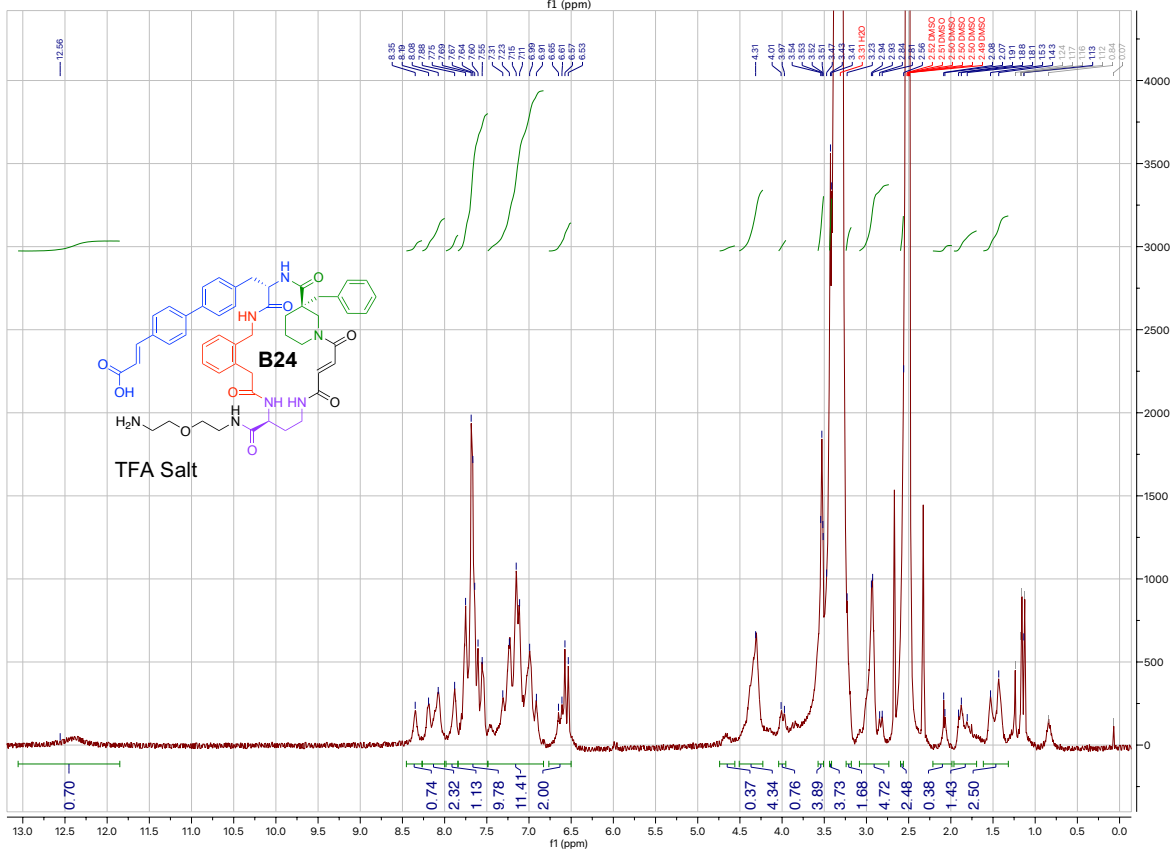
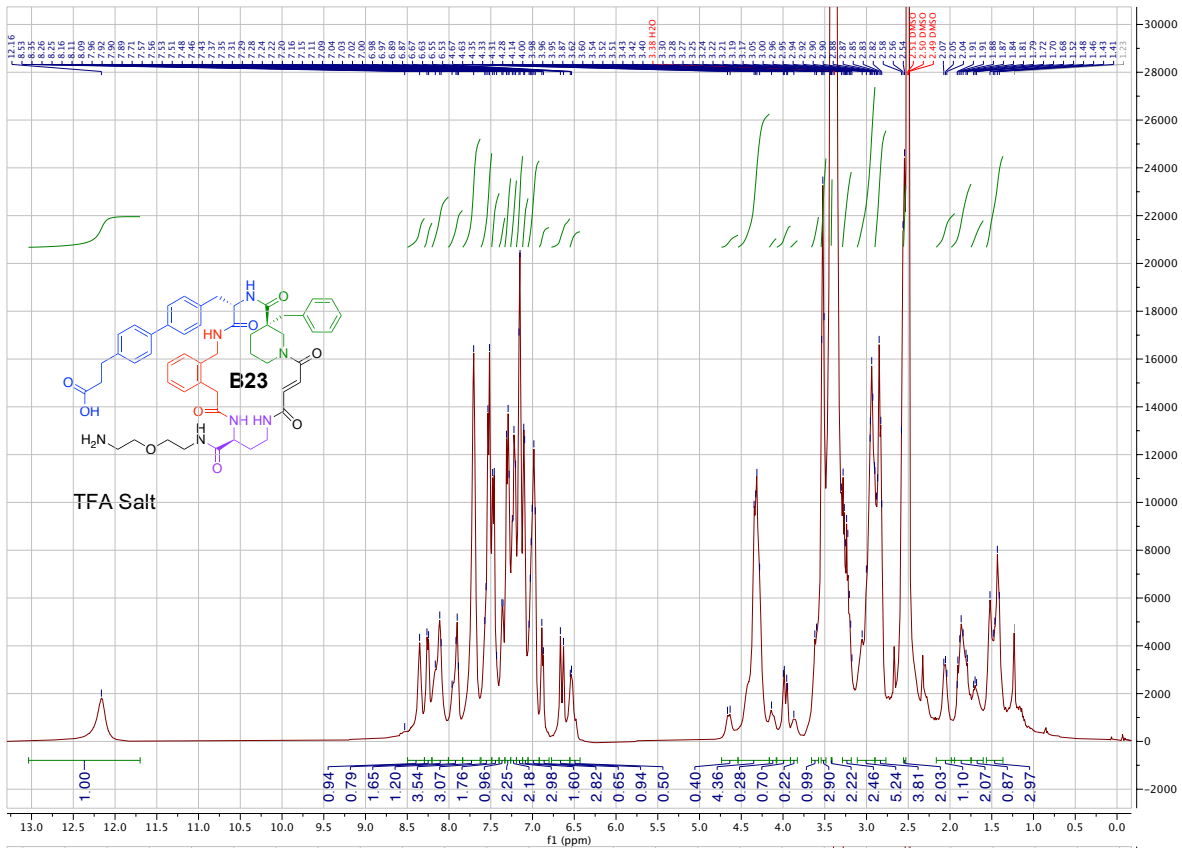


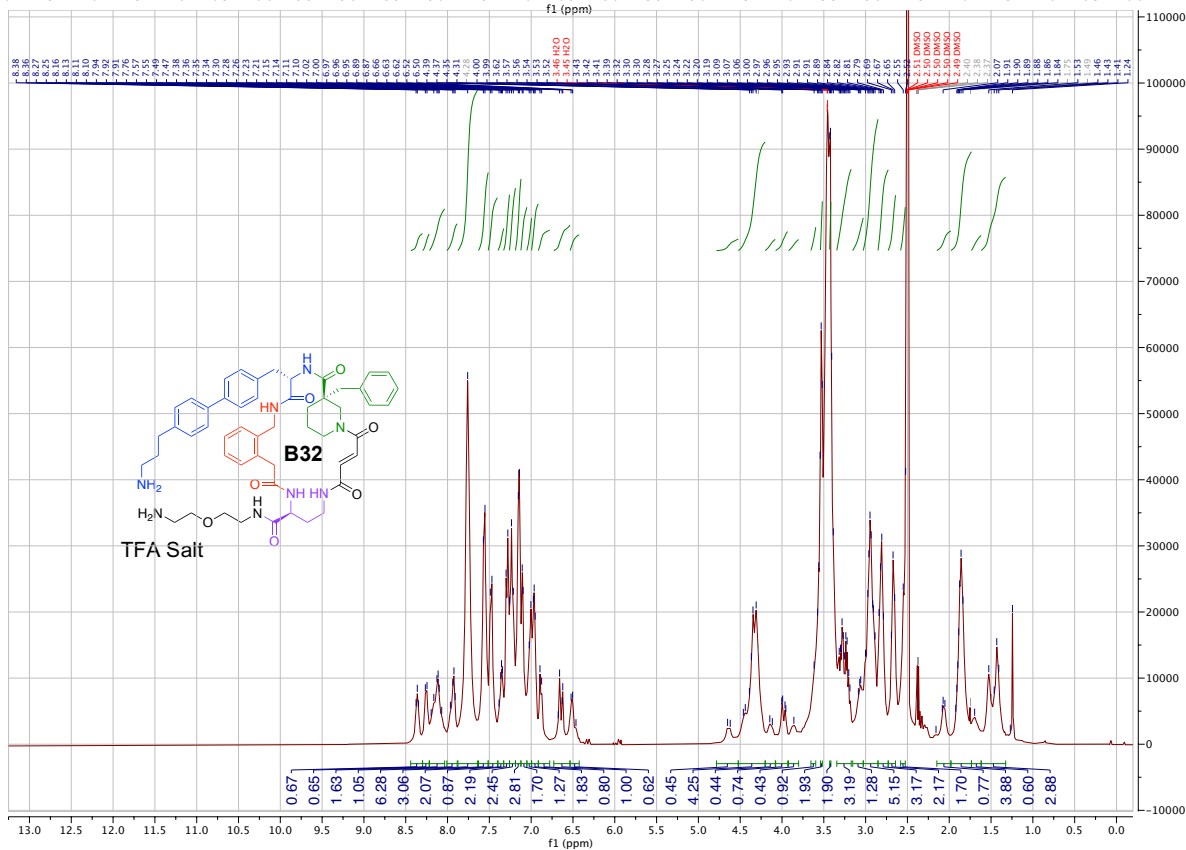
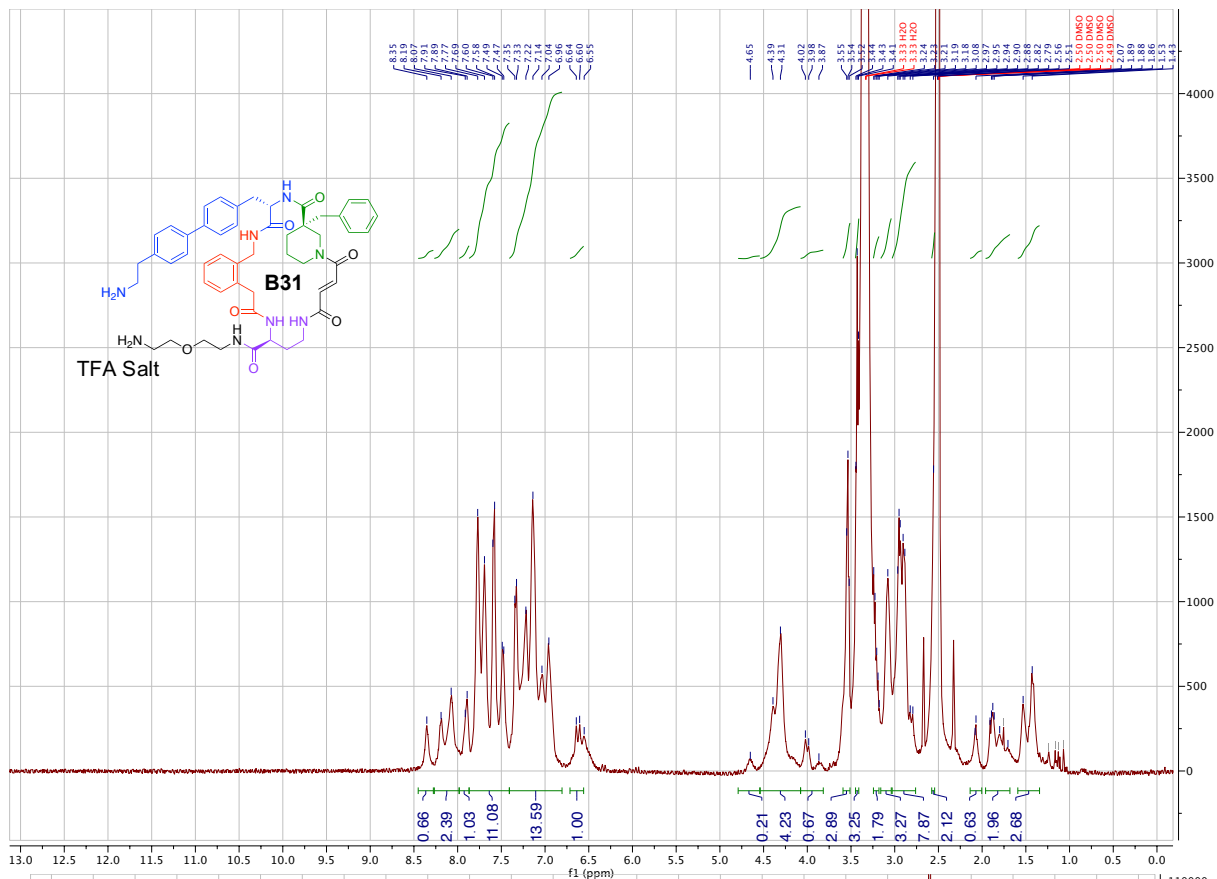


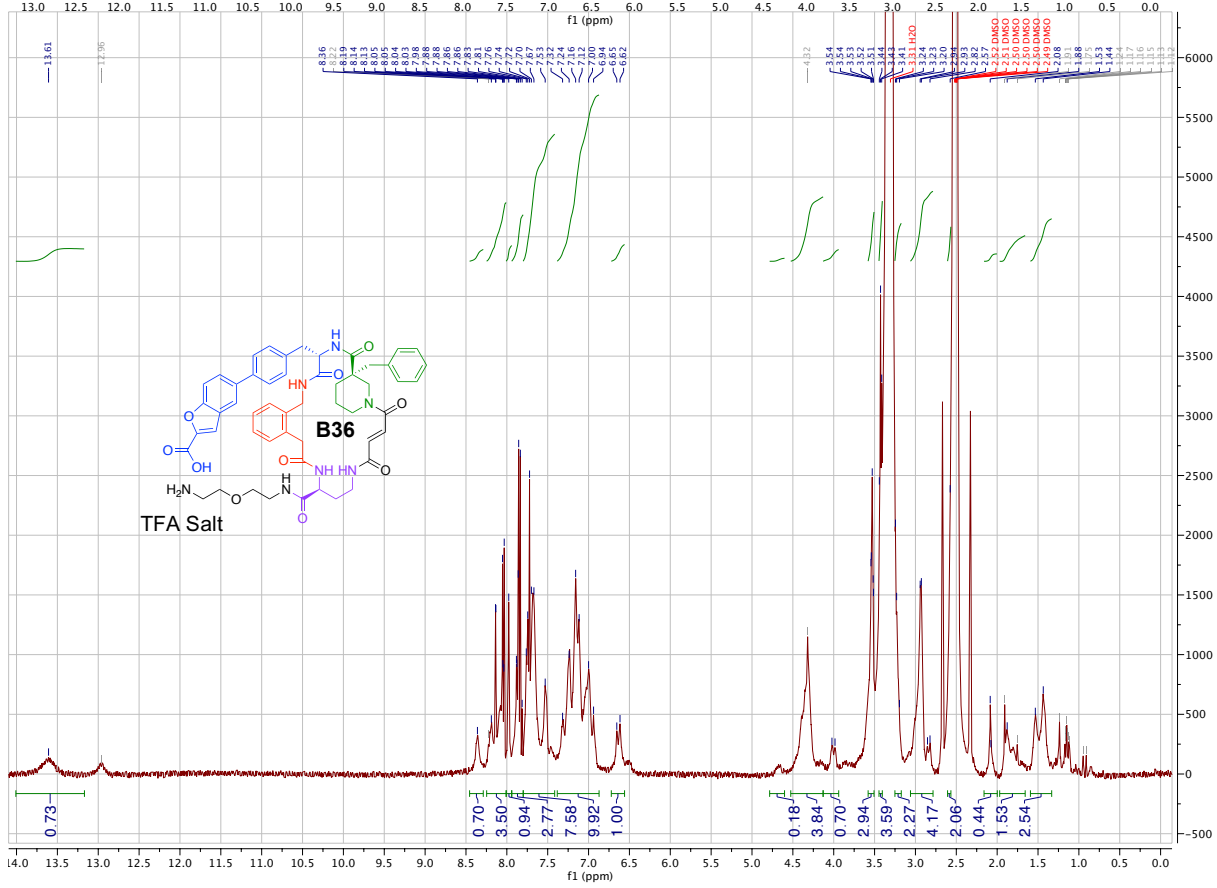
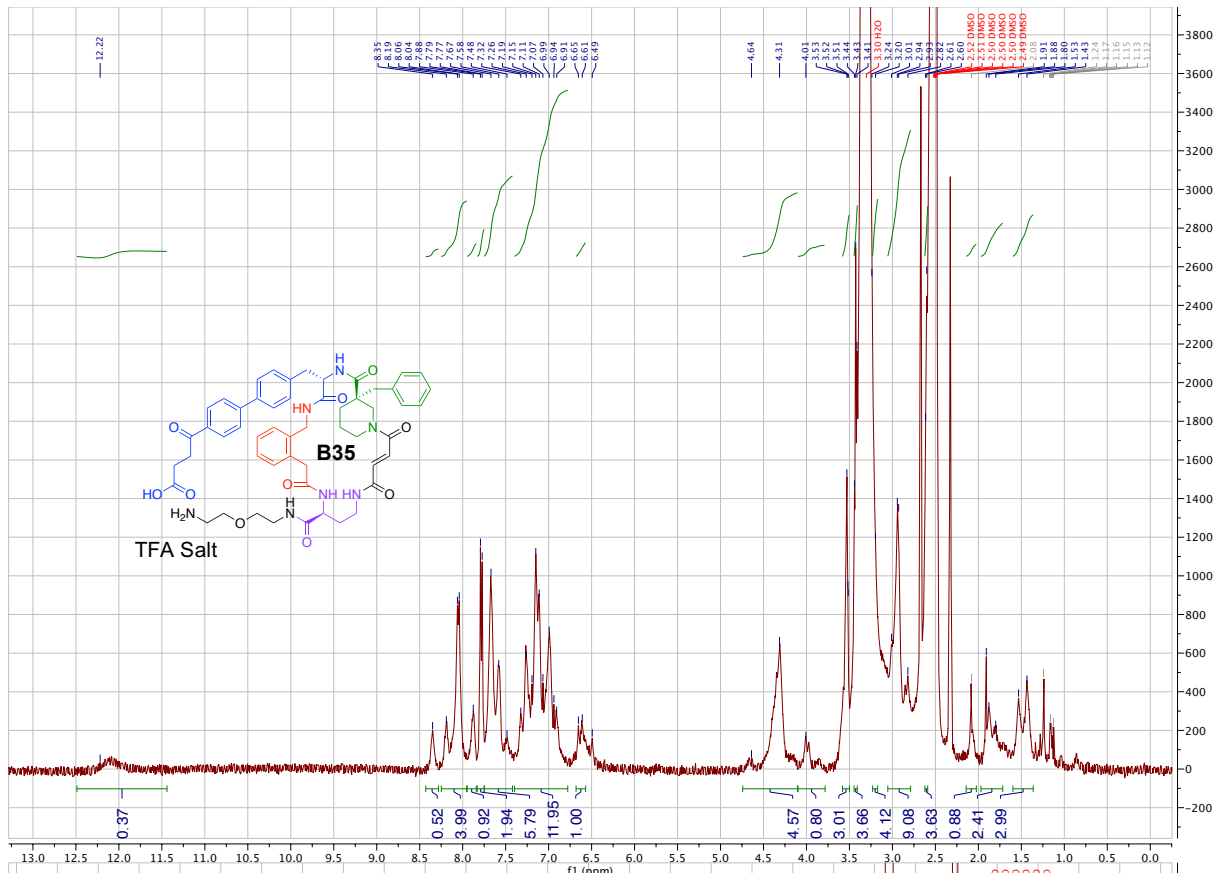


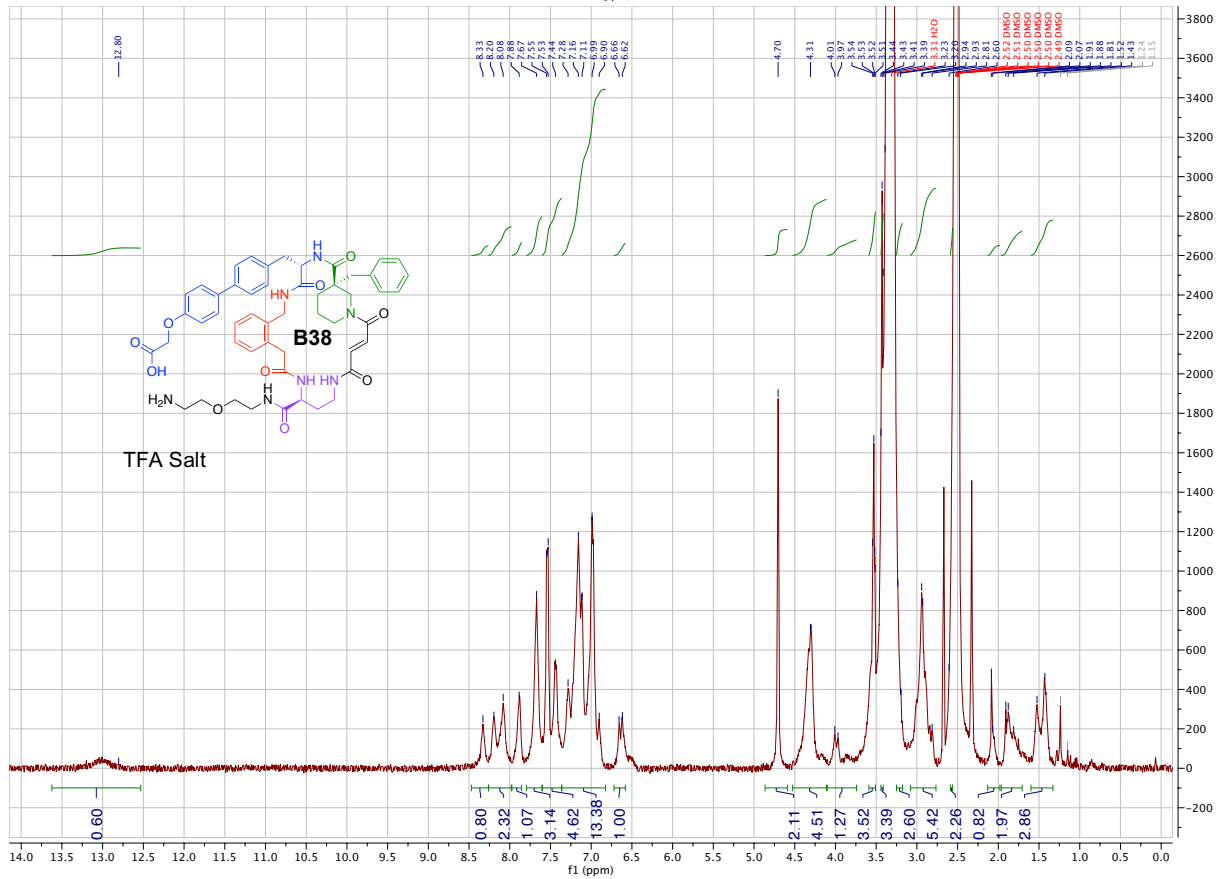
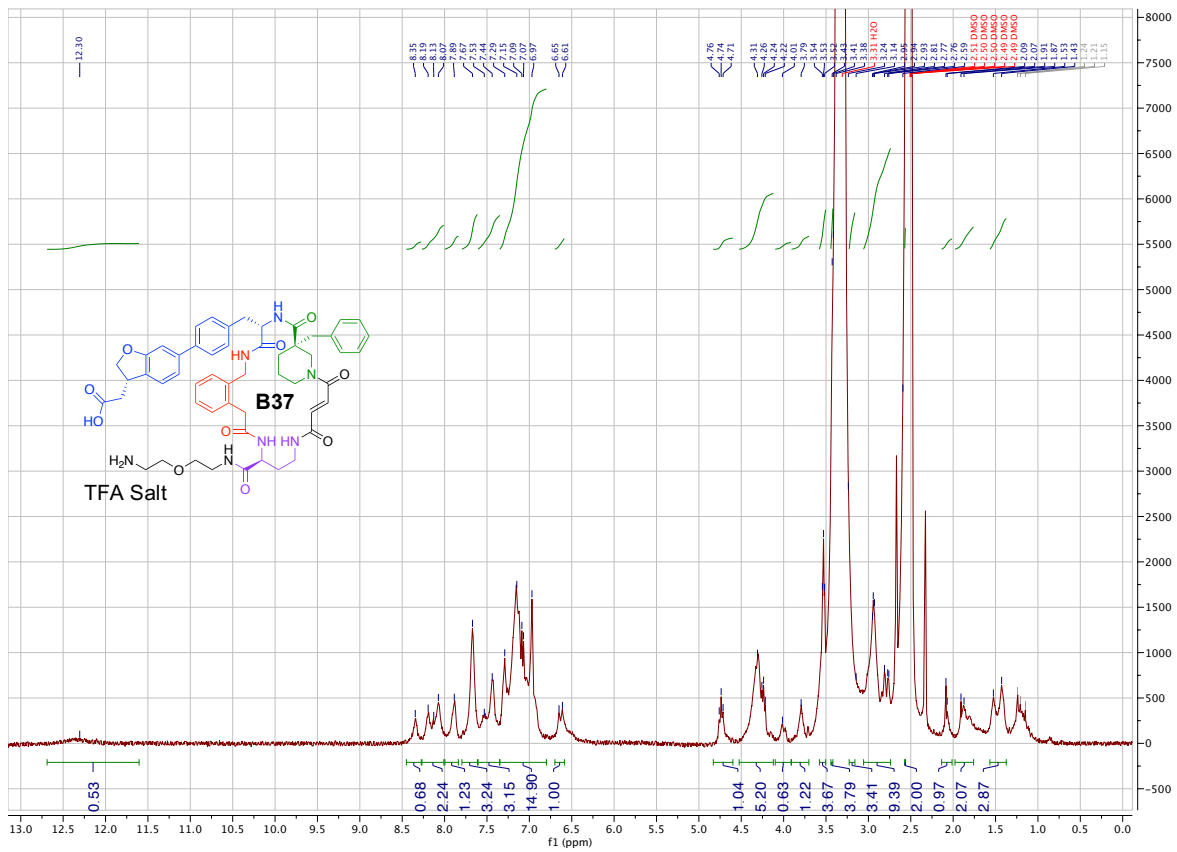


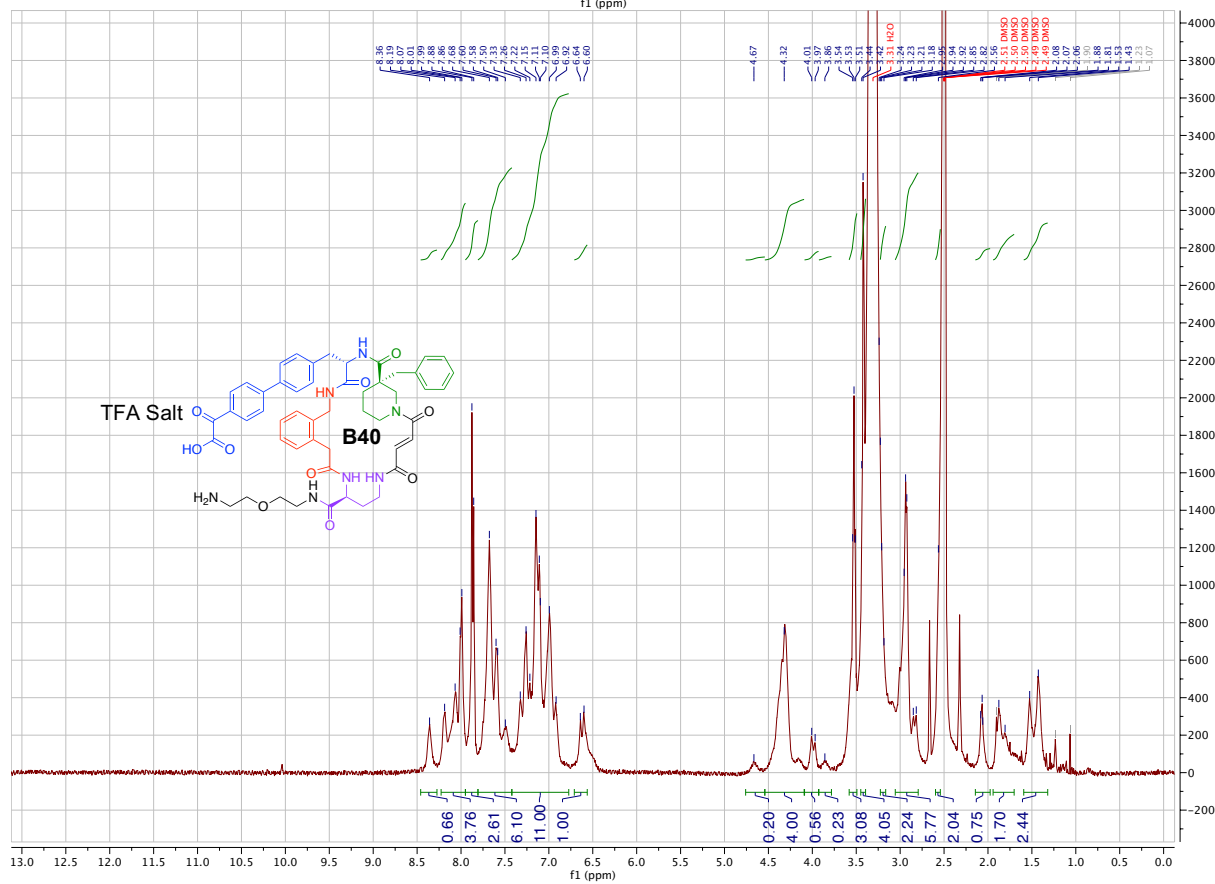
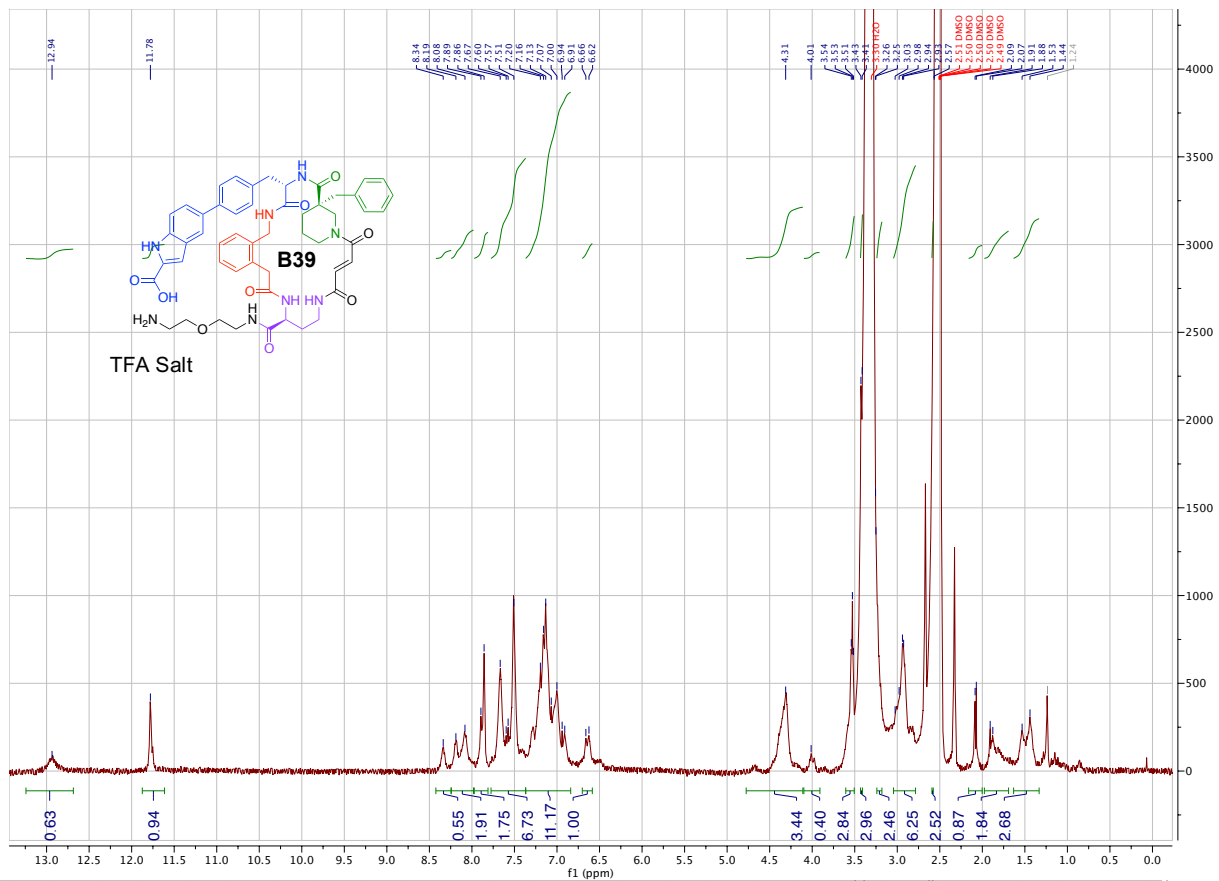


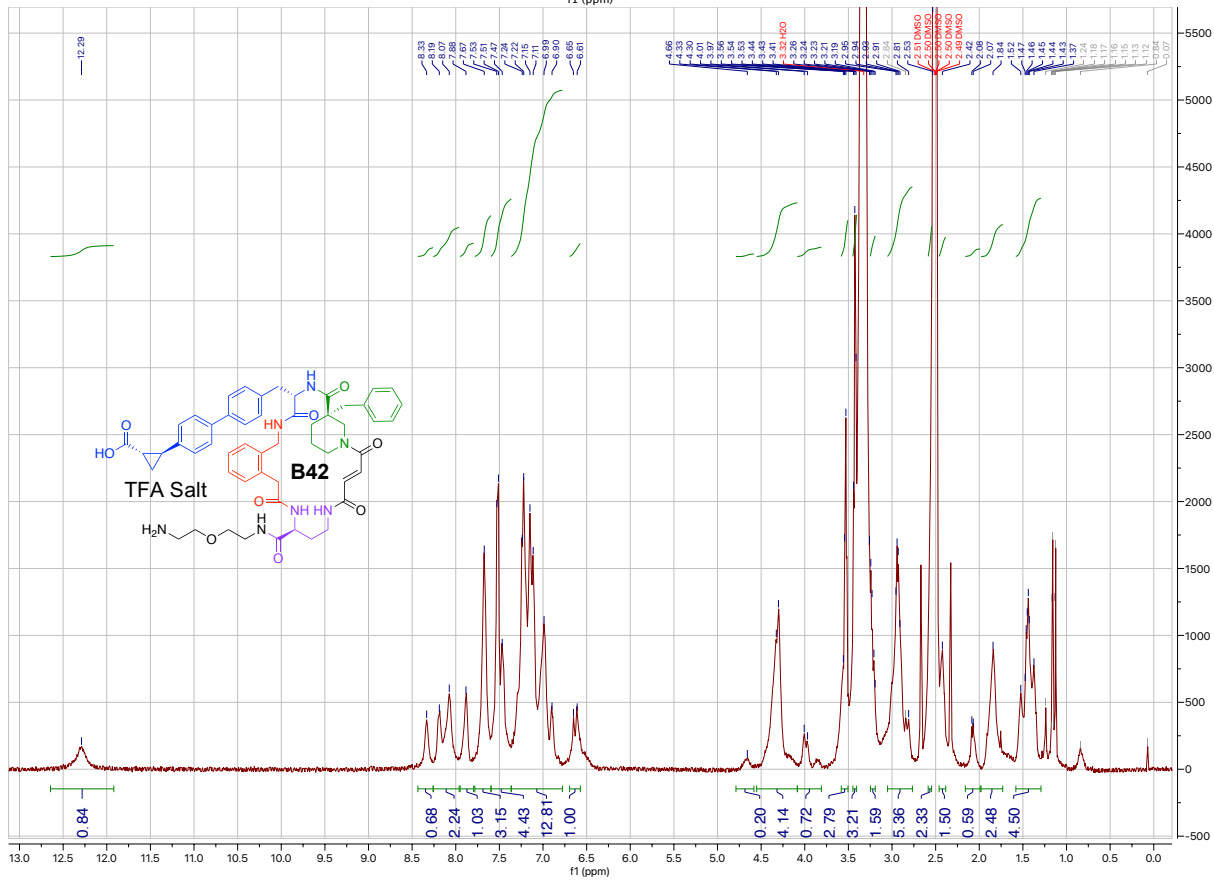
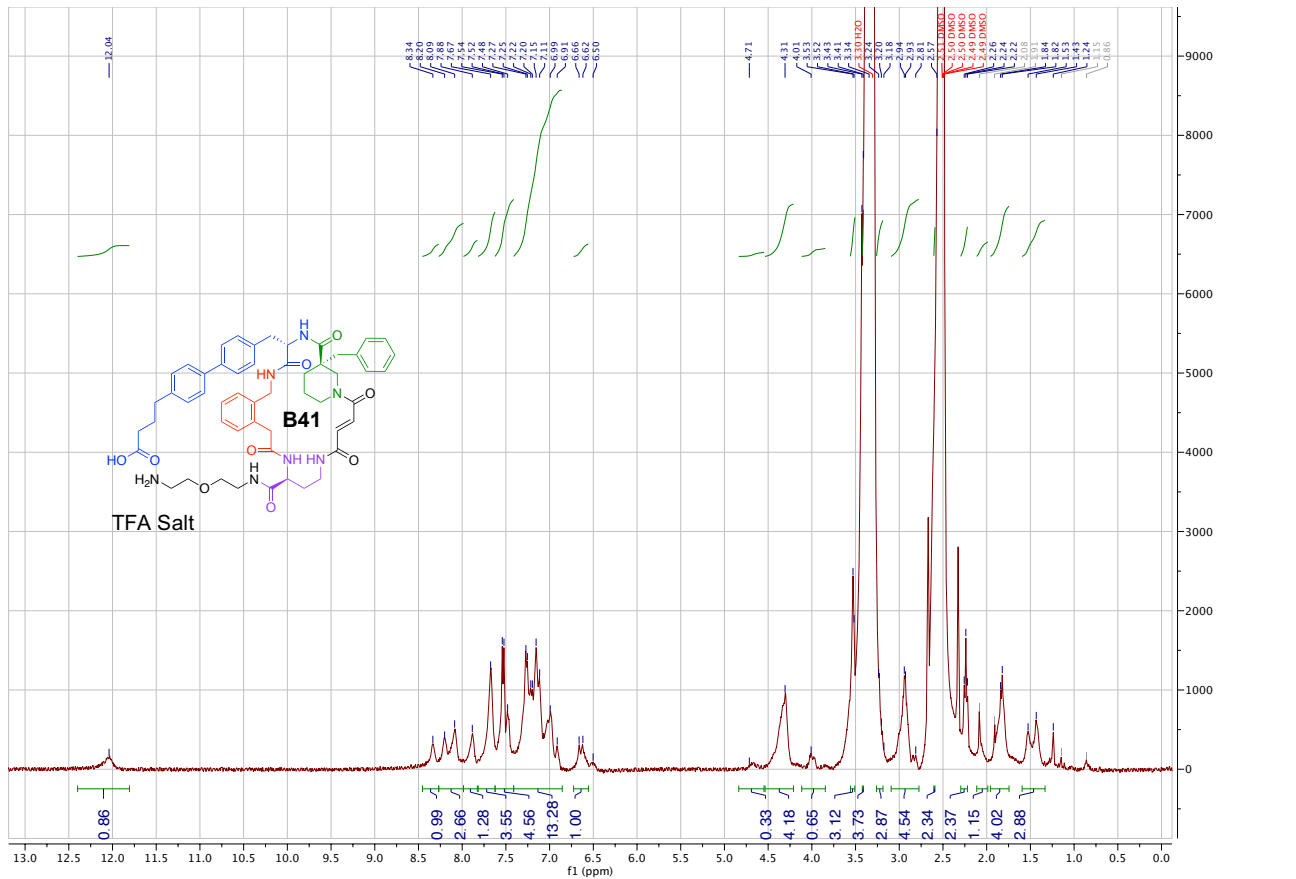


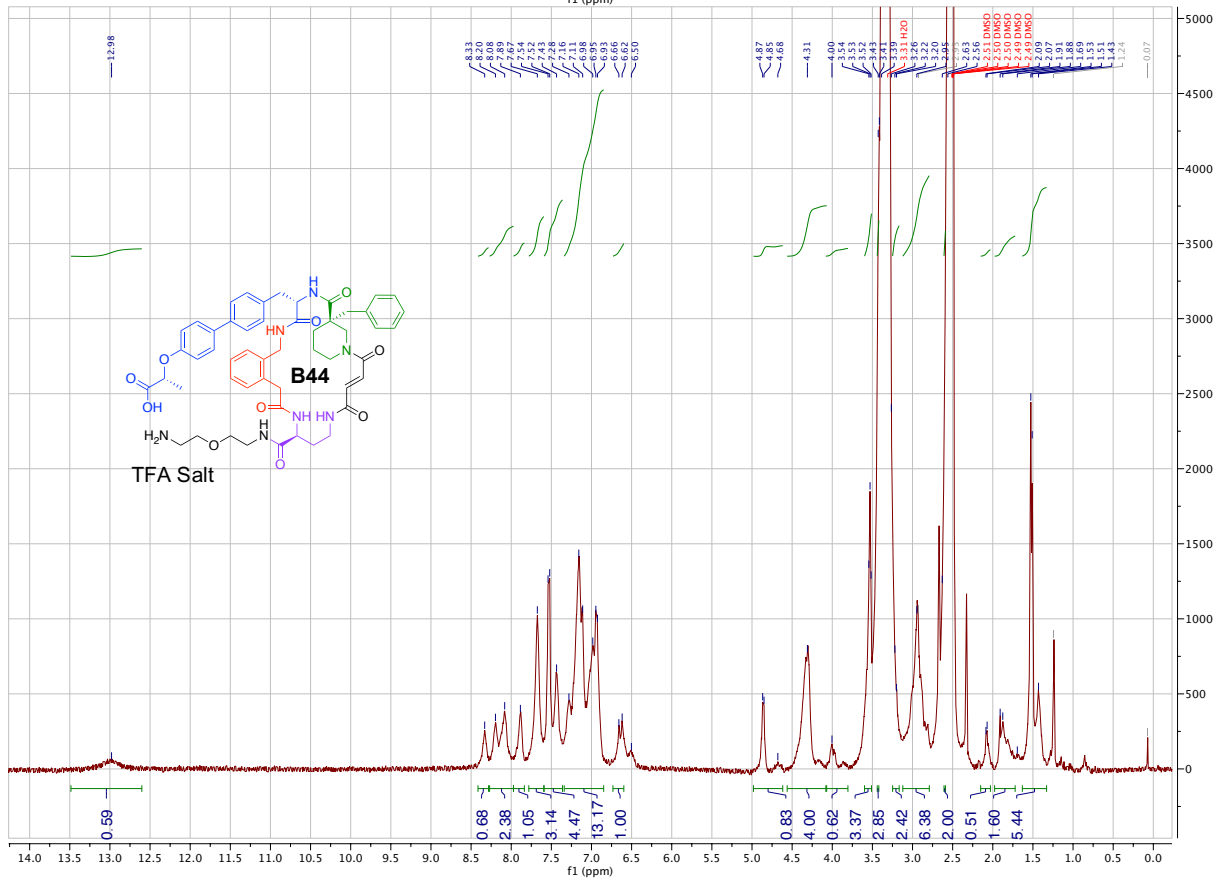
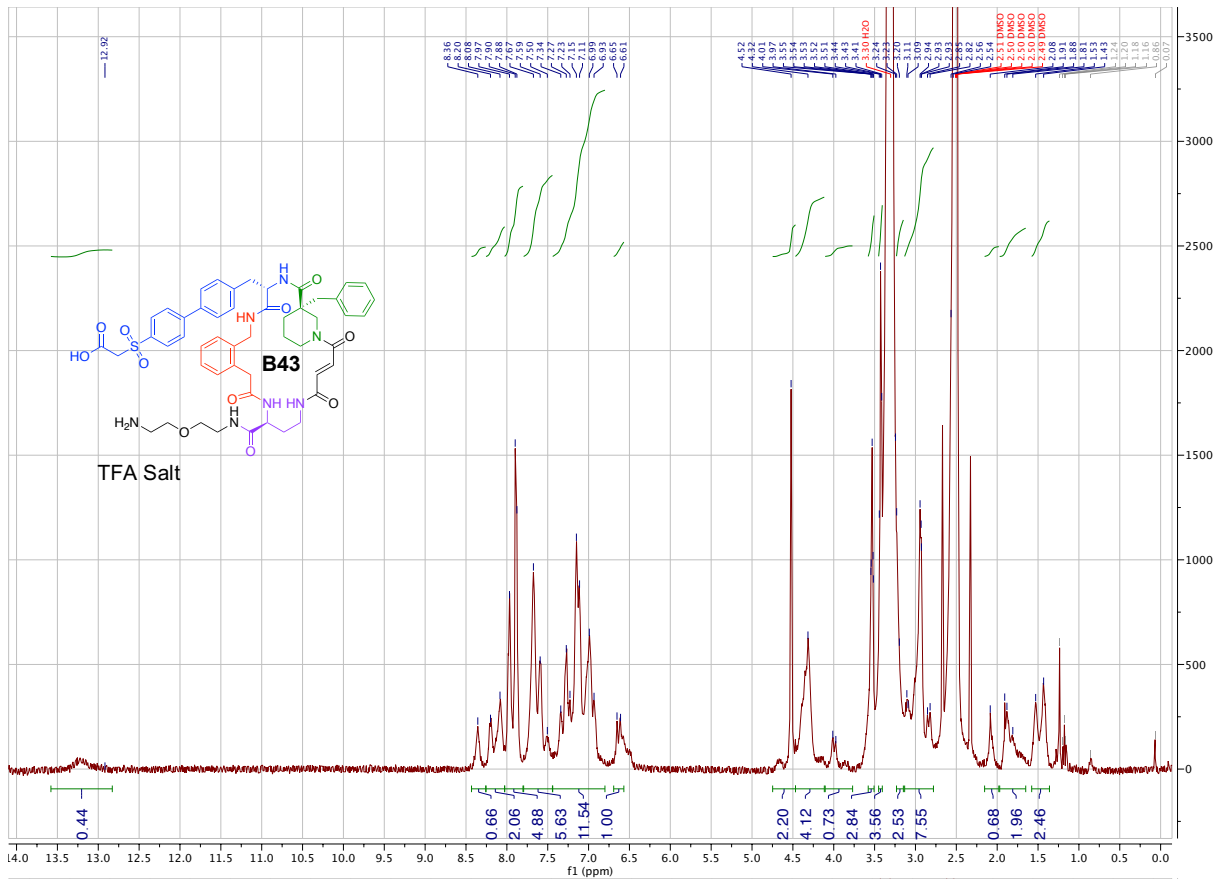


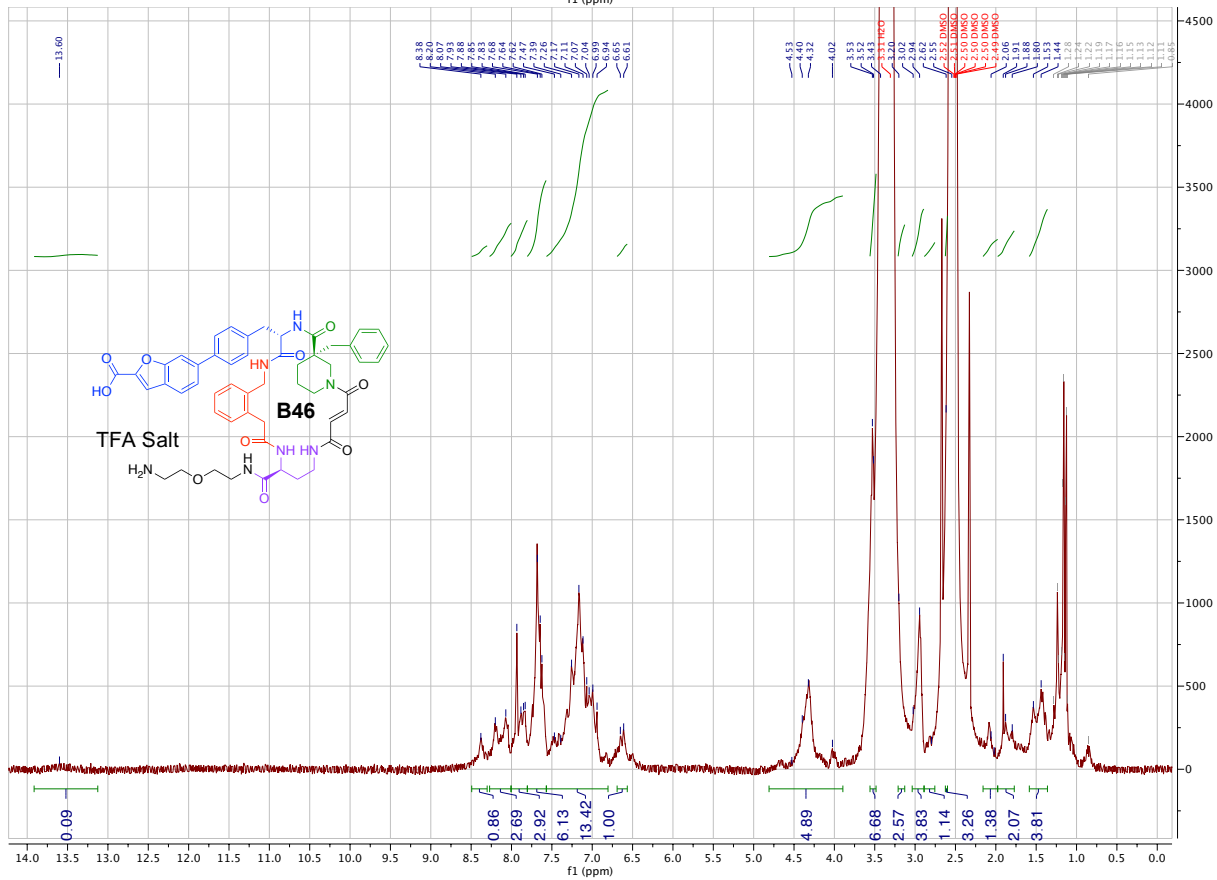
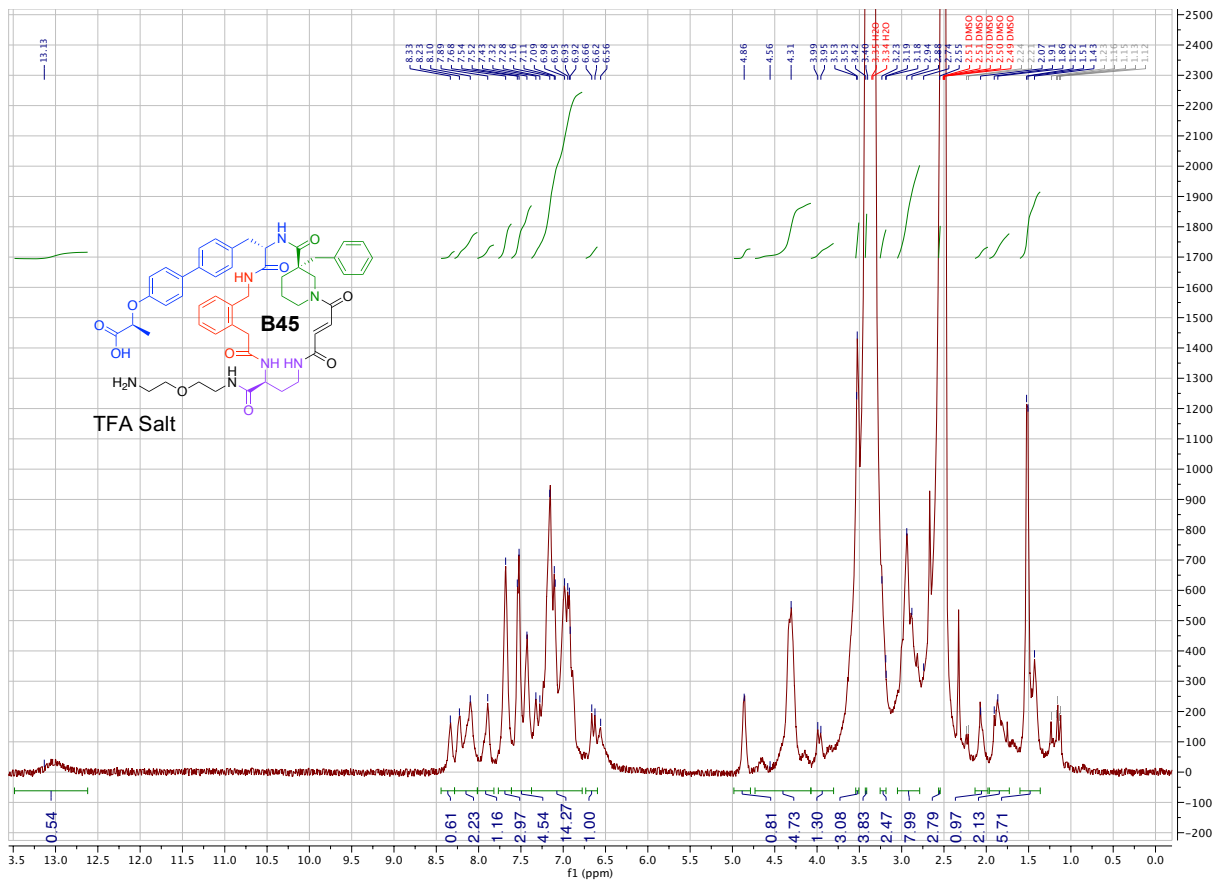


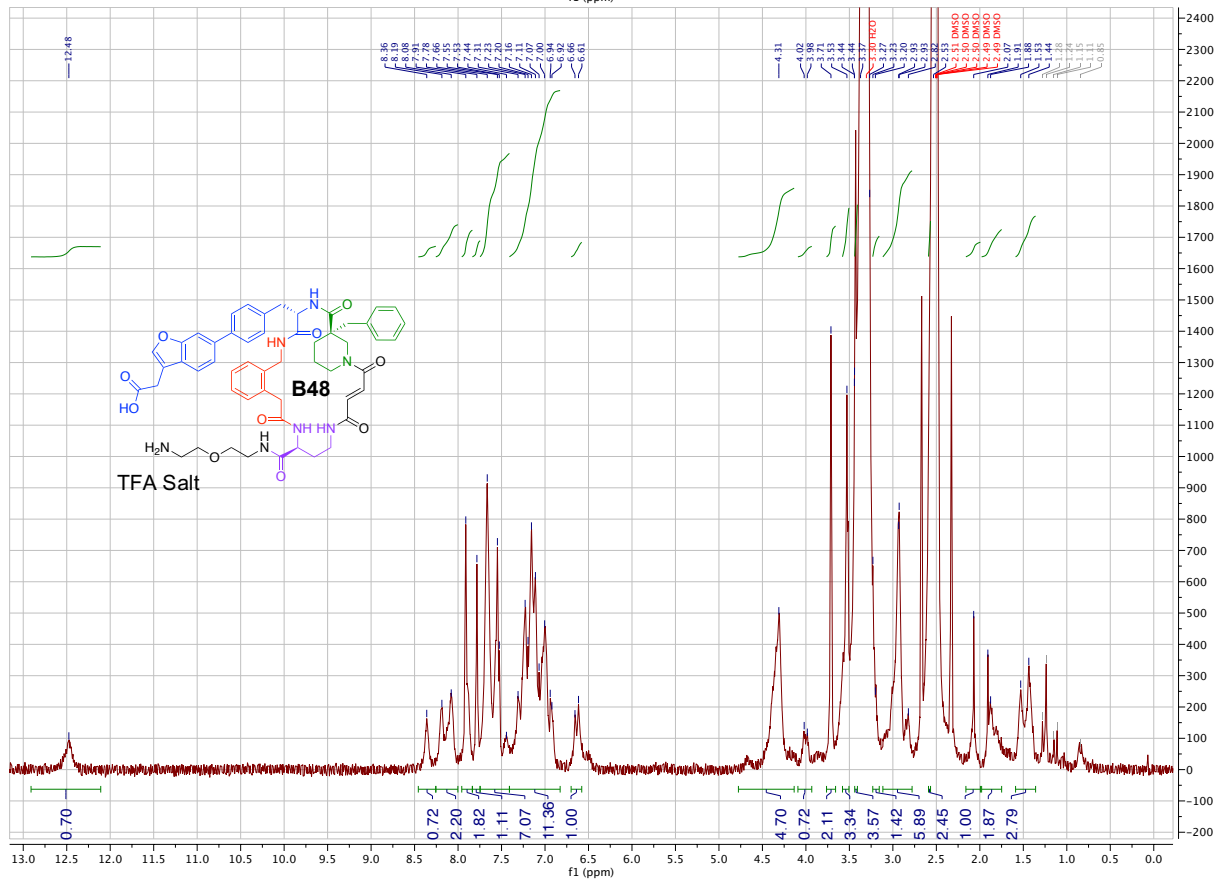
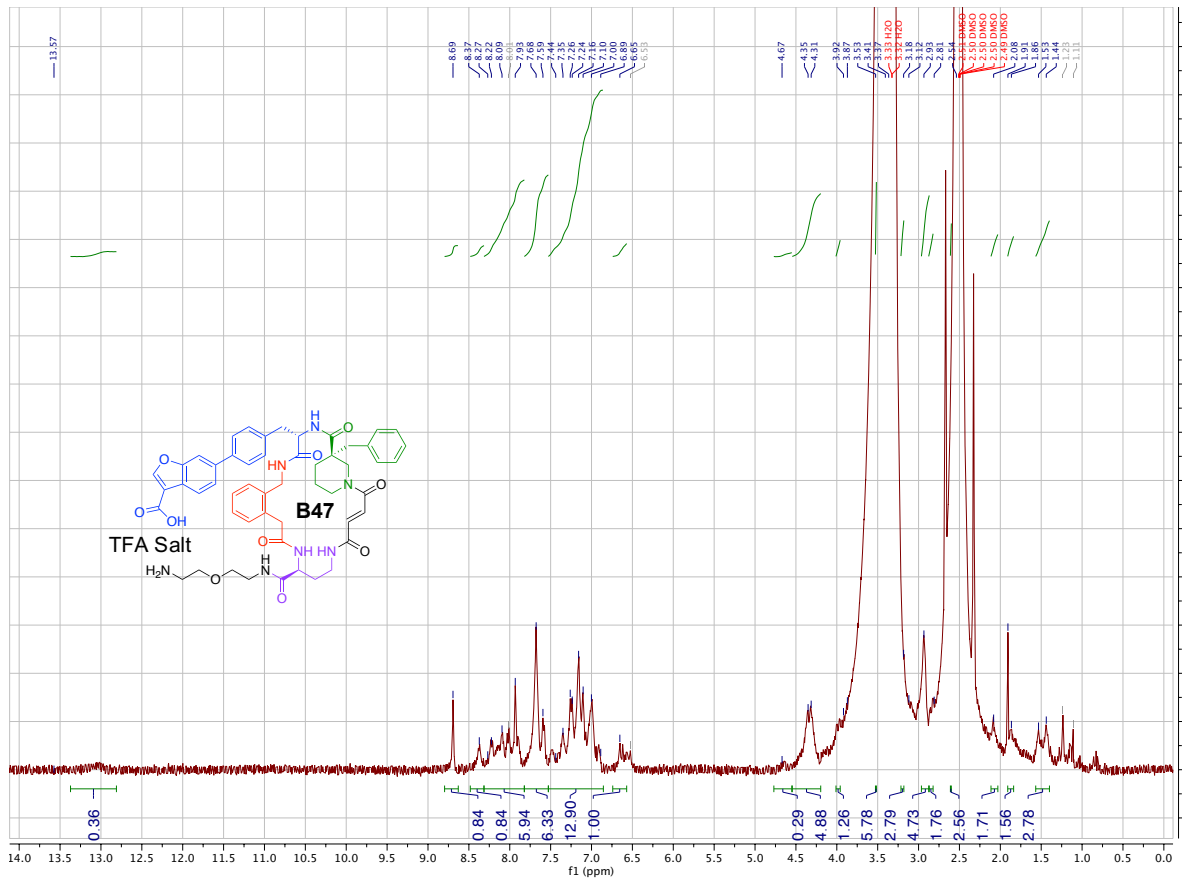


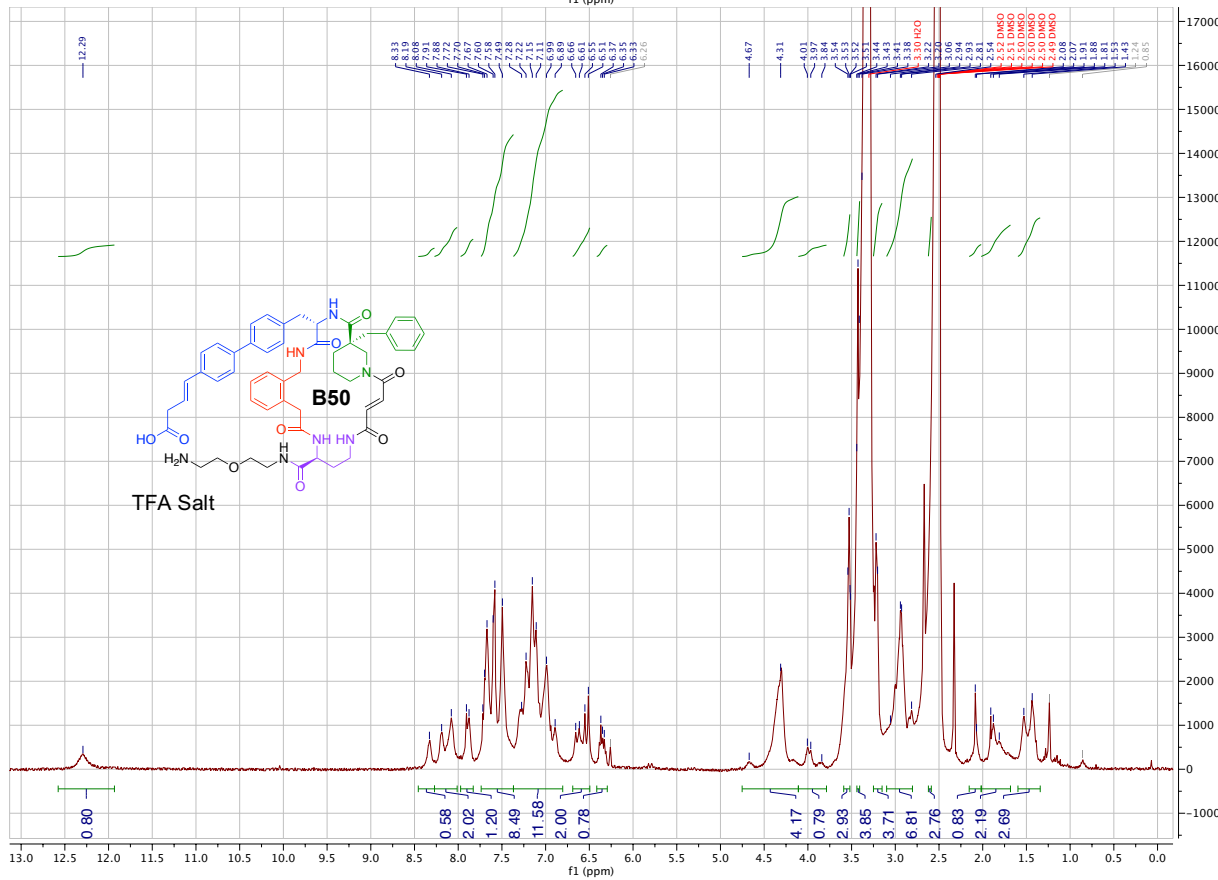
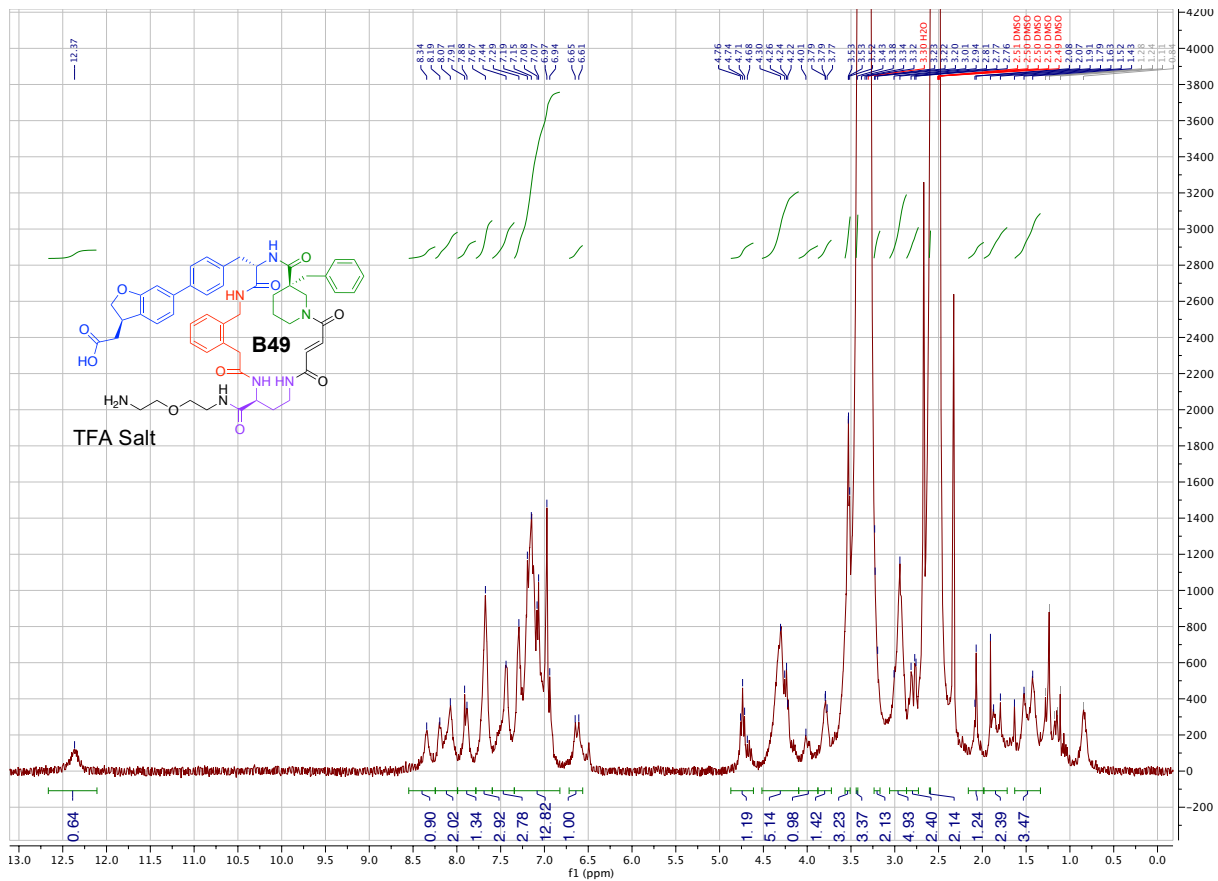


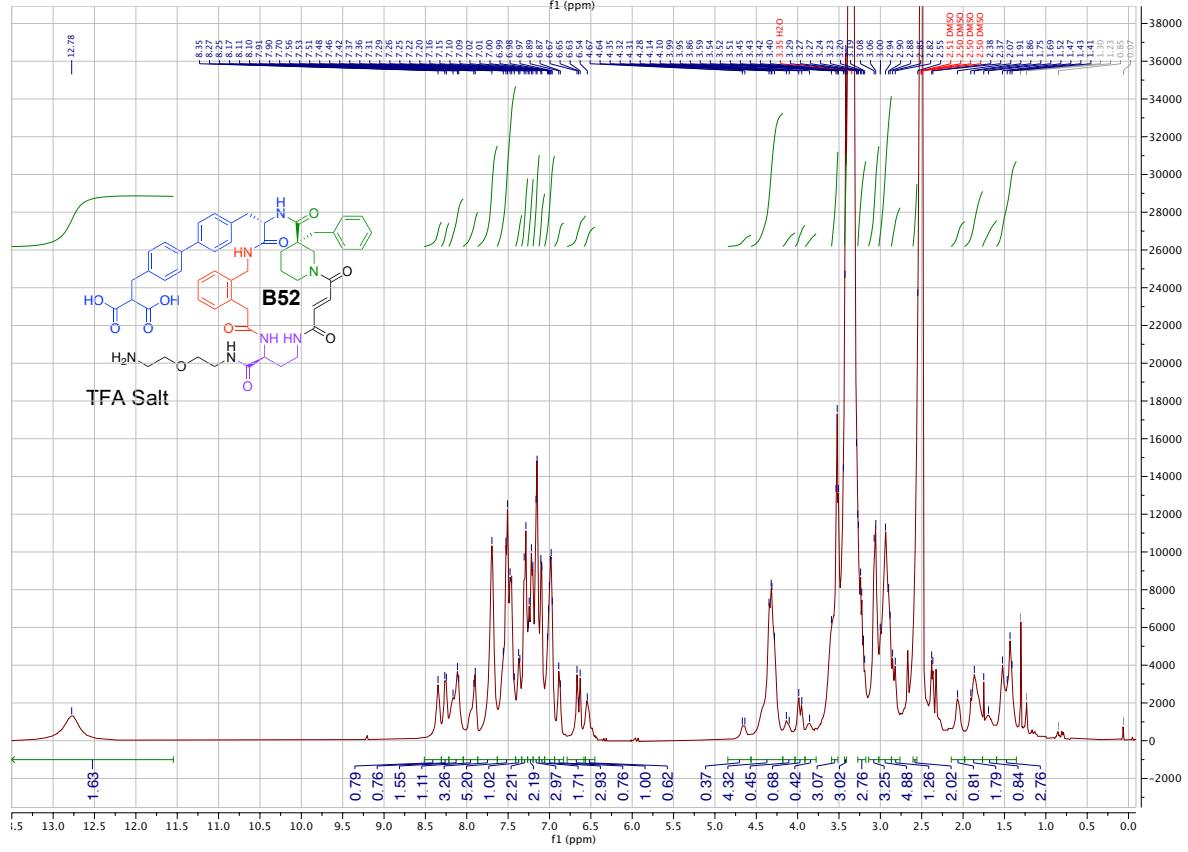
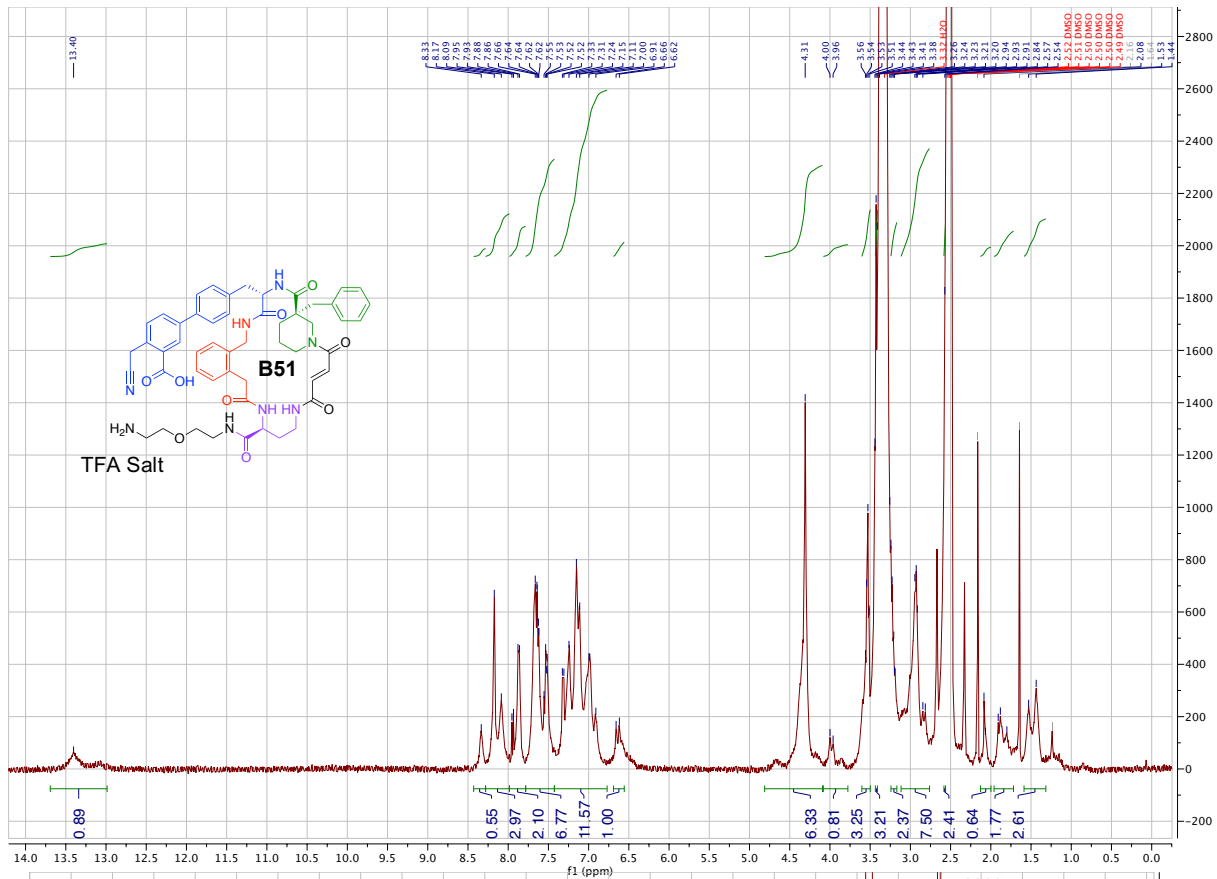


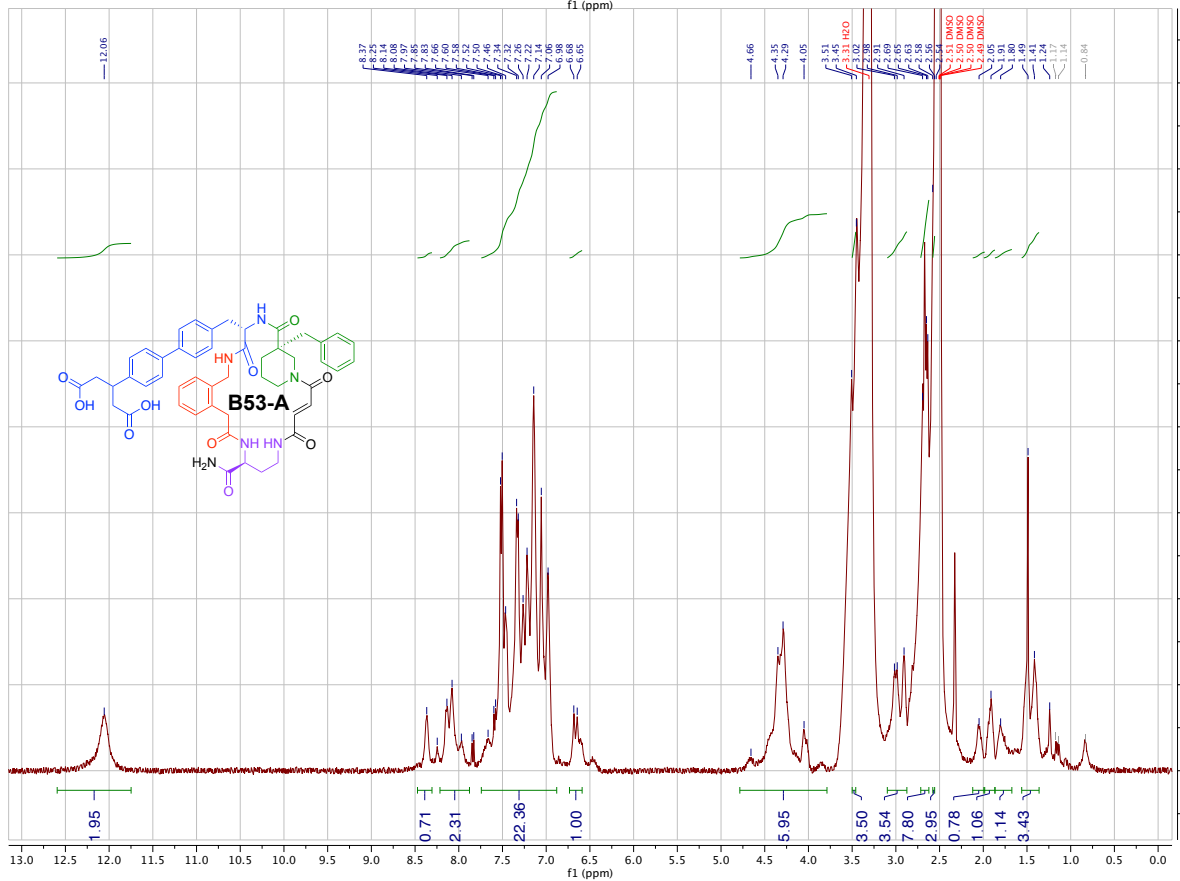
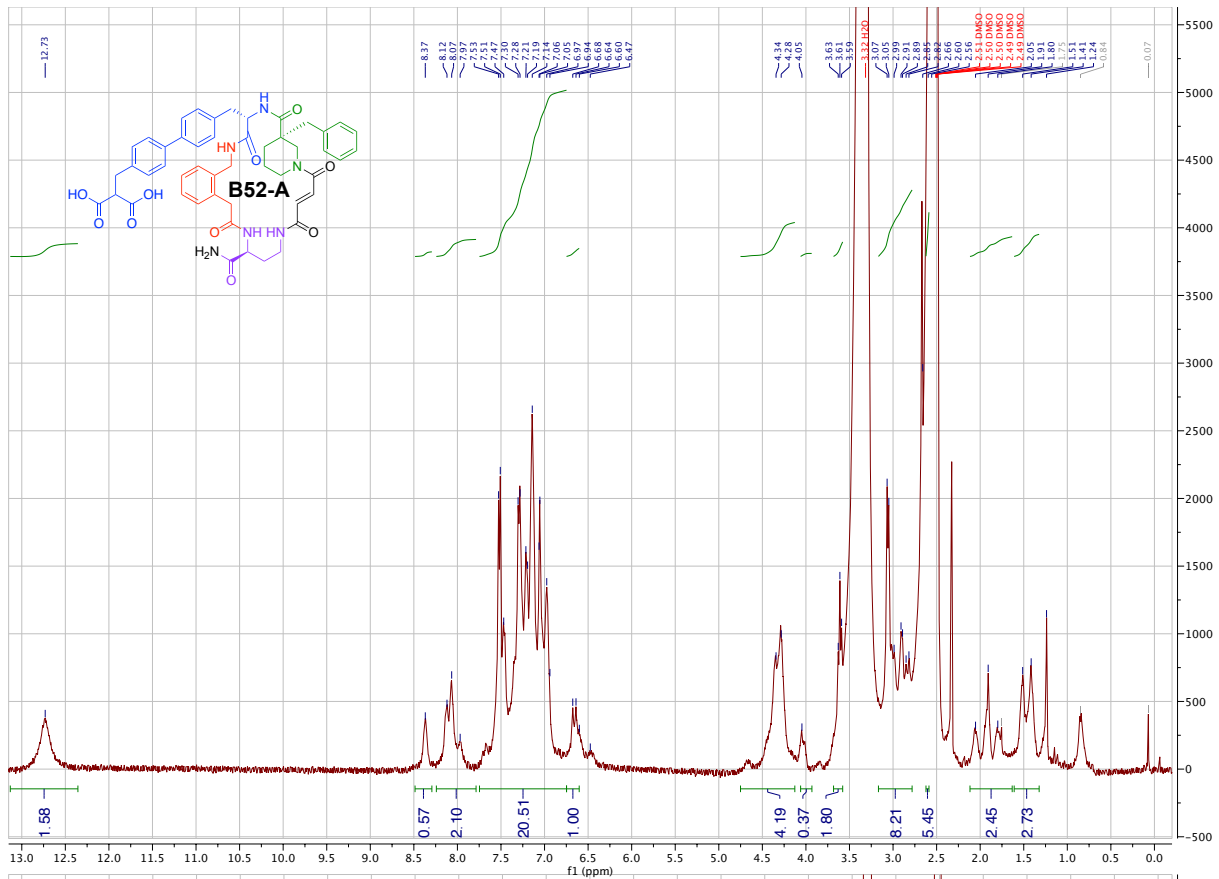


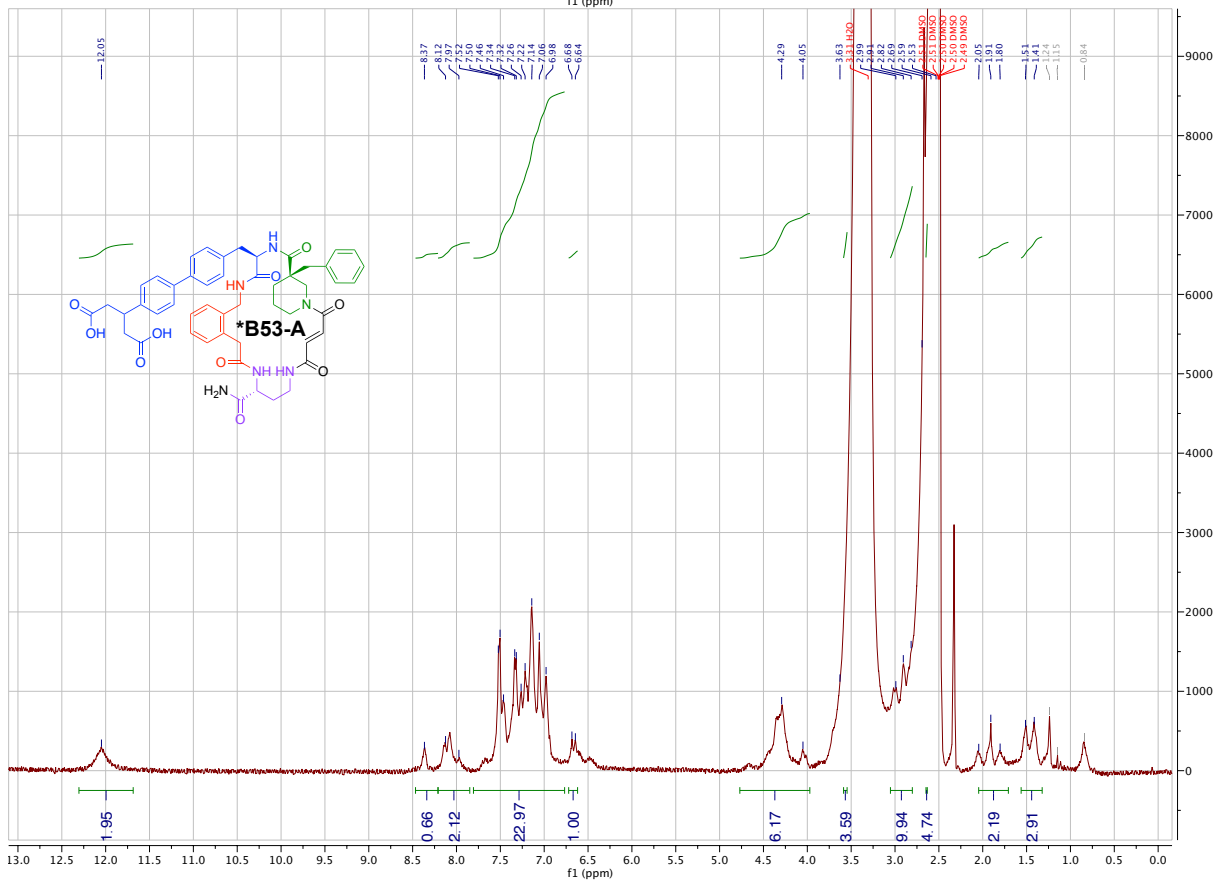
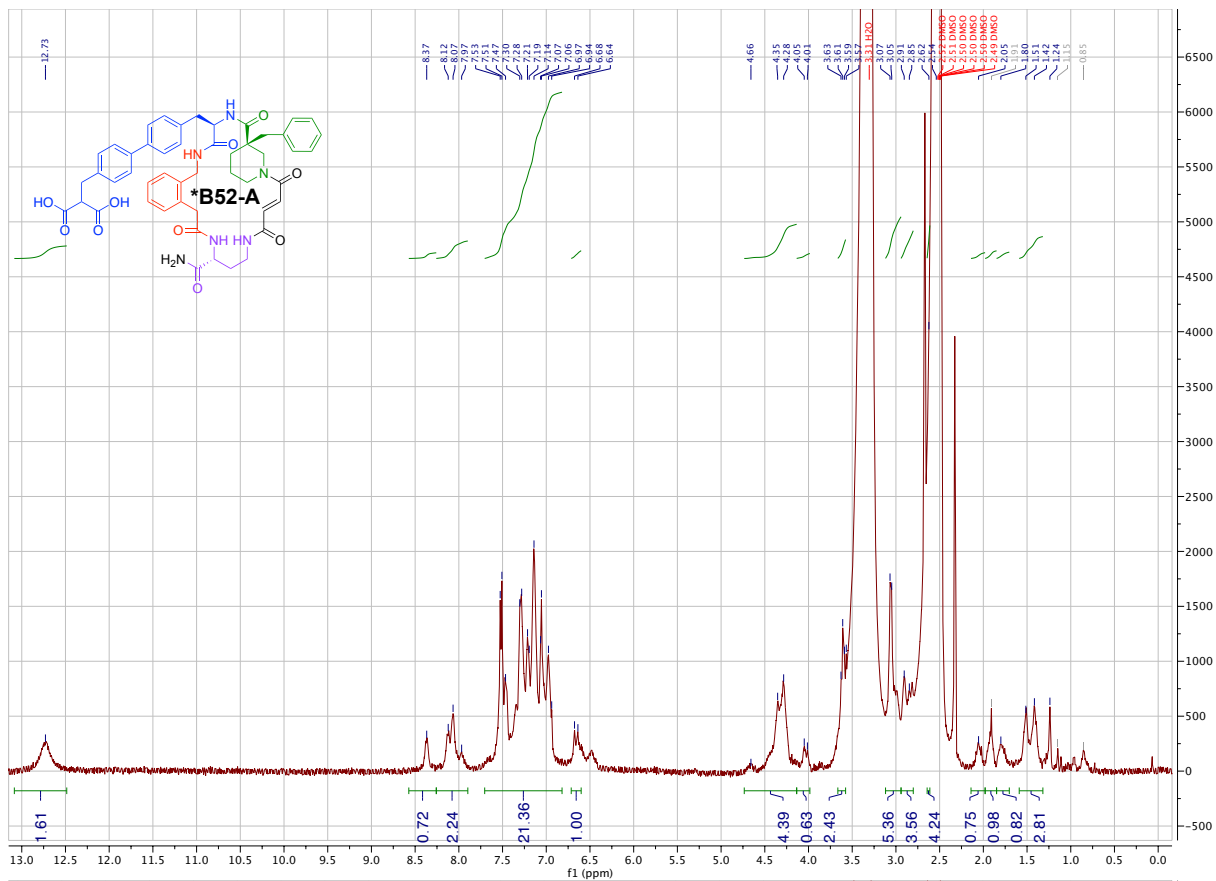


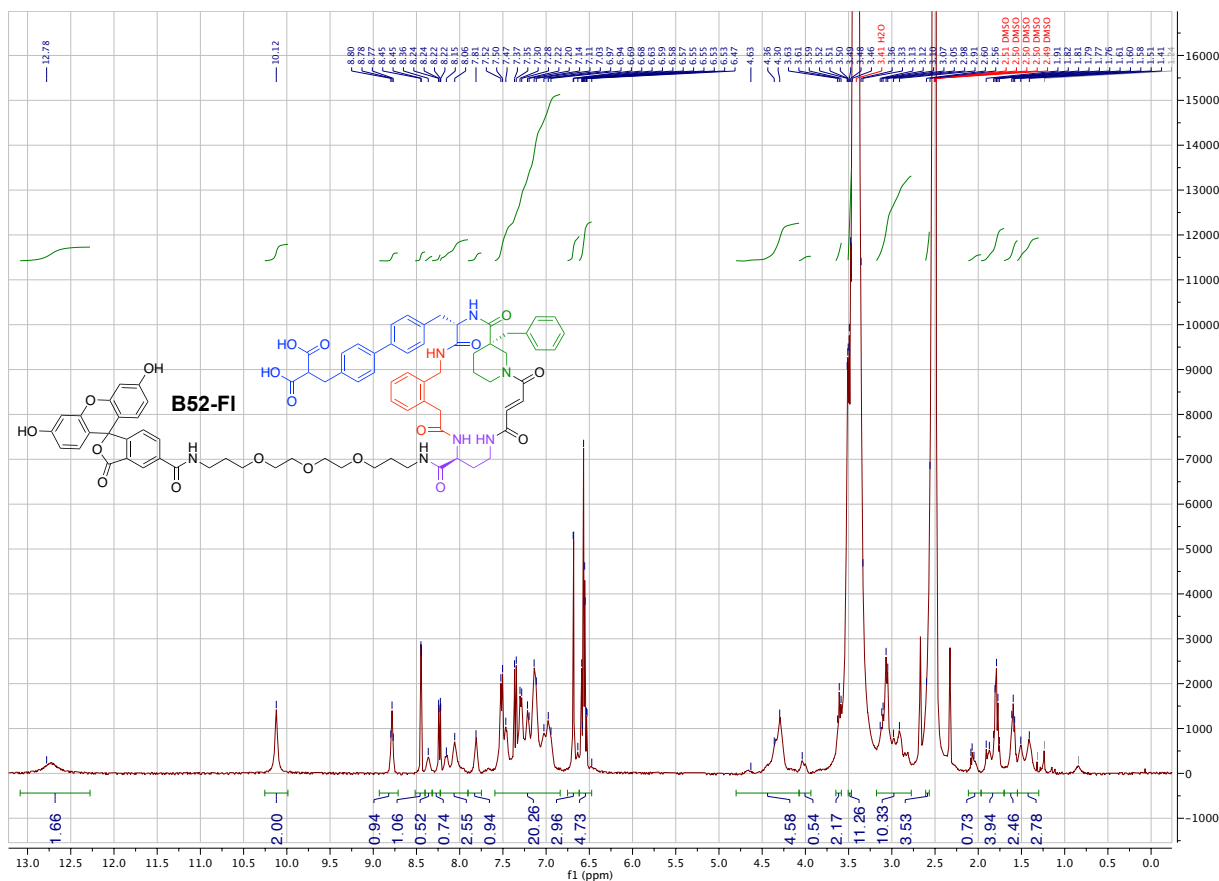
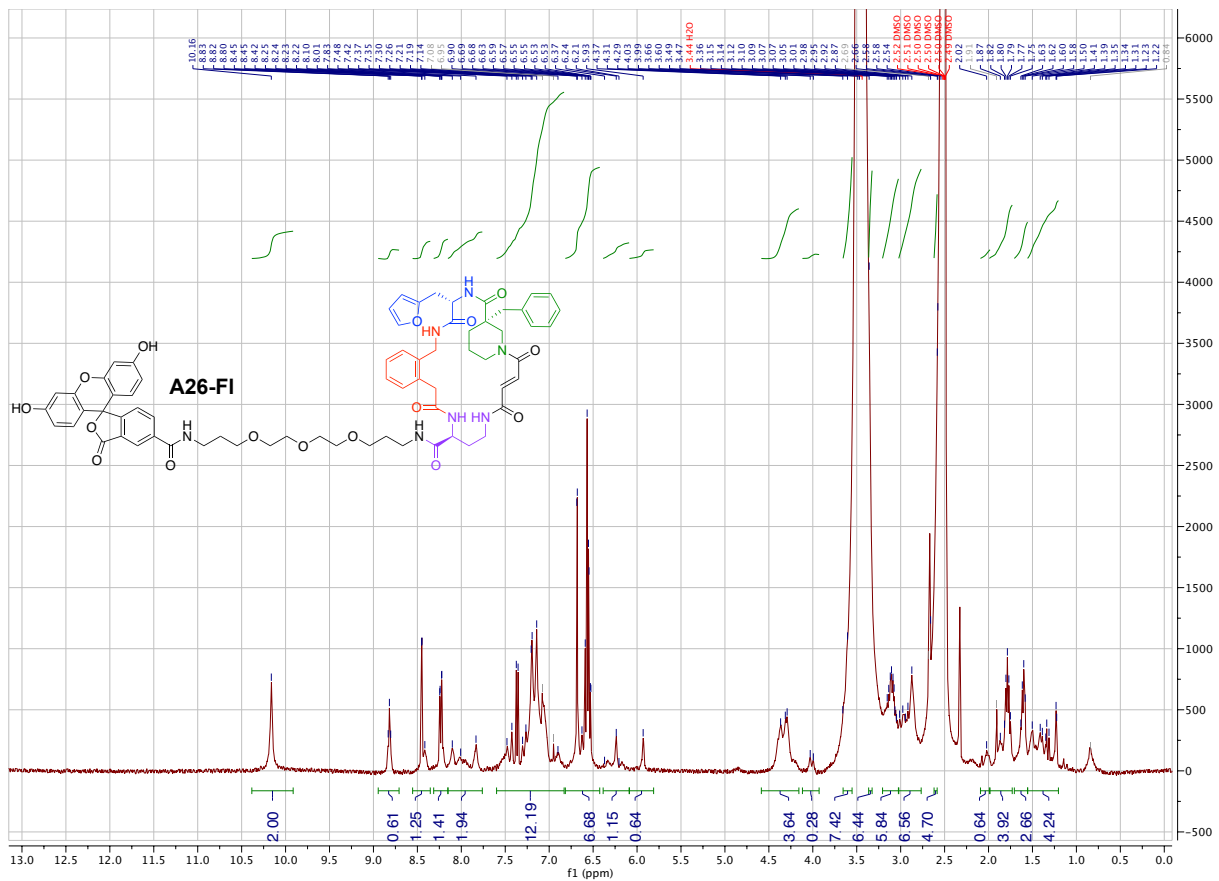


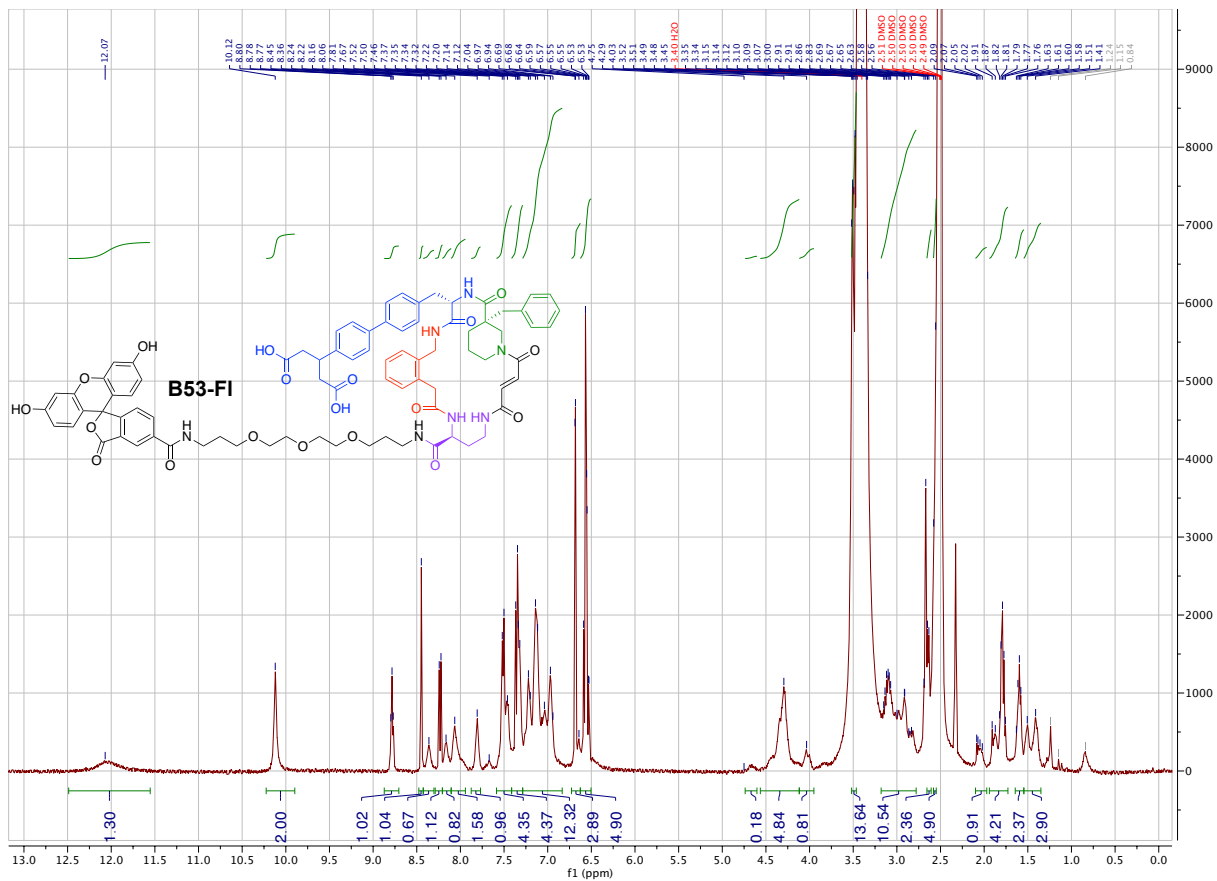


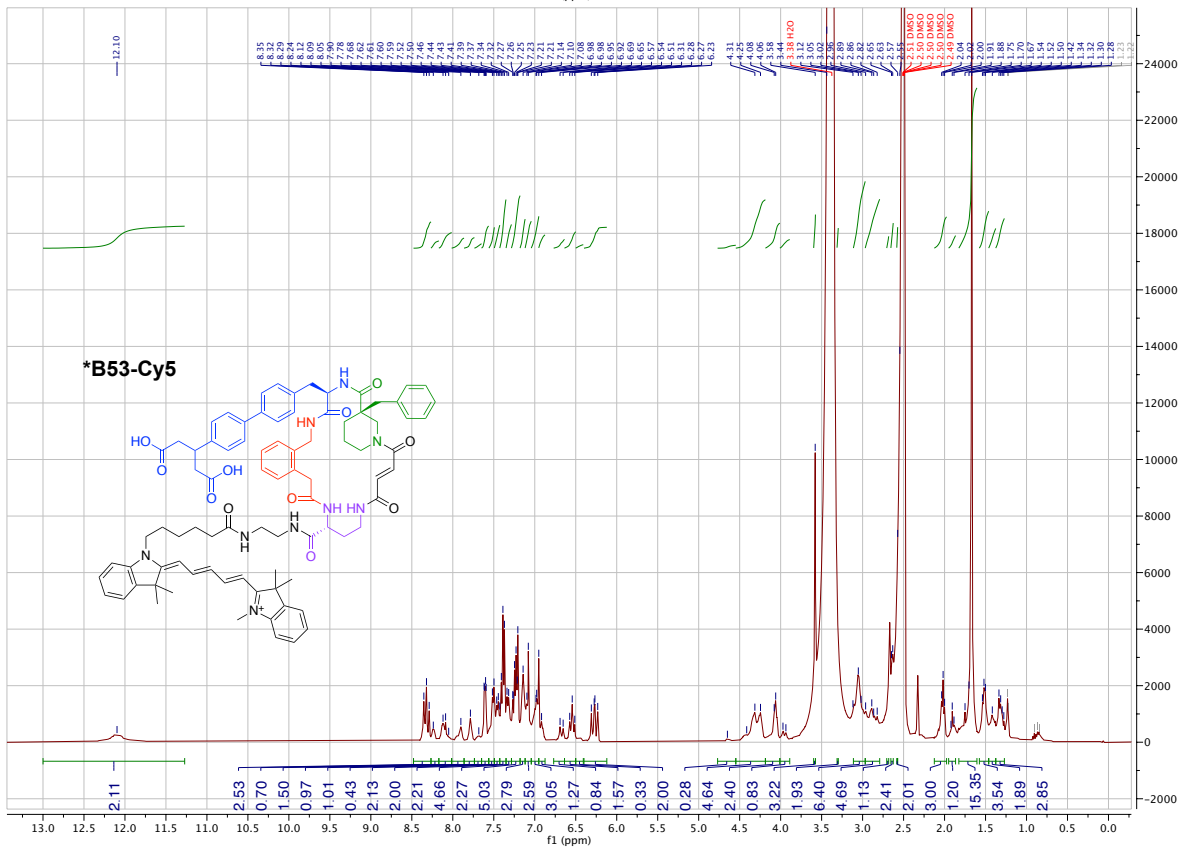
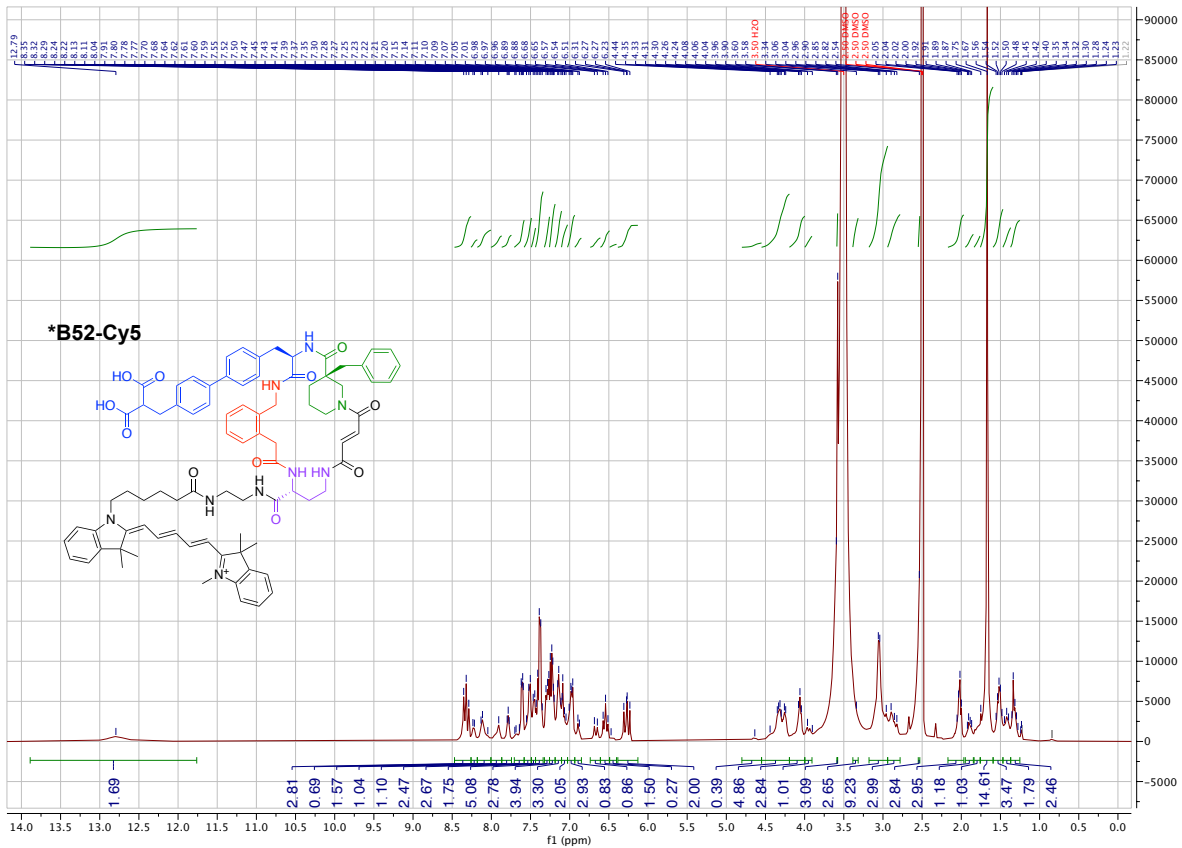


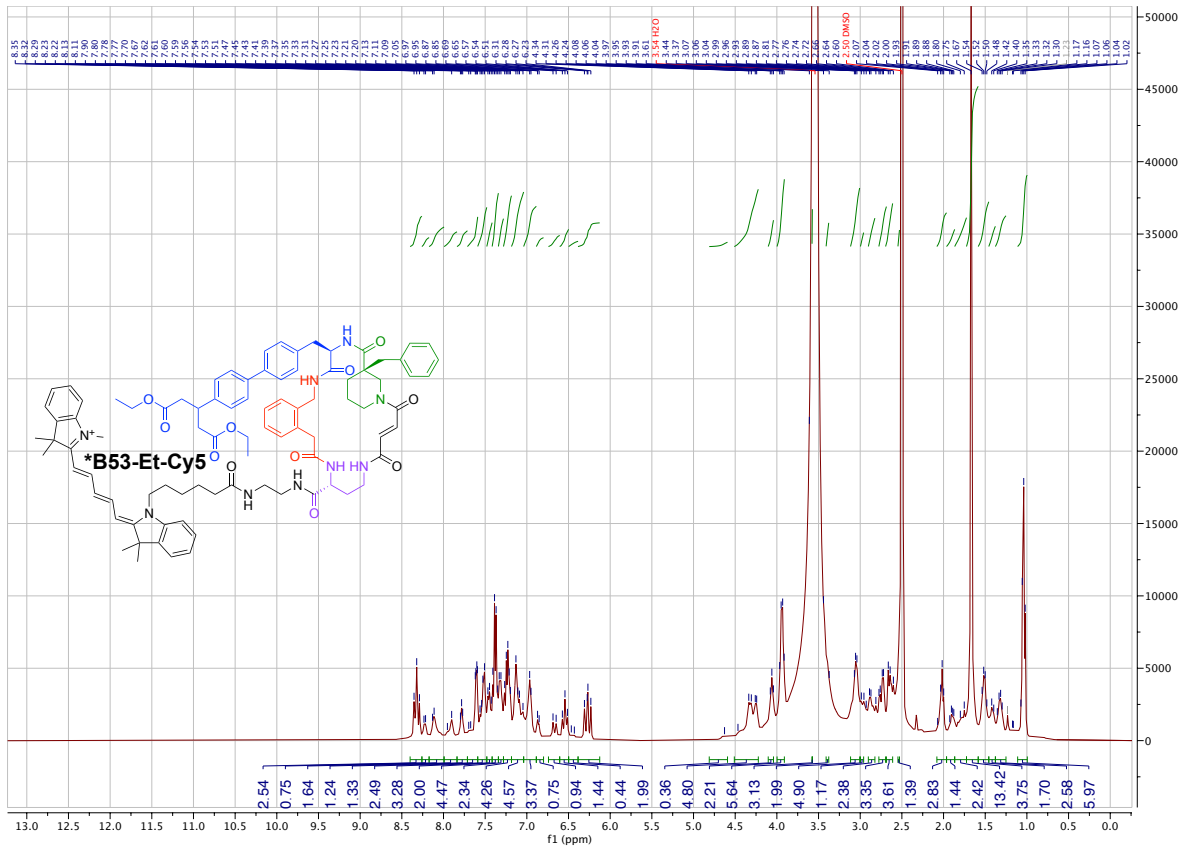
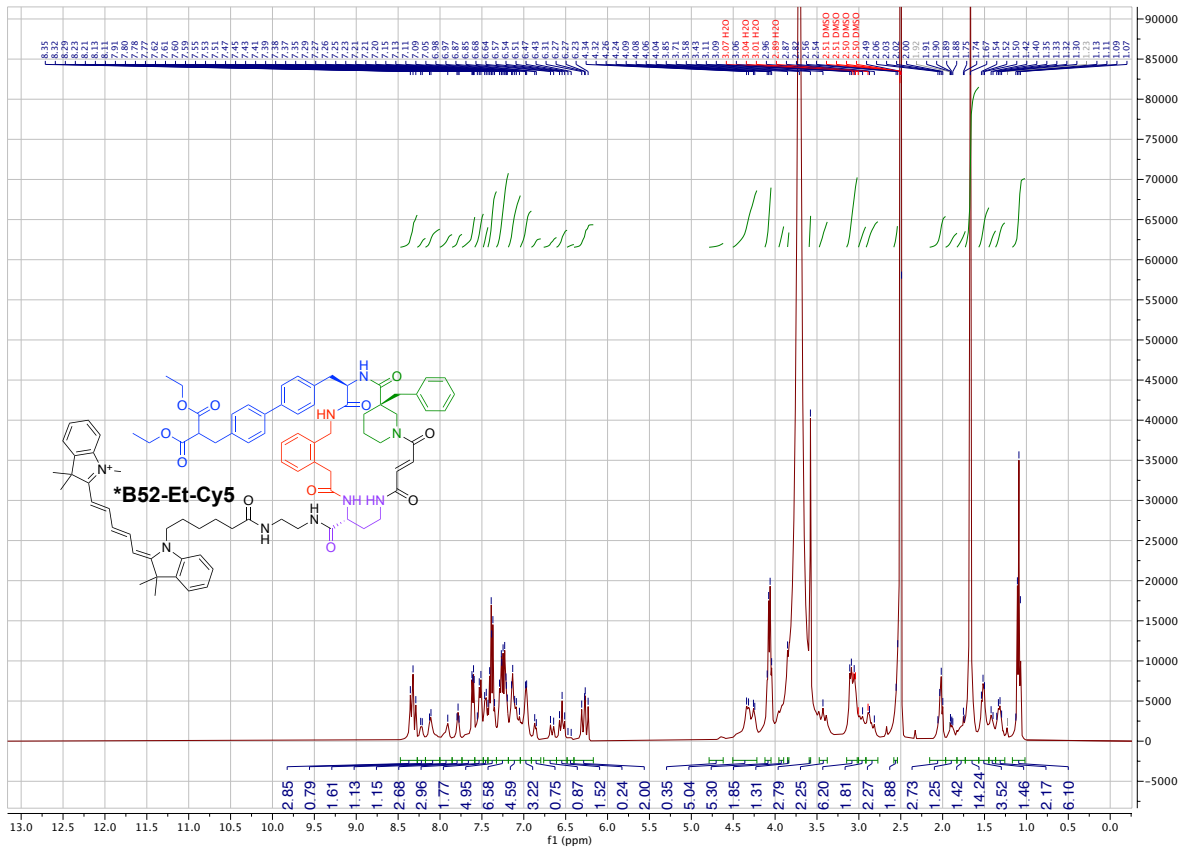


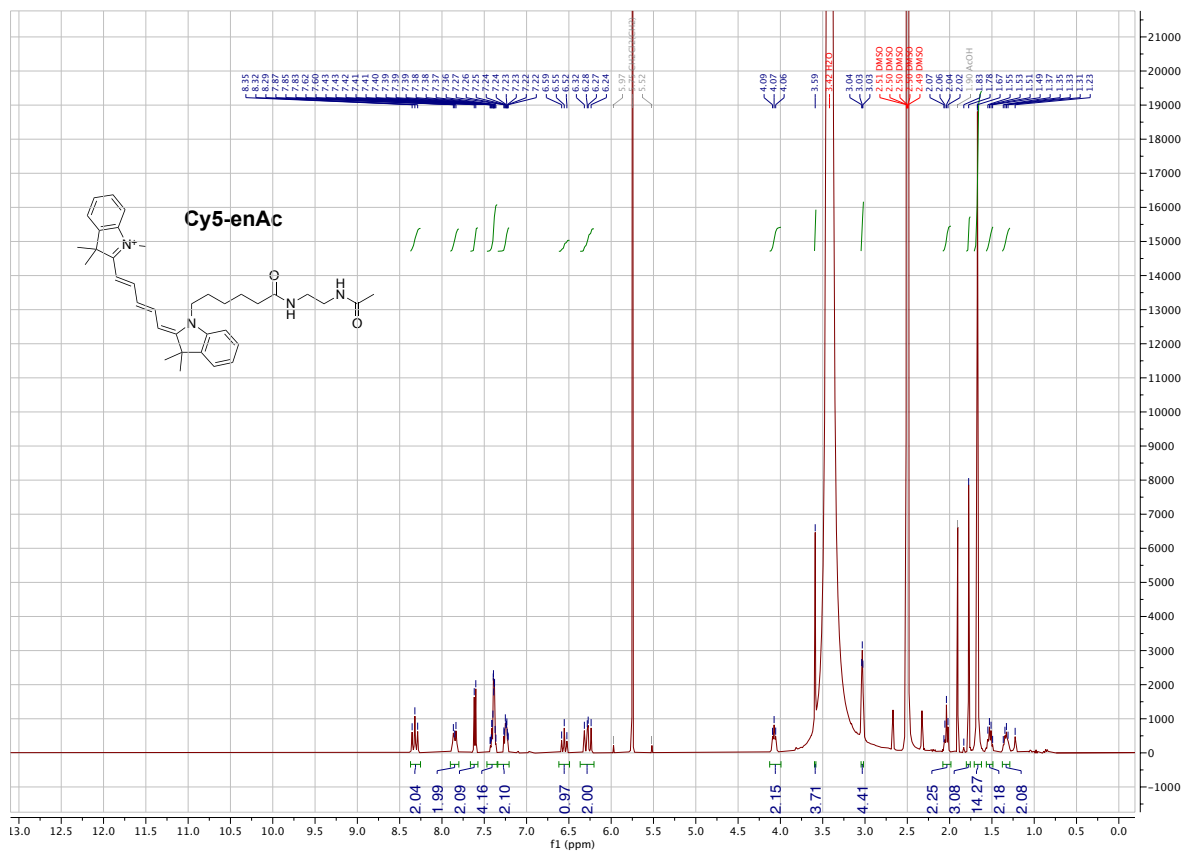


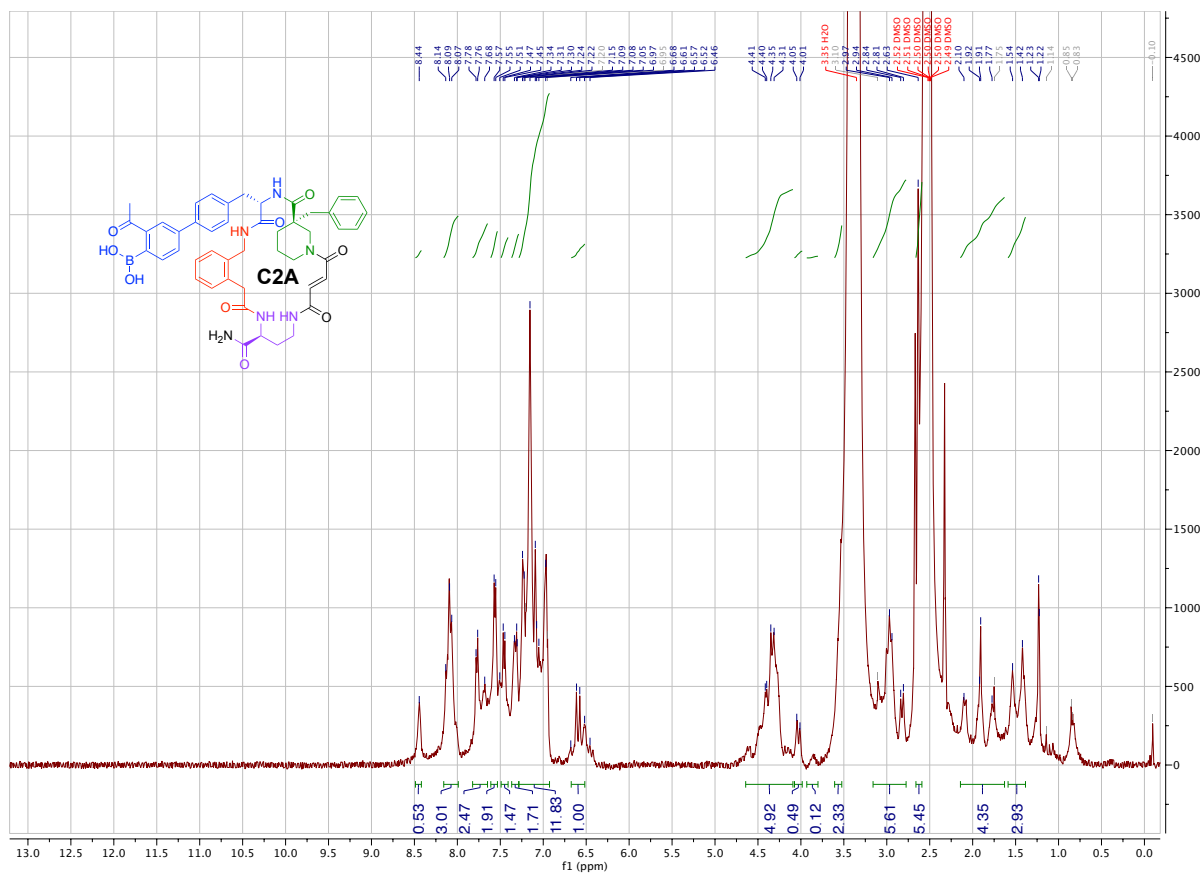
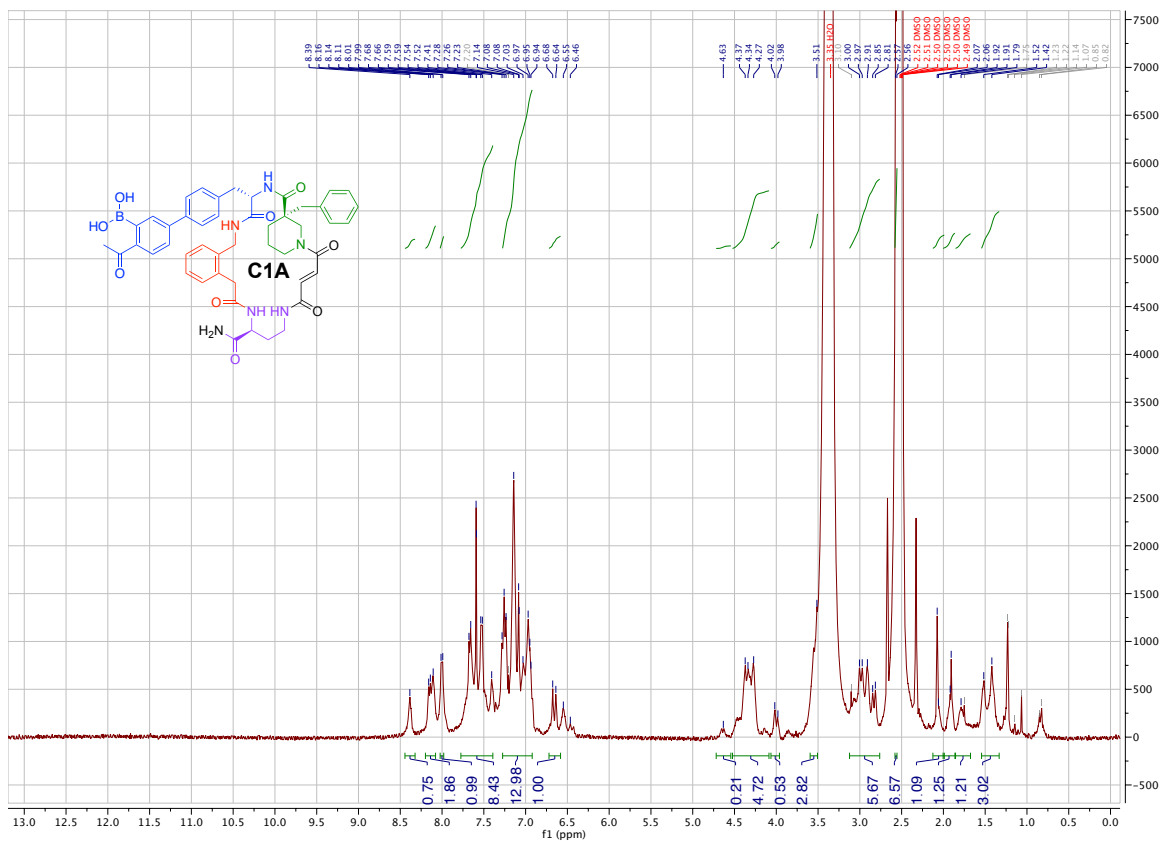


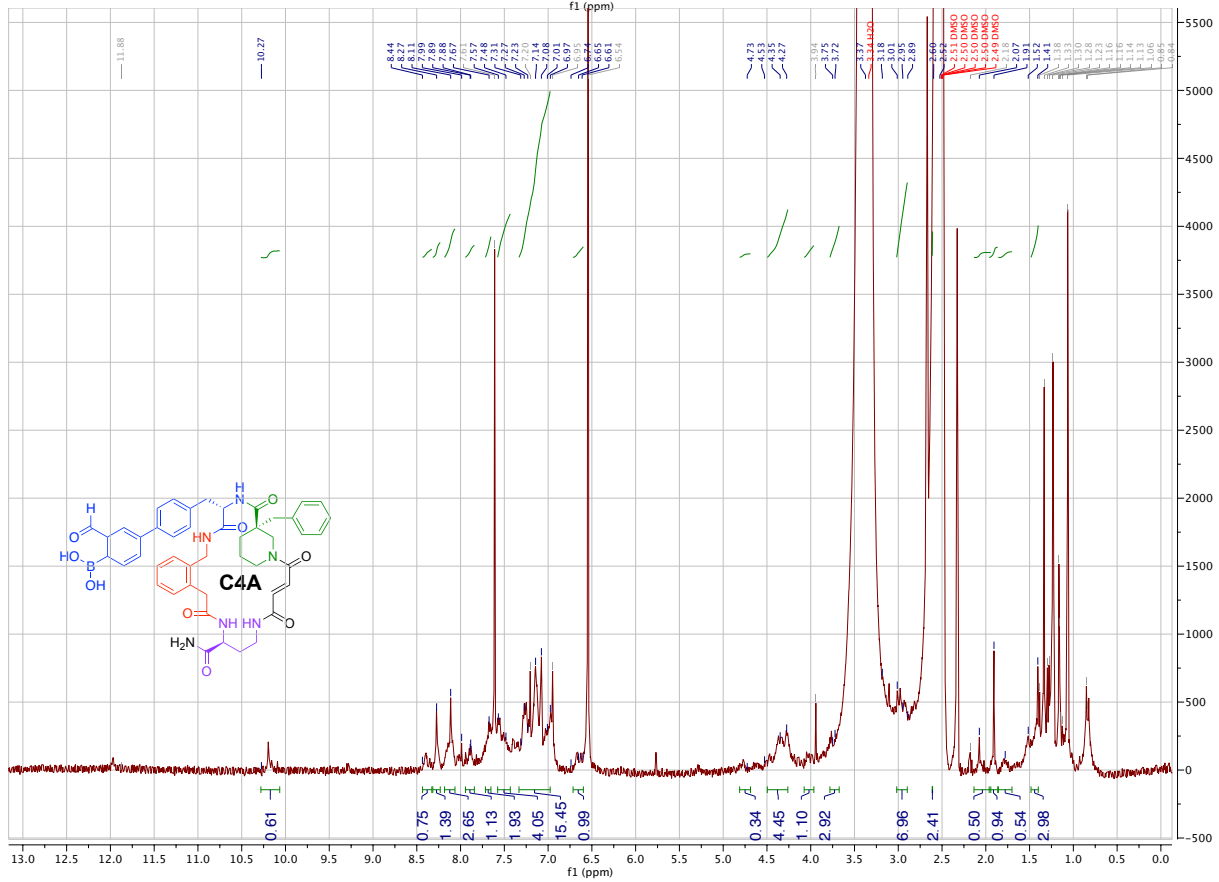
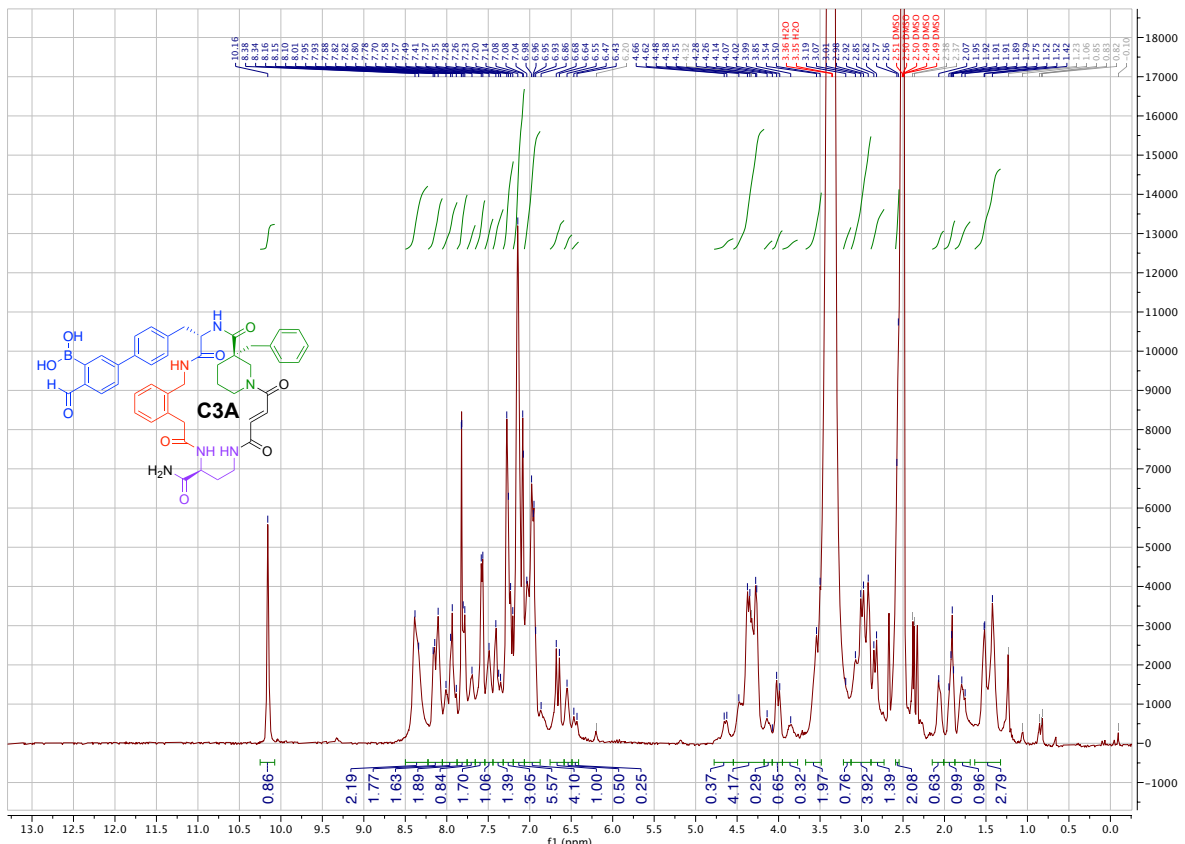


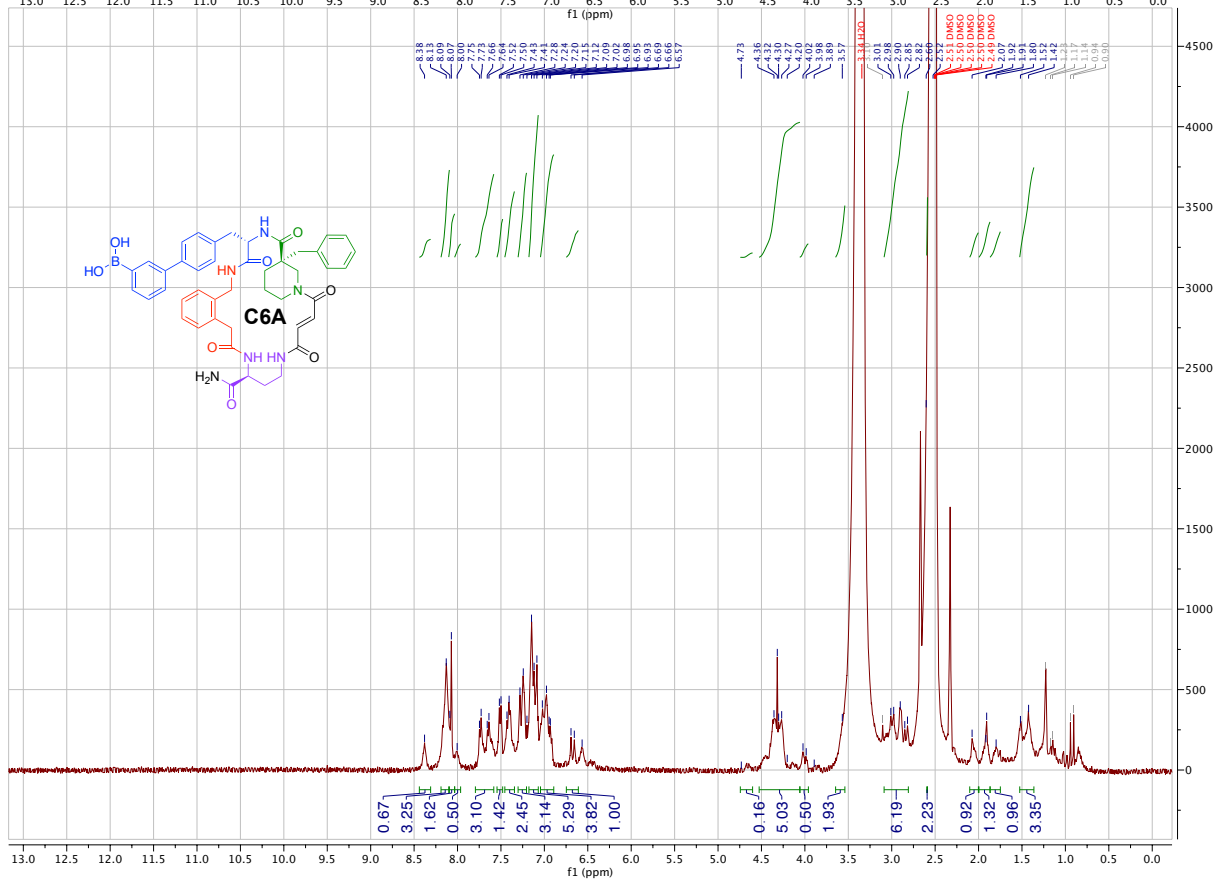
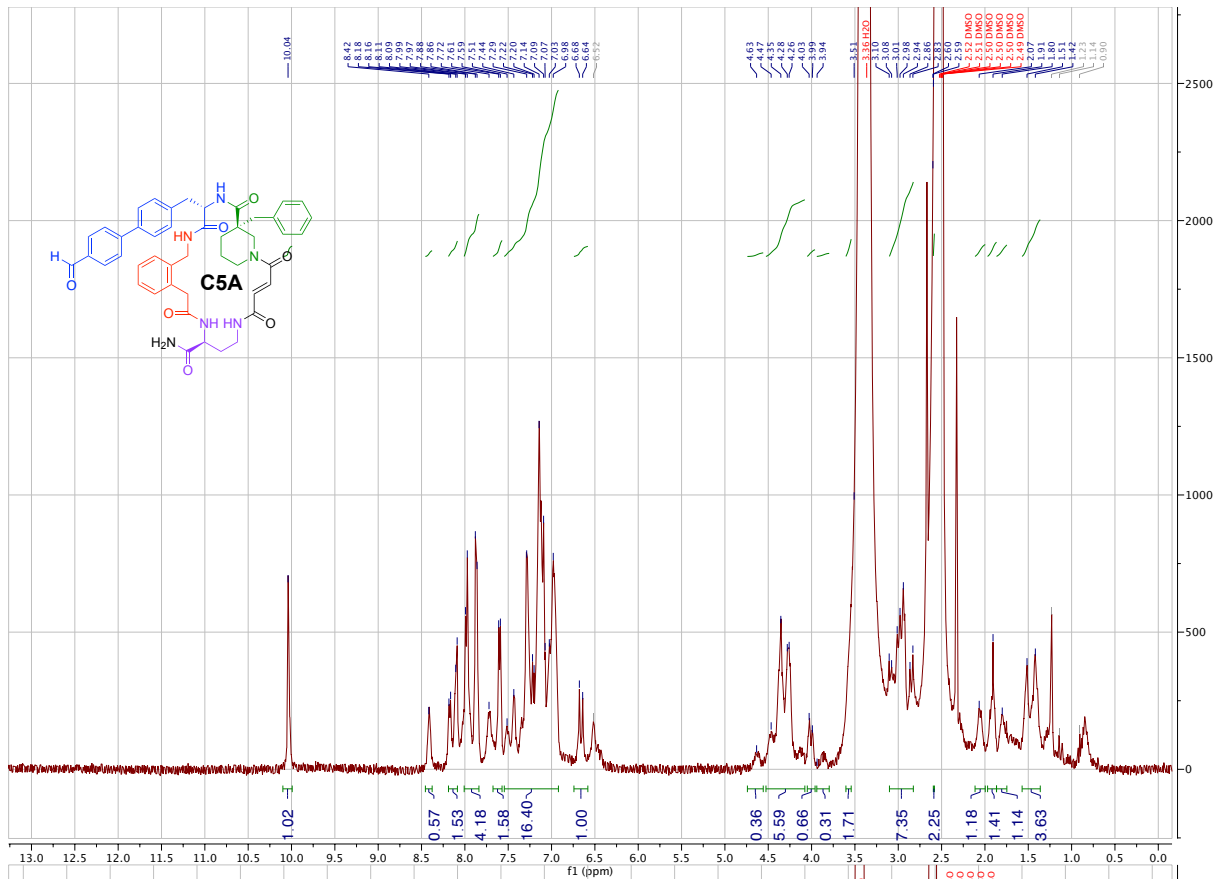


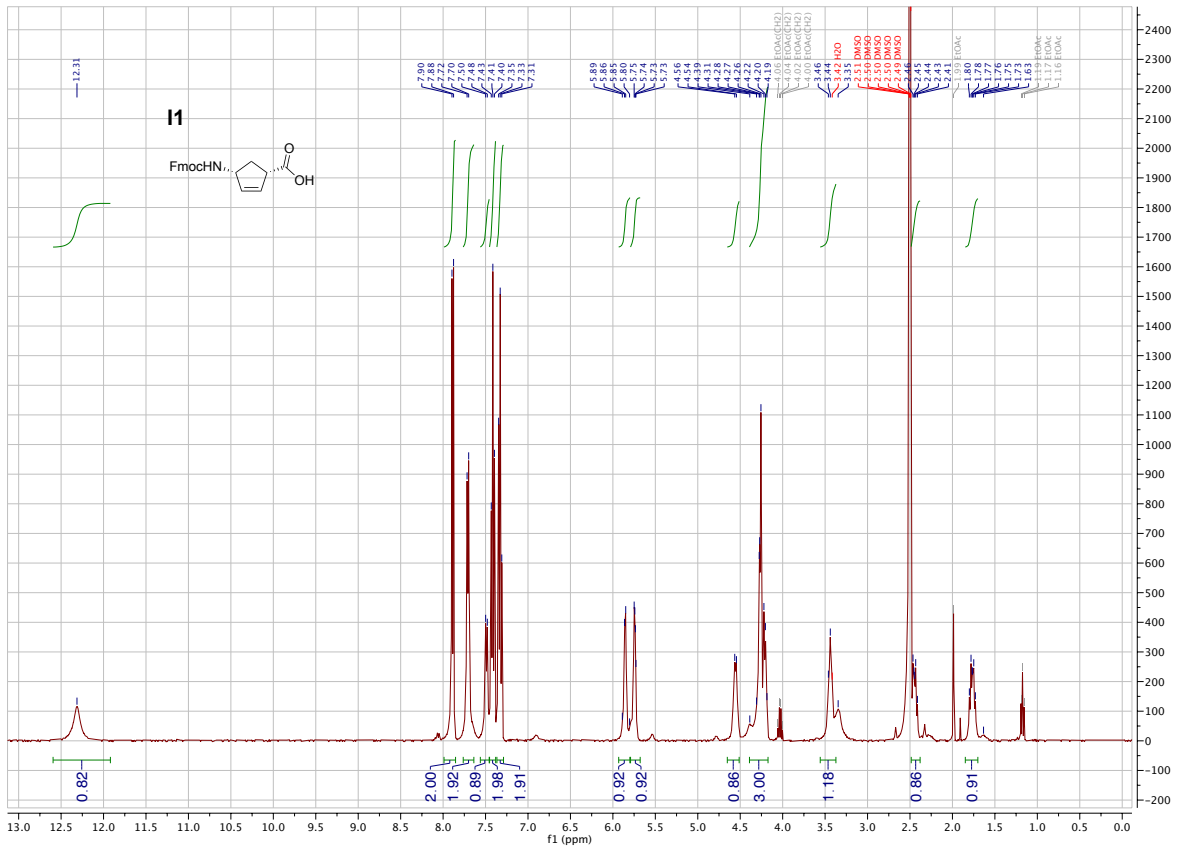
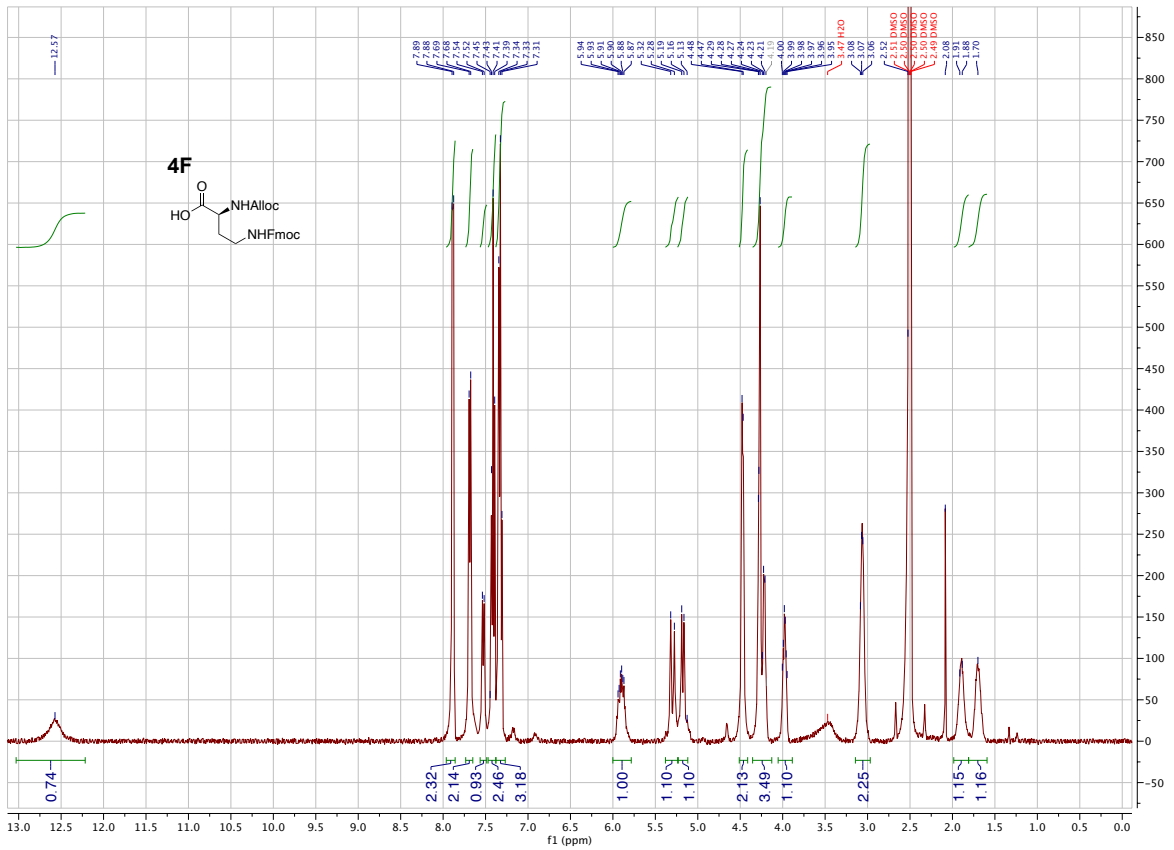


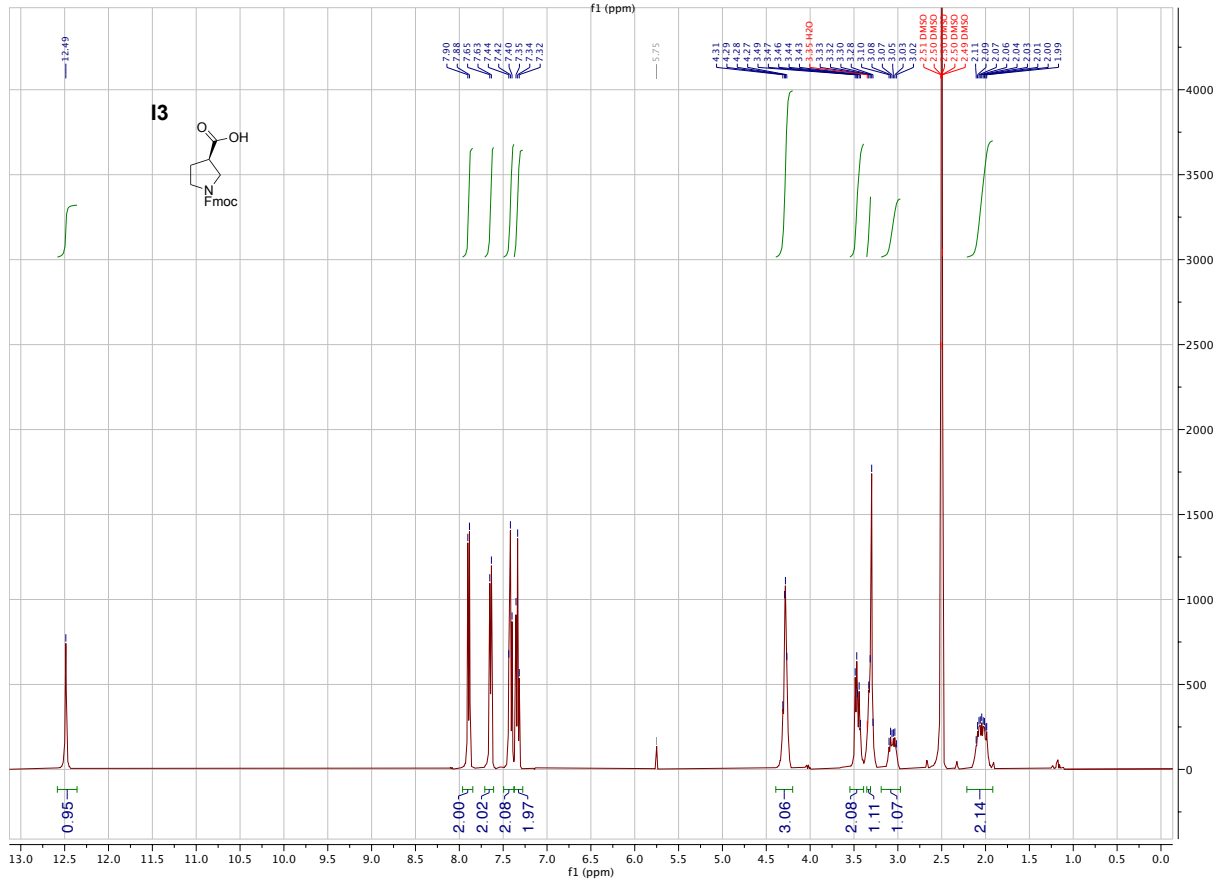
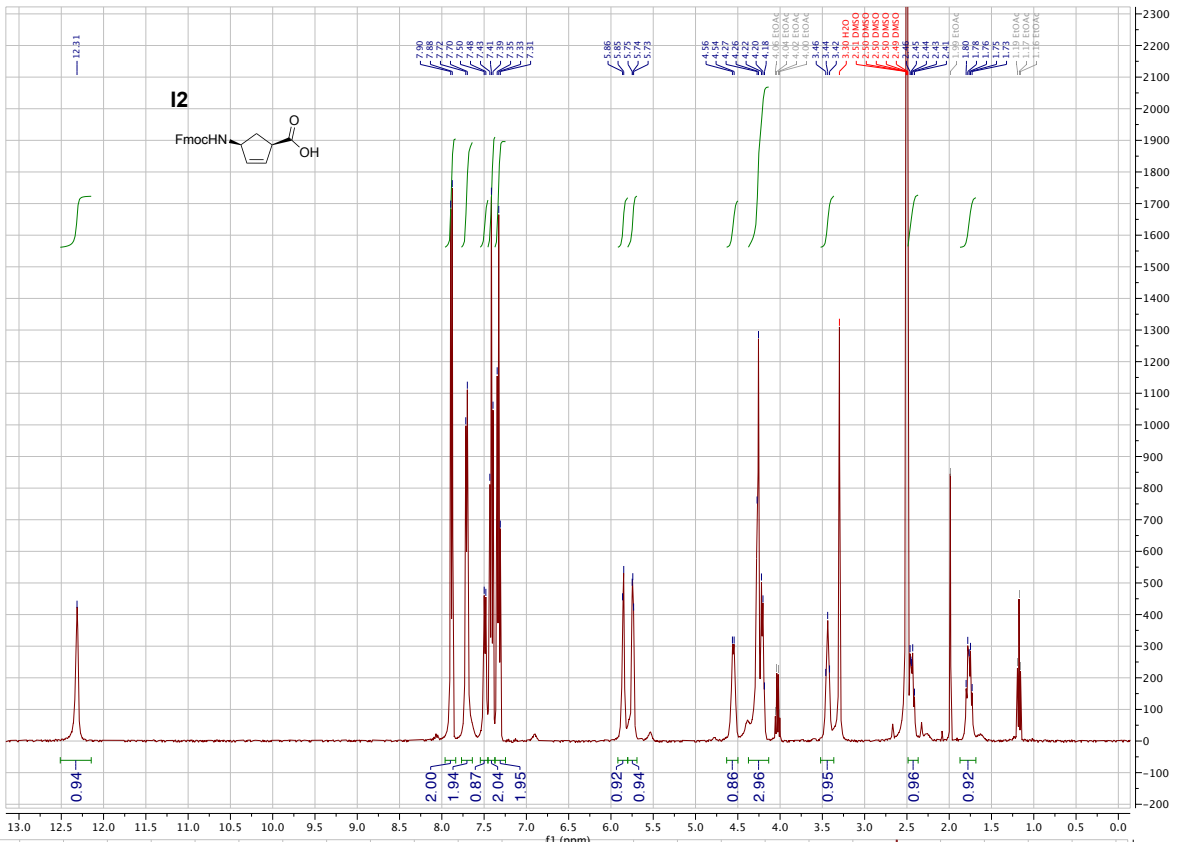


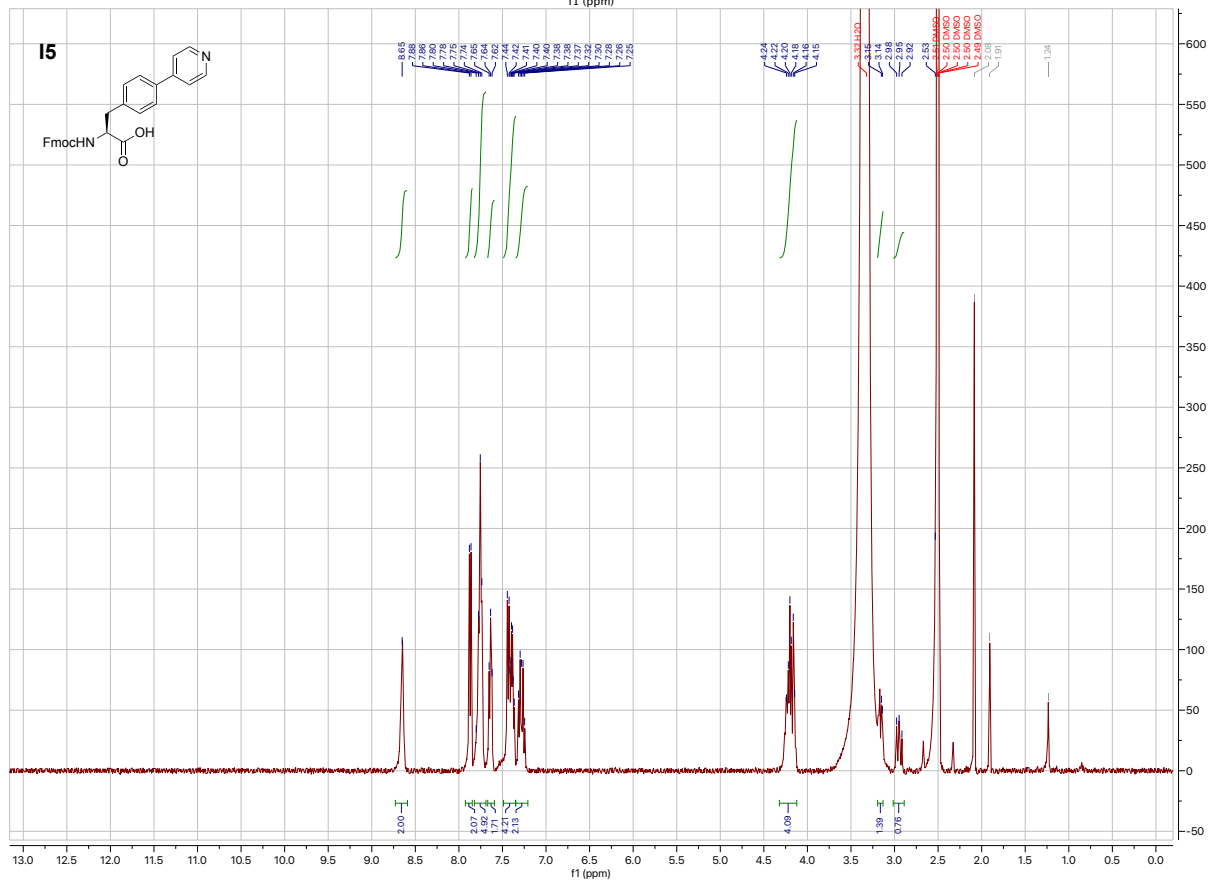
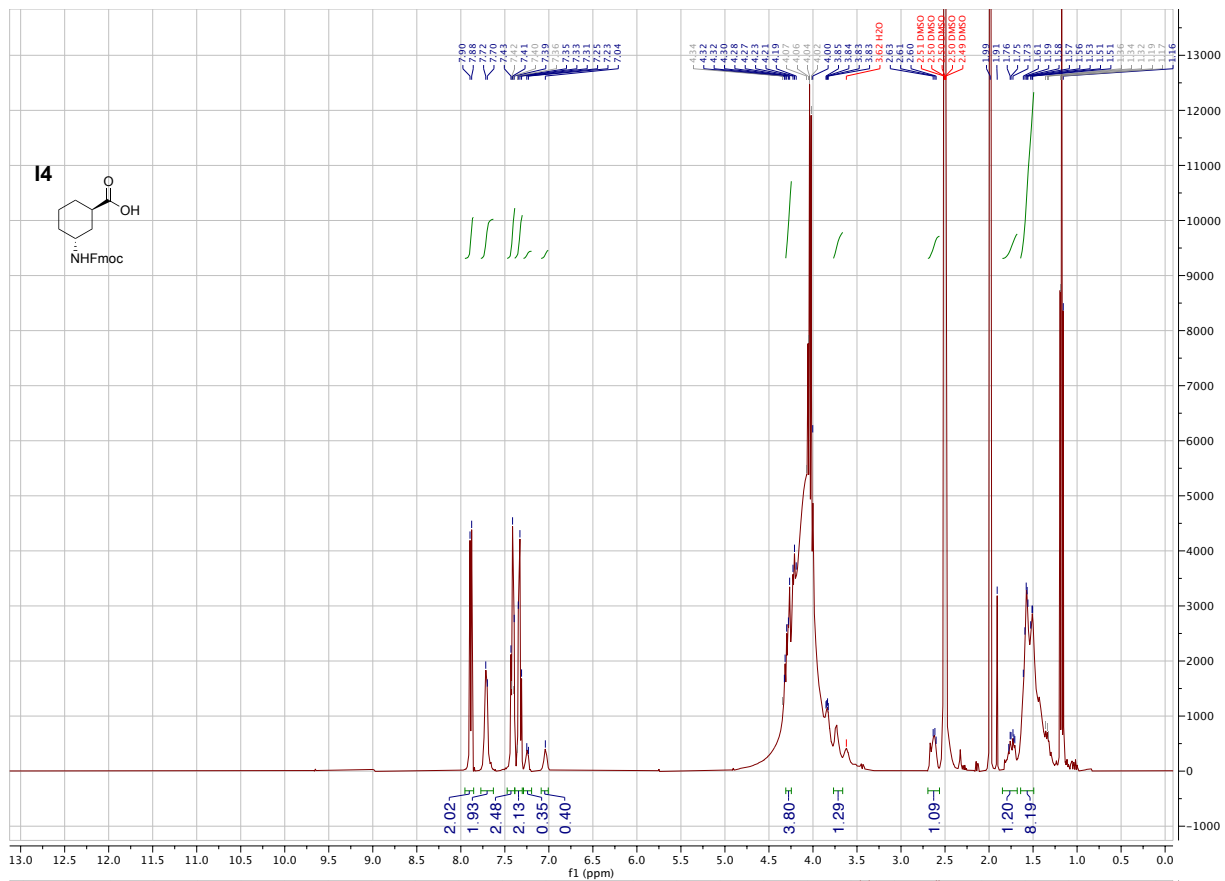


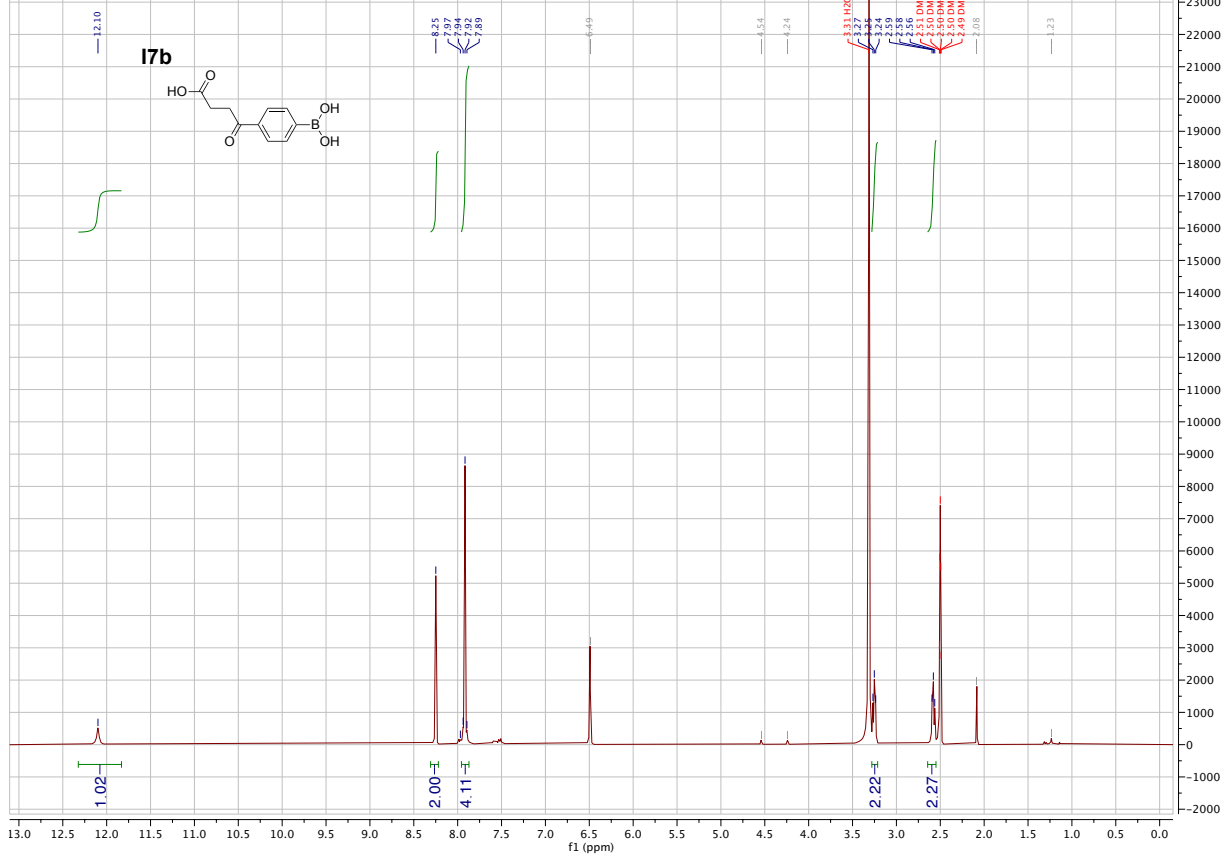
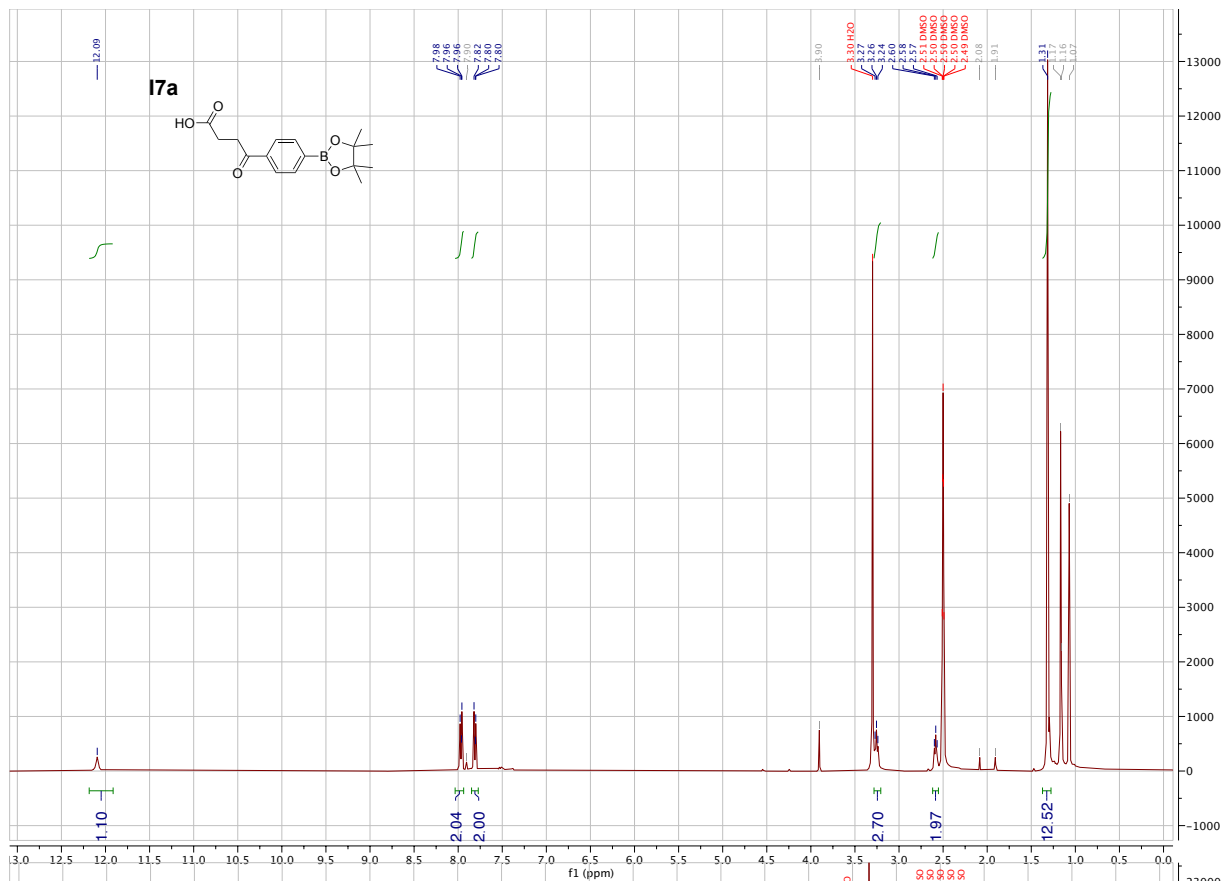


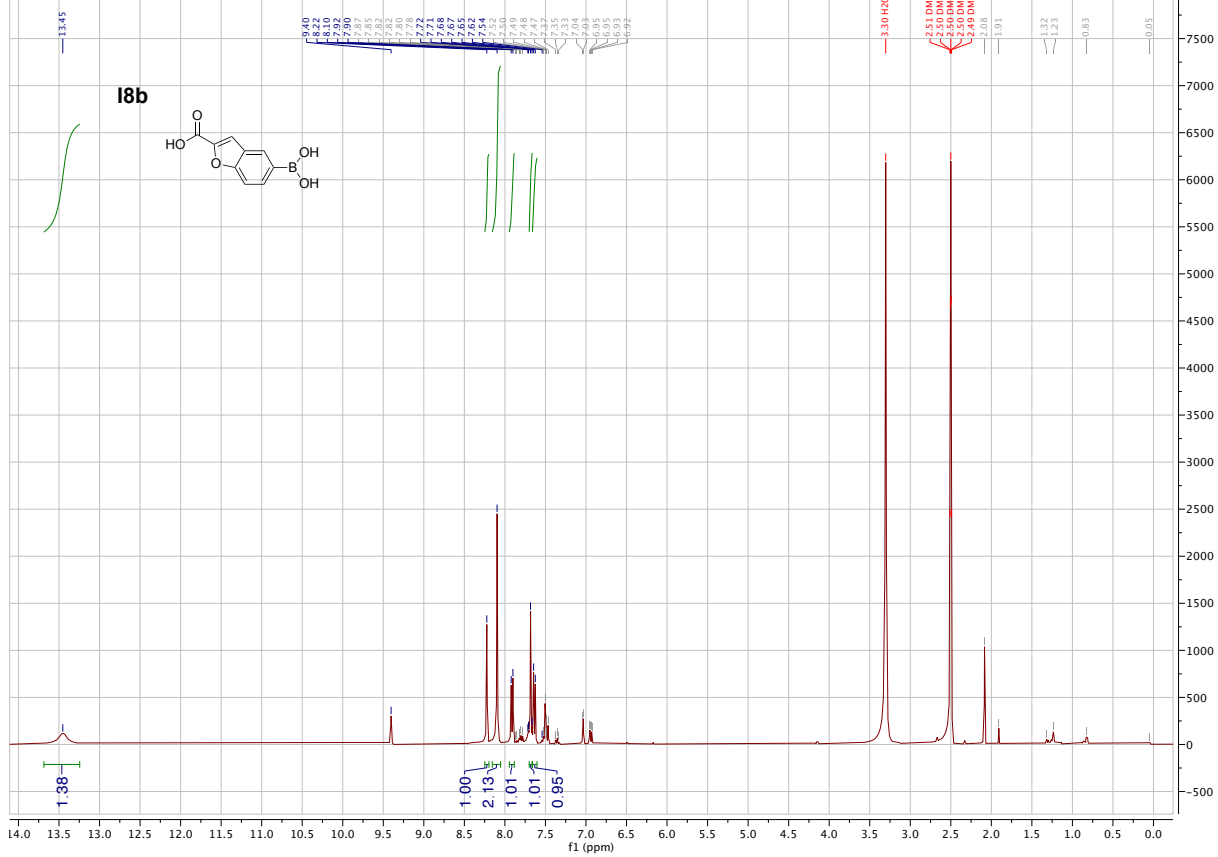
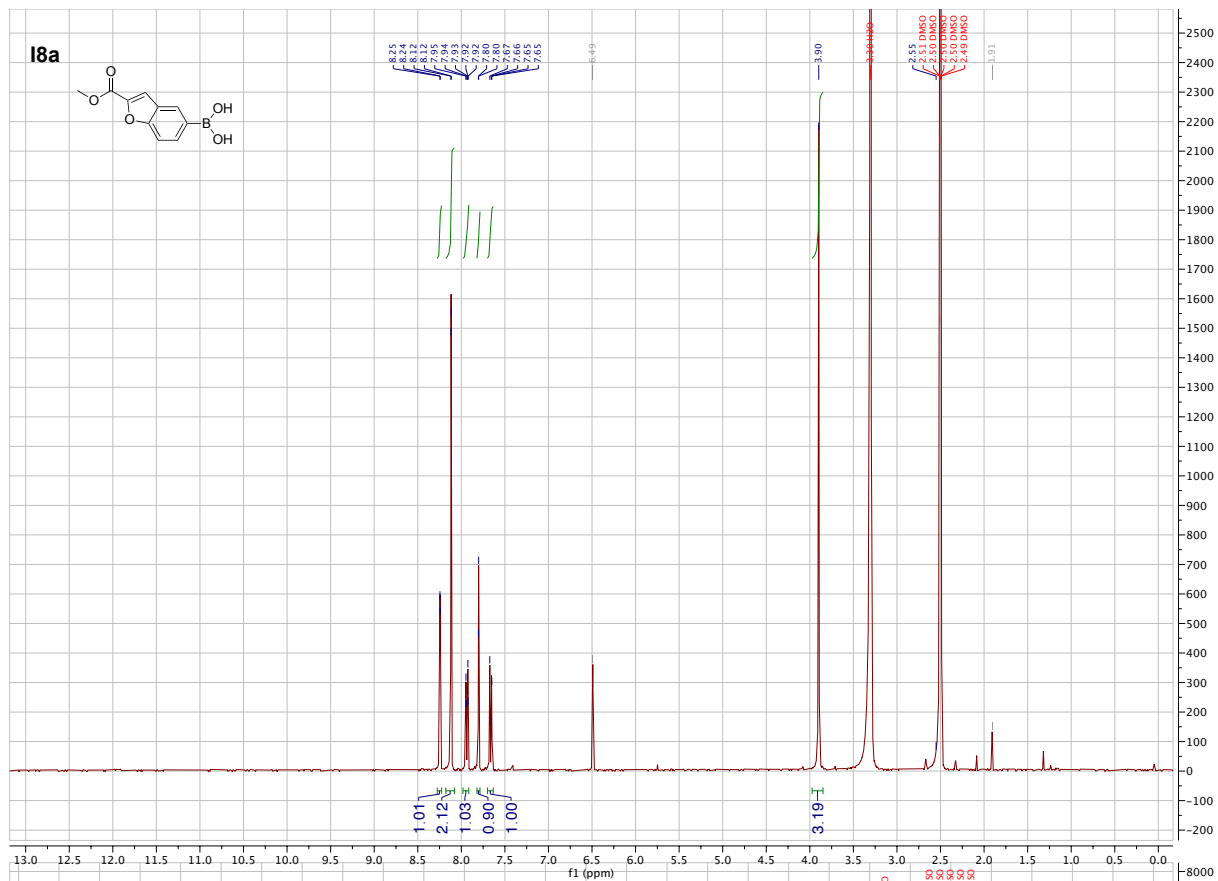


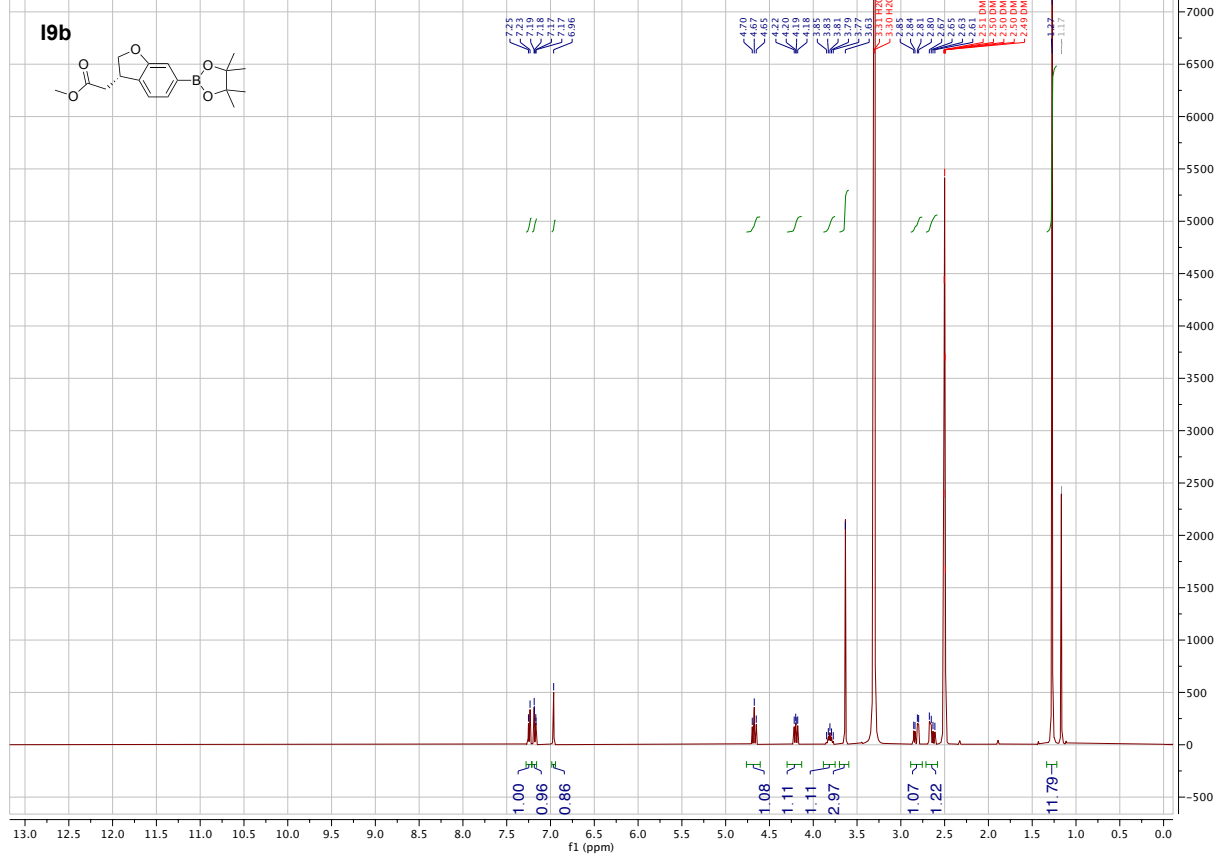
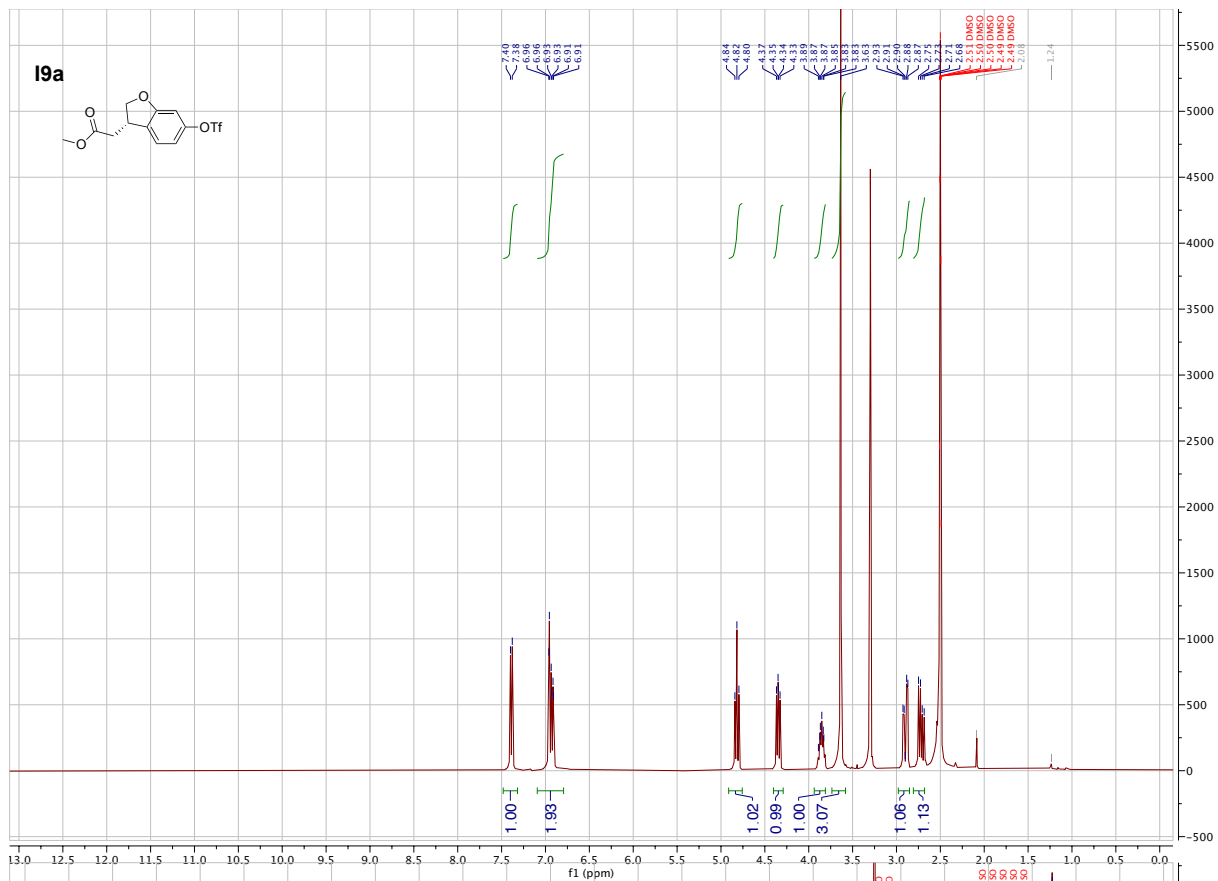


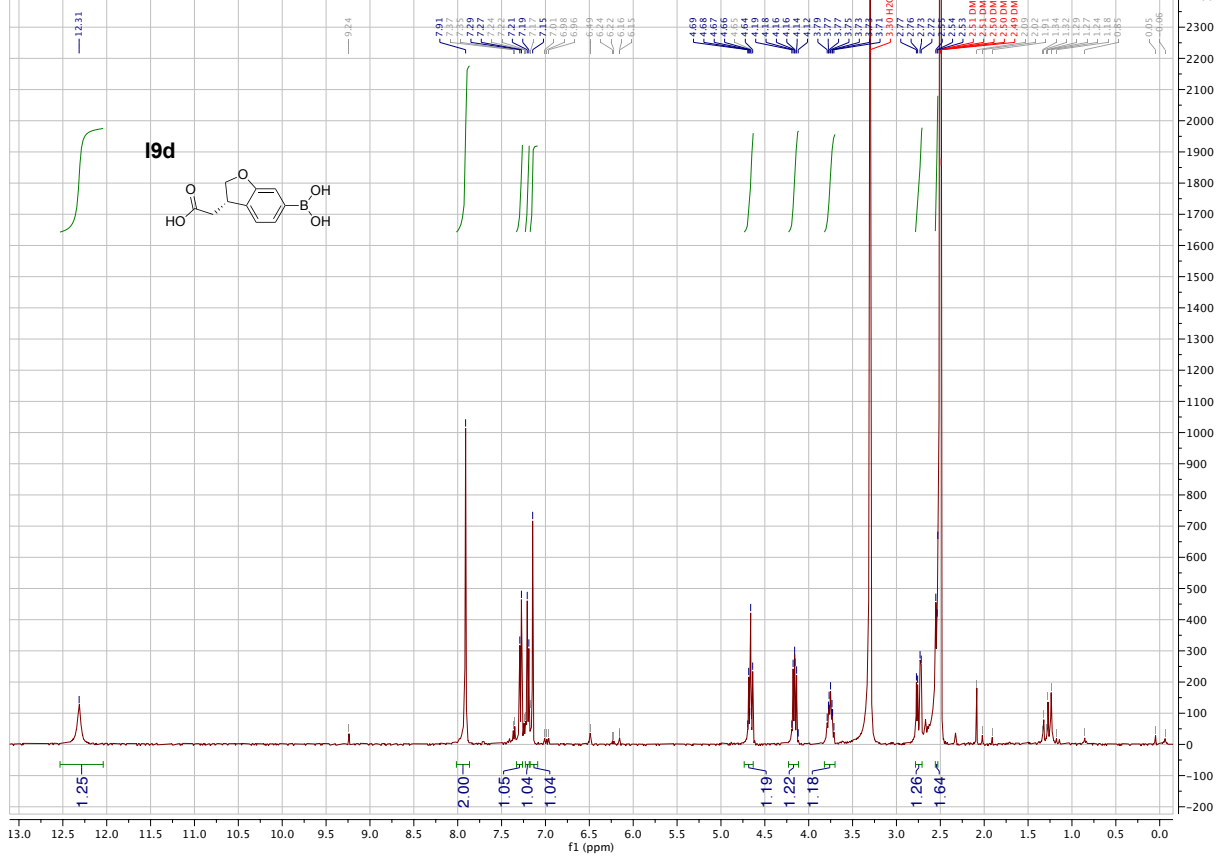
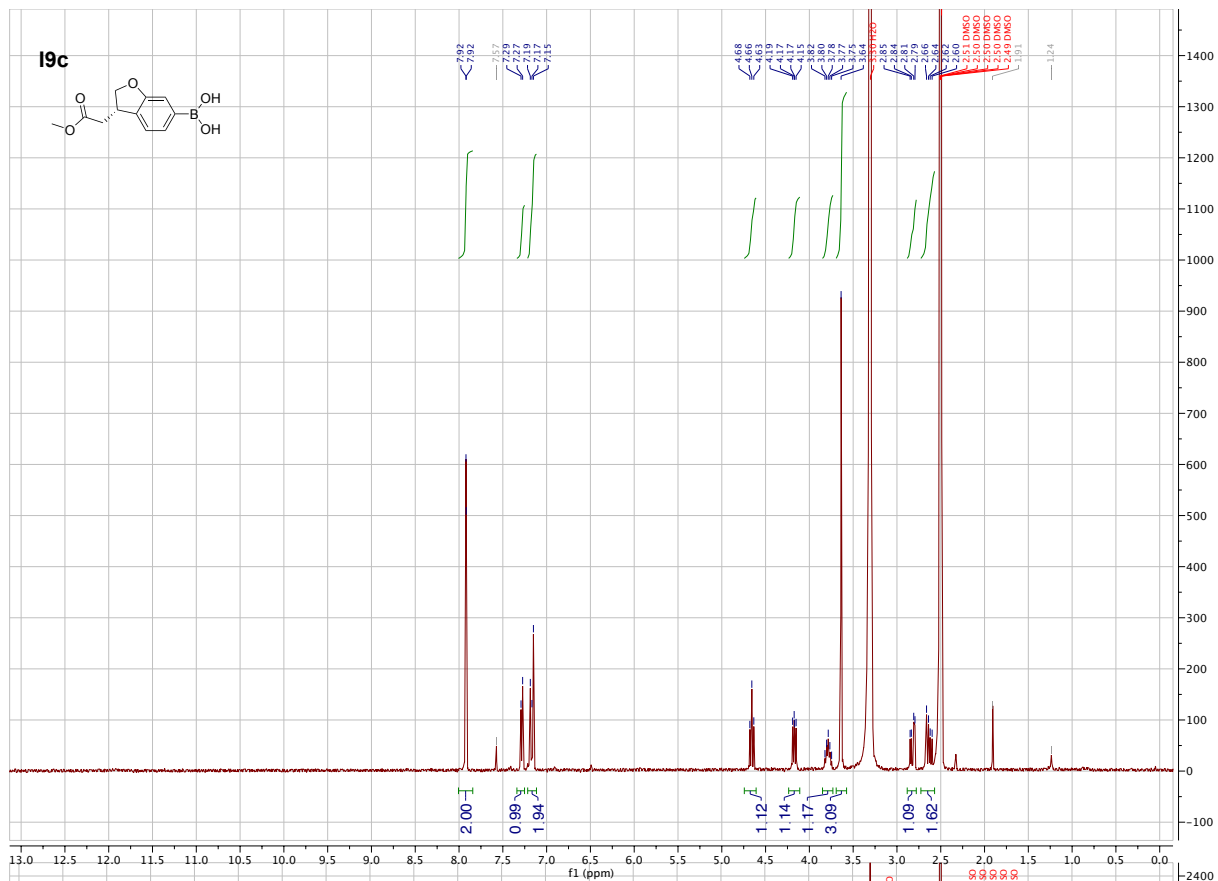


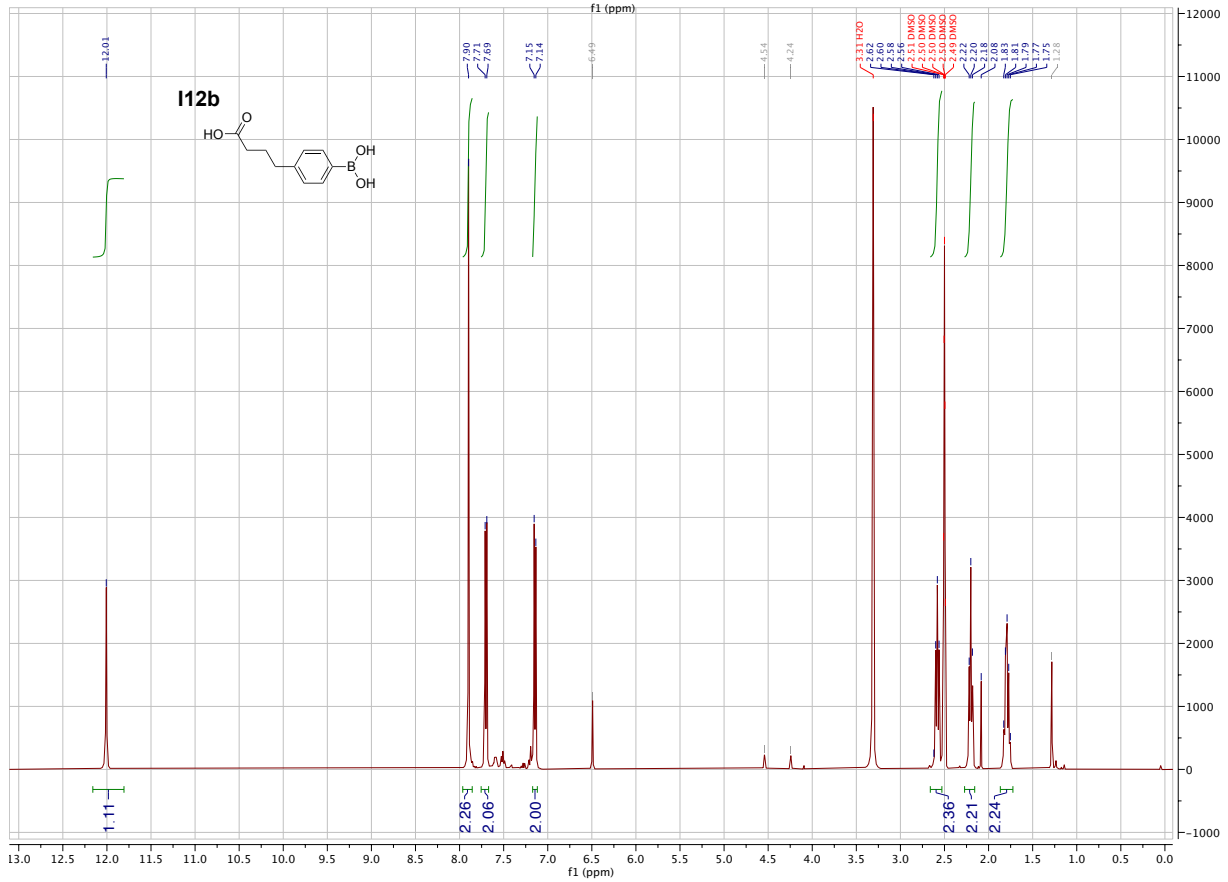
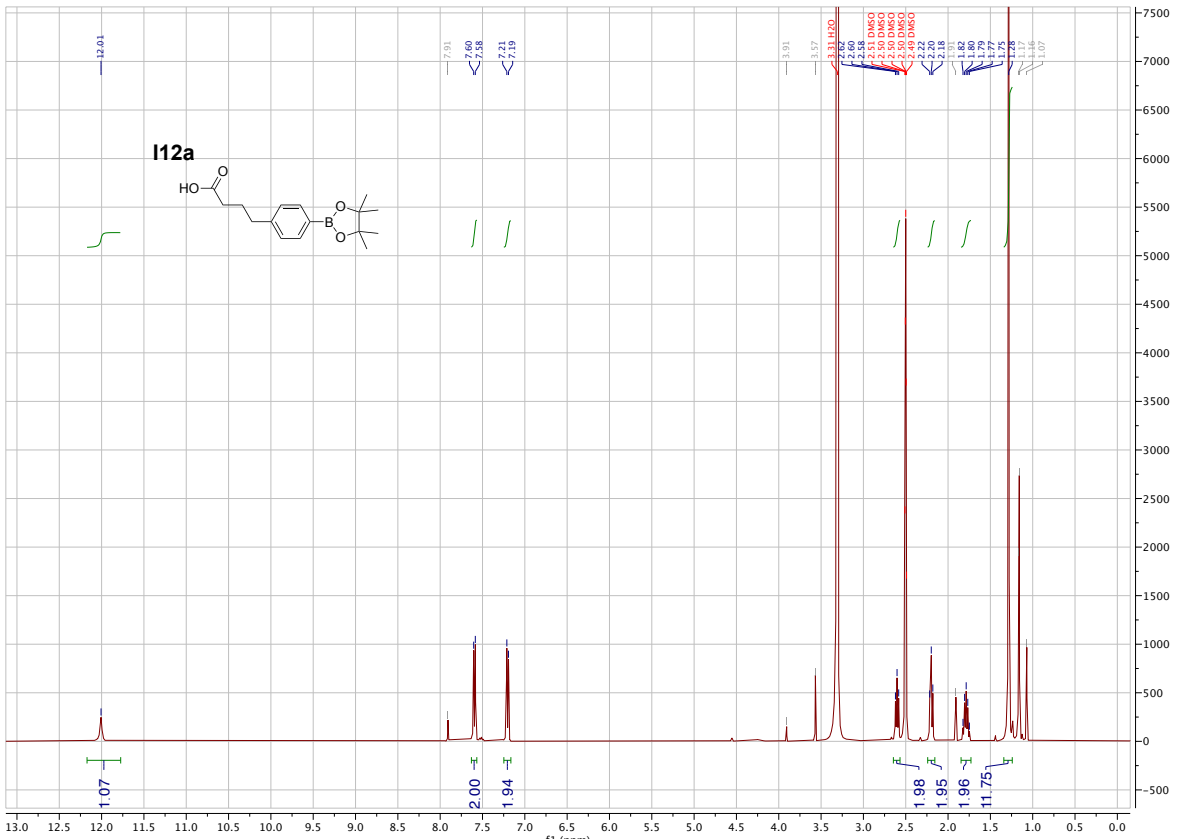


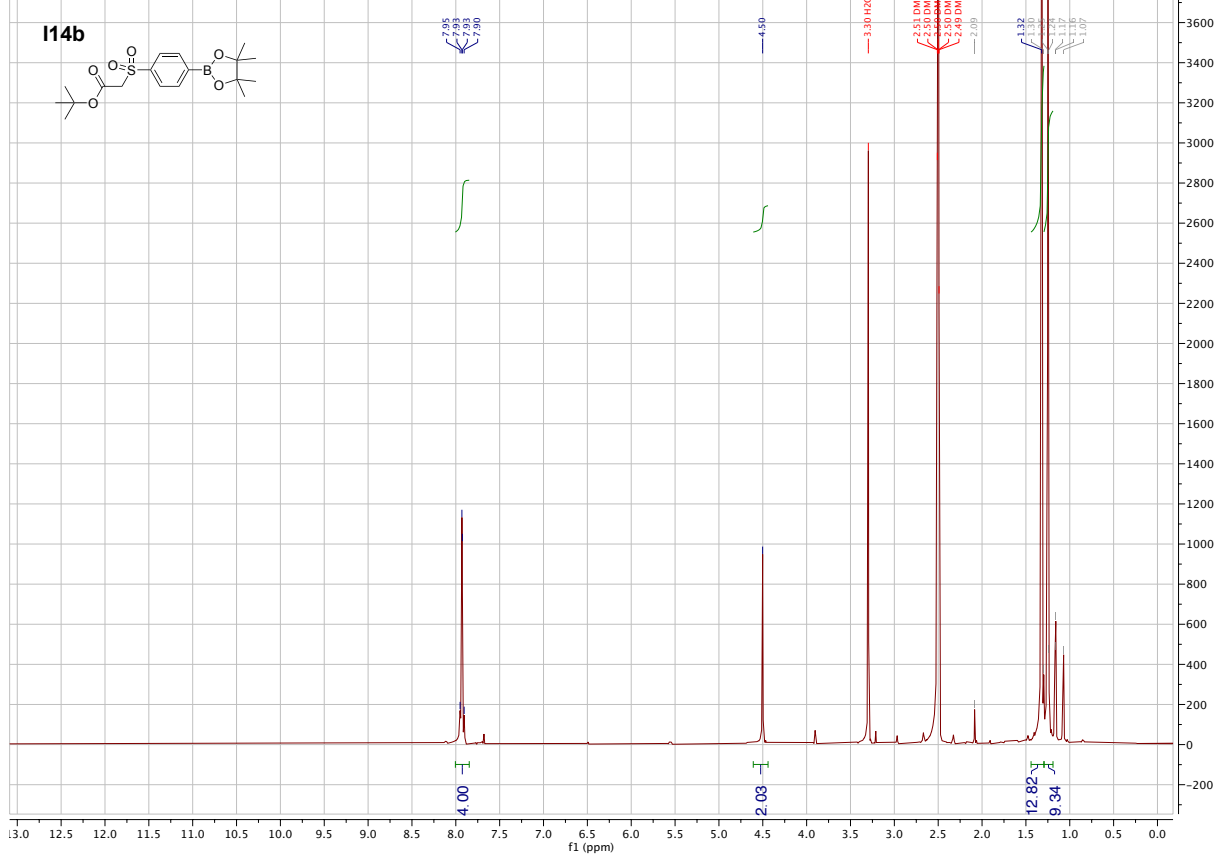
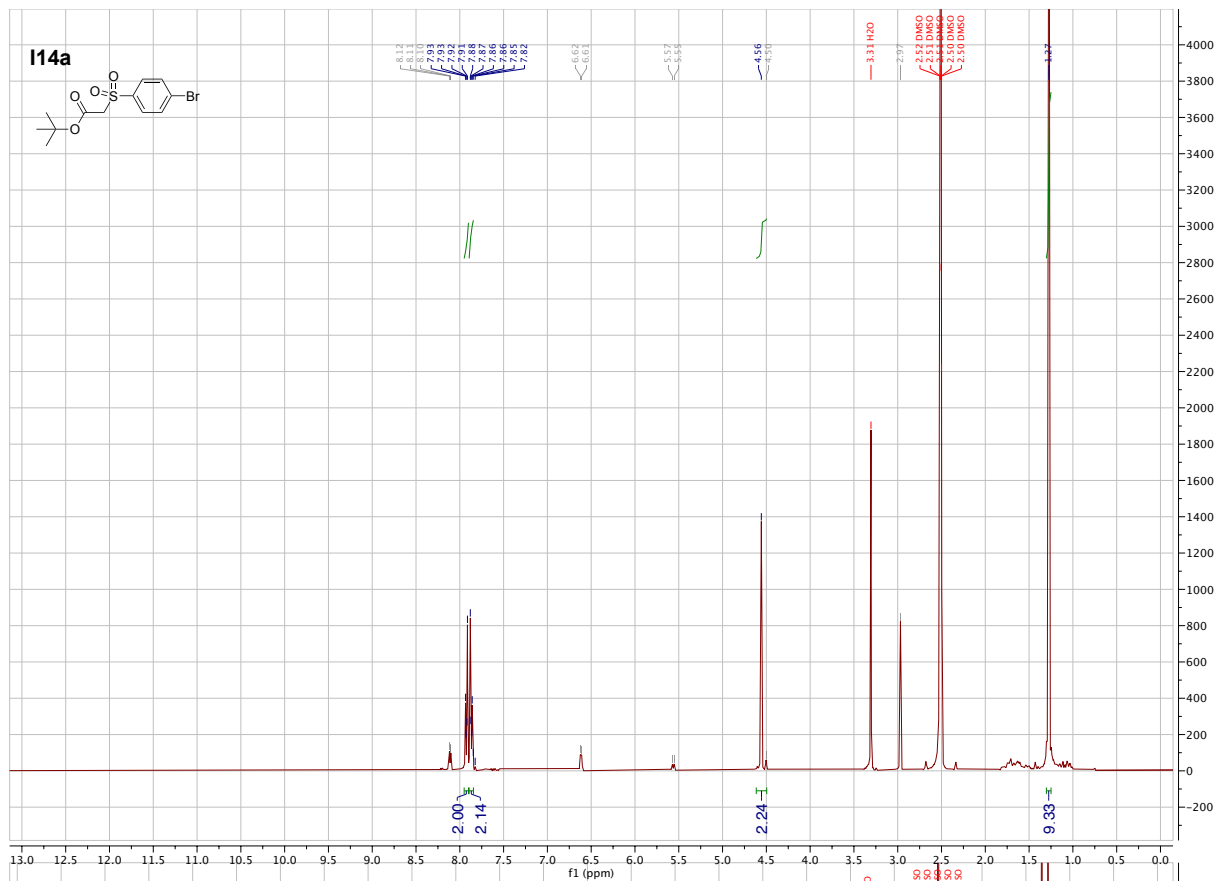


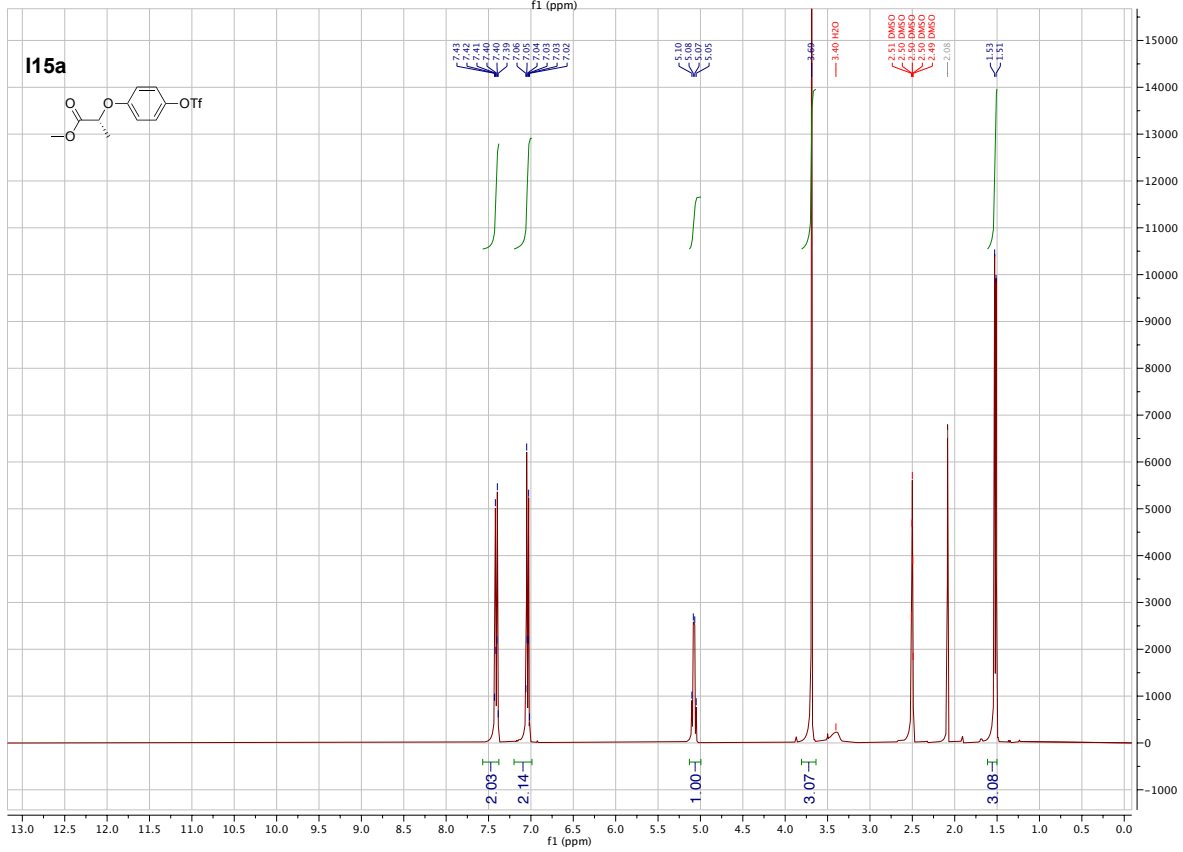
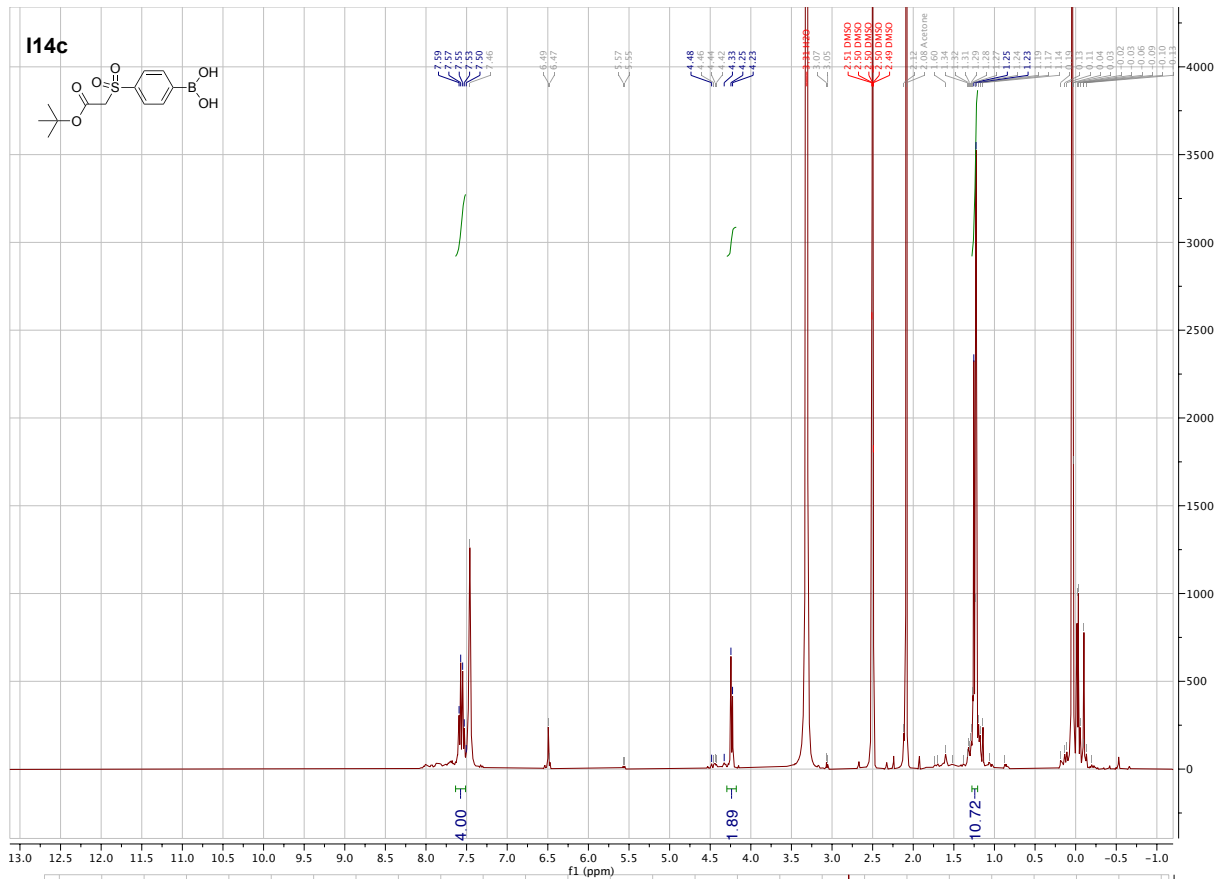


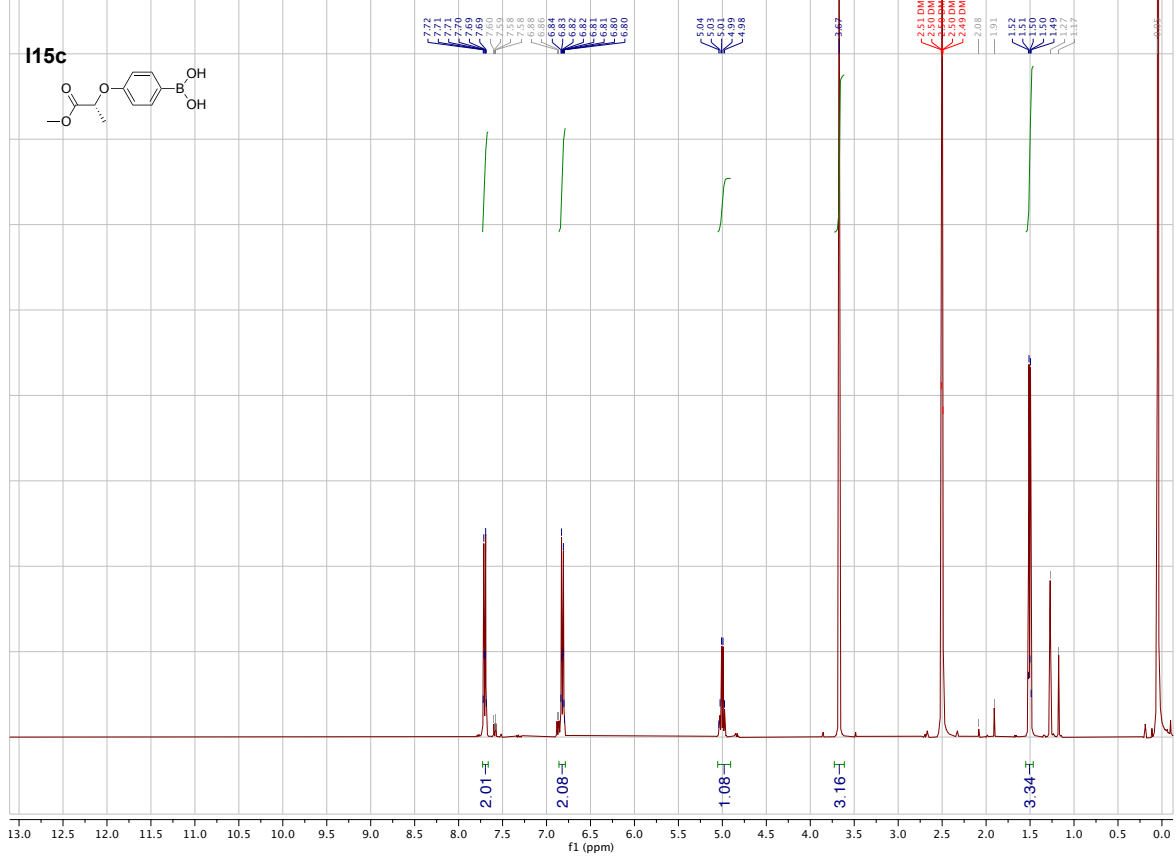


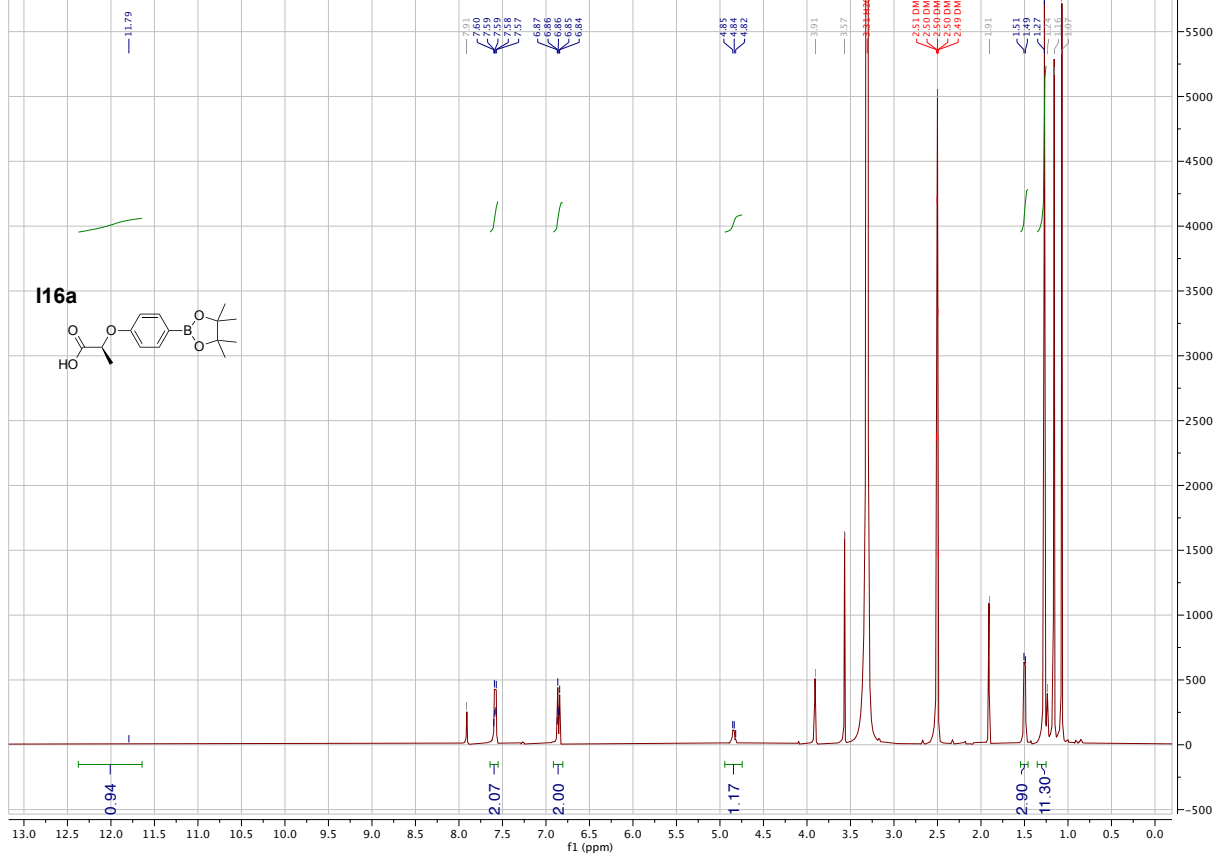
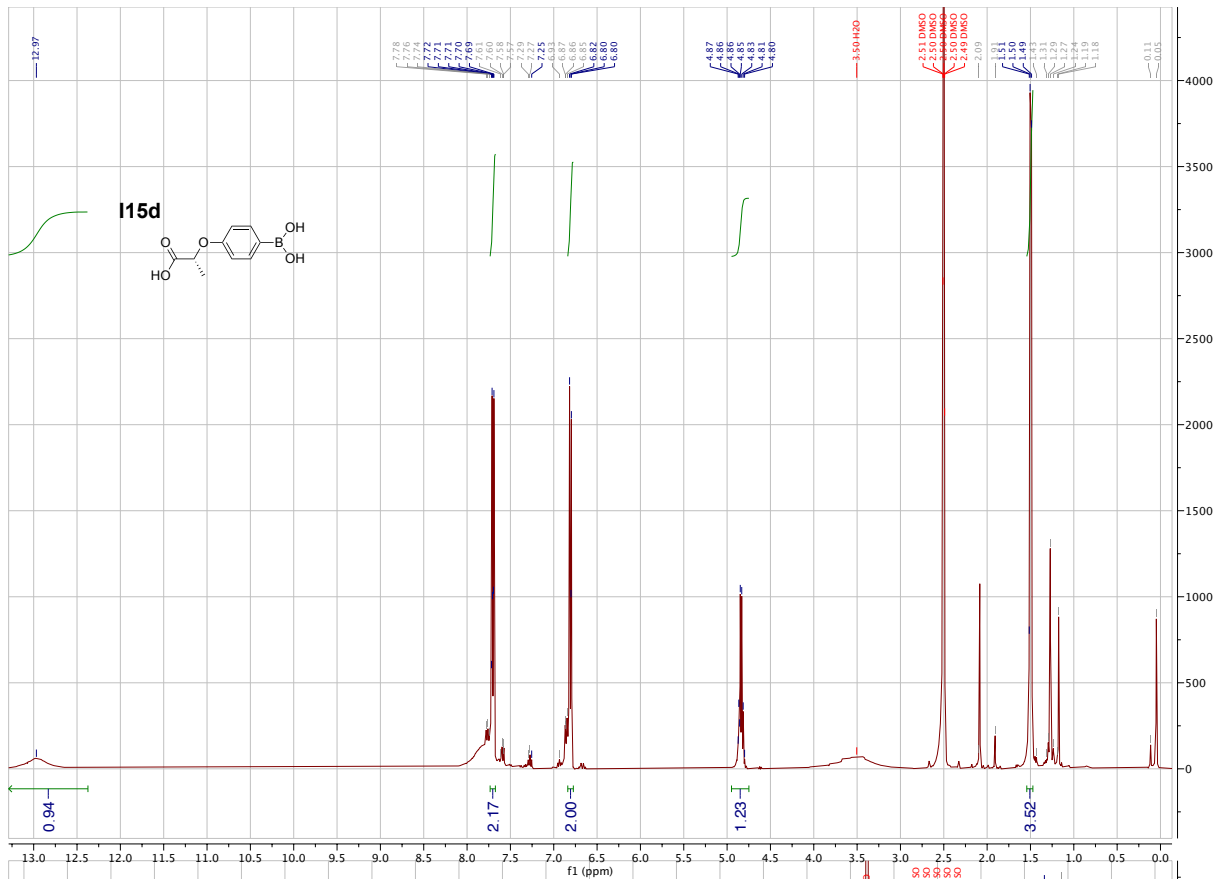


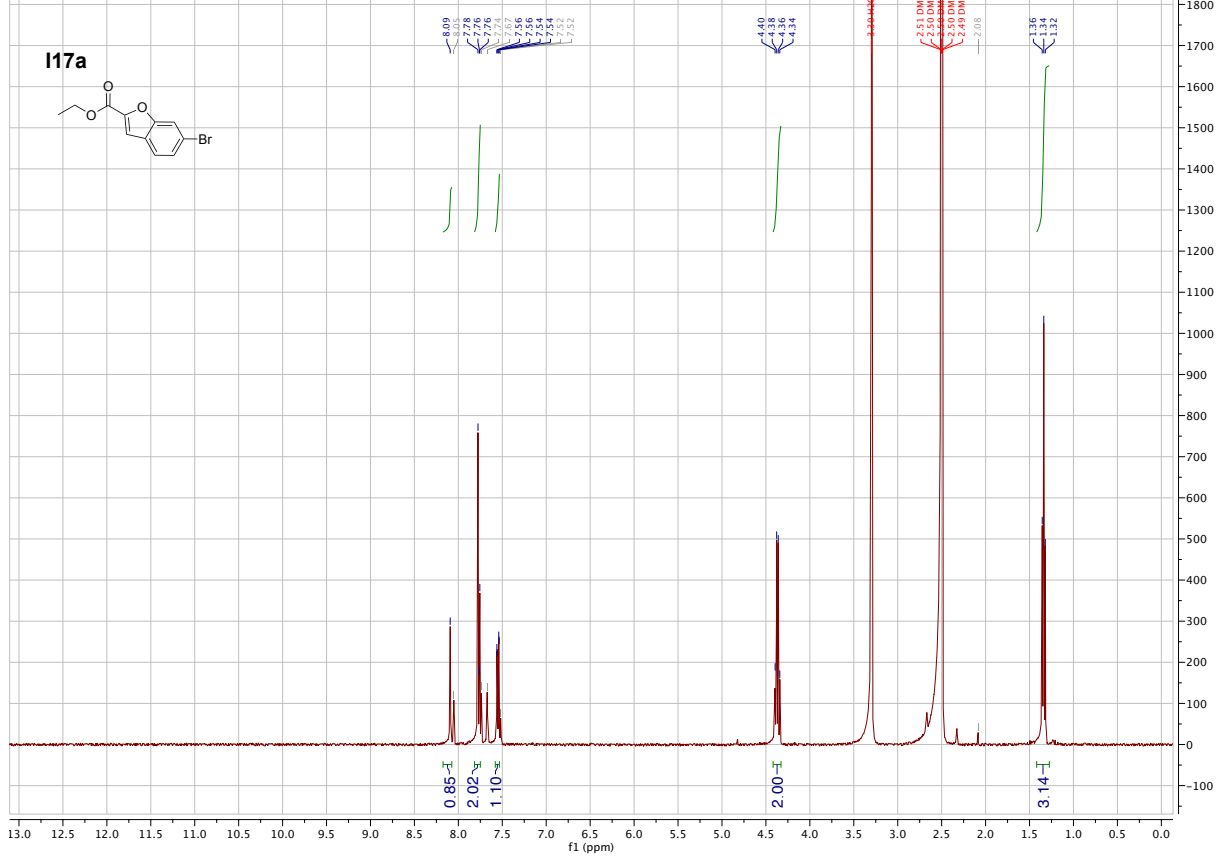
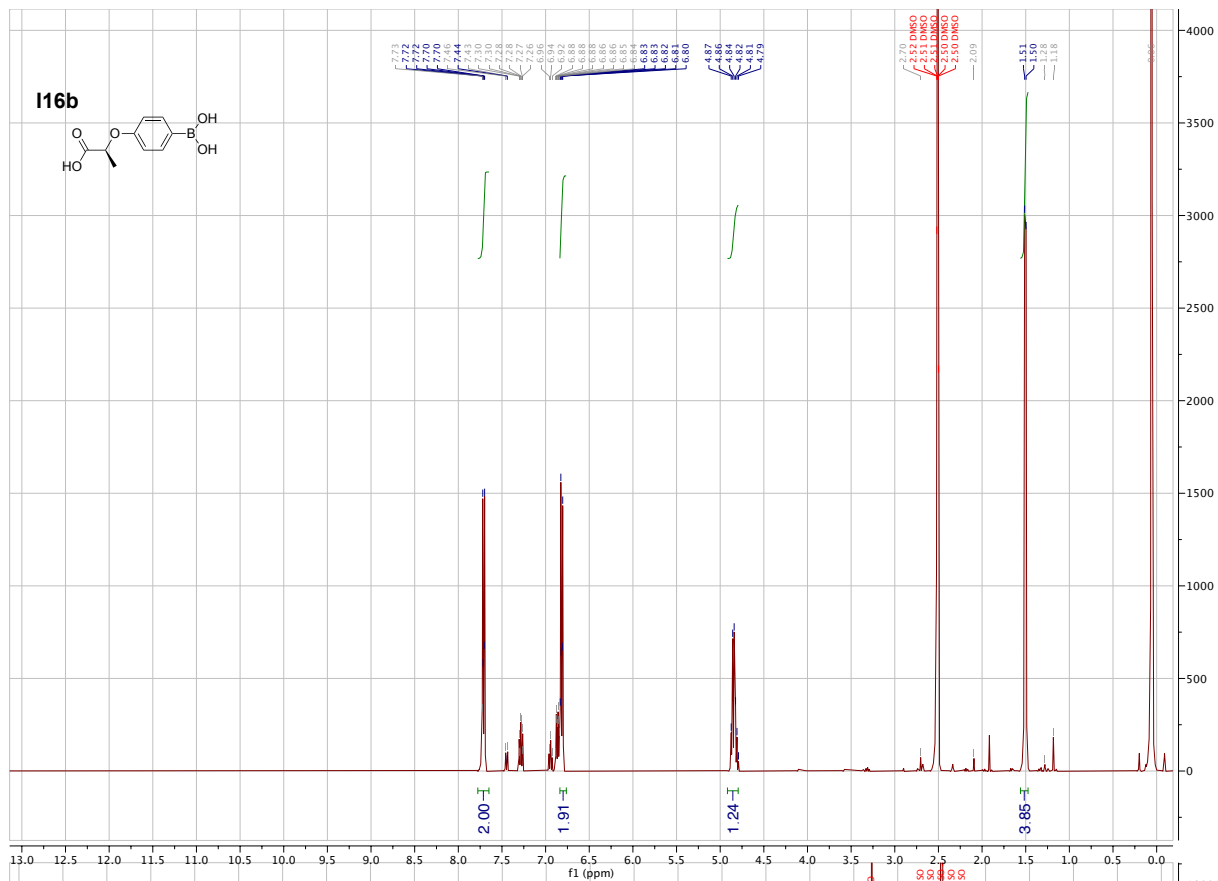


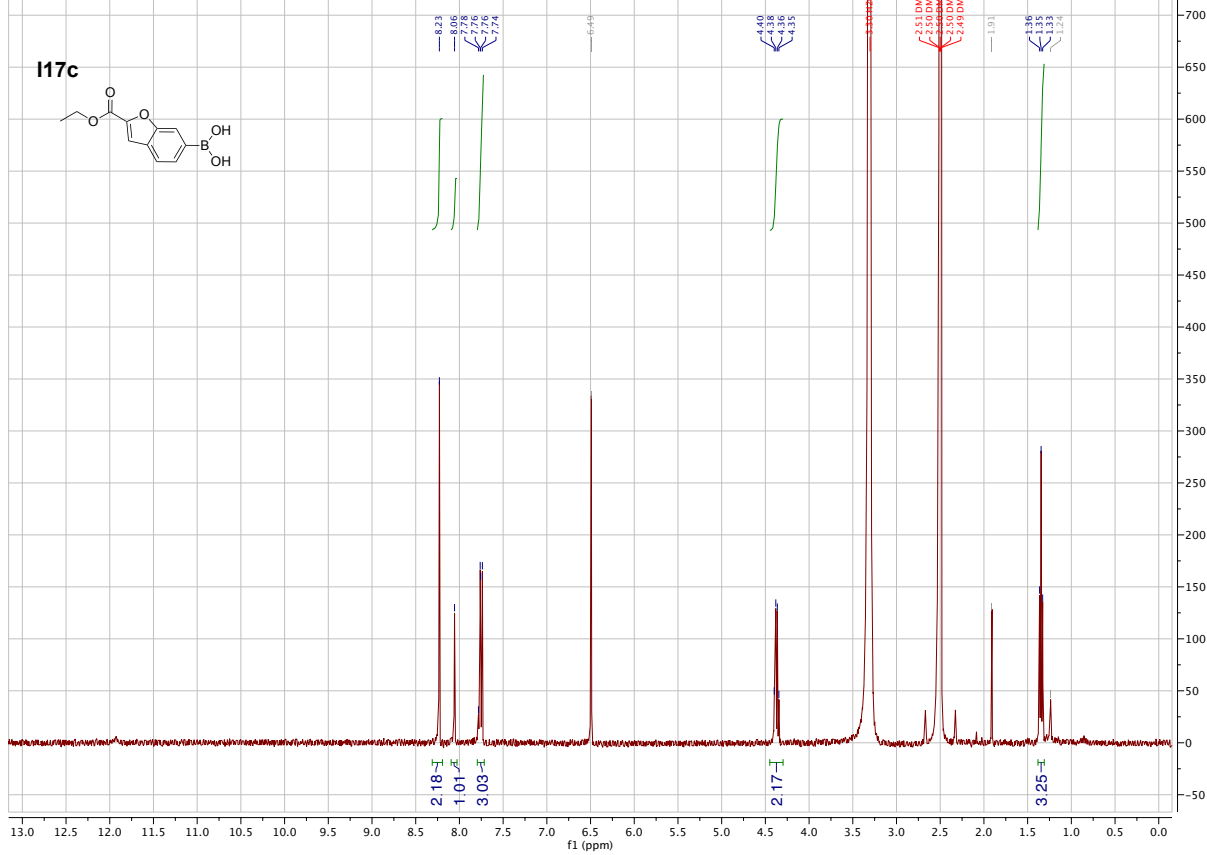
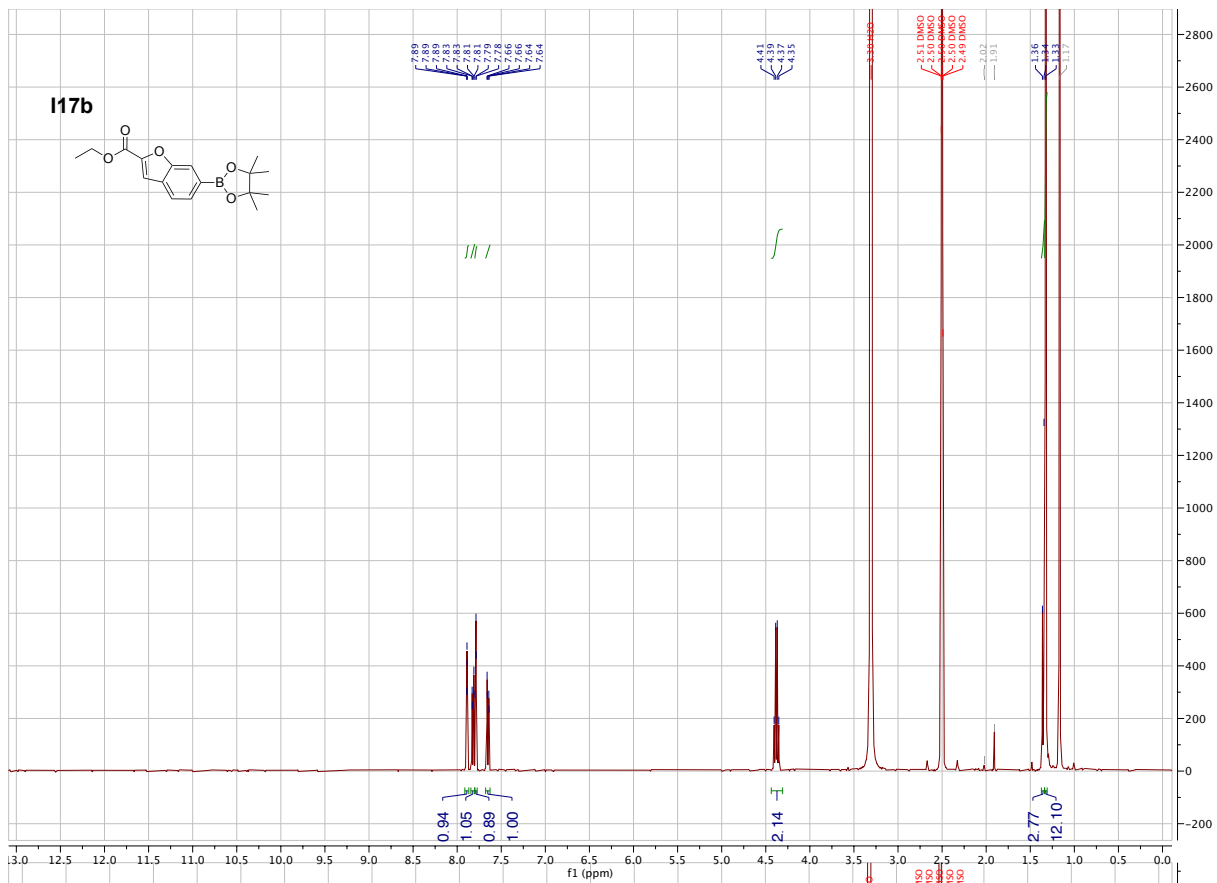


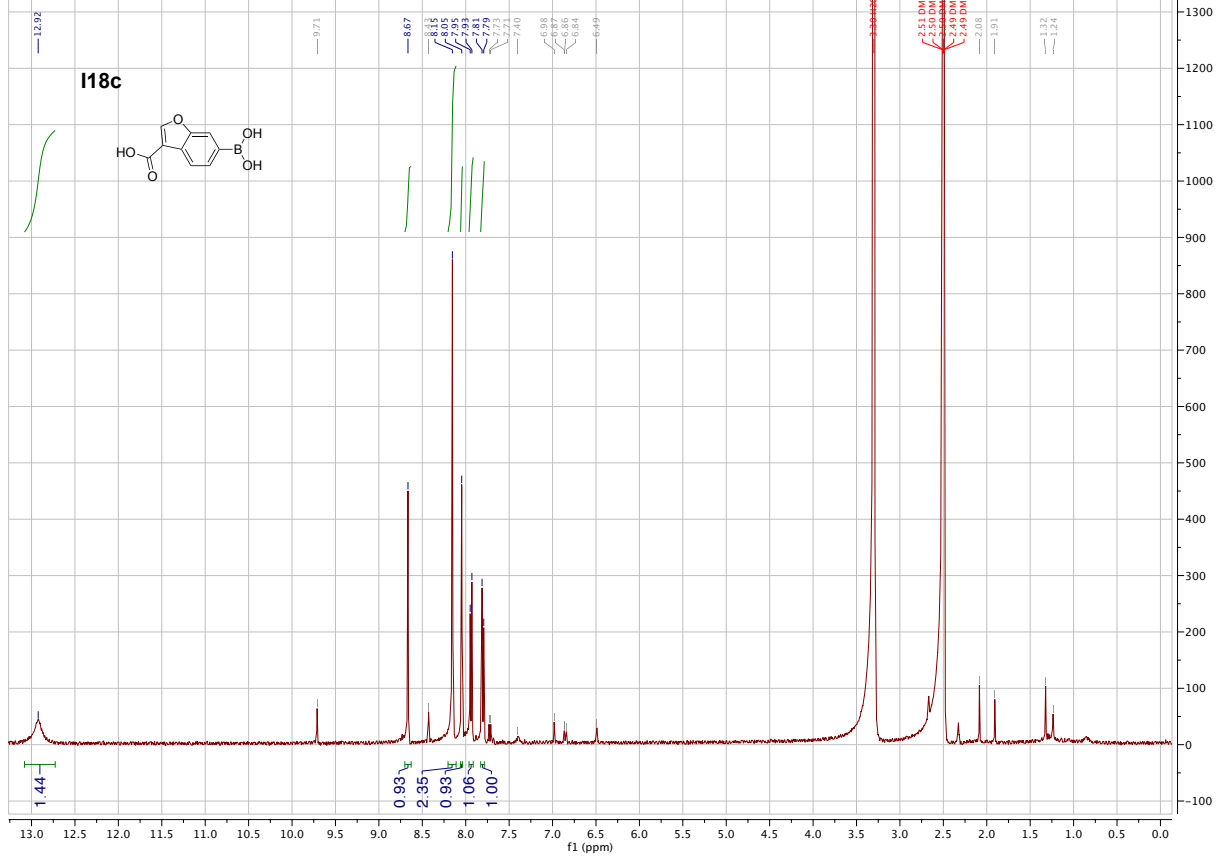
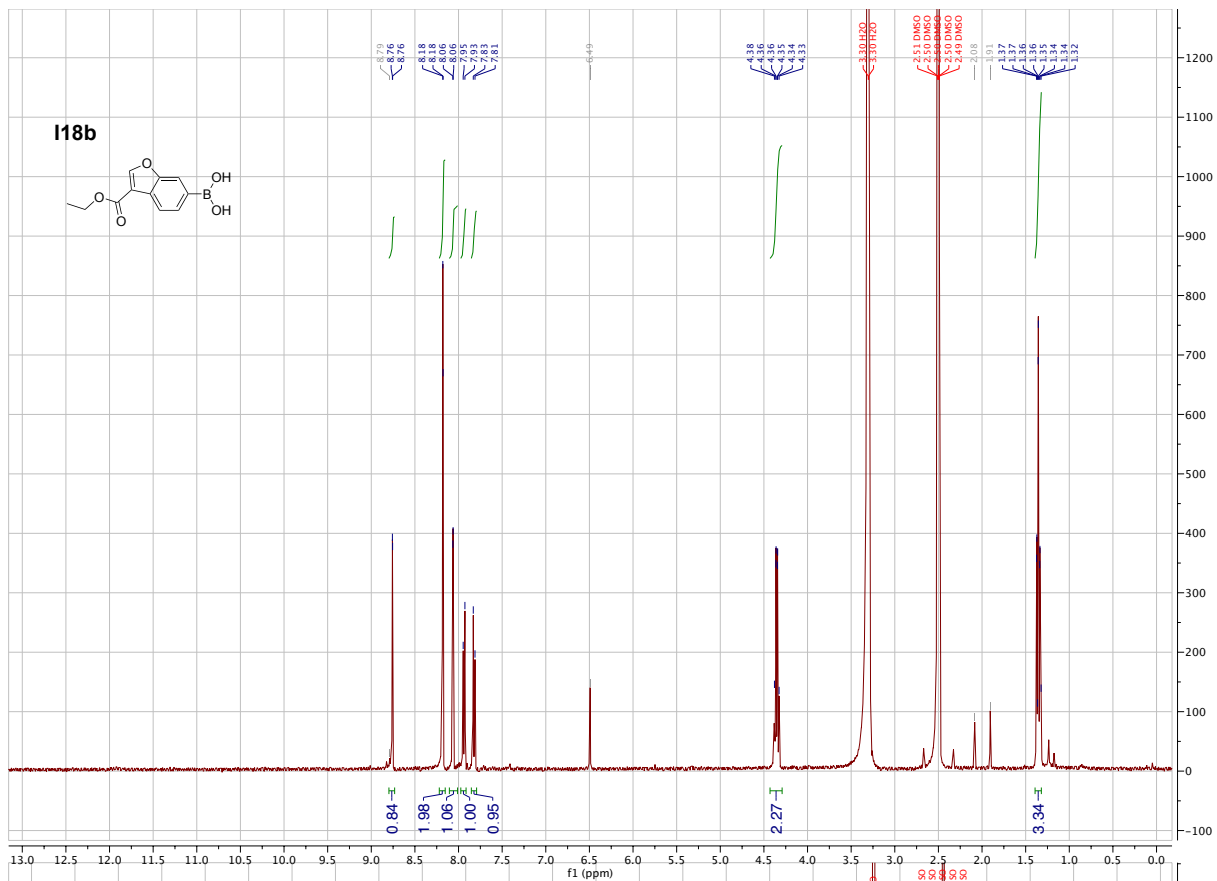


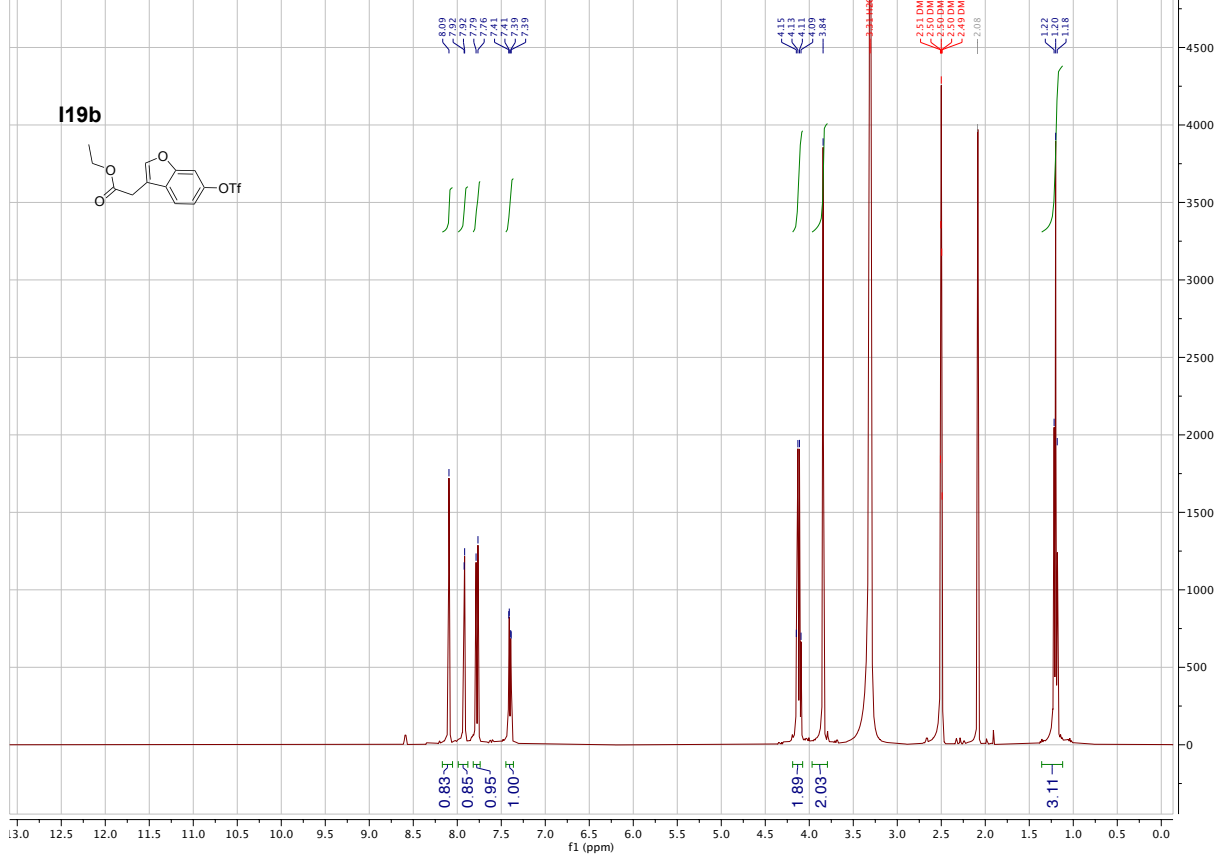
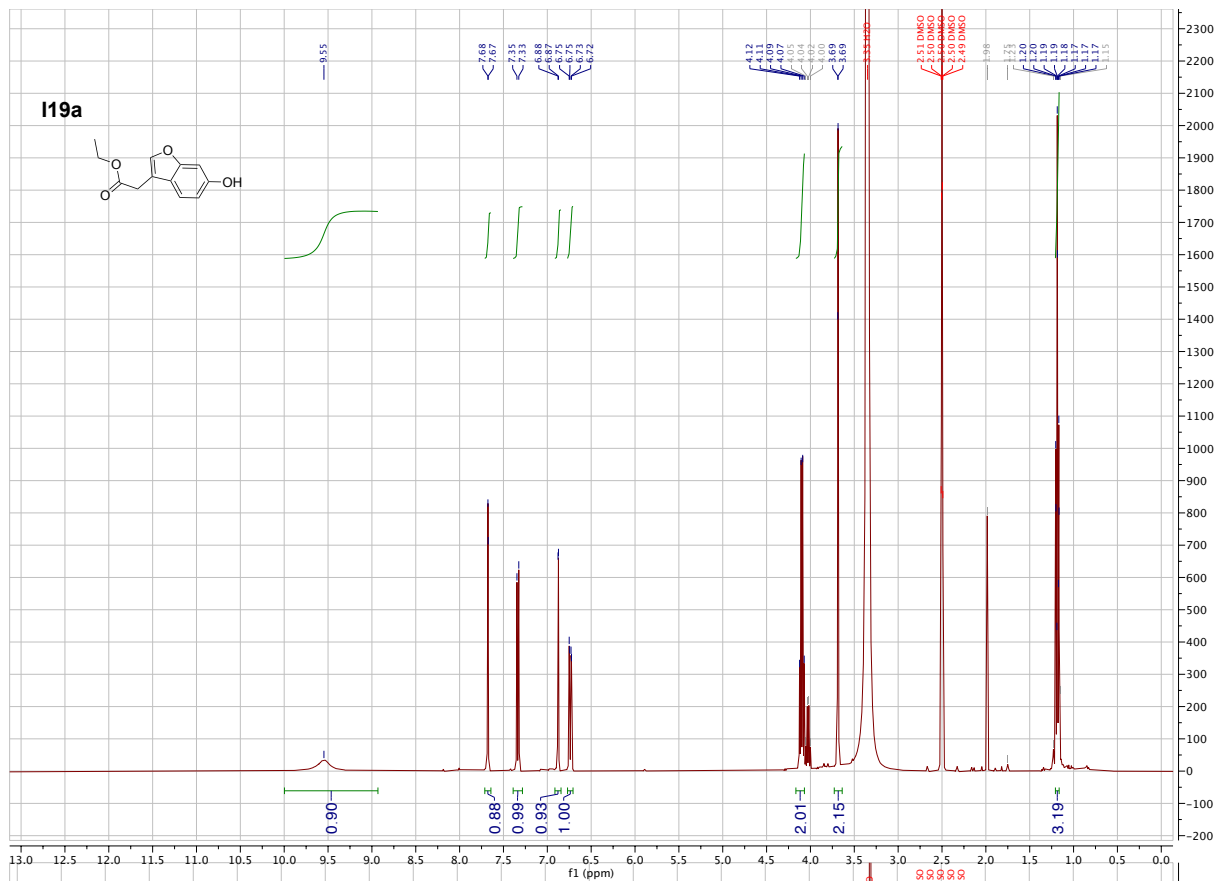


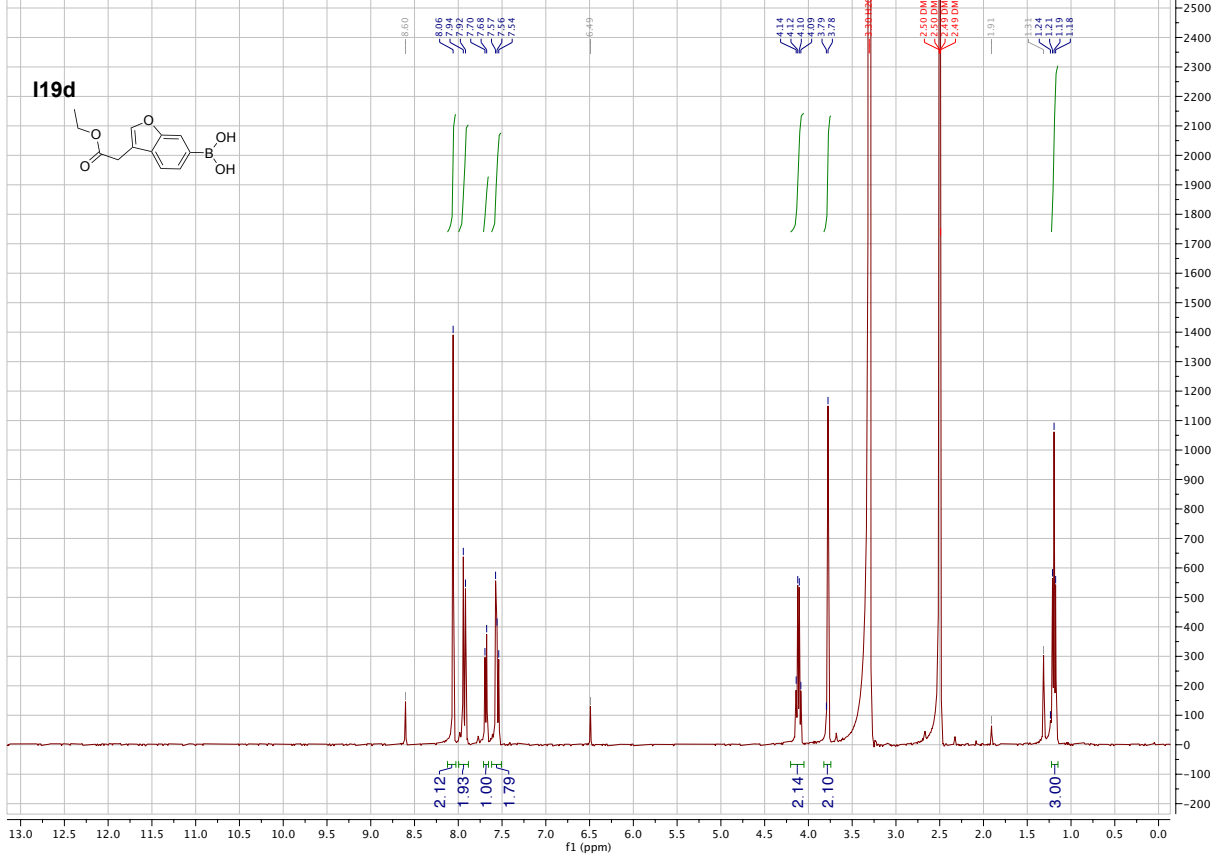
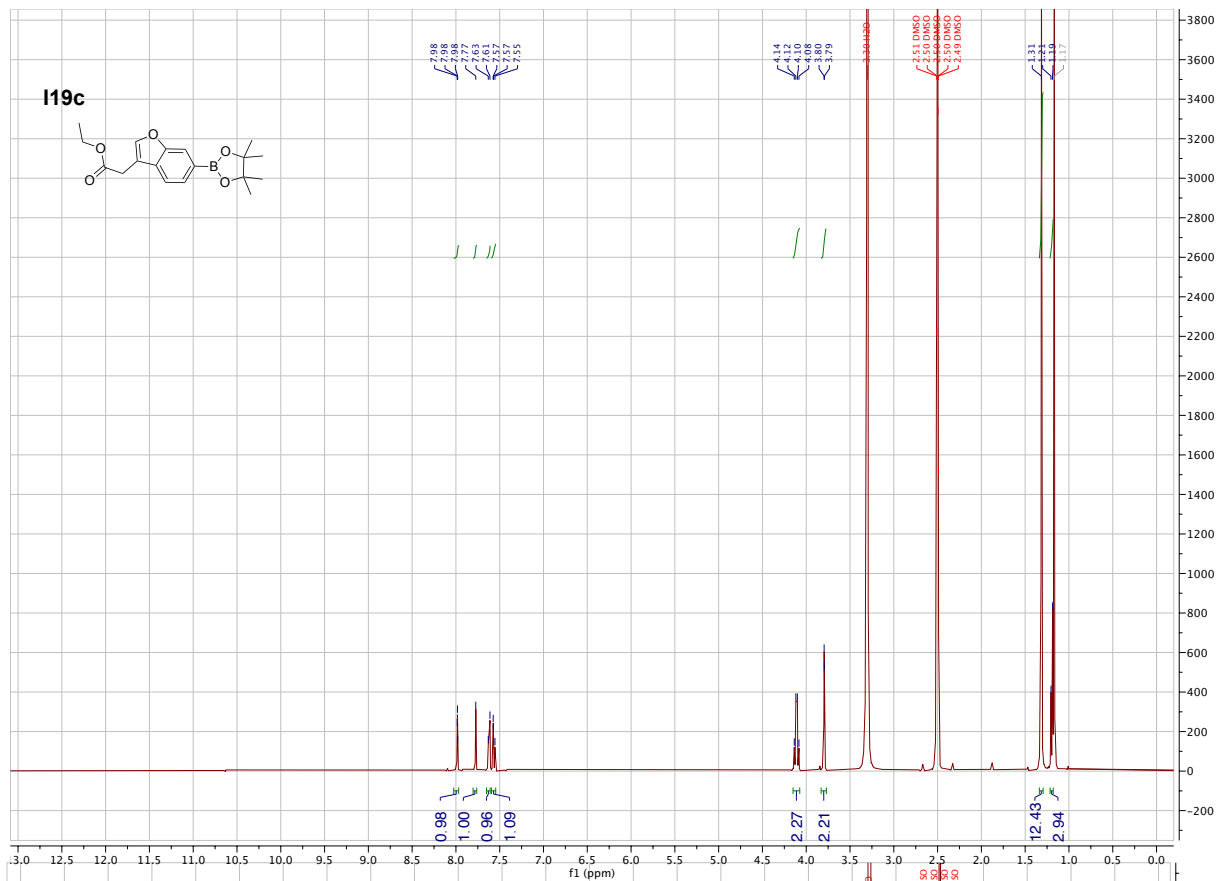


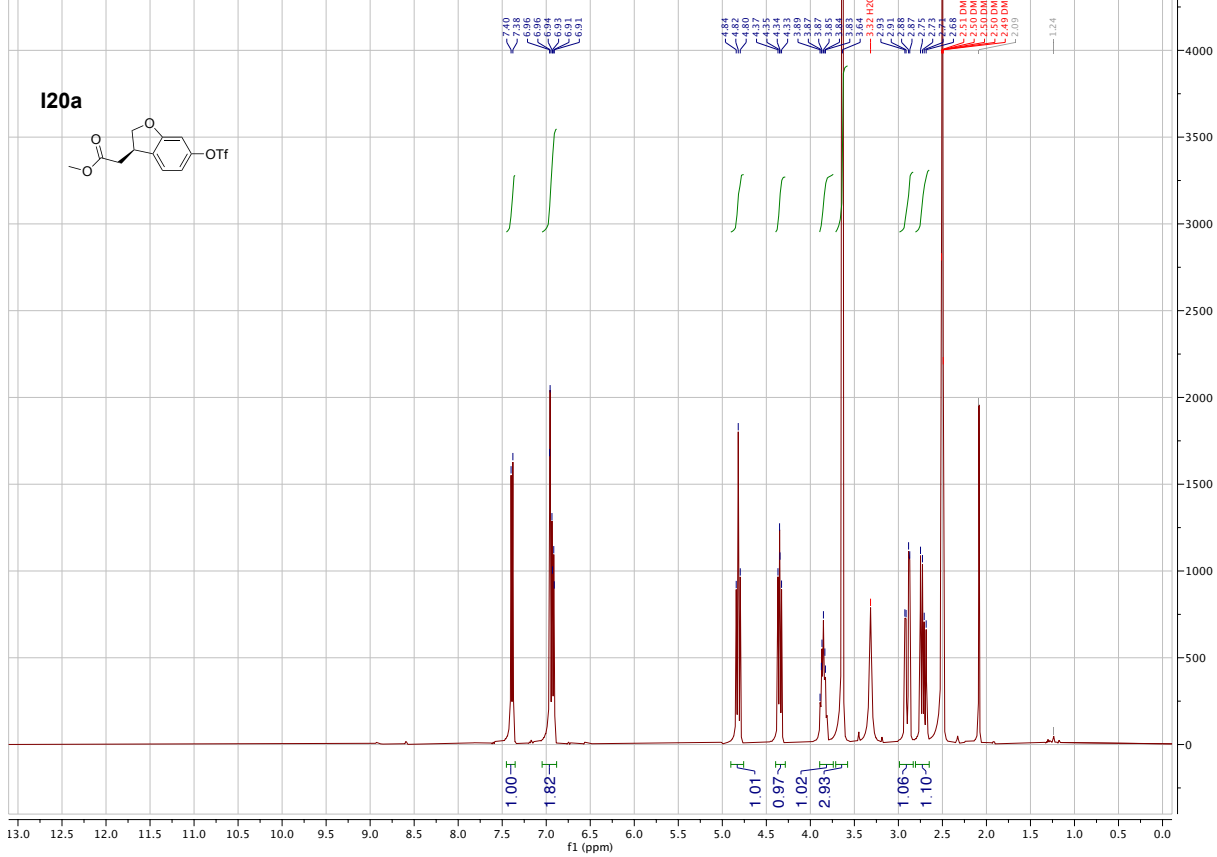
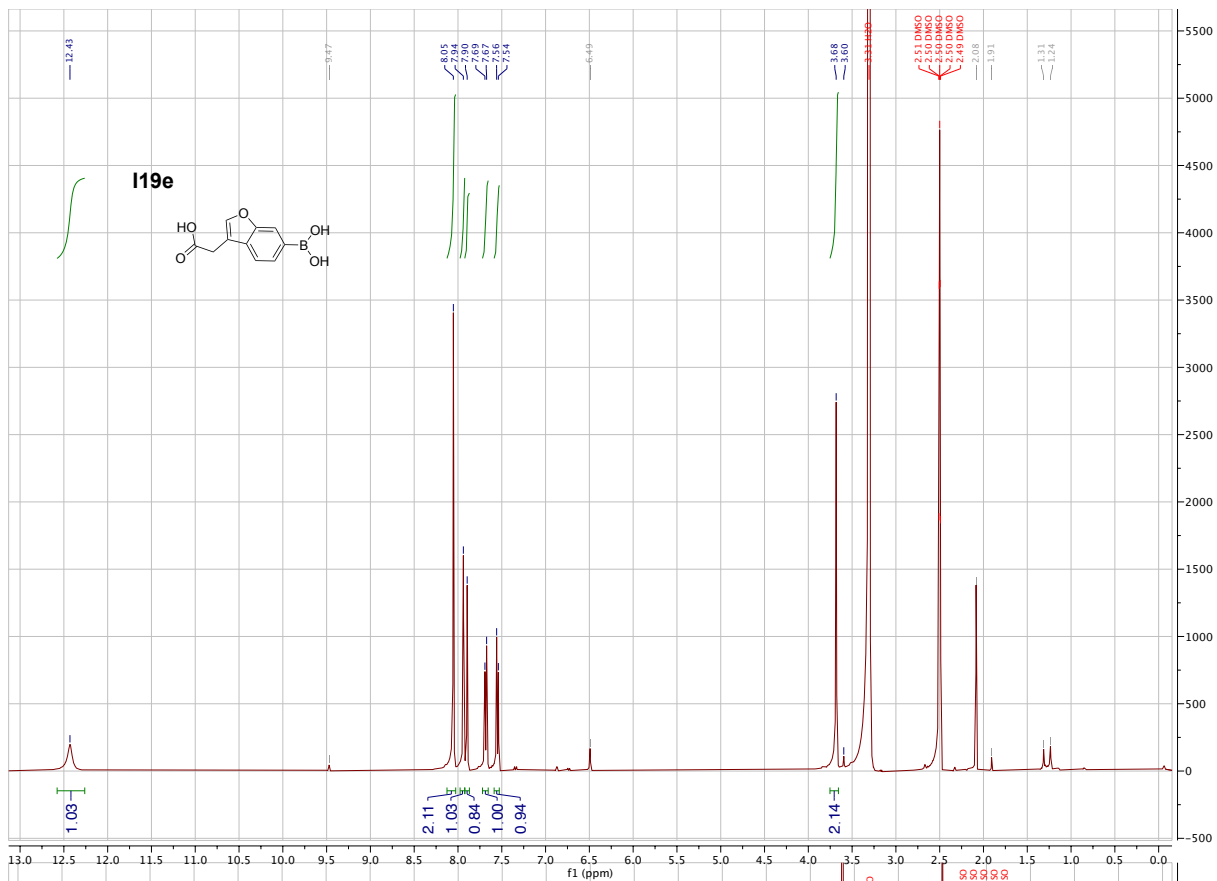


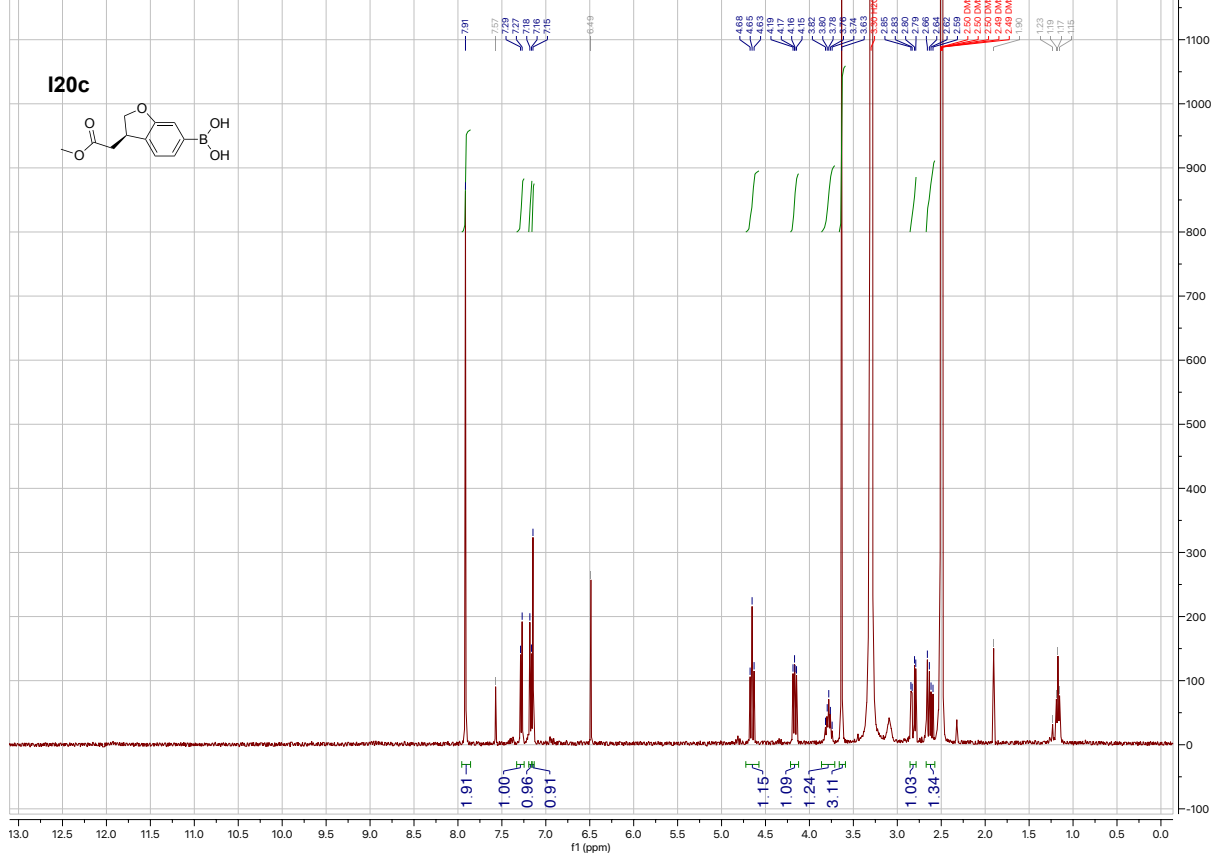
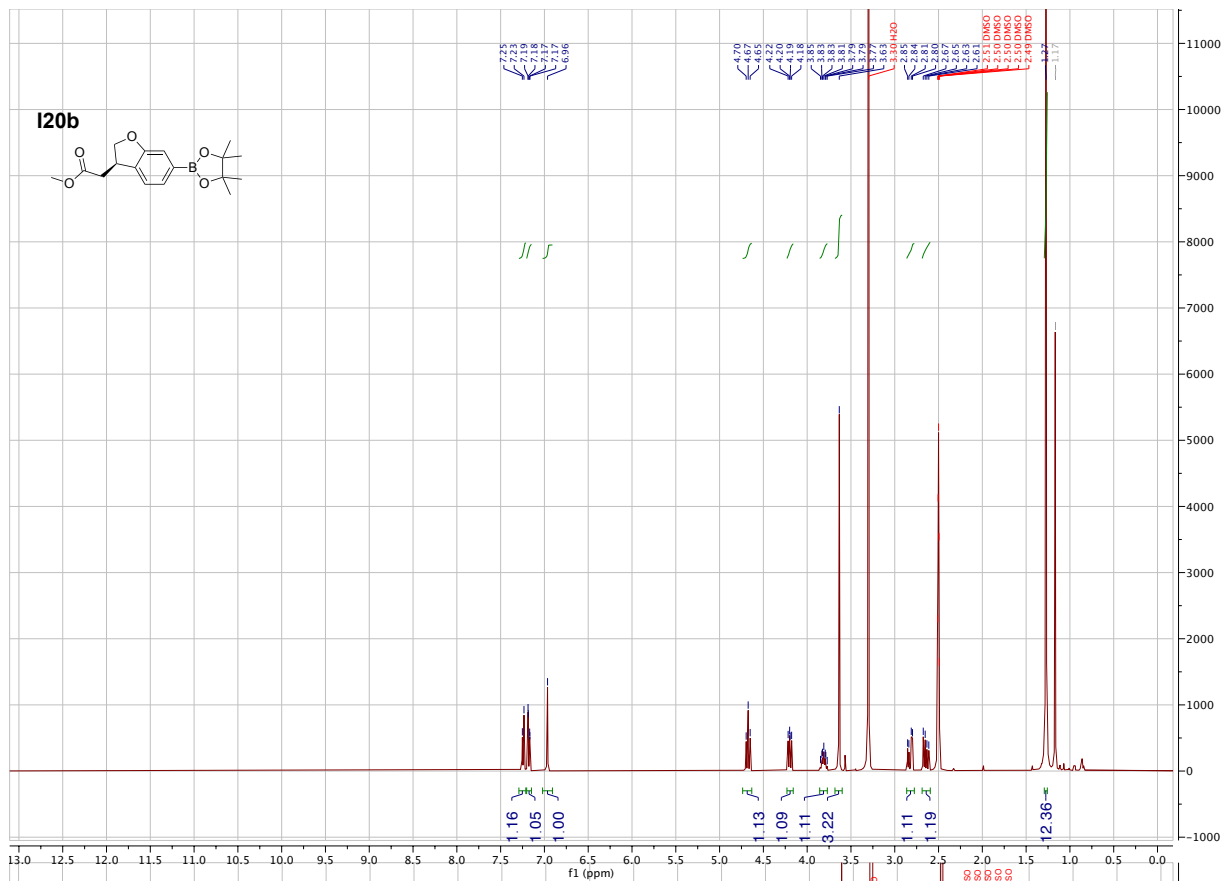


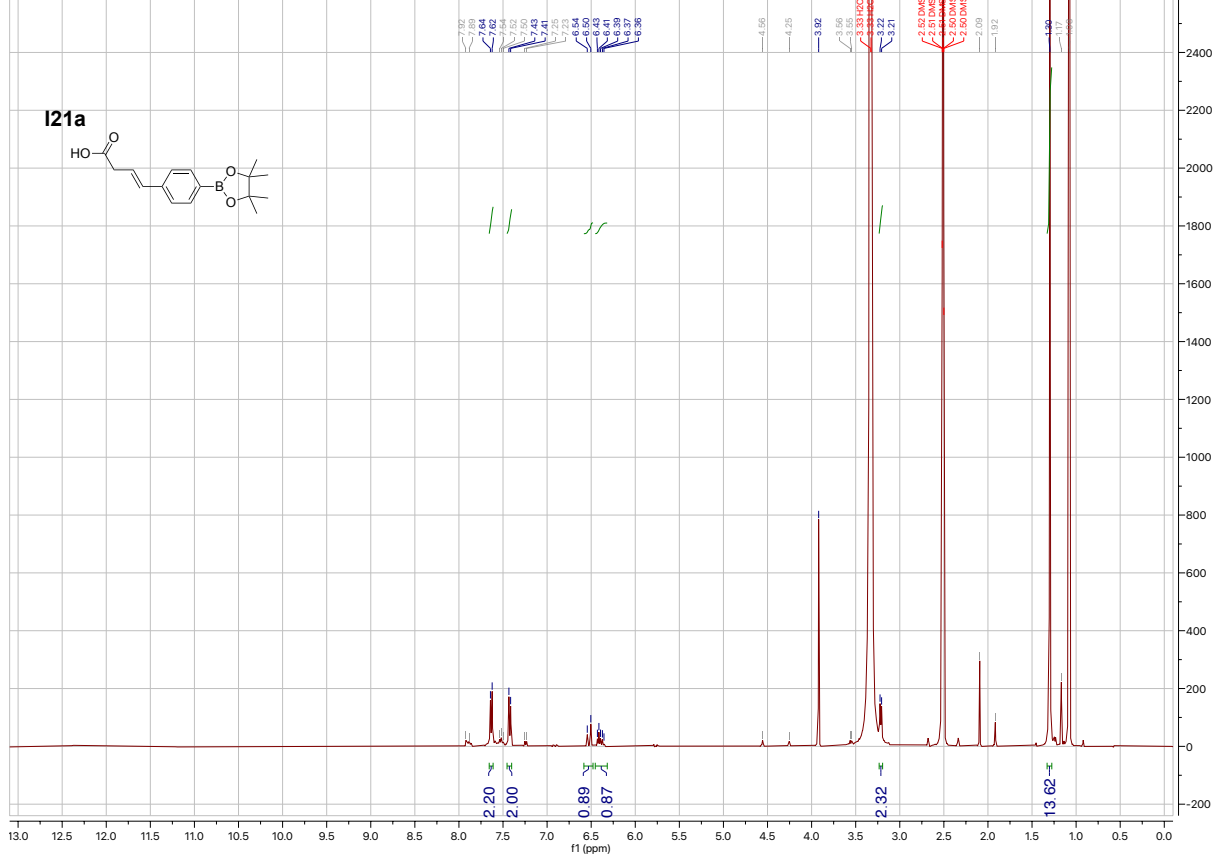
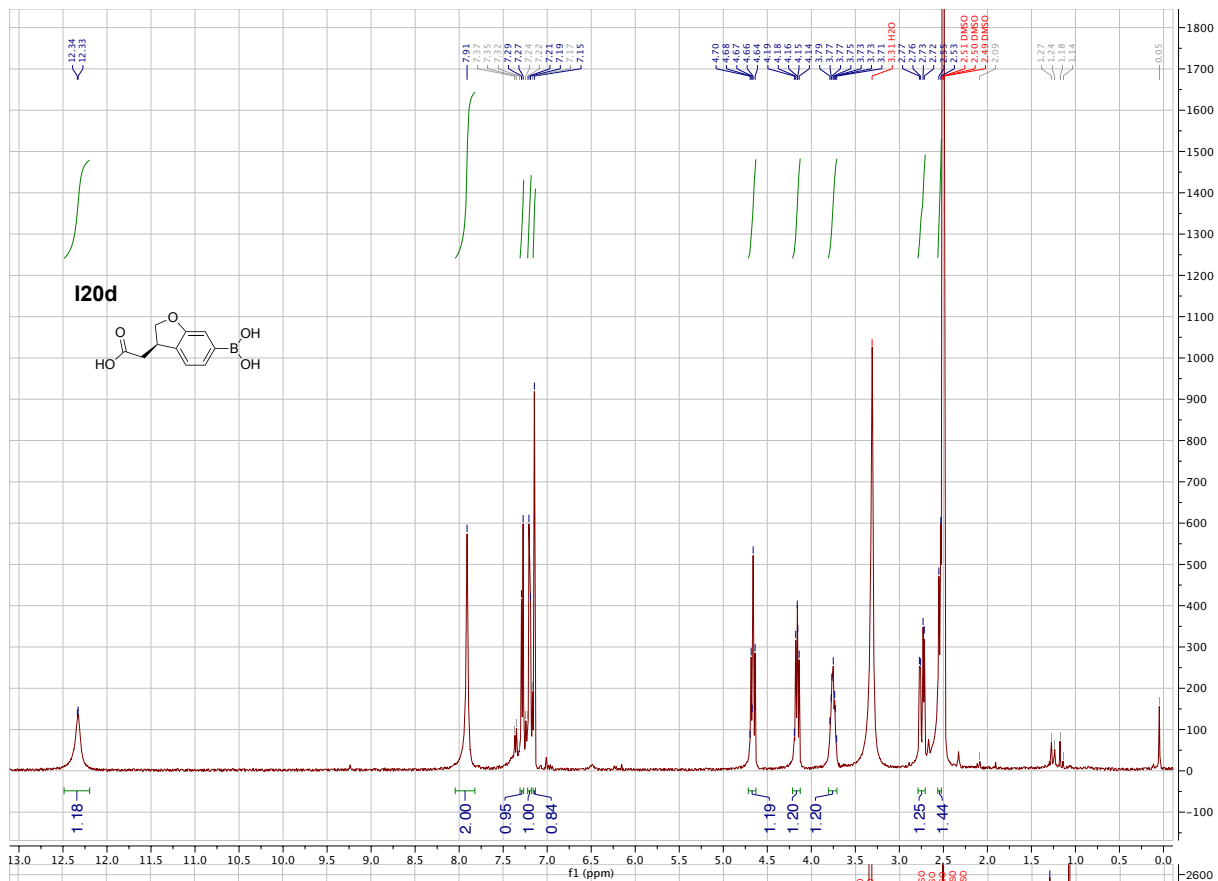


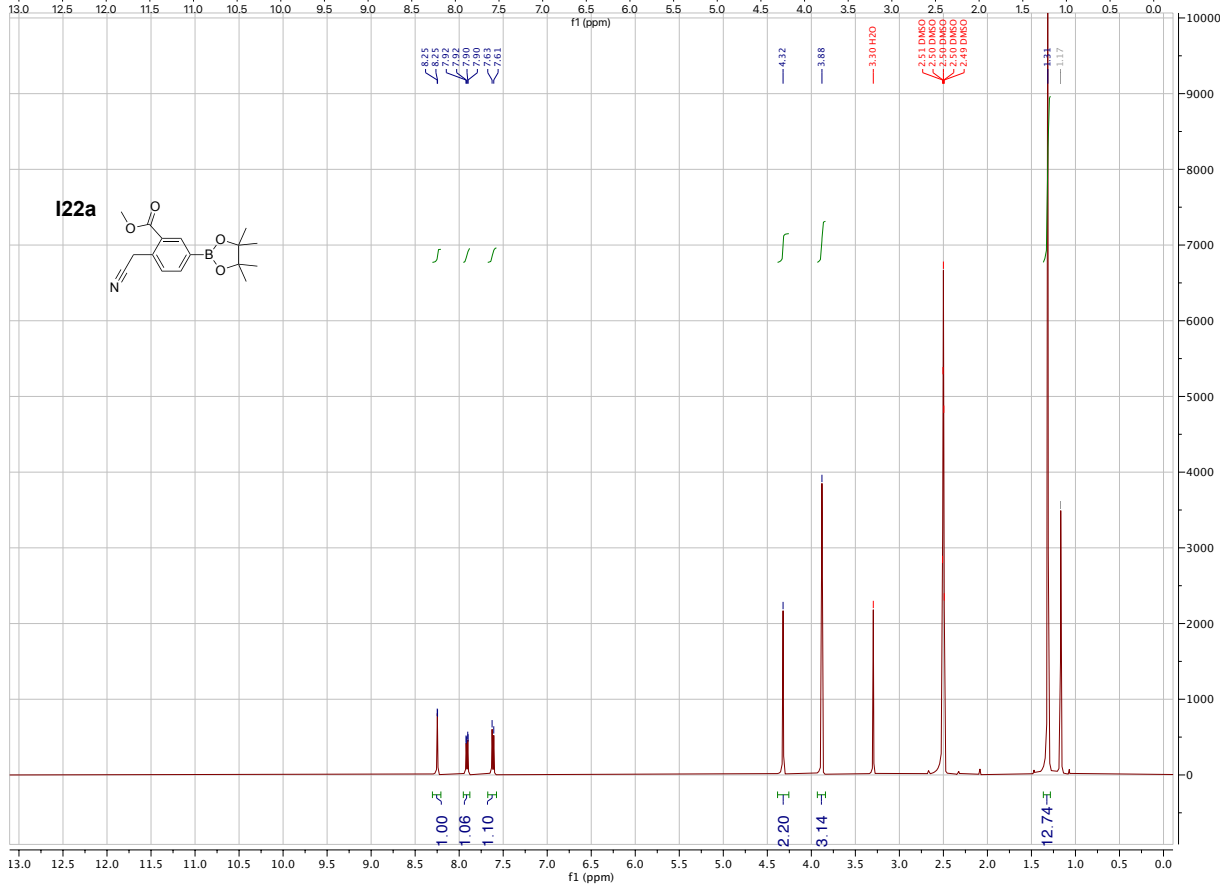
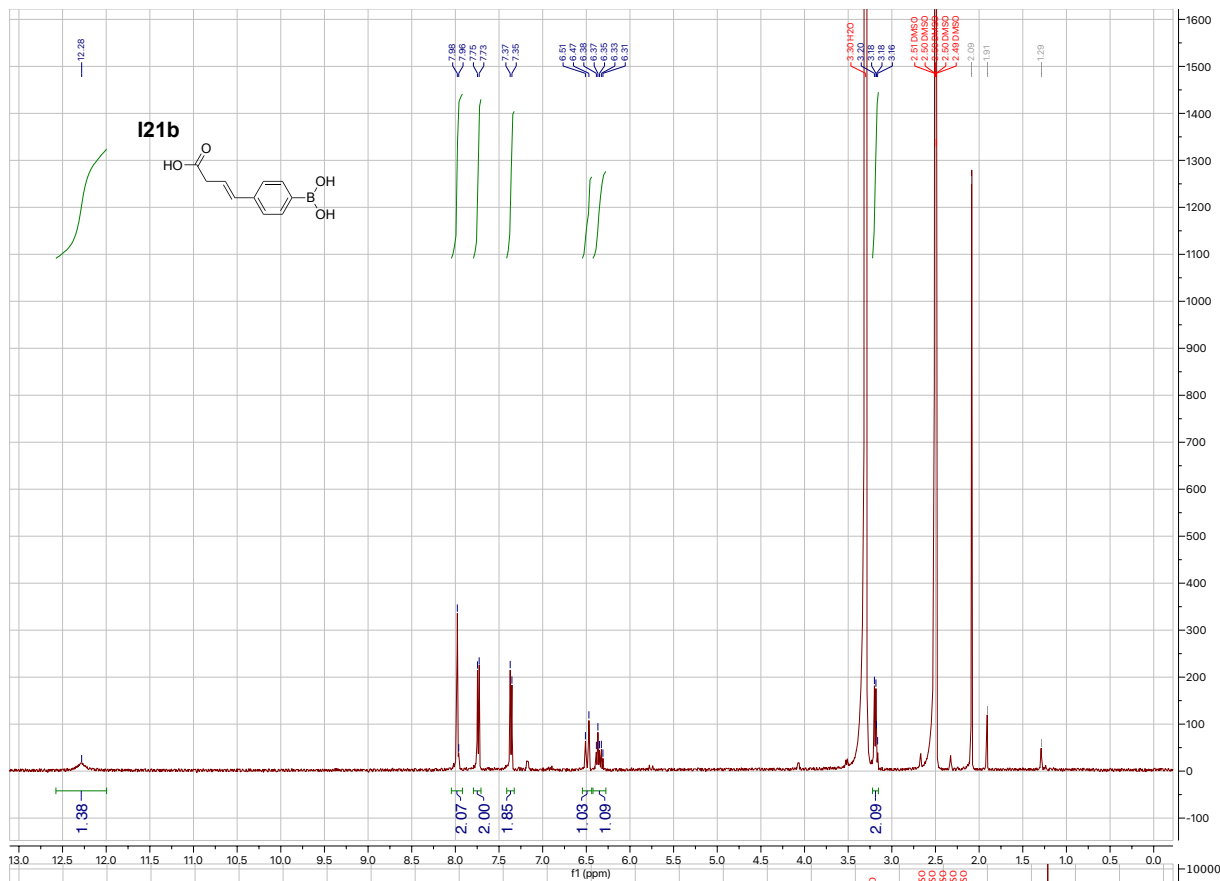


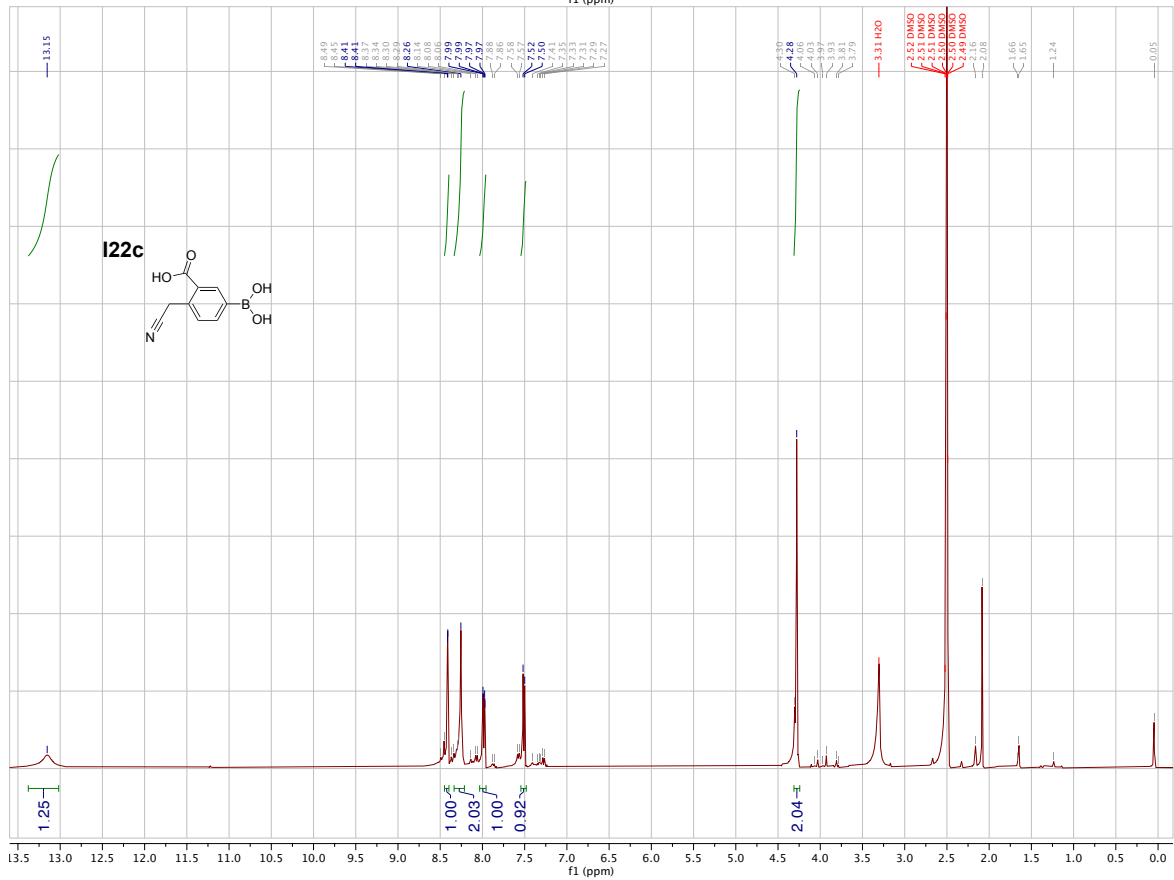
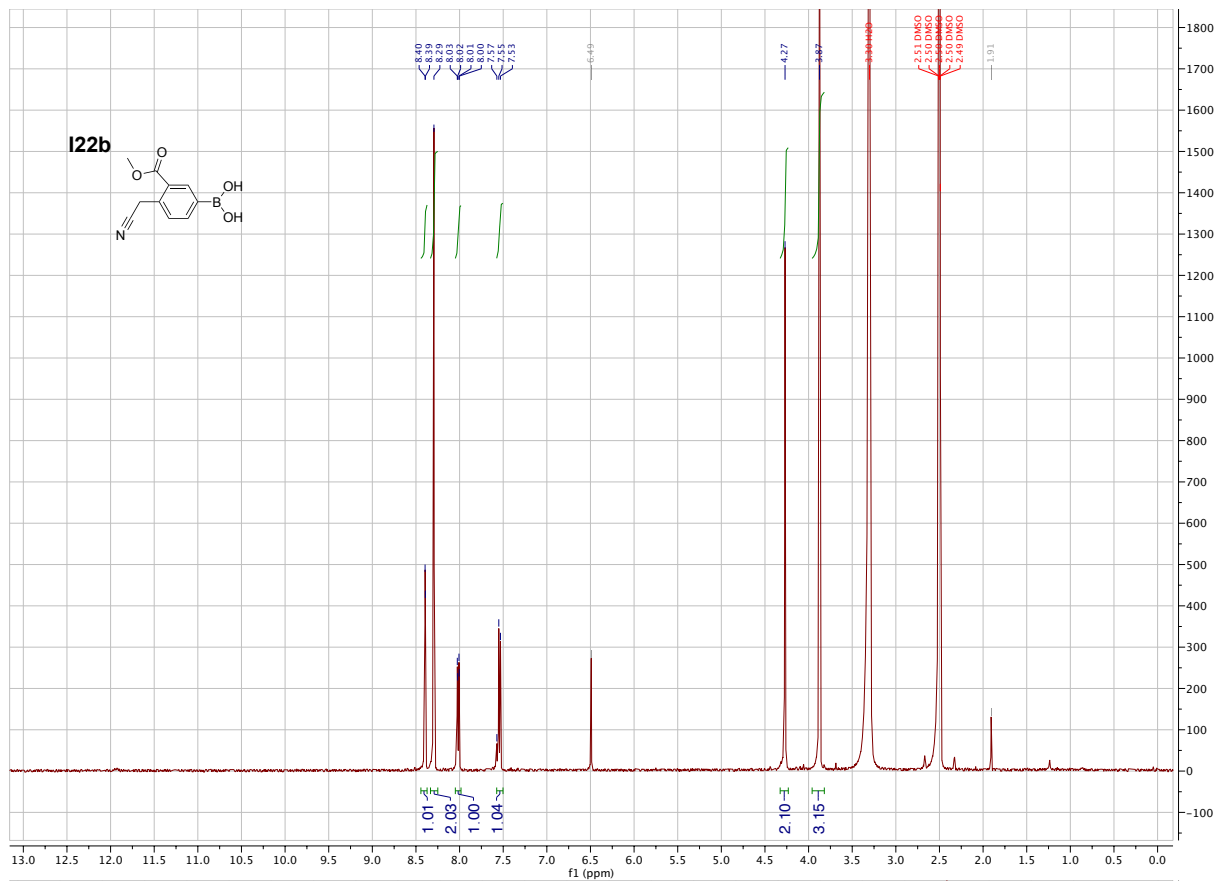


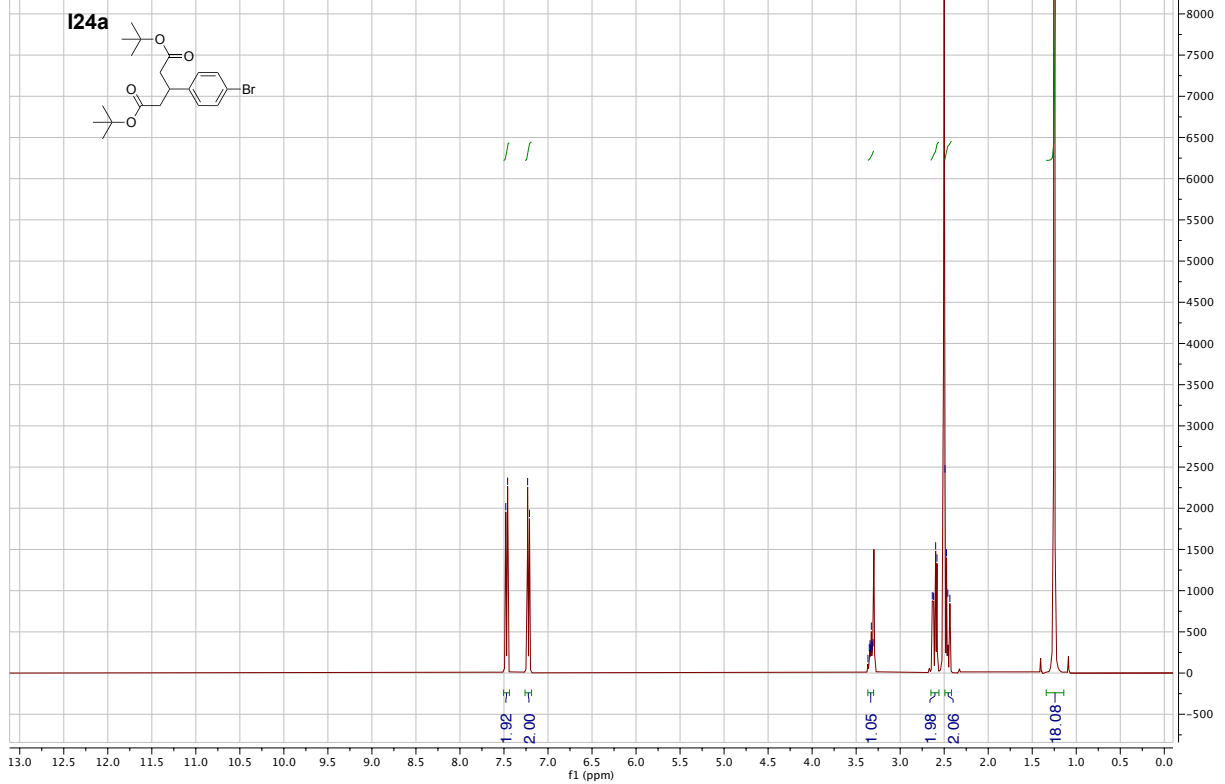
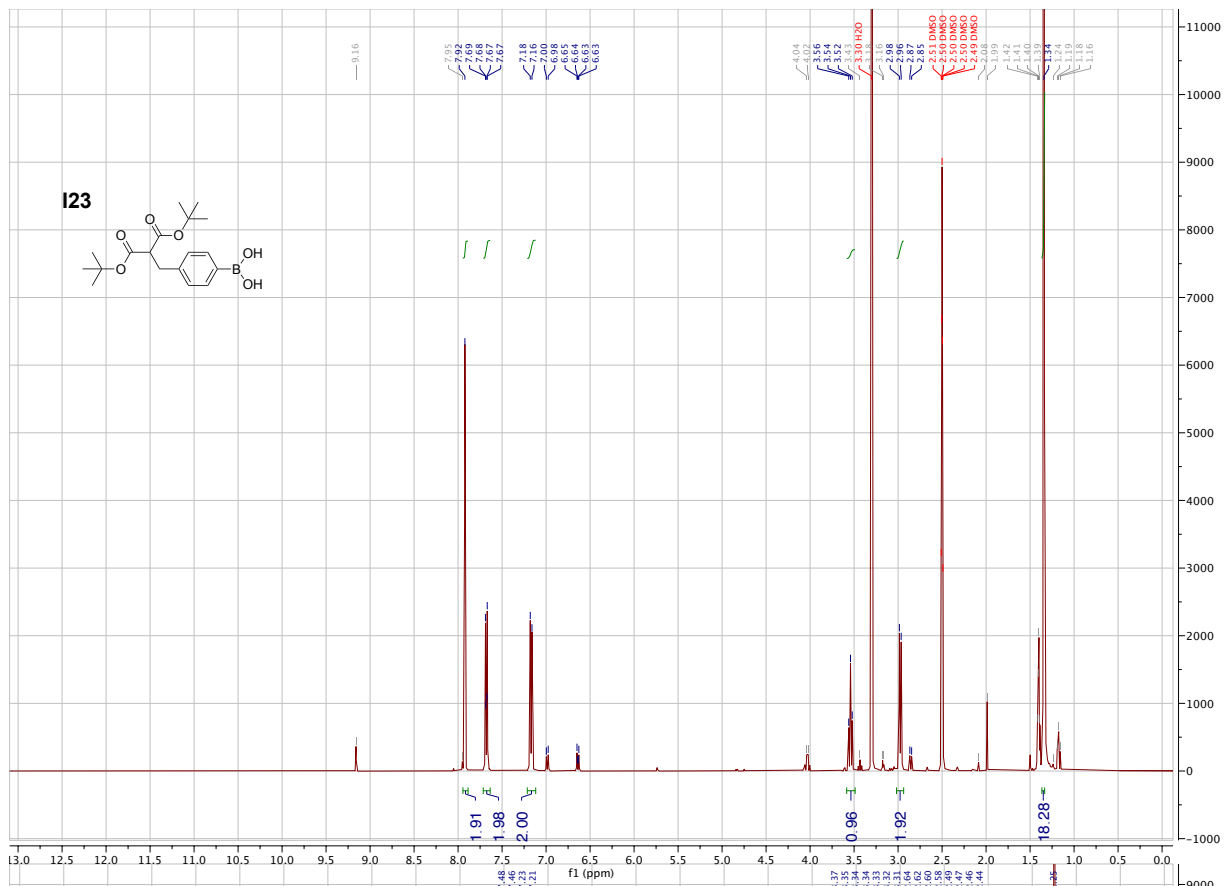


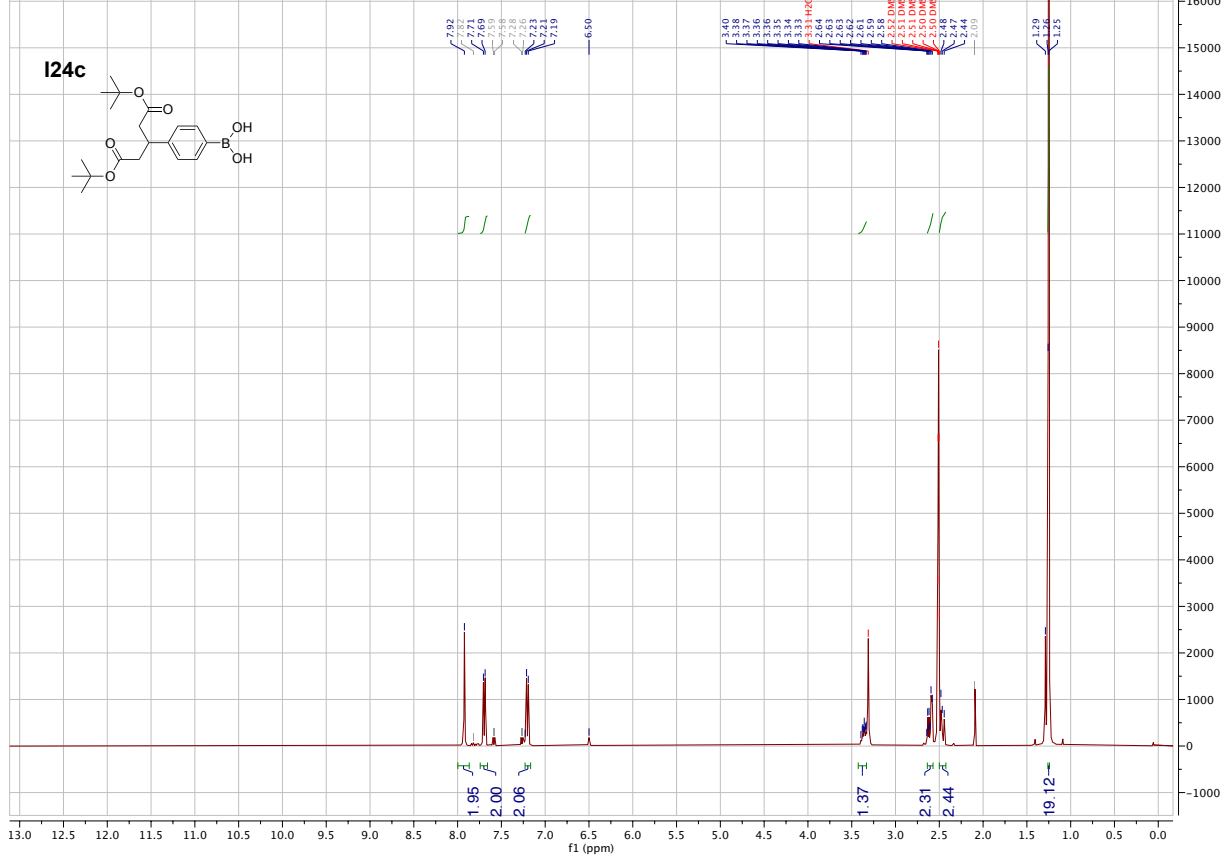
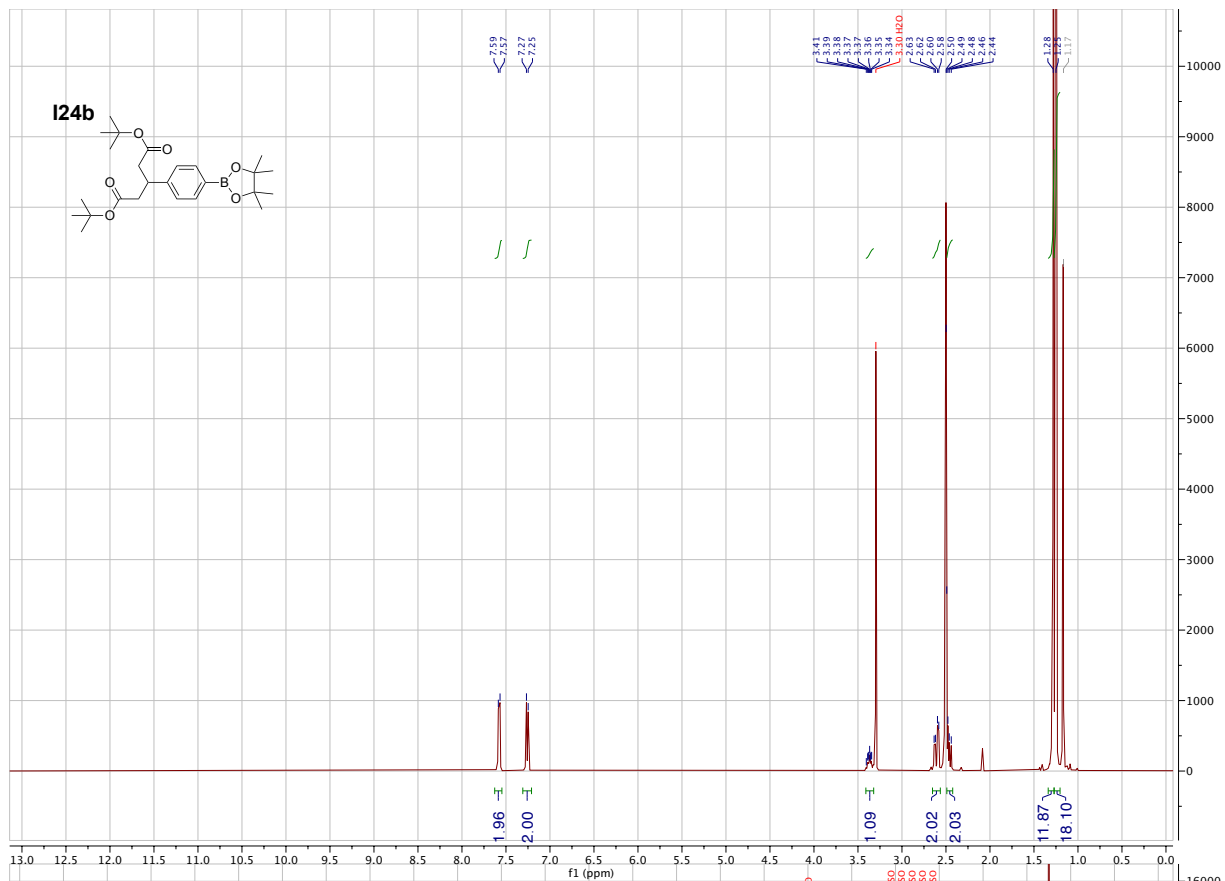


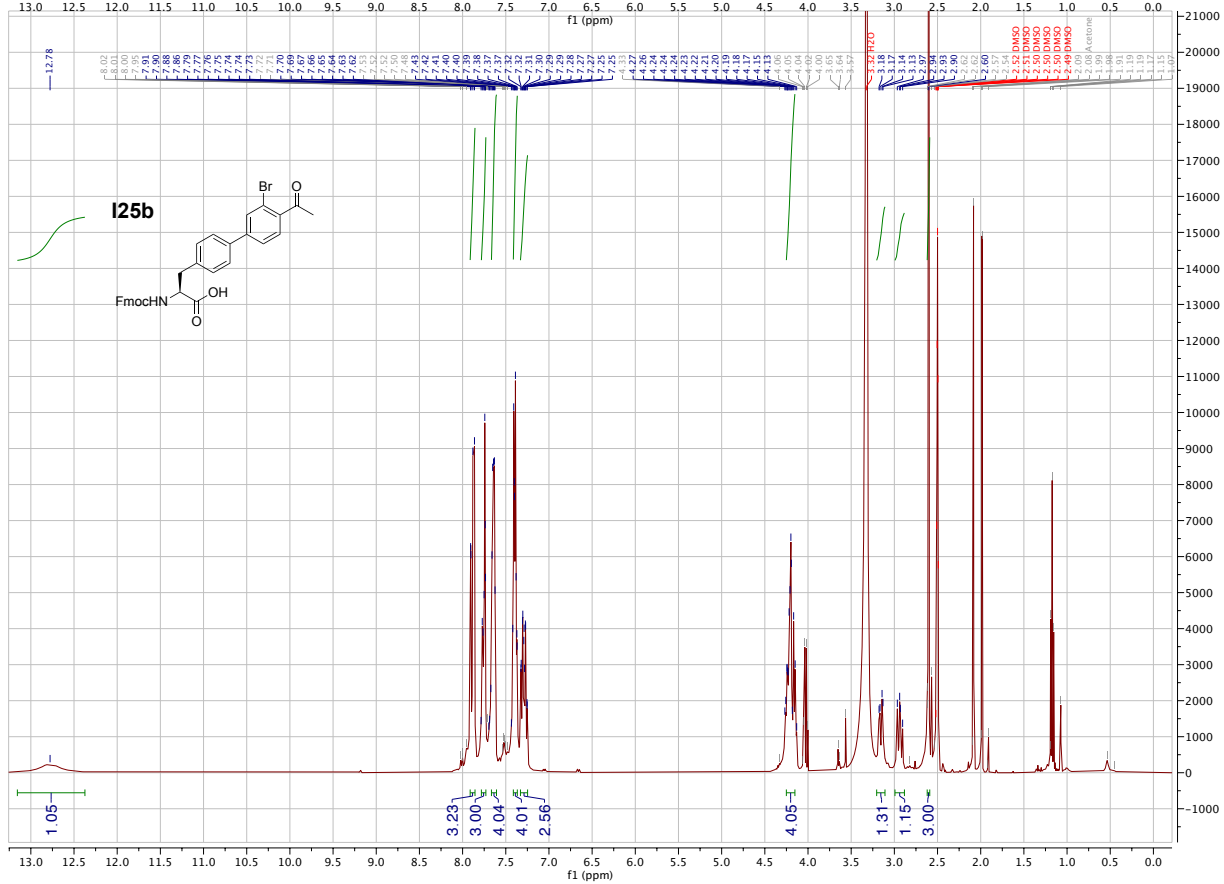
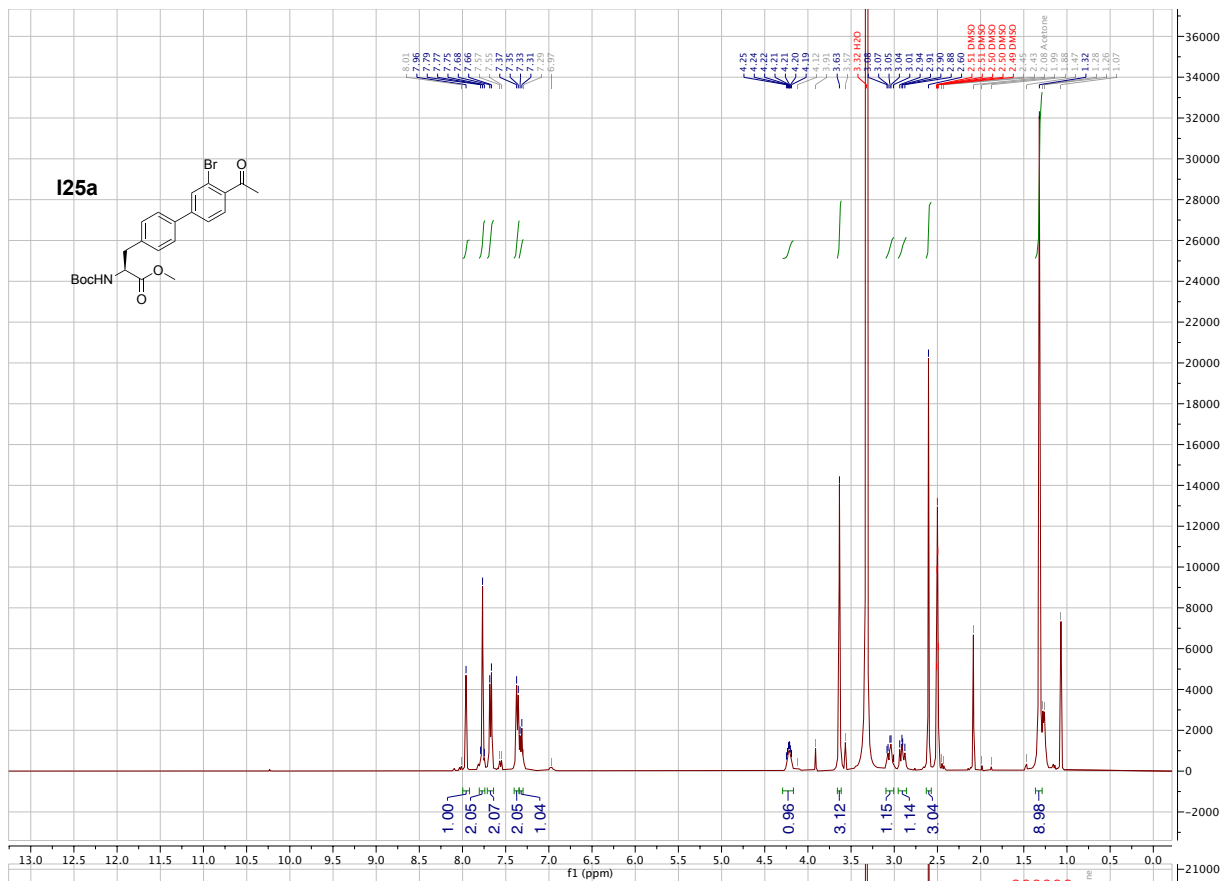


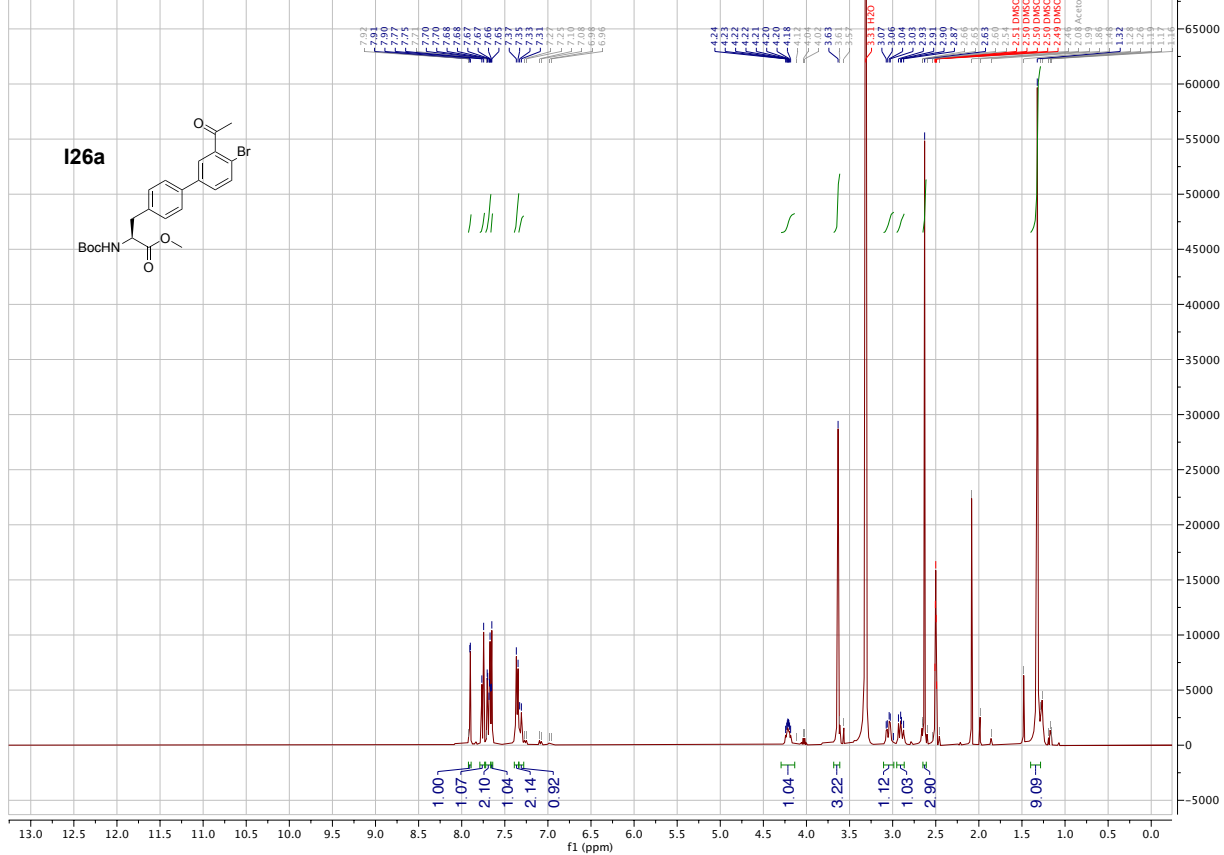
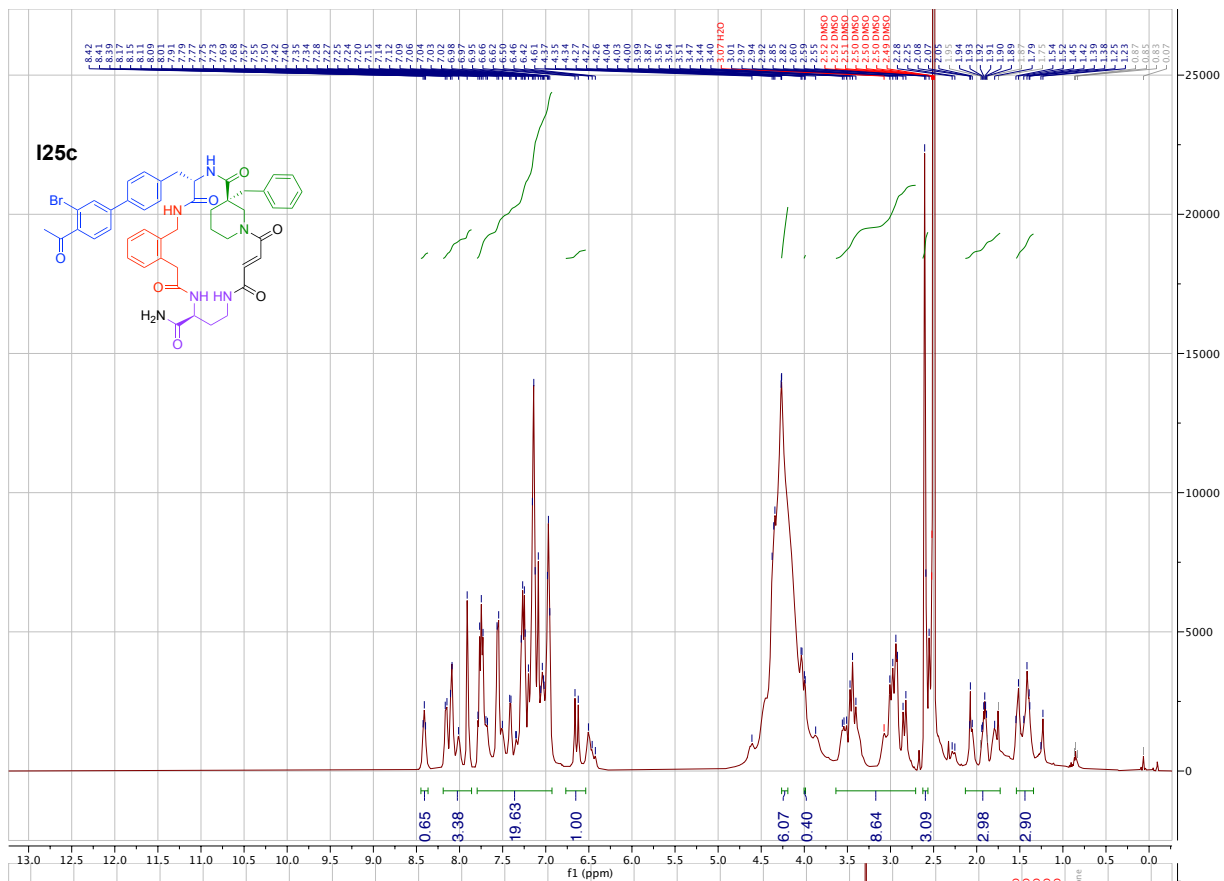


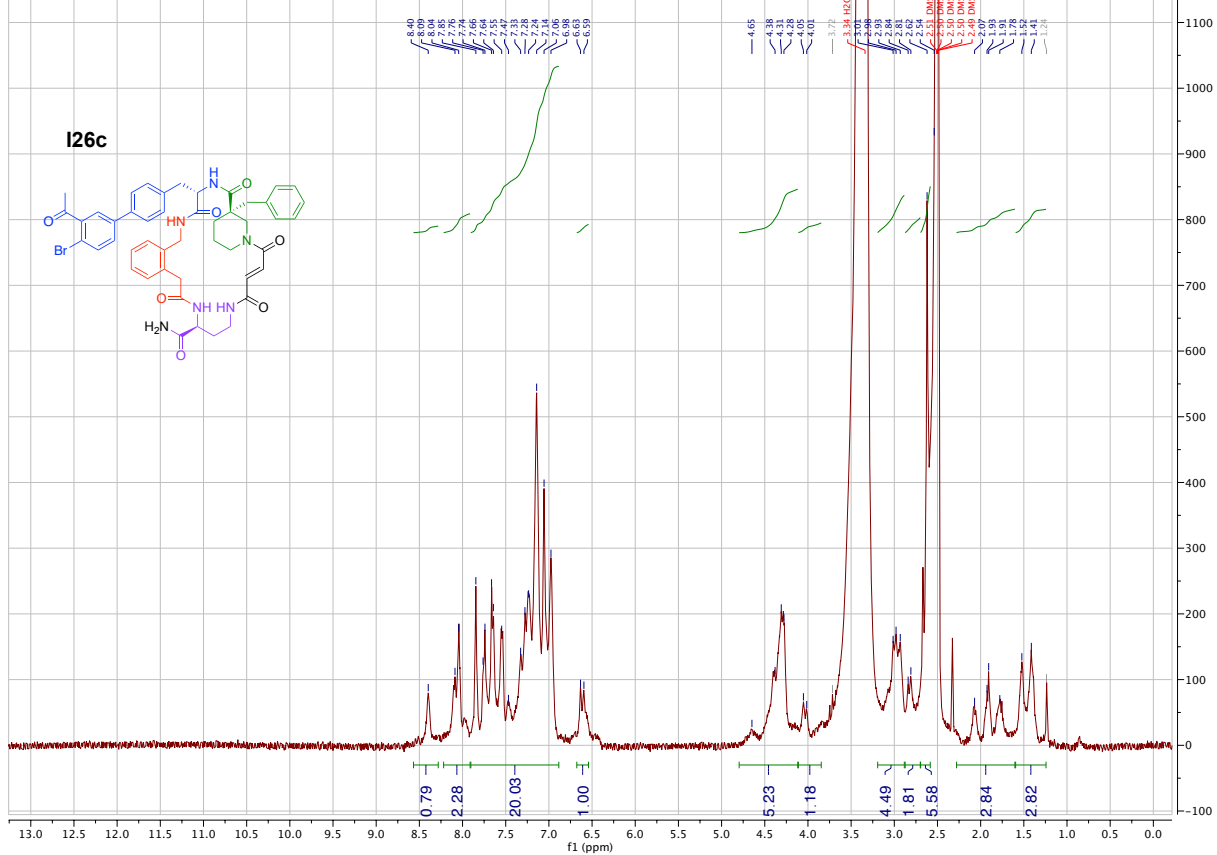
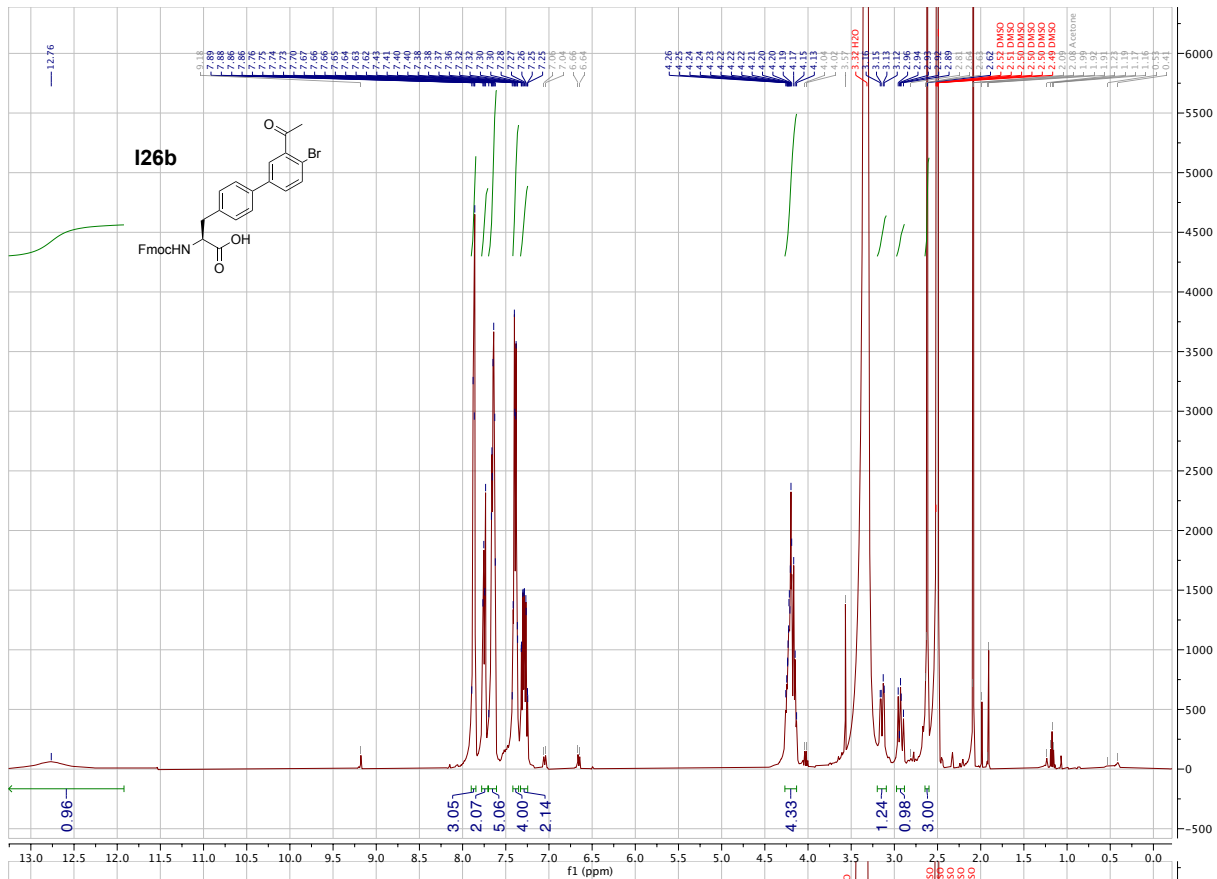


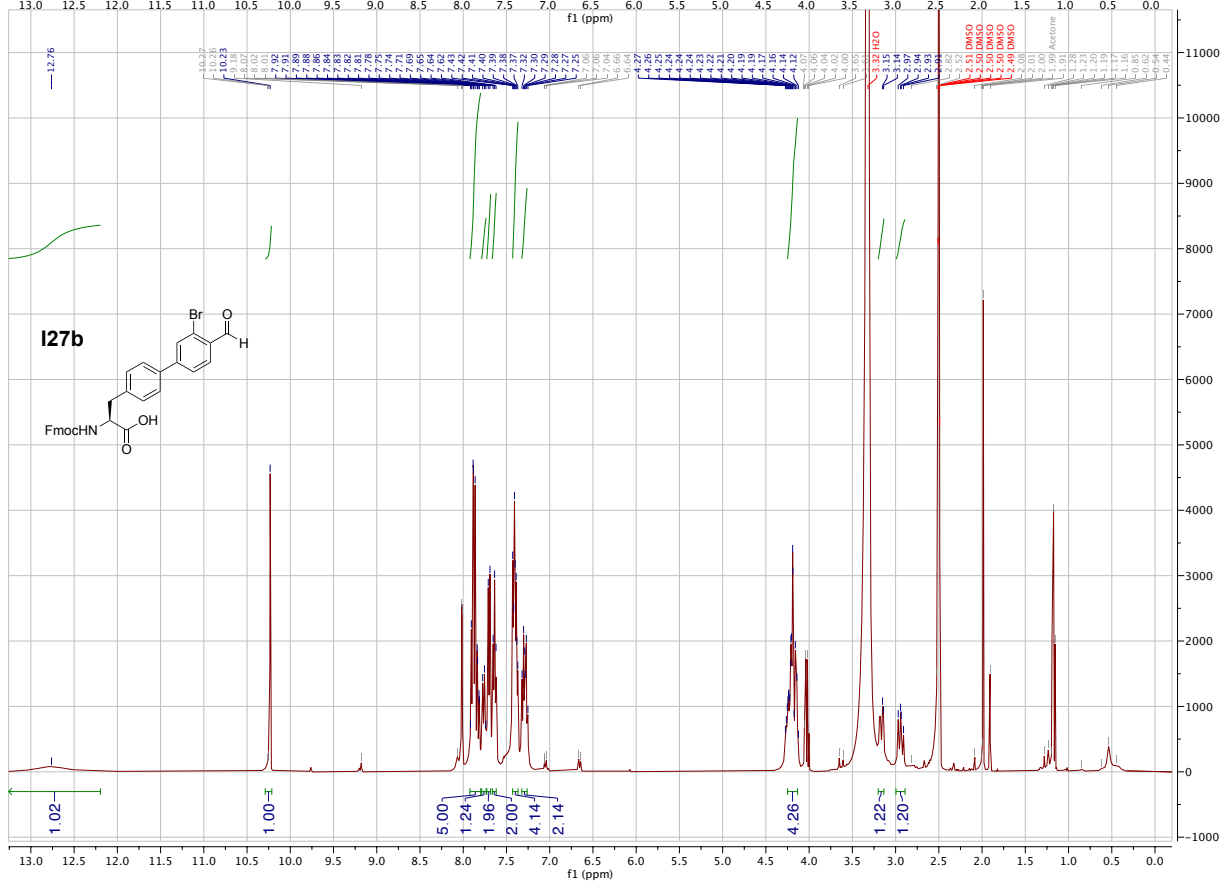
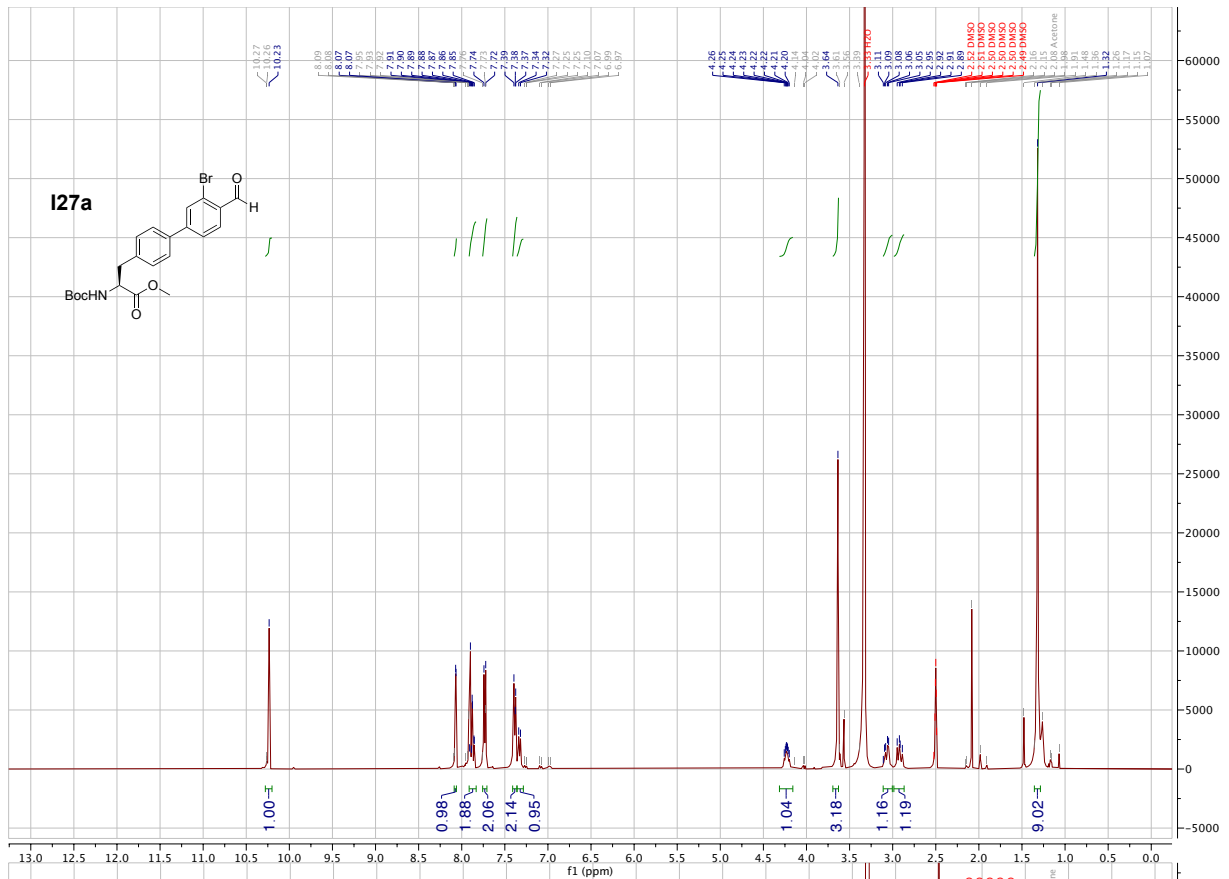




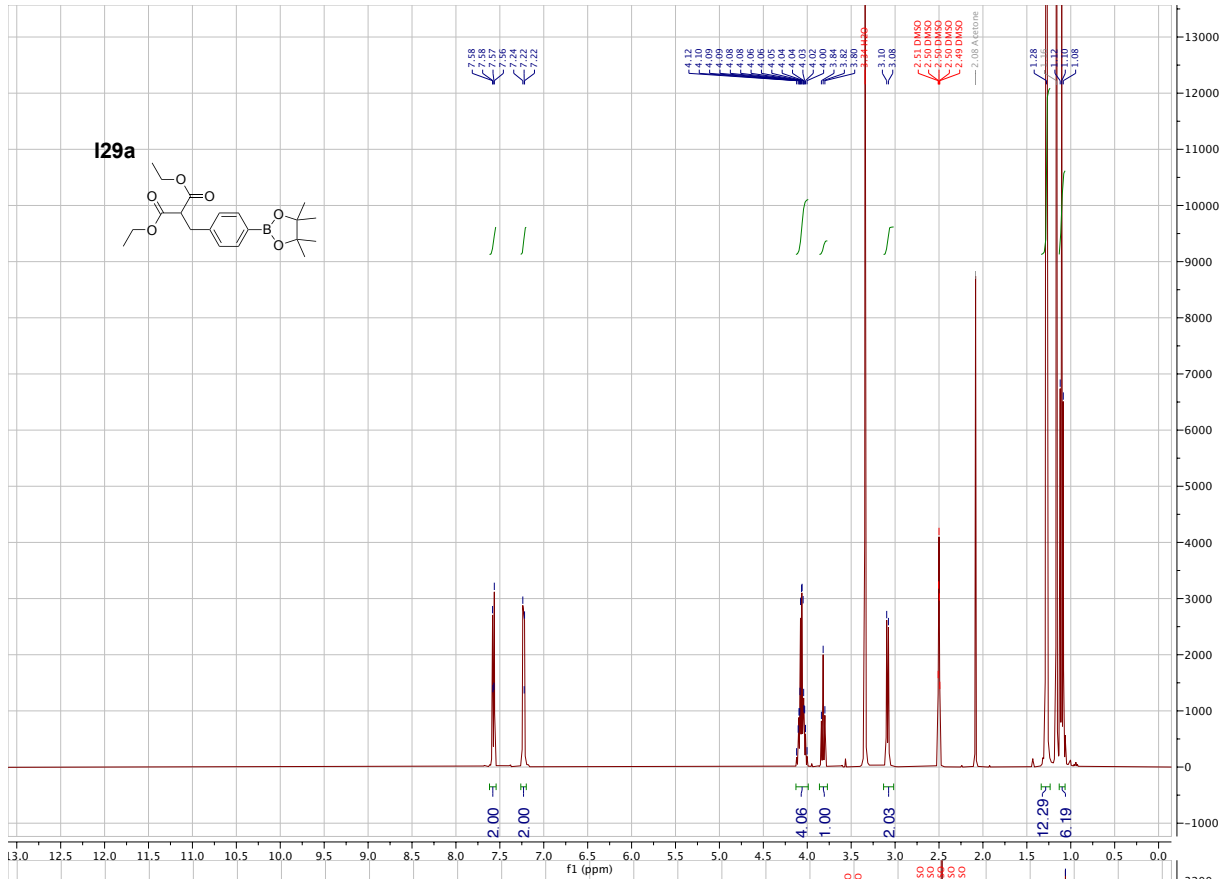
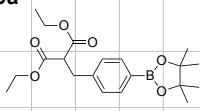




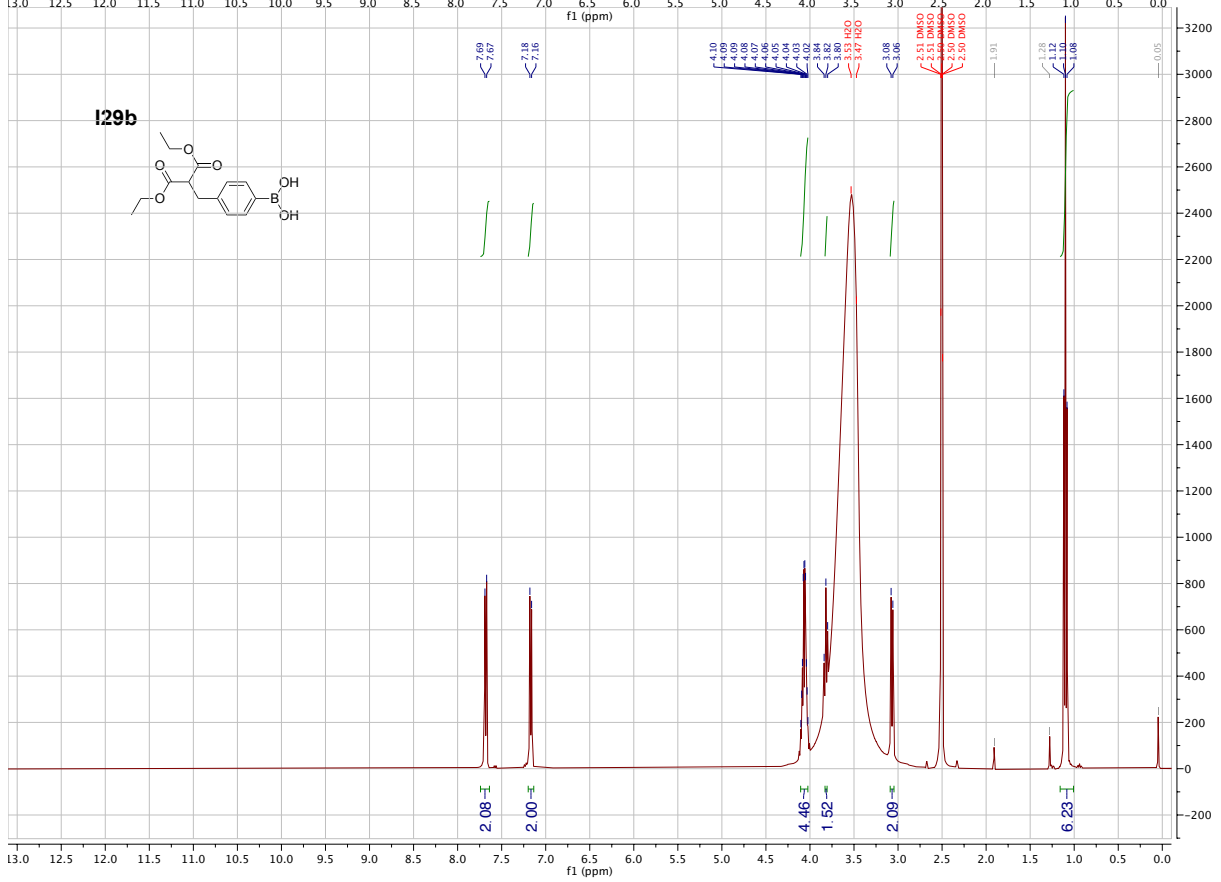
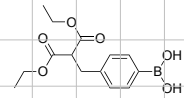


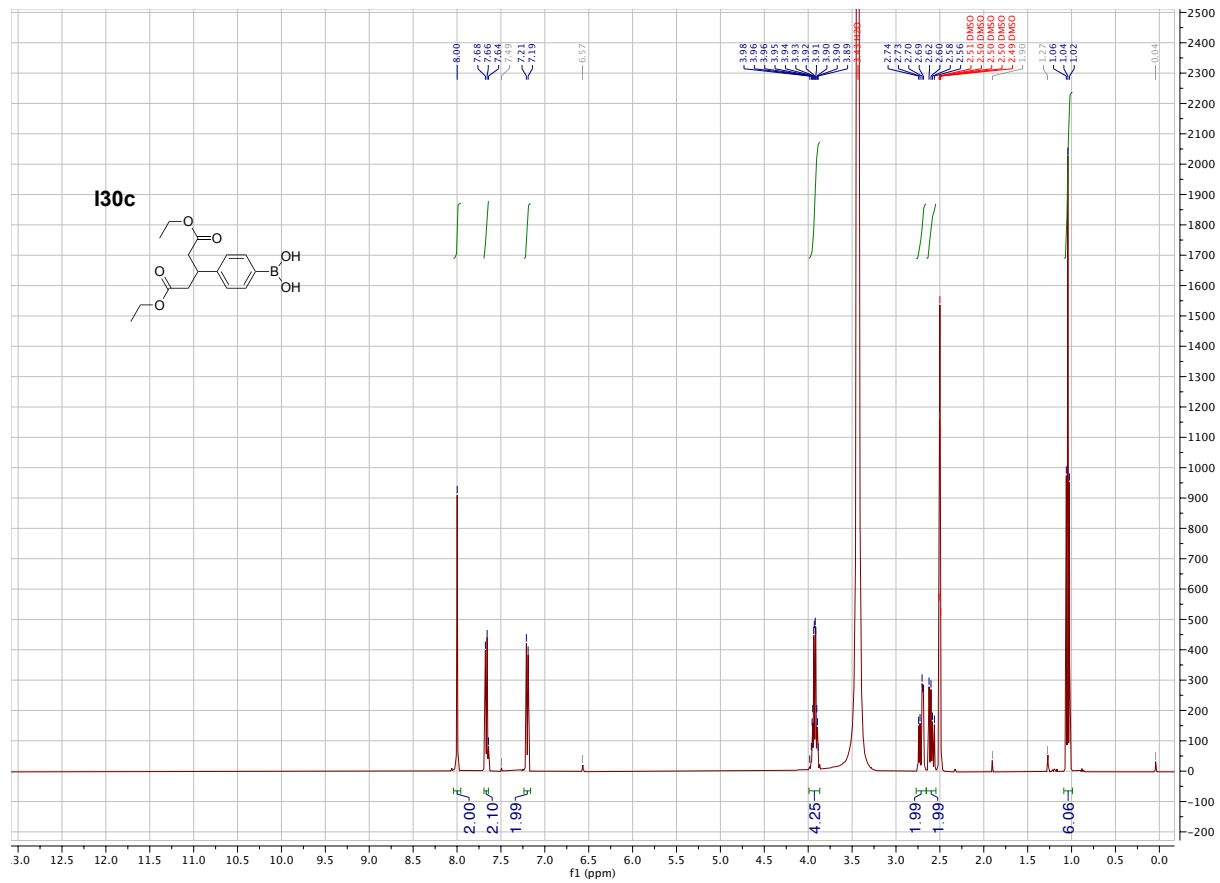


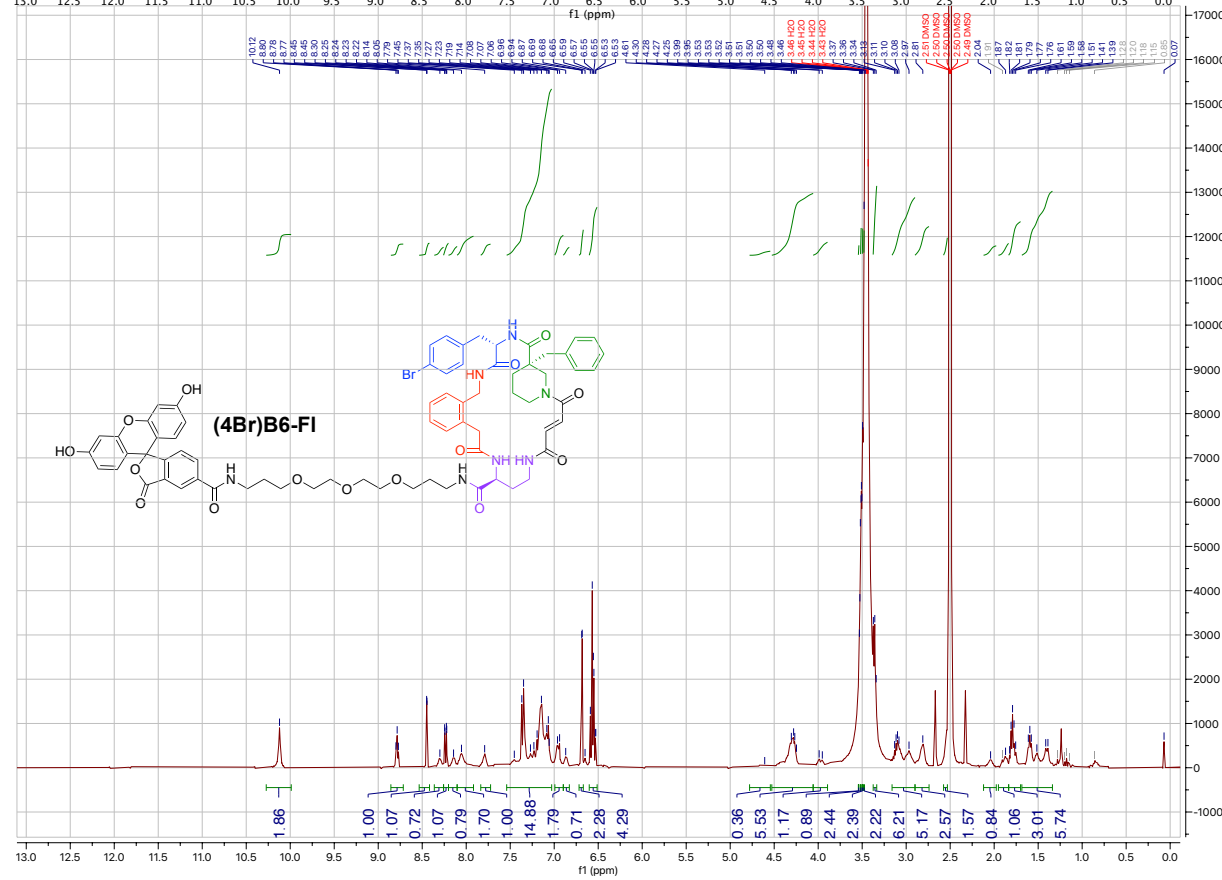
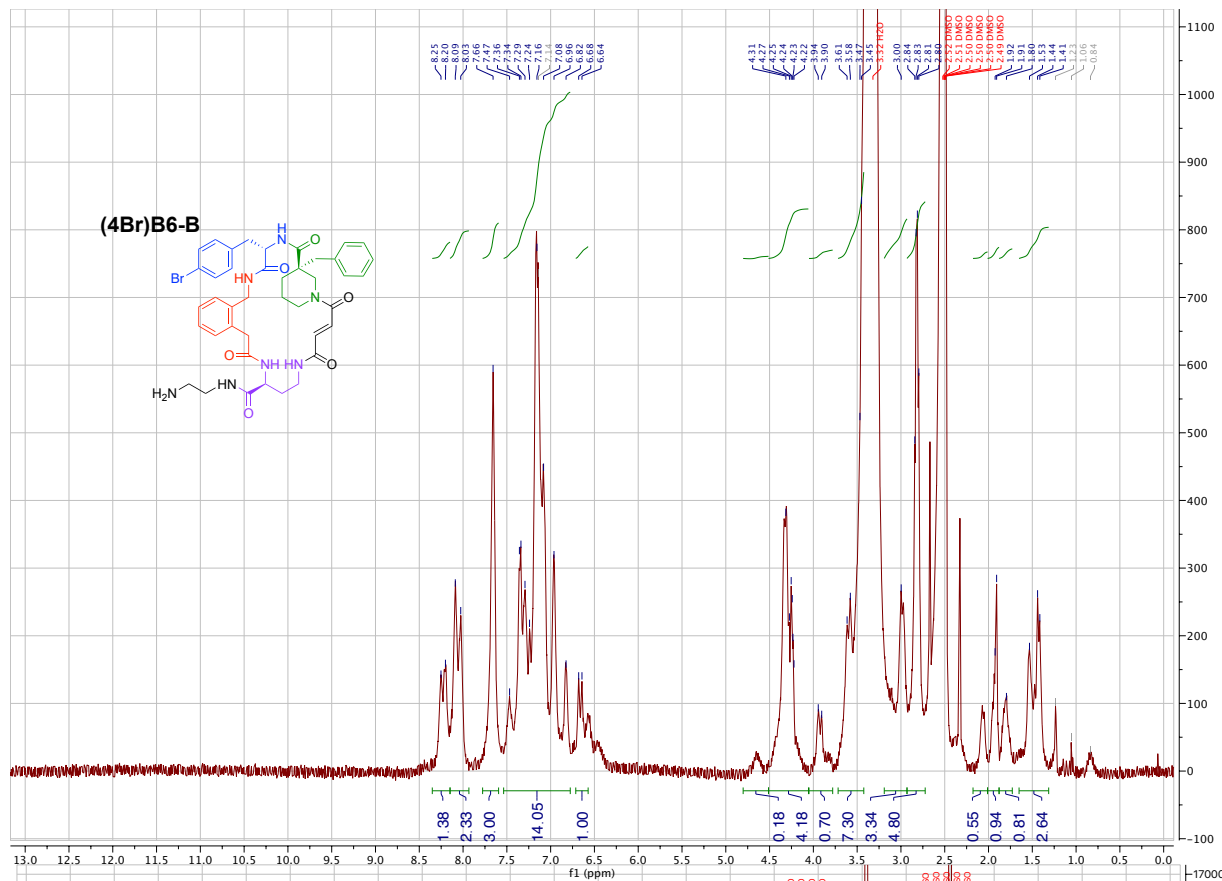
129a

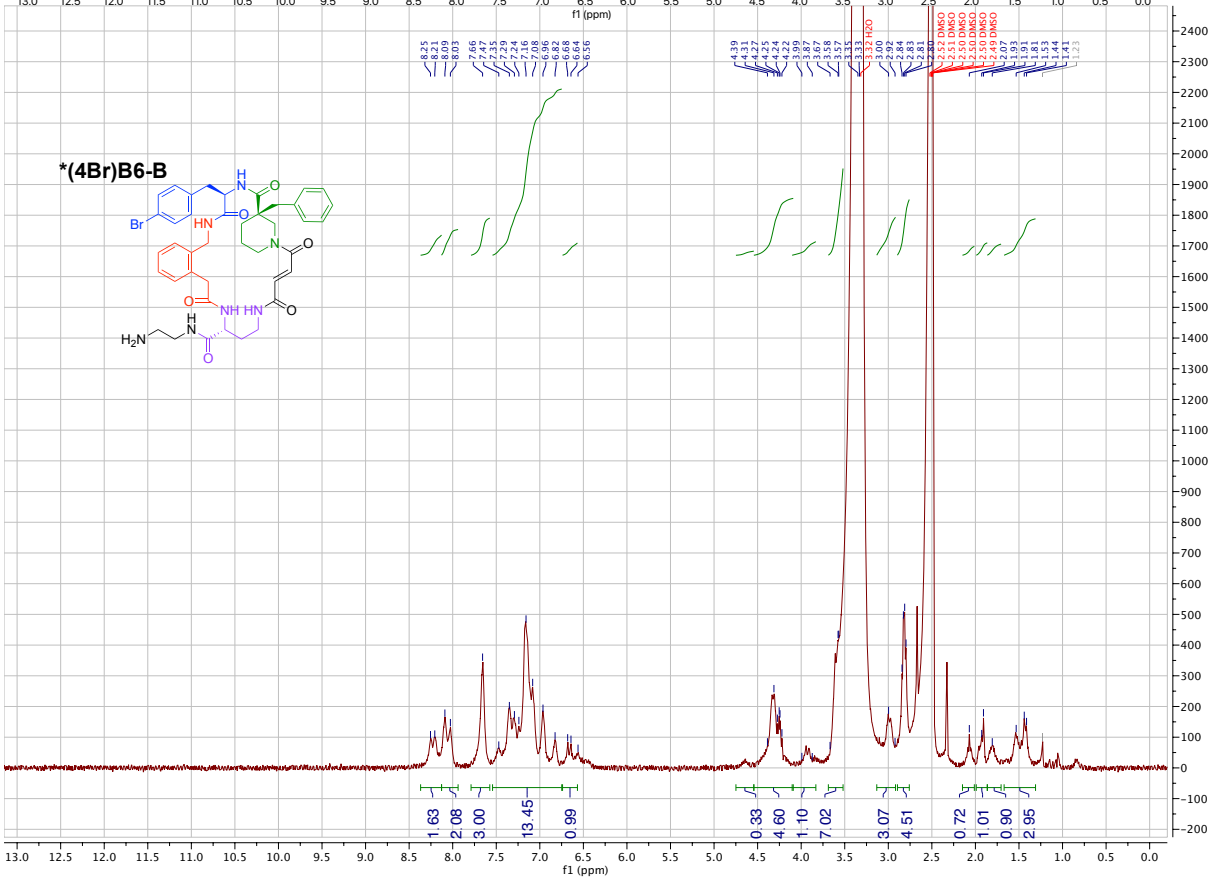
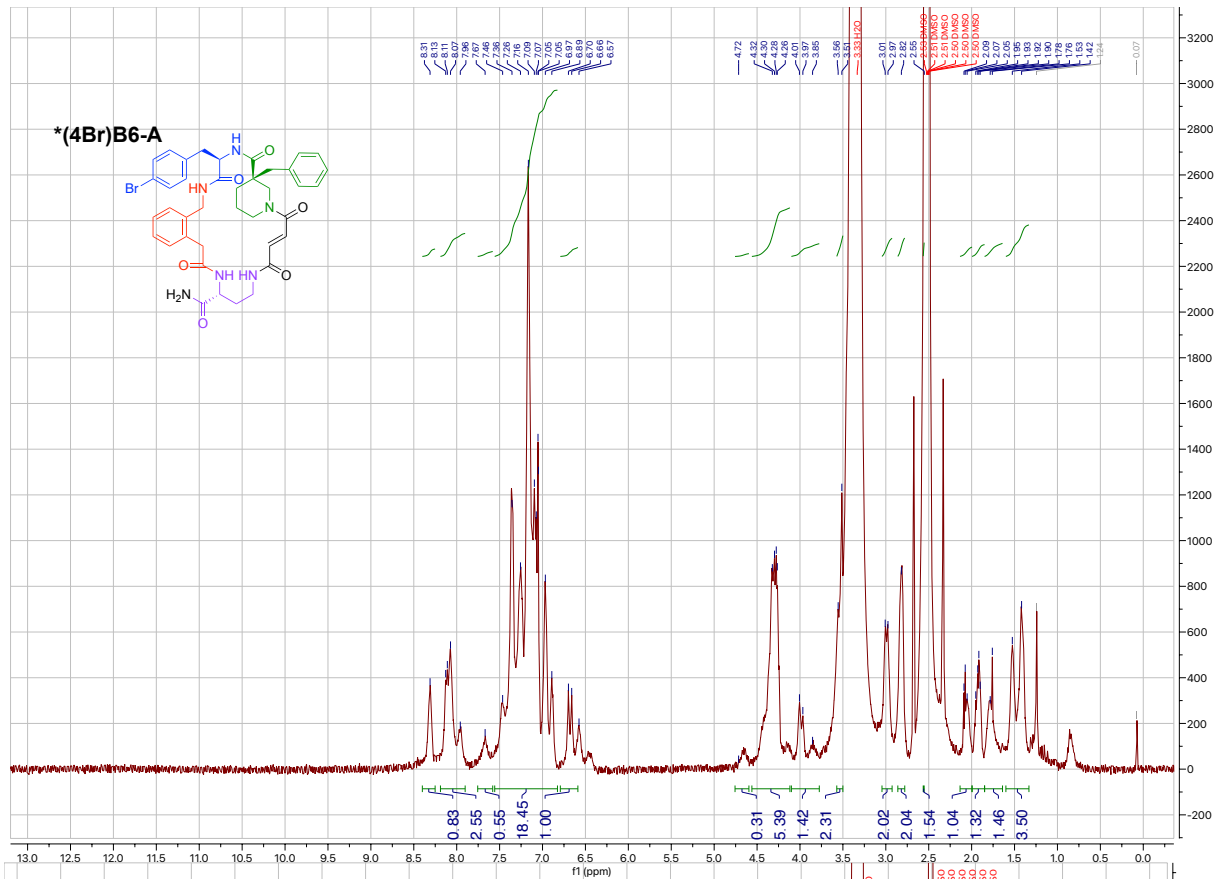


129b









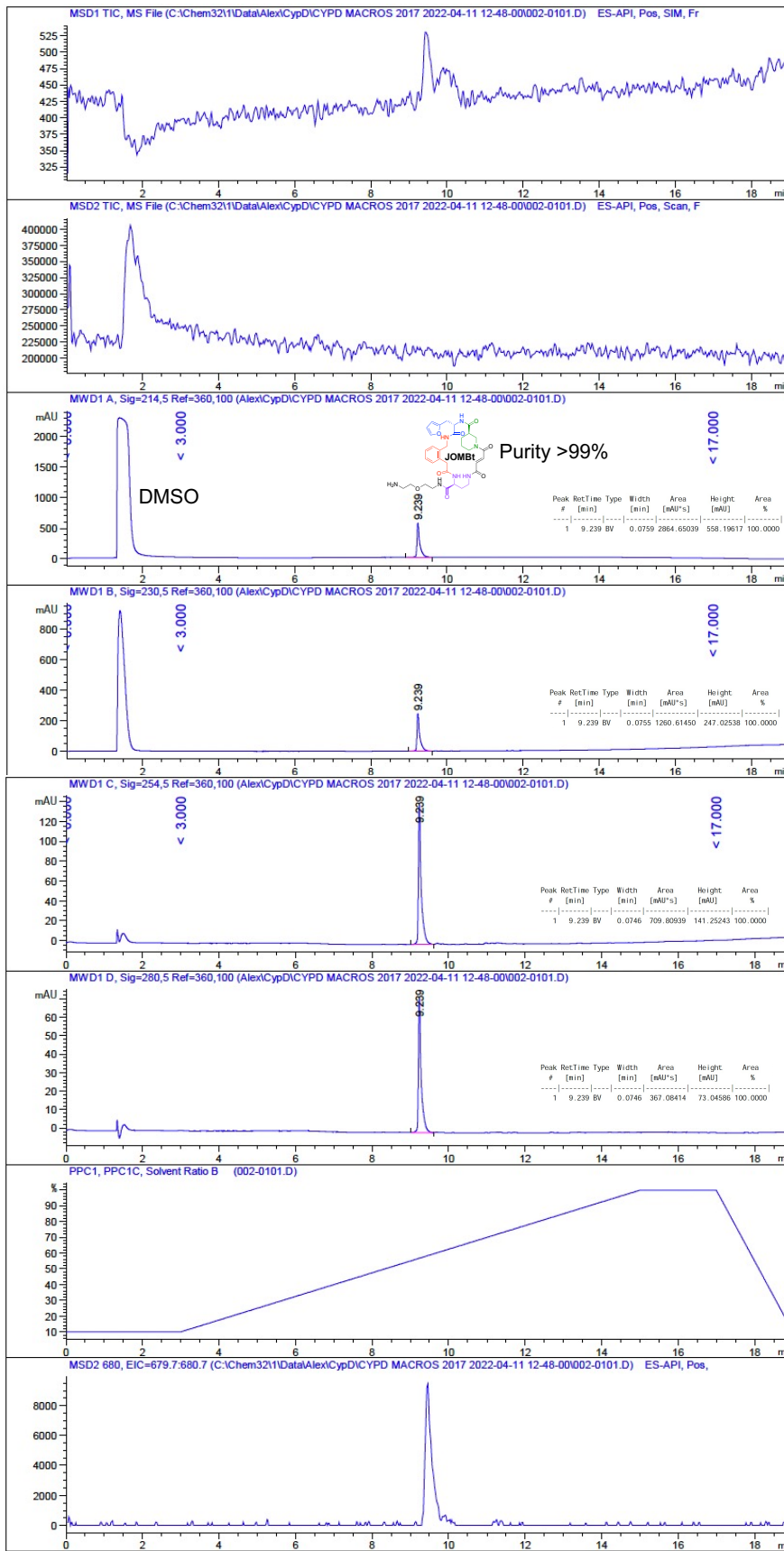
HPLC Chromatograms

Panels from top→bottom:

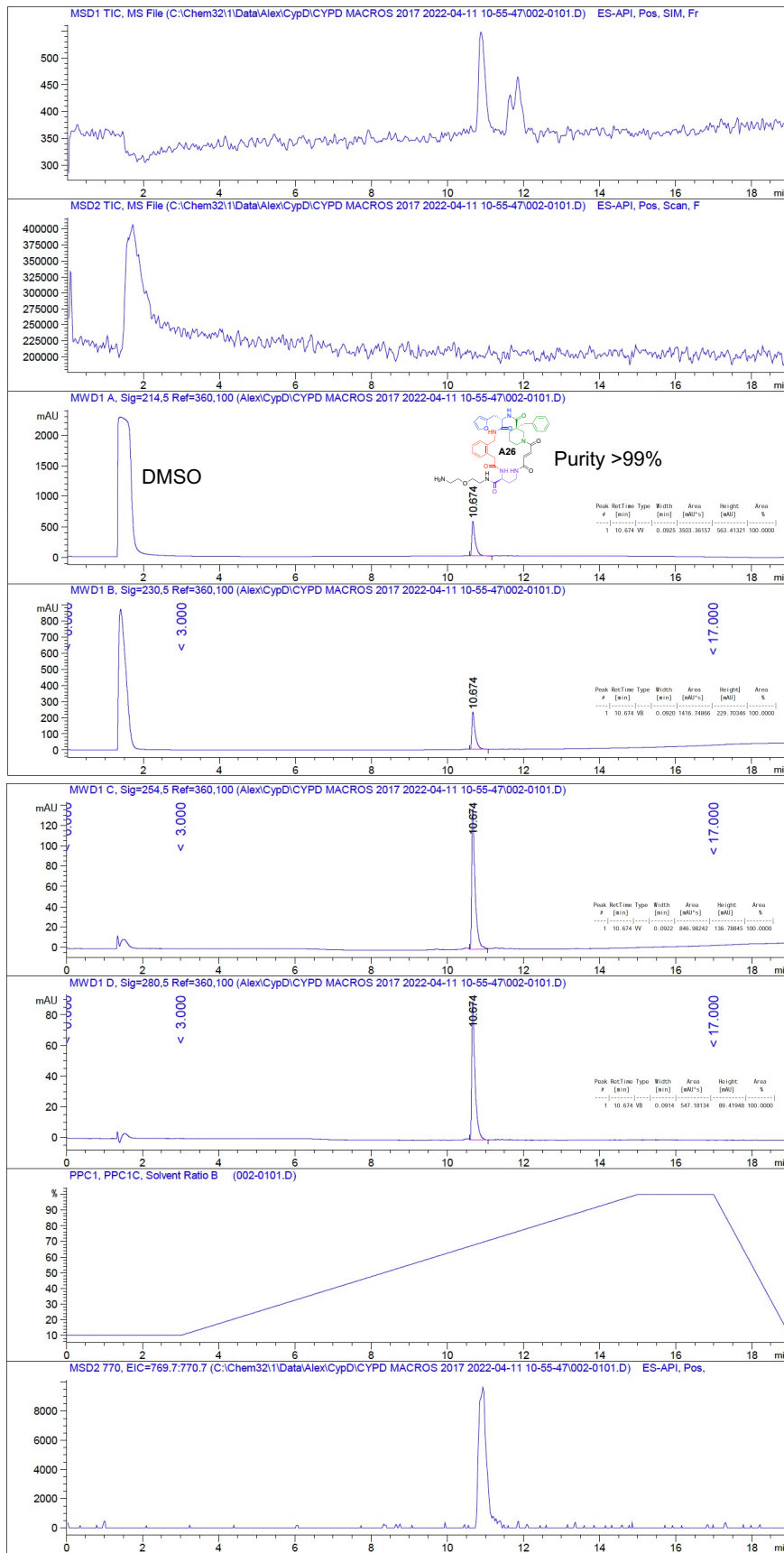
1. MS trace for compound ions (M, M+H⁺, M+Na⁺)
2. MS scan trace for all ions
3. Absorbance at 214 nM
4. Absorbance at 230 nM
5. Absorbance at 254 nM
6. Absorbance at 280 nM
7. Solvent gradient, with % acetonitrile shown on y-axis
8. Extracted ion chromatogram for M+H⁺ ion

Purity of compound was determined by % area of the indicated compound peak at 214 nM relative to all identified peaks between 3 and 17 minutes. DMSO peak occurs at 1.5 minutes.

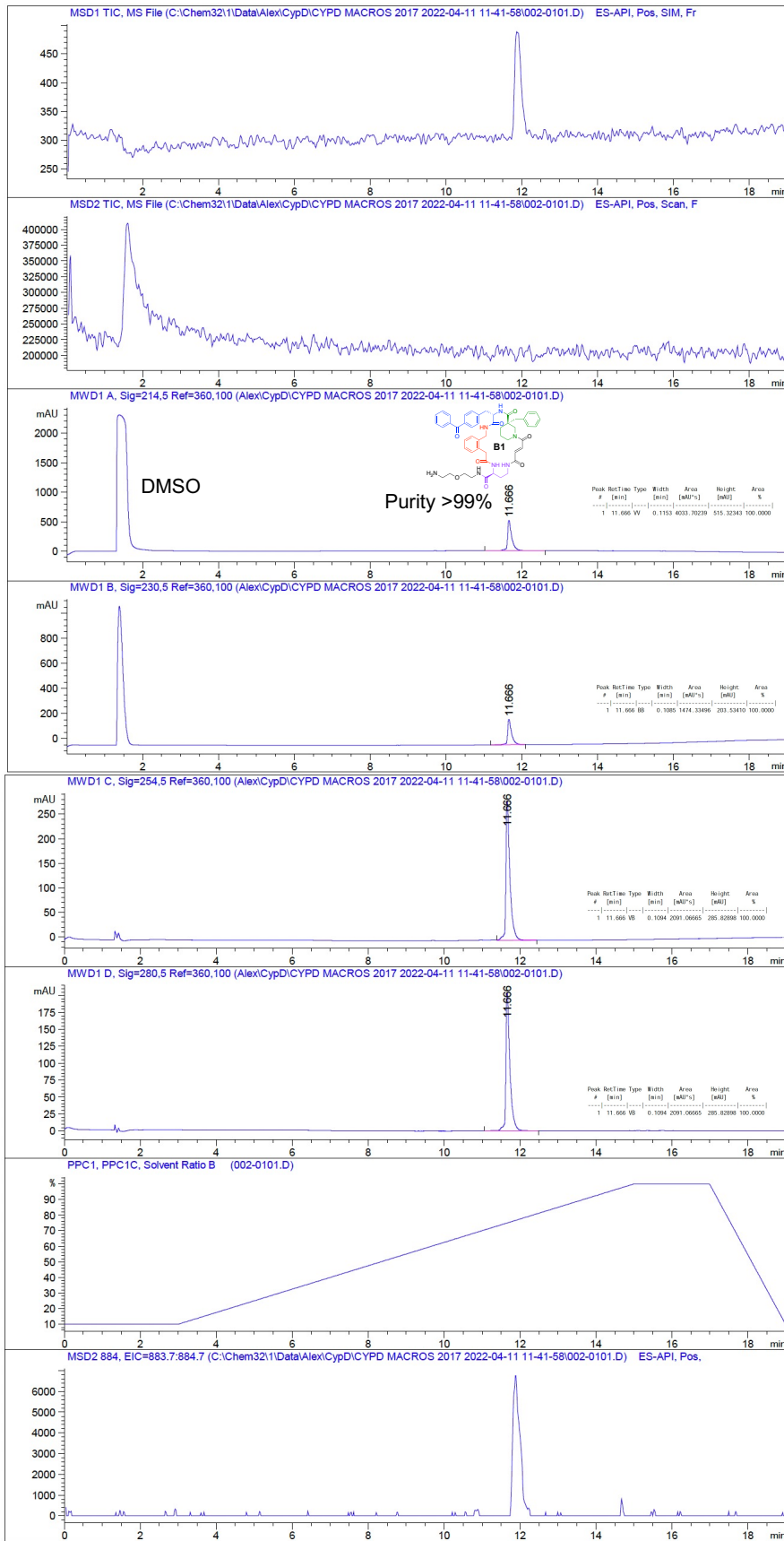
JOMBt



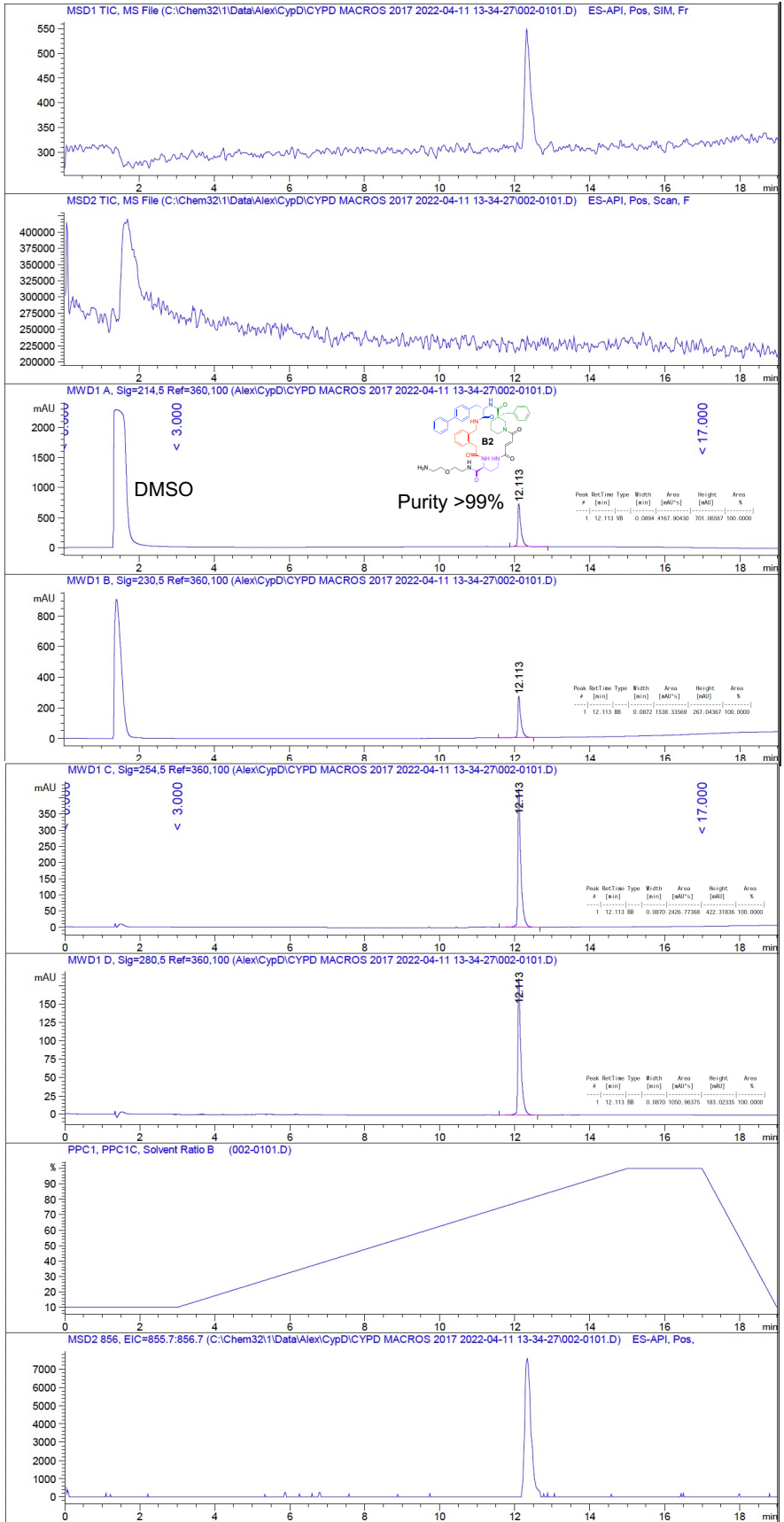
A26



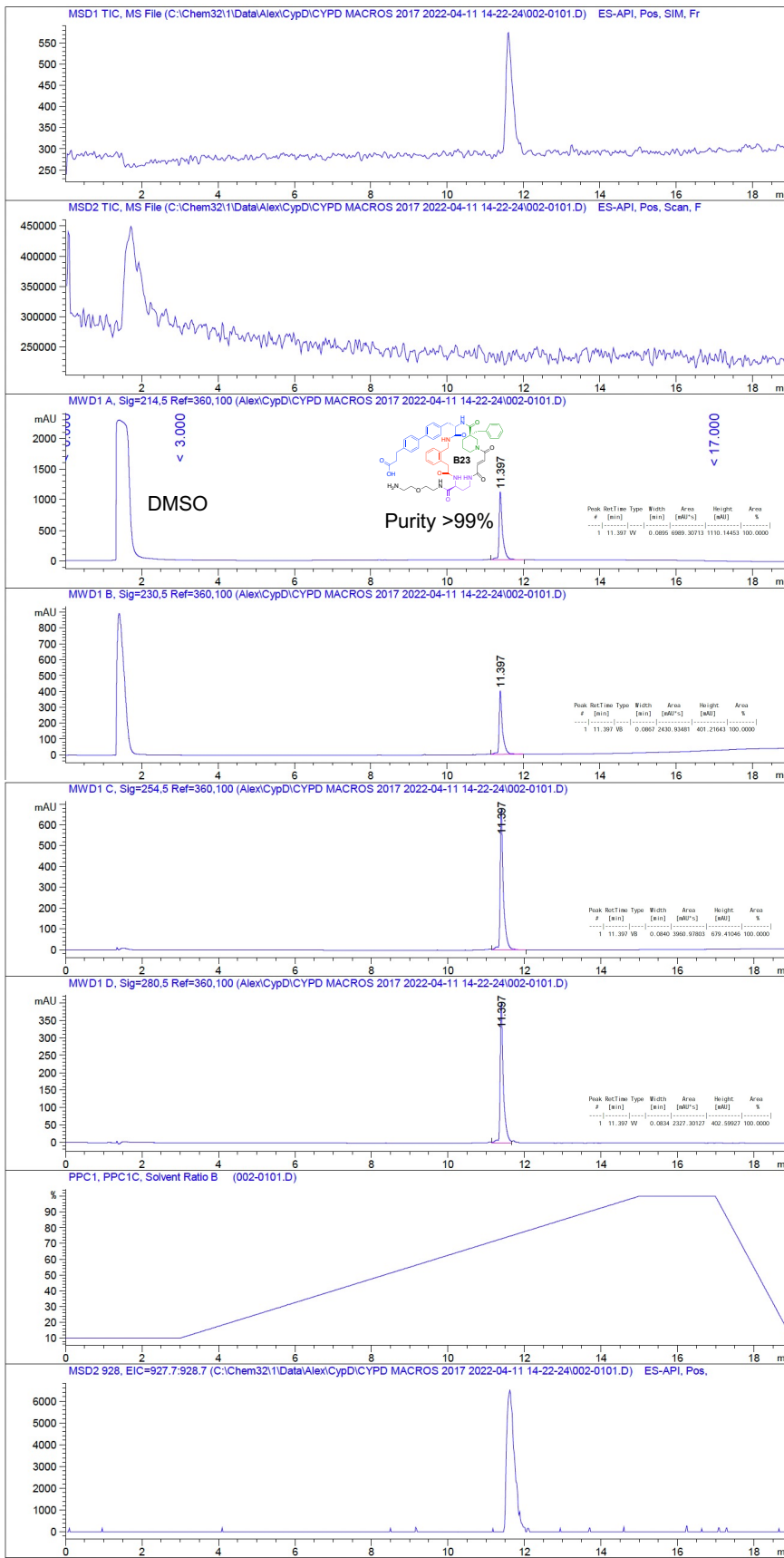
B1



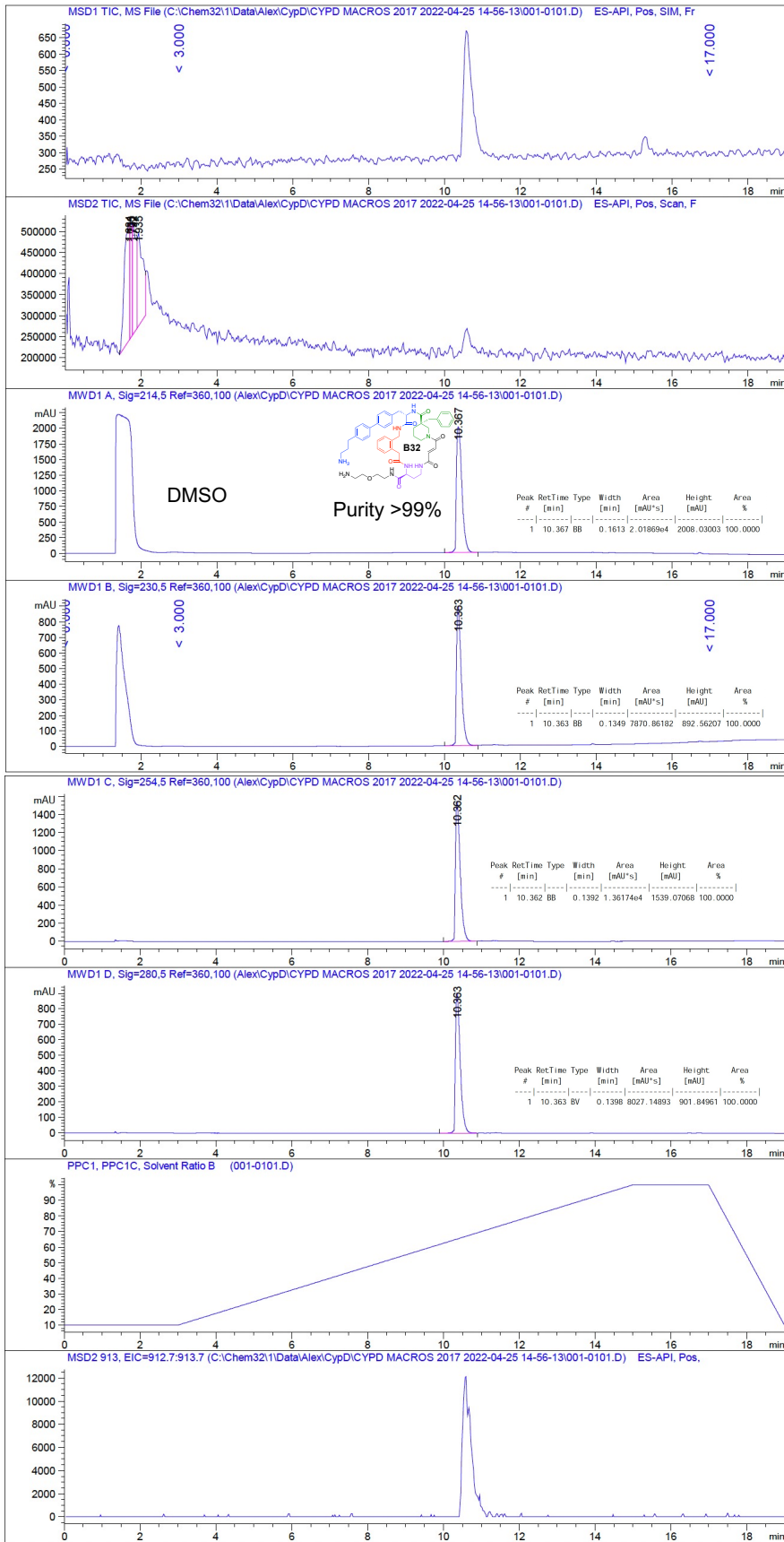
B2



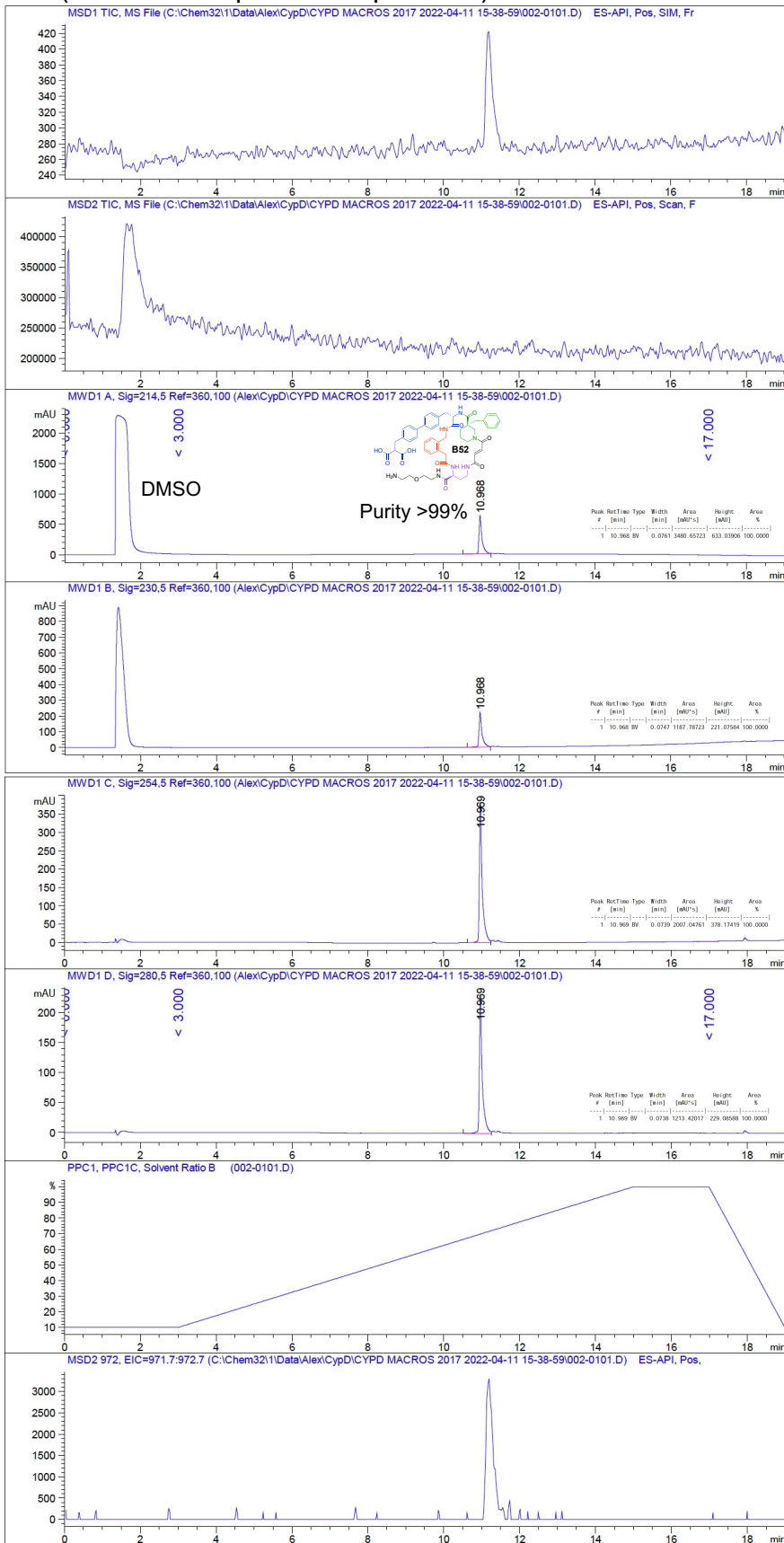
B23



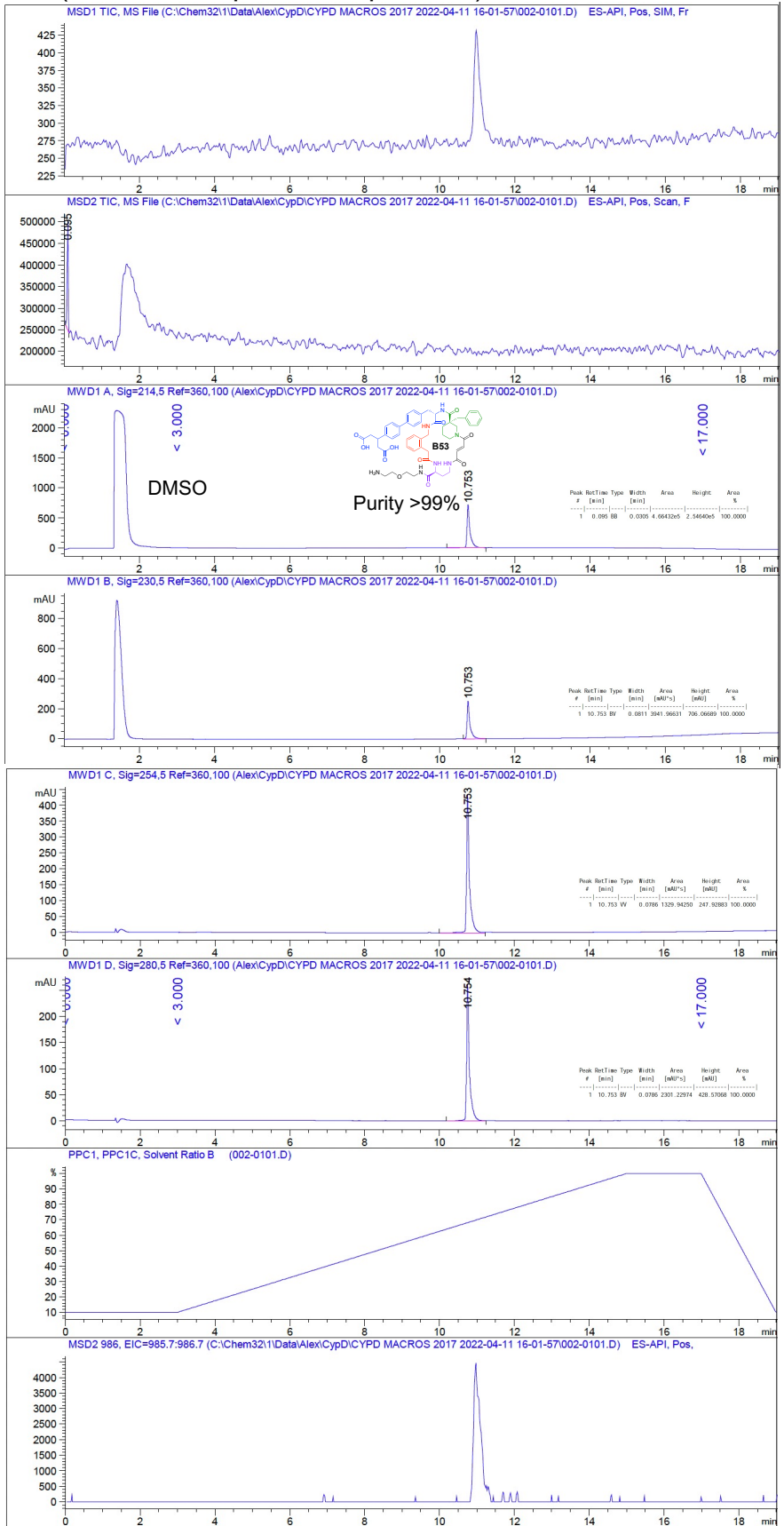
B32



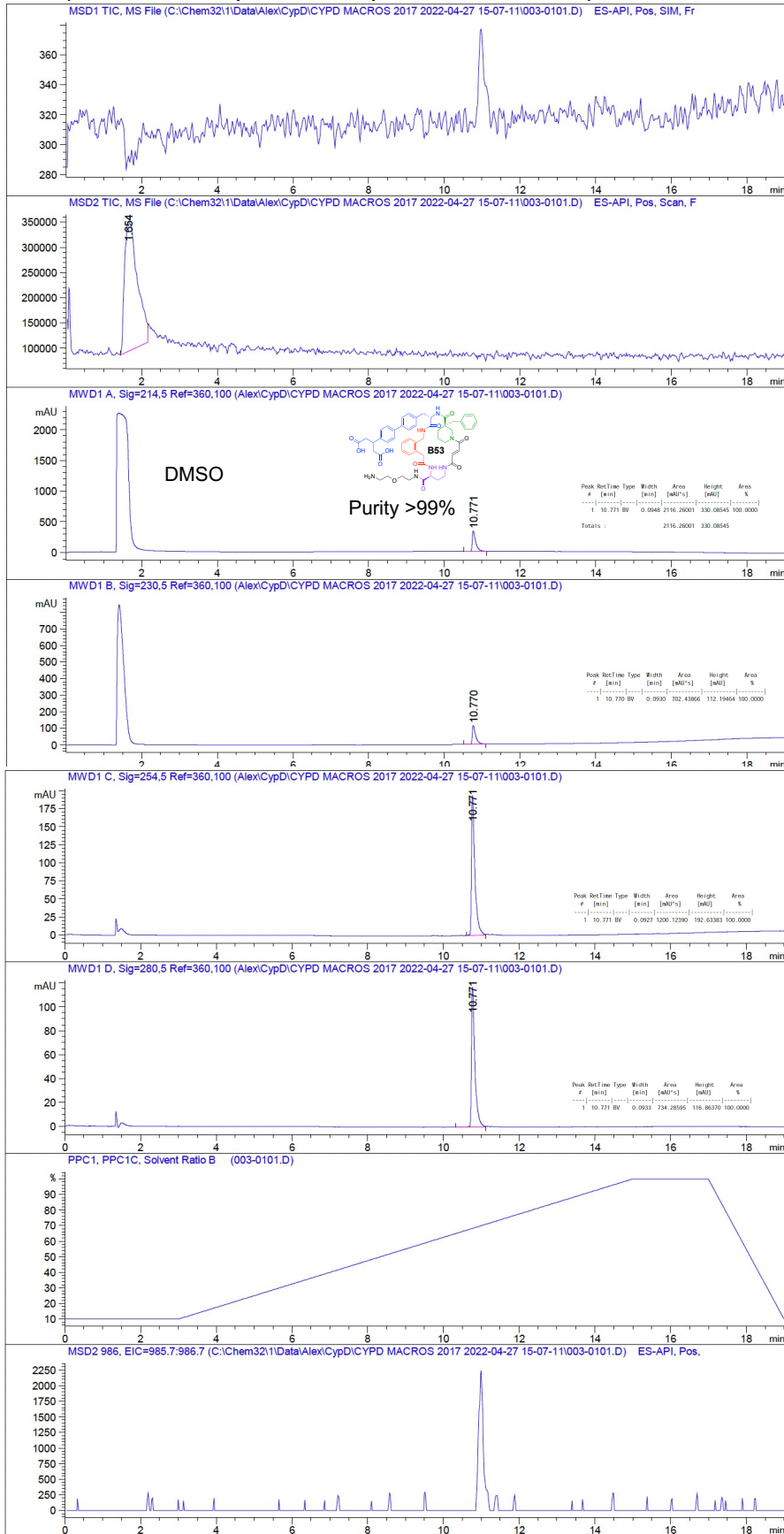
B52 (used for independent replicate 1)



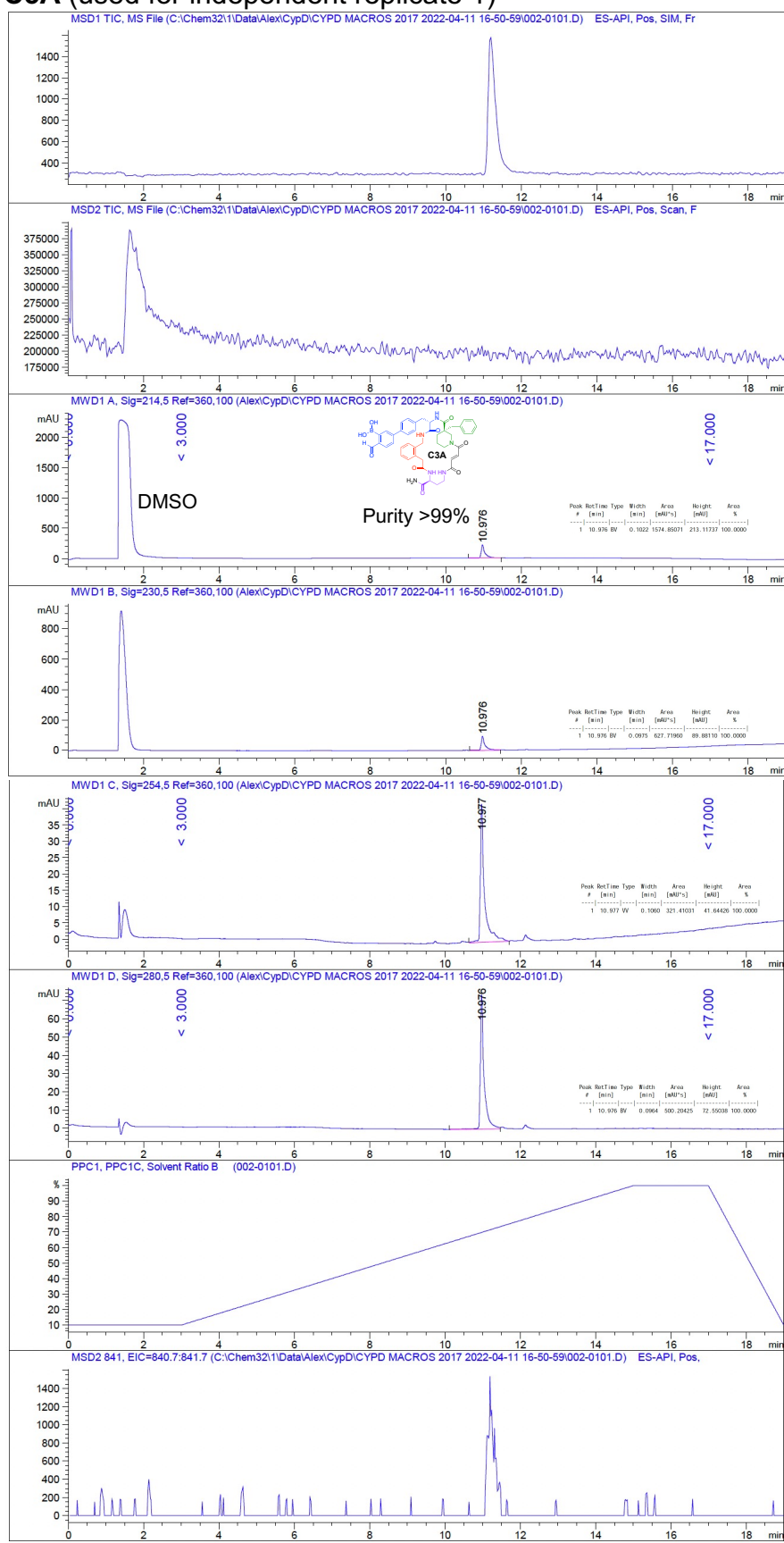
B53 (used for independent replicate 1)



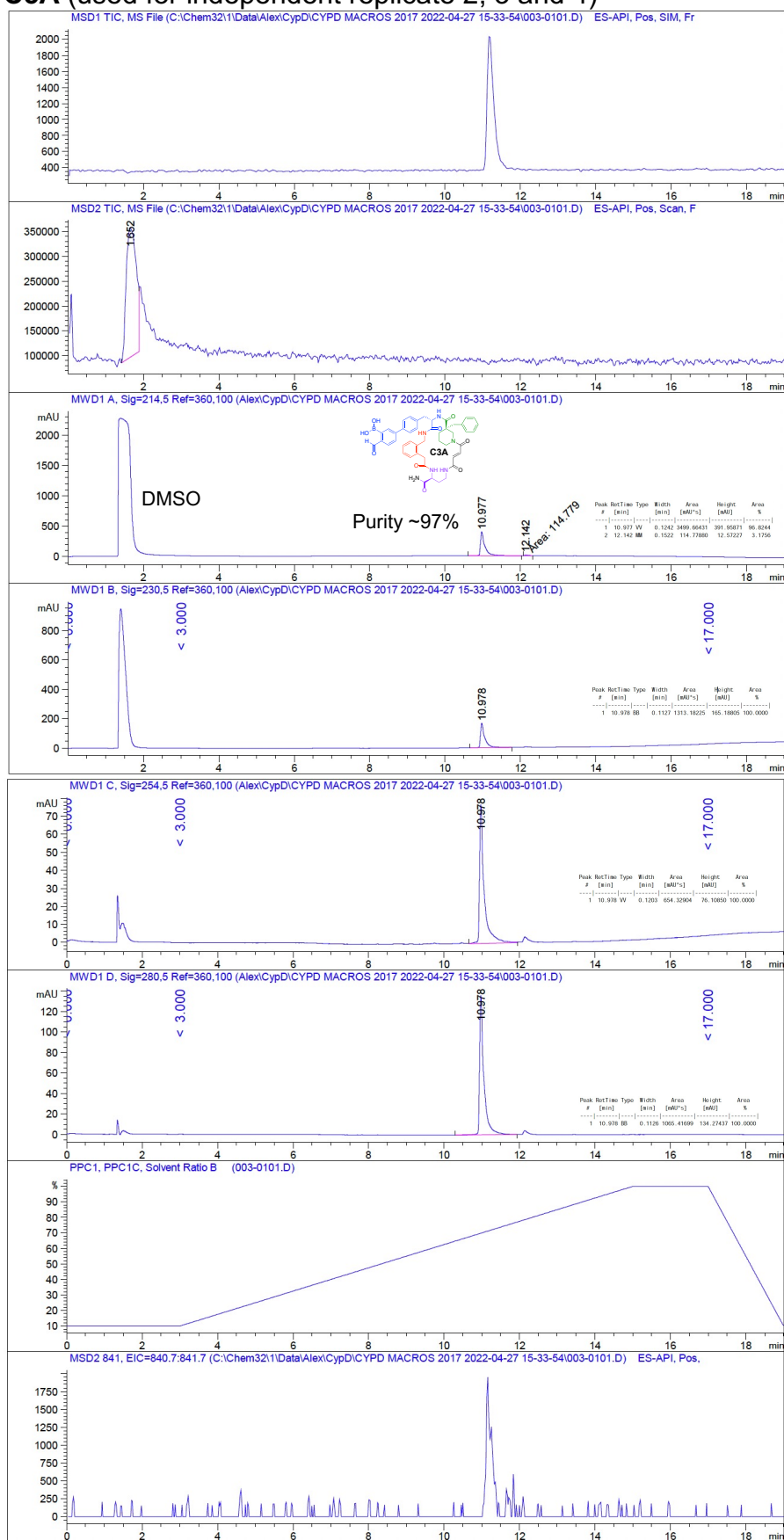
B53 (used for independent replicate 2, 3 and 4)



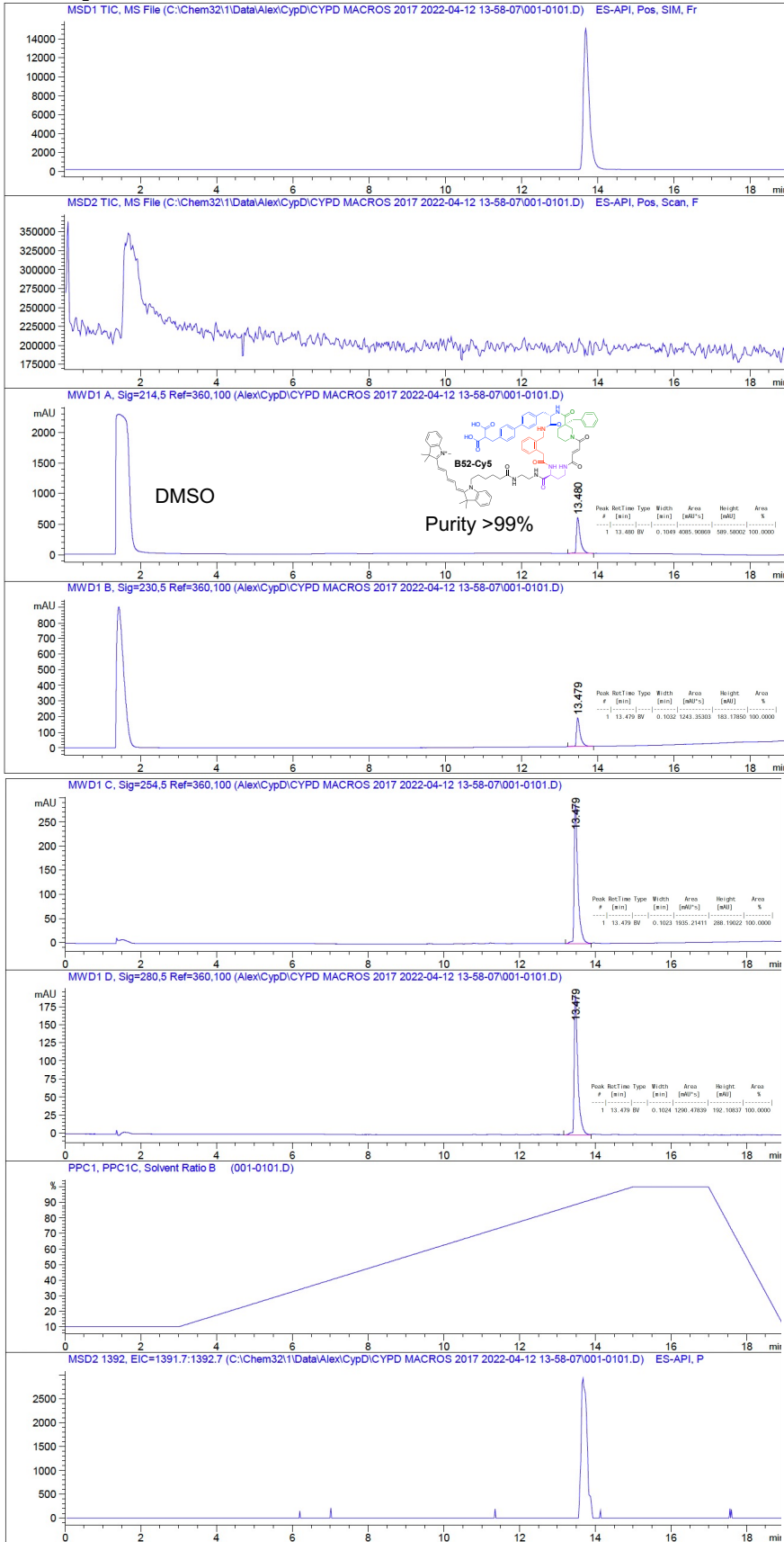
C3A (used for independent replicate 1)



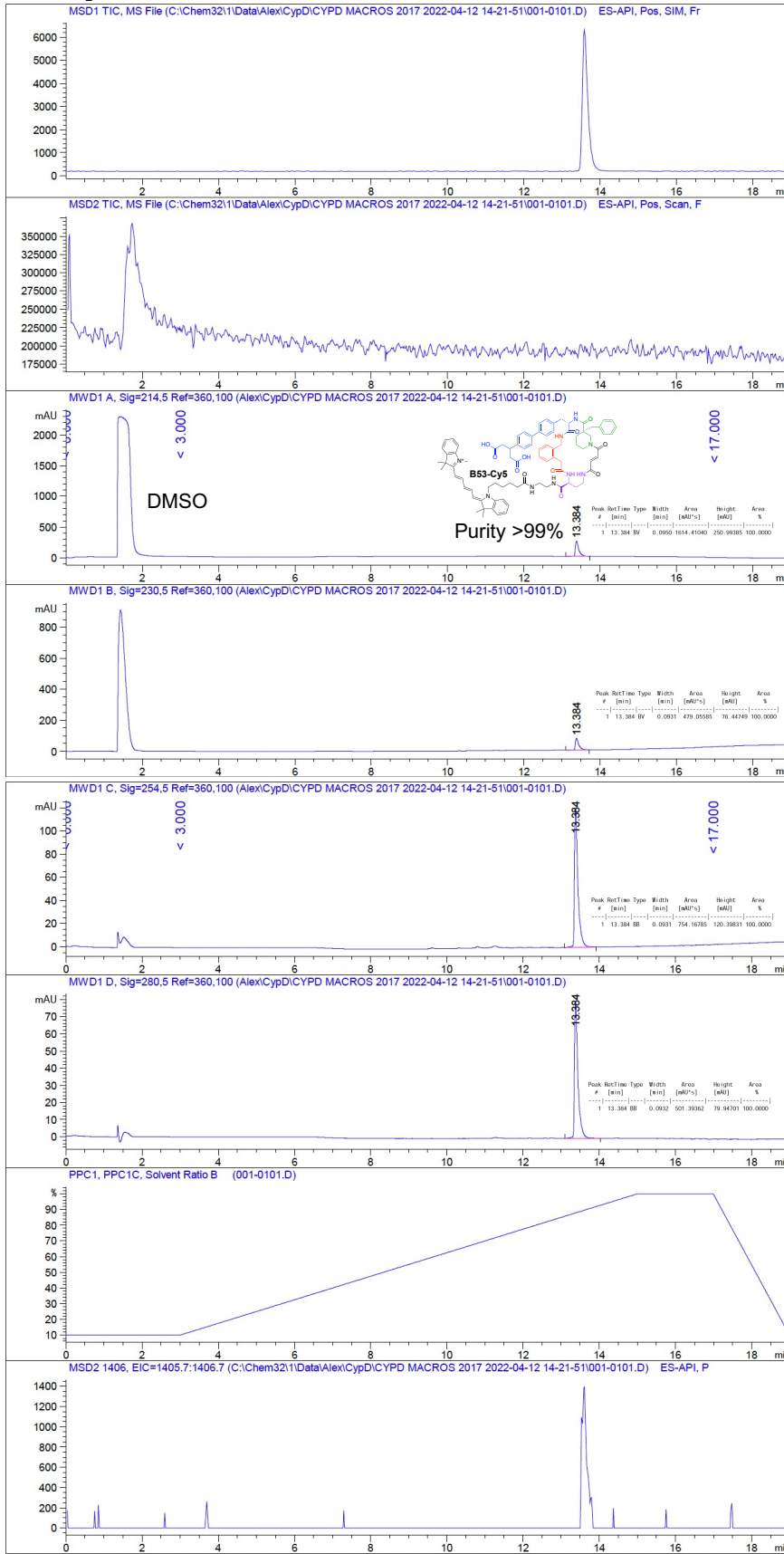
C3A (used for independent replicate 2, 3 and 4)



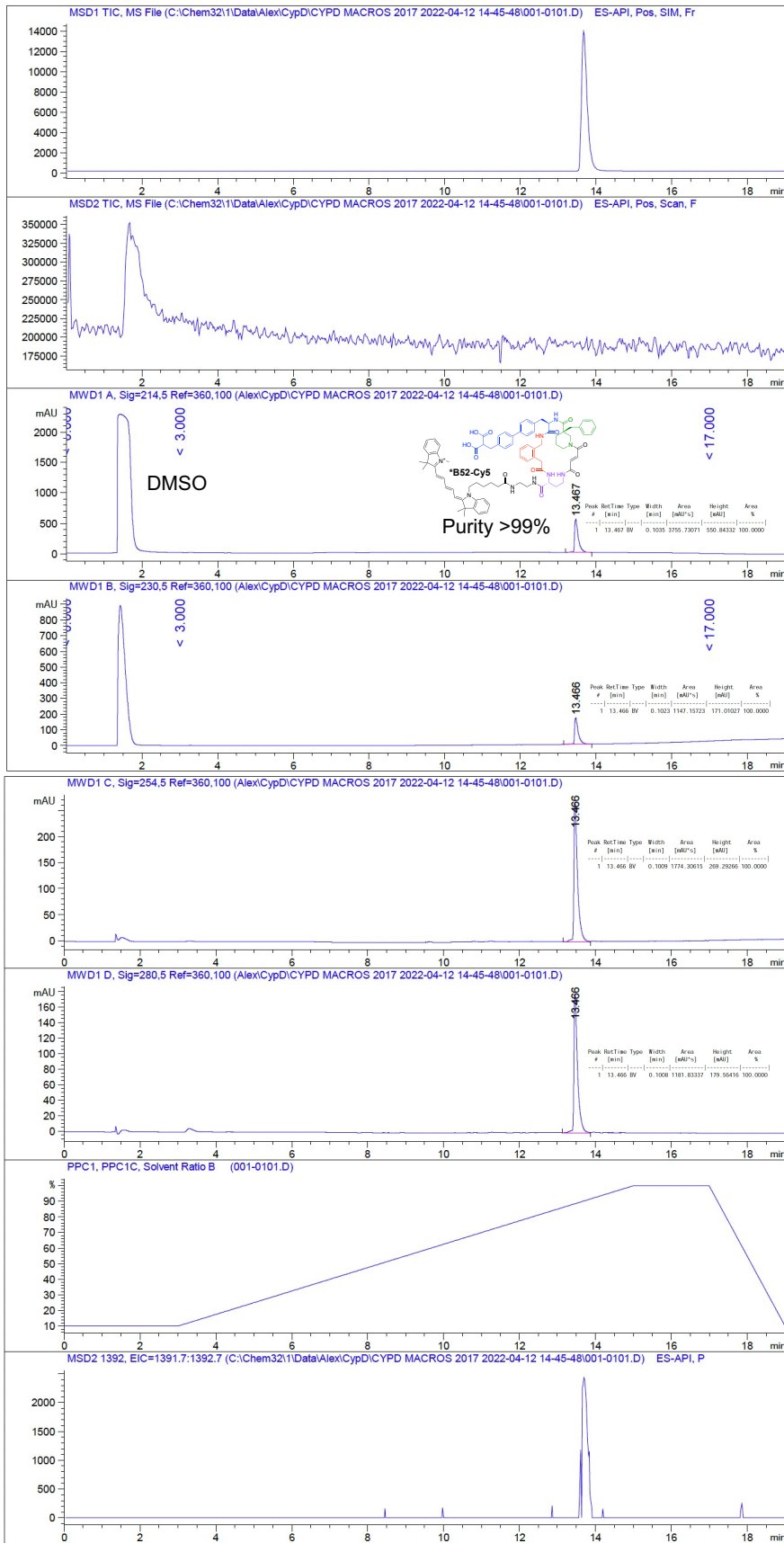
B52-Cy5



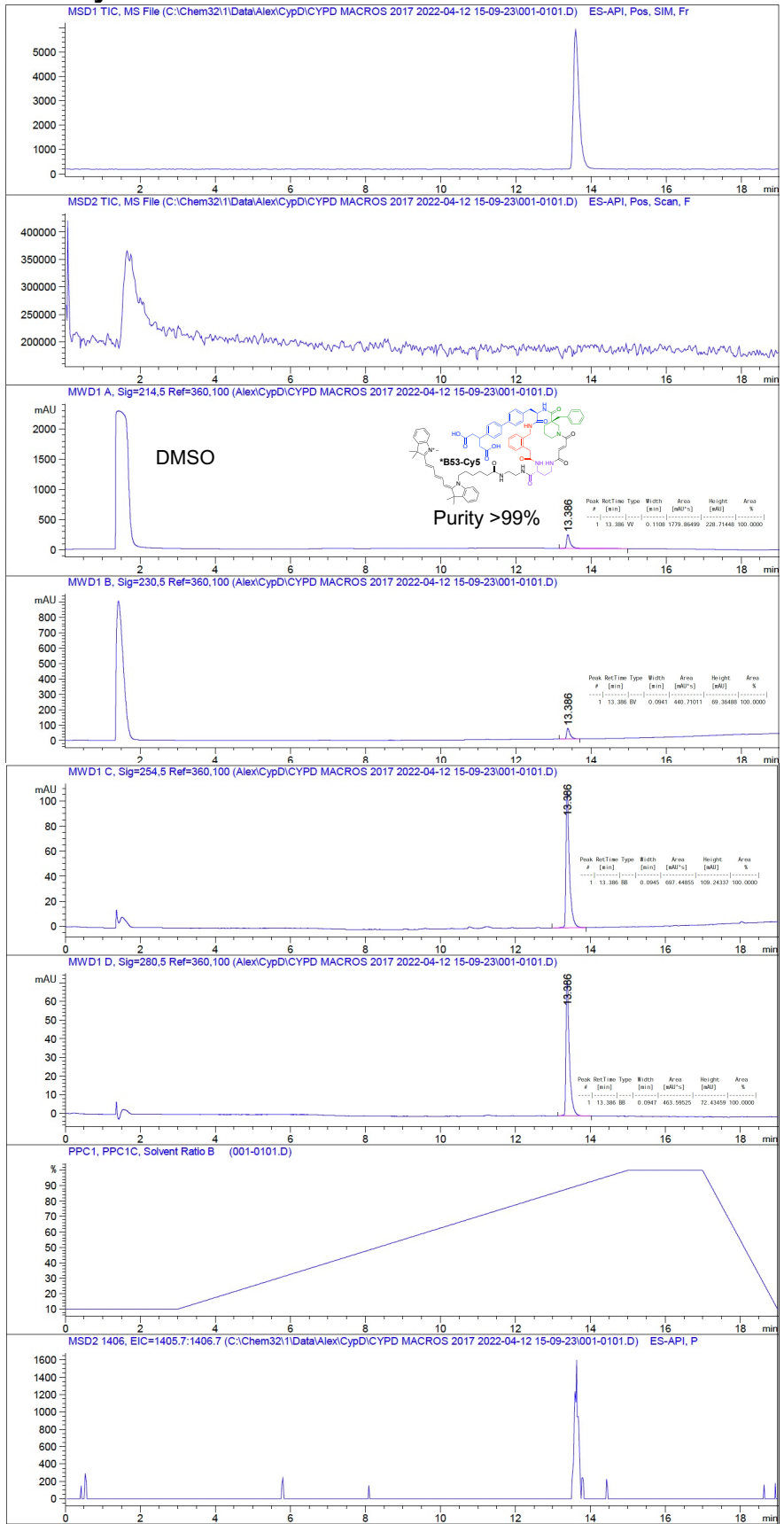
B53-Cy5



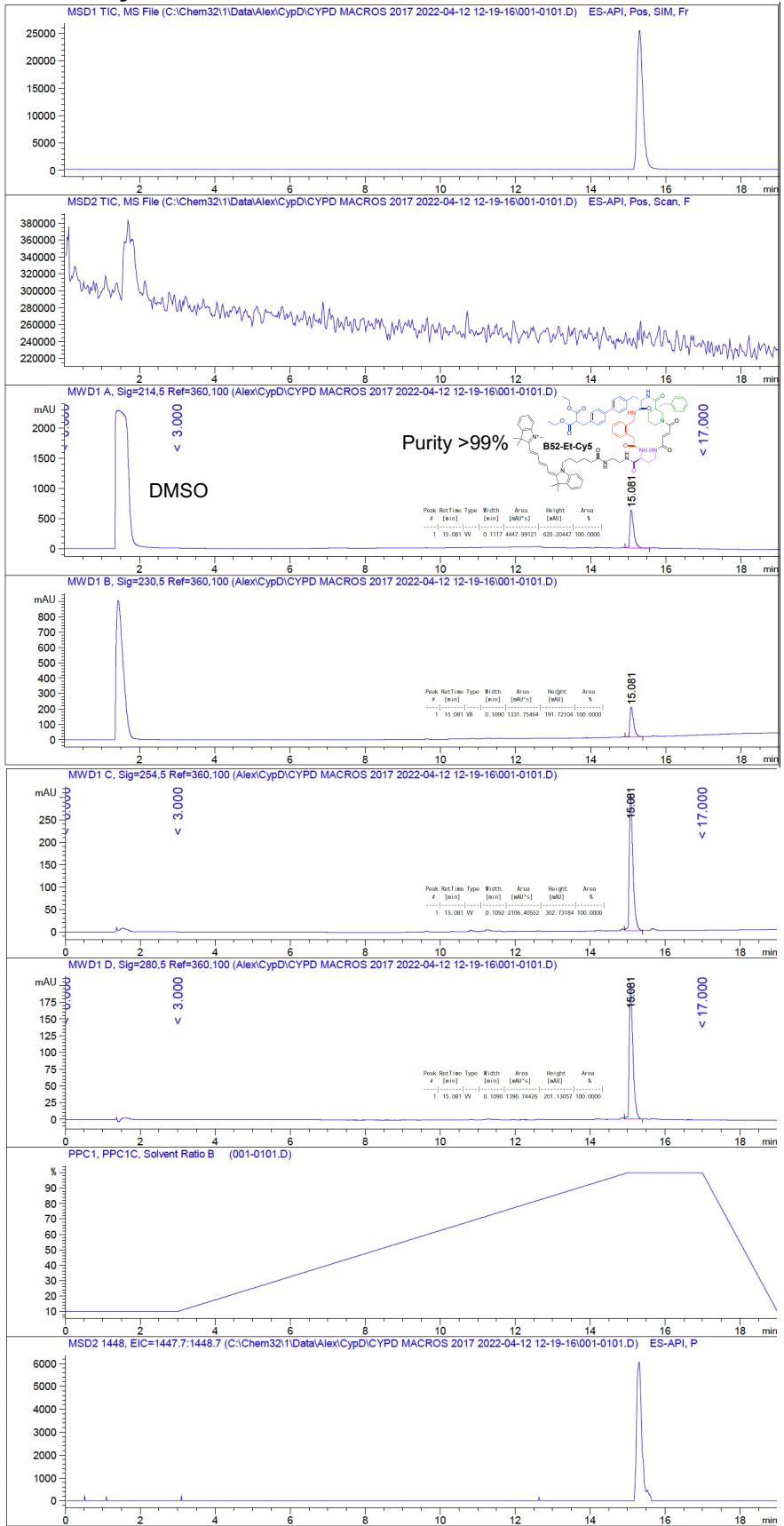
***B52-Cy5**



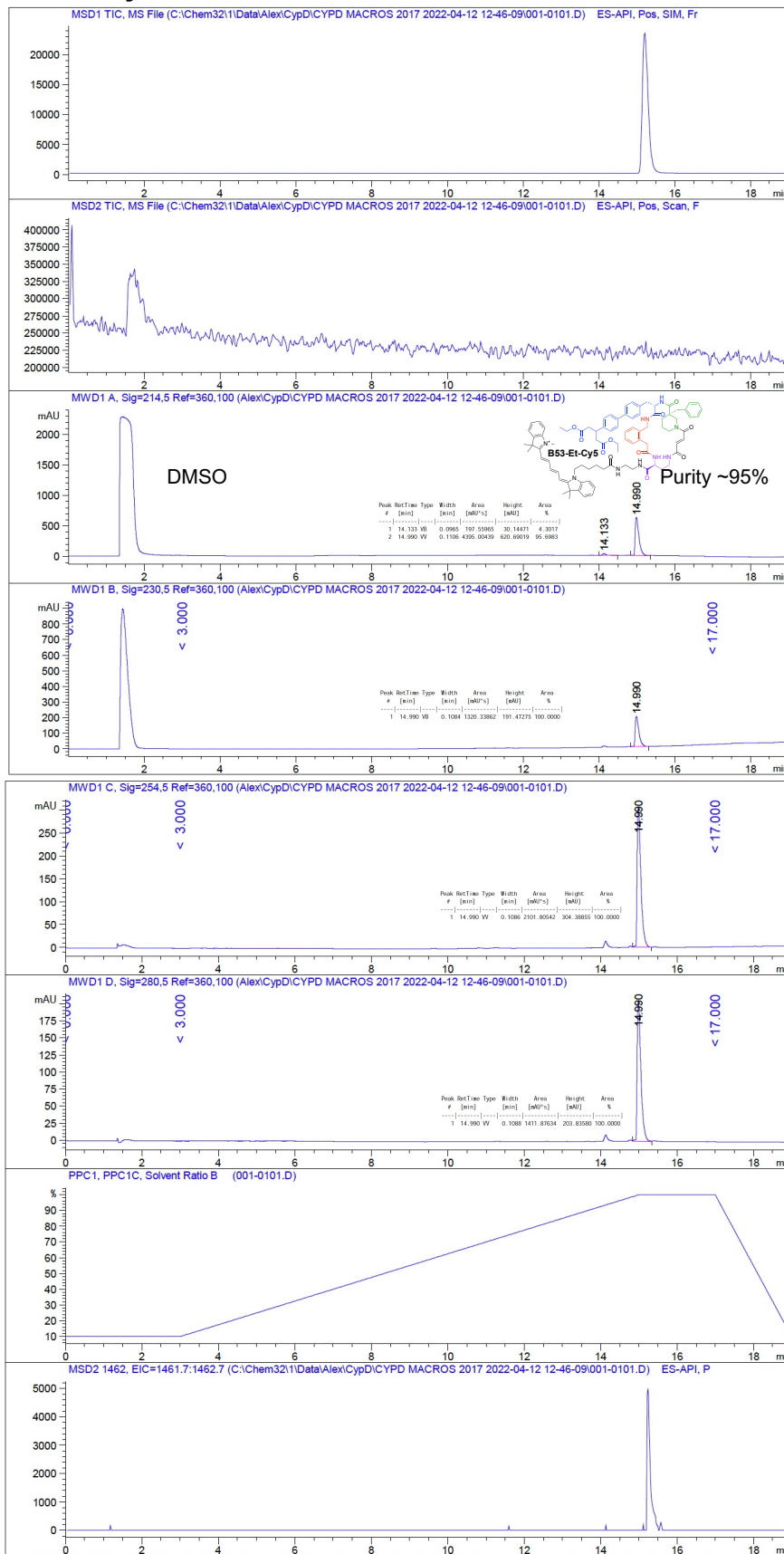
***B53-Cy5**



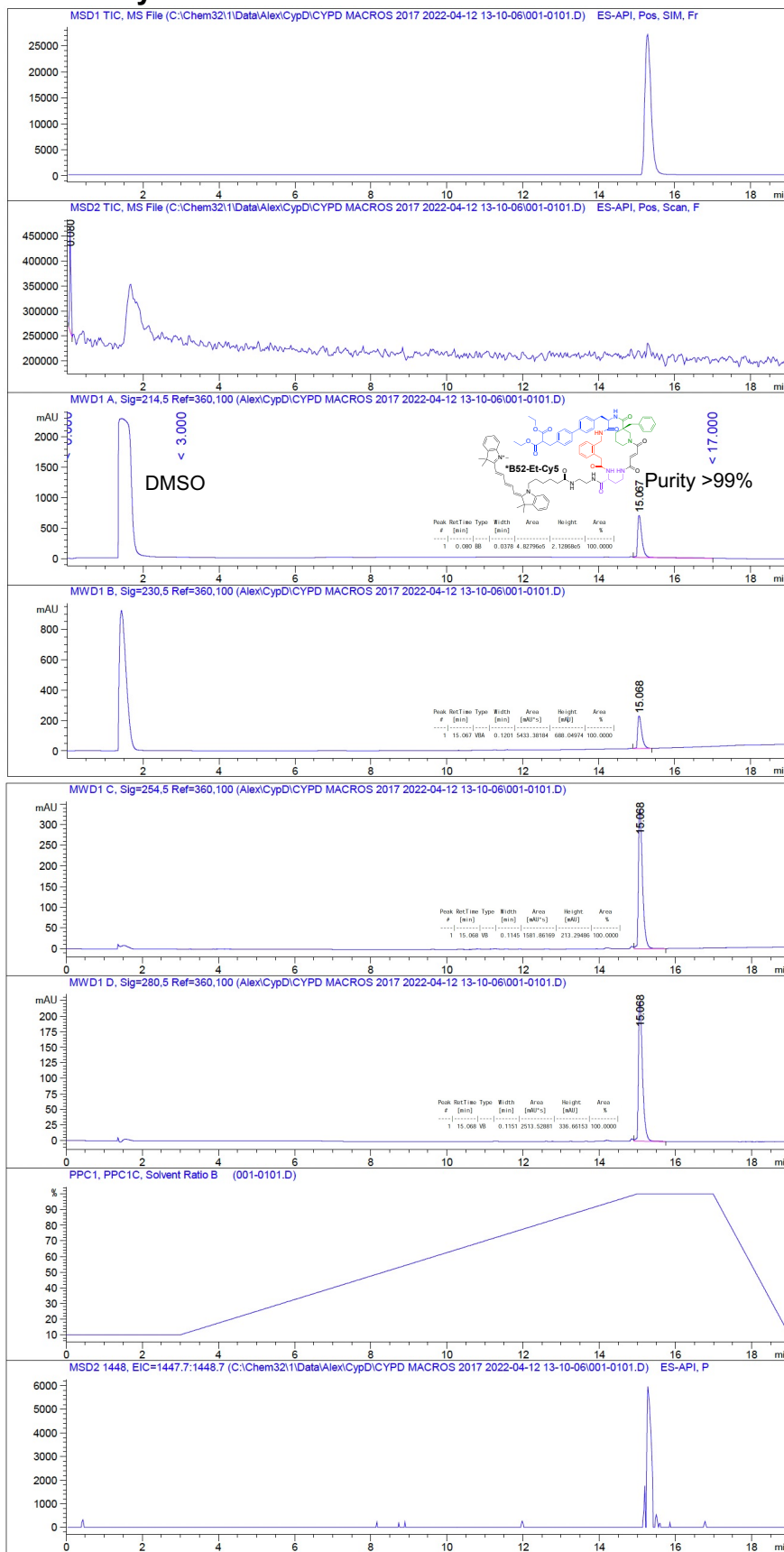
B52-Et-Cy5



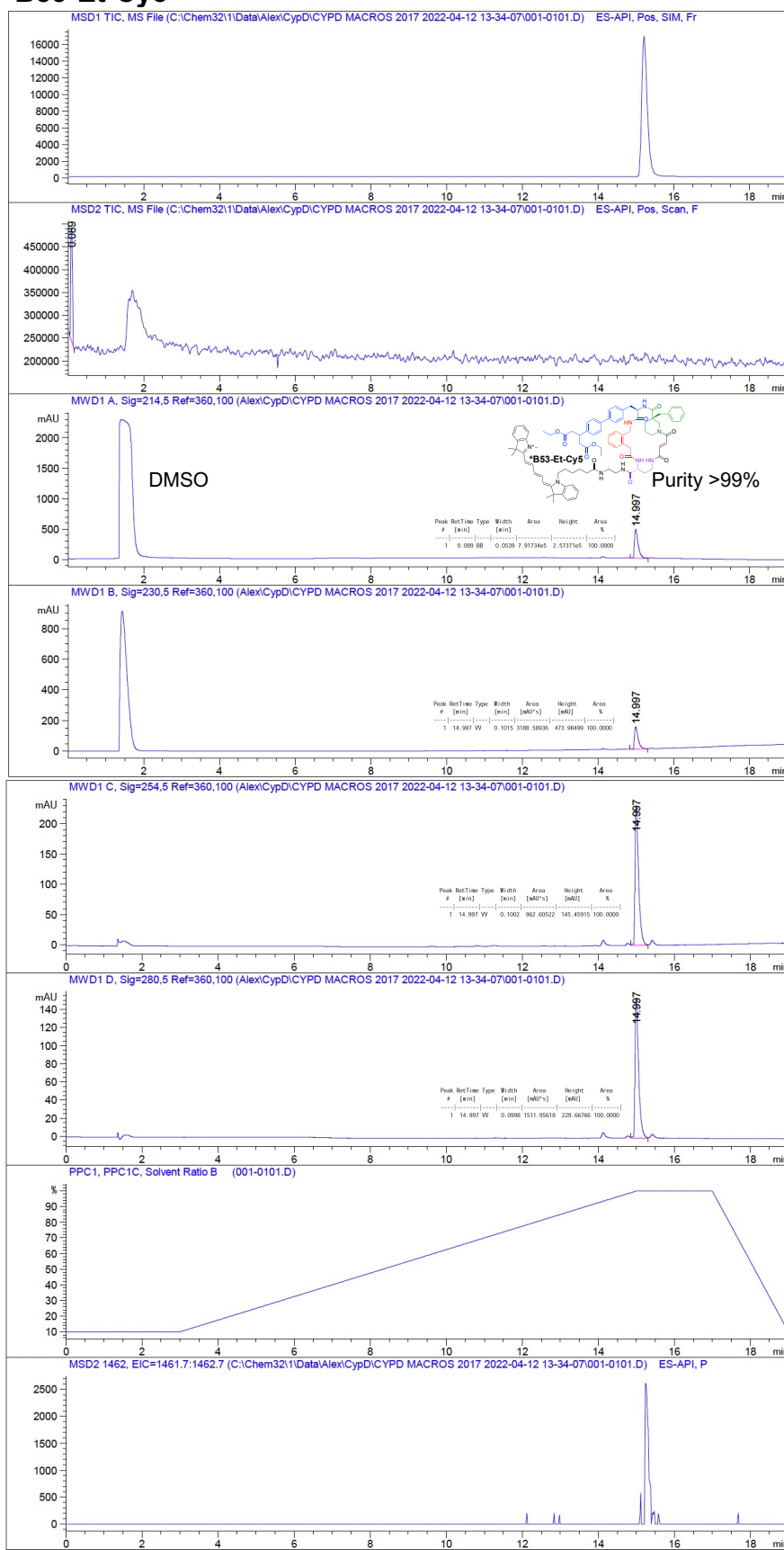
B53-Et-Cy5



***B52-Et-Cy5**



***B53-Et-Cy5**



Supplementary References

1. Usanov, D. L., Chan, A. I., Maianti, J. P. & Liu, D. R. Second-generation DNA-templated macrocycle libraries for the discovery of bioactive small molecules. *Nat. Chem.* **10**, 1–11 (2018).
2. Qiao, J. X. *et al.* Synthesis of Fmoc-Protected Arylphenylalanines (Bip Derivatives) via Nonaqueous Suzuki-Miyaura Cross-Coupling Reactions. *J. Org. Chem.* **81**, 9499–9506 (2016).
3. Hinkes, S. P. A. & Klein, C. D. P. Virtues of Volatility: A Facile Transesterification Approach to Boronic Acids. *Org. Lett.* **21**, 3048–3052 (2019).
4. Fretz, Heinz; Lyothier, Isabelle; Pothier, Julien; Richard-Bildstein, Sylvia; Sifferlen, Thierry; Wyder Peterson, Lorenza; Pozzi, D. & Corminboeuf, O. N-SUBSTITUTED INDOLE DERIVATIVES AS PGE2 RECEPTOR MODULATORS. (2017). doi:WO 2017/085198A1
5. Yang, D. *et al.* Synthesis and characterization of chiral N-O turns induced by α -aminoxy acids. *J. Org. Chem.* **66**, 7303–7312 (2001).
6. Wilent, J. & Petersen, K. S. Enantioselective desymmetrization of diesters. *J. Org. Chem.* **79**, 2303–2307 (2014).
7. Lunn, D. J. *et al.* Scalable synthesis of an architectural library of well-defined poly(acrylic acid) derivatives: Role of structure on dispersant performance. *J. Polym. Sci. Part A Polym. Chem.* **57**, 716–725 (2019).
8. Quach, D. *et al.* Strategic Design of Catalytic Lysine-Targeting Reversible Covalent BCR-ABL Inhibitors. *Angew. Chemie - Int. Ed.* **60**, 17131–17137 (2021).
9. Crudden, C. M. *et al.* Iterative protecting group-free cross-coupling leading to chiral multiply arylated structures. *Nat. Commun.* **7**, 1–7 (2016).